

**VIRIDIOFUNGINS AND XENIOLIDE F:
TARGET ORIENTED SYNTHESIS USING DIFFERENT REARRANGEMENT
REACTIONS OF A COMMON SUBSTRATE CLASS**

DISSERTATION

zur Erlangung des akademischen Grades

Doctor rerum naturalium

(Dr. rer. nat.)

vorgelegt

der Fakultät Mathematik und Naturwissenschaften
der Technischen Universität Dresden

von

Diplom-Chemikerin ANNETT POLLEX

geboren am 14.01.1978 in Dresden

Gutachter: 1)
 2)
 3)

Eingereicht am:

Tag der Verteidigung:

Dresden 2006

The present Ph.D. thesis work was realized based upon a suggestion and under the guidance of Prof. M. Hiersemann between September 2003 and September 2006 at the Technische Universität Dresden.

I thank Prof. M. Hiersemann for giving me the opportunity to work on this interesting project and for his constant support and advice.

To My Parents & Patrick

Table of Contents

| | | |
|-----------------------------|---|----|
| 1 | The Task..... | 1 |
| Part 1: Viridiofungins..... | | 5 |
| 2 | Introduction..... | 7 |
| 2.1 | Fungi: Versatile Multi-Purpose Organism with Fundamental Importance..... | 7 |
| 2.2 | Trichoderma Viride..... | 9 |
| 2.3 | Viridiofungins..... | 11 |
| 2.3.1 | Viridiofungin A – an Alkyl Citrate..... | 11 |
| 2.3.2 | Viridiofungins – Biological Activity..... | 14 |
| 2.3.3 | Proposed Biosynthesis of Viridiofungins..... | 18 |
| 2.3.4 | Published Total Syntheses of Viridiofungins..... | 19 |
| 3 | Retrosynthetic Analysis of Viridiofungin A..... | 27 |
| 4 | Ester Dienolate [2,3]-Wittig Rearrangement..... | 30 |
| 4.1 | Historical Development, Main Characteristics and Heteroatom Analogues..... | 30 |
| 4.1.1 | The Carbanion Stabilizing Group G..... | 32 |
| 4.1.2 | Formation of the Carbanion..... | 34 |
| 4.2 | Mechanism and Simple Diastereoselectivity..... | 36 |
| 4.3 | Induced Diastereo- and Enantioselectivity during [2,3]-Wittig Rearrangements.... | 41 |
| 4.3.1 | Substrate-Induced Diastereo- and Enantioselectivity: 1,3-Chirality Transfer and Remote Stereocontrol..... | 41 |
| 4.3.2 | Auxiliary-Induced Diastereoselectivity..... | 44 |
| 4.3.3 | Reagent-Induced Enantioselectivity..... | 46 |
| 4.3.4 | Catalyst-Induced Enantioselectivity..... | 47 |
| 4.4 | Ester Enolate [2,3]-Wittig Rearrangement..... | 49 |
| 4.5 | Ester Dienolate [2,3]-Wittig Rearrangement..... | 50 |
| 5 | Synthesis of the Eastern Half..... | 56 |
| 6 | Synthesis of the Western Half..... | 60 |
| 7 | Synthesis of the Viridiofungin A, A ₂ and A ₄ Triesters..... | 66 |
| 8 | Verification of the Proposed Structure of Viridiofungin A Triester (–)-65a..... | 75 |

| | |
|--|-----|
| Part 2: (+)-Xeniolide F | 81 |
| 9 Introduction | 83 |
| 9.1 Xenias: Soft Corals of the Genus Anthozoa – their Biology and the Resulting Potential as Sources of Pharmaceutical Interesting Natural Products..... | 83 |
| 9.2 Xenicane Diterpenes | 88 |
| 9.2.1 Xeniolide F – One Bioactive Representative of the Xenicane Diterpenes | 88 |
| 9.2.2 Proposed Biosynthesis of (+)-Xeniolide F | 91 |
| 9.2.3 Published Total Synthesis of Xenicane Diterpenes..... | 93 |
| 10 Retrosynthetic Analysis of Xeniolide F | 96 |
| 11 The Catalytic Asymmetric Claisen Rearrangement (CAC) | 102 |
| 11.1 Historical Development and Important Variations | 102 |
| 11.2 Mechanism and Simple Diastereoselectivity | 105 |
| 11.2.1 Mechanism | 105 |
| 11.2.2 Simple Diastereoselectivity (Syn-/Anti-Selectivity)..... | 107 |
| 11.2.3 Strategies for the Diastereoselective Formation of the Vinyl Ether Double Bond | 109 |
| 11.3 Induced Diastereo- and Enantioselectivity during Claisen Rearrangements | 112 |
| 11.3.1 Substrate-Induced Diastereo- and Enantioselectivity: 1,3-Chirality Transfer and Remote Stereocontrol..... | 112 |
| 11.3.2 Auxiliary-Induced Diastereoselectivity..... | 113 |
| 11.3.3 Reagent-Induced Enantioselectivity..... | 116 |
| 11.3.4 Catalyst-Induced Enantioselectivity..... | 119 |
| 12 Copper(II) Bis(oxazoline) Complexes | 136 |
| 13 Stereoselective Synthesis of the Allylic Alcohol | 144 |
| 13.1 Butyrolactone Route..... | 144 |
| 13.2 Cross-Coupling Approach..... | 147 |
| 13.2.1 Stille Cross-Coupling | 149 |
| 13.2.2 Negishi and Suzuki-Miyaura Cross-Coupling | 152 |
| 14 Stereoselective Synthesis of Allyl Vinyl Ethers via Horner-Wadsworth-Emmons Olefination..... | 160 |
| 14.1 Rhodium-Catalyzed OH-Insertion | 161 |
| 14.1.1 Synthesis of the Phosphonates | 166 |
| 14.1.2 Application of the Rhodium-Catalyzed OH-Insertion | 167 |
| 14.2 Horner-Wadsworth-Emmons Olefination | 168 |
| 15 Catalytic Asymmetric Claisen Rearrangement (CAC) | 172 |
| 16 Side Chain Synthesis and Introduction | 185 |
| 17 Preliminary Experiments for the Envisaged Nozaki-Hiyama-Kishi Reaction..... | 195 |
| 18 Summary and Future Prospects..... | 197 |

| | | |
|--------|--|-----|
| 19 | Verification of the Proposed Structure..... | 200 |
| | Part 3: Experimental Section..... | 207 |
| 20 | Experimental Section | 209 |
| 20.1 | General Experimental Methods..... | 209 |
| 20.2 | Viridiofungins | 214 |
| 20.2.1 | Synthesis of the Eastern Half | 214 |
| 20.2.2 | Synthesis of the Western Half..... | 224 |
| 20.2.3 | Synthesis of the Viridiofungin A, A ₄ , A ₂ Triesters | 234 |
| 20.3 | (-)-Xeniolide F..... | 251 |
| 20.3.1 | Stereoselective Synthesis of the Allylic Alcohol | 251 |
| 20.3.2 | Synthesis of the Allyl Vinyl Ether, Synthesis of the Catalyst, Claisen Rearrangement and Further Steps toward (-)-Xeniolide F | 267 |
| 20.3.3 | Side Chain Synthesis | 291 |
| 21 | Appendix | 304 |

1 The Task

The viridifungins (-)-A, (-)-A₂ and (-)-A₄ (Figure 1, right) and (+)-xeniolide F (Figure 1, left) are members of very different natural product classes. While the viridifungins **1** are members of the alkyl citrate natural product family, (+)-xeniolide F (**2a**) is a xenicane diterpene.

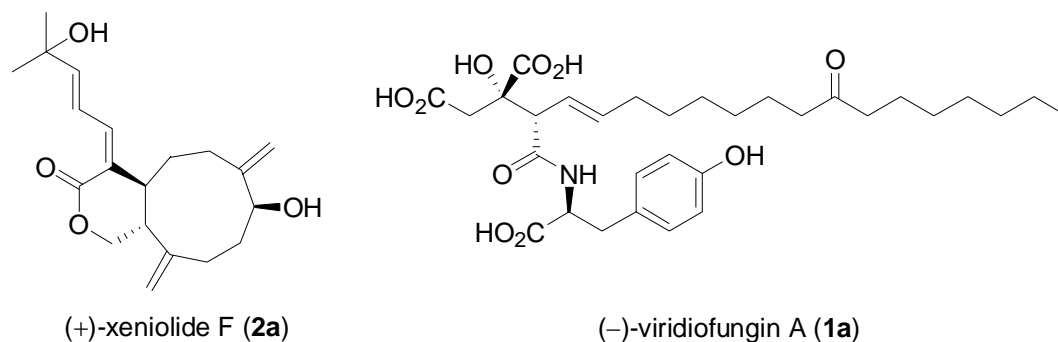
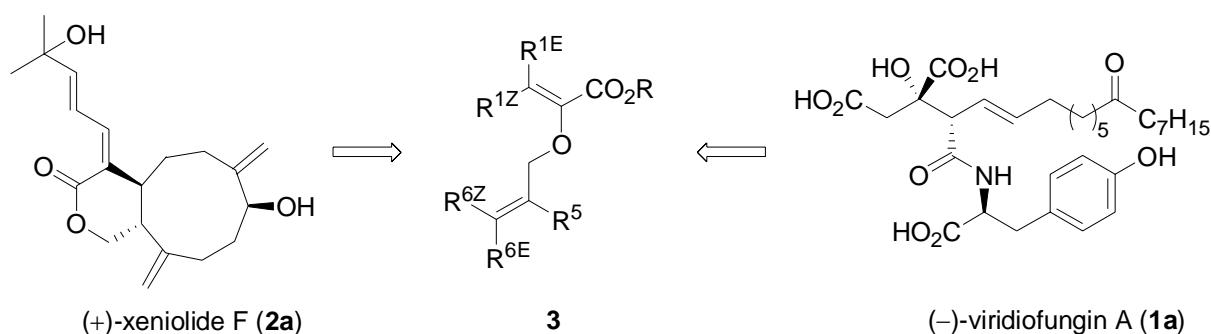


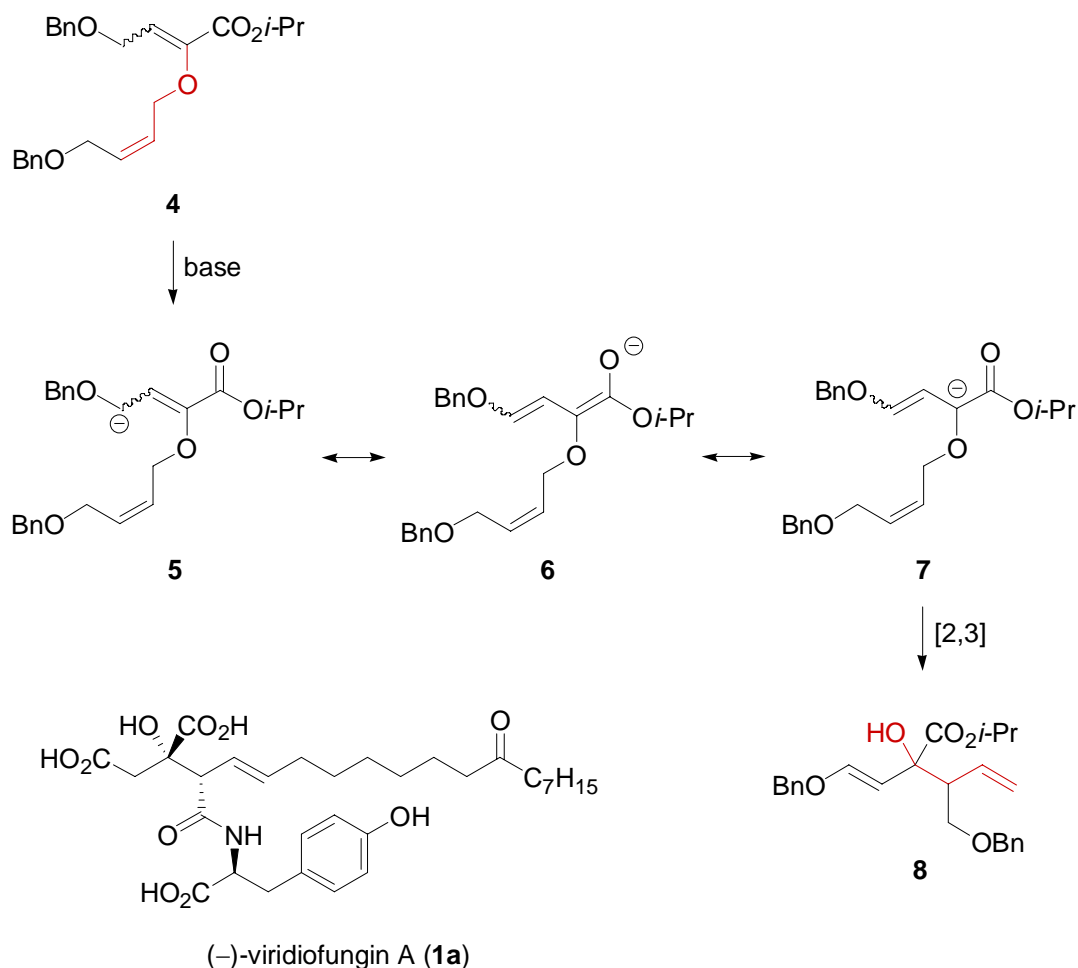
Figure 1

At first sight, these natural products do not have a lot in common except two adjacent stereogenic centers. The substitution patterns at the stereogenic centers are significantly different. The polar head group of the viridifungins (e.g. **1a**) includes a quaternary stereogenic center and shows a high degree of oxidation. In contrast, (+)-xeniolide F (**2a**) is characterized by two vicinal tertiary stereogenic centers. Nevertheless, we proposed that both natural products may be synthesized from a common starting material – the α,β -unsaturated esters **3** (Scheme 1).



Scheme 1: Retrosynthetic analysis of (+)-xeniolide F (**2a**) and (-)-viridifungin A (**1a**) lead in both cases to α,β -unsaturated esters **3**.

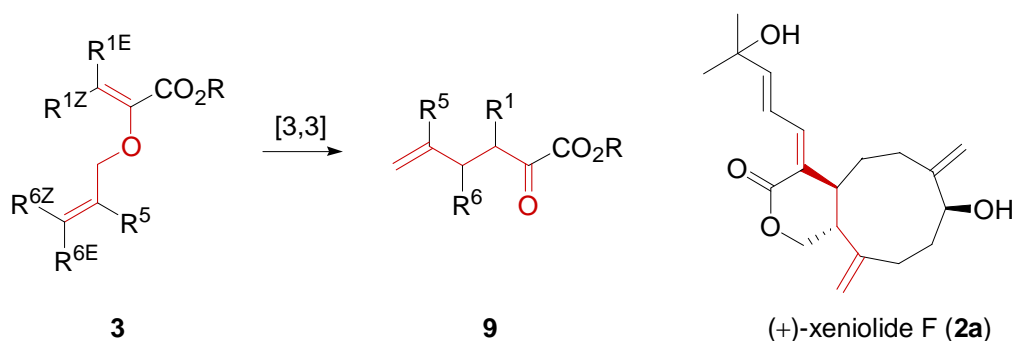
The α -allyloxy-substituted α,β -unsaturated esters **3** are precursors of α -allyloxy-substituted carbanions (e.g. **7**) which are prone to undergo a [2,3]-Wittig rearrangement. Deprotonation of **4** and resonance stabilization of **5** provides **7** (Scheme 2).



Scheme 2: Identification of the [2,3]-Wittig retron in **8** - a precursor for the synthesis of (-)-viridifungin A (**1a**).

Structural similarities between the rearrangement product **8** and the polar head group of the target molecule **1a** are clearly visible. The three carboxylic acid groups of **1a** are introduced as an ester, an enol ether and a protected alcohol. This would allow the chemoselective transformation of each of the three prospective carboxylic acid groups individually.

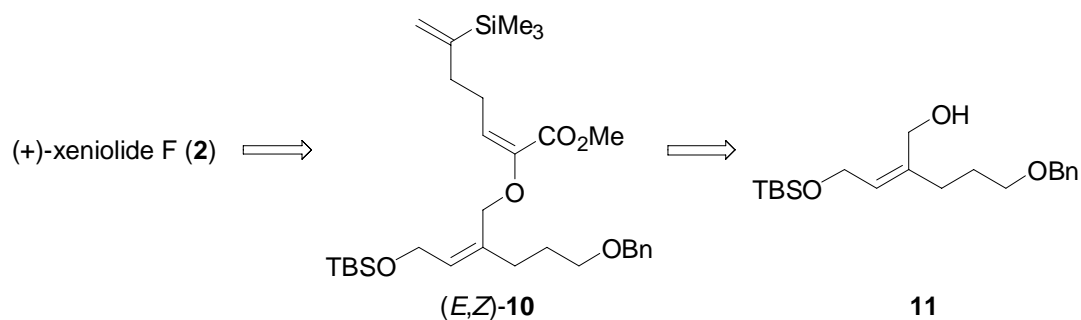
Furthermore, since α -allyloxy-substituted α,β -unsaturated esters **3** contain an allyl vinyl ether element, they are prone to undergo Claisen rearrangements. The transformation results in γ,δ -unsaturated α -keto esters **9**. The Claisen retron is highlighted in Scheme 3. Consequently, by using an appropriately substituted α,β -unsaturated ester **3** the total synthesis of the natural product **2a** may be realized.



Scheme 3: Identification of the Claisen retron in (+)-xeniolide F (**2a**).

The aim of this work was the completion of the total synthesis of the viridiofungin A, A₂ and A₄ triesters with an ester dienolate [2,3]-Wittig rearrangement as key CC-connecting step. Fundamental work for this part of the project has been performed previously by Lars Abraham – a former Ph.D. student in our research group¹ - and his contributions to the successful completion of the total synthesis is gratefully acknowledged.

In a second part of my Ph.D. thesis work the total synthesis of the diterpene (+)-xeniolide F (**2a**) should be investigated. Utilization of the catalytic asymmetric Claisen rearrangement (CAC) as key CC-connecting step for the enantioselective generation of the two adjacent stereogenic centers of the target molecule **2a** was envisioned. In the context of this work, a stereoselective route toward the *Z*-configured allylic alcohol **11** had to be developed. Additionally, 2-alkoxycarbonyl-substituted allyl vinyl ethers **10** should be synthesized utilizing a new, stereoselective strategy for the generation of the *E*-configured vinyl ether double bond.



Scheme 4: Retrosynthetic analysis of **2a** involves the (*E,Z*)-**10** and the *Z*-configured allylic alcohol **11**.

For the benefit of a concise presentation of the results achieved during my Ph.D. thesis, the viridiofungins and (+)-xeniolide F will be addressed individually.

¹ Deceased on a motorcycle accident in September 2003.

Part 1: Viridifungins

2 Introduction

2.1 Fungi: Versatile Multi-Purpose Organism with Fundamental Importance.

Fungi are one of the five kingdoms of life. There are over 100,000 known species of fungi.² The most familiar fungi are mushrooms and mold fungi (Image 1).



Image 1: Familiar phenotypes of fungi: mold (middle) and mushrooms (left and right).³

According to their lack of chlorophyll they depend on organic food sources. Most of them are saprophytes which means that they are living off of dead organisms decaying the organic material. They are especially important for the digestion of cellulose the main organic component of fouling plants. By breaking down the organic material of dead animals and plants, they are of fundamental importance in continuing the circle of nutrients through ecosystems. Despite this ecological relevance as recyclers, various beneficial applications of fungi play highly desirable roles in human life (Image 2). Mushrooms for example - the edible fungi - comprise some species being very popular among gourmets (e.g. cep or truffle). Yeast and barm fungi are essentially involved in the production of bread, wine and beer. Special molds are used for the fabrication of various cheese types (e.g. Roquefort or Camembert).

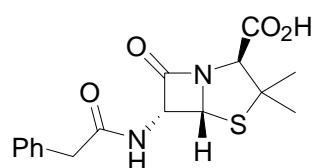
² (a) Alexopoulos, C. J.; Mims, C. W.; Blackwell, M. *Introductory Mycology (4th Ed.)*. John Wiley and Sons, New York, USA, **1996**. (b) Schwantes, H. O. *Biologie der Pilze – eine Einführung in die angewandte Mykologie (3rd Ed)*, Ulmer, Stuttgart, Germany, **1996**.

³ The images have been obtained from the following web pages (from left to right): (a) http://www.grossschutzgebiete.brandenburg.de/np_nllr/_fotos/Pilze-1.jpg; 25.05.2006 (b) <http://www.ib-rauch.de/Beratung/schim/schimpi01.jpg>; 25.05.2006 (c) <http://www.christoph-schnauss.de/misc/pilze/braun.jpg>; 25.05.2006



Image 2: Desirable applications of fungi are found in food production.⁴

Another example of a highly useful application derived from fungi is penicillin **12** (Figure 2), the outset and first example of an antibiotic, which was isolated from the fungal strain *Penicillium chrysogenum*.⁵



penicillin G (**12**)

Figure 2

On the other side, fungi infestation is known to cause severe harvest losses. Some toxins produced by such fungi are severely pathogenic. Examples are aflatoxins which are produced by *Asparagyllus* sp. that regularly affects cereals and nuts; or ergot toxins – alkaloids found in *Claviceps purpurea* (ergot) that often infects rye (Image 3).



Image 3: From left to right: *Claviceps purpurea*, ergot on rye spikes, corn infected by *Asparagyllus flavus*, and a microscopic image of the ascospores of the latter.⁶

⁴ The images have been obtained from the following web pages: from left to right (a) <http://www.provence-personally.com/images/truffle.jpg>; 25.05.2006 (b) <http://www.frencheese.co.uk/cheeses/photos/roquefort.jpg>; 25.05.2006 (c) <http://www.fraenkische-schweiz.com/info/images/bierglas.jpg>; 25.05.2006 (d) <http://www.uni-ulm.de/LiLL/forschendeslernen/europakontakte/brot.jpg>; 25.05.2006

⁵ <http://en.wikipedia.org/wiki/Penicillin>

⁶ The images have been obtained from the following web pages (left to right): (a) <http://www.dipbot.unict.it/sistematica/Immagini/13002.JPG>; 25.05.2006 (b) http://www.grzyby.pl/foto/ww/w_Claviceps_purpurea_030704_01.jpg; 25.05.2006 (c)

Mold infestation in human dwellings is known to cause allergic reactions in sensitive people. Infections can result from fungal contact, with ringworm and athlete's foot being probably the most widespread diseases in connection with fungal infection.

2.2 *Trichoderma Viride*

Trichoderma viride is one of the most commonly reported and widely distributed of all soil fungi (Image 4).⁷



Image 4: Microscopic image of *Trichoderma viride*: Hyphae (elongated filamentous forms) with conidia (spores) at the tips.⁸

Colonies of *Trichoderma viride* grow rapidly. Due to the filamentous consistence, they appear woolly and become compact in time.⁹ The filaments are colorless. The eponymous dark teal to greenish color (viridis (lat.) = green) is derived from the formation of conidia.



Image 5: Typical instars of *Trichoderma viride*.¹⁰

<http://www.viarural.com.ar/viarural.com.ar/agricultura/aa-enfermedades/aspergillus-spp.-01.jpg>; 25.05.2006 (d)
http://index.hu/cikkepek/0410/belfold//asp_flavus.jpg; 25.05.2006

⁷ Lieckfeldt, E.; Samuels, G. J.; Nirenberg, H.I.; Petrini, O. *Appl. Environ. Microbiol.* **1999**, *65*, 2418-2428.

⁸ The picture was obtained from the following web page: http://botit.botany.wisc.edu/Toms_fungi/nov2004.html; 25.05.2006

⁹ <http://www.doctorfungus.org/thefungi/Trichoderma.htm>

¹⁰ The pictures have been obtained from the following web pages (from left to right): (a) http://www.nahuby.sk/sk/images/fotosutaz/2006/oldrich_roucka2006_28138_t.jpg; 25.05.2006 (b) http://www.nahuby.sk/sk/images/fotosutaz/2005/oldrich_roucka2005_24301_t.jpg; 25.05.2006 (c) http://www.nahuby.sk/sk/images/fotosutaz/2004/milan_novotny2004_9222_t.jpg; 25.05.2006

Its natural habitats are found throughout the world spanning all different climatic zones. Predominant is the ability to digest chitin and cellulose. As a result of these nutritional preferences *Trichoderma* sp. are commonly found growing on fouling wood and plant material but as well on damp wall paper and paper boards. In fact, due to its highly developed cellulose digestion ability the fungi are an important source for cellulases - enzymes that degrade cellulose.¹¹ The proteins are obtained from biotechnologically cultured strains of *Trichoderma viride*.¹² They may be used for hydrolization and degradation of cellulotic materials from a wide variety of sources. The paper producing industry uses these cellulases extensively to avoid environmental pollution. Sludge and pulp waste can be degraded into fermentable sugars.¹³ Efforts have been made to use this process to reveal new resources for sugar production that might be used as renewable energy resources for e.g. bio-ethanol production.¹⁴ Often, the biotechnologically cultured fungi themselves are used for the biodegradation (e.g. transformation of banana waste into sugar,¹⁵ biodegradation of waste paper¹⁶ and agro waste¹⁷). An interesting application of the cellulases of *Trichoderma* sp. which furnishes a commonplace object of everyday use can be found in the fabrication of the so-called 'stone-washed jeans'. The popular effect is a result of the partially but irregularly cotton digestion conducted by cellulases.¹⁸

The other important enzyme class present in *Trichoderma viride* is the class of chitinases. These enzymes enable the fungi to be parasites of other fungi which cell walls are primarily composed of chitin.¹⁸ This ability was used for a number of agricultural applications. The fungi offered an attractive and non-toxic alternative to control various pathogenic fungal plant diseases, e.g. black seed rot disease and dry basal rot of oil palm trees,¹⁹ infection by *Fusarium moniliform*²⁰ and blight.²¹ This method of biological control is considered a more natural and environmentally acceptable alternative to the existing chemical treatment.¹⁹ Chitinases were as well used for the biodegradation of shrimp shell waste into sugars.²²

¹¹ <http://schimmel-schimmelpilze.de/schimmelpilz/trichoderma-viride.html>

¹² For a detailed description of cellulase separation see: Selby, K; Maitland, C. C. *Biochem. J.* **1967**, *104*, 716-724.

¹³ van Wyk, J. P. H.; Mohulatsi, M. *J. Polym. Env.* **2003**, *11*, 23-28.

¹⁴ Zayed, G.; Meyer, O. *Appl. Microbiol. Biotechn.* **1996**, *45*, 551-555.

¹⁵ Majid, M. A.; Khan, M. R. *Science Internat. (Lahore)* **2003**, *15*, 287-288.

¹⁶ van Wyk, J. P. H.; Mogale, A. M.; Seseng, T. A. *J. Solid Waste Techn. Manag.* **2001**, *27*, 82-86.

¹⁷ Tabassum, B.; Saleem, M.; Kausar, T. *Science Internat. (Lahore)* **2003**, *15*, 97-101.

¹⁸ http://botit.botany.wisc.edu/Toms_fungi/nov2004.html

¹⁹ Eziashi, E. I.; Uma, N. M. A.; Airede, C. E. *Afr. J. Biotechn.* **2006**, *5*, 703-706.

²⁰ Yates, I.; Meredith, F.; Smart, W.; Bacon, C.; Jaworski, A. *J. Food Prot.* **1999**, *62*, 1326-1332.

²¹ Hou, C. T.; Ciegler, A.; Hesseltine, C. W. *Appl. Microbiol.* **1972**, 183-185.

²² (a) Shindia, A. A.; El Hawa, M. I. A.; Shalaby, K. El-S. M. *Egypt. J. Microbiol.* **2001**, *36*, 119-134. (b) Shindia, A. A.; El Hawa, M. I. A.; Shalaby, K. El-S. M. *Egypt. J. Bot.* **2001**, *39*, 219-132.

Efforts have been made to take advantage of the high tolerance of fungi with respect of heavy metal pollution and the known phenomenon of bioaccumulation of these metals. This characteristic might be used for waste water treatment of sewage contaminated with heavy metals.²³

2.3 Viridiofungins

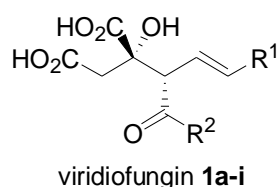
2.3.1 Viridiofungin A – an Alkyl Citrate

In 1993, Merck Research Laboratories reported the isolation and structure elucidation of several members of a novel family of amino alkyl citrates.²⁴ The screening was part of a bioassay-guided search for inhibitors of the squalene synthase as cholesterol lowering agents and antifungal drugs. Originally, the filamentous soil fungi of the strain *Trichoderma viride* attracted attention due to their broad spectrum antifungal activity which was later found to be the consequence of the inhibition of the serine palmitoyltransferase.²⁵ Viridiofungins, obtained from fermentation of this mold are summarized in Table 1. Beside viridiofungin A-C (entry 1-3, Table 1), a compounds **1d-1i** have been isolated as minor components (entry 4-9, Table 1).

²³ Bishnoi, N. R.; Garima, S. *J. Sci. Ind. Res.* 2005, *64*, 93-100.

²⁴ Harris, G. H.; Turner Jones, E. T.; Meinz, M. S.; Nallin-Omstead, M.; Helms, G. L.; Bills, G. F.; Zink, D.; Wilson, K. E. *Tetrahedron Lett.* **1993**, *34*, 5235-5238. The term 'alkyl citrate' is commonly used for citrate analogues alkylated or alkenylated in 2-position. It does *not* reflect an alkyl ester of a citrate as it might be concluded from the term 'alkyl citrate'.

²⁵ Mandala, S. M.; Thornton, R. A.; Frommer, B. R.; Dreikorn, S.; Kurtz, M. B. *J. Antibiotics* **1997**, *50*, 339-343.



| Entry | Compound | R ¹ | R ² | Viridiofungin |
|-------|-----------|--|----------------|----------------|
| 1 | 1a | | tyr= | A |
| 2 | 1b | | phe= | B |
| 3 | 1c | | trp= | C |
| 4 | 1d | | tyr | A ₁ |
| 5 | 1e | (CH ₂) ₁₃ CH ₃ | tyr | A ₂ |
| 6 | 1f | (CH ₂) ₁₃ CH ₃ | phe | B ₂ |
| 7 | 1g | (CH ₂) ₁₃ CH ₃ | OH | Z ₂ |
| 8 | 1h | | tyr | A ₃ |
| 9 | 1i | | tyr | A ₄ |

Table 1: Structure of viridiofungins **1a-i**.

The viridiofungins belong to the amino alkyl citrates. The common feature of the members of this family of natural products is a citric acid structural element **13** (Figure 3) that is alkylated in 2-position.

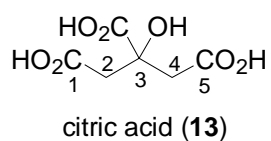


Figure 3

Naturally occurring agaricic (**14**) and caperatic acid (**15**) (Figure 4)²⁶ that are collagen cross linking inhibitors are commonly used as additives in the cosmetic industry for the fabrication of crèmes and sun protecting lotions.²⁷ The cross linking inhibition may be attributed to the structural similarities between the alkyl citrates and the important membrane component ceramide (**16**) which both consist of a lipophilic tail attached to a polar head group.²⁷

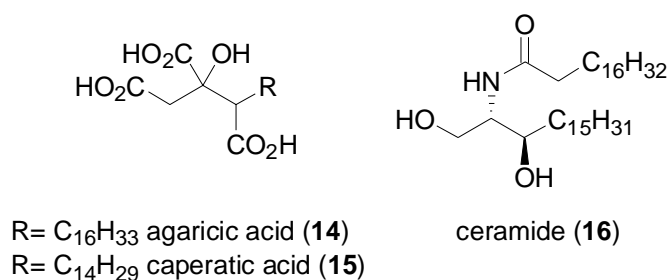


Figure 4: Structural similarities of the simple alkyl citrates agaricic (**14**) and caperatic acids (**15**) and the sphingolipid ceramide (**16**).

Other representatives of this class of secondary metabolites are the highly oxygenated zaragozic acid A (**17**)²⁸ which was found to be a very potent squalene synthase inhibitor, trachyspic acid (**18**),^{29,30} the acyclic L-731,120 (**19**),³¹ and the citrafungines (**20**)³² (Figure 5). These natural products were all isolated from fermented fungal strains.

²⁶ Lichen is the common source of agaricic and caperatic acid.

²⁷ Rona, C.; Vailati, F.; Berardesca, E. *J. Cosm. Derm.* **2004**, *3*, 26-34.

²⁸ Wilson, K. E.; Burk, R. M.; Biftu, T.; Ball, R. G.; Hoogsteen, K. *J. Org. Chem.* **1992**, *57*, 7151-7158. For reviews covering total synthesis of zaragozic acids, see: (a) Jotterand, N.; Vogel, P. *Curr. Org. Chem.* **2001**, *5*, 637-661. (b) Nadin, A.; Nicolaou, K. C. *Angew. Chem.* **1996**, *108*, 1733-1760; *Angew. Chem., Int. Ed.* **1996**, *35*, 1622-1656. For biosynthetic studies, see: (c) Byrne, K. M.; Arison, B. H.; Nallin-Omstead, M.; Kaplan, L. *J. Org. Chem.* **1993**, *58*, 1019-1024.

²⁹ Isolation: Shiozawa, H.; Takahashi, M.; Takatsu, T.; Kinoshita, T.; Tanzawa, K.; Hosoya, T.; Furuya, K.; Takahashi, S.; Furihata, K.; Seto, H. *J. Antibiotics* **1995**, *48*, 357-362.

³⁰ Total synthesis: (a) Hirai, K.; Ooi, H.; Esumi, T.; Iwabuchi, Y.; Hatakeyama, S. *Org. Lett.* **2003**, *5*, 857-859. (b) Zammit, S. C.; White, J. M.; Rizzacasa, M. A. *Org. Biomol. Chem.* **2005**, *3*, 2073-2074.

³¹ Harris, G. H.; Dufresne, C.; Joshua, H.; Koch, L. A.; Zink, D. L.; Salmon, P. M.; Goklen, K. E.; Kurtz, M. M.; Rew, D. J.; Bergstrom, J. D.; Wilson, K. E. *Bioorg. Med. Chem. Lett.* **1995**, *5*, 2403-2408.

³² Singh, S. B.; Zink, D. L.; Doss, G. A.; Polishook, J. D.; Ruby, C.; Register, E.; Kelly, T. M.; Bonfiglio, C.; Williamson, J. M.; Kelly, R. *Org. Lett.* **2004**, *6*, 337-340.

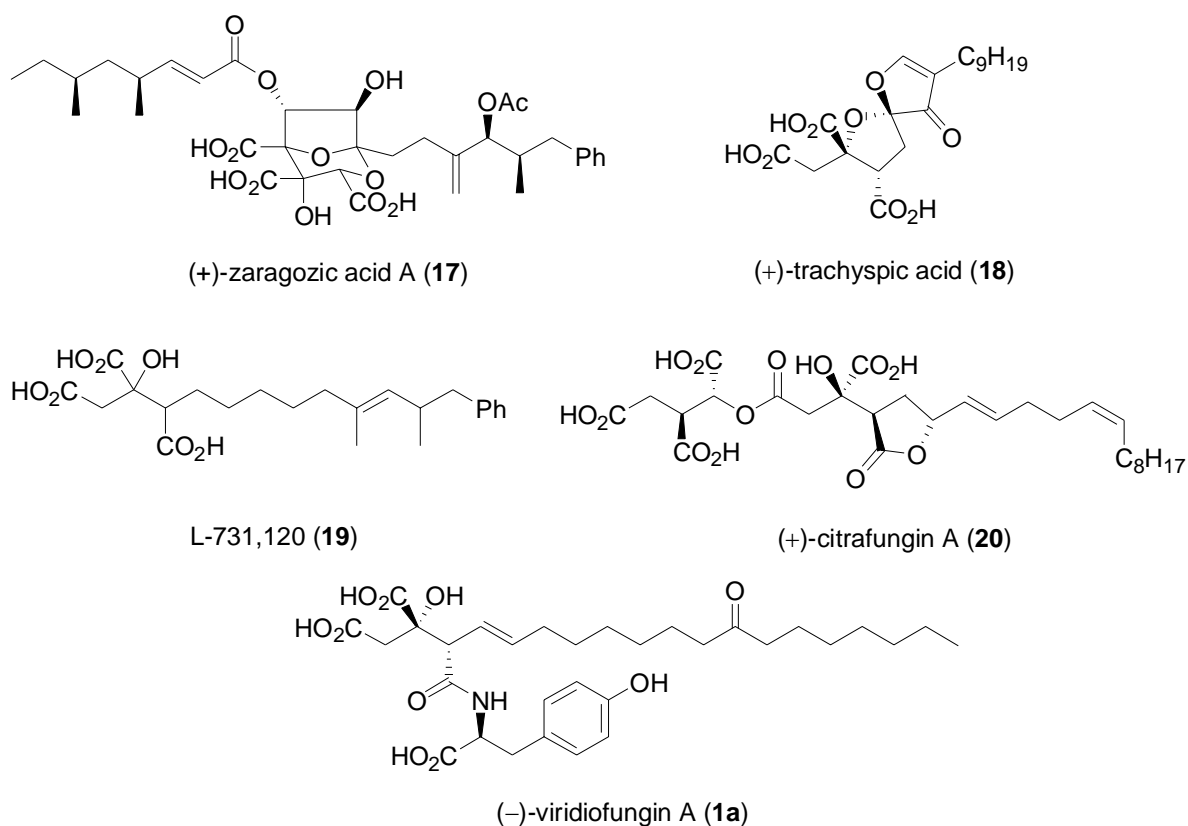


Figure 5: Representative examples of alkyl citrates.

2.3.2 Viridifungins – Biological Activity

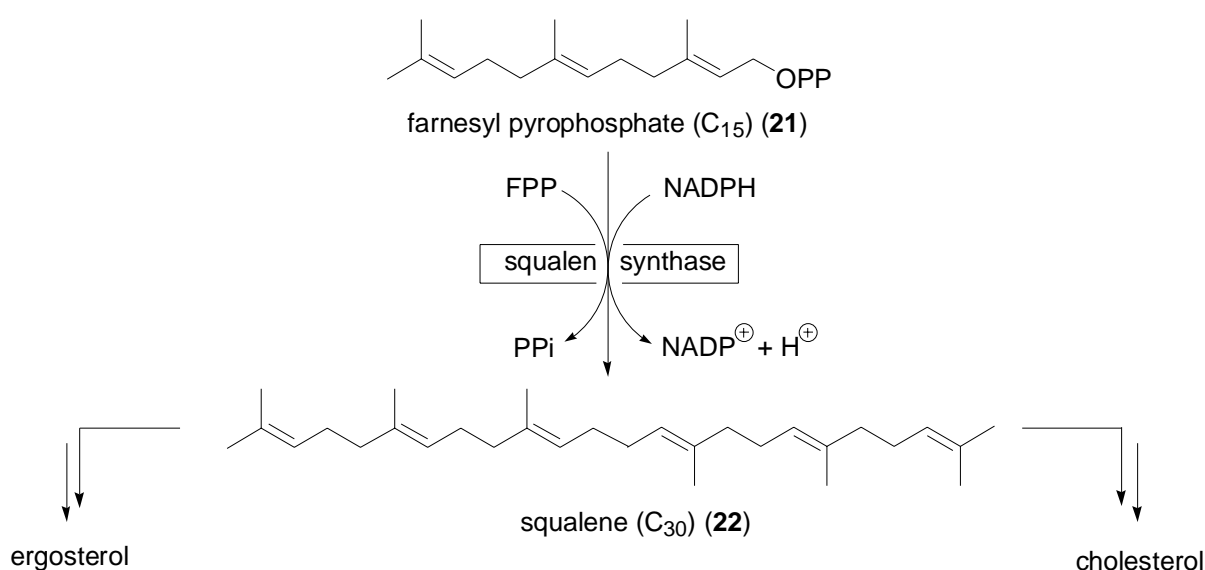
As mentioned earlier, viridifungin A (VF_A) was found to be an inhibitor of the squalene synthase.³³ The activity was found to be 1000-fold lower than for zaragozic acid A (**17**) (Table 2).²⁴

| Entry | Compound | Inhibition of the squalene synthase IC ₅₀ [μM] | |
|-------|--------------------------------|---|-------------------------|
| | | <i>Saccaramyces cerevisiae</i> | <i>Candida albicans</i> |
| 1 | Zaragozic acid A (17) | 1.0·10 ⁻⁴ | 1.7·10 ⁻⁴ |
| 2 | VF _A (1a) | 12.0 | 11.8 |
| 3 | VF _B (1b) | 1.7 | 11.3 |
| 4 | VF _C (1c) | 0.35 | 11.4 |

Table 2: In vitro inhibition of the squalene synthase.

³³ Inhibitors of the squalen synthase have been reviewed: Abe, I.; Tomesch, J. C.; Wattanasin, S.; Prestwich, G. D. *Nat. Prod. Rep.* **1994**, *11*, 279-302.

However, in vitro inhibition of squalene synthase of *S. cerevisia* and *C. albicans* successfully realized in micromolar concentrations still appears to be an attractive and promising activity for reasonable applications as a pharmaceutical candidate.³⁴ The squalene synthase is involved in the formation of squalene by reductive dimerization of two molecules farnesyl pyrophosphate (FPP) (**21**). As shown in Scheme 5, squalene (**22**) is a precursor for the de novo cholesterol synthesis. Therefore, inhibition of the squalene formation is believed to offer a versatile possibility to treat hypercholesterolemia (high cholesterol levels in human blood).³⁴ This diagnostic finding is known to be one of the prime risk factors for cardiovascular diseases such as arteriosclerosis and heart attack.



Scheme 5: Reductive head-to-head dimerization of two molecules FPP resulted in the formation of squalene a precursor for the *de novo* cholesterol (mammalian) and ergosterol (fungal) biosynthesis.

The molecular mode of action of the zaragozic acids **17** has been investigated.³⁵ Due to structural similarities, the biological activity of the viridifungins may be based on the same strategy. Thus, the inhibition may be attributed to a mimicking effect of the viridifungins **1** that may result in a competitive inhibition of the enzyme.³⁶

³⁴ Meinz, M. S.; Pelaez, F.; Omstead, M. N.; Milligan, J. A.; Diez, M. T.; Onishi, J. C.; Bergstrom, J. D.; Jenkins, R. F.; Harris, G. H.; Jones, E. T. T.; Huang, L.; Kong, Y. L.; Lingham, R. B.; Zink, D. Eur. Pat. Appl. EP 526,936 (Cl. C07C235/76), 1993; *Chem. Abstr.* **1993**, 118, 183428t.

³⁵ Hasumi, K.; Tachikawa, K.; Sakai, K.; Murakawa, S.; Yoshikawa, N.; Kumazawa, S.; Endo, A. *J. Antibiotics* **1993**, 46, 689-91. (b) Bergstrom, J. D.; Kurtz, M. M.; Rew, D. J.; Amend, A. M.; Karkas, J. D.; Bostedor, R. G.; Bansal, V. S.; Dufresne, C.; VanMiddlesworth, F. L.; O.D., H. *Proc. Natl. Acad. Sci. USA* **1993**, 90, 80-84. (c) Bergstrom, J. D.; Dufresne, C.; Bills, G. F.; Nallin-Omstead, M.; Byrne, K. *Annu. Rev. Microbiol.* **1995**, 49, 607-639.

³⁶ (a) Lindsey, S.; Harwood, H. J., Jr. *FASEB J.* **1994**, 8, A1285. (b) Lindsey, S.; Harwood, H. J., Jr. *J. Biol. Chem.* **1995**, 270, 9083-9096. (c) Ref. 28b.

Later it was demonstrated, that the potent antifungal activity³⁷ of the viridifungins in vivo is triggered by the nanomolar inhibition of the serine palmitoyltransferase SPT (Table 3).^{38,39}

| Entry | Compound | Inhibition of the SPT IC ₅₀ [nM] |
|-------|---------------------------------|---|
| 1 | VF Z ₂ (1g) | 3817 |
| 2 | VF B ₂ (1f) | 62.5 |
| 3 | VF _A (1a) | 13.1 |
| 4 | VF A ₄ (1i) | 3.2 |

Table 3: In vitro inhibition of the serine palmitoyltransferase SPT tested for *C. albicans*.

Obviously, the absence of the carbonyl group in the lipophilic tail resulted in significantly reduced inhibitory activity (entry 1, Table 3). Interestingly, the elongated side chain of the minor component VF A₄ (**1i**) caused an enhanced activity against the SPT of *C. albicans* (entry 4, Table 3). This pyridoxal 5'-phosphate-dependent enzyme catalyzes the first step of the de novo synthesis of sphingosines (**25**).⁴⁰ The sphingosines are intermediates of the ceramide (**16**) biosynthesis (Scheme 6), the latter being precursors for a range of different cytoplasmic membrane components (e.g. sphingomyeline, glycosphingolipides, cerebroside, gangliosides and neuramine acids) that have structural functions and are involved in cell-cell recognition and signal transduction. Furthermore, the ceramides and sphingosines themselves are essentially involved as second messengers in the regulation of enzyme activity and for the control of cell cycle processes such as growth, differentiation, cell cycle arrest and programmed cell death (apoptosis).⁴¹

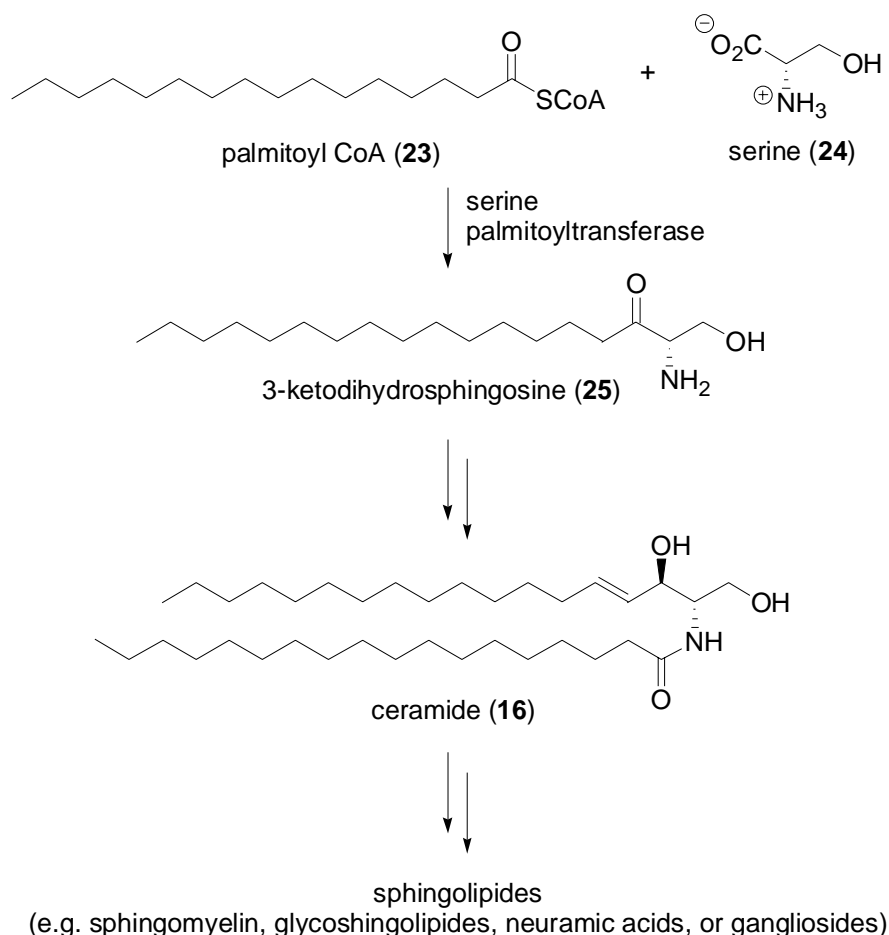
³⁷ For an instructive review covering different potential targets for antifungal development, see: Wills, E. A.; Redinbo, M. R.; Perfect, J. R.; Del Poeta, M. *Emerg. Ther. Targ.* **2000**, *4*, 1-32.

³⁸ Tested in vitro for *Candida albicans* and HeLa cells. See reference 25.

³⁹ For serine palmitoyltransferase inhibitors other than alkyl citrates, see: (a) Sundaram, K. S.; Lev, M. *J. Neurochem.* **1984**, *42*, 577-581. (b) Sundaram, K. S.; Lev, M. *Lipid Res.* **1985**, *26*, 473-477. (c) Medlock, K. A.; Merrill, A. H., Jr. *Biochemistry* **1988**, *27*, 7079-7084. (d) Holleran, W. M.; Williams, M. L.; Gao, W. N.; Elias, P. M. *J. Lipid. Res.* **1990**, *31*, 1655-1661. (e) Zweerink, M. M.; Edison, A. M.; Wells, G. B.; Pinto, W.; Lester, R. L. *J. Biol. Chem.* **1992**, *267*, 25032-25038. (f) Horn, W. S.; Smith, J. L.; Bills, G. F.; Raghoobar, S. L.; Helms, G. L.; Kurtz, M. B.; Marrinan, J. A.; Frommer, B. R.; Thornton, R. A.; Mandala, S. M. *J. Antibiotics* **1992**, *45*, 1692-1696. (g) Horvath, A.; Sütterlin, C.; Manning-Krieg, U.; Movva, N. R.; Riezmann, H. *EMBO J.* **1994**, *13*, 3687-3695. (h) Nakamura, S.; Kozutsumi, Y.; Sun, Y.; Miyake, Y.; Fujita, T.; Kawasaki, T. *J. Biol. Chem.* **1996**, *271*, 1255-1257. (i) Mandala, S. M.; Frommer, B. R.; Thornton, R. A.; Kurtz, M. B.; Young, N. M.; Cabello, M. A.; Genilloud, O.; Liesch, J. M.; Smith, J. L.; Horn, W. S. *J. Antibiotics* **1994**, *47*, 376-379.

⁴⁰ For reviews concerning the biosynthesis and biological function of sphingolipids, see: (a) Kolter, T.; Sandhoff, K. *Angew. Chem.* **1999**, *111*, 1632-1670; *Angew. Chem., Int. Ed. Engl.* **1999**, *38*, 1532-1568. (b) Chen, J. K.; Lane, W. S.; Schreiber, S. L. *Chem. Biol.* **1999**, *6*, 221-235. (c) Linn, S. C.; Kim, H. S.; Keane, E. M.; Andras, L. M.; Wang, E.; Merrill, A. H. *Biochem. Soc. Trans.* **2001**, *29*, 831-835. (d) Merrill, A. H. *J. Biol. Chem.* **2002**, *277*, 25843-25846. (e) Radin, N. S. *Biochem. J.* **2003**, *371*, 243-256.

⁴¹ Merrill, A. H., Jr.; Sandhoff, K. in *Biochemistry of Lipids, Lipoproteins and Membranes (4th Edn.)* Vance, D. E.; Vance, J. E. (Eds.) **2002**, Elsevier Science, B.V. pp. 373-407.



Scheme 6: Serine palmitoyl transferase catalyzes the first step of the *de novo* ceramide biosynthesis.

As part of the membranes, glycosphingolipide play an essential role for cell recognition and immune response. In this respect, the pharmacological effect of SPT inhibitors (cell wall destabilisation/disintegration and immuno suppression) can be easily rationalized. Recently, studies with NA 255 (**26**) – a compound closely related to the viridofungins - have been performed (Figure 6).⁴²

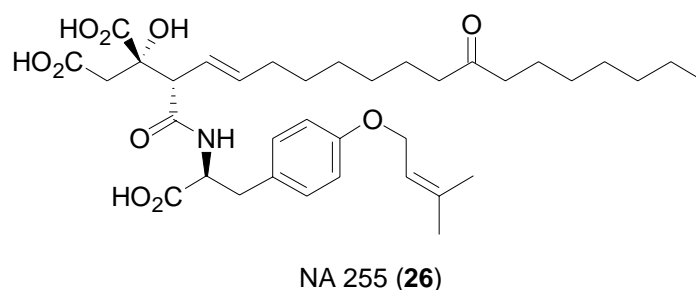


Figure 6

⁴² Sakamoto, H.; Okamoto, K.; Aoki, M.; Kato, H.; Katsume, A.; Ohta, A.; Tsukuda, T.; Shimma, N.; Aoki, Y.; Arisawa, M.; Kohara, M.; Sudoh, M. *Nat. Chem. Biol.* **2005**, *1*, 333-337.

It was shown, that as a result of the serine palmitoyltransferase inhibition the formation of the so-called lipid rafts – microdomains of the cell membranes that are enriched with cholesterol, shingolipides and phospholipides⁴³ – is disrupted. A potential application was found in the treatment of earlier stages of hepatitis C virus (HCV) infections since the inhibition of liquid raft formation interferes with the association of non-structural proteins of the virus, preventing its proliferation inside the host. Hence, this biological activity suggests, that inhibition of sphingolipide metabolism may provide a new therapeutic strategy for the treatment of HCV infections.⁴²

The ability to inhibit the farnesyl transferase is another characteristic of the viridifungins.⁴⁴ Farnesylation of the oncogenic Ras protein was found to be involved in the transformation of normal cells into cancer cells.^{45,34} Thus, the inhibition of the farnesyl transferase may block this transformation and natural products that are able to inhibit such enzymes are potentially useful for cancer treatment.^{34,46}

2.3.3 Proposed Biosynthesis of Viridifungins

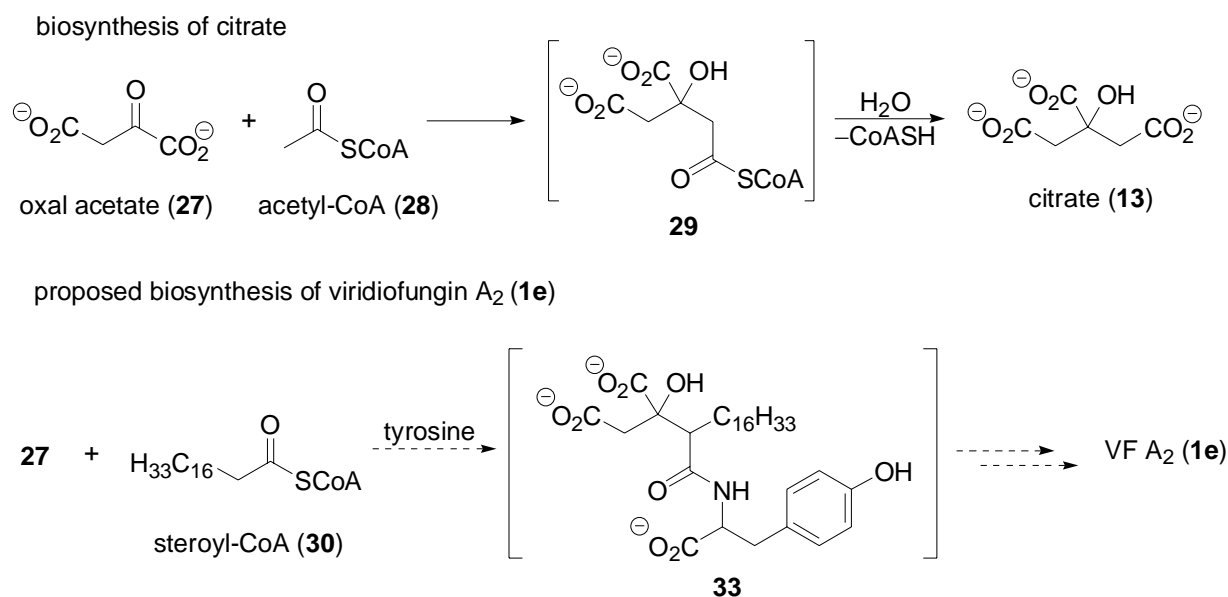
The biosynthesis of the viridifungins (**1**) is assumed to proceed in close analogy with the formation of citrate itself during the citrate cyclus.^{24,28c} Instead of acetyl CoA (**28**) an activated ester of the appropriated fatty acid (e.g. **30**) would be employed. Condensation of oxalacetate (**27**) with the α -methylene group of the fatty acid **30** followed by the displacement of the activated ester with an aromatic amino acid should finally generate the viridifungin **1e**. This hypothetical biosynthetic pathway allows the easy rationalisation of the amino acid position.

⁴³ http://en.wikipedia.org/wiki/Lipid_raft

⁴⁴ Appels, N. M. G. M.; Beijnen, J. H.; Schellens, J. H. M. *Oncologist* **2005**, *10*, 565-578.

⁴⁵ Cancer types wherein this transformation was found to be involved are e.g. colorectal carcinoma, exocrine pancreatic carcinoma and myeloid leukaemia.

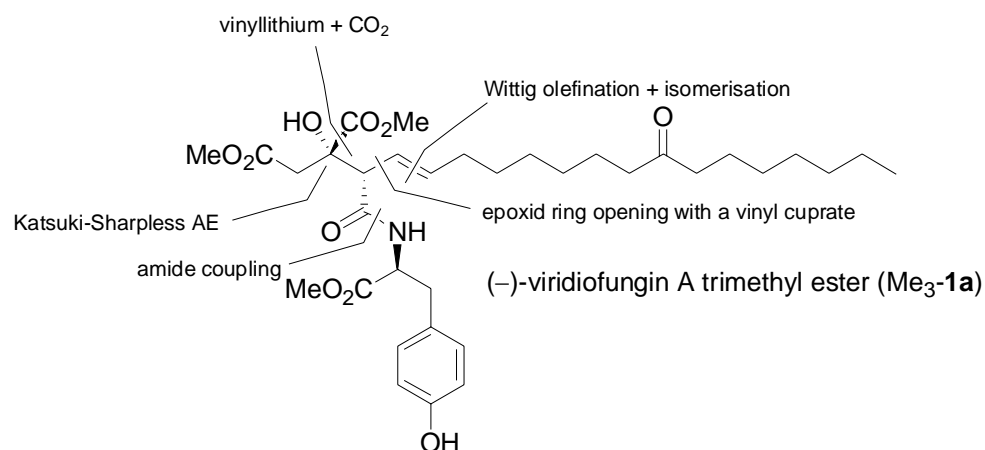
⁴⁶ For reviews covering the potential of farnesyl transferase inhibitors in cancer chemotherapy, see: Wittinghofer, A.; Waldmann, H. *Angew. Chem.* **2000**, *112*, 4360-4383; *Angew. Chem., Int. Ed.* **2000**, *39*, 4192-4214. (b) Bell, I. M. *J. Med. Chem.* **2004**, *47*, 1869-1878.



Scheme 7: Biosynthetically, the viridiofungins **1** may be produced analogue to citrate (**13**) itself.

2.3.4 Published Total Syntheses of Viridiofungins

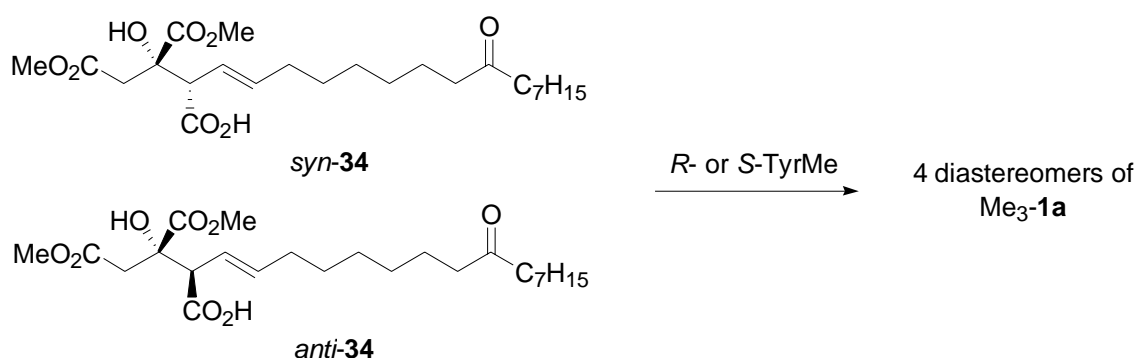
In an earlier attempt the research group of Hatakeyama and co-workers successfully realized the total synthesis of (–)-viridiofungin A trimethyl ester Me₃-**1a** (Scheme 8).⁴⁷



Scheme 8: Important reactions involved in the first published total synthesis of (–)-viridiofungin A trimethyl ester (Me₃-**1a**) by Hatakeyama.

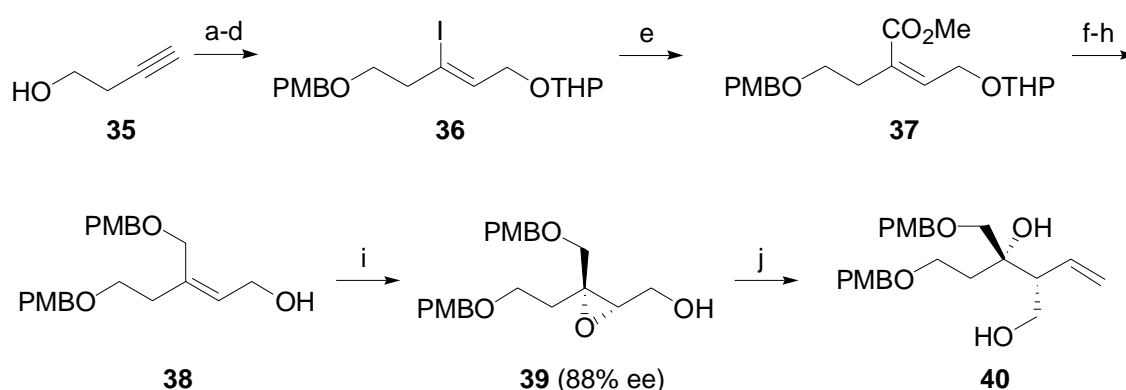
Two diastereomers (*syn*-**34** and *anti*-**34**) were synthesized and then coupled with enantiomerically pure methyl ester of the amino acids *S*-tyrosine (*S*-TyrMe) or *R*-tyrosine (*R*-TyrMe) to afford four distinct diastereomers (Scheme 9).

⁴⁷ Esumi, T.; Iwabuchi, Y.; Irie, H.; Hatakeyama, S. *Tetrahedron Lett.* **1998**, *39*, 877-880.



Scheme 9: Four diastereomers of **Me₃-1a** have been synthesized and their analytical data used for comparison with semi-synthetic **Me₃-1a**.

Comparison of the optical rotation values and spectroscopic data of these synthetic diastereomers with semi-synthetic **Me₃-1a** was utilized for the assignment of the relative and absolute configuration of naturally occurring VF_A (**1a**). The total synthesis of **Me₃-1a** was realized with a longest linear sequence of 27 steps. The crucial absolute configuration at the stereogenic quaternary carbon atom C3 was set by a Katsuki-Sharpless asymmetric epoxidation⁴⁸ (88% ee) (Scheme 10).



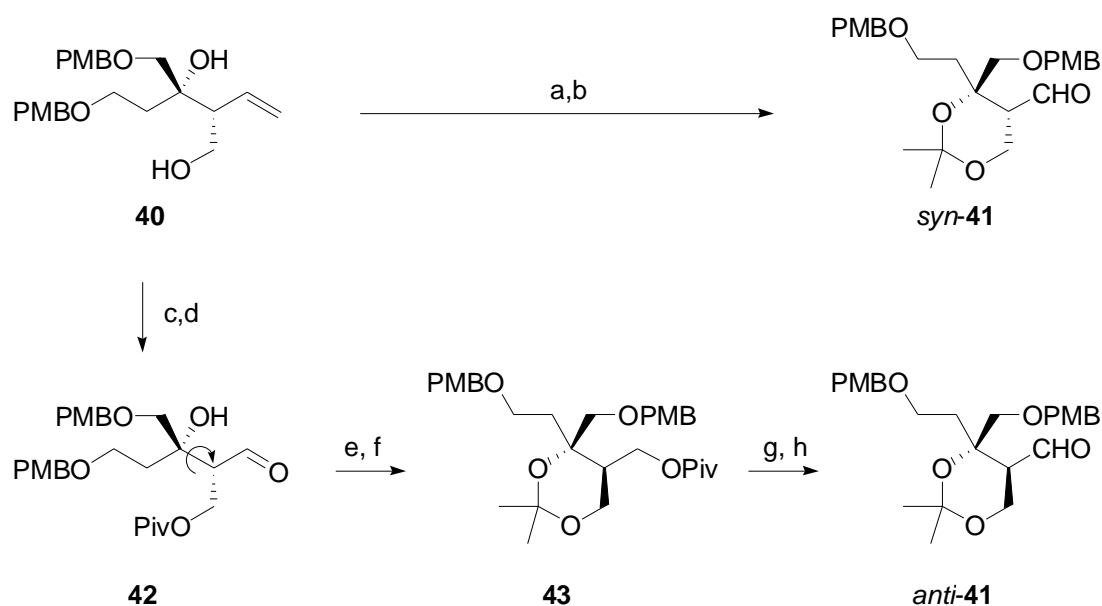
Scheme 10: Synthesis of intermediate **40** bearing two of the three stereogenic centers of the natural product: a) *p*-(MeO)₆C₆H₄CH₂Cl (PMBCl), NaH, *n*-Bu₄NI, THF; b) *n*-BuLi, (CH₂O)_{*n*}, THF, 75% (two steps); c) Red-Al, Et₂O, 0 °C to rt, then I₂, -50 °C to rt; d) pyridinium *p*-toluene sulfonic acid (PPTS), dihydropyranone (DHP), CH₂Cl₂, 78% (two steps); e) *t*-BuLi, CO₂, Et₂O, -78 °C, then MeI, DMF, 96%; f) DIBAL-H, CH₂Cl₂, -78 °C; g) PMBCl, NaH, *n*-Bu₄NI, THF, reflux; h) PPTS, MeOH, reflux, 72% (three steps); i) diisopropyl L-tartrate (0.09 eq), Ti(O*i*-Pr)₄ (0.07 eq), *t*-BuOOH, (2.0 eq), 4 Å molecular sieves, CH₂Cl₂, -30 °C, 92%; j) CH₂=CHMgBr, CuI, THF, -25 °C, 93%.

Protection of the hydroxyl group of **35** (a), nucleophilic addition of the deprotonated alkyne to paraformaldehyde (b), stereoselective reduction of the corresponding propargylic alcohol with subsequent iodine trapping of the aluminium intermediate (c) and protection of the hydroxyl

⁴⁸ Katsuki, T.; Sharpless, K. B. *J. Am. Chem. Soc.* **1980**, *102*, 5974-5976.

group (d) afforded the vinyl iodide **36**. Halogen lithium exchange and subsequent reaction with carbon dioxide (e) afforded **37**. Reduction (f), protection (g) and cleavage of the ether (h) provided allylic alcohol **38** that was successfully subjected to the conditions of a Katsuki-Sharpley asymmetric epoxidation (i).⁴⁸ The epoxide **39** was formed with an enantiomeric excess of 88% ee. Regio- and stereoselective nucleophilic ring opening with vinyl magnesium bromide (j) provided **40** with good yields.

Wittig olefination and subsequent double bond isomerization was utilized for the generation of the isolated *E*-configured double bond. The synthesis of the starting materials, aldehyde *syn*- and *anti*-**41** is depicted in Scheme 11.



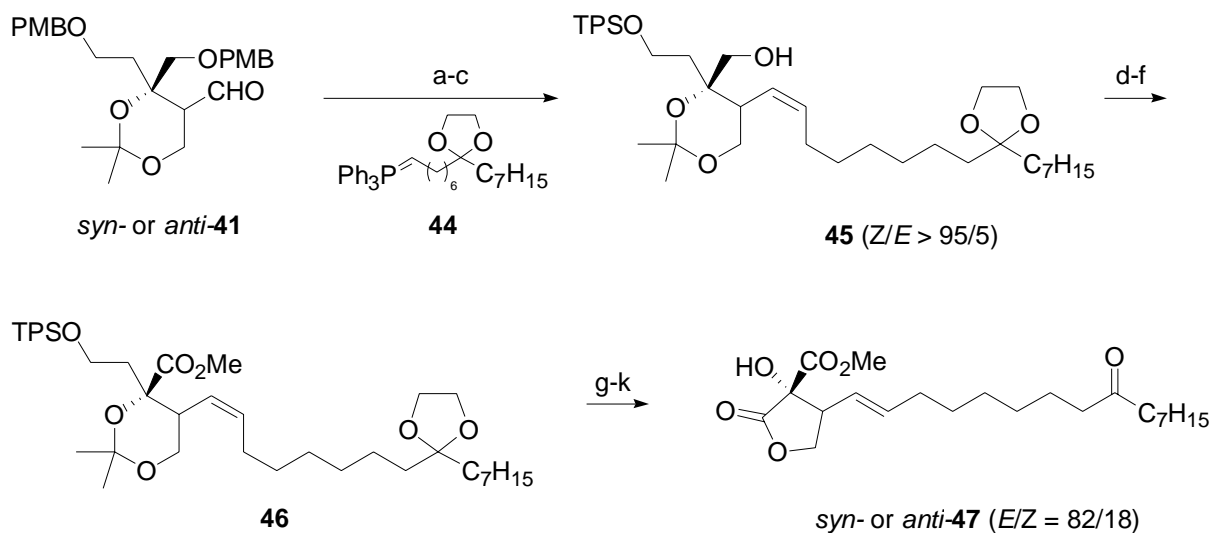
Scheme 11: Formation *syn*-**41** and its diastereomer *anti*-**41**: a) $(\text{MeO})_2\text{CMe}_2$, PPTS, benzene, reflux; b) OsO_4 , NMO, THF/ H_2O 3/1, then NaIO_4 , 83% (two steps); c) PivCl , Et_3N , CH_2Cl_2 ; d) OsO_4 , NMO, THF/ H_2O 3/1, then NaIO_4 ; e) NaBH_4 , MeOH; f) $(\text{MeO})_2\text{CMe}_2$, PPTS, CH_2Cl_2 , 31% (four steps); g) NaOH , MeOH; h) $(\text{COCl})_2$, DMSO, Et_3N , CH_2Cl_2 , -60°C to rt, 60% (two steps).

Aldehyde *syn*-**41** was generated by transketalization of diol **40** with acetone dimethyl acetal (a) followed by Lemieux-Johnson oxidation (b).⁴⁹ The corresponding diastereomer *anti*-**41** was generated by a six-step procedure as depicted in Scheme 11. After protection of the primary hydroxyl group as pivatoyl-ester (c), Lemieux-Johnson oxidation (d)⁴⁹ afforded the aldehyde **42** that was reduced to the corresponding alcohol (e) and protected as ketal **43** (f). Finally, ester cleavage (g) and oxidation (h) afforded the aldehyde *anti*-**41**.

The formation of the *E*-configured double bond of **Me**₃-**1a** was realized by Wittig olefination followed by a double bond isomerization which was realized after some manipulation of the

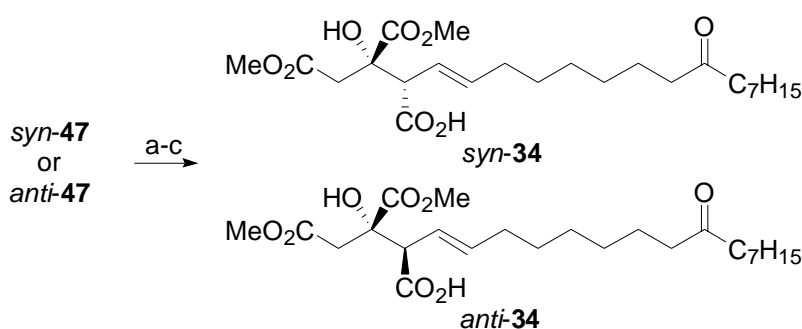
⁴⁹ Pappo, R.; Allen, D.; Lemieux, R.; Johnson, W. *J. Org. Chem.* **1956**, *21*, 478-479.

olefination product (Scheme 12). The isomerization - initialized by exposure to UV radiation in the presence of PhSSPh - afforded the desired pure *E*-isomers *syn*- and *anti*-**47** after chromatographic separation of the 82/18 mixture of double bond isomers.



Scheme 12: Construction of the *E*-configured double bond by Wittig olefination and subsequent *E/Z*-isomerization: a) **44**, THF, 0 °C, 80%; b) Li, THF, liq. NH₃, -33 °C; c) TPSCl, Et₃N, CH₂Cl₂, 86% (two steps); d) (COCl)₂, DMSO, Et₃N, CH₂Cl₂, -60 °C to rt; e) NaClO₂, NaH₂PO₄, 2-methyl-2-butene, *t*-BuOH/H₂O 4/1; f) CH₂N₂, Et₂O, 96% (three steps); g) conc. HCl, *t*-BuOH; h) 46% HF/MeCN 1/7; i) H₂CrO₄, aq acetone, -10 °C; j) CH₂N₂, Et₂O, 50% (four steps); k) *hν*, PhSSPh, cyclohexane, 100%.

Final steps afforded the diastereomers *syn*- and *anti*-**34** ready for amid formation (Scheme 13).

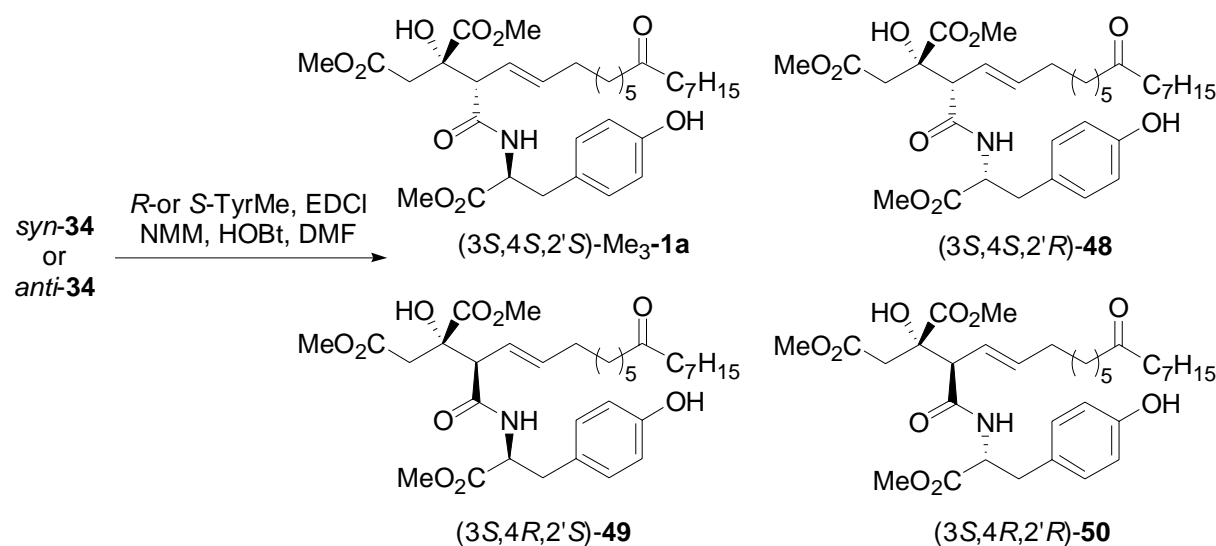


Scheme 13: Final steps for the generation of the acids *syn*- and *anti*-**34**: a) NaOH, MeOH; b) CH₂N₂, Et₂O; c) H₂CrO₄, aq acetone, -10 °C (yields given in Table 4).

Both diastereomers *syn*- and *anti*-**34** were subjected to either *R*-tyrosine methyl ester or *S*-tyrosine methyl ester using EDCI,⁵⁰ 1-hydroxybenzotriazole (HOBt) and *N*-methylmorpholine

⁵⁰ EDCI = (1-(3-(dimethylamino)-propyl)-3-ethylcarbodiimide hydrochloride (Me₂N(CH₂)₃N=C=NEt·HCl).

(NMM) to induce the amide formation (Table 4). The specific rotation as well as spectroscopic data of the amide coupling product between *syn*-**34** and *S*-tyrosine methyl ester were in good agreement with results obtained for semi-synthetic Me₃-**1a**. Therefore, it was concluded that the absolute configuration of the natural product is (3*S*,4*S*,2'*S*).



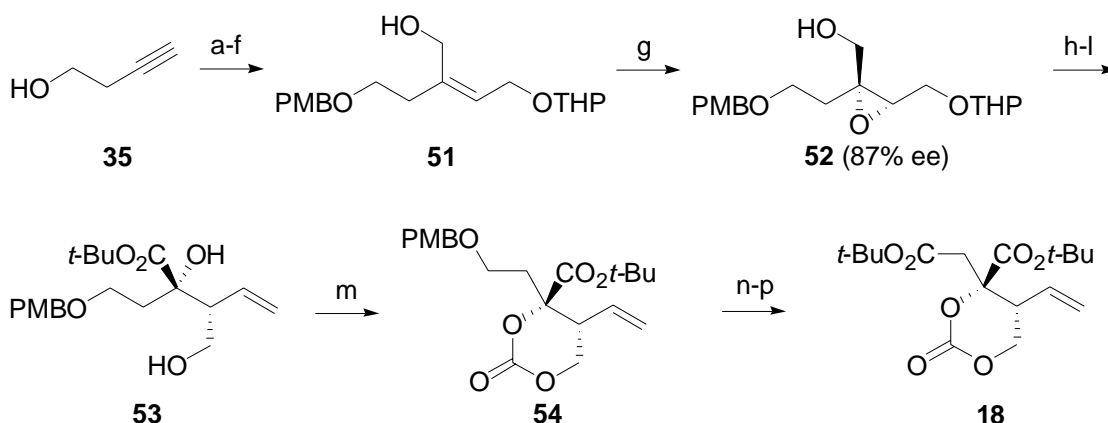
| Entry | Starting material | Tyrosine methyl ester | Yield [%] | Product | Optical rotation in MeOH |
|-------|-------------------------|-----------------------|-----------------|---|--------------------------|
| 1 | <i>syn</i> - 34 | <i>S</i> -TyrMe | 48 | 3 <i>S</i> ,4 <i>S</i> ,2' <i>S</i> | -19.1 (<i>c</i> 0.43) |
| 2 | <i>syn</i> - 34 | <i>R</i> -TyrMe | 38 | 3 <i>S</i> ,4 <i>S</i> ,2' <i>R</i> | -15.5 (<i>c</i> 0.43) |
| 3 | <i>anti</i> - 34 | <i>S</i> -TyrMe | 8 ^a | 3 <i>S</i> ,4 <i>R</i> ,2' <i>S</i> | +33.3 (<i>c</i> 0.47) |
| 4 | <i>anti</i> - 34 | <i>R</i> -TyrMe | 10 ^a | 3 <i>S</i> ,4 <i>R</i> ,2' <i>R</i> | +31.6 (<i>c</i> 0.47) |
| 5 | - | - | - | semisynthetic Me ₃ - 1a | -23.0 (<i>c</i> 0.47) |

Table 4: Results of the amid formation.^a From *anti*-**41** (15 steps); EDCI= Me₂N(CH₂)₃N=C=NEt·HCl; NMM= *N*-methylmorpholine; HOBt= 1-hydroxy-benzotriazole, TyrMe= tyrosine methyl ester, DMF= dimethylformamide.

In 2005, a second generation synthesis of **1a** was published.⁵¹ Formation of *tert*-butyl ester instead of methyl ester allowed the generation of unprotected natural occurring **1a** after deprotection under acid conditions as final step. In this improved synthesis 22 steps were required for the generation of VF_A (**1a**). The first steps parallel the earlier published strategy (Scheme 14). Using a more efficient strategy, the protection-deprotection sequence prior to the Katsuki-Sharplees epoxidation was avoided. Replacement of the ketal protection group by

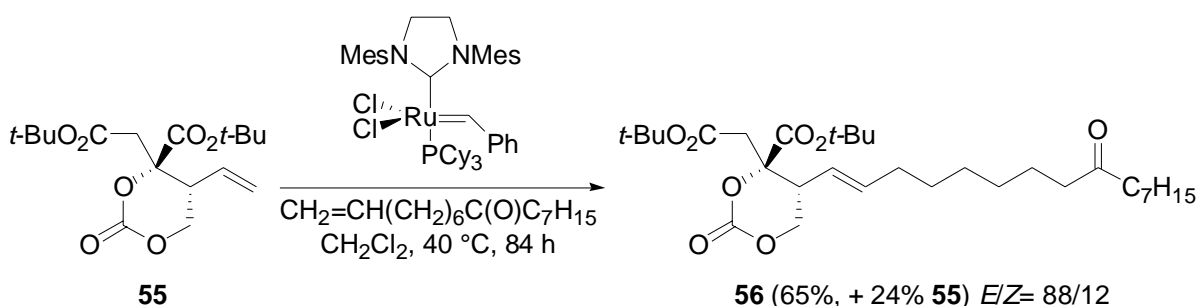
⁵¹ Morekuma, K.; Takahashi, K.; Ishihara, J., Hatakeyama, S. *Chem. Comm.* **2005**, 2265-2267.

a cyclic carbonate avoided the yield limiting lactonization step in the previously described synthesis.



Scheme 14: First steps of the improved synthesis of **1a**: a) PMBCl, NaH, *n*-Bu₄NI, THF; b) *n*-BuLi, (CH₂O)_n, THF; c) Red-Al, Et₂O, 0 °C to rt, then I₂, -50 °C to rt; d) PPTS, DHP, CH₂Cl₂; e) *t*-BuLi, CO₂, Et₂O, -78 °C, then MeI, DMF; f) DIBAL-H, CH₂Cl₂, -78 °C, 56% (six steps); g) diisopropyl L-tartrate (0.3 eq), Ti(O-*i*-Pr)₄ (0.25 eq), *t*-BuOOH, (2.0 eq), 4 Å molecular sieves, CH₂Cl₂, -20 °C, 100%; h) SO₃·pyridine, Et₃N, DMSO, CH₂Cl₂; i) NaClO₂, NaH₂PO₄, 2-methyl-2-butene, *t*-BuOH/H₂O 4/1; j) *N,N'*-diisopropyl-*O*-2-*tert*-butylisourea, CH₂Cl₂; k) PPTS, MeOH, 74% (four steps); l) CH₂=CHMgBr, CuI, THF, -26 °C, 71%; m) triphosgene, pyridine, THF; n) DDQ, CH₂Cl₂/H₂O 20/1, 79% (two steps); o) H₂CrO₄, aq. acetone, -10 °C; p) *N,N'*-diisopropyl-*O*-2-*tert*-butylisourea, CH₂Cl₂, 84% (two steps).

For the construction of the of the isolated C5/C6 double bond a cross metathesis strategy was successfully employed. Reaction of **55** with hexadec-15-en-8-one resulted in the formation of the desired *E*-configured coupling product *E*-**56** together with the *Z*-configured isomer thereof and unreacted starting material **55** (Eq. 1).⁵²

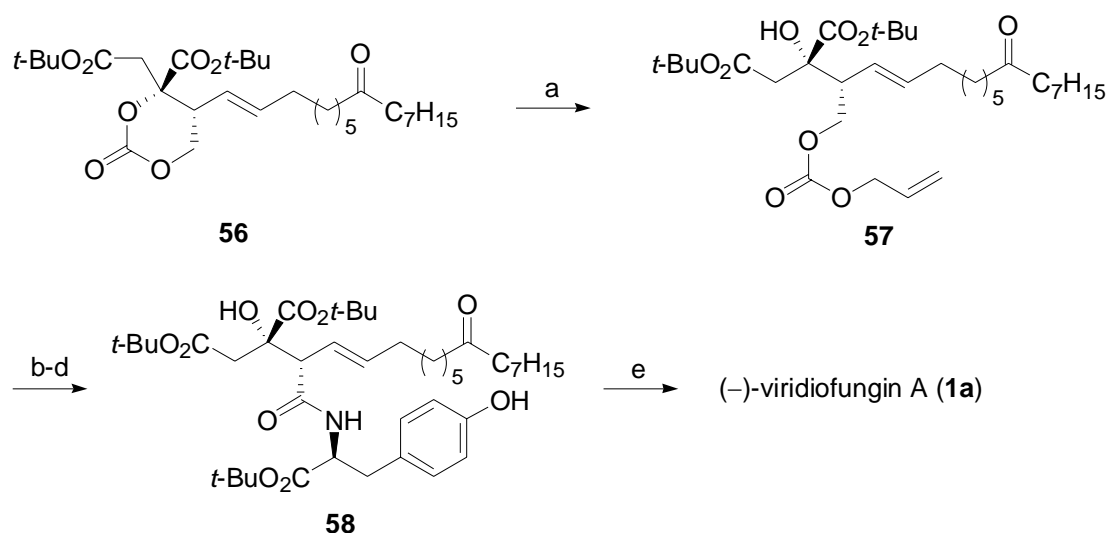


Eq. 1 Mes= mesityl, Cy= cyclohexyl.

The cleavage of the carbonate was realised by formation of the allyl carbonate **57** (a) followed by palladium-catalyzed deallylation (b) affording the corresponding alcohol. Jones oxidation (c) gave the corresponding carboxylic acid which was amidated (d) under the conditions

⁵² Separation of the double bond isomers *E*-**56** and *Z*-**56** is not explicitly explained. Possibly it was achieved during the final reversed phase chromatography.

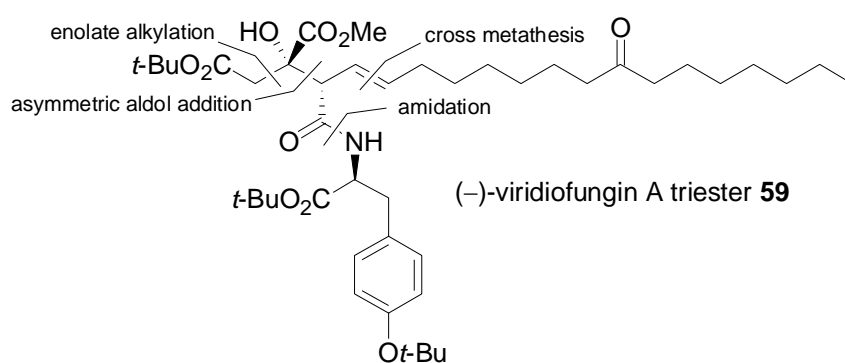
described previously to provide **58**. Final cleavage of all *tert*-butyl ester groups in formic acid (e) afforded (–)-viridifungin A (**1a**) (Scheme 15).



Scheme 15: Final steps for the total synthesis of viridifungin A (**1a**): a) K_2CO_3 , $\text{CH}=\text{CHCH}_2\text{OH}$, $-20\text{ }^\circ\text{C}$, 80%; b) HCO_2NH_4 (3 eq), Ph_3P (0.3 eq), $\text{Pd}(\text{PPh}_3)_4$ (0.1 eq), THF, 98%; c) H_2CrO_4 , aq. acetone, $-10\text{ }^\circ\text{C}$; d) *S*-tyrosine *tert*-butyl ester, EDCI, NMM, HOBT, DMF, 78%; e) HCO_2H , 74%.

With the successful total synthesis of VF_A the absolute configuration proposed previously could be unambiguously verified.

Very recently, a short and simple route toward viridifungin trimerster **59** was published (Scheme 16).⁵³

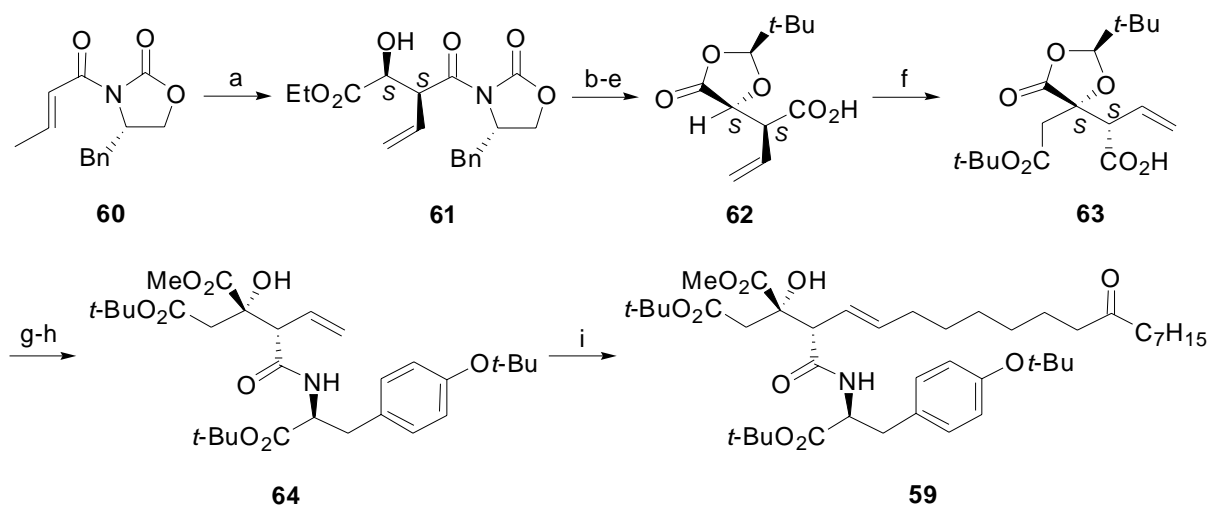


Scheme 16: Important reactions involved in the recently published total synthesis of the viridifungin A triester **59**.

Asymmetric aldol reaction⁵⁴ and enolate alkylation were employed as key CC-connection steps. The isolated double bond was generated by cross metathesis.

⁵³ Goldup, S. M.; Pilkington, C. J.; White, A. J. P.; Burton, A.; Barrett, A. G. M. *J. Org. Chem.* **2006**, *71*, 6185-6191.

Starting from oxazolidinone precursor **60**⁵⁵ reaction with glyoxylate (a) afforded the *syn*-aldol product **61**. Cleavage of the chiral auxiliary (b), saponification of the ethyl ester (c) and treatment with trimethylchlorosilane (d) and pivaldehyde (e) afforded dioxolane **62**. Conversion to **63** was realized by deprotonation of **62** with LiHMDS and subsequent reaction with *tert*-butyl- α -bromo acetate (f). Final steps include transesterification (g), amide coupling (h) and cross-metathesis (i).



Scheme 17: Synthesis of intermediate **59**: a) Bu_2BOTf , Et_3N , CH_2Cl_2 , $-78\text{ }^\circ\text{C}$ to $0\text{ }^\circ\text{C}$; EtO_2CCHO , $-78\text{ }^\circ\text{C}$ to $0\text{ }^\circ\text{C}$, 72%; b) LiOH , H_2O_2 , $\text{THF}/\text{H}_2\text{O}$ 3/1, $0\text{ }^\circ\text{C}$; c) LiOH , $\text{MeOH}/\text{H}_2\text{O}$ 1/1, $0\text{ }^\circ\text{C}$ to rt, 85% (two steps); d) Me_3SiCl , $(i\text{-Pr})_2\text{NEt}$, THF , rt; e) $t\text{-BuCHO}$, Me_3SiOTf (20 mol%), CH_2Cl_2 , $-35\text{ }^\circ\text{C}$, 79% (two steps); f) LiHMDS , DMF , $-70\text{ }^\circ\text{C}$, 50 min; $\text{BrCH}_2\text{CO}_2t\text{-Bu}$, $-70\text{ }^\circ\text{C}$, 15 min, 61%; g) K_2CO_3 , MeOH , $0\text{ }^\circ\text{C}$ to rt; h) $4\text{-}t\text{-BuOC}_6\text{H}_4\text{CH}_2\text{CH}(\text{CO}_2t\text{-Bu})\text{NH}_2\cdot\text{HCl}$, HOBT , HBTU ,⁵⁶ $(i\text{-Pr})_2\text{NEt}$, DMF , $0\text{ }^\circ\text{C}$, 28% (two steps); i) hexadec-15-ene-8-one, Grela catalyst⁵⁷ (20 mol%), CH_2Cl_2 , $55\text{ }^\circ\text{C}$ (microwaves), 54%.

⁵⁴ For a review concerning asymmetric aldol reactions, see: Palomo, C.; Oiarbide, M.; Garcia, J. M. *Chem. Soc. Rev.* **2004**, *33*, 65-75.

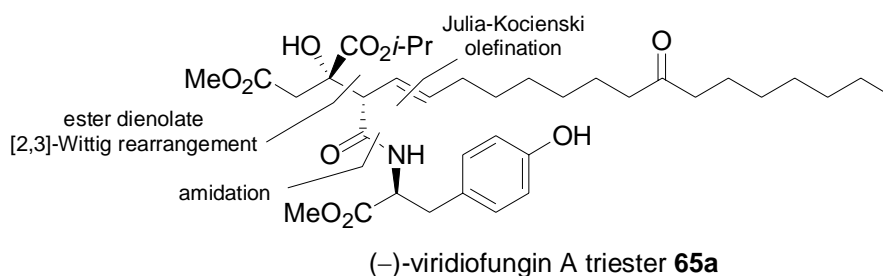
⁵⁵ Evans, D. A.; Bartroli, J.; Shih, T. L. *J. Am. Chem. Soc.* **1981**, *103*, 2127-2129.

⁵⁶ HOBT= 1-hydroxy-1,2,3-benzotriazole; HBTU= 2-(1*H*-benzo-triazol-1-yl)-1,1,3,3-tetramethyluronium hexafluorophosphate.

⁵⁷ Michrowska, A.; Bujok, R.; Harutyunyan, S.; Sashuk, V.; Dolgonos, G.; Grela, K. *J. Am. Chem. Soc.* **2004**, *126*, 9318-9325.

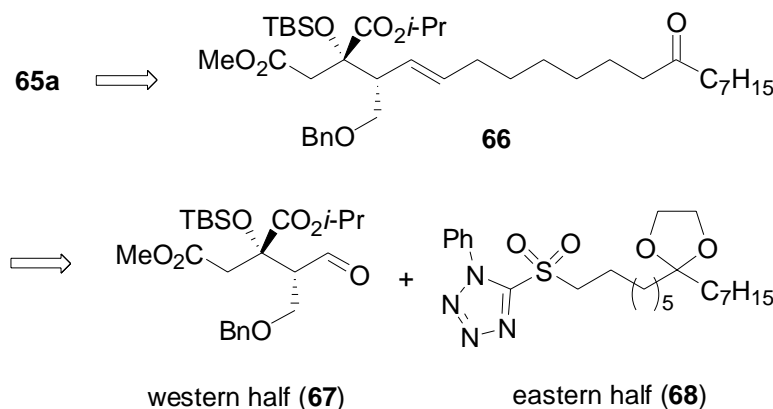
3 Retrosynthetic Analysis of Viridifungin A

Viridifungin A consists of a highly functionalized, polar head group connected with a lipophilic tail. Beside the amide functionality, two additional sites for a retrosynthetic disconnection were identified (Scheme 18). The *E*-configured C5/C6 double bond may be generated by an inherently *E*-selective Julia-Kocienski olefination.⁵⁸ For the formation of the two neighboured stereogenic centers of the polar head group utilization of the ester dienolate [2,3]-Wittig rearrangement was envisioned.⁵⁹



Scheme 18: Retrosynthetic analysis of (-)-viridifungin A triester **65a**.

According to this plan, the target molecule was disassembled into two fragments that are named ‘eastern half’ and ‘western half’ (Scheme 19).⁶⁰



Scheme 19: **65** may be generated by the coupling of the western half with the eastern half. TBS= *tert*-butyldimethylsilyl [Si(*t*-Bu)Me₂], Bn= benzyl.⁶¹

⁵⁸ Blakemore, P. R.; Cole, W. J.; Kocienski, P. J.; Morley, A. *Synlett* **1998**, 26-28.

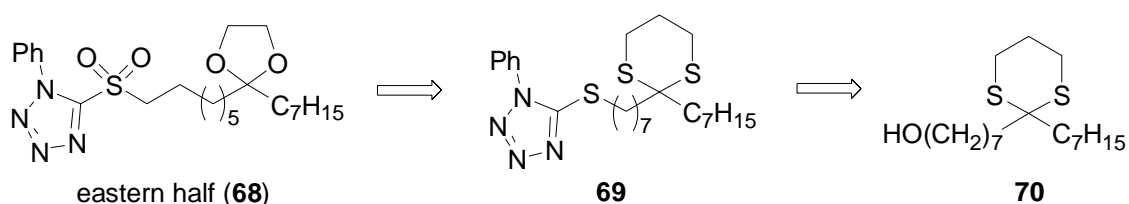
⁵⁹ (a) Hiersemann, M. *Tetrahedron* **1999**, 55, 2625-2638. (b) Hiersemann, M.; Lauterbach, C.; Pollex, A. *Eur. J. Org. Chem.* **1999**, 2713-2724. (c) Hiersemann, M.; Abraham, L.; Pollex, A. *Synlett* **2003**, 1088-1095.

⁶⁰ For concise reasons, solely the retrosynthetic analysis of VF_A (**1a**) will be discussed in this chapter.

⁶¹ The depicted protecting groups reflect the realized synthetic strategy. For details, see page 56 ff.

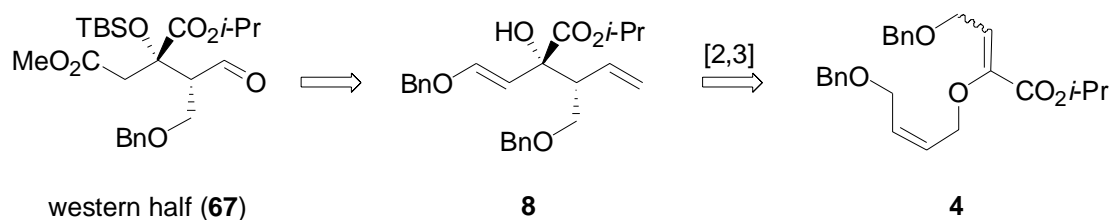
This highly convergent strategy enables the straight forward synthesis of various natural and non-natural analogues of VF_A (**1a**) simply by using different coupling partners **68**. The easy synthesis of minor components owning interesting biological activities (e.g. VF A₄ (**1i**), see Table 3) that are difficult to obtain from fermentation processes is one of the possible applications of this strategy. Furthermore, non-natural analogues – often advantageously for studying the molecular mode of action of a specific substance – may be prepared. Accordingly triesters of the viridiofungin A and the minor components A₄ and A₂ were chosen to prove the versatility of this synthetic strategy. The synthesis of **65a** is required for data comparison.

For the synthesis of the eastern half (**68**), a sequential alkylation of 1,3-dithiane⁶² and the introduction of the sulfanyl-1-phenyl-1*H*-tetrazole by the application of a Mitsunobu redox-condensation was envisioned (Scheme 20).⁶³



Scheme 20: Retrosynthetic analysis of the eastern half (**68**).

The highly functionalized western half (**67**) might be disassembled to **71** containing the retron of an ester dienolate [2,3]-Wittig rearrangement. An appropriated α -allyloxy-substituted α,β -unsaturated ester **4** should represent a possible synthon for this purpose (Scheme 21).

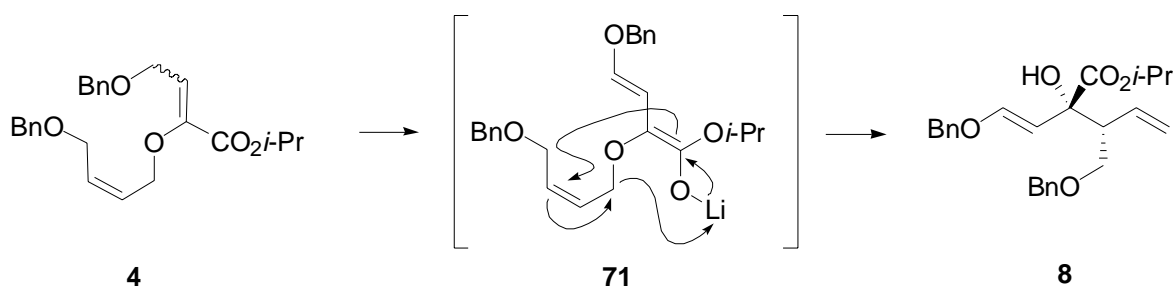


Scheme 21: Retrosynthetic analysis of the western half (**67**). TBS= *tert*-butyldimethylsilyl [Si(*t*-Bu)Me₂], Bn= benzyl.

⁶² For reviews concerning the utilization of 1,3-dithianes in natural product synthesis, see: (a) Smith, A. B.; Adams, C. M. *Acc. Chem. Res.* **2004**, *37*, 365-377. (b) Yus, M.; Najera, C.; Foubelo, F. *Tetrahedron* **2003**, *59*, 6147-6212. (c) Smith, A. B.; Condon, S. M.; McCauley, J. A. *Acc. Chem. Res.* **1998**, *31*, 35-46.

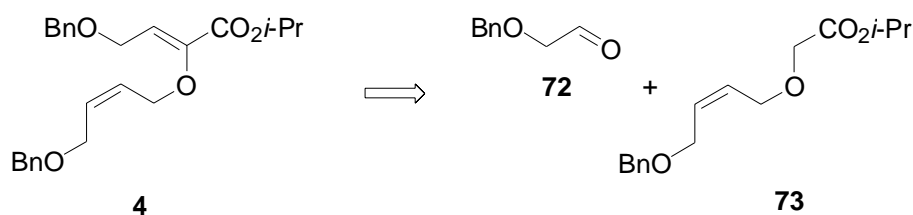
⁶³ Mitsunobu, O.; Yamada, M. *Bull. Chem. Soc. Jpn.* **1967**, *40*, 2380-2382.

Deprotonation of **4** would provide ester dienolate **71** which is prone to undergo [2,3]-Wittig rearrangement to afford the 1,5-hexadienes **8** as depicted in Scheme 22.



Scheme 22: Proposed synthesis of **8** utilizing an ester dienolate [2,3]-Wittig rearrangement. Bn= benzyl.

Generation of the α -allyloxy-substituted α,β -unsaturated ester **4** may be realized by the application of an aldol-condensation strategy between ester **73** and aldehyde **72** (Scheme 23) that is well established in our research group and was successfully employed for various similar α -allyloxy-substituted α,β -unsaturated esters.⁶⁴



Scheme 23: Aldol condensation strategy.

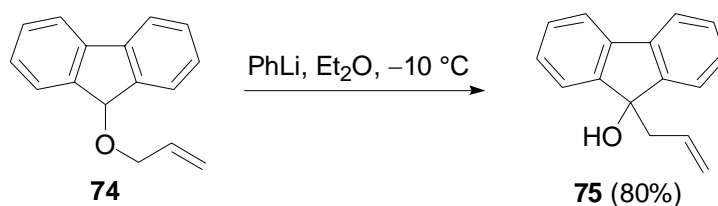
In the following section (23 pages) I will outline important characteristics of the key CC-connecting step: the ester dienolate [2,3]-Wittig rearrangement. The historical development as well as mechanistic considerations will be covered. Those readers who are mainly interested in the synthetic strategy and the results of the present work are referred to chapter 5 (page 56).

⁶⁴ Hiersemann, M. *Synthesis* **2000**, 1279-1290.

4 Ester Dienolate [2,3]-Wittig Rearrangement

4.1 Historical Development, Main Characteristics and Heteroatom Analogues

In 1949, Wittig *et al.* reported that treatment of 9-allyloxy-9*H*-fluorene (**74**) with phenyl lithium resulted in the formation of 9-allyl-9*H*-fluoren-9-ol (**75**) (Eq. 2)

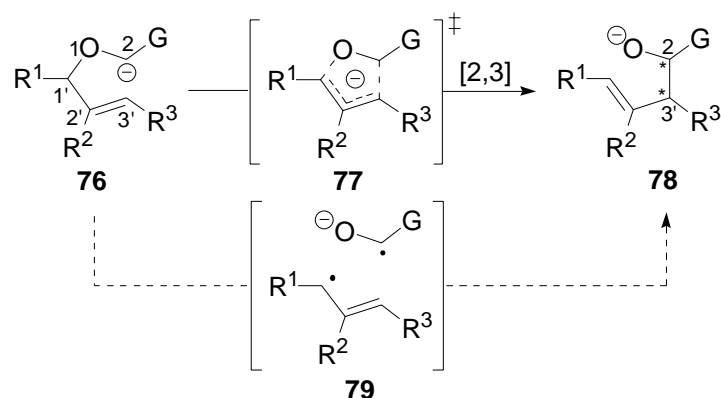


Eq. 2

This reaction is the prototype for the [2,3]-Wittig rearrangement – a term that is used for [2,3]-sigmatropic rearrangements of α -allyloxy-substituted carbanions **76** to afford homoallylic alcohols **78** (Scheme 24). It allows the formation of a carbon-carbon σ -bond starting from an easier accessible carbon-oxygen bond. Since its discovery, the [2,3]-Wittig rearrangement has been developed as a powerful tool for the stereoselective generation of homoallylic alcohols. In various natural product syntheses the potential of this transformation has been proven.⁶⁵ At low temperatures, the pericyclic reaction proceeds through a six-electron five-membered cyclic transition state **77** in a concerted fashion (Scheme 24). The competing diradical pathway **79** can be prevented by running the reaction at low temperatures.⁶⁶

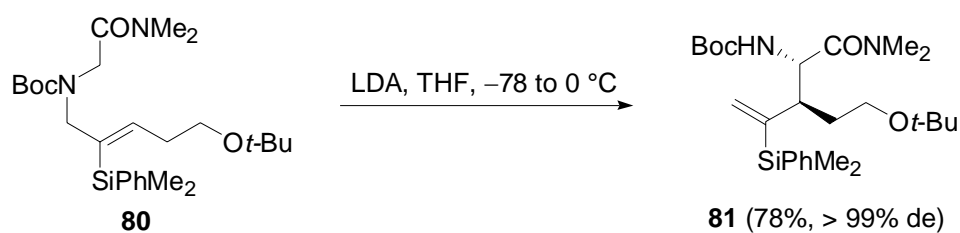
⁶⁵ For examples, see: (a) Midland, M.; Gabriel, J. *J. Org. Chem.* **1985**, *50*, 1143-1144. (b) Kiyota, H.; Ueda, R.; Oritani, T.; Kuwahara, S. *Synlett*, **2003**, 219-220. (c) Anderson, J. C.; Whiting, M. *J. Org. Chem.* **2003**, *68*, 6160-6163. (d) Berberich, S. M.; Cherney, R. J.; Colucci, J.; Courillon, C.; Geraci, L. S.; Kirkland, T. A.; Marx, M. A.; Schneider, M. F.; Martin, S. F. *Tetrahedron* **2003**, *59*, 6819-6832. (e) Audrain, H.; Skrydstrup, T.; Ulibarri, G.; Riche, C.; Chiaroni, A.; Grierson, David S. *Tetrahedron* **1994**, *50*, 1469-1502. (f) Watanabe, K.; Iwasaki, K.; Abe, T.; Inoue, M.; Ohkubo, K.; Suzuki, T.; Katoh, T. *Org. Lett.* **2005**, *7*, 3745-3748. (g) Ng, F. W.; Lin, H.; Danishefsky, S. J. *J. Am. Chem. Soc.* **2002**, *124*, 9812-9824. (h) Abe, T.; Iwasaki, K.; Inoue, M.; Suzuki, T.; Watanabe, K.; Katoh, T. *Tetrahedron Lett.* **2006**, *47*, 3251-3255. (i) Nakamura, Y.; Kiyota, H.; Ueda, R.; Kuwahara, S. *Tetrahedron Lett.* **2005**, *46*, 7107-7109. (j) Pollex, A.; Abraham, L.; Müller, J.; Hiersemann, M. *Tetrahedron Lett.* **2004**, *45*, 6915-6918. (k) Pollex, A.; Millet, A.; Müller, J.; Hiersemann, M.; Abraham, L. *J. Org. Chem.* **2005**, *70*, 5579-5591.

⁶⁶ For reviews, see: (a) Marshall, J. A. In *Comprehensive Organic Synthesis*; Trost, B. M.; Fleming, I., Eds.; Pergamon: Oxford **1991**; Vol. 3, p. 975-1014. (b) Nakai, T.; Koichi, M. In *Organic Reactions*, Paquette, L. A., Ed.; Wiley: New York **1994**; Vol. 46, p. 105-209. (c) Nakai, T.; Mikami, K. *Chem. Rev.* **1986**, *86*, 885-902. (d) Kallmerten, J. In *Houben Weyl, Methods of Organic Chemistry*; Helmchen, G.; Hoffmann, R. W.; Mulzer, J.; Schaumann, E., Eds; Thieme: Stuttgart, **1995**; Vol. E21, p. 3757-3809. (e) Mikami, K.; Nakai, T. *Synthesis* **1991**, 594-604. (f) Brückner, R. *Nachr. Chem. Techn. Lab.* **1990**, *38*, 1506-1510.

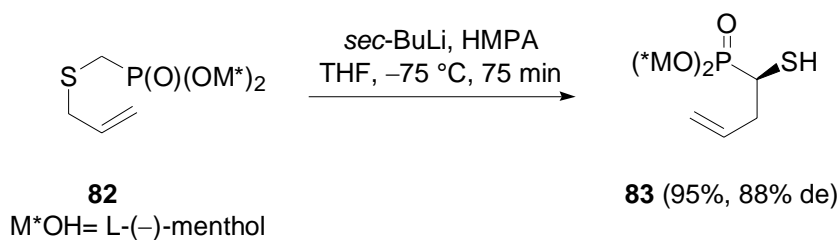


Scheme 24: Competing mechanism for the [2,3]-Wittig rearrangement: concerted (top) or a stepwise (bottom). At the low temperatures the concerted mechanism is preferred. G= carbanion stabilizing group.⁶⁷

The driving force of this rearrangement is the transformation of a carbanion into a more stable oxyanion. By replacing the ether oxygen by other hetero atoms, (e.g. sulphur or nitrogen) aza⁶⁸ and thio⁶⁹ analogues have been developed. Representative examples are depicted in Eq. and Eq. 4.



Eq. 3 Boc= *tert*-butyloxy carbonyl, LDA= lithium diisopropylamide.



Eq. 4: HMPA= hexamethylphosphoramide $\{[(\text{CH}_3)_2\text{N}]_2\text{PO}\}$.

⁶⁷ The equilibrium between the starting material and the transition state is not explicitly depicted. We have chosen this formulation for it allows a concise representation of the transformation proceeding through the corresponding transition states. The placing of the transition state formula within the arrow is used to emphasize that the transition state must not be seen as intermediate.

⁶⁸ For recent examples, see: (a) Anderson, J. C.; Siddons, D. C.; Smith, S. C.; Swarbrick, M. E. *J. Org. Chem.* **1996**, *61*, 4820-4823. (b) Anderson, J. C.; Flaherty, A.; Swarbrick, M. E. *J. Org. Chem.* **2000**, *65*, 9152-9156. (c) Anderson, J. C.; Whiting, M. *J. Org. Chem.* **2003**, *68*, 6160-6163. (d) Åhman, J.; Jarevång, T.; Somfai, P. *J. Org. Chem.* **1996**, *61*, 8148-8159. (e) Åhman, J.; Somfai, P. *Tetrahedron Lett.* **1996**, *37*, 2495-2498. (f) Anderson, J. C.; Ford, J. G.; Whiting, M. *Org. Biomol. Chem.* **2005**, *3*, 3734-3748. For a review, see: Vogel, C. *Synthesis* **1997**, 497-505.

⁶⁹ (a) Marchand, P.; Gulea, M.; Masson, S.; Saquet, M.; Collignon, N. *Org. Lett.* **2000**, *2*, 3757-3759. (b) Emde, H. v. d.; Brückner, R. *Tetrahedron Lett.* **1992**, *33*, 7323-7326. (c) Brickmann, K.; Brückner, R. *Chem. Ber.* **1993**, *126*, 1227-1239. (d) Uneyama, K.; Ohkura, H.; Hao, J.; Amii, H. *J. Org. Chem.* **2001**, *66*, 1026-1029.

4.1.1 The Carbanion Stabilizing Group G

Alkyl Groups

The group G may be simply an alkyl group. However, such carbanions are highly unstable and afford special conditions for their formation. Methods for the generation of these unstabilized carbanions will be discussed in chapter 4.1.2.

Aryl-, Vinyl- and Alkynyl-Groups

Various [2,3]-Wittig rearrangements have been reported that employ aryl-, vinyl- and propargyl-groups as carbanion stabilizing group G (Figure 7).

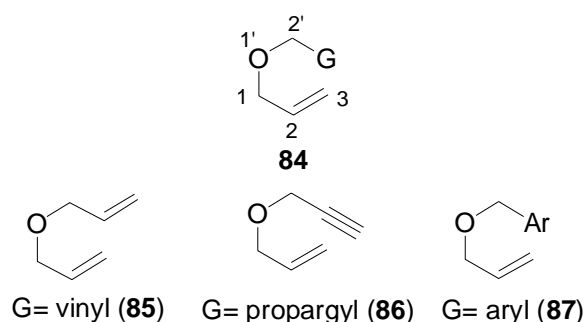
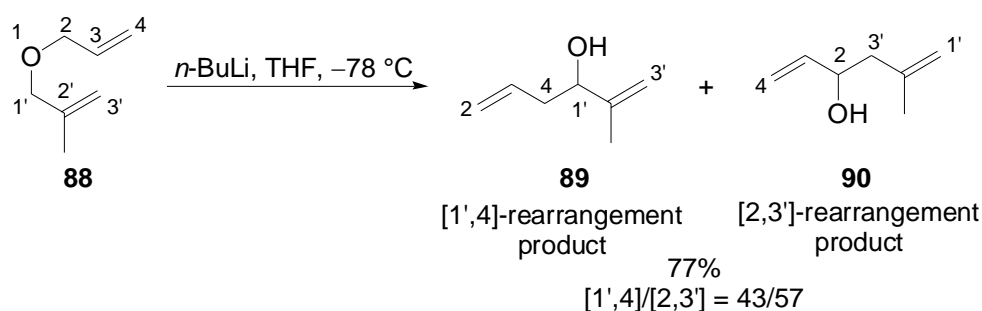


Figure 7

For unsymmetrical bisallylic ethers (G= vinyl), a regioselectivity problem arises (Eq. 5). Either of the allylic positions may be deprotonated and, consequently, both of the possible rearrangement products could be generated. Eq. 5 outlines a representative example.⁷⁰

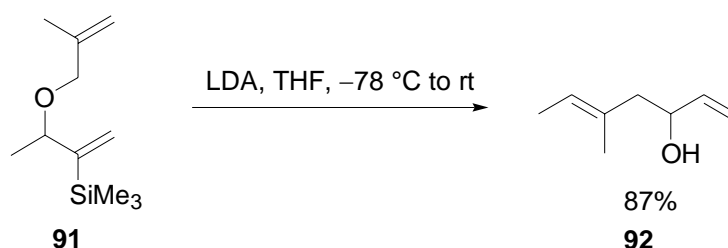


Eq. 5

However, it was shown, that the carbanion is usually generated at the less sterically hindered allyl fragment. Therefore, if appropriately substituted bisallyl ethers are employed, the

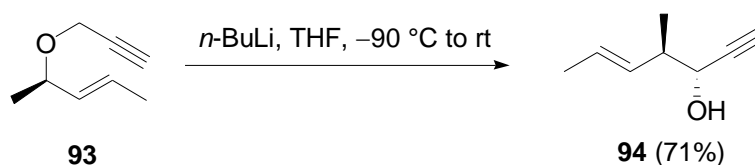
⁷⁰ Nakai, T.; Mikami, K.; Taya, S.; Fujita, Y. *J. Am. Chem. Soc.* **1981**, *103*, 6492-6494.

reaction proceeds with good regioselectivity.⁷¹ Rearrangement of bisallyl ether **91** afforded **92** as the only product of the transformation (Eq. 6).^{71c}



Eq. 6: LDA= lithium diisopropylamide.

An application of the [2,3]-Wittig rearrangement of an allyl propargyl ether **93** is shown in Eq. 7.⁷² **94** was formed as single diastereomer and enantiomer with the latter being the consequence of 1,3-chirality transfer.⁷³



Eq. 7

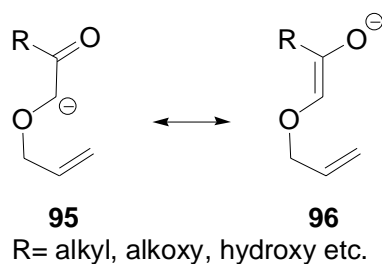
π -Acceptors

Functional groups that allow stabilization of the carbanion by resonance were also used as group G (Scheme 25). Noteworthy examples are ketones (or the hydrazone derivatives thereof), nitriles, phosphonates, and carboxylic acid derivatives (e.g. esters, amides, or oxazolines).

⁷¹ For recent examples, see: (a) Dorling, E. K.; Thomas, A. P.; Thomas, E. J. *Tetrahedron Lett.* **1999**, *40*, 475-476. (b) Spino, C.; Godbout, C.; Beaulieu, C.; Harter, M.; Mwene-Mbeja, T. M.; Boisvert, L. *J. Am. Chem. Soc.* **2004**, *126*, 13312-13319. (c) Tomooka, K.; Igarashi, T.; Kishi, N.; Nakai, T. *Tetrahedron Lett.* **1999**, *40*, 6257-6260.

⁷² Liang, J.; Hoard, D. W.; Khau, V. V.; Martinelli, M. J.; Moher, E. D.; Moore, R. E.; Tius, M. A. *J. Org. Chem.* **1999**, *64*, 1459-1463.

⁷³ 1,3-chirality transfer as an useful tool during substrate induced stereoselectivity will be discussed in more detail in chapter 4.3.1.



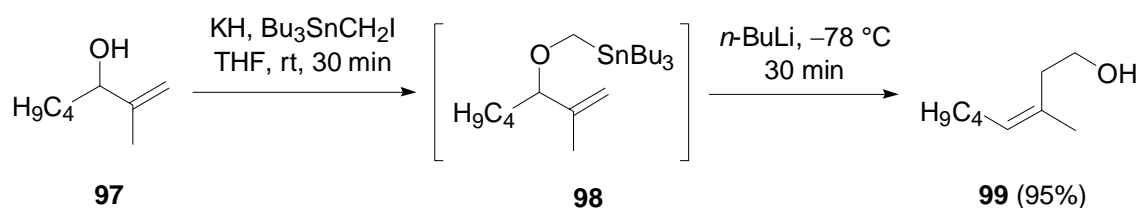
Scheme 25: Representative example for the carbanion stabilization by resonance employing an adjacent carbonyl group.

4.1.2 Formation of the Carbanion

There are different strategies for the formation of the carbanion. Unstabilized carbanions (G= alkyl, H) are most commonly generated by transmetalation of stannanes or reductive lithiation of *S,O*-acetals. Stabilized carbanions (G≠ alkyl or H) are usually formed by the treatment of the substrate with a base causing deprotonation.

Transmetalation and reductive lithiation of *S,O*-acetals

In 1978, the introduction of the Still-variation was an important breakthrough for the development of the [2,3]-Wittig rearrangement as an useful tool in organic synthesis. It allowed the selective formation of carbanions lacking any stabilizing groups under mild conditions (Scheme 26).⁷⁴

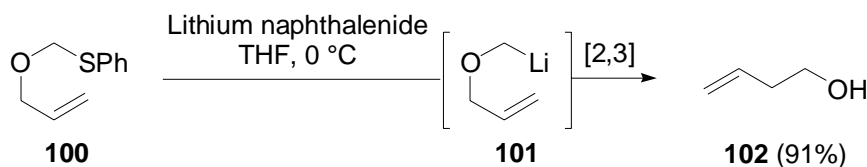


Scheme 26: [2,3]-Wittig rearrangement according to Still.

The carbanion is formed by transmetalation of a tin organyl to afford a lithium organyl that readily undergoes the rearrangement at low temperatures.

⁷⁴ Still, W. C.; Mitra, A. *J. Am. Chem. Soc.* **1978**, *100*, 1927-1928.

Later, Brückner and Broka independently used the reductive lithiation of *S,O*-acetals - originally developed by Cohen and co-workers for the formation of α -allyloxy-substituted organo lithium compounds⁷⁵ - as preliminary step for [2,3]-Wittig rearrangement (Eq. 8^{76a}).⁷⁶



Eq. 8

This intriguing alternative to the highly toxic alkyl tin compounds significantly increased the scope of the reaction because it allowed the incorporation of various substituents on the carbanionic center. Later, methods were developed to generate secondary and tertiary stannanes making secondary and tertiary lithium organyls accessible by transmetallation.⁷⁷

Mulzer reported a transmetallation strategy employing a silicon-lithium exchange.⁷⁸

Deprotonation

A very common method for the formation of the carbanion is the deprotonation facilitated by the presence of a carbanion stabilizing group. Carbonyl groups in particular are frequently applied. Applications of this method will be discussed later (chapter 4.3-4.5).

Miscellaneous

Further variations for the formation of the carbanion include lithium-halogen exchange,⁷⁹ fluoride induced desilylation⁸⁰ and SET-induced formation of carbanions using SmI_2 .⁸¹

The α -allyloxy-substituted anions, prone to undergo the [2,3]-sigmatropic rearrangement may as well be formed by the reaction of allyl ethers with metal carbenes. Versatile starting materials are diazocarbonyl compounds that readily produce the required metal carbenes upon

⁷⁵ (a) Cohen, T.; Daniewski, W. M.; Weisenfeld, R. B. *Tetrahedron Lett.* **1978**, *49*, 4665-4668. (b) Cohen, T.; Matz, J. R. *Synth. Comm.* **1980**, *10*, 311-317. (c) Cohen, T.; Matz, J. R. *J. Am. Chem. Soc.* **1980**, *102*, 6900-6902.

⁷⁶ (a) Broka, C. A.; Shen, T. *J. Am. Chem. Soc.* **1989**, *111*, 2981-2984. (b) Kruse, B.; Brückner, R. *Chem. Ber.* **1989**, *122*, 2023-2025.

⁷⁷ Hoffmann, R.; Brückner, R. *Angew. Chem.* **1992**, *104*, 646-648, *Angew. Chem., Int. Ed. Engl.* **1992**, *31*, 647-649. For a more detailed discussion, see chapter 4.3.1.

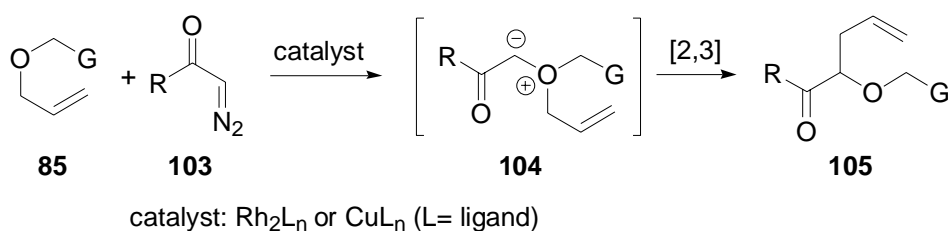
⁷⁸ Mulzer, J.; List, B. *Tetrahedron Lett.* **1996**, *37*, 2403-2404.

⁷⁹ Maciá, B.; Gómez, C.; Yus, M. *Tetrahedron Lett.* **2005**, *46*, 6101-6104.

⁸⁰ Malezcka, R. E., Jr.; Geng, F. *Org. Lett.* **1999**, *1*, 1111-1113.

⁸¹ Kunishima, M.; Hioki, K.; Kono, K.; Kato, A.; Tani, S. *J. Org. Chem.* **1997**, *62*, 7542-7543.

treatment with rhodium(II) or copper(I) complexes.⁸² Intermediary, ylides are generated (Scheme 27).



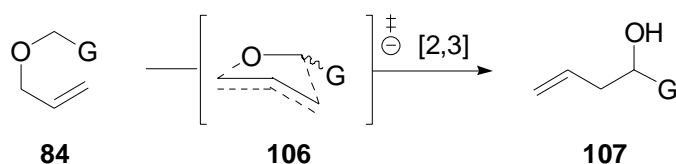
Scheme 27: Charge accelerated [2,3]-sigmatropic rearrangement of oxonium ylides is similar to the [2,3]-Wittig rearrangement.

The present discussion will concentrate on the [2,3]-Wittig rearrangement of α -allyloxy-substituted carbanions. Therefore, neither the heteroatom analogues nor the charge accelerated [2,3]-sigmatropic rearrangement of ylides will be discussed in more detail.

4.2 Mechanism and Simple Diastereoselectivity

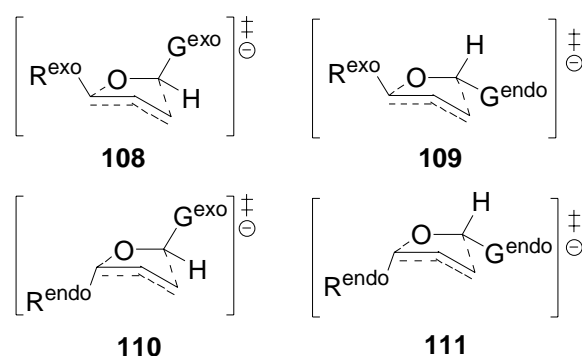
As a result of the rearrangement, up to two vicinal stereogenic centers and one stereogenic double bond are formed. Similar to the [3,3]-sigmatropic rearrangements the [2,3]-Wittig rearrangement proceeds through a highly ordered cyclic transition state. Consequently, attempts have been made to develop models that allow the explanation and reliable prediction of the stereochemical outcome of the rearrangement. However, models developed so far are not as self-consistent and highly intuitive as the well defined and energetically distinct conformations of a cyclohexane system used to describe the transition state of [3,3]-sigmatropic rearrangements. The reaction is believed to proceed through an envelope-like transition state rather than through a transition state with half chair conformation. However, the energetic differences between the different possible low energy conformations are very small. Of the five possible envelope conformations, the conformer with the terminal vinyl residue adopting an out of plane orientation (Scheme 28) is in good agreement with experimental evidence and is commonly used for the projection of the stereochemical consequences.⁶⁶

⁸² For the first examples of the [2,3]-sigmatropic rearrangement of oxonium ylides, see: (a) Pirrung, M. C.; Werner, J. A. *J. Am. Chem. Soc.* **1986**, *108*, 6060-6062. (b) Roskamp, E. J.; Johnson, C. R. *J. Am. Chem. Soc.* **1986**, *108*, 6062-6063.



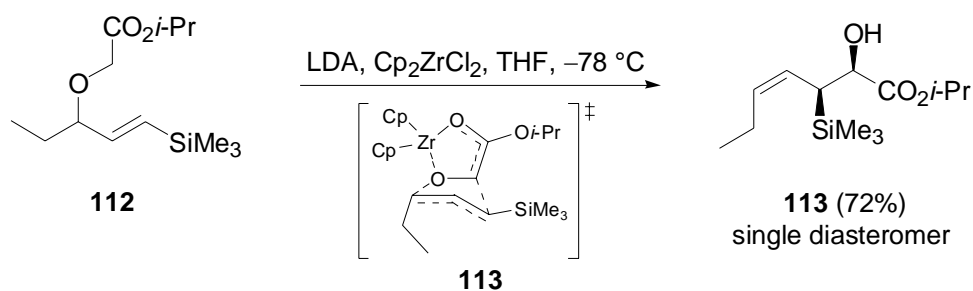
Scheme 28: Commonly used projection to describe the transition state of the [2,3]-Wittig rearrangement.

The presence of an allylic substituent and a carbanion stabilization group G results in different conformations with the substituents being in *exo* (toward the convex face of the cyclopentane frame) or *endo* (directed toward the concave face of the cyclopentane ring) position (Scheme 29).



Scheme 29: Possible transition states if an additional allylic substituent is present.

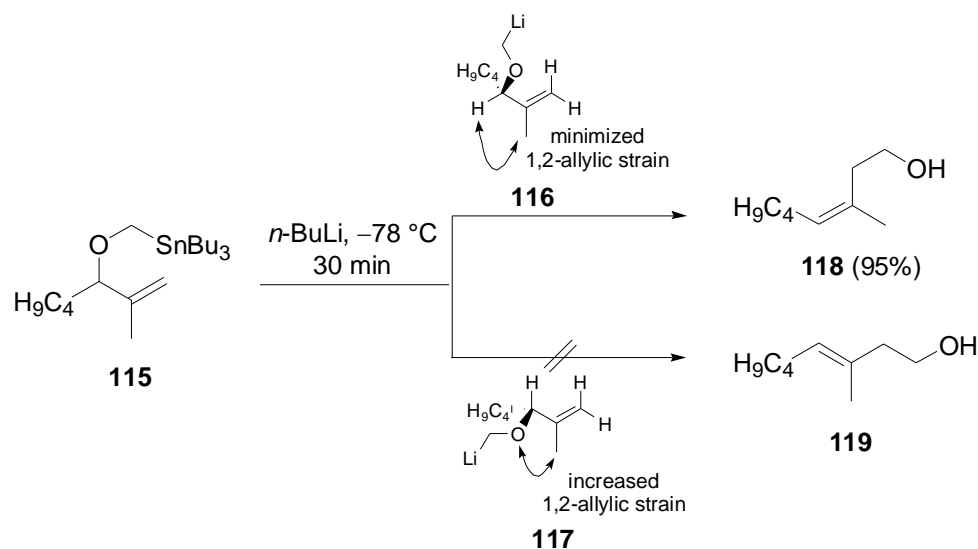
In most cases the allylic substituent prefers an *exo*-orientation toward the convex face of the cyclopentane frame (R^{exo}). Consequently, an *E*-configured double bond is preferentially formed. However, there are exceptions of this general rule. One example for such an unusual *Z*-selectivity is the rearrangement of zirconium ester enolates which exclusively affords *Z*-alkenes. This result may be accounted to unfavourable steric interactions between the ethyl residue and the sterically demanding cyclopentadienyl ligands (Eq. 9Eq.).⁸³



Eq. 9 LDA= lithium diisopropylamide, Cp= cyclopentadienyl.

⁸³ Kuroda, S.; Katsuki, T.; Yamaguchi, M. *Tetrahedron Lett.* **1987**, *28*, 803-804.

In the following example, the unusual formation of the *Z*-configured double bond is the result of the presence of an additional substituent at C-2 of the double bond (Scheme 30). Due to the absence of a substituent $R^3 \neq H$ at C-3 the 1,3-allylic strain is expected to be less important for the stereochemical outcome of the rearrangement. In contrast, the presence of the methyl group at C-2 increases the relevance of the 1,2-allylic strain. For the formation of *E*-configured **118**, the rearrangement would have to proceed through a transition state with maximized 1,2-allylic strain while for the generation of *Z*-configured **119** a transition state conformation with minimized 1,2-allylic strain would be adopted.

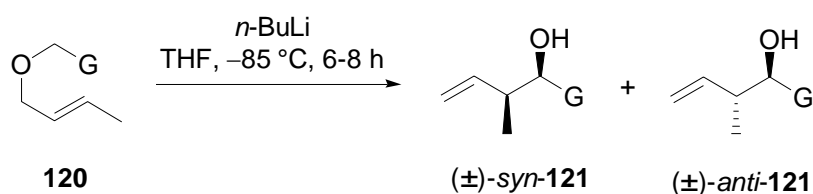


Scheme 30: The preferred formation of the rearrangement product with *Z*-configured double bond is the consequence of unfavourable steric interactions.

The diastereoselectivity is influenced by the carbanion stabilizing group G and the double bond configuration. The general rules can be summarized as following (Table 5):

- If non-carbonyl anion-stabilizing groups are employed, *E*-configured starting material will rearrange to give the *anti*-products while *Z*-configured alkenes will afford *syn*-products.⁸⁴
- For substrates in which the carbanion is stabilized by a carbonyl group the *syn/anti*-diastereoselectivity is reversed.

⁸⁴ [2,3]-Wittig rearrangement with phosphorus anion stabilizing groups afforded *anti*-configured rearrangement products regardless what the double bond configuration was. See: Denmark, S.; Miller, P. C. *Tetrahedron Lett.* **1995**, *36*, 6631-6634.



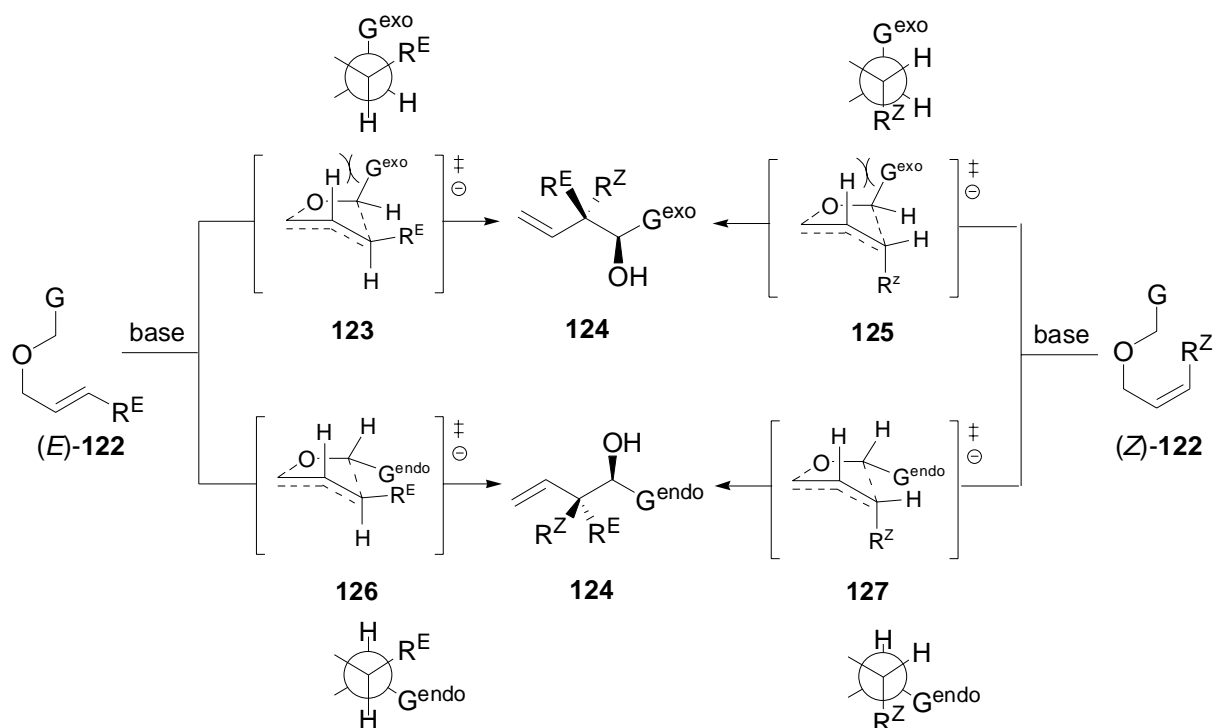
| Entry | G | <i>E/Z</i> (starting material) | <i>syn/anti</i> |
|-------|--------------------|-----------------------------------|-----------------|
| 1 | C≡CH | 93/7 | 7/93 |
| 2 | | 2/98 | 88/12 |
| 3 | CH=CH ₂ | 93/7 | 21/79 |
| 4 | | 5/95 | 88/12 |
| 5 | Ph | 93/7 | 63/37 |
| 6 | | 5/95 | 93/7 |
| 7 | CO ₂ H | 93/7 | 88/12 |
| 8 | | 5/95 | 25/75 |

Table 5: Dependence of the diastereoselectivity from the nature of the carbanion stabilizing group G and the double bond configuration.⁸⁵

If G is an alkynyl group, comparable diastereoselectivities for both double bond isomers were observed (Table 5, entry 1 and 2). However, if phenyl was used as carbanion stabilizing group the *E*-configured starting material rearranged with significantly lower diastereoselectivity (Table 5, entry 5 and 6). With vinyl groups employed as G slightly improved diastereoselectivities are observed (Table 5, entry 3 and 4). In case of the acid (Table 5, entry 7 and 8) the diastereoselectivity was reversed.

A model was developed that nicely explains these results. Thus, the orientation of the carbanion stabilizing group G on the envelope-like transition state is decisive (Scheme 31).

⁸⁵ Obtained from reference 66c.



Scheme 31: Analysis of the possible transition state conformations with respect to the carbanion stabilizing group G. The Newman projection illustrates steric interactions along the newly formed bond.

Stronger pseudo-1,3-diaxial interactions in transition states **123/125** were accounted for a preferred *endo* orientation of G (G^{endo}). The transition state **126** only suffers from a *gauche* interaction between G and R^{E} . Consequently, sterically higher demanding groups G would cause stronger steric *gauche* interactions along the newly formed bond what would lead to a decreased *syn/anti*-selectivity overall but especially if the double bond is *E*-configured (entry 3 and 5, Table 5).

In the case of G containing a carbonyl group, calculations of the relative energy revealed the preference of the opposite orientation (G^{exo}) on the cyclopentane frame.⁸⁶ The presence of the carbonyl group might render transition states **126/127** - resulting in significant *gauche* interactions between $R^{\text{E/Z}}$ and G^{endo} along the newly formed bond - less favourable than the corresponding transition state **123/125**. Consequently, the *syn/anti*-selectivity is reversed. As well, better diastereoselectivities are expected for the rearrangement of *Z*-configured starting materials (entry 7, Table 5) because transition state **125** profits from a favourable *antiperiplanar* arrangement of R^{Z} and G^{exo} .

⁸⁶ Wu, Y.-D.; Houk, K. N.; Marshall, J. A. *J. Org. Chem.* **1990**, *55*, 1421-1423.

4.3 Induced Diastereo- and Enantioselectivity during [2,3]-Wittig Rearrangements

Beside the simple diastereoselectivity, affords have been made to develop enantioselective and/or diastereoselective variations. There are four different possible strategies for the induction of enantio- or diastereoselectivity:

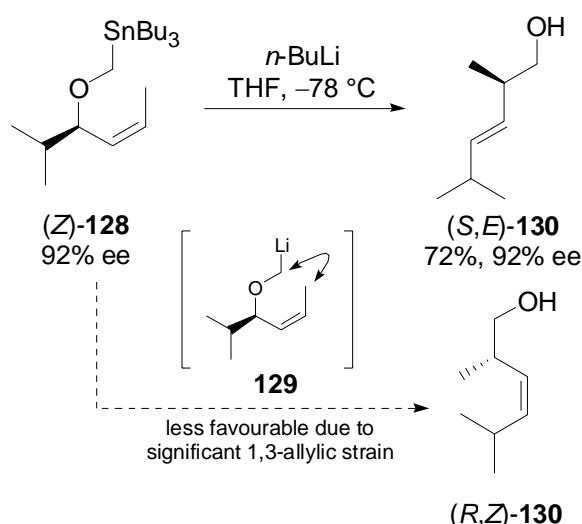
- substrate induction (4.3.1),
- auxiliary induction (4.3.2),
- reagent induction (4.3.3),
- or catalyst induction (4.3.4).

4.3.1 Substrate-Induced Diastereo- and Enantioselectivity: 1,3-Chirality Transfer and Remote Stereocontrol

Due to the highly ordered transition state, the possibilities for chirality transfer are similar to those known for the related [3,3]-sigmatropic events. Various successful applications of the 1,3-chirality transfer employed in the [2,3]-Wittig rearrangement of allylic ethers of secondary alcohols proved the value of this strategy.⁸⁷ The extent of asymmetric induction during the self-immolative chirality transfer is generally very high (>95%). An example is depicted in Scheme 32.⁸⁸

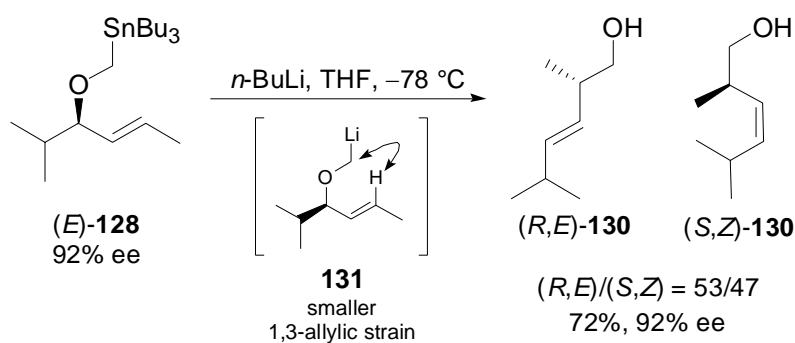
⁸⁷ For examples, see: (a) Scheuplein, S. W.; Kusche, A.; Brückner, R.; Harms, K. *Chem. Ber.* **1990**, *123*, 917-925. (b) Hoffmann, R.; Brückner, R. *Angew. Chem.* **1992**, *104*, 646-648, *Angew. Chem., Int. Ed. Engl.* **1992**, *31*, 647-649. (c) Uchikawa, M.; Katsuki, T.; Yamaguchi, M. *Tetrahedron Lett.* **1986**, *27*, 4581-4582. (d) Balestra, M.; Kallmerten, J. *Tetrahedron Lett.* **1988**, *29*, 6901-6904. (e) Tsai, D. J. S.; Midland, M. M. *J. Org. Chem.* **1984**, *49*, 1842-1843. (f) Marshall, J. A.; Jenson, T. *J. Org. Chem.* **1984**, *49*, 1707-1712. (g) Sayo, N.; Kitahara, E.; Nakai, T. *Chem. Lett.* **1984**, 259-262. (h) Tsubuki, M.; Okita, H.; Kamata, T.; Ohinata, A.; Kaneko, K.; Honda, T. *Tetrahedron: Asymmetry* **2000**, *11*, 4725-4736. (i) Uchiyama, M.; Kimura, Y.; Ohta, A. *Tetrahedron Lett.* **2000**, *41*, 10013-10017.

⁸⁸ Midland, M. M.; Kwon, Y. C. *Tetrahedron Lett.* **1985**, *26*, 5013-5016.



Scheme 32: An unfavourable 1,3-allylic strain in **129** may be accounted for the preferred formation of $(S,E)\text{-130}$.

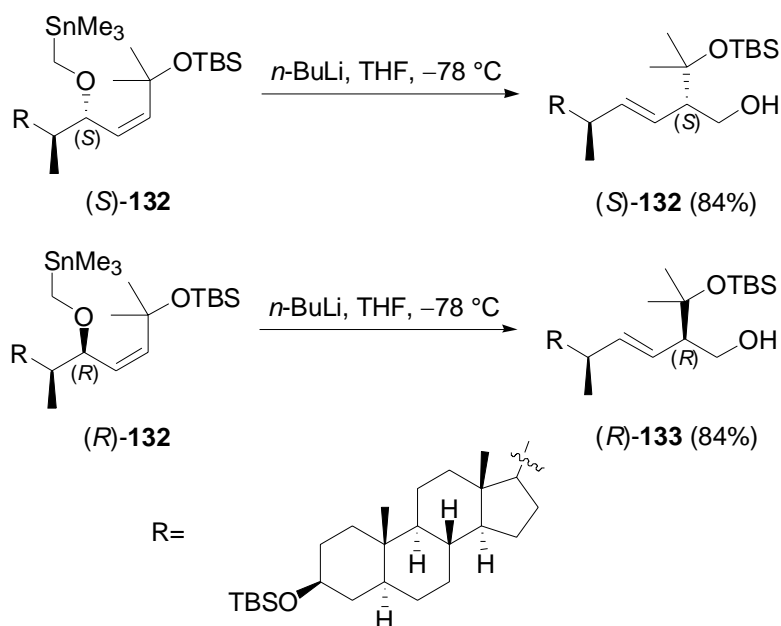
The preferred formation of the *E*-configured rearrangement product $(S,E)\text{-130}$ can be accounted to a strong 1,3-allylic strain provoked by the presence of the methyl group at C-3 that render **129** less favourable. In contrast, if *E*-configured $(E)\text{-128}$ is rearranged, decreased *E/Z*-selectivities were observed (Eq. 10). $(R,E)\text{-130}$ and $(S,Z)\text{-130}$ are formed in roughly equal amounts (Eq. 10). The decreased *E/Z*-selectivities may be rationalized by the decreased 1,3-allylic strain between $R^{3Z} = \text{H}$ and the substituent in allylic position compared to $R^{3Z} = \text{Me}$ in the above example. Note that even though the *E/Z*-selectivity is low the chirality transfer is comparable to the above example given in Scheme 32.



Eq. 10

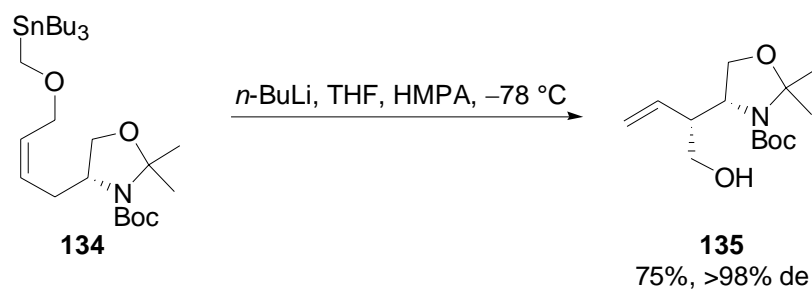
Inversion of the directing allylic stereogenic center represents an effective strategy to generate the opposite enantiomer. This strategy was successfully employed in the synthesis of steroidal side chains.⁸⁹ Representative examples – the formation of campestone $(S)\text{-133}$ and ergostane steroids $(R)\text{-133}$ – are shown in Scheme 33.

⁸⁹ (a) Castedo, L.; Granja, J. R.; Mouriño, A. *Tetrahedron Lett.* **1985**, *26*, 4959-4960. (b) Castedo, L.; Granja, J. R.; Mouriño, A.; Pumar, M. *Synth. Comm.* **1987**, *17*, 251-256. (c) Midland, M. M.; Kwon, Y. C. *Tetrahedron*



Scheme 33: 1,3-chirality transfer was employed as powerful tool for the side chain formation of steroids. TBS= *tert*-butyldimethylsilyl [$\text{Si}(t\text{-Bu})\text{Me}_2$].

Remote stereocontrol was found to be another powerful tool to control the diastereoselectivity of the reaction.⁹⁰ Eq. 11 shows an instructive example for the potent control of the diastereofacial selectivity.⁹¹



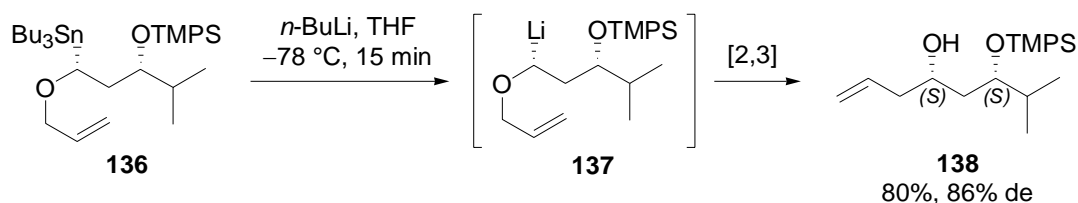
Eq. 11 HMPA= hexamethylphosphoramide $\{[(\text{CH}_3)_2\text{N}]_2\text{PO}\}$, Boc= *tert*-butyloxycarbonyl.

Lett. **1985**, *26*, 5017-5020. (d) Midland, M. M.; Kwon, Y. C. *Tetrahedron Lett.* **1985**, *26*, 5021-5024. (e) Mikami, K.; Kawamoto, K.; Nakai, T. *Tetrahedron Lett.* **1985**, *26*, 5799-5802. (f) Mikami, K.; Kawamoto, K.; Nakai, T. *Tetrahedron Lett.* **1986**, *27*, 4899-4902. (g) Koreeda, M.; Ricca, D. J. *J. Org. Chem.* **1986**, *51*, 4090-4092. (h) Tsubuki, M.; Ohinata, A.; Tanaka, T.; Takahashi, K.; Honda, T. *Tetrahedron Lett.* **2005**, *61*, 1095-1100.

⁹⁰ For selected examples, see: (a) Balnaves, A. S.; McGowan, G.; Shapland, P. D. P.; Thomas, E. J. *Tetrahedron Lett.* **2003**, *44*, 2713-2716. (b) Mulzer, J.; List, B. *Tetrahedron Lett.* **1994**, *35*, 9021-9024. (c) Keegan, D. S.; Midland, M. M.; Werley, R. T.; McLoughlin, J. I. *J. Org. Chem.* **1991**, *56*, 1185-1191. (d) Abe, T.; Iwasaki, K.; Inoue, M.; Suzuki, T.; Watanabe, K.; Katoh, T. *Tetrahedron Lett.* **2006**, *47*, 3251-3255. (e) Ghosh, A. K.; Wang, Y. *Tetrahedron* **1999**, *55*, 13369-13376. (f) Dorling, E. K.; Thomas, A. P.; Thomas, E. J. *Tetrahedron Lett.* **1999**, *40*, 475-476.

⁹¹ Priepke, H.; Brückner, R.; Harms, K. *Chem. Ber.* **1990**, *123*, 555-563.

Finally, the possibility to employ a configurationally defined secondary or tertiary lithium organyls should be mentioned. This strategy relies on configurationally defined secondary stannanes and *S,O*-acetals which upon lithiation form a configurationally defined lithium organyl which in turn undergoes the rearrangement (Eq. 12).^{92a}



Eq. 12 TMPS= [dimethyl-(1,1,2-trimethylpropyl)]-silyl.

4.3.2 Auxiliary-Induced Diastereoselectivity

If the group G is a π -acceptor, chiral auxiliaries are easy to introduce. Chiral esters, amides, oxazolines, hydrazones and phosphonates have been successfully employed. The auxiliary-induced diastereoselectivities were usually moderate to good.⁹³ A selection of representative examples is given below.⁹⁴

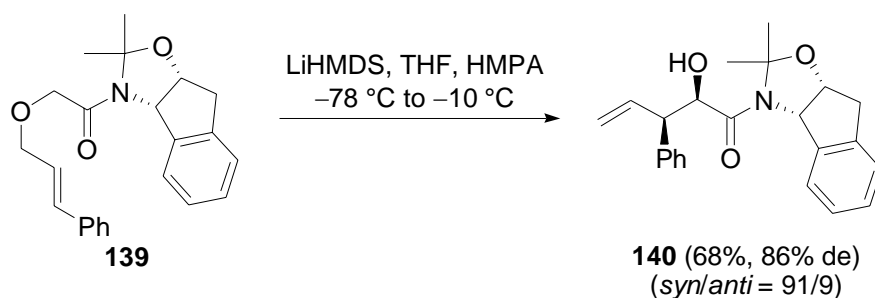
The research group of Kress *et al.* utilized chiral amino indanoles as auxiliaries for an amide enolate [2,3]-Wittig rearrangement (Eq. 13).⁹⁵

⁹² (a) Ref. 77 (b) Tomooka, K.; Igrashi, T.; Watanabe, M.; Nakai, T. *Tetrahedron Lett.* **1992**, *33*, 5795-5798. (c) Verner, E. J.; Cohen, T. J. *J. Am. Chem. Soc.* **1992**, *114*, 375-377.

⁹³ Usually, both the simple diastereoselectivities and the auxiliary induced diastereoselectivities have to be considered. To allow the reader an easy appreciation of the auxiliary induced diastereoselectivity the latter is given as 'de' in the following equations while the simple diastereoselectivity is documented by the *syn/anti*-relation in parantheses. For a more detailed discussion of scope and limitations of the descriptors de and ee, see: Gawley, R. E. *J. Org. Chem.* **2006**, *71*, 2411-2416.

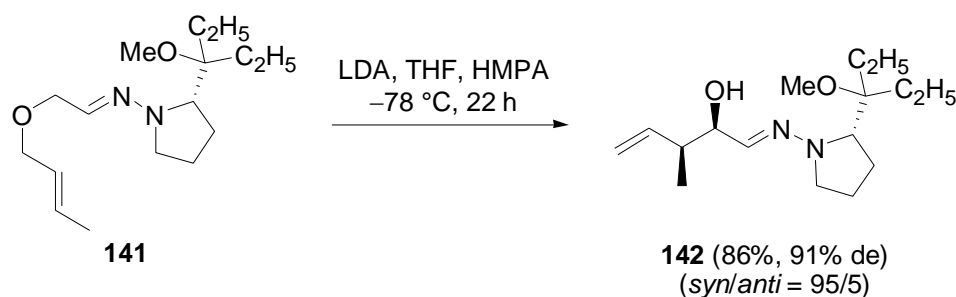
⁹⁴ For a review concerning asymmetric [2,3]-Wittig reactions, see: Nakai, T.; Tomooka, K. *Pure & Appl. Chem.* **1997**, *69*, 595-600.

⁹⁵ Kress, M. H.; Yang, C.; Yasuda, N.; Grabowski, E. J. *J. Tetrahedron Lett.* **1997**, *38*, 2633-2636. For additional examples of asymmetric amide enolate [2,3]-Wittig rearrangement, see: (a) Mikami, K.; Takahashi, O.; Kasuga, T.; Nakai, T. *Chem. Lett.* **1985**, 1729-1732. (b) Uchikawa, M.; Hanamoto, T.; Katsuki, T.; Yamaguchi, M. *Tetrahedron Lett.* **1986**, *27*, 4577-4580.



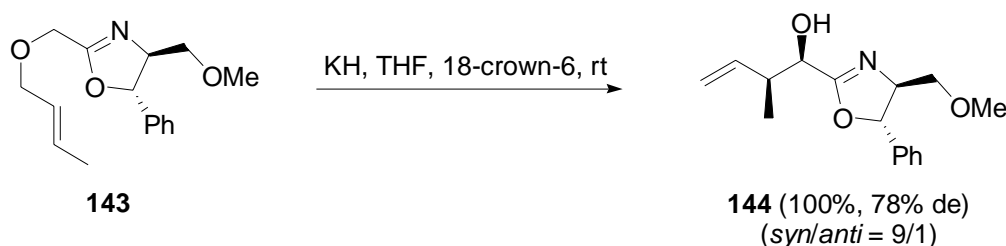
Eq. 13: LiHMDS= Li[N(SiMe₃)₂], HMPA= hexamethylphosphoramide {[(CH₃)₂N]₂PO }.

Transformation of ketones into the corresponding chiral hydrazones and subsequent [2,3]-Wittig rearrangement resulted in auxiliary-induced diastereoselectivities up to 92% de (Eq. 14).⁹⁶



Eq. 14: HMPA= hexamethylphosphoramide {[(CH₃)₂N]₂PO }, LDA= lithium diisopropylamide.

Chiral oxazolines used as carbanion stabilizing group G as well induced diastereoselectivity with reasonable success.⁹⁷ Nakai *et al.* found enhanced diastereoselectivities in the presence of 18-crown-6 (Eq. 15).^{97f}

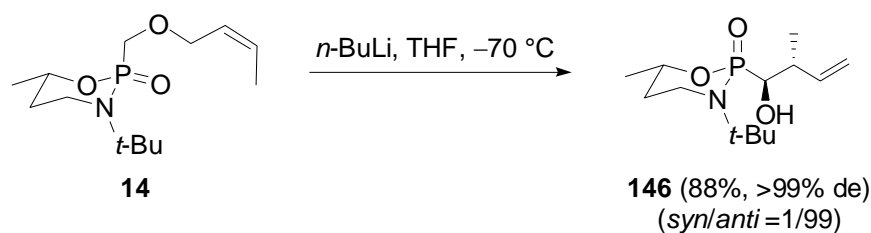


Eq. 15

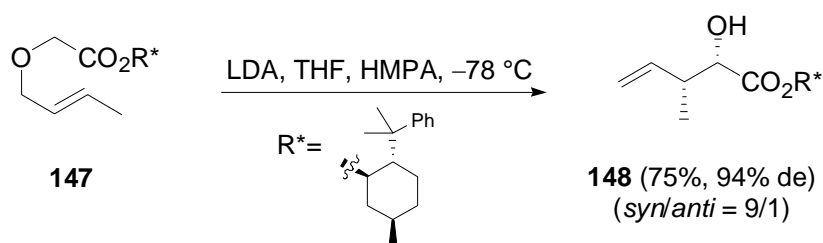
⁹⁶ Enders, D.; Backhaus, D.; Runsink, J. *Angew. Chem.* **1994**, *106*, 2167-2170; *Angew. Chem., Int. Ed. Engl.* **1994**, *33*, 2098-2100. For further examples, see: (a) Luengo, J. L.; Koreeda, M. *J. Org. Chem.* **1989**, *54*, 5415-5417. (b) Enders, D.; Bartsch, M.; Backhaus, D.; Runsink, J.; Raabe, G. *Synthesis* **1996**, 1438-1442. (c) Enders, D.; Backhaus, D.; Runsink, J. *Tetrahedron* **1996**, *52*, 1503-1528. (d) Enders, D.; Backhaus, D. *Synlett* **1995**, 631-632.

⁹⁷ (a) Mikami, K.; Fujimoto, K.; Nakai, T. *Tetrahedron Lett.* **1983**, *24*, 513-516. (b) Mikami, K.; Fujimoto, K.; Kasuga, T.; Nakai, T. *Tetrahedron Lett.* **1984**, *25*, 6011-6014. (c) Rossano, L. T.; Plata, D. J.; Kallmerten, J. *J. Org. Chem.* **1988**, *53*, 5189-5191. (d) Kress, M. H.; Haller, B. F.; Kishi, Y. *Tetrahedron Lett.* **1993**, *34*, 8047-8050. (e) Sudo, Y.; Hashimoto, Y.; Kimoto, H.; Hayashi, K.; Saigo, K. *Tetrahedron: Asymmetry* **1994**, *5*, 1333-1346. (f) Mikami, K.; Kasuga, T.; Fujimoto, K.; Nakai, T. *Tetrahedron Lett.* **1986**, *27*, 4185-4188.

A very good auxiliary-induced diastereoselectivity was reported for the use of phosphonates. The rearrangement products have been obtained with up to 99% de (Eq. 16).^{98a}



Eq. 17 illustrates an ester enolate [2,3]-Wittig rearrangement incorporating a chiral ester alcohol residue.⁹⁹



4.3.3 Reagent-Induced Enantioselectivity

The reagent-induced enantioselectivity is less frequently employed for asymmetric variations of the [2,3]-Wittig rearrangement. Chiral lithium amides have been used.¹⁰⁰ However, appreciable enantioselectivities were observed only for specific cyclic substrates.

Chiral ligands such as (-)-sparteine¹⁰¹ or bis(oxazolines)¹⁰² have been employed. Enantioselectivities up to 50% ee could be realized by using (-)-sparteine for the rearrangement of allyl heteroaryl ethers (Eq. 18).

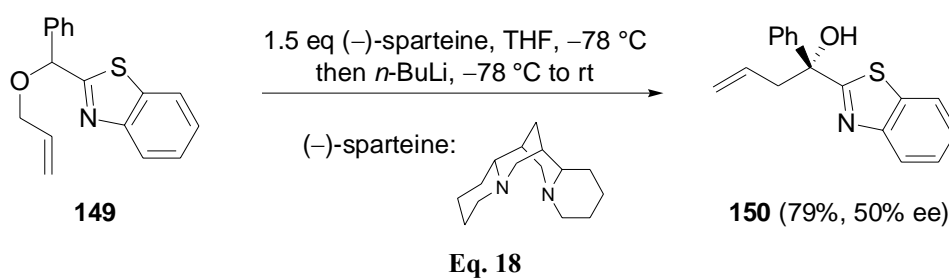
⁹⁸ For representative examples using phosphonates, see: (a) Denmark, S. E.; Miller, P. A. *Tetrahedron Lett.* **1995**, *36*, 6631-6634. (b) Gulea-Purcarescu, M.; About-Jaudet, E.; Collignon, N. *Tetrahedron Lett.* **1995**, *36*, 6635-6638.

⁹⁹ Takahashi, O.; Mikami, K.; Nakai, T. *Chem. Lett.* **1987**, 69-72.

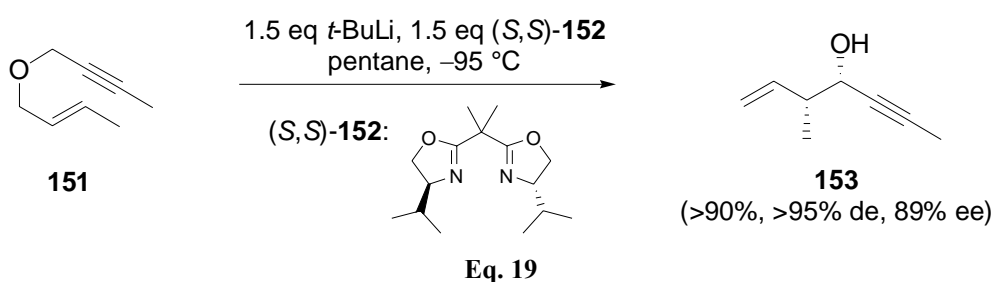
¹⁰⁰ (a) Marshall, J. A.; Lebreton, J. *Tetrahedron Lett.* **1987**, *28*, 3323-3326. (b) Marshall, J. A.; Lebreton, J. *J. Org. Chem.* **1988**, *53*, 4108-4112.

¹⁰¹ For recent examples, see: (a) Capriati, V.; Florio, S.; Ingrosso, G.; Granito, C.; Troisi, L. *Eur. J. Org. Chem.* **2002**, 478-484. (b) Kawasaki, T.; Kimachi, T. *Tetrahedron* **1999**, *55*, 6847-6862.

¹⁰² (a) Tomooka, K.; Komine, N.; Nakai, T. *Tetrahedron Lett.* **1998**, *39*, 5513-5516. (b) Barrett, I. M.; Breeden, S. W. *Tetrahedron: Asymmetry* **2004**, *15*, 3015-3017.



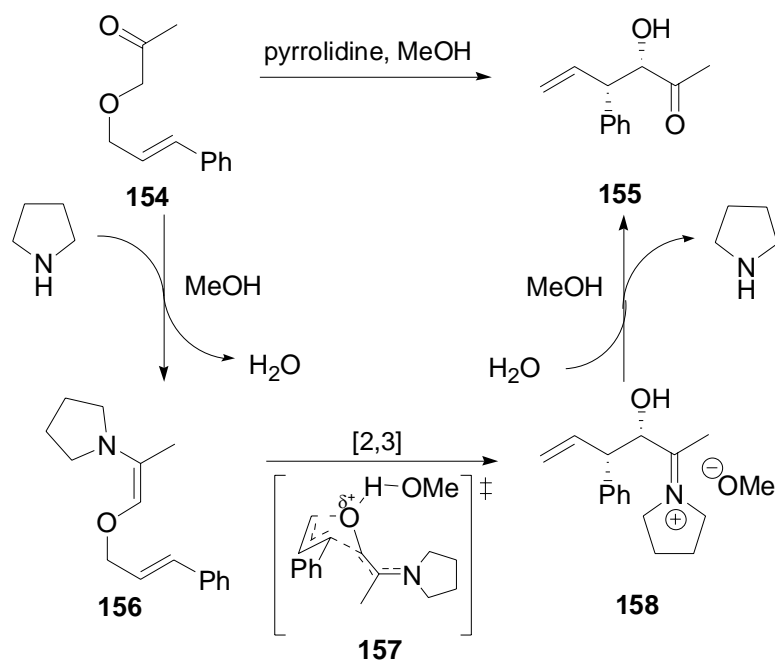
Bis(oxazoline) ligands have been used for reagent induced enantioselectivity during the rearrangement of crotyl propargyl ethers. The corresponding [2,3]-Wittig rearrangement products could be obtained in up to 89% ee (Eq. 19).¹⁰²



4.3.4 Catalyst-Induced Enantioselectivity

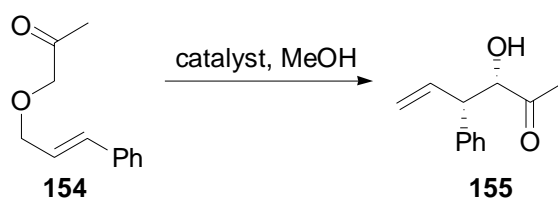
Examples of catalyzed [2,3]-Wittig rearrangements are very rare. Recently, the first organocatalytic version of the [2,3]-Wittig rearrangement has been reported.¹⁰³ Gaunt and co-workers utilized cyclic secondary amines for their approach. The catalytic activity of the amine is based on the formation of an enamine (Scheme 34).

¹⁰³ McNally, A.; Evans, B.; Gaunt, M. J. *Angew. Chem.* **2006**, *118*, 2170-2173; *Angew. Chem., Int. Ed.* **2006**, *45*, 2116-2119.



Scheme 34: Mechanism of the organo catalytic [2,3]-Wittig rearrangement: formation of an enamine initialized the reaction.

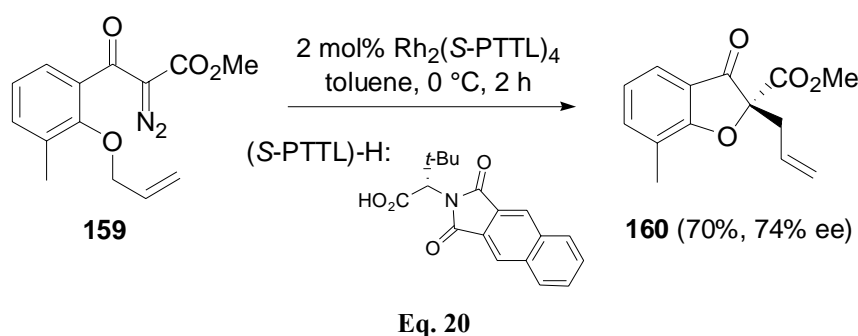
It was shown, that 5 mol% of pyrrolidine was a sufficient amount to induce the rearrangement. Low temperatures (below $-5\text{ }^{\circ}\text{C}$) were required to obtain the rearrangement product with significant diastereoselectivity (Table 6, entry 4). In a preliminary experiment the potential of a catalytic asymmetric process was investigated. When a chiral diamine was utilized, ambient temperatures were required (Table 6, entry 5). Consequently, the diastereoselectivity was only low. Nevertheless, an intriguing 60% ee could be obtained which makes this access an exciting lead for prospective developments in this field.



| Entry | Catalyst | Catalyst loading [mol%] | Temperature [$^{\circ}\text{C}$] | Reaction time [h] | <i>syn/anti</i> |
|-------|-------------|----------------------------|---------------------------------------|----------------------|-----------------|
| 1 | pyrrolidine | 20 | 23 | 0.5 | 3/1 |
| 2 | pyrrolidine | 20 | -5 | 24 | 6.5/1 |
| 3 | pyrrolidine | 20 | -25 | 90 | 10/1 |
| 4 | pyrrolidine | 5 | -5 | 96 | 8/1 |
| 5 | | 20 | 23 | 120 | 2/1 (60% ee) |

Table 6: [2,3]-Wittig rearrangement by way of enamine catalysis.

No metal catalysed variation has been reported for the [2,3]-Wittig rearrangement. Only for the charge accelerated [2,3]-sigmatropic rearrangement of ylides considerable success has been achieved and should be mentioned in this context. As it was pointed out earlier, the carbanion is formed by the reaction of a rhodium-¹⁰⁴ or copper-carbene¹⁰⁵ with the oxygen of an allyl ether. If chiral ligands are used to form the catalyst complex, catalytic asymmetric variations could be realized.¹⁰⁶ Doyle *et al.* reported remarkable enantioselectivities up to 98% ee for an intermolecular reaction, although yields were low (about 30%).¹⁰⁷ In contrast, an intramolecular reaction provided the resulting cyclic ethers with good yields but moderate enantioselectivities (Eq. 20).



4.4 Ester Enolate [2,3]-Wittig Rearrangement

In the 1980ies different research groups reported successful ester enolate [2,3]-Wittig rearrangements. The formation of the carbanion is facilitated by the presence of the carbonyl group. However, since the carbanion is highly stabilized, it exhibited only limited reactivity. Increased reaction rates at low temperatures were realized by the addition of the co-solvent HMPA.¹⁰⁸ Without the co-solvent, reaction temperatures of 0 °C were required.¹⁰⁹ In a different approach the lithium enolate is transformed into a zirconium enolate prior to the rearrangement. The transmetalation facilitated the subsequent rearrangement (Eq. 21).¹¹⁰ The unusual formation of the *Z*-configured double bond is the result of a chelated transition state

¹⁰⁴ Kitagaki, S.; Yanamoto, Y.; Tsutsui, H.; Anada, M.; Nakajima, M.; Hashimoto, S. *Tetrahedron Lett.* **2001**, *42*, 6361-6364.

¹⁰⁵ Clark, J. S.; Fretwell, M.; Whitlock, G. A.; Burns, C. J.; Fox, D. N. A. *Tetrahedron Lett.* **1998**, *39*, 97-100.

¹⁰⁶ For reviews, see: (a) Li, A.-H.; Dai, L.-X.; Aggarwal, V. K. *Chem. Rev.* **1997**, *97*, 2341-2372. (b) Hodgson, D. M.; Pierard, F. Y. T. M.; Stuppel, P. A. *Chem. Soc. Rev.* **2001**, *30*, 50-61.

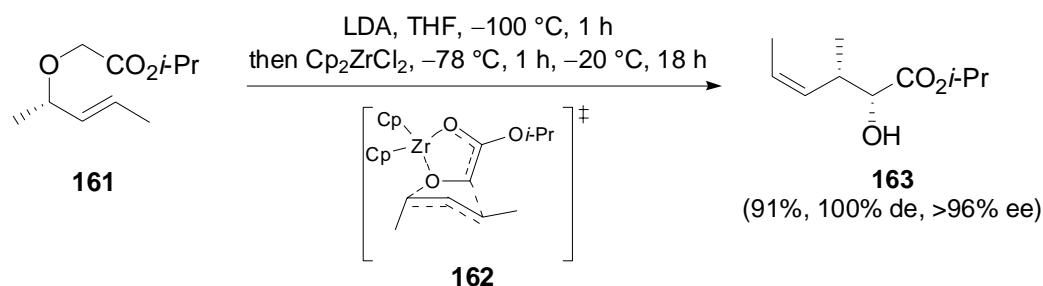
¹⁰⁷ Doyle, M. P.; Forbes, D. C.; Vasbinder, M. M.; Peterson, C. S. *J. Am. Chem. Soc.* **1998**, *120*, 7653-7654.

¹⁰⁸ Takahashi, O.; Saka, T.; Mikami, K.; Nakai, T. *Chem. Lett.* **1986**, 1599-1602.

¹⁰⁹ Raucher, S.; Gustavson, L. M. *Tetrahedron Lett.* **1986**, *27*, 1557-1560.

¹¹⁰ Uchikawa, M.; Katsuki, T.; Yamaguchi, M. *Tetrahedron Lett.* **1986**, *27*, 4581-4582.

and the steric demanding cyclopentadienyl ligands. Noteworthy is the excellent diastereoselectivity as well as the high degree of chirality transfer.



Eq. 21 LDA= lithium diisopropylamide, Cp= cyclopentadienyl.

In the following years, numerous examples of the ester enolate [2,3]-Wittig rearrangement have been reported and are covered by comprehensive review articles.⁶⁶ Powerful asymmetric versions involve chirality transfer¹¹¹ and auxiliary induced diastereoselectivity.¹¹²

4.5 Ester Dienolate [2,3]-Wittig Rearrangement

The first example of an ester *dienolate* [2,3]-Wittig rearrangement was reported in 1999.^{59a,113} In this version the easy and regioselective formation of the carbanion was combined with the higher reactivity of bisallyl ethers. No donor solvent or metal salt addition was required to trigger the rearrangement. Quantum chemical calculations revealed a smaller energy gap between the HOMO and the LUMO of the ester dienolate compared to the HOMO-LUMO gap of the corresponding ester enolate.^{59b} This finding may be accounted for the observed higher reactivities of the ester dienolates. The rearrangement of *Z*-configured substrate **164** afforded the rearrangement product *anti*-**165** with high diastereoselectivity (Eq. 22).¹¹⁴ In contrast but not unexpected, the auxiliary induced diastereoselectivity was rather low.¹¹⁵

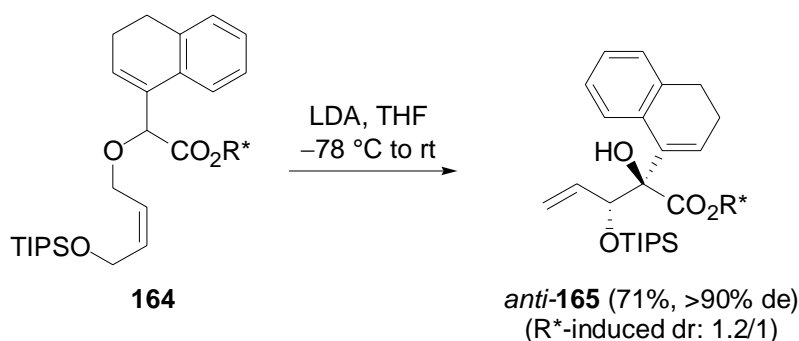
¹¹¹ For a successful application in target oriented synthesis, see: Mulzer, J.; Riether, D. *Org. Lett.* **2000**, *2*, 3139-3141.

¹¹² An example for the auxiliary induced diastereoselectivity was given in Eq. 17.

¹¹³ For examples of conceptual different dienolate [2,3]-Wittig rearrangements, see: (a) Li, Y.-J.; Lee, P.-T.; Yang, C.-M.; Chang, Y.-K.; Weng, Y.-C.; Liu, Y.-H. *Tetrahedron Lett.* **2004**, *45*, 1865-1868. (b) Pevet, I.; Meyer, C.; Cossy, J. *Tetrahedron Lett.* **2001**, *42*, 5215-5218.

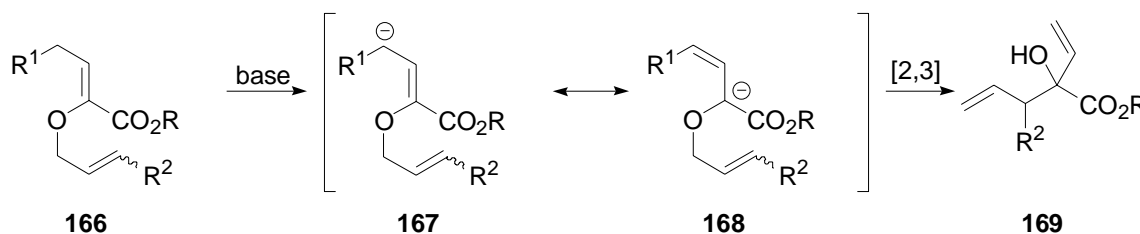
¹¹⁴ The terms *syn* and *anti* refer to the projection of the product as substituted pentenoic acid as depicted in Eq. 22. This representation is used throughout chapter 4.5. In the following sections and in accordance to the projected total synthesis of viridifungins **1**, the structure that is formed by the [2,3]-Wittig rearrangement and that mirrors a central element of the viridifungins **1** will be represented as a 1,5-diene backbone. The preferred *anti*-configuration was confirmed by 2D-NMR experiments of a lactone derivative (formed by a one-pot desilylation/lactonization sequence of the rearrangement product).

¹¹⁵ In the following example 'de' reflects the result of the simple (*syn/anti*) diastereoselectivity.



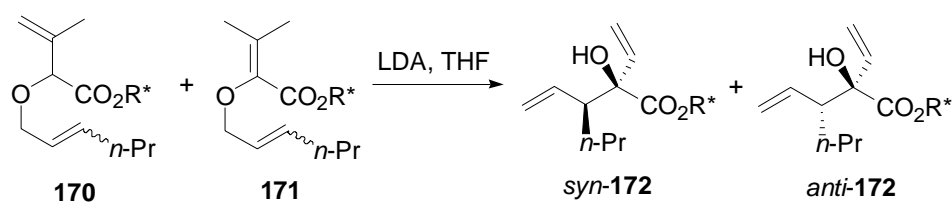
Eq. 22: HOR* = (-)-menthol, TIPS = triisopropylsilyl [Si(*i*-Pr)₃], LDA = lithium diisopropylamide.

Furthermore, it was shown, that α,β -unsaturated esters possessing γ -protons can undergo the ester dienolate [2,3]-Wittig rearrangement. Formation of the α -carbanion can be rationalized by the resonance concept (Scheme 35).



Scheme 35: 2-alkoxycarbonyl substitute AVEs as substrates for ester dienolate [2,3]-Wittig rearrangements.

Subsequently, results were published that confirmed the previously reported stereochemical rule [(*E*) to *syn* and (*Z*) to *anti*]⁶⁶ directed by the allyl double bond configuration.^{59b,116}



| Entry | Substrate | Reaction conditions | Yield [%] | <i>syn/anti</i> |
|-------|--------------------------------|--------------------------------|-----------|-----------------|
| 1 | (<i>E</i>)- 170/171 - | -78 °C, 12 h | 90 | 93/7 |
| 2 | (<i>Z</i>)- 170/171 | -78 °C, 10 min, then 0 °C, 1 h | 78 | 6/94 |

Table 7: ‘[(*E*) to *syn* and (*Z*) to *anti*]’ selectivity observed for the rearrangement of **170/171**. HOR* = (-)-menthol, LDA = lithium diisopropylamide.

¹¹⁶ Hiersemann, M. *Synlett* **2000**, 415-417.

Small changes in the substitution pattern can have a strong influence both for the diastereoselectivity and the reactivity (Table 8).^{59c}

| Entry | R ¹ | R ² | R ³ | Yield [%] | <i>syn/anti</i> |
|-------|----------------|----------------|-----------------|-----------|-----------------|
| 1 | H | H | (<i>E</i>)-Et | 90 | 91/9 |
| 2 | H | H | (<i>Z</i>)-Et | 92 | 14/86 |
| 3 | H | Me | (<i>Z</i>)-Et | 83 | 5/95 |
| 4 | Ph | H | (<i>E</i>)-Et | 91 | 79/21 |
| 5 | Me | H | (<i>E</i>)-Et | 40 | 92/8 |
| 6 | OBn | H | (<i>E</i>)-Et | 20-50 | 80/20 |
| 7 | OTPS | H | (<i>E</i>)-Et | n.r. | - |
| 8 | H | H | OBn | 65 | 72/28 |
| 9 | H | H | OTPS | 81 | >95/5 |

Table 8: Dependency of the stereochemical result and the reactivity from the substituents present on the substrate. LDA= lithium diisopropylamide.

Substrates **173/174** containing a *Z*-configured allylic ether double bond rearranged with lower diastereoselectivity than the corresponding *E*-configured substrates (Table 8, entry 1 and 2). However, if a methyl group was introduced at C2 improved diastereoselectivities were observed (Table 8, entry 3). If a R¹-substituent other than hydrogen was used, reduced diastereoselectivities were observed in most cases (Table 8, entry 5-7). Noteworthy is the reduced reactivity observed for those cases. Entry 8 and 9 impressively show how the change of the nature of the protecting group can have a strong effect on the diastereoselectivity.

A qualitative model was developed to explain the stereochemical course of the ester dienolate [2,3]-Wittig rearrangement.⁵⁹ Based on a favourable formation of a chelate, it is conceivable to assume the formation of a *Z*-configured enolate **176** (Figure 8).

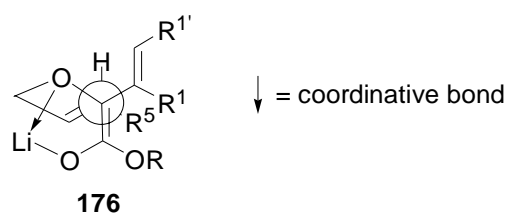


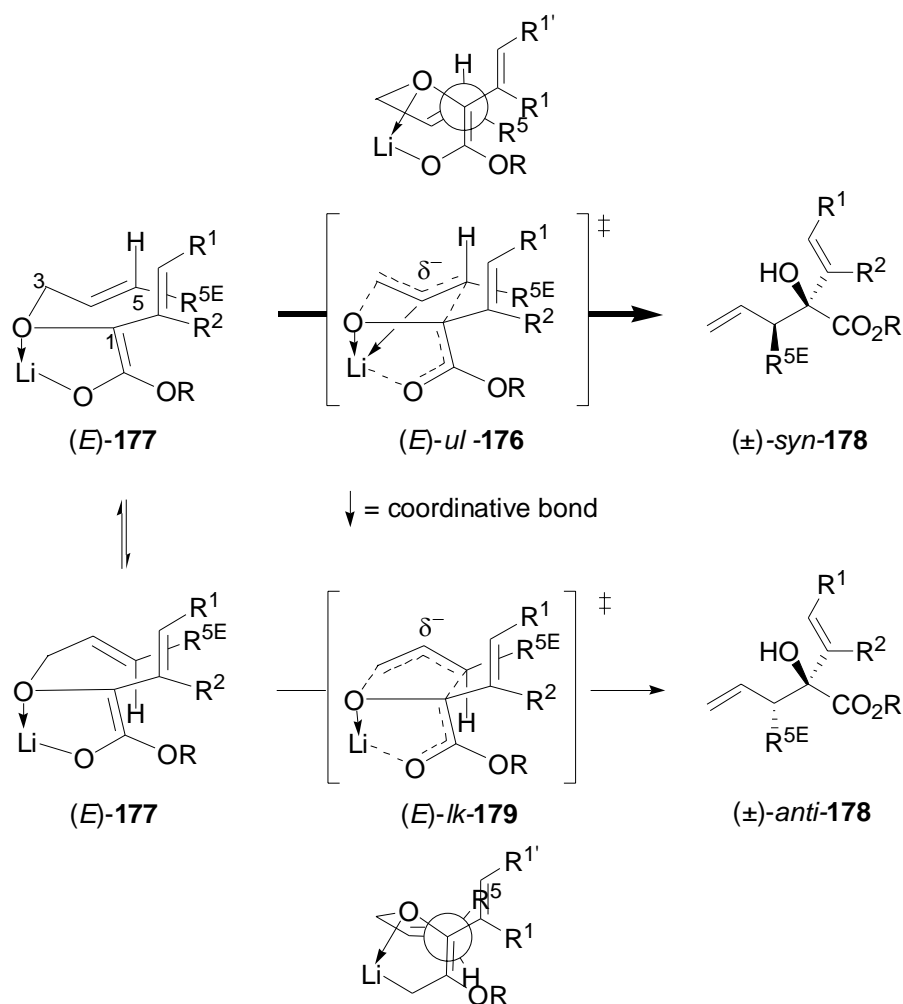
Figure 8: Preferred formation of a *Z*-configured enolate **176** as a result of favourable chelate formation.

For the rearrangement of each of the dienolates (*E*)-**177** and (*Z*)-**177** two different transition states (*E*)- or (*Z*)-*ul* (**176** and **181**) and (*E*)- or (*Z*)-*lk* (**179** and **180**) may be postulated (Scheme 36 and Scheme 37).¹¹⁷

Considering (*E*)-**177** as starting material, the *E*-configured double bond should result in a less dominant 1,3-allylic strain. As well, the 1,2-allylic strain is expected to be rather small for each of the possible transition states (*E*)-*ul*-**176** and (*E*)-*lk*-**179**. Consequently 1,2-relations along the newly formed bond have to be considered. The transition state **179** is destabilized by steric interactions between the substituents on C1 and C5 with pseudo-*eclipsed* arrangement and a pseudo-transannular-diaxial interaction between the H-atom on C5 and the ester enolate unit. The pseudo-*gauche* arrangement of the C1 and C5 substituent in **176** should be more favourable. Furthermore, the partial negative charge at the center of the allyl fragment might be stabilized by an attractive interaction with the lithium cation.¹¹⁸ Due to the smaller distance between lithium cation and the allyl ether moiety, this stabilizing interaction should be significantly higher for **176**. Therefore, rearrangement of (*E*)-**177** preferentially gives (\pm)-*syn* **178** (Scheme 36).

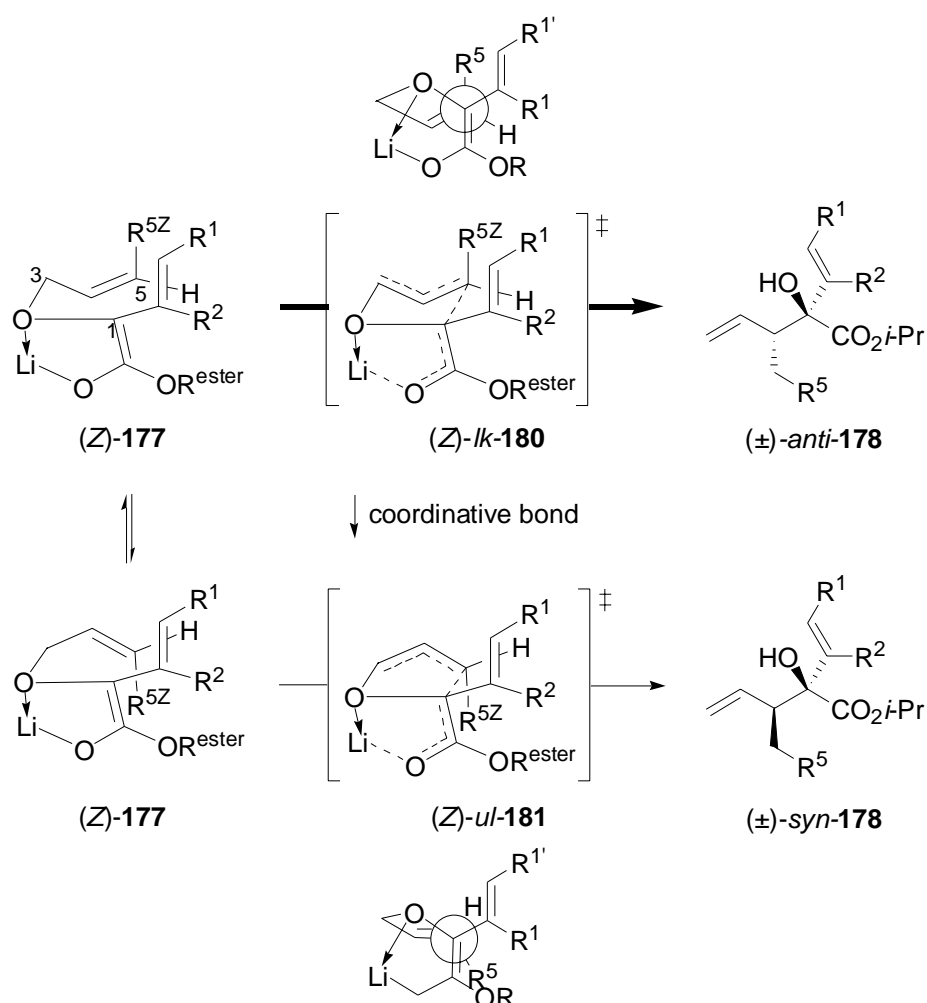
¹¹⁷ For a detailed discussion of the *lk/ul* descriptors, see: Seebach, D.; Prelog, V. *Angew. Chem.* **1982**, *94*, 696-702; *Angew. Chem., Int. Ed. Eng.* **1982**, *21*, 654-660.

¹¹⁸ (a) Okajima, T.; Fukuzawa, Y. *Chem. Lett.* **1997**, 81-82. (b) Mikami, K.; Uchida, T.; Hirano, T.; Wu, Y.; Houk, K. N. *Tetrahedron* **1994**, *50*, 5917-5926.



Scheme 36: Proposed qualitative transition state model for the ester dienolate [2,3]-Wittig rearrangement of (*E*)-**177**. *ul* = unlike *lk* = like

Analogue to the arguments outlined in the preceding paragraph, the rearrangement of (*Z*)-**177** should proceed through the transition state (*Z*)-*lk*-**180** rather than through (*Z*)-*ul*-**181** giving (*±*)-*anti*-**178** as major product (Scheme 37). However, (*Z*)-*lk*-**180** suffers from a stronger 1,3-allylic strain between R^{5Z} and the substituents at C3. This can result in decreased diastereoselectivities (Table 8, entry 1 and 2).



Scheme 37: The [2,3]-Wittig rearrangement of ester dienolates with *Z*-configured double bond preferentially gave *anti*-products.

Having discussed the theoretical background of the ester dienolate [2,3]-Wittig rearrangement, the following chapter will cover the results of the realized total synthesis of the triesters of viridifungin A, A₂ and A₄ as well as the non-natural diastereomers thereof. The underlying synthetic plan was outlined previously and – if required – the interested reader is kindly referred to chapter 3 (page 27) to recapitulate the intended strategy.

5 Synthesis of the Eastern Half

For the attempted total synthesis of the viridifungins A, A₂ and A₄ three different sulfones **68a-c** were required (Table 9).

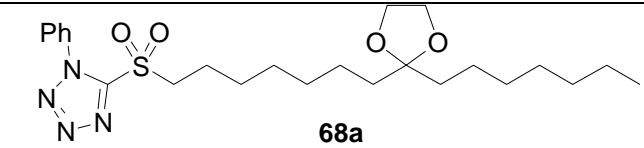
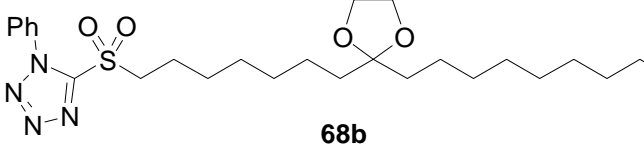
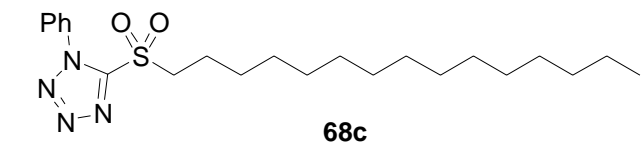
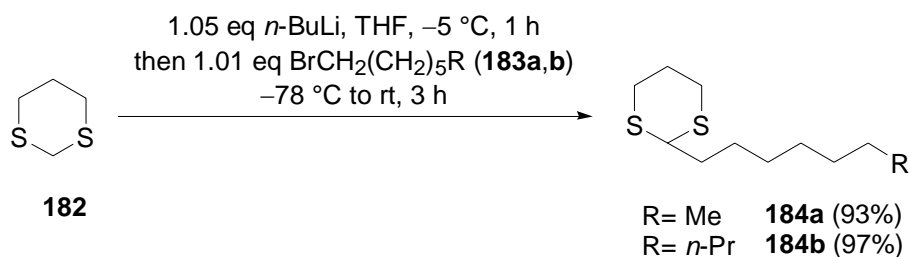
| Viridifungin | Required sulfone = eastern half |
|----------------|---|
| A |  <p style="text-align: center;">68a</p> |
| A ₄ |  <p style="text-align: center;">68b</p> |
| A ₂ |  <p style="text-align: center;">68c</p> |

Table 9

Pentadecanol (**70c**), the starting material for the formation of **68c**, is commercially available. For sulfone **68a** and **68b** the required alcohols may be generated by sequential alkylation of 1,3-dithiane (**182**) and subsequent cleavage of the thioketale.

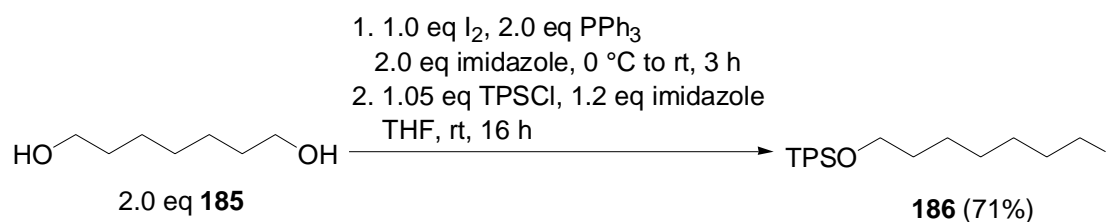
In the first alkylation step 1,3-dithiane (**182**) was subjected to *n*-BuLi and 1-bromoheptane (**183a**) or 1-bromononane (**183b**) respectively (Scheme 38).¹¹⁹



Scheme 38

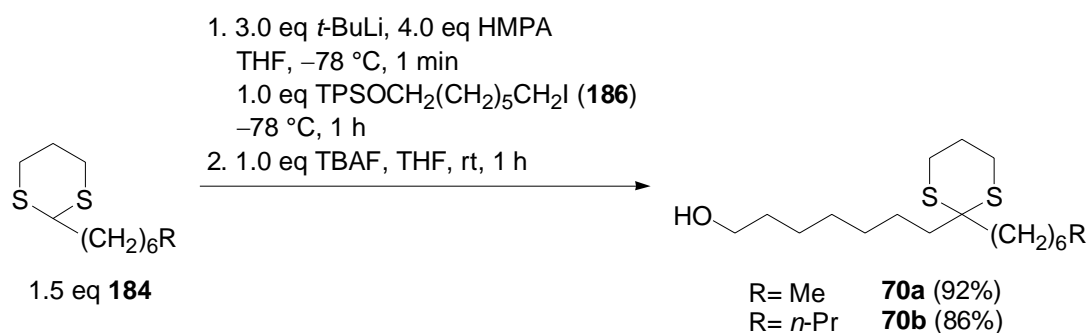
Iodide **186**, required for the second alkylation step was obtained in two steps. After functional group exchange the free hydroxyl group was protected as silyl ether¹²⁰ (Scheme 39).

¹¹⁹ (a) Corey, E. J.; Seebach, D. *Angew. Chem.* **1965**, *77*, 1134-1135; *Angew. Chem., Int. Ed. Engl.* **1965**, *4*, 1077-1078. (b) Seebach, D.; Corey, E. J. *J. Org. Chem.* **1975**, *40*, 231-237.



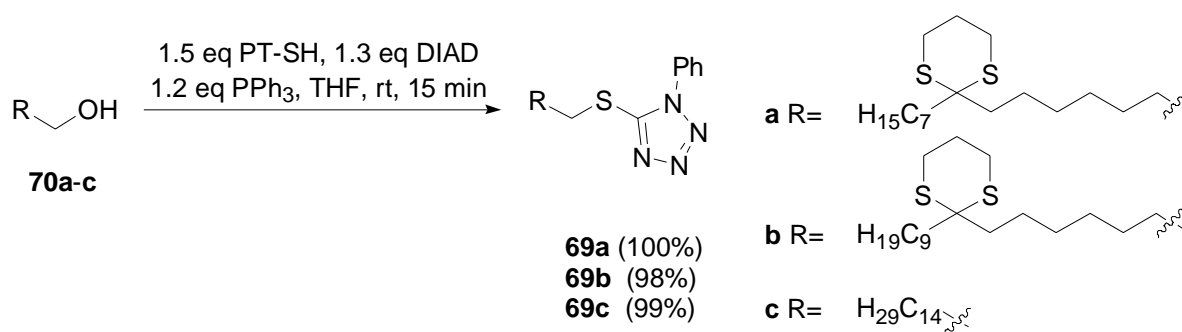
Scheme 39 TPS= *tert*-butyldiphenylsilyl [Si(*t*-Bu)Ph₂].

For the second alkylation step a stronger base was required.¹²¹ Thus, **184a,b** were treated with *t*-BuLi to generate the carbanion that in turn was alkylated by the iodide **186**. Since we were unable to purify the reaction product after this step, the crude material was deprotected using TBAF. Deprotected alcohols **70a,b** were easily separable from excess of **184** by flash chromatography (Scheme 40).



Scheme 40 TPS= *tert*-butyldiphenylsilyl [Si(*t*-Bu)Ph₂], TBAF= tetrabutyl ammonium fluoride [(*n*-Bu)₄NF], HMPA= hexamethylphosphoramide {(CH₃)₂N₂PO}.

Alcohols **70a-c** were converted into the 5-alkylsulfanyl-1-phenyl-1*H*-tetrazole derivatives **69a-c**. Again, a Mitsunobu procedure was successfully employed and afforded **69a-c** in almost quantitative yield (Scheme 41).

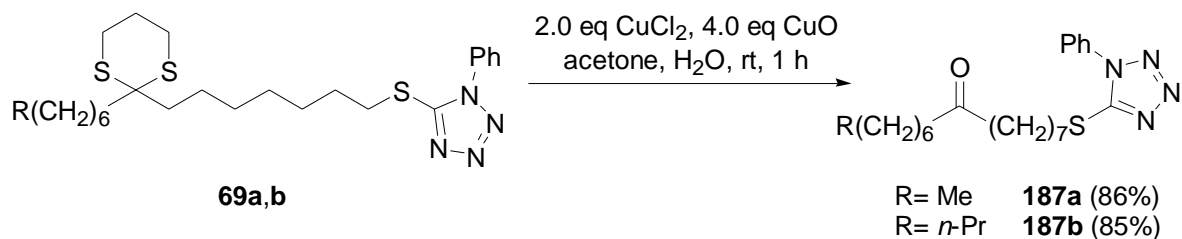


Scheme 41 PT-SH= 1-phenyl-1*H*-tetrazole-5-thiol, DIAD= diisopropyl azodicarboxylate.

¹²⁰ Hanessian, S.; Lavallee, P. *Can. J. Chem.* **1975**, *53*, 2975-2977.

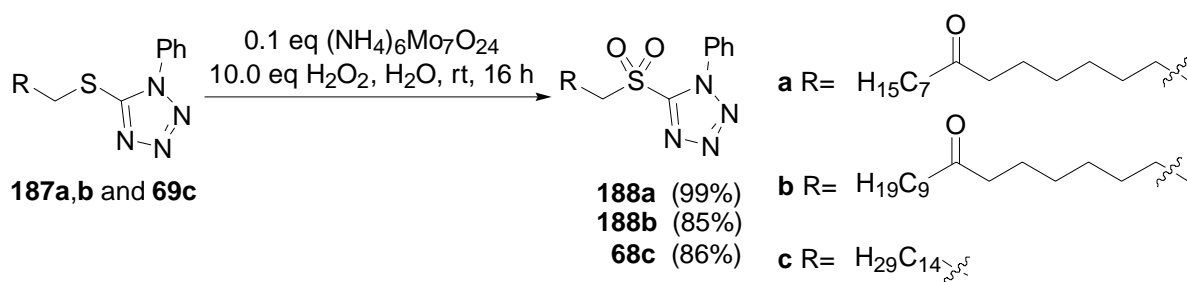
¹²¹ Williams, D. R.; Sit, S. Y. *J. Am. Chem. Soc.* **1984**, *106*, 2949-2954.

Since the chemoselective oxidation of the sulfide in the presence of the thioetale proved to be unsuccessful, the thioetale cleavage was performed first. Treatment of **69a,b** with Cu^{II} in water resulted in the formation of the ketones **187a,b** (Scheme 42).¹²²



Scheme 42

The following oxidation step of the sulfides **187a-c** afforded the corresponding sulfones **188a,b** and **68c** (Scheme 43).

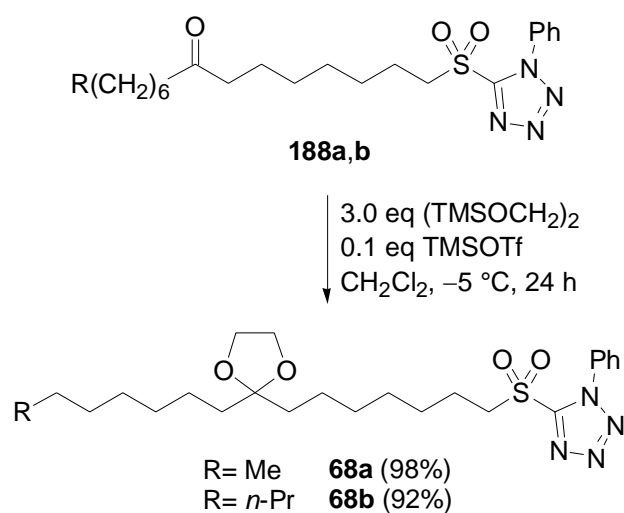


Scheme 43

Finally, the carbonyl groups of **188a,b** were converted into cyclic ketales **68a,b** (Scheme 44). We found the Noyori conditions¹²³ for the generation of the ketales **68a,b** a more reliable alternative than the conventional method of ketalization using 1,2-ethandiol under acidic conditions.

¹²² Mukaiyama, T.; Narasaka, K.; Furusato, M. *J. Am. Chem. Soc.* **1972**, *94*, 8641-8642.

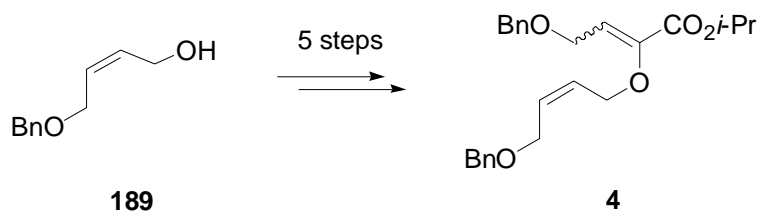
¹²³ Tsunoda, T.; Suzuki, M.; Noyori, R. *Tetrahedron Lett.* **1980**, *21*, 1357-1358.



Scheme 44 TMS= trimethylsilyl [SiMe₃], TMSOTf= trimethylsilyloxy trifluoromethane sulfonic acid [Me₃SiOSO₂CF₃].

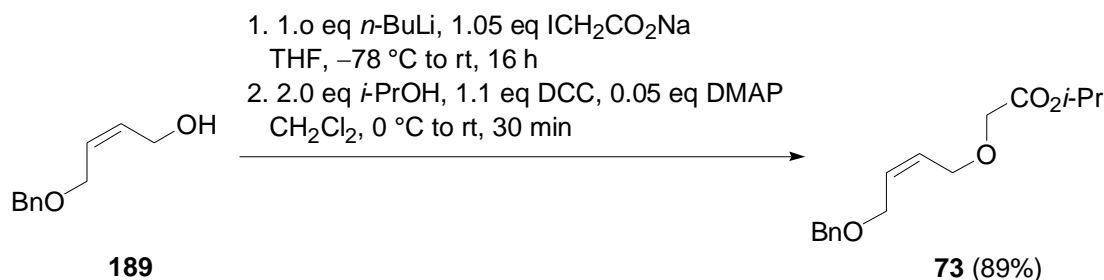
6 Synthesis of the Western Half

The synthesis of the α -allyloxy-substituted α,β -unsaturated ester **4** was realized by the well established aldol condensation strategy.⁶⁴ This convenient multigram access was routinely performed on a 10 g scale. Starting from commercially available compounds, five steps were required for the synthesis of **4** (Scheme 46).



Scheme 45

Etherification of mono-benzylated (*Z*)-2-butene-1,4-diol **189**¹²⁴ was followed by esterification with *iso*-propanol (Scheme 46).¹²⁵

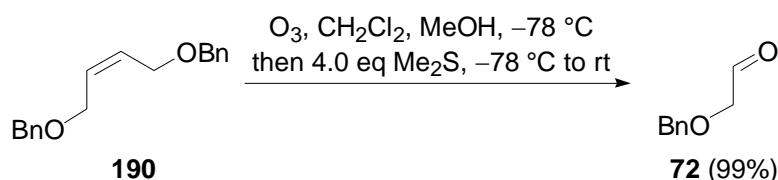


Scheme 46: DCC= dicyclohexylcarbodiimide, DMAP= *N,N*-dimethyl-4-aminopyrriidine.

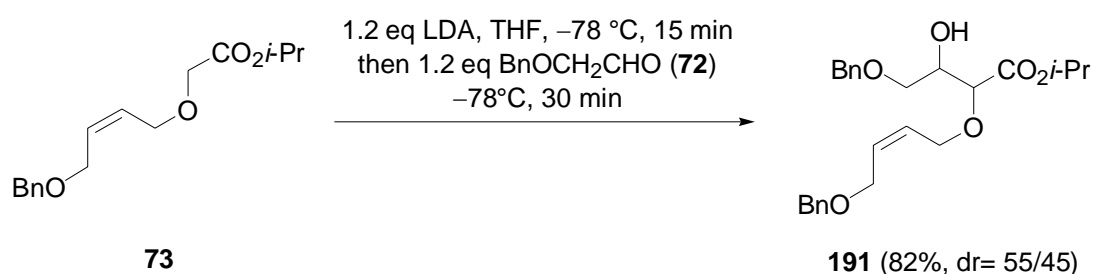
Aldol condensation of the α -allyloxy-substituted ester **73** with benzyloxy acetaldehyde **72** was employed for the generation of the vinyl ether double bond. Ozonolysis of dibenzylated (*Z*)-2-butene-1,4-diol **190** was recruited to provide the required aldehyde **72** (Eq. 23).

¹²⁴ Both mono- and dibenzylated 2-butene-1,4-diol (**189** and **190**) are commercially available from Aldrich, ACROS and others (~8 €/g and ~9 €/g respectively). Both were required for our synthesis. For economical reasons we synthesized **189** and **190** starting from (*Z*)-2-butene-1,4-diol by mono- and dibenylation. The dibenzylated side product of the monobenylation could be combined with the main product of the dibenylation and vice versa. For details. See: Experimental Section.

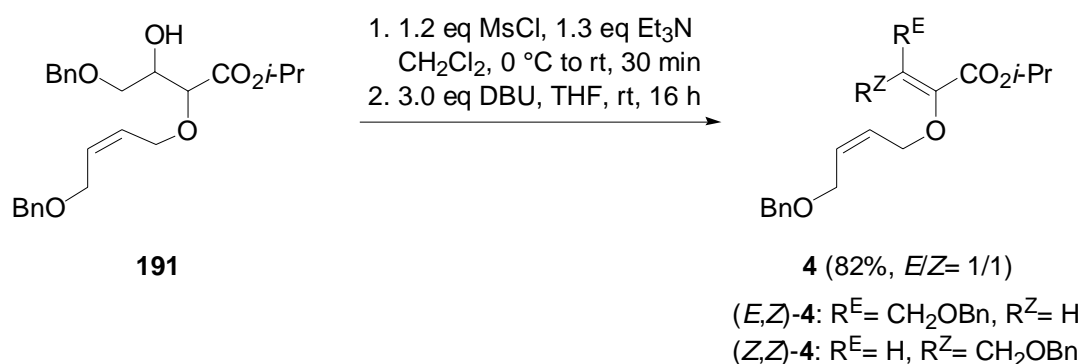
¹²⁵ Neises, B.; Steglich, W. *Angew. Chem.* **1978**, *90*, 556-557; *Angew. Chem., Int. Ed. Eng.* **1978**, *17*, 522-524.



The α -allyloxy substituted ester **73** was deprotonated with LDA and subsequently subjected to the aldehyde **72** (Eq. 24). As it was pointed out earlier, ester enolates exhibit reduced reactivity with respect to the [2,3]-Wittig rearrangement. Therefore, this competing side reaction could be efficiently prevented by keeping the reaction at low temperatures.



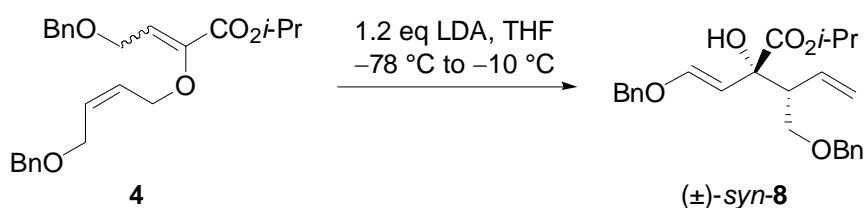
The resulting diastereomeric β -hydroxyl esters **191** were mesylated to enable DBU-mediated elimination (Scheme 47). The α -allyloxy-substituted α,β -unsaturated ester **4** was obtained as 1/1 mixture of double bond isomers (*E,Z*)- and (*Z,Z*)-**4** which may be separated by preparative HPLC or carefully performed flash chromatography.¹²⁶



With the successfully realized synthesis of **4**, the crucial [2,3]-Wittig rearrangement was performed next. It was found that slight excess of LDA in concert with THF as solvent and a

¹²⁶ For details, see: Experimental Section.

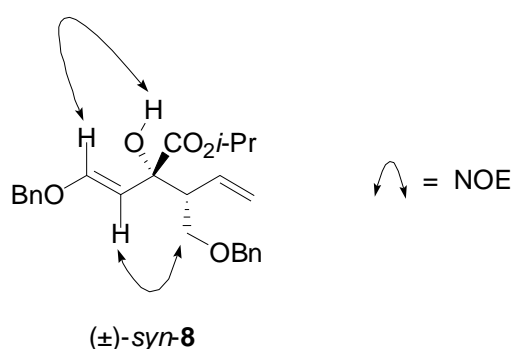
reaction temperature of $-78\text{ }^{\circ}\text{C}$ which was slowly warmed to $-10\text{ }^{\circ}\text{C}$ gave the best results for the transformation.¹²⁷ We expected that both double bond isomers should lead to the same rearrangement product (\pm)-*syn*-**8**. Indeed, *syn*-/*anti*-selectivity was found to be 95/5 or higher for both cases and afforded the desired *syn*-diastereomer (\pm)-*syn*-**8**.¹²⁸ However, (*E,Z*)-**4** exhibited considerably lower chemoselectivity than (*Z,Z*)-**4**. Low yields were isolated together with varying amounts of reisolated starting material and several unidentified side products (Table 10, entry 1). In contrast, (*Z,Z*)-**4** rearranged to the desired *syn*-product (\pm)-*syn*-**8** with acceptable yields (Table 10, entry 2).



| Entry | Substrate | Yield | <i>syn/anti</i> |
|-------|---------------------------|-------|-----------------|
| 1 | (<i>E,Z</i>)- 48 | 9 | >95/5 |
| 2 | (<i>Z,Z</i>)- 48 | 57 | 95/5 |

Table 10: Unexpected different chemoselectivities were observed for the rearrangement of (*E,Z*)-**4** and (*Z,Z*)-**4**. LDA= lithium diisopropylamide, Bn= benzyl.

The enol ether was formed with *E*-configuration exclusively. Selected NOEs are presented Scheme 48.



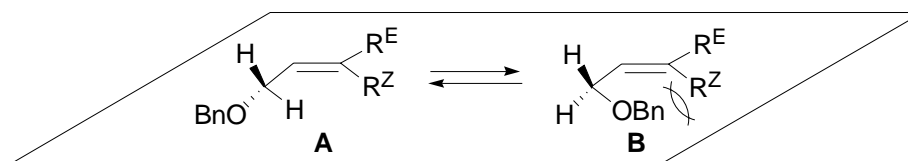
Scheme 48: Selected NOEs for (\pm)-*syn*-**8**.

¹²⁷ Different bases, solvents and temperature protocols were tested. Abraham, L., unpublished results.

¹²⁸ In accordance to the projected total synthesis and the structure element of the viridifungines that is formed by the rearrangement event we will use a 1,5-diene backbone to illustrate the rearrangement product in the following sections. Using this projection instead of the previously described pentenoic acid backbone applied in chapter 4.3-4.5 consequently resulted in a 'Z to *syn*-' instead of 'Z to *anti*-selectivity'. Even though we are aware of the inconvenience of this change that is attributed to the softness of the stereochemical descriptors we prefer this projection in this context for it results in a representation that guides the reader to the similarities between the rearrangement product and the target molecule. However, for the discussion of general trends and stereoselectivities of the [2,3]-Wittig rearrangement such a projection would not have been useful.

The exact reason(s) for the observed finding of the different chemoselectivities for (*E,Z*)-**4** and (*Z,Z*)-**4** remain speculative. We assume that the deprotonation to the ester dienolate rather than the consecutive rearrangement is influenced by the configuration of the vinyl ether double bond.^{65k} The following model is recruited to consider possible reasons for the different behaviour of the double bond isomers as well as for a reasonable explanation of the preferred formation of an *E*-configured double bond.

The vinyl ether double bond and the carbonyl group adopt a planar arrangement to allow resonance stabilization. During the transition state of the deprotonation event, the leaving proton would be oriented in right angle with respect to the plane of the present sp^2 -configured carbon atoms to allow the overlap of the p-orbital (formed by the hybridisation change from sp^3 to sp^2) with the p-orbitals of the already existing π -bonds. At the same time this allows the delocalisation of the negative charge by resonance. To minimize the 1,3-allylic strain, the benzyloxy substituent would be expected to prefer conformation **A** finally resulting in an *E*-configured enol ether rather than conformation **B** that would lead to a *Z*-configured enol ether (Scheme 49).¹²⁹



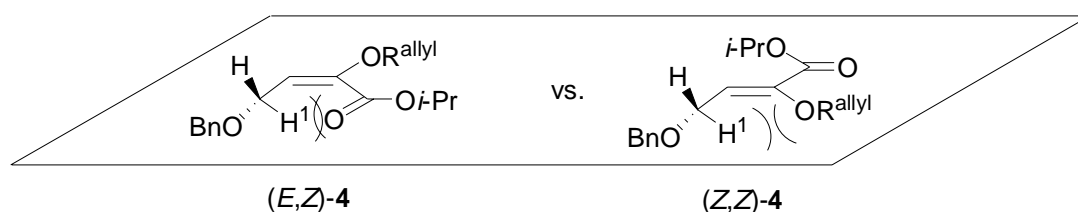
Scheme 49: Possible conformations of **4** that would lead to either *E*-configured enol ethers (**A**) or *Z*-configured enol ethers (**B**).

To rationalize the different behaviours of (*E,Z*)-**4** and (*Z,Z*)-**4**, structure **A** requires a more detailed analysis. Some features may be emphasized (Scheme 50):

- As discussed earlier, in the transition state of the deprotonation the leaving proton has to adopt a right angular out of plane orientation.
- It appears reasonable to argue that the 1,3-allylic strain between the remaining hydrogen-atom at C1'' and the allyloxy substituent of *Z*-**4** ($R^Z = OR^{\text{allyl}}$, $R^E = CO_2i\text{-Pr}$) (Scheme 50, right) would be significantly smaller than the 1,3-allylic strain between the hydrogen atom and the ester group of *E*-**4** ($R^Z = CO_2i\text{-Pr}$, $R^E = OR^{\text{allyl}}$) (Scheme 50, left). In the former case, repulsion results from the steric interaction of the hydrogen atom with the lone pairs of the sp^3 -configured ether oxygen-atom. In contrast, in the latter case, the trigonal planar sp^2 -configured carbon-atom bears two substituents (carbonyl oxygen and *Oi*-Pr). Additionally,

¹²⁹ It can not be excluded, that the preferred formation of the *E*-configured enol ether is the result of a thermodynamic equilibrium of the dienolate.

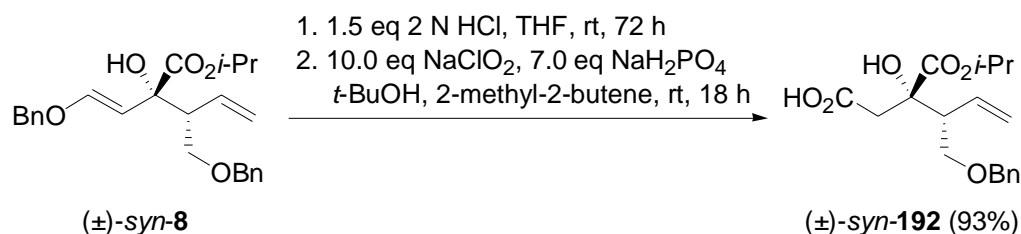
due to the possible resonance stabilization of the vinyl ether double bond and the carbonyl bond a planar arrangement is preferred what would further increase the disadvantageous 1,3-allylic strain. Therefore, the adoption of a conformation required for a successful deprotonation is more unfavourable for *E*-4 than for *Z*-4. In summary, the above reasons should increase the activation barrier for the deprotonation of (*E,Z*)-4 compared to (*Z,Z*)-4 and could therefore be accounted for the different behaviours of the double bond isomers (*E,Z*)-4 and (*Z,Z*)-4 with respect to the [2,3]-Wittig rearrangement.



Scheme 50: Rationalization of the different behaviours of (*E,Z*)-4 compared to (*Z,Z*)-4 by consideration of the 1,3-allylic strain.

However, it should be emphasized once again, that the above described model is speculative and was only employed to rationalize the observed finding. No further experiments or calculations have been undertaken to support the above assumption.

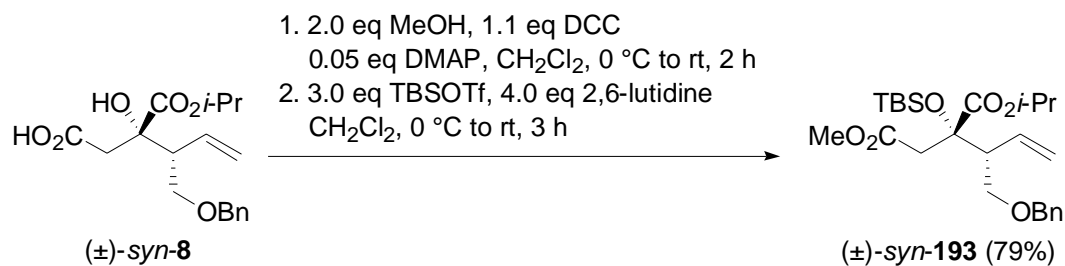
For the construction of the carboxylic group at C1 the benzyl enol ether of the rearrangement product (\pm)-*syn*-8 was cleaved under acidic conditions. The resulting aldehyde was immediately oxidized to the corresponding acid (\pm)-*syn*-192 (Scheme 51). At this step, the cleaved benzyl alcohol of the preliminary step had to be carefully removed to prevent its interference during the following esterification.¹³⁰



Scheme 51

¹³⁰ If benzylalcohol is not completely removed by flash chromatography it could form the benzyl ester under the conditions of the following esterification.

Esterification of (\pm)-*syn*-**192** was followed by protection of the tertiary alcohol as silyl ether¹³¹ using TBSOTf and 2,6-lutidine to afford (\pm)-*syn*-**193** (Scheme 52).¹³² Preparation of the western half may be completed by ozonolysis of the terminal double bond to provide the desired aldehyde (\pm)-*syn*-**67**. However, (\pm)-*syn*-**67** was found to be unstable. Consequently, it was generated prior to the following Julia-Kocienski olefination and used immediately without further purification.



Scheme 52 TBS= *tert*-butyldimethylsilyl, OTf= trifluoromethanesulfonyl, DCC= dicyclohexylcarbodiimide, DMAP= *N,N*-dimethyl-4-aminopyridine.

¹³¹ Nelson, T. D.; Crouch, R. D. *Synthesis* **1996**, 1031-1069.

¹³² Corey, E. J.; Cho, H.; Rücker, C.; Hua, D. H. *Tetrahedron Lett.* **1981**, 22, 3455-3458.

7 Synthesis of the Viridiofungin A, A₂ and A₄ Triesters

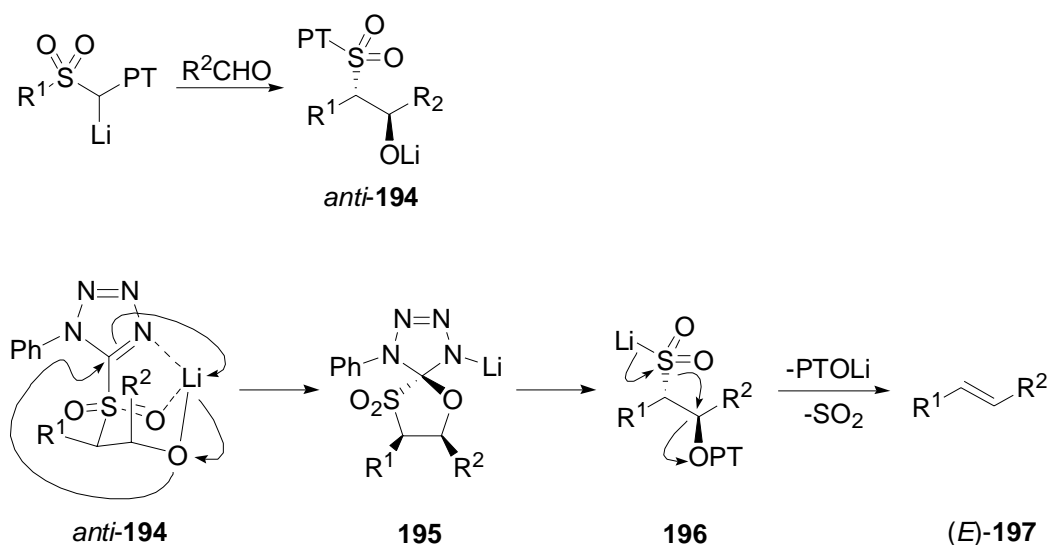
Completion of the carbon skeleton of the viridiofungins was attempted next. The polar head group and the lipophilic tail are connected by an isolated, *E*-configured double bond. Following our synthetic plan, Julia-Kocienski olefination was identified as a prospective synthetic tool for the formation of the isolated C5-C6 double bond. Kocienski's modification¹³³ of the classical Julia olefination¹³⁴ allows the transformation to be completed in one step. This attractive improvement has been frequently employed for the construction of isolated *E*-configured double bonds.¹³⁵ The preferred formation of the *E*-configuration was accounted to the kinetically controlled diastereoselective addition of the metallated alkyl 1-phenyl-1*H*-tetrazol-5-yl sulfones to the aldehyde affording *anti*- β -alkoxysulfones *anti*-**194**.¹³⁵ This inherently unstable addition product undergoes a Smiles rearrangement¹³⁶ that affects the transfer of the heterocycle from sulfur to oxygen. The rearrangement proceeds through the spirocyclic intermediate **195**. The resulting sulfinate **196** readily eliminates sulfur dioxide and lithium phenyltetrazolone. *Anti*-elimination of the two leaving groups which are in *antiperiplanar* arrangement yields the *E*-configured olefin (*E*)-**197** (Scheme 53).¹³⁵

¹³³ (a) Kocienski, P. J.; Lythgoe, B.; Ruston, S. *J. Chem. Soc., Perk. Trans. 1* **1978**, 829-834. (b) Kocienski, P. J.; Lythgoe, B.; Roberts, D. A. *J. Chem. Soc., Perk. Trans. 1* **1978**, 834-837. (c) Kocienski, P. J.; Lythgoe, B.; Waterhouse, I. *J. Chem. Soc., Perk. Trans. 1* **1980**, 1045-1050. (d) Kocienski, P. J.; Lythgoe, B.; Ruston, S. *J. Chem. Soc., Perk. Trans. 1* **1979**, 1290-1293.

¹³⁴ Julia, M.; Paris, J.-M. *Tetrahedron Lett.* **1973**, *14*, 4833-4836.

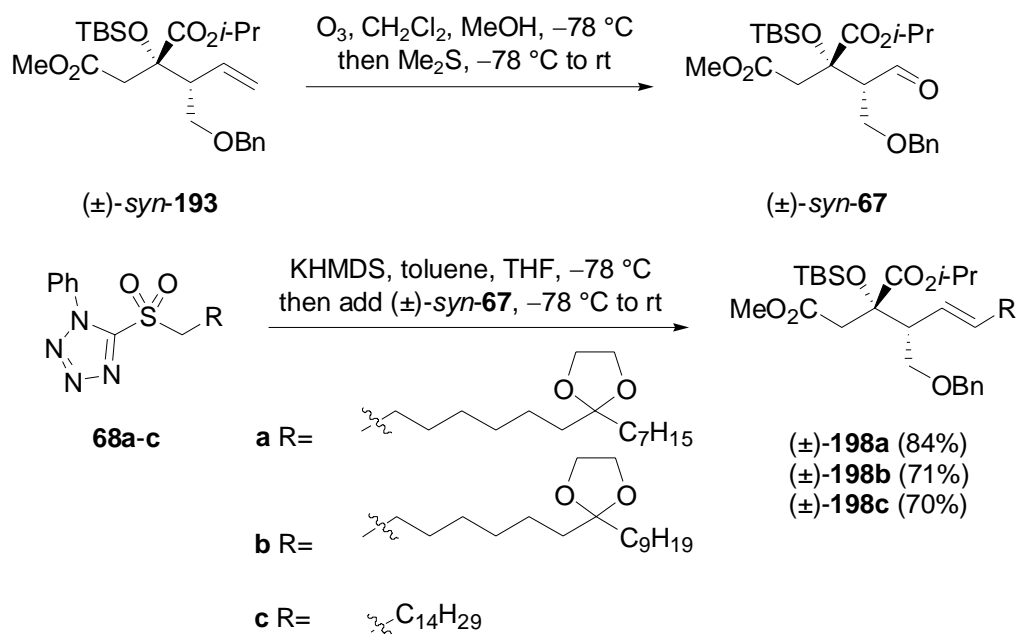
¹³⁵ For a review concerning the modified Julia-olefination, see: Blakemore, P. R. *J. Chem. Soc., Perk. Trans. 1* **2002**, 2563-2585.

¹³⁶ Levy, A. A.; Rains, H. C.; Smiles, S. *J. Chem. Soc.* **1991**, 3264-3269.



Scheme 53: Mechanism of the Julia-Kocienski olefination. Highly diastereoselective formation of *anti*-**194** during the initial addition was accounted for the overall *E*-selectivity of the olefination. PT= 1-phenyl-1*H*-tetrazol-5-yl.

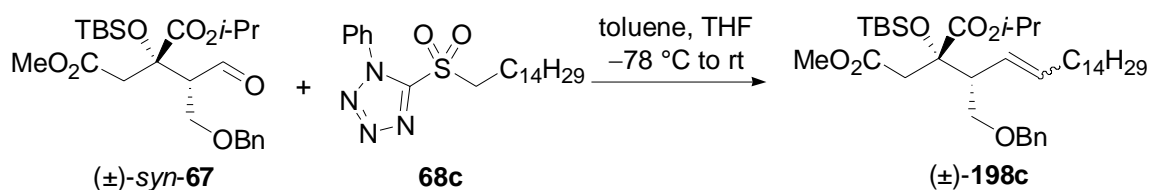
In the course of our synthetic effort, sulfones **68a-c** were treated with potassium hexamethyl disilazide (KHMDS) at $-78\text{ }^{\circ}\text{C}$ and then subjected to the aldehyde (\pm)-*syn*-**67**. (Scheme 54) The reaction afforded the corresponding coupling products (\pm)-**198a-c** as single double bond isomers.



Scheme 54: Julia-Kocienski olefination.¹³⁷ KHMDS= potassium hexamethyl disilazide [K(N(SiMe₃)₂)], TBS= *tert*-butyldimethylsilyl [Si(*t*-Bu)Me₂], Bn= benzyl.

¹³⁷ For the utilized ratios of the starting materials, see: Experimental section.

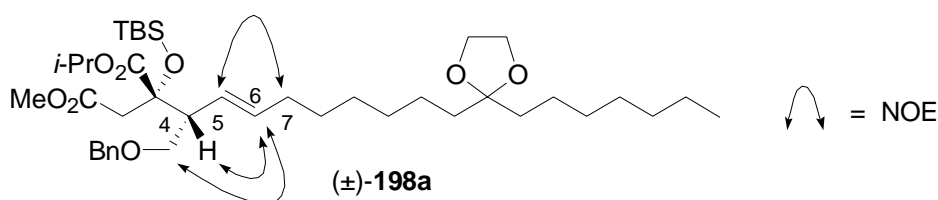
Application of LiHMDS instead of KHMDS as deprotonation agent for the Julia-Kocienski olefination led to inferior *E/Z*-selectivities (Table 11).



| Entry | Base | Yield [%] | <i>E/Z</i> |
|-------|--------|-----------|------------|
| 1 | KHMDS | 70 | >95/5 |
| 2 | LiHMDS | 47 | 2/1 |

Table 11: Utilization of LiHMDS instead of KHMDS led to inferior *E/Z*-selectivities for the Julia-Kocienski olefination. KHMDS= potassium hexamethyl disilazide, LiHMDS= lithium hexamethyl disilazide.

The exclusive formation of the *E*-configured double bond was verified for the coupling product (±)-**198a** by NOE-experiments (Table 12).

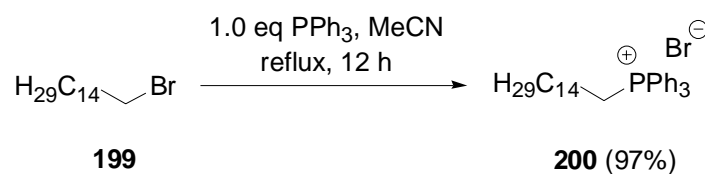


| Entry | NOE cross peaks between | Conclusion |
|-------|---|------------|
| 1 | 4-H (2.68-2.57 ppm) 6-H (5.44 ppm) | <i>5-E</i> |
| 2 | 5-H (5.24 ppm) 7-CH ₂ (1.98-1.86 ppm) | <i>5-E</i> |
| 3 | 4'-H (3.32 ppm) 6-H (5.44 ppm) | <i>5-E</i> |

Table 12: Selected NOEs for (±)-**57a**

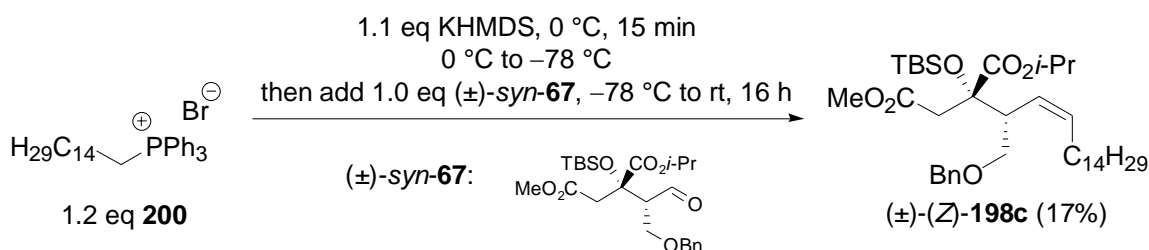
In an additional experiment, *Z*-configured double bond isomer (*Z*)-**198c** was synthesized by application of the inherently *Z*-selective Wittig olefination for the formation of the double bond. The required Wittig-salt **200** was easily accessible by the reaction of 1-bromopentadecane (**199**) with triphenylphosphine in acetonitrile (Eq. 25).¹³⁸

¹³⁸ Kumar, V.; Dev, S. *Tetrahedron* **1987**, *43*, 5933-5948.



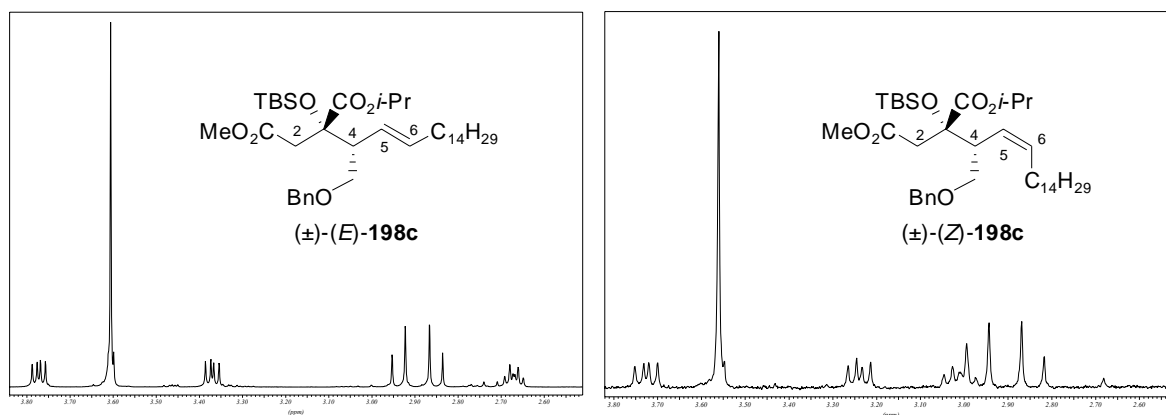
Eq. 25

Reaction of aldehyde (\pm)-*syn*-**67** with deprotonated **200** provided (\pm)-(*Z*)-**198c** in 17% non-optimized yield (Eq. 26).



Eq. 26 KHMDS= potassium hexamethyl disilazide $\text{K}[\text{Si}(\text{NMe}_3)_2]$, TBS= *tert*-butyldimethylsilyl $[\text{Si}(t\text{-Bu})\text{Me}_2]$, Bn= benzyl.

A significant downfield shift was found for 4-CH of (\pm)-(*Z*)-**198c** (Scheme 55, Table 13). Comparison of the coupling constants of the vinylic protons supported the assignment of the double bond configuration (Table 13).



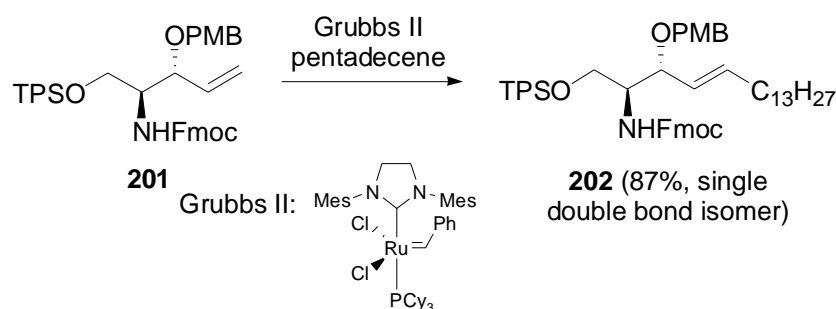
Scheme 55: Detail of the ¹H NMR spectra of (\pm)-(*E*)-**198c** and (\pm)-(*Z*)-**198c**.

| Entry | C-atom | (±)-(<i>E</i>)- 198c | | (±)-(<i>Z</i>)- 198c | |
|-------|-------------------|-------------------------------|--------------------------------------|-------------------------------|--------------------------------------|
| | | Chemical shift [ppm] | Multiplicity, coupling constant [Hz] | Chemical shift [ppm] | Multiplicity, coupling constant [Hz] |
| 1 | 5-CH= | 5.24 | dd, $J = 15.2, 9.6$ | 5.27 | dd, $J = 10.7, 10.7$ |
| 2 | 6-CH= | 5.44 | ddd, $J = 15.0, 6.5, 6.5$ | 5.45 | ddd, $J = 11.3, 7.2, 7.2$ |
| 3 | 2-CH ₂ | 2.80 | $d^{AB} = 15.3$ | 2.84 | $d^{AB} = 15.2$ |
| | | 2.89 | $d^{AB} = 15.3$ | 2.97 | $d^{AB} = 15.3$ |
| 4 | 4-CH | 2.57-2.68 | m | 2.97-3.05 | m |

Table 13: Selected ¹H NMR signals of (±)-(*E*)-**198c** and (±)-(*Z*)-**198c**.

The vinylic protons at C5 and C6 have significantly higher coupling constants for (±)-(*E*)-**198c** than for (±)-(*Z*)-**198c** (Table 13, entry 1 and 2). As it would be expected, the analytical data for the protons bond to C2 are similar for both double bond isomers (Table 13, entry 3). In contrast, the signal of the proton bound to C4 shows a significant downfield shift for (±)-(*Z*)-**198c**.

The recently published viridiofungin syntheses^{51,53} as well as the synthesis of the sphingolipide backbone¹³⁹ involved a cross-metathesis reaction as key CC-connecting reaction for the generation of the isolated double bond (Eq. 27).

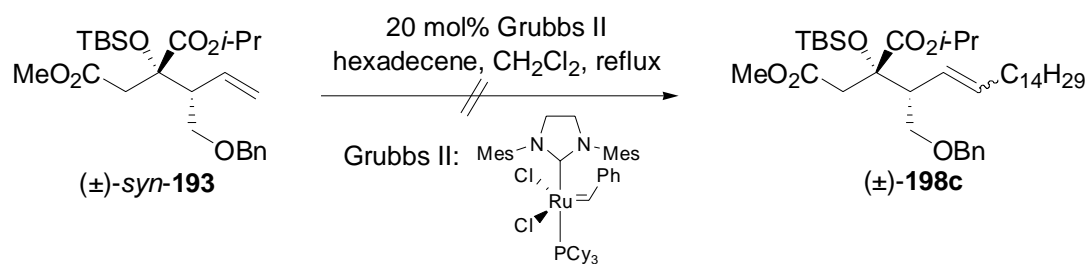


Eq. 27: Fmoc= fluoromethyloxycarbonyl, TPS= *tert*-butyldiphenylsilyl [Si(*t*-Bu)Ph₂], PMB= *p*-methoxybenzyl, Mes= mesityl.

It was tried, to employ this strategy for the installation of the *E*-configured double bond of the viridiofungins. However, reaction of (±)-*syn*-**193** with 1-hexadecen in the presence of Grubbs

¹³⁹ Rai, A. N.; Basu, A. *Org. Lett.* **2004**, *6*, 2861-2863.

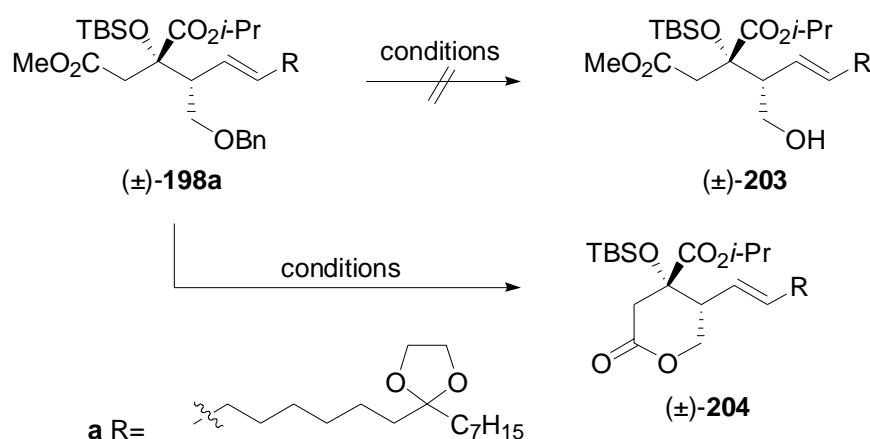
catalyst (2nd generation) resulted in the homo-coupling of 1-hexadecen and reisolation of (±)-*syn*-**193**.



Eq. 28 TBS= *tert*-butyldimethylsilyl [Si(*t*-Bu)Me₂], Bn= benzyl, Mes= mesityl.

Cross metathesis is known to be strongly dependent from the steric demand of the substituents present at the substrates. Manipulation of (±)-*syn*-**193** might render the metathesis successful. However, since the Julia-Kocienski olefination provided an reliable tool for the stereoselective formation of the C5/C6 double bond, no further experiments were performed for the cross metathesis.

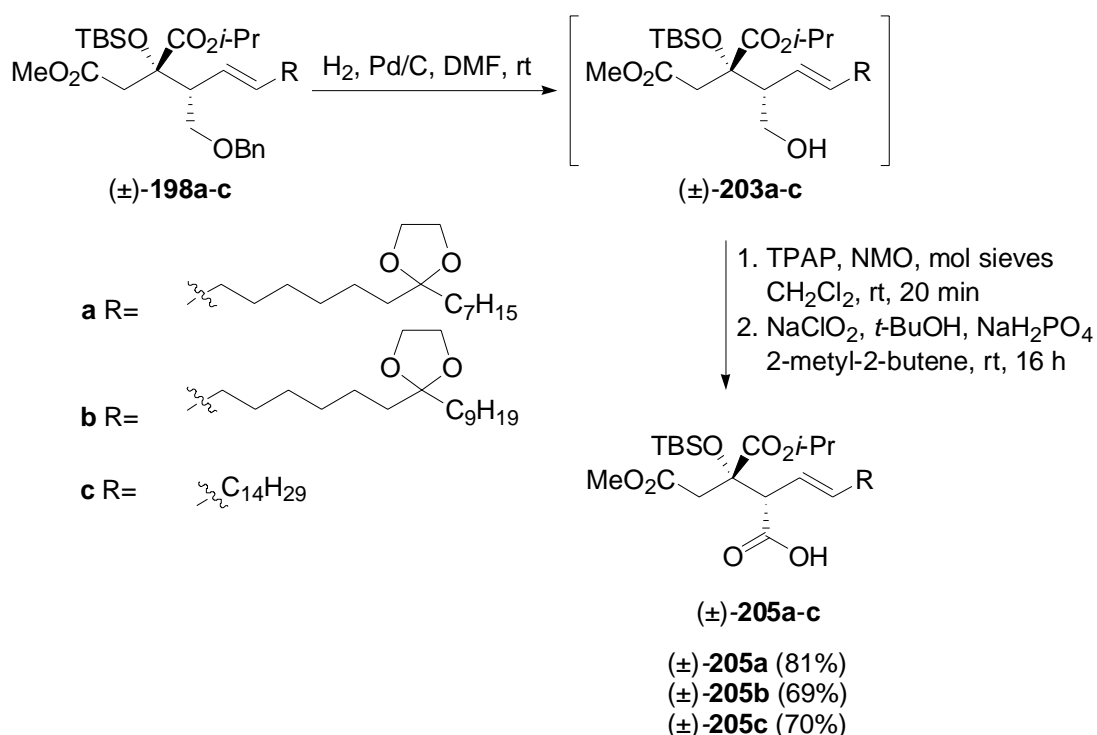
For the completion of the synthesis of the viridiofungins A, A₄ and A₂ the third carboxylic acid functionality had to be constructed starting from a protected alcohol. Standard debenzylation procedures were tested (DDQ, Li/NH₃, LiDBB, cyclohexa-1,4-diene/Pd/C).¹⁴⁰ However, formation of the lactone (±)-**204a** circumvented these methods. Any attempts of lactone cleavage failed to provide the desired deprotected alcohol (±)-**203a** (Scheme 56).¹⁴⁰



Scheme 56: Undesired lactonization has to be considered as side reaction during debenzylation of (±)-**198**. TBS= *tert*-butyldimethylsilyl [Si(*t*-Bu)Me₂], Bn= benzyl.

¹⁴⁰ Abraham, L. unpublished results.

Finally, it was found that hydrogenolysis using simply hydrogen in concert with palladium on activated carbon allowed the chemoselective debenzoylation in the presence of the isolated double bond. Careful monitoring of the reaction using TLC provided (±)-**203a-c** within a view minutes. Without further purification¹⁴¹ the primary alcohols (±)-**203a-c** were subjected to tetra-*n*-propyl-ammonium perruthenate (TPAP) and *N*-methylmorpholine *N*-oxide (NMO). The raw aldehydes were immediately oxidized to the corresponding stable acids (±)-**205a-c** (Scheme 57).

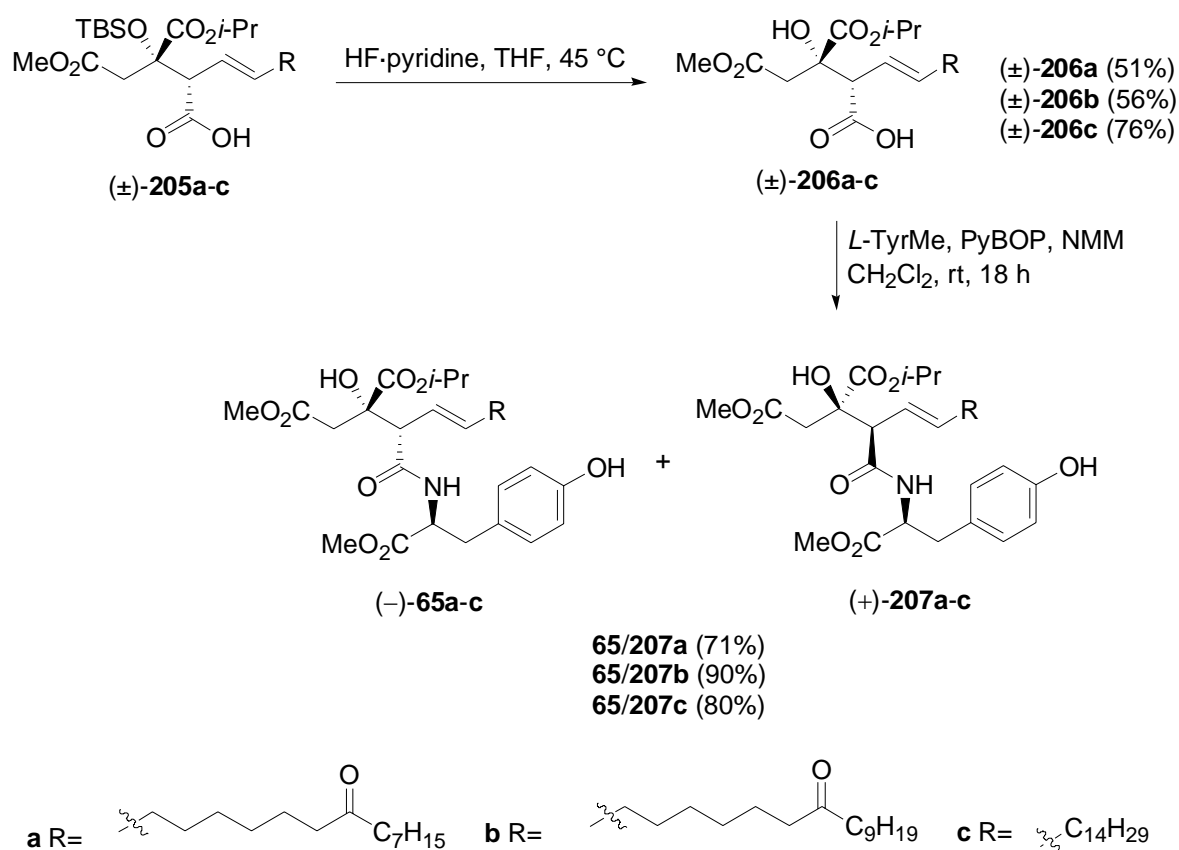


Scheme 57: Formation of the acids (±)-**205a-c** by deprotection and sequential oxidation. TBS= *tert*-butyldimethylsilyl [Si(*t*-Bu)Me₂], Bn= benzyl, TPAP= tetra-*n*-propylammoniumperruthenate, NMO= *N*-methylmorpholine *N*-oxide.

Utilization of HF·pyridine for the deprotonation of the tertiary alcohol cleaved the ketal protection groups as well. The deprotected acids (±)-**206a-c** were then subjected to several peptide coupling reagents and conditions.¹⁴² Benzotriazolylxytris(pyrrolidino)phosphonium hexafluorophosphate (PyBOP) in concert with *N*-methylmorpholine (NMM) was identified to provide the most convenient reaction conditions for the coupling of racemic acids (±)-**206a-c** with enantiomerically pure, commercially available *S*-tyrosine methyl ester (*S*-TyrMe) (Scheme 58).

¹⁴¹ Attempts to purify the alcohol (±)-**203** led to the lactonization product (±)-**204**.

¹⁴² Abraham, L. unpublished results. For a review concerning peptide coupling reagent, see: Han, S.-Y.; Kim, Y.-A. *Tetrahedron* **2004**, *60*, 2447-2467.



Scheme 58: TBS= *tert*-butyldimethylsilyl [Si(*t*-Bu)Me₂], *S*-TyrMe= *S*-tyrosine methyl ester, PyBOP= Benzotriazoloyloxytris(pyrrolidino)phosphonium hexafluorophosphate, NMM= *N*-methylmorpholine.

The resulting mixtures of viridiofungin A, A₄ and A₂ triester diastereomers **65/207a-c** could be separated by reversed phase HPLC. Figure 9 - Figure 11 show the chromatograms of the separation of the viridiofungin triester **65/207a-c** by analytical HPLC.

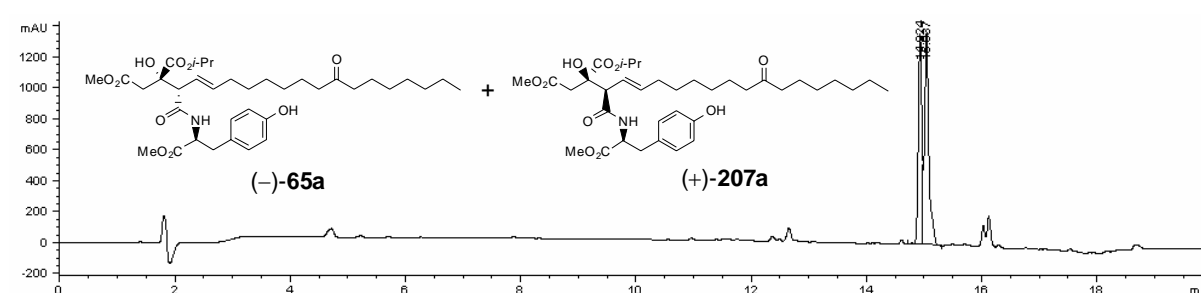


Figure 9: Chromatogram for the separation of **65a/207a** by analytical HPLC (reversed phase) isocratic A/B = 60/40 (R_t (-)-**65a**: 14.9 min, R_t (+)-**207a**: 15.0 min).¹⁴³

¹⁴³ Analytical HPLC (reversed Phase): Column: ECLIPSE XDB-C8, 4.6 × 150 mm, 5 μm; Eluent: isocratic A/B (solvent A: H₂O + 0.1 % TFA, solvent B: CH₃CN + 0.1 % TFA, 1 ml/min).

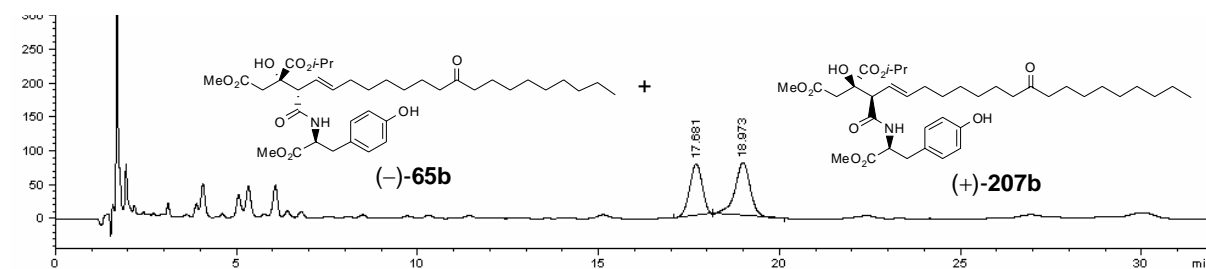


Figure 10: Chromatogram for the separation of **65b/207b** by analytical HPLC (reversed phase) isocratic A/B = 60/40 (R_t (-)-**65b**: 17.7 min, R_t (+)-**207b**: 19.0 min).¹⁴³

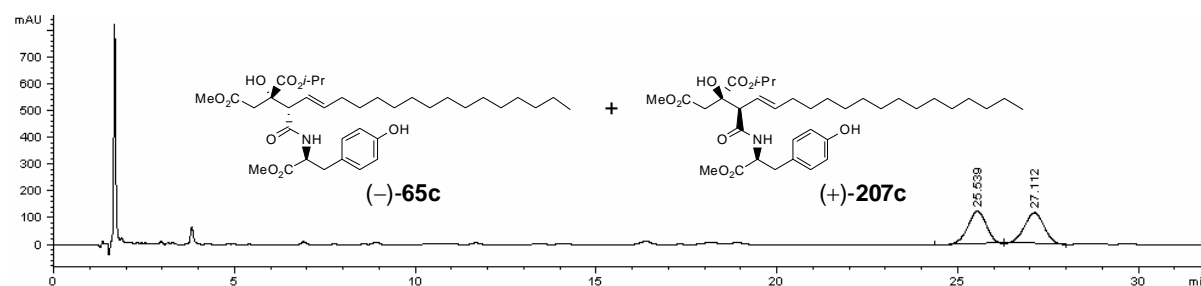


Figure 11: Chromatogram for the separation of **65c/207c** by analytical HPLC (reversed phase) isocratic A/B = 71/29. (R_t (-)-**65c**: 25.6 min, R_t (+)-**207c**: 27.1 min).¹⁴³

Application of the optimized conditions for the preparative HPLC afforded the triesters of natural (-)-viridiofungin A (**65a**), (-)-A₄ (**65b**) and (-)-A₂ (**65c**) as well as the nonnatural diastereomers thereof ((+)-**207a-c**).¹⁴⁴ The assignment of (-)-**65a** as the diastereomer with the natural configuration was based on the comparison with reported data of synthetic Me₃-**1a** and (*t*-Bu)₃-**1a**.¹⁴⁵ The configuration of viridiofungin A₂ and A₄ was assigned in analogy to the known configuration of viridiofungin A. Since we expect the chemical and physical properties of the natural products being closely related we propose **65b,c** as the diastereomers with the absolute configuration of the natural diastereomers even though no analytical data are available that would allow verification by comparison.

¹⁴⁴ Diastereomeric ratio >9:1 concluded from 500 MHz ¹H NMR of the separated diastereomers.

¹⁴⁵ For a detailed justification of the assigned constitution and configuration, see chapter 8.

8 Verification of the Proposed Structure of Viridiofungin A Triester (–)-65a

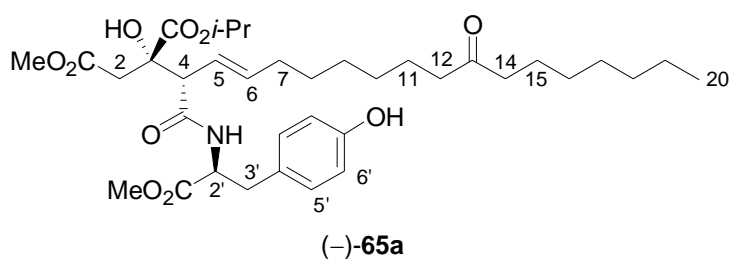
The diastereomer (–)-**65a** which exhibits the configuration of the natural product VF_A is chosen for the approval of the proposed structure. The IR-spectrum of (–)-**65a** includes the following characteristic signals: peaks at 1742 and 1715 cm⁻¹ indicate the presence of at least two ester carbonyl groups while the low carbonyl band at 1642 cm⁻¹ indicates the presence of an amide. Several additional signals between 2859 and 2932 cm⁻¹ show the presence of aliphatic CH-bond vibrations. A broad peak at 3372 cm⁻¹ indicates the presence of a hydroxyl group.

Analysis of the ¹³C NMR spectrum of (–)-**65a** shows signals of non-hydrogen-substituted carbon atoms of carbonyl groups at 213.4, 172.2, 171.6, 170.6, and 170.5 ppm. The significant downfield shift of the first of these five signals indicates the presence of a ketone, while the latter signals may result from ester or amide group carbonyl carbon atoms. Two non-hydrogen-substituted aromatic carbon atoms were detected at 155.4 and 127.3 ppm. The first of these two signals is shifted downfield due to an adjacent oxygen atom. Further aromatic signals are present at 130.4 and 115.5 ppm. Each of these peaks represents two equivalent aromatic CH-groups. Two olefinic carbon atoms each bearing one hydrogen atom (5- and 6-CH=) gave signals located at 137.8 and 122.4 ppm. Non-aromatic carbon atoms directly connected with an oxygen atom gave signals at 76.1, 70.2, 52.3 and 51.8 ppm. The first of these four signals is a non-hydrogen-substituted carbon atom. Therefore, the signal is attributed to 3-C. The other three signals represent CH- or CH₃-carbon atoms of ester alcohol residues. Two CH-carbon atoms neighbored to carbonyl groups were detected at 57.6 (4-CH) and 53.3 (2'-CH) ppm as well as three CH₂-carbon atoms adjacent to a carbonyl group at 43.0, 42.7 and 41.6 ppm. The first two of these three signals were assigned as carbon atoms 12-CH₂ and 14-CH₂ by HSQC analysis and the latter as 2-CH₂. Additional prominent CH₂-signals were found at 36.6 and 32.5 ppm (3'- and 7-CH₂). The slight downfield shift is a result of the adjacent unsaturated carbon atoms. Due to γ -effect¹⁴⁶ 18-CH₂ resulted in the unusual high ppm value found for this group (31.7 ppm). Eight further CH₂ groups gave signals between 29.7 and 22.6 that could not be assigned to an individual carbon atom by 2D-NMR

¹⁴⁶ Kalinowski, H.-O.; Berger, S.; Braun, S. *¹³C-NMR-Spektroskopie* Thieme: Stuttgart, New York **1984**; p.93-101.

analysis. The isopropyl-CH₃ groups resulted in two separated signals at 21.7 and 21.6 ppm. The signal with the smallest ppm-value can be attributed to the terminal methyl group.

The ¹H-NMR spectrum of (-)-**65a** shows the following signals: a doublet of the amide and a singlet of the aromatic hydroxyl group are located at 6.67 and 6.34 ppm. Four aromatic protons were found at 6.95 and 6.76 ppm each showing doublet-multiplicity. Due to the distinct multiplicities the olefinic signals at 5.63 and 5.49 ppm could be assigned as 6-CH= (ddd) and 5-CH (dd) respectively. The characteristic septet signal of the isopropylester was identified at 5.05 ppm. The next upfield signal belongs to 2'-CH with the high ppm value of 4.74 being the result of the nitrogen and the carbonyl group adjacent to the CH-group. The singlet at 4.49 is the signal of the OH-group at 3-C. Further singlets at 3.72 and 3.65 indicate the presence of OCH₃-groups. Several doublets between 3.09 and 2.42 ppm were identified as 4-CH, 2-CH₂ and 3'-CH₂ by the analysis of COSY- and HSQC-spectra. The latter two have AB-system character. Two triplets with similar chemical shifts at 2.42 and 2.41 were assigned as the CH₂-groups adjacent to the ketone (12- and 14-CH₂). A multiplet between 2.01 and 1.92 may be attributed to 7-CH₂ with the slight downfield shift being the consequence of the neighbored double bond. Two multiplets between 1.59-1.48 and 1.34-1.18 cover 11- and 15-CH₂ and 20 protons of the seven remaining CH₂-groups and the two CH₃-groups of the isopropyl ester respectively. The triplet at 0.86 ppm belongs to the terminal CH₃-group at C-20.



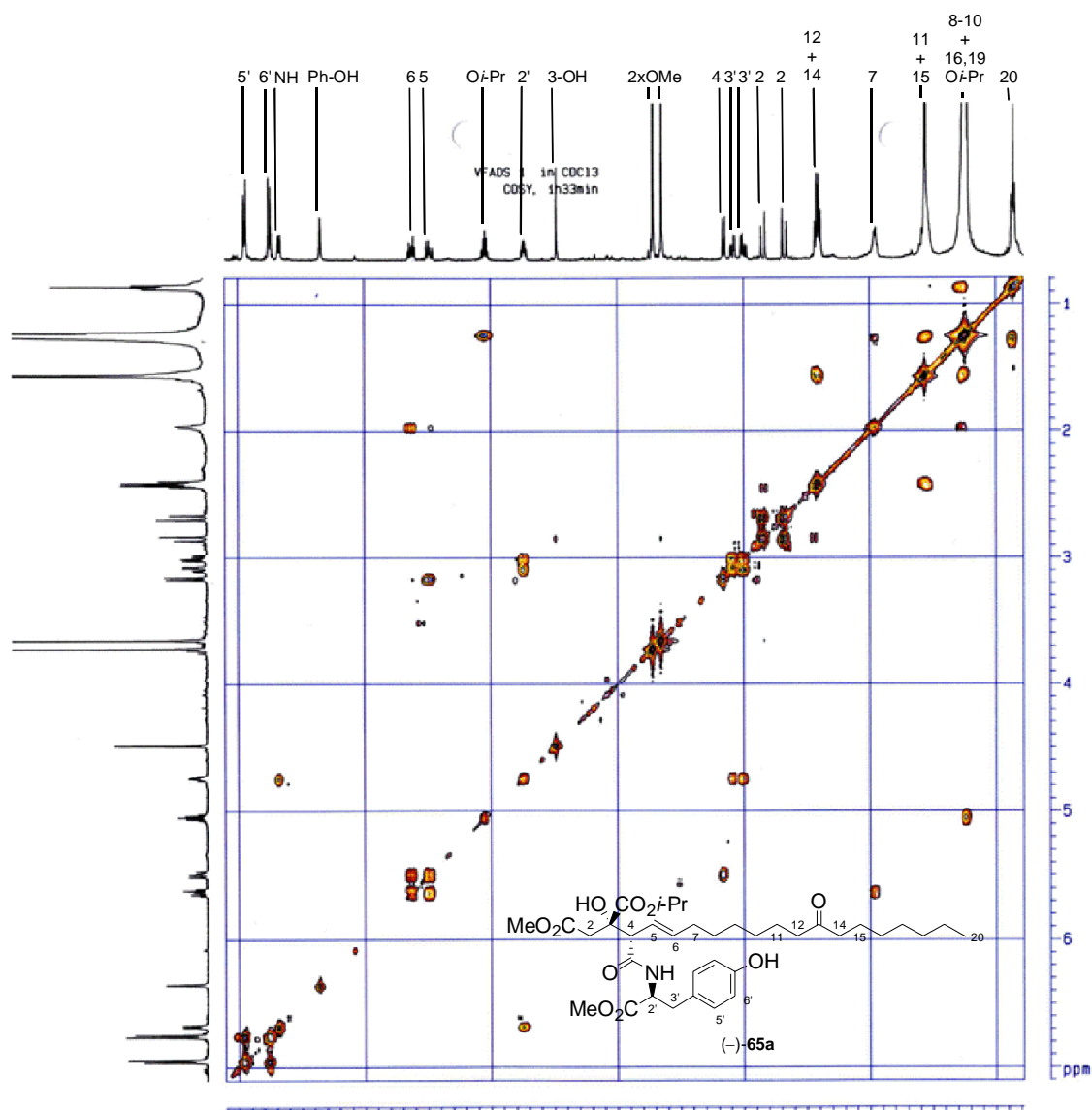
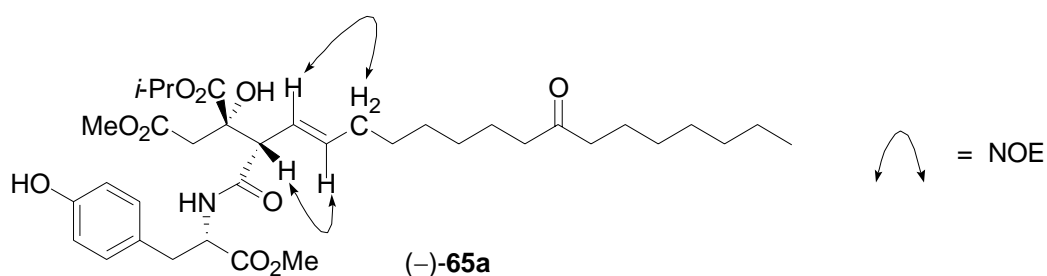


Figure 12: COSY spectrum (500 MHz, CDCl_3) of (-)-65a: signals from left to right 5'-CH, 6'-CH, NH, Ph-OH, 6-CH=, 5-CH=, OiPr-CH, 2'-CH, 3-OH, 1'-OMe, 1-OMe, 4-CH, 3'-CH₂, 2-CH₂ (1H), 2-CH₂ (1H), 12- and 14-CH₂, 7-CH₂, 11- and 15-CH₂, 8-9,10,16- to 19-CH₂ and OiPr-CH₃, 20-CH₃.

NOE cross peaks between 5-CH= and 7-CH₂ as well as between 4-CH and 6-CH₂ verified the *E*-configuration of the double bond. The *syn*-configuration of C3 and C4 was assigned in analogy to experiments published earlier.^{59a}



Scheme 59: Selected NOEs for (-)-65a.

The assignment of the absolute configuration was made by comparison of optical rotation value and spectroscopic signals with data reported. Table 14 compares ^1H NMR data of viridiofungin A triester (–)-**65a** (Table 14, middle column) with its unnatural diastereomer (+)-**207a** (Table 14, right column) and the reported data for Me_3 -**1a** (Table 14, left column).

| Viridiofungin A trimethylester Me_3 - 1a in CD_3OD ⁴⁷ | Viridiofungin A triester (–)- 65a in CD_3OD | Viridiofungin A triester (+)- 207a in CD_3OD |
|---|---|--|
| 0.90 (t, $J = 7.5$ Hz, 3H) | 0.97 (t, $J = 7.0$ Hz, 3H) | 0.97 (t, $J = 6.4$ Hz, 3H) |
| – | 1.30 (d, $J = 6.3$ Hz, 3H) | 1.30 (d, $J = 5.8$ Hz, 3H) |
| – | 1.32 (d, $J = 6.3$ Hz, 3H) | 1.32 (d, $J = 6.1$ Hz, 3H) |
| 1.29 (m, 14H) | 1.36 (m, 14 H) | 1.36 (m, 14H) |
| 1.53 (m, 4H) | 1.60 (m, 4H) | 1.61 (m, 4H) |
| 1.98 (m, 2H) | 2.06 (m, 2H) | 2.01 (m, 2H) |
| 2.43 (t, $J = 7.5$ Hz, 4H) | 2.51 (t, $J = 7.4$ Hz, 4H) | 2.51 (t, $J = 7.3$ Hz, 4H) |
| 2.60 (d, $J = 16.0$ Hz, 1H) | 2.65 (d, $J = 15.8$ Hz, 1H) | 2.67 (d, $J = 15.8$ Hz, 1H) |
| 2.87 (dd, $J = 14.5, 8.5$ Hz, 1H) | 2.94 (dd, $J = 14.5, 8.7$ Hz, 1H) | 2.85 (d, $J = 15.8$ Hz, 1H) |
| 2.92 (d, $J = 16.0$ Hz, 1H) | 2.97 (d, $J = 15.9$ Hz, 1H) | 2.95 (dd, $J = 14.0, 9.0$ Hz, 1H) |
| 3.07 (dd, $J = 14.5, 5.0$ Hz, 1H) | 3.15 (dd, $J = 14.1, 5.1$ Hz, 1H) | 3.16 (dd, $J = 14.0, 5.1$ Hz, 1H) |
| 3.19 (d, $J = 8.5$ Hz, 1H) | 3.26 (d, $J = 8.7$ Hz, 1H) | 3.20 (d, $J = 9.1$ Hz, 1H) |
| 3.64 (s, 3H) | – | – |
| 3.70 (s, 3H) | 3.71 (s, 3H) | 3.70 (s, 3H) |
| 3.71 (s, 3H) | 3.79 (s, 3H) | 3.78 (s, 3H) |
| 4.61 (dd, $J = 8.5, 5.0$ Hz, 1H) | 4.68 (dd, $J = 9.1, 5.2$ Hz, 1H) | 4.69 (dd, $J = 8.9, 5.1$ Hz, 1H) |
| – | 5.06 (sept, $J = 6.3$ Hz, 1H) | 5.01 (sept, $J = 6.2$ Hz, 1H) |
| 5.51 (m, 2H) | 5.60 (m, 2H) | 5.58 (m, 2H) |
| 6.67 (d, $J = 8.5$ Hz, 2H) | 6.74 (d, $J = 8.5$ Hz, 2H) | 6.78 (d, $J = 8.5$ Hz, 2H) |
| 6.98 (d, $J = 8.5$ Hz, 2H) | 7.06 (d, $J = 8.5$ Hz, 2H) | 7.08 (d, $J = 8.5$ Hz, 2H) |

Table 14: Comparison of ^1H NMR signals found for (–)-**65a** and its diastereomer (+)-**207a** with data reported for Me_3 -**1a**.

In the table below ^{13}C NMR data (diagnostic signals) and optical rotation values are listed for reported Me_3 -**1a**, (*t*-Bu)₃-**1a** and viridiofungin A triester (–)-**65a** (Table 15).

| | Viridiofungin A trimethylester (Me ₃ - 1a) in CD ₃ OD ⁴⁷ | Viridiofungin A tri- <i>tert</i> - butylester (<i>t</i> -Bu ₃ - 1a) in CD ₃ OD ⁵¹ | Viridiofungin A triester (–)- 65a in CD ₃ OD |
|---|---|--|--|
| Optical rotation [α] _D ²⁶ | –19.1° (<i>c</i> 0.43, MeOH) | –8.3° (<i>c</i> 1.16, MeOH) | –6.6 (<i>c</i> 0.15, CHCl ₃) |
| ¹³ C-NMR data (diagnostic signals) | 212.3 174.3 173.4 173.3 171.9 157.5 137.7 131.3 128.4 124.6 116.2 - - - 78.3 - 58.3 55.2 | 212.8 171.9 170.5 170.4 169.5 155.4 137.0 130.6 127.5 122.5 115.3 83.0 82.1 81.4 75.6 - 58.1 54.0 | 212.9 172.0 171.8 171.6 170.4 156.0 136.3 129.8 127.2 123.0 114.8 - - - 76.3 69.4 56.7 53.2 |

Table 15: Comparison of ¹³C NMR signals and optical rotation values of Me₃-**1a**, (*t*-Bu)₃-**1a** and viridiofungin A triester (–)-**65a**.

Part 2: (+)-Xeniolide F

9 Introduction

9.1 *Xenias*: Soft Corals of the Genus *Anthozoa* – their Biology and the Resulting Potential as Sources of Pharmaceutical Interesting Natural Products

The first report covering the isolation of pharmaceutical interesting natural products from a marine source dates back to the 1950s.¹⁴⁷ This early discovery has stimulated an ever increasing interest in marine organism as sources of potent pharmaceuticals.¹⁴⁸ Marine invertebrates were found to produce a variety of secondary metabolites with promising anti-bacterial, anti-fungal, and especially anti-cancer properties.¹⁴⁹ In recent years many marine natural products which are promising candidates for new drugs have been discovered (Table 16).¹⁵⁰

| Entry | Potentially useful for the treatment of | Compound | Organism | Origin |
|-------|---|--|----------|--------------------|
| 1 | Cancer | Bryostatin 1 | Bryozoan | Gulf of California |
| 2 | Cancer | Dolastatin 10 | Sea hare | Indian Ocean |
| 3 | Cancer | Ecteinascidin-743 (ET-743, Trabectedin, Yondelis TM) | Tunicate | Caribbean |
| 4 | Cancer | Halichondrin B | Sponge | Okinawa |
| 5 | Cancer | Kahalaide F | Mollusc | Hawaii |
| 6 | HIV | Cyclodidemniserinol trisulfate | Tunicate | Palau |
| 7 | Nematode infection | Dithiocyanates | Sponge | Australia |
| 8 | Asthma | Contignasterol | Sponge | Papua, New Guinea |
| 10 | Pain | Conotoxins | Snail | Australia |

Table 16: Marine natural products as potential therapeutic compounds (in clinical trials: phase II and III).

¹⁴⁷ Bergmann, W. W.; Jeffrey, C.; Stempfen, M. F., Jr. *J. Org. Chem.* **1957**, *22*, 1308-1313.

¹⁴⁸ Newman, D. J.; Cragg, G. M. *J. Nat. Prod.* **2004**, *67*, 1216-1238.

¹⁴⁹ Swartsmann, G.; Ratain, M. J.; Cragg, G. M.; Wong, J. E.; Saijo, N.; Parkinson, D. R.; Fujiwara, Y.; Pazdur, R.; Newman, D. J.; Dagher, R.; Di Leone, L. *J. Clin. Oncol.* **2002**, *20*, 47S-59S.

¹⁵⁰ Kijjoo, A.; Sawangwong, P. *Mar. Drugs* **2004**, *2*, 73-82.

The focus of pharmaceutical companies and marine chemists screening and evaluating natural products is concentrated on organism lacking physical protection. For their survival they strongly rely on a chemical defence.¹⁵¹ Soft corals have been found to be a rich source of interesting natural products.¹⁵² These polypoid cnidarians belong to the class *Anthozoa* which is often called *Octocorallia*. This reflects the typical eightfold radial symmetry of the organisms.¹⁵³ The polyp consists essentially of a hollow cylinder with a fringe of eight tentacles around the mouth – the opening on the top of the polyp.¹⁵⁴ The tentacles are pinnate – small branches come off of the main tentacles creating a fragile and feather-like appearance of the soft coral (Image 6).



Image 6: Pinnated tentacles of different *Octocorallia* species.¹⁵⁵

The animals live together in soft, fleshy, irregularly shaped colonies (Image 7, left) with each polyp being attached to a connecting tissue called conenchyme. The colony is sessile in its nature and ones attached to the surface it usually remains sedentary for the whole span of its life.¹⁵⁶ It can reproduce both sexually and asexually. For sexual reproduction, mature colonies release gametes into the water (spawning) that form planula larvae after fertilisation. The planula then settles on a new substrate and develops a polyp. Starting from a single polyp, the colony growth occurs asexually by budding (Image 7, right).

¹⁵¹ (a) Kelman, D.; Benayahu, Y.; Kashman, Y. *J. Exp. Mar. Biol. Ecol.* **1999**, *238*, 127-137. (b) *Drugs from the sea, will the next penicillin come from a sponge?* by Kerr, R.: <http://www.science.fau.edu/drugs.htm>; 04.07.2006

¹⁵² Faulkner, D. J. *Nat. Prod. Rep.* **2002**, *19*, 1-48.

¹⁵³ *Introduction to the Octocorallia*: <http://www.ucmp.berkeley.edu/cnidaria/octocorallia.html>

¹⁵⁴ *Soft corals* by Shimek, R.: http://www.reefs.org/library/aquarium_net/0998/0998_5.html; 24.04.2006

¹⁵⁵ The pictures have been obtained from the following web pages (from left to right): (a) <http://www.nanoreef.it/immagini/schede/invertebrati/xenia3.jpg>; 26.04.2006 (b) <http://www.pbs.org/kcet/shapeoflife/imaganim/cnidaria2.jpg>; 25.04.2006; (c) http://www.bellsouthpwp.net/1/o/loguell/Saltwater/100gRR/Xenia_coral_03.jpg; 25.04.2006

¹⁵⁶ *Coral ecosystems* at the web page of the Australian Institute of Marine Science (<http://www.aims.gov.au>): *General biology*: <http://www.aims.gov.au/pages/reflib/bigbank/pages/bb-09g.html>

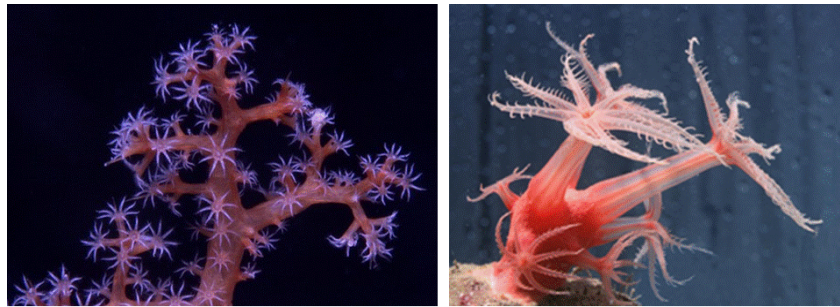


Image 7: A soft coral colony (left) and budding of a soft coral (right).¹⁵⁷

The family *Xeniidae* was found to have a unique mode of reproduction: the colonies produce elongate excrescences similar to runners of strawberry plants. Another colony forms on the end. After some time the connection withers, resulting in two separate colonies.¹⁵⁸

Soft corals are filter-feeders harvesting plankton from the water flowing around the colony. However, most of them live in a symbiotic relationship with unicellular dinoflagellates called zooxanthellae (or *Symbiodinium*). They are responsible for the bright colors found among the soft corals (Image 8).

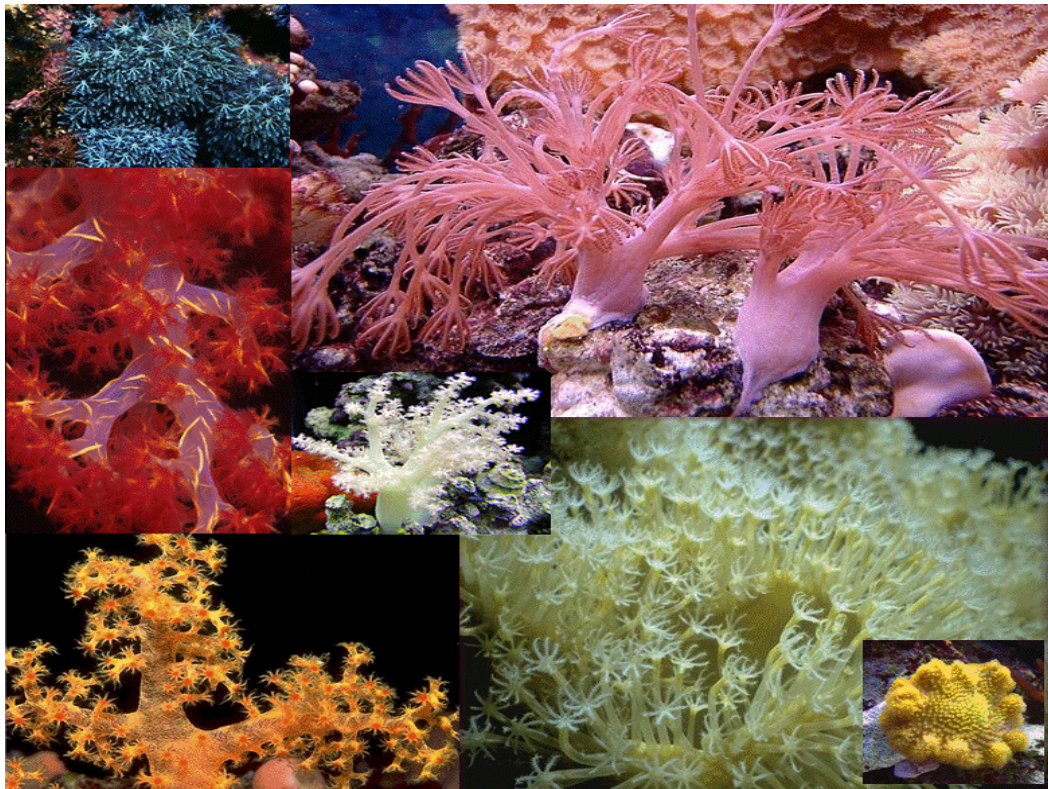


Image 8: The bright colors of soft corals are the result of symbiotic zooxanthellae.¹⁵⁹

¹⁵⁷ The pictures have been obtained from the following web pages (from left to right): (a) http://www.wetpixel.com/legacy/reviews/10duk_smith/images/soft%20coral%20at%20night.jpg; 25.04.2006 (b) <http://www.mar.dfo-mpo.gc.ca/oceans/e/essim/gully/images/softcoral2.jpg>; 25.04. 2006

¹⁵⁸ *Coral ecosystems* at the web page of the Australian Institute of Marine Science (<http://www.aims.gov.au>):
 Reproduction: <http://www.aims.gov.au/pages/reflib/bigbank/pages/bb-09i.html>

The zooxanthellas play an essential role for the biology of their host organism. It is agreed that at least a few of the secondary metabolites found in soft corals are produced by the zooxanthellae.¹⁶⁰ External stress (increased temperature, pollution, salinity shock or high UV radiation) may lead to the ejection of the symbiotic algae resulting in the known phenomenon of the so called coral bleaching.¹⁶¹ Although it is known that corals can survive and recover from short time bleaching events,¹⁶² distortion of the whole colony will occur if the reason for the bleaching maintains.^{160,163} Under healthy conditions the soft corals nutrition often relies on a combination of plankton digestion and supplements from the photosynthetic activities of the symbionts. The algae on the other hand profits from the digestion waste produced by the coral, for despite their impressive biodiversity, the coral ecosystems are in fact characterized by a low level of anorganic nutrients.¹⁶⁴ Indeed, over-nutrition can cause the distortion of a reef ecosystem for it may result in the overgrowth with algae.¹⁶⁵

Members of the genus *Xenia* are relatively autonomic from phytoplankton as source for nutrition and strongly rely on the photosynthetic products of their symbiotic partners.¹⁶⁶ This is reflected in the preferred shallow water habitats of *Xenia* soft corals. There, sufficient amounts of light enable photosynthetic activity. The independence from external food sources stimulated the widespread popularity of the organisms among aquarists for light is much easier provided in an artificial environment than it would be to install a reasonable phytoplankton source.¹⁶⁷

¹⁵⁹ The pictures have been obtained from the following web pages: top left: <http://www.coralreefnetwork.com/stender/marine/cnidaria/Anthelia%20edmondsoni.jpg>; 26.04.2006; top right: <http://www.reef-eden.com/Xenia%20pulse%20coral.jpg>; 26.04.2006; middle left: <http://www.uga.edu/cuda/images/HLsoftcoralCU72.jpg>; 26.04.2006; middle centre: <http://www.premiumaquatics.com/softcoral/tonga.jpg>; 26.04.2006; bottom left: http://www.imagequest3d.com/pages/articles/articleofmonth/softcoral/rstn_sfl.jpg; 26.04.2006; bottom right: http://www.tauchfoto.de/03_15.jpg; 27.04.2006; bottom small picture: <http://www.reef-encounters.com/Livestock%20subpages/Soft%20coral%.jpg>; 27.04.2006

¹⁶⁰ (a) König, G. M.; Kehraus, S.; Seibert, S. F.; Abdel-Lateff, A.; Müller, D. *ChemBioChem* **2006**, *7*, 229-238. (b) Proksch, R.; Edrada, R. A.; Ebel, R. *Appl. Microbiol. Biotechnol.* **2002**, *59*, 125-134. (c) Kokke, W. C. M. C.; Epstein, S.; Look, S. A.; Rau, G. H.; Fenical, W.; Djerassi, C. *J. Biol. Chem.* **1984**, *259*, 8168-8173. (d) *The ecology and biochemistry of soft corals* by Michalek-Wagner, K. on the web page of the reef research center: <http://www.reef.crc.org.au/aboutreef/coral/softcoralbiochem.html>; 27.04.2006

¹⁶¹ Buddemeier, R. W.; Fautin, D. G. *BioScience* **1993**, *43*, 320-326. and references therein.

¹⁶² *Status of coral reefs in the world: 1998* by Wilkinson, C. at the web page of the Australian Institute of Marine Science (<http://www.aims.gov.au>): *Executive Summary: How coral reefs respond to stress*: <http://www.aims.gov.au/pages/research/coral-bleaching/scr-004.html>

¹⁶³ (a) Strychar, K. B.; Coates, M.; Sammarco, P. W.; Piva, T. J. *J. Exp. Mar. Biol. Ecol.* **2004**, *304*, 99-121. (b) *Spawning Studies Investigate Bleaching Effects* by Ashworth, T. at the web page of the reef research centre: <http://www.reef.crc.org.au/publications/explore/feat19.html>; 27.04.2006

¹⁶⁴ <http://netpet.org/fish/fishnews/articles/hermatypic.html>

¹⁶⁵ Barber, R. T.; Hilding, A. K.; Hayes, M. L. *Human Ecol. Risk Manag.* **2001**, *7*, 1255-1270.

¹⁶⁶ http://www.augsburg.edu/biology/aquaria/SpeciesInfoFiles/soft_XeniaElongata.html

¹⁶⁷ <http://www.dtplankton.com/phytoplankton/articles/sandbeds.html>

In contrast to the closely related reef building *Scleractinians* (hard corals), soft corals lack the protective calcium carbonate skeleton. Therefore, *Octocorallia* would be expected to be an attractive food source for predators. However, surveys revealed that the rate of predation is surprisingly low.¹⁶⁸ The organism developed some efficient weapons to defend themselves not only against predators but as well against competitors for space, invasions of algae, and against bacterial or viral infections. The chemical defence of these sessile animals that lack physical protection and that literally are unable to run away is highly developed. A large number of soft corals produce noxious chemicals. Storing of those compounds is a useful defence against predators by rendering the coral distasteful or unpalatable for grazing animals. Since the soft corals possess only a very simple immune system the defence against infection and fouling strongly relies on bioactive chemicals.^{163b} Therefore, it was not surprising that a range of different anti-fouling agents with anti-bacterial and anti-fungal characteristics were isolated during the screenings. However, defence is required not only against those immanent dangers. The organisms live in a constant battle against competitors for food and light. Cytotoxic secondary metabolites are often secreted into the water to interfere the growing and/or to inhibit the settling of other marine organism.¹⁶⁹ Those compounds that interfere with quickly proliferating cells are interesting potential therapeutics for cancer treatment since cancer cells as well exhibit high cell proliferation rates. Apparently, the chemicals produced by the coral provide an effective defence even in the high dilution of the aquatic environment. Consequently, they are expected to be highly active inducing the desired response if administered in very small dosages what makes them interesting targets for pharmaceutical research and as potential drug candidates.¹⁷⁰

¹⁶⁸ (a) Davies-Coleman, M. T.; Beukes, D. R. *S. Afr. J. Sci.* **2004**, *100*, 539-544. (b) *Coral ecosystems* at the web page of the Australian Institute of Marine Science (<http://www.aims.gov.au>): *Predation and defence*: <http://www.aims.gov.au/pages/reflib/bigbank/pages/bb-09j.html>

¹⁶⁹ Artificial delocated soft corals were found to induce necrosis in neighbouring hard corals due to excreted allelopathic substances: Alino, P. M.; Sammarco, P. W.; Coll, J. C. *Mar. Ecol. Prog. Ser.* **1992**, *81*, 129-145.

¹⁷⁰ Conotoxin (ziconotideTM) for example – a pain killer and analgesic isolated from the venom of a marine snail proved to be 1000 times more active than morphine. McCleskey, E. W.; Fox, A. P.; Feldman, D.; Cruz, L. J.; Olivera, B. M.; Tsien, R. W.; Yoshikami, D. *Proc. Natl. Acad. Sci. USA* **1987**, *84*, 4327-4331.

9.2 Xenicane Diterpenes

9.2.1 Xeniolide F – One Bioactive Representative of the Xenicane Diterpenes

(+)-Xeniolide F (**2a**) belongs to the xenicane diterpenes (Figure 13). These secondary metabolites have been isolated from brown algae and cnidarians. Especially soft corals of the genus *Xenia* were found a rich source of these natural products.¹⁷¹ The characteristic feature of the xenicane diterpene class is the presence of a nine membered carbocyclus that is usually annulated with a second ring to form a bicyclic frame.¹⁷²

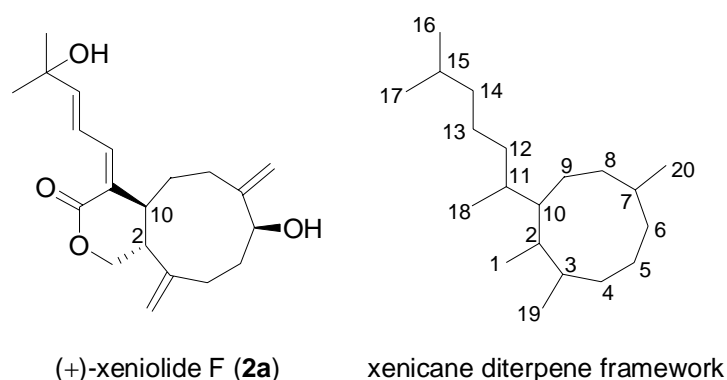


Figure 13

The xenicane diterpenes are divided into five types depending on the additional functional groups present in the molecule. The xenicines **208**,¹⁷³ xeniolides **2**,¹⁷⁴ and xeniaethers **209**¹⁷⁵ possess an oxabicyclic skeleton. They are distinguished by the oxidation states of the carbon atoms in α -position to the oxygen atom (Figure 14).

¹⁷¹ For recent reports on the isolation of xenicanes from *Xenia* sp., see: (a) Duh, C.-Y.; Li, C.-H.; Wang, S.-K.; Dai, C.-F. *J. Nat. Prod.* **2006**, *69*, 1118-1192. (b) Cheng, Y.-B.; Jang, J.-Y.; Khalil, A. T.; Kuo, Y.-H.; Shen, Y.-C. *J. Nat. Prod.* **2006**, *69*, 675-678. (c) El-Gamal, A. A. H.; Chiang, C.-Y.; Huang, S.-H.; Wang, S.-K.; Duh, C.-Y. *J. Nat. Prod.* **2005**, *68*, 1336-1340. (d) El-Gamal, A. A. H.; Wang, S.-K.; Duh, C.-Y. *J. Nat. Prod.* **2006**, *69*, 338-341. (e) Shen, Y.-C.; Lin, Y.-C.; Ahmed, A. F.; Kuo, Y.-H. *Tetrahedron Lett.* **2005**, *46*, 4793-4796.

¹⁷² We suggest the numbering depicted in Figure 13 for it reflects the proposed biosynthesis of the diterpene with geranylgeranyl diphosphate as starting material. For details, see chapter 9.2.2.

¹⁷³ Xenicin (**208**), the first isolated xenicane diterpene was reported in 1977: Vanderah, K. J.; Steudler, P. A.; Ciereszko, L. S.; Schmitz, F. J.; Ekstrand, J. D.; van der Helm, D. *J. Am. Chem. Soc.* **1977**, *99*, 5780-5784.

¹⁷⁴ The first reported xeniolide (**2b**) was isolated by Kashman *et al.*: Kashman, Y.; Groweiss, A. *Tetrahedron Lett.* **1978**, *19*, 4833-4836.

¹⁷⁵ Xeniaether A (**209**), the first xenicane diterpene containing the 9-membered carbocyclus fused to a tetrahydrofuran, was isolated in 1995: Iwagawa, T.; Amano, Y.; Hase, T.; Shiro, M. *Tetrahedron* **1995**, *51*, 11111-11118.

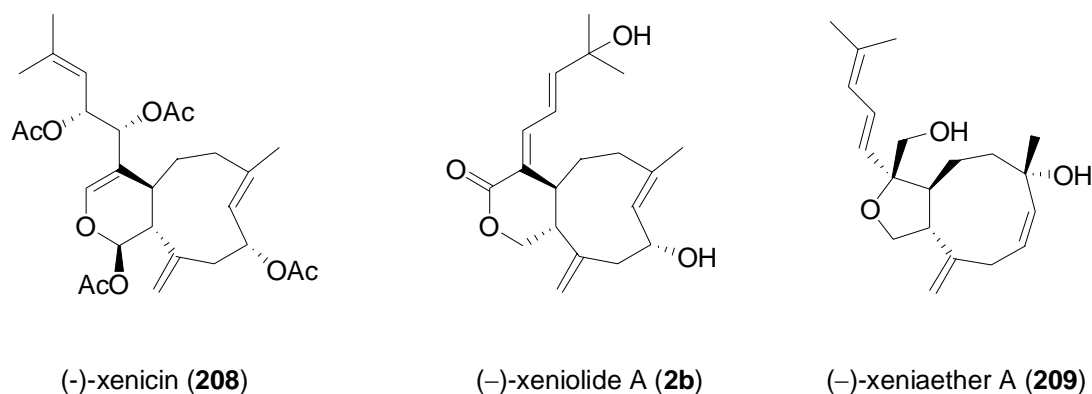


Figure 14: Ac= acetyl.

Xenicane diterpenes with a bicyclo[7.2.0]undecane skeleton are named xeniaphyllanes **210** (Figure 15, left).¹⁷⁶ The monocyclic azamilides **211** represent the most recently discovered group of xenicane diterpenes.¹⁷⁷ They are usually acylated with saturated C16-C20 fatty acids (Figure 15, right).

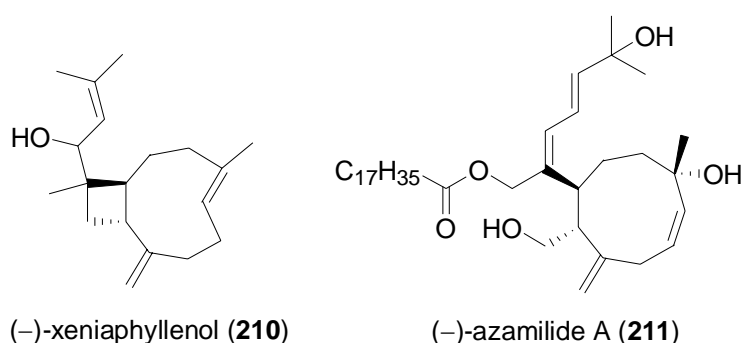


Figure 15

Xenicane diterpenes have shown interesting biological activities in vitro, e.g. cytotoxic potential which was tested against different cancer cell lines,¹⁷⁸ antibacterial activity,¹⁷⁹ inhibitory activity against farnesyl protein transferase (FPT) and antiangiogenic activity thus significantly inhibiting the tube formation of the human umbilical vein endothelial cell (HUVEC) induced by the basic fibroblast growth factor (bFGF),¹⁸⁰ anti-inflammatory¹⁸¹ and anti-fungal activity.¹⁸²

¹⁷⁶ The first reported xeniaphyllenol (**210**) was isolated in 1978: Groweiss, A.; Kashman, Y. *Tetrahedron Lett.* **1978**, *19*, 2205-2208.

¹⁷⁷ For the isolation and structure elucidation of the first azamilide (**211**), see: Iwagawa, T.; Amano, M.; Nakatani, M.; Hase, T. *Bull. Chem. Soc. Jpn.* **1996**, *69*, 1309-1312.

¹⁷⁸ (a) Reference 171a (b) El-Gamal, A. A. H.; Wang, S.-K.; Duh, C.-Y. *Tetrahedron Lett.* **2005**, *46*, 4499-4500. (c) Duh, C.-Y.; El-Gamal, A. A. H.; Chiang, C.-Y.; Chu, C.-J.; Wang, S.-K.; Dai, C.-F. *J. Nat. Prod.* **2002**, *65*, 1882-1885.

¹⁷⁹ (a) Iwagawa, T.; Kawasali, J.-i.; Hase, T. *J. Nat. Prod.* **1998**, *61*, 1513-1515. (b) Iwagawa, T.; Masuda, T.; Okamura, H.; Nakatani, M. *Tetrahedron* **1996**, *52*, 13121-13128.

¹⁸⁰ Rho, J.-R.; Oh, M.-S.; Jang, K. H.; Cho, K. W.; Shin, J. *J. Nat. Prod.* **2001**, *64*, 540-543.

(+)-Xeniolide F (**2a**) was isolated from a not yet classified *Xenia* species collected near the Togeian islands (Image 9)¹⁸³ - a remarkably diverse archipelago of coral and volcanic isles near Sulawesi (Indonesia).



Image 9: *Xenia* sp.¹⁸⁴ of which xeniolide F (**2a**) was isolated was collected from coral reefs near the Togeian islands.¹⁸⁵

Extraction of 300 g of the animal afforded 0.41 g of a diterpene enriched mixture of organic material. Flash chromatography and reversed phase HPLC resulted in the isolation of 4.7 mg of (+)-xeniolide F. The molecular formula of the diterpene was determined by electron spray mass spectroscopy (ESMS) and high resolution FAB molecular spectroscopy (HRFABMS). The constitution and relative configuration was solved by 1D and 2D NMR methods. The absolute configuration of (+)-xeniolide F (**2a**) was not explicitly determined. However, the depicted absolute configuration at C2 and C10 is in agreement with the results obtained by Yamada *et al.*¹⁸⁶ As a result of these studies, the absolute configuration of xeniolide A, xenialactol and xeniaoxolane was determined by the application of the modified Mosher's

¹⁸¹ (a) Hooper, G. J.; Davies-Coleman, M. T.; Schleyer, M. *J. Nat. Prod.* **1997**, *60*, 889-893. (b) Hooper, G. J.; Davies-Coleman, M. T. *Tetrahedron* **1995**, *51*, 9973-9984.

¹⁸² Fusetani, N.; Asano, M.; Matsunga, S.; Hashimoto, K. *Tetrahedron* **1989**, *45*, 1647-1652.

¹⁸³ Anta, C.; González, N.; Santafé, G.; Rodríguez, J.; Jiménez, C. *J. Nat. Prod.* **2002**, *65*, 766-768.

¹⁸⁴ We thank Professor Carloz Jiménez for kindly providing us with the above picture of the *Xenia* sp. from which the natural product was originally isolated. As well he has sent copies of the NMR spectra of xeniolide F what is gratefully acknowledged.

¹⁸⁵ The map has been obtained from the following web site: <http://www.wrm.org.uy/Indonesia/Togeian5.jpg>; 11.05.2006.

¹⁸⁶ (a) Miyaoka, H.; Mitome, H.; Nakano, M.; Yamada, Y. *Tetrahedron* **2000**, *56*, 7737-7740. (b) Miyaoka, H.; Nakano, M.; Iguchi, K.; Yamada, Y. *Tetrahedron* **1999**, *55*, 12977-12982.

method¹⁸⁷ while the absolute configuration of xenadiol was resolved by the application of the lactone sector rule.¹⁸⁸ For two crystalline xenicane diterpenes isolated independently in two different research groups single crystal X-ray analysis were performed revealing as well the represented absolute configuration.¹⁸⁹ Moderate Cytotoxic activity was found during in vitro tests against the human cancer cell lines A-549 (lung adenocarcinoma), HT-29 (colon cancer) and MEL-28 (melanoma) as well as against murine cell line P-388 (lymphocytic leukaemia). As for various other natural products of marine origin, an unsolved supply issue complicates the further investigation of the mode of action and the development into clinical candidates.¹⁹⁰ Beside their interesting structural features this justifies them as attractive targets for synthetic oriented research groups.

9.2.2 Proposed Biosynthesis of (+)-Xeniolide F

Although no biosynthetic studies have been undertaken for xenicane diterpenes so far, it is believed that they are derived from transannular carbocation cyclization of the common diterpene precursor geranylgeranyl diphosphate (GGPP) (**212**) (Scheme 60).¹⁹¹ The analogue biosynthesis of the related sesquiterpene caryophyllane was verified by isotopic labelling studies.¹⁹²

¹⁸⁷ Ohtani, I.; Kusumi, T.; Kashman, Y.; Kakisawa, H. *J. Am. Chem. Soc.* **1991**, *113*, 4092-4096.

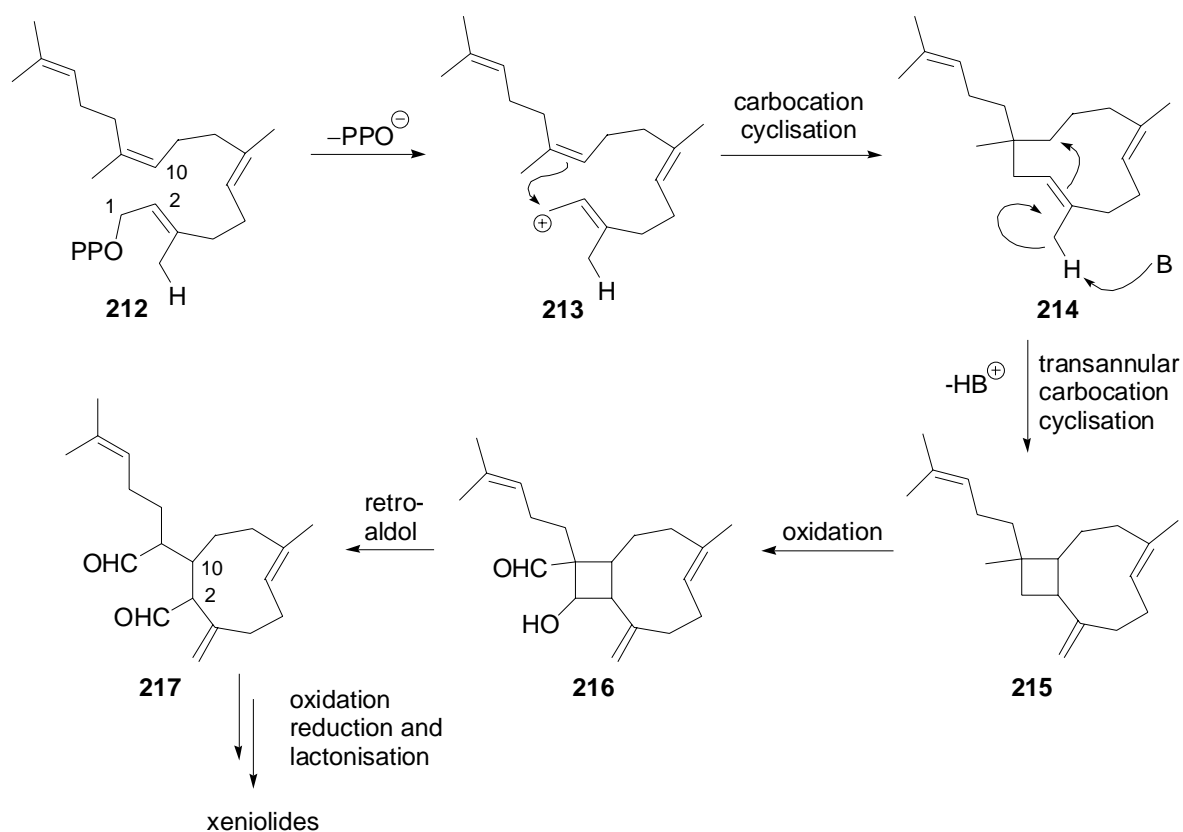
¹⁸⁸ (a) Jennings, J. P.; Klyne, W.; Scopes, P. M. *J. Chem. Soc.* **1965**, 7211-7242. (b) Shalon, Y.; Yanuka, Y.; Sarel, S. *Tetrahedron Lett.* **1969**, *10*, 957-960. (c) Melton, L. D.; Morris, E. R.; Rees, D. A.; Thom, D. *J. Chem. Soc., Perkin Trans. 2* **1979**, 10-17.

¹⁸⁹ (a) Lelong, H.; Ahond, A.; Chiraroni, A.; Poupar, C.; Riche, C.; Potier, P.; Pusset, J.; Pusset, M.; Laboute, P.; Menou, J. L. *J. Nat. Prod.* **1987**, *50*, 203-210. (b) König, G. M.; Coll, J. C.; Bowden, B. F.; Gublis, J. M.; MacKay, M. F.; La Barre, S. C.; Laurent, D. *J. Nat. Chem.* **1989**, *52*, 294-299.

¹⁹⁰ (a) König, G. M.; Wright, A. D. *Planta Med.* **1996**, *62*, 193-211. (b) See reference 160.

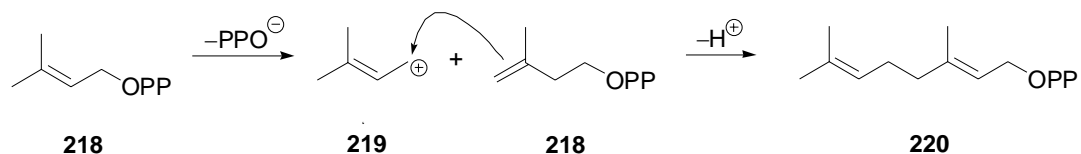
¹⁹¹ (a) Green, D.; Carmely, Y. B.; Kashman, Y. *Tetrahedron Lett.* **1988**, *29*, 1605-1608. (b) Kashman, Y.; Rudi, A. *Phytochem. Rev.* **2004**, *3*, 309-323.

¹⁹² (a) Croteau, R.; Gundy, A. *Arch. Biochem. Biophys.* **1984**, *233*, 838-841. (b) Cane, D. E. *Acc. Chem. Res.* **1985**, *18*, 220-226.



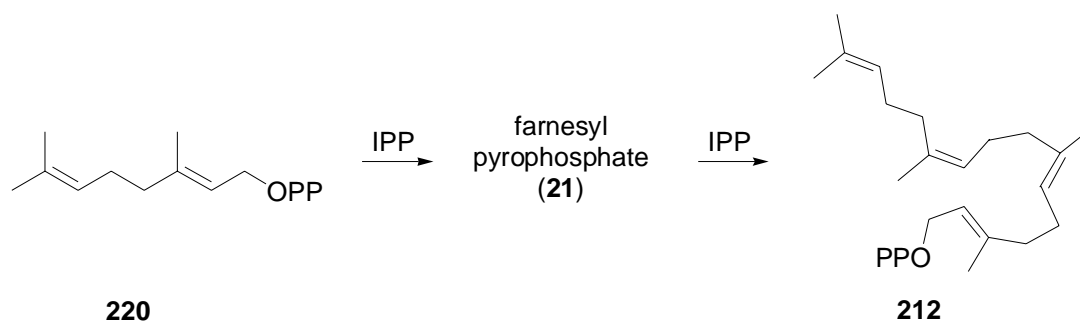
Scheme 60: Proposed biosynthesis of xeniolides starting from geranylgeranyl pyrophosphate GGPP (**212**). PP= pyrophosphate, B= base.

Starting from dimethylallyl pyrophosphate DMAPP (**218**) the biosynthesis of GGPP (**112**) is initiated by the formation of the allyl cation **219**. The cation **219** may then be attacked by isopentenyl pyrophosphate IPP (**218**) affording geranyl pyrophosphate GPP (**220**) after the loss of a proton from the primary addition product (Scheme 61).



Scheme 61: Biosynthesis of geranyl pyrophosphate GPP (**220**). PP= pyrophosphate.

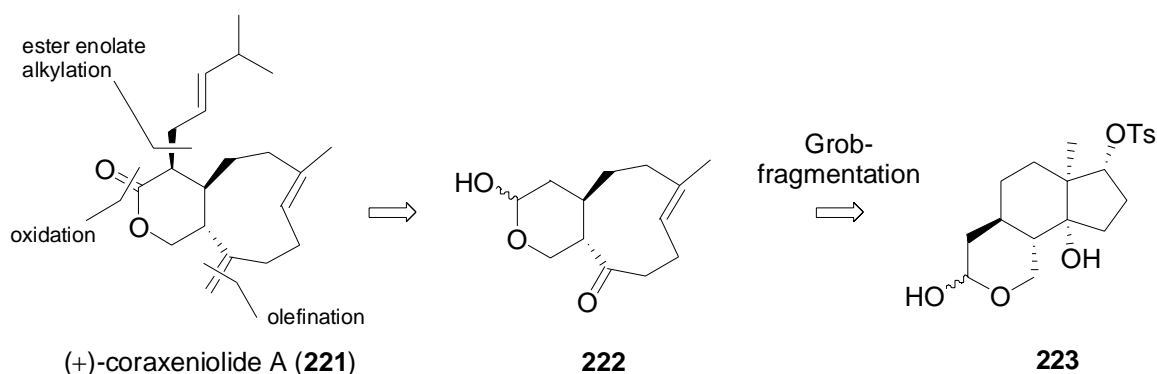
Propagation with another molecule **218** generates farnesyl pyrophosphate FPP (**21**) and one additional propagation step finally produces geranylgeranyl diphosphate (**212**) (Scheme 62).



Scheme 62: With two additional propagation steps **220** may be transformed to **212**. PP= pyrophosphate.

9.2.3 Published Total Synthesis of Xenicane Diterpenes

The only realized total synthesis of a xenicane diterpene was published by Leumann *et al.*¹⁹³ The synthesis of (+)-coraxeniolide A (**221**) was based on the pioneering synthesis of caryophyllene by Corey and co-workers.¹⁹⁴ The synthetic strategy rests on a Grob-fragmentation¹⁹⁵ of an appropriated functionalized tricyclus **223** for the stereospecific construction of the nine-membered ring **222** (Scheme 63).



Scheme 63: Retrosynthetic analysis of coraxeniolide A (**221**). Ts= *para*-toluene sulfonyl.

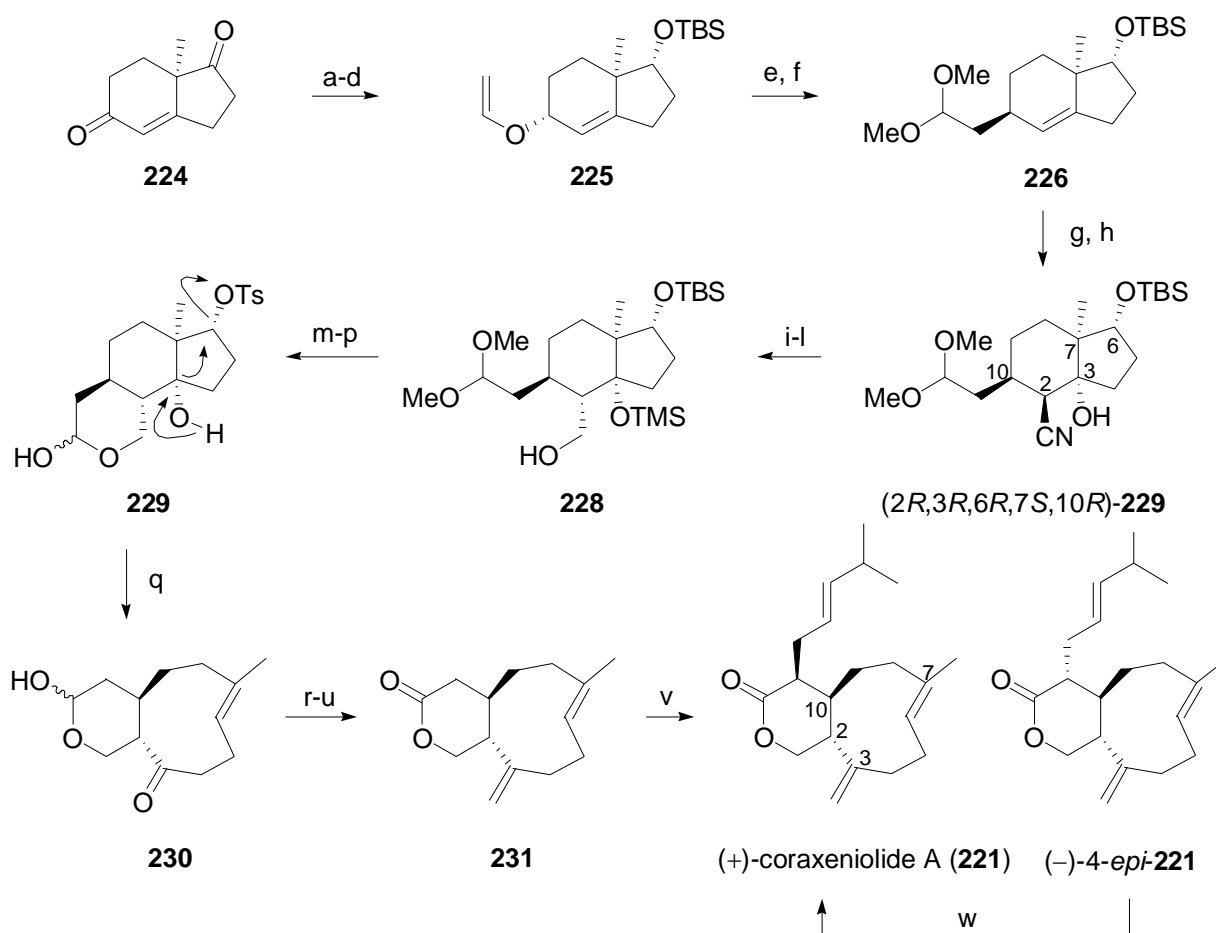
As starting material enantiomerically pure Hajos-Parrish diketone **224**¹⁹⁶ was utilized. The single asymmetric center allowed the diastereoselective formation of all remaining stereogenic centers as shown in Scheme 64.

¹⁹³ Renneberg, D.; Pfander, H.; Leumann, C. J. *J. Org. Chem.* **2000**, *65*, 9069-9079.

¹⁹⁴ Corey, E. J.; Mitra, R. B.; Uda, H. *J. Am. Chem. Soc.* **1964**, *86*, 485-492.

¹⁹⁵ (a) Grob, C. A.; Baumann, W. *Helv. Chim. Acta* **1955**, *38*, 594-610. (b) Grob, C. A. *Angew. Chem., Int. Ed. Engl.* **1969**, *8*, 535-546; *Angew. Chem.* **1969**, *81*, 543-554.

¹⁹⁶ (a) Hajos, Z. G.; Parrish, D. R. *J. Org. Chem.* **1974**, *39*, 1612-1615. (b) Hajos, Z. G.; Parrish, D. R. *J. Org. Chem.* **1974**, *39*, 1615-1621.



Scheme 64: Total synthesis of coraxeniolide A (**221**) was realized as following. a) NaBH_4 , EtOH, -10 - 5 °C, 94%; b) TBSCl, imidazole, DMAP, CH_2Cl_2 , 82%; c) LiAlH_4 , Et_2O , -78 °C, 90%; d) $\text{C}_2\text{H}_5\text{OC}_2\text{H}_3$, $\text{Hg}(\text{OAc})_2$, 40 °C, 80%; e) $\text{Mg}(\text{ClO}_4)_2$, CH_3NO_2 , 83%; f) $\text{CH}(\text{OCH}_3)_3$, montmorillonite clay K-10; Et_2O , 98%; g) *m*-CPBA, CH_2Cl_2 , -5 - 0 °C, 80%; h) LiCN, THF, reflux, 84%; i) KOH, EtOH, 69%; j) TMSCl, imidazole, DMAP, CH_2Cl_2 , 99%; k) DIBAL-H, hexane, 76%; l) NaBH_4 , EtOH, -10 °C, 89%; m) HCl, THF; n) Ag_2CO_3 on Celite, benzene, reflux, 61% (two steps); o) TsCl, pyrridine, CHCl_3 , 92%; p) DIBAL-H, CH_2Cl_2 , -65 °C, 98%; q) NaH, DMSO 88%; r) TBSCl, imidazole, CH_2Cl_2 , 98%; s) $\text{TiCp}_2\text{CH}_2\text{ClAlMe}_3$, THF, pyrridine, -5 °C to rt, 70%; t) TBAF, THF, 85%; u) Ag_2CO_3 on Celite, benzene, 60 °C, 89%; v) LDA, 1-bromo-4-methylpent 2-ene, THF, DMPU, -78 to -69 °C, 50%; w) TBD, toluene, 80%. TBS= *tert*-butyldimethylsilyl [$\text{Si}(\textit{t}\text{-Bu})\text{Me}_2$], DMAP= *N,N*-dimethylamino-4-pyridine, Ac= acetyl, *m*-CPBA= *meta*-chlor perbenzoic acid, TMS= trimethylsilyl [SiMe_3], DIBAL-H= diisobutyl aluminium hydride, Ts= *para*-toluene sulfonyl, DMSO= dimethyl sulfoxide, Cp= cyclopentadienyl, TBAF= tetrabutyl ammonium fluoride [$(\textit{t}\text{-Bu})_4\text{NF}$], LDA= lithium diisopropylamide, DMPU= dimethylpropylenurea, TBD= 1,5,7-triazabicyclo[4.4.0]dec-5-ene.

Chemo- and diastereoselective reduction of the isolated carbonyl functionality of **224** (a), protection of the resulting hydroxyl group (b) and reduction of the conjugated carbonyl group (c) followed by mercuric acetate catalyzed transesterification (d)¹⁹⁷ resulted in the allyl vinyl

¹⁹⁷ Watanabe, W. H.; Conlon, L. E. *J. Am. Chem. Soc.* **1957**, *79*, 2828-2833.

ether **225** that, when treated with $\text{Mg}(\text{ClO}_4)_2$, underwent [1,3] sigmatropic rearrangement¹⁹⁸ to form an aldehyde (e). This aldehyde was protected as dimethylacetale **226** (f). After epoxidation of the double bond (g), treatment with LiCN resulted in regioselective ring opening to afford the β -hydroxynitrile **226** stereoselectively (h). Epimerisation of (2*R*,3*R*,6*R*,7*S*,10*R*)-**227** to the thermodynamically more stable nitrile (2*S*,3*R*,6*R*,7*S*,10*R*)-**227** (i), protection of the hydroxyl group (j) and reduction of the nitrile functionality afforded the corresponding aldehyde (k). After the reduction of this aldehyde functionality to the corresponding alcohol **228** (l), treatment with 2 N HCl resulted in global deprotection (m) and formation of a hemiacetale that was oxidized to a lactone employing the very mild oxidation reagent silver carbonate on Celite (n)¹⁹⁹ which allowed the selective oxidation of the acetale in the presence of a secondary alcohol. The lactone was then tosylated (o) and reduced to the lactol **229** (p). Treatment with methylsulfinyl carbanion²⁰⁰ resulted in the fragmentation reaction to form **230** (q). Final steps included protection (r), Tebbe olefination²⁰¹ of the ketocarbonyl group (s), deprotection (t) and oxidation (u). The lacton **231** was then deprotonated with LDA and subjected to 1-bromo-4-methylpent 2-ene (v). The alkylation products (+)-**221** and (-)-*epi*-**221** were formed in a 1/5.7 ratio and could be separated by column chromatography. Equilibration of 4-*epi*-coraxeniolide A with 1,5,7-triazabicyclo[4.4.0]dec-5-ene (TBD) afforded (+)-**221** and (-)-*epi*-**221** as 3/1 mixture (w).

In conclusion, the synthesis of coraxeniolide A (**221**) was realized with a longest linear sequence of 25 steps in an overall yield of 1.6%. This synthetic approach seems to offer a reasonable solution for various xeniolides with a C6/C7 endocyclic double bond. However, xeniolides with an exocyclic C7/C20 double bond have to be synthesized on a different route.

¹⁹⁸ Grieco, P. A.; Clark, J. D.; Jagoe, C. T. *J. Am. Chem. Soc.* **1991**, *113*, 5488-5489.

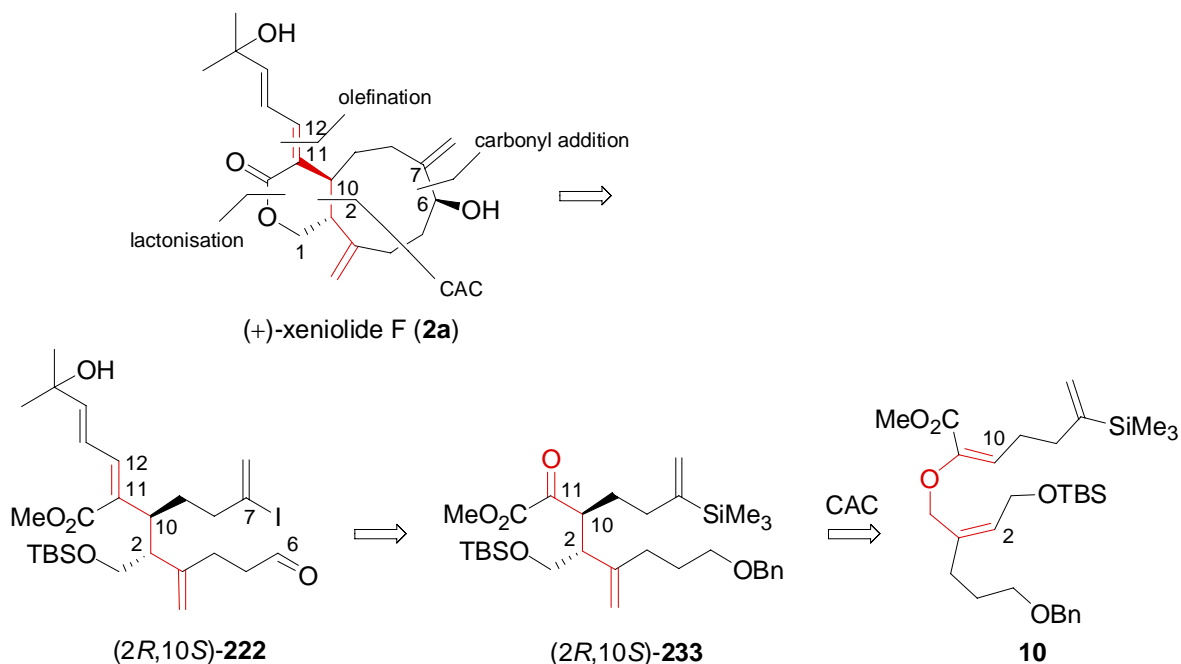
¹⁹⁹ (a) Fétizon, M.; Golfier, M.; Louis, J.-M. *Tetrahedron* **1975**, *31*, 171-176. (b) Fétizon, M.; Golfier, M.C.R. *Hebd. Seances, Acad. Sci.; Ser. C.* **1968**, *267*, 900-903.

²⁰⁰ Corey, E. J.; Chaykovsky, M. *J. Am. Chem. Soc.* **1965**, *87*, 1345-1353.

²⁰¹ Tebbe, F. N.; Parshall, G. W.; Reddy, G. S. *J. Am. Chem. Soc.* **1978**, *100*, 3611-3613.

10 Retrosynthetic Analysis of Xeniolide F

The retrosynthetic analysis of xeniolide F (**2a**) is build upon our recently developed catalytic asymmetric Claisen rearrangement (CAC)²⁰² as the key CC-connecting step (Scheme 65).



Scheme 65: Retrosynthetic analysis of (+)-xeniolide F (**2a**) led to acyclic allyl vinyl ether **10**. CAC= catalytic asymmetric Claisen rearrangement, Bn= benzyl, TBS= *tert*-butyldimethylsilyl [$\text{Si}(t\text{-Bu})\text{Me}_2$].²⁰³

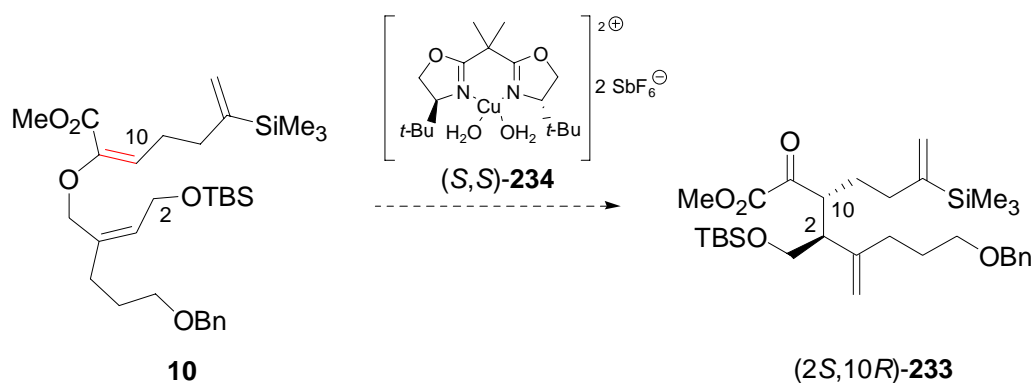
In one step the two neighboured stereogenic carbon atoms C2 and C10 of the α -keto ester **233** could be generated enantioselectively. The diastereoselectivity would be the result of the concerted nature and the chair-like geometry of the transition state of the Claisen rearrangement of acyclic allyl vinyl ether **10**. Best results for the diastereoselectivity are expected for allyl vinyl ethers with *Z*-configured allyl ether double bonds.²⁰⁴ To obtain the

²⁰² (a) Abraham, L.; Czerwonka, R.; Hiersemann, M. *Angew. Chem. Int. Ed.* **2001**, *40*, 4700-4703; *Angew. Chem.* **2001**, *113*, 4835-4837. (b) Hiersemann, M.; Abraham, L. *Eur. J. Org. Chem.* **2002**, 1461-1471. (c) Abraham, L.; Körner, M.; Schwab, P.; Hiersemann, M. *Adv. Synth. Catal.* **2004**, *346*, 1281-1294. (d) Abraham, L.; Körner, M.; Hiersemann, M. *Tetrahedron Lett.* **2004**, *45*, 3647-3650. For recent successful application in target oriented synthesis, see: (e) Pollex, A.; Hiersemann, M. *Org. Lett.* **2005**, *7*, 5705-5708. (f) Körner, M.; Hiersemann, M. *Synlett* **2006**, 121-123.

²⁰³ The depicted protecting groups reflect our realized synthetic route (see chapter 13.2.2). Chemoselective deprotection of the benzyl group in the presence of isolated double bonds might be realized using an oxidative cleavage strategy. Utilization of the TBS-group for the protection of the allyl alcohol functionality was performed with respect to a previously described synthesis of an analogue intermediate (see chapter 13.2).

²⁰⁴ For a more detailed analysis and discussion of the simple diastereoselectivity as a result of the double bond geometry see chapter 11.2.

desired *anti*-selectivity,²⁰⁵ an *E*-configured vinyl ether double bond is required. Since the starting material is achiral, an external chiral inductor is required to control the absolute configuration of the rearrangement product. For this purpose, we envisioned the application of the chiral Lewis acid [Cu{(S,S)-*t*-Bu-box}](SbF₆)₂(H₂O)₂²⁰⁶ [(S,S)-**234a**] that promotes the CAC. Unfortunately, application of the easily accessible (S,S)-**234** to (*E,Z*)-AVE **10** would deliver α -keto ester (2*S*,10*R*)-**233** with reversed absolute configuration with respect to the *assumed* absolute configuration of the natural product (Eq. 29).²⁰⁷



Eq. 29: Bn= benzyl, TBS= *tert*-butyldimethylsilyl [Si(*t*-Bu)Me₂].

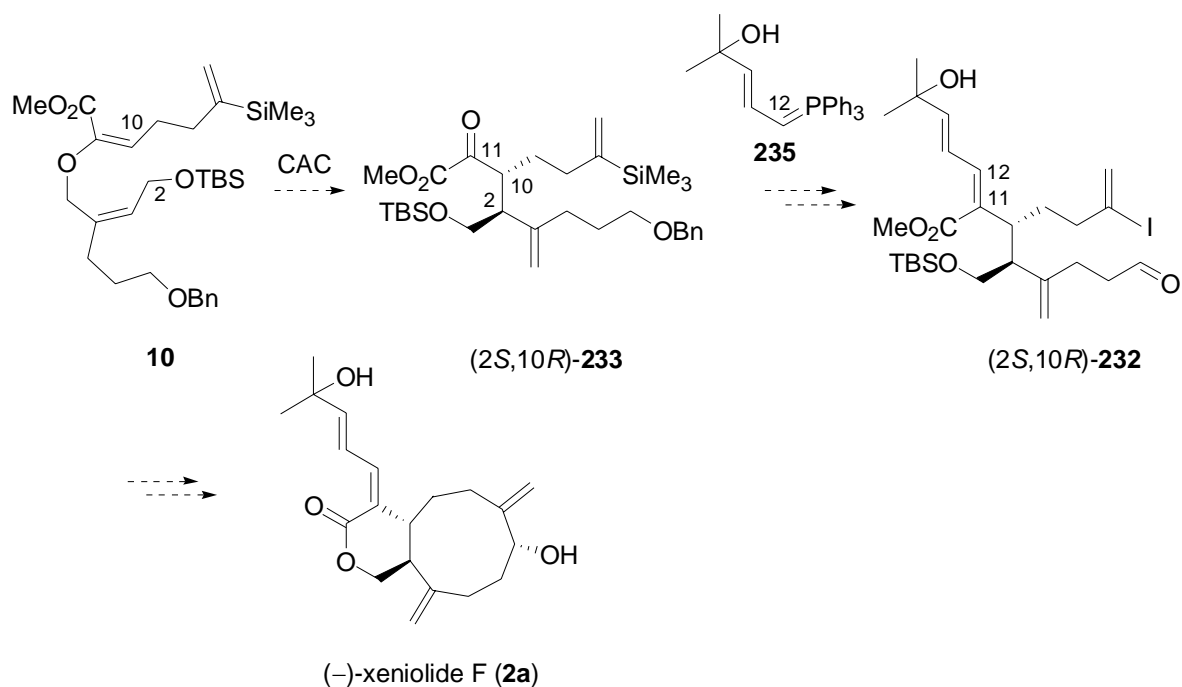
For the total synthesis of (+)-xeniolide F (**2a**) [Cu{(R,R)-*t*-Bu-box}](SbF₆)₂(H₂O)₂ [(R,R)-**234a**] with reversed absolute configuration would be required. However, this catalyst would be disproportionately more expensive.²⁰⁸ Therefore, we decided to perform the initial synthetic studies toward (-)-xeniolide F with the less expensive (S,S)-**234a** (Scheme 66). With an established route to the target molecule, the synthesis of the natural product may be realised by an analogue route employing (R,R)-**234a** as catalyst for the CAC.

²⁰⁵ The term '*anti*' is used to describe the relative configuration at the two neighboured stereogenic centers in a 'zigzag' presentation of the molecule as represented in Scheme 65.

²⁰⁶ For reviews see: (a) Johnson, J. S.; Evans, D. A. *Acc. Chem. Res.* **2000**, *33*, 325-335. (b) Evans, D. A.; Rovis, T.; Johnson, J. S. *Pure Appl. Chem.* **1999**, *71*, 1407-1415. (c) Jørgensen, K. A. *Angew. Chem.* **2000**, *112*, 3702-3733; *Angew. Chem., Int. Ed.* **2000**, *39*, 3558-3588. (d) Gosh, A. K.; Mathivanan, P.; Cappiello, J. *Tetrahedron: Asymmetry* **1998**, *9*, 1-45.

²⁰⁷ This assumption is made in analogy to results obtained earlier in our research group. See reference 202.

²⁰⁸ Starting material for the synthesis of the (S,S)-**234a** [(S)-*t*-leucine] is available from Aldrich (236,20 €/ 0.5 kg) while the (R)-*t*-leucine is about 100-times more expensive (242.00 €/ 5 g).



Scheme 66: Synthetic plan for (–)-**2a**. Bn= benzyl, TBS= *tert*-butyldimethylsilyl [Si(*t*-Bu)Me₂].

Starting from the α -keto ester **233**, we planned to introduce the side chain at C11 by olefination chemistry.²⁰⁹ The formation of the nine-membered carbocycle of (–)-**2a** should be addressed by an intramolecular addition of a vinyl anion at C7 to an aldehyde functionality at C6.²¹⁰ The aldehyde group may be generated by deprotection of the alcohol functionality at C6 and subsequent oxidation of the hydroxyl group. For the formation of the vinyl anion we envisioned a sequence of iododesilylation²¹¹ and halogen-lithium exchange. Starting from vinyl iodide **232**, the carbonyl addition might as well be performed under Nozaki-Hiyama-Kishi conditions.²¹² The latter method was found to be especially useful for the formation of medium sized rings – a synthetic challenge for which only limited reliable solutions were

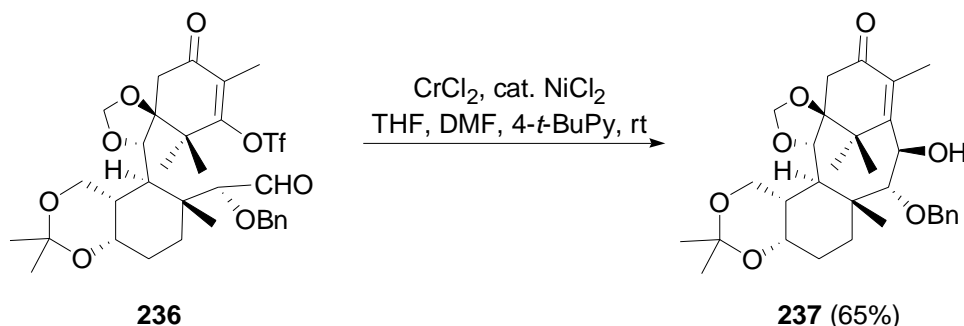
²⁰⁹ For Wittig olefinations involving unprotected hydroxy groups, see: (a) Maryanoff, B. E.; Reitz, A. B.; Dahl-Emswiler, B. A. *J. Am. Chem. Soc.* **1985**, *107*, 217-226. (b) Maryanoff, B. E.; Reitz, A. B.; Dahl-Emswiler, B. A. *Tetrahedron Lett.* **1983**, *24*, 2477-2480. For a Wittig olefination involving a very similar, unsaturated Wittig salt with an unprotected OH-group, see: (c) Taber, D.; Teng, D. *J. Org. Chem.* **2002**, *67*, 1607-1612. (Eq. 61, page 186).

²¹⁰ We are aware of a possible intramolecular Michael addition between the vinyl anion and carbon atom C12. For alternative strategies to generate the nine-membered ring, see chapter 18.

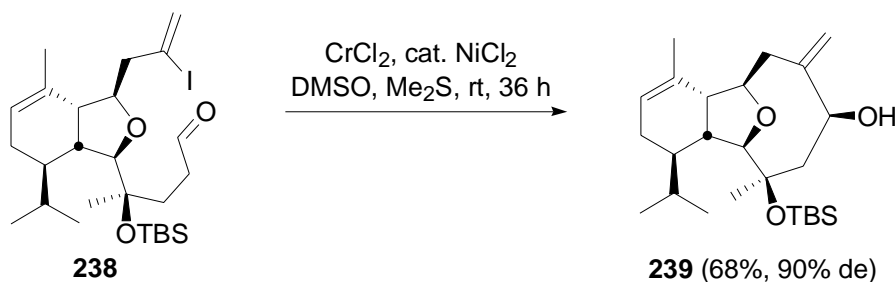
²¹¹ The iododesilylation as tool for the formation of vinyl iodides is known. For references, see chapter 17.

²¹² (a) Stamos, D. P.; Sheng, X. C.; Chen, S. S.; Kishi, Y. *Tetrahedron Lett.* **1997**, *38*, 6355-6358. (b) Takai, K.; Tagashira, M.; Kuroda, T.; Oshima, K.; Utimoto, K.; Nozaki, H. *J. Am. Chem. Soc.* **1986**, *108*, 6048-6050. (c) Jin, H.; Uenishi, J.; Christ, W. J.; Kishi, Y. *J. Am. Chem. Soc.* **1986**, *108*, 5644-5646. (d) Takai, K.; Kimura, K.; Kuroda, T.; Hiyama, T.; Nozaki, H. *Tetrahedron Lett.* **1983**, *24*, 5281-5284. (e) Kress, M. H.; Ruel, R.; Miller, W. H.; Kishi, Y. *Tetrahedron Lett.* **1993**, *34*, 5999-6003. (f) Kress, M. H.; Ruel, R.; Miller, W. H.; Kishi, Y. *Tetrahedron Lett.* **1993**, *34*, 6003-6007. For a review, see: (g) Takai, K.; Nozaki, H. *Proceed. Jpn. Acad. B* **2000**, *76B*, 123-131. For recent applications of the NHK, see: (h) Mi, B.; Maleczka, E., Jr. *Org. Lett.* **2001**, *3*, 1491-1494. (i) Corminboeuf, O.; Overman, L. E.; Pennington, L. D. *J. Am. Chem. Soc.* **2003**, *125*, 6650-6652. (j) Venkatraman, L.; Aldrich, C. C.; Sherman, D. H.; Fecik, R. A. *J. Org. Chem.* **2005**, *70*, 7267-7272. (k) Bian, J.; Van Wingerden, M.; Ready, J. M. *J. Am. Chem. Soc.* **2006**, *128*, 7428-7429.

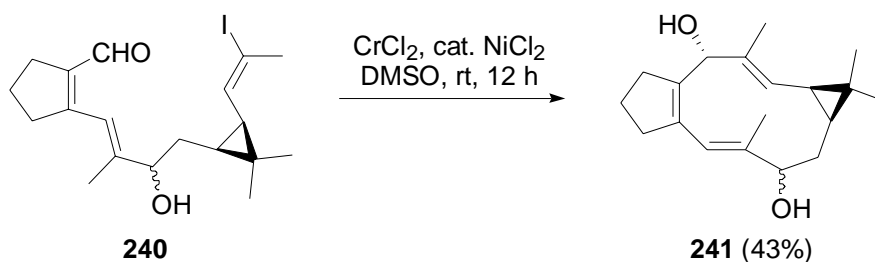
found.²¹³ Instructive examples for the successful application of the Nozaki-Hiyama-Kishi (NHK) coupling in the formation of eight-^{212a}, nine-²¹⁴, and eleven-²¹⁵ rings are given below (Eq. 30 -Eq. 32).



Eq. 30: Formation of an eight-membered ring by the NHK-reaction. Bn= benzyl, Tf= trifluoromethane sulfonyl (CF₃SO₂), DMF= dimethyl formamide, 4-*t*-BuPy= 4-*tert*-butylpyridine.



Eq. 31: Formation of a nine-membered ring by the NHK-reaction. TBS= *tert*-butyldimethylsilyl [Si(*t*-Bu)Me₂], DMSO= dimethyl sulfoxide.



Eq. 32: Formation of an eleven-membered ring by the NHK-reaction. DMSO= dimethyl sulfoxide.

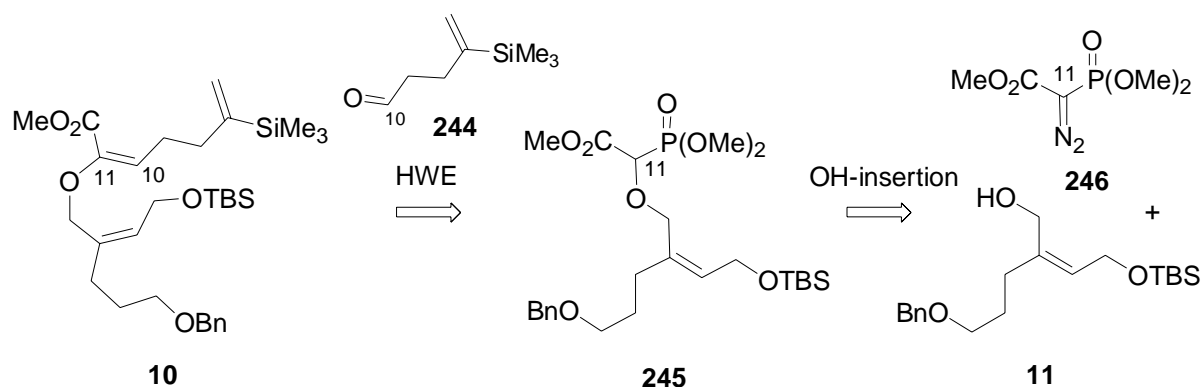
Pivotal for the success of our envisioned synthesis of (–)-**2a** is an efficient access to the achiral 2-alkoxycarbonyl substituted allyl vinyl ether (AVE) **10** with defined double bond configuration. Retrosynthetically, we selected the inherently *E*-selective Horner-Wadsworth-

²¹³ (a) Fürstner, A. *Chem. Rev.* **1999**, *99*, 991-1045. (b) Yet, L. *Chem. Rev.* **2000**, *100*, 2963-3007.

²¹⁴ MacMillan, D. W. C.; Overman, L. E.; Pennington, L. D. *J. Am. Chem. Soc.* **2001**, *123*, 9033-9044.

²¹⁵ Yamamura, S.; Matsuura, T.; Terada, Y. *Tetrahedron Lett.* **2000**, *41*, 2189-2192.

Emmons olefination²¹⁶ as useful transform for the generation of the vinyl ether double bond of AVE **10**. For the synthesis of the required phosphonate **245** a rhodium(II)-catalysed OH-insertion between diazo phosphonate **246** and allylic alcohol **11** might be utilized (Scheme 67). The application of a sequence of a rhodium(II)-catalyzed OH-insertion²¹⁷ and a Horner-Wadsworth-Emmons olefination for the synthesis of alkoxy carbonyl-substituted vinyl ether double bonds was first reported by Sinaÿ and co-workers.²¹⁸ Further successful applications of this two step strategy were realised independently by Ganem,²¹⁹ and Berchtold.²²⁰ An intramolecular approach was developed by Moody and co-workers.²²¹



Scheme 67: Retrosynthetic analysis led to allyl alcohol **11**. TBS= *tert*-butyldimethylsilyl [$\text{Si}(t\text{-Bu})\text{Me}_2$], Bn= benzyl, HWE= Horner-Wadsworth-Emmons olefination.

For the synthesis of the crucial *Z*-configured allylic alcohol **11** a *B*-alkyl Suzuki-Miyaura cross coupling²²² between boron **247** and vinyl iodide **248** might be attempted (Scheme 68).

²¹⁶ (a) Horner, L.; Hoffmann, H.; Wippel, H. G.; Klahre, G. *Chem. Ber.* **1959**, *92*, 2449-2507. (b) Wadsworth, W. S.; Emmons, W. D. *J. Am. Chem. Soc.* **1961**, *83*, 1733-1738.

²¹⁷ For a review concerning the OH-insertion see: Miller, D. J.; Moody, C. J. *Tetrahedron* **1995**, *51*, 10821-10843.

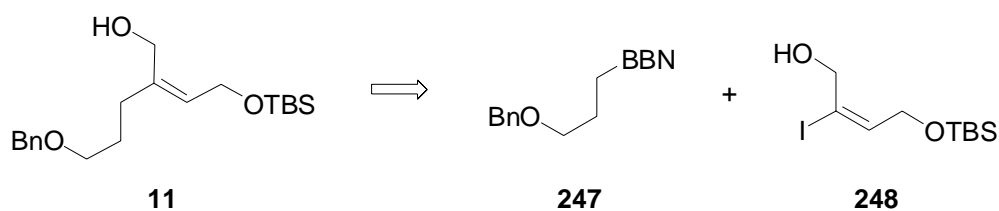
²¹⁸ (a) Paquet, F.; Sinaÿ, P. *Tetrahedron Lett.* **1984**, *25*, 3071-3074. (b) Paquet, F.; Sinaÿ, P. *J. Am. Chem. Soc.* **1984**, *106*, 8313-8315. See: Scheme 119, page 162.

²¹⁹ Wood, H. W.; Buser, H. P.; Ganem, B. *J. Org. Chem.* **1992**, *57*, 178-184.

²²⁰ (a) Pawlak, J. L.; Berchtold, G. A. *J. Org. Chem.* **1987**, *52*, 1765-1771. (b) Lesuisse, D.; Berchtold, G. A. *J. Org. Chem.* **1988**, *53*, 4992-4997. (c) Mattia, K. M.; Ganem, B. *J. Org. Chem.* **1994**, *59*, 720-728.

²²¹ (a) Davies, M. J.; Moody, C. J. *J. Chem. Soc., Perkin Trans. 1* **1991**, 1-8. (b) Davies, M. J.; Moody, C. J. *J. Chem. Soc., Perkin Trans. 1* **1991**, 9-17.

²²² Miyaura, N.; Ishiyama, T.; Ishikawa, M.; Suzuki, A. *Tetrahedron Lett.* **1986**, *27*, 6369-6372.



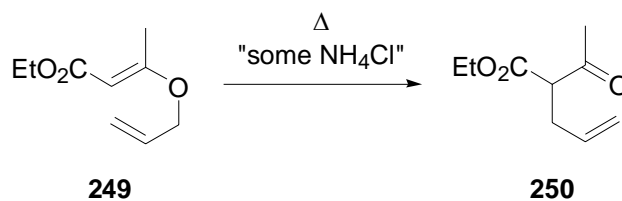
Scheme 68: Retrosynthetic analysis of allylic alcohol **11**. BBN= borabicyclo[3.3.1]nonane, TBS= *tert*-butyldimethylsilyl [Si(*t*-Bu)Me₂], Bn= benzyl.

In the following section (37 pages) I will outline important characteristics of the key CC-connecting step: the aliphatic Claisen rearrangement. The historical development as well as mechanistic considerations will be discussed. A particular focus is set on the simple and the induced diastereo- and enantioselectivity and especially the catalytic asymmetric Claisen rearrangement CAC. Furthermore, characteristics and recent applications of the essentially involved copper(II)-bis(oxazoline) complex (*S,S*)-**234a** are covered. Readers who are mainly interested in the synthetic strategy and the results of the present work are referred to chapter 13 (page 144).

11 The Catalytic Asymmetric Claisen Rearrangement (CAC)

11.1 Historical Development and Important Variations

The term ‘Claisen rearrangement’²²³ is used for the [3,3]-sigmatropic rearrangement²²⁴ of allyl vinyl ethers generating γ,δ -unsaturated carbonyl compounds.²²⁵ The first example was reported by Ludwig Claisen in 1912 (Eq. 33).²²⁶ The distillation of *O*-allylated ethyl acetoacetate **249** in the presence of NH_4Cl afforded the γ,δ -unsaturated ketone **250**.



Eq. 33

During the nine decades after its discovery, the reaction has gained a lot of attention and today, certainly belongs to the most important synthetic methods for CC-bond formation. The major strengths of the transformation can be summarized as following:

- An easier accessible C-Het-bond is transformed into a CC- σ -bond that is usually more difficult to install.
- Up to two adjacent chirality centres and one stereogenic double bond are formed with high diastereoselectivity.
- The reaction conditions are tolerable for a wide range of different functional groups.

A great number of variations have been developed. Replacing the oxygen atom by other heteroatoms, aza-²²⁷ and thio-analogues²²⁸ were introduced. Utilization of alternative starting materials for the Claisen rearrangement allowed the access to other useful target structures.

²²³ The present discussion covers exclusively the aliphatic Claisen rearrangement.

²²⁴ The description of the Claisen rearrangement as a [3,3]-sigmatropic event refers to a numeration which focus the bond that will be broken. The atoms that form that bond are given the numbers 1 and 1' respectively. Consequently, the new bond is formed between the atom C3 and C3'.

²²⁵ For reviews see: (a) Castro, A. M. M. *Chem. Rev.* **2004**, *104*, 2939-3002. (b) Ziegler, F. E. *Chem. Rev.* **1988**, *88*, 1423-1452.

²²⁶ Claisen, L. *Ber. Dtsch. Chem. Ges.* **1912**, *45*, 3157-3167.

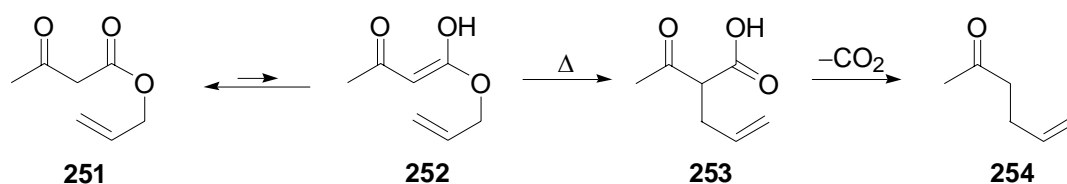
²²⁷ Bennett, G. B. *Synthesis* **1977**, 589-606.

²²⁸ Takahashi, H.; Oshima, K.; Yamamoto, H.; Nozaki, H. *J. Am. Chem. Soc.* **1973**, *95*, 5803-5804.

Often, intermediary formed ketene acetals were employed. For some of the most noteworthy examples the basic structural features and typical reaction conditions are given below.

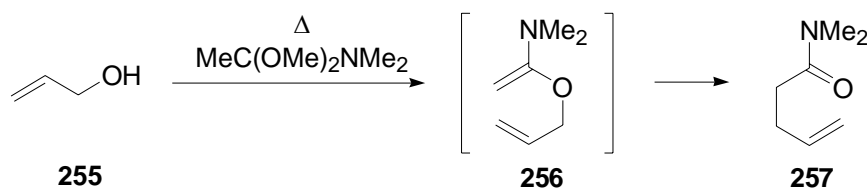
Carroll-Claisen rearrangement

In 1940 the thermal rearrangement of β -keto esters **251** was described.²²⁹ The reaction is terminated by the decarboxylation of **253** yielding γ,δ -unsaturated ketones **254** (Eq. 34).



Eschenmoser-Claisen rearrangement

Eschenmoser reported the [3,3]-sigmatropic rearrangement of *N,O*-ketene acetals **256** which were formed intermediary upon heating of a mixture of an amide acetale and an allylic alcohol **255**.²³⁰ The products of these transformations are γ,δ -unsaturated amides **257** (Eq. 35).



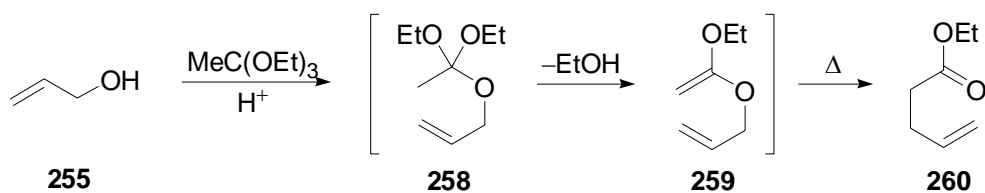
Johnson-Claisen rearrangement

In the attempt of Johnson and co-workers in 1970, allylic alcohols **255** were subjected to an orthoacetate in the presence of trace amounts of a weak acid.²³¹ The intermediary formed ketene acetals **259** rearranged to yield γ,δ -unsaturated esters **260** (Eq. 36).

²²⁹ (a) Carroll, M. F. *J. Chem. Soc.* **1940**, 704-706. (b) Carroll, M. F. *J. Chem. Soc.* **1940**, 1266-1268. (c) Carroll, M. F. *J. Chem. Soc.* **1941**, 507-510.

²³⁰ (a) Wick, A. E.; Felix, D.; Steen, K.; Eschenmoser, A. *Helv. Chim. Acta.* **1964**, *47*, 2425-2429. (b) Wick, A. E.; Felix, D.; Gschwend-Steen, K.; Eschenmoser, A. *Helv. Chim. Acta.* **1969**, *52*, 1030-1042.

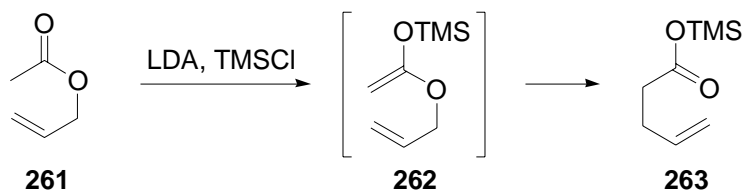
²³¹ Johnson, W. S.; Werthemann, L.; Bartlett, W. R.; Brocksom, T. J.; Li, T. T.; Faulkner, D. J.; Peterson, M. R. *J. Am. Chem. Soc.* **1970**, *92*, 741-743.



Ireland-Claisen rearrangement

The Ireland Claisen rearrangement, introduced in 1972,²³² has attracted great attention especially in recent efforts to develop asymmetric variations of the Claisen rearrangement.²³³

Allyl trimethylsilyl ketene acetals **262** underwent the [3,3]-rearrangement at low temperatures (ambient temperature or below). As a result of the transformation γ,δ -unsaturated silyl esters **263** are formed (Eq. 37).



The major advantage of these substrates is the possibility to control the vinyl ether double bond configuration simply by the choice of the deprotonation conditions.²³⁴ The Ireland Claisen rearrangement proceeds under basic or neutral conditions and at exceptionally low temperatures. It was later expanded to allylic ester enolates of various other metals used as Lewis acid accelerators of the reaction.²³⁵

Miscellaneous

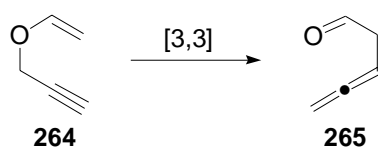
The Claisen rearrangement of propargyl vinyl ethers results in the formation of allenes (Eq. 38).

²³² (a) Ireland, R. E.; Mueller, R. H. *J. Am. Chem. Soc.* **1972**, *94*, 5897-5898. (b) Ireland, R. E.; Willard, A. K. *Tetrahedron Lett.* **1975**, *46*, 3975-3978. (c) Ireland, R. E.; Mueller, R. H.; Willard, A. K. *J. Am. Chem. Soc.* **1976**, *98*, 2868-2877.

²³³ For a more detailed discussion, see chapter 11.3.3.

²³⁴ For a more detailed discussion, see chapter 11.2.3.

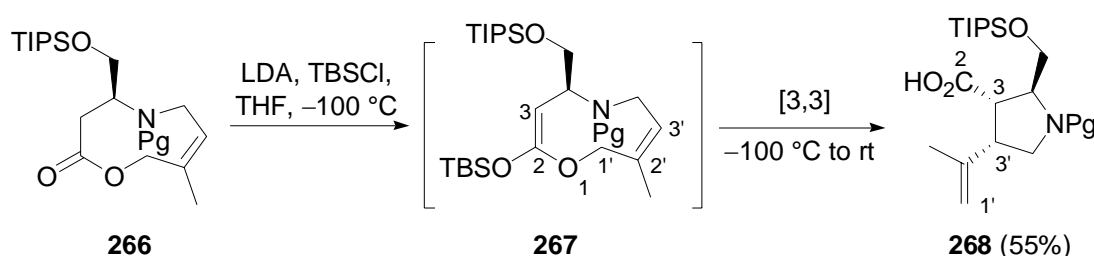
²³⁵ Examples of the Lewis acid accelerated Claisen rearrangement are discussed in chapter 11.3.3.



Eq. 38

Although the rearrangement of such systems usually affords special conditions (e.g. microwave irradiation) interesting target-orientated applications for highly functionalized starting materials have been reported.²³⁶

In some examples transannular variations were described.²³⁷ In these cases the allyl vinyl ether is part of a ring. The rearrangement causes ring contraction. An instructive example is given in Scheme 69.^{237c}



Scheme 69: Transannular Claisen rearrangement according to Knight *et al.*^{237c} Pg= CO₂Et, LDA= lithium diisopropylamide, TBS= *tert*-butyldimethylsilyl [Si(*t*-Bu)Me₂], TIPS= triisopropylsilyl [Si(*i*-Pr)₃].

11.2 Mechanism and Simple Diastereoselectivity

11.2.1 Mechanism

Although the mechanism of the Claisen rearrangement has been in the focus of numerous methodical²³⁸ and theoretical²³⁹ studies, the exact structure of the transition state can not be

²³⁶ Durand-Reville, T.; Gobbi, L. B.; Gray, B. L.; Ley, S. V.; Scott, J. S. *Org. Lett.* **2002**, *4*, 3847-3850.

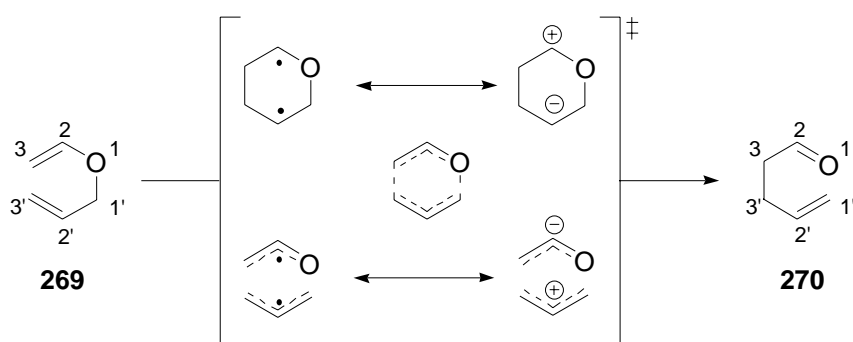
²³⁷ For some instructive examples see: (a) Frank, S. A.; Works, A. B.; Roush, W. R. *Can. J. Chem.* **2000**, *78*, 757-771. (b) Corey, E. J.; Kania, R. S. *J. Am. Chem. Soc.* **1996**, *118*, 1229-1230. (c) Cooper, J.; Knight, D. W.; Gallagher, P. T. *J. Chem. Soc., Perkin Trans. 1* **1992**, 553-559.

²³⁸ (a) Burrows, C. J.; Carpenter, B. K. *J. Am. Chem. Soc.* **1981**, *103*, 6983-6984. (b) Burrows, C. J.; Carpenter, B. K. *J. Am. Chem. Soc.* **1981**, *103*, 6984-6986. (c) Curran, D. P.; Suh, Y.-G. *J. Am. Chem. Soc.* **1984**, *106*, 5002-5004. (d) Wilcox, C. S.; Babston, R. E. *J. Am. Chem. Soc.* **1986**, *108*, 6636-6642. (e) Coates, R. M.; Rogers, B. D.; Hobbs, S. J.; Curran, D. P.; Peck, D. R. *J. Am. Chem. Soc.* **1987**, *109*, 1160-1170. (f) Gajewski, J. J.; Jurayj, J.; Kimbrough, D. R.; Gande, M. E.; Ganem, B.; Carpenter, B. K. *J. Am. Chem. Soc.* **1987**, *109*, 1170-1186.

²³⁹ (a) Carpenter, B. K. *Tetrahedron* **1978**, *34*, 1877-1884. (b) Dewar, M. J. S.; Healy, E. F. *J. Am. Chem. Soc.* **1984**, *106*, 7127-7131. (c) Vance, R. L.; Rondan, N. G.; Houk, K. N.; Bordan, W. T. *J. Am. Chem. Soc.* **1988**, *110*, 2314-2315. (d) Wiest, O.; Black, K. A.; Houk, K. N. *J. Am. Chem. Soc.* **1994**, *116*, 10336-10337. (e) Wiest, O.; Houk, K. N.; Black, K. A.; Thomas, B. *J. Am. Chem. Soc.* **1995**, *117*, 8594-8599. (g) Wiest, O.; Montiel, D. C.; Houk, K. N. *J. Phys. Chem. A* **1997**, *101*, 8378-8388. (h) Meyer, M. P.; DelMonte, A. J.; Singleton, D. A. *J.*

exactly defined. The bond breaking and bond formation are concerted. Ideally, the concerted bond reorganisation proceeds through a quasi aromatic transition state (Scheme 70, middle). However, in most cases bond breaking and bond formation are not equally advanced resulting in two mechanistic borderline cases:

- If the bond formation is more advanced than the bond breaking the transition state can be described as a 1,4-diyli (Scheme 70, top).
- In contrast, if the bond breaking is further advanced than the bond formation, the transition state is best represented by a bisallyl (Scheme 70, bottom).



Scheme 70: The bond reorganisation of the Claisen rearrangement is concerted. Two mechanistic borderline cases are possible to describe the nature of the transition state.

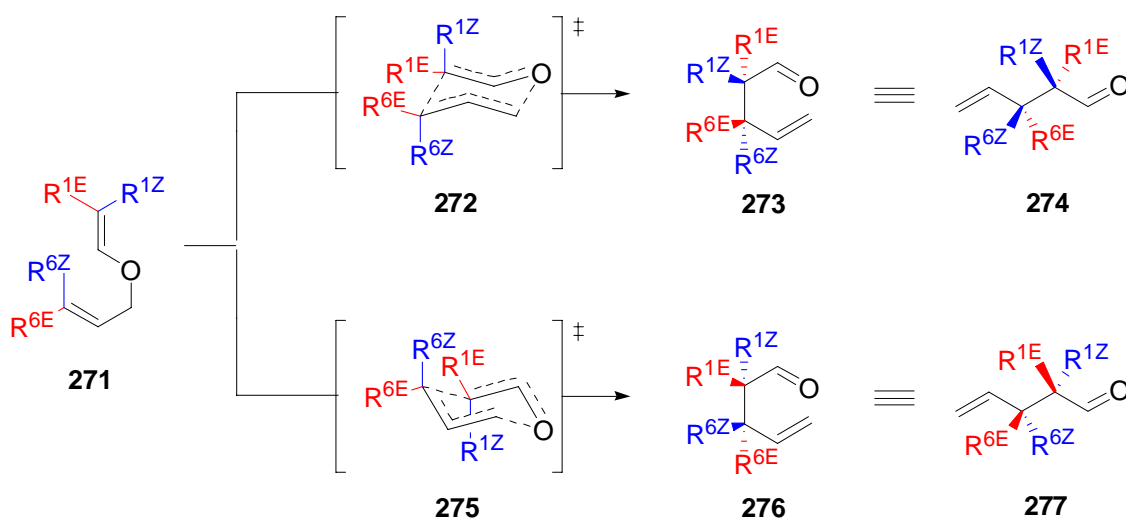
The real structure of the transition state can be visualized with a More-O'Ferrall-Jencks diagram.²⁴⁰ The location of the transition state within this plot depends both on the substitution patterns and the reaction conditions.

Am. Chem. Soc. **1999**, *121*, 10865-10874. (i) Guner, V.; Khuong, K.S.; Leach, A.G.; Lee, P. S.; Bartberger, M. D.; Houk, K. N. *J. Phys. Chem. A* **2003**, *107*, 11445-11459. (j) Dewar, M. J. S.; Jie, C. *J. Am. Chem. Soc.* **1989**, *111*, 511-519. (k) Gajewski, J. J.; Gee, K. R.; Jurayj, J. *J. Org. Chem.* **1990**, *55*, 1813-1882. (l) Sehgal, A.; Shao, L.; Gao, J. *J. Am. Chem. Soc.* **1995**, *117*, 11337-11340. (m) Hrovat, D. A.; Beno, B. R.; Lange, H.; Yoo, H. J.; Houk, K. N. *J. Am. Chem. Soc.* **1999**, *121*, 10529-10537. (n) Coates, R. M.; Rogers, B. D.; Hobbs, S. J.; Peck, D. R.; Curran, D. P. *J. Am. Chem. Soc.* **1987**, *109*, 1160-1170. (o) Yoo, H. Y.; Houk, K. N. *J. Am. Chem. Soc.* **1997**, *119*, 2877-2884. (p) Aviyente, V.; Yoo, H. Y.; Houk, K. N. *J. Org. Chem.* **1997**, *62*, 6121-6128. (q) Aviyente, V.; Houk, K. N. *J. Phys. Chem. A* **2001**, *105*, 383-391. (r) Severance, D. L.; Jørgensen, W. L. *J. Am. Chem. Soc.* **1992**, *114*, 10966-10968. (s) Wiest, O.; Houk, K. N. *J. Org. Chem.* **1994**, *59*, 7582-7584. (t) Yoo, H. Y.; Houk, K. N. *J. Am. Chem. Soc.* **1994**, *116*, 12047-12048. (u) Yamabe, S.; Okumoto, S.; Hayashi, T. *J. Org. Chem.* **1996**, *61*, 6218-6226. (v) Gajewski, J. J. *Acc. Chem. Res.* **1997**, *30*, 219-225. (w) Khaledy, M. M.; Kalani, M.Y. S.; Khuong, K. S.; Houk, K. N.; Aviyente, V.; Neier, R.; Soldermann, N.; Velker, J. *J. Org. Chem.* **2003**, *68*, 572-577.

²⁴⁰ (a) More O'Farrell, R. A. *J. Chem. Soc. B* **1970**, 274-277. (b) Jencks, W. P. *Chem. Rev.* **1972**, *72*, 705-718.

11.2.2 Simple Diastereoselectivity (*Syn*-/*Anti*-Selectivity)

It is agreed that as a [3,3]-sigmatropic pericyclic reaction the Claisen rearrangement of acyclic allyl vinyl ethers shows a high preference for a chair-like transition state (Scheme 71).^{225b} If the allyl vinyl ether is substituted in 1 and 6 position the relative configuration (*syn/anti*)²⁴¹ of the newly generated chirality centers is controlled by the configuration of the stereogenic double bonds.

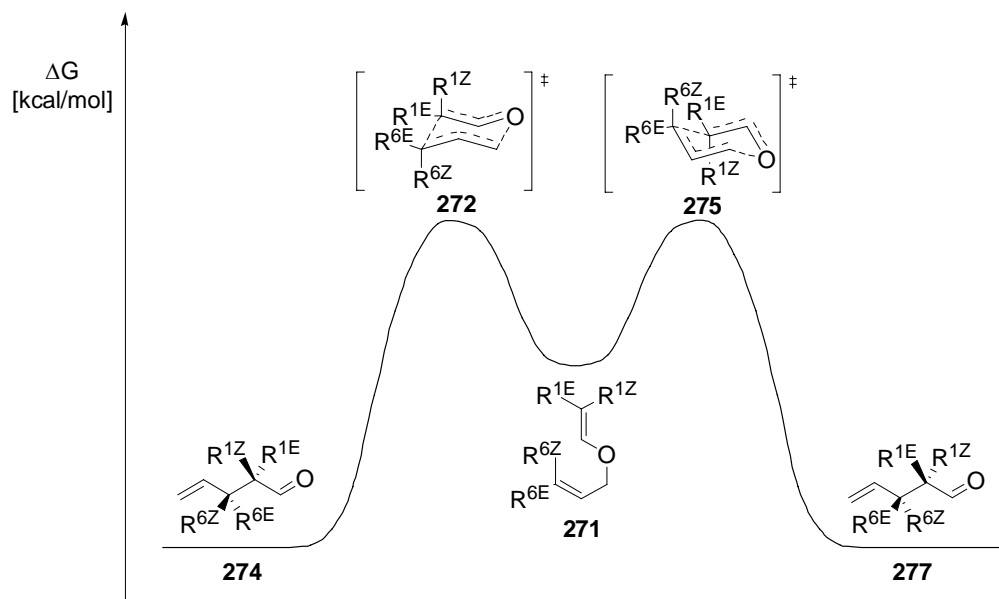


Scheme 71: Idealized presentation of the concerted nature of the transition state of the Claisen rearrangement: Both enantiomeric transition states are shown for allyl vinyl ether **271** substituted in 1- and 6-position.²⁴²

As illustrated in Scheme 72, the rearrangement of **271** proceeds through either of the two possible enantiomeric transition states **272** or **275** possessing identical energies. Therefore, the Claisen rearrangement of achiral allyl vinyl ethers affords racemic products.

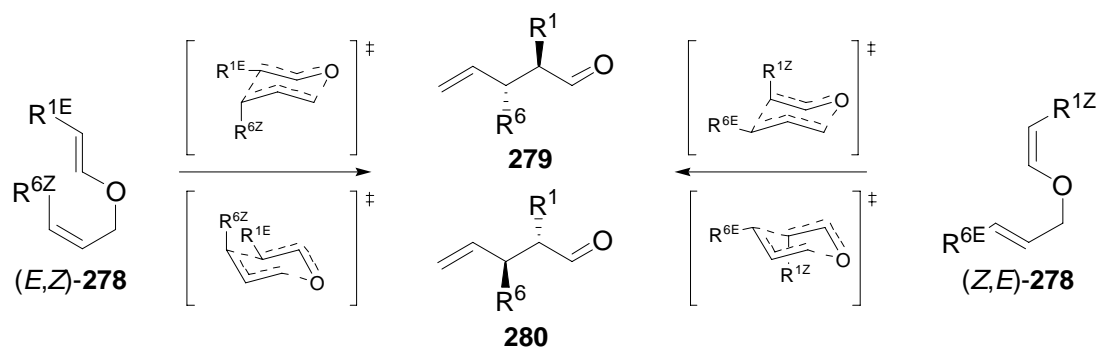
²⁴¹ The terms '*syn*' and '*anti*' are employed with respect to the relative configuration of the substituents at C1 and C6 adopted in a zigzag presentation of the molecule.

²⁴² The equilibrium between the starting material and the transition state is not explicitly depicted. We have chosen this formulation for it allows a concise representation of the transformation proceeding through the corresponding transition states. The placing of the transition state formula within the arrow is used to emphasize that the transition state must not be seen as intermediate.



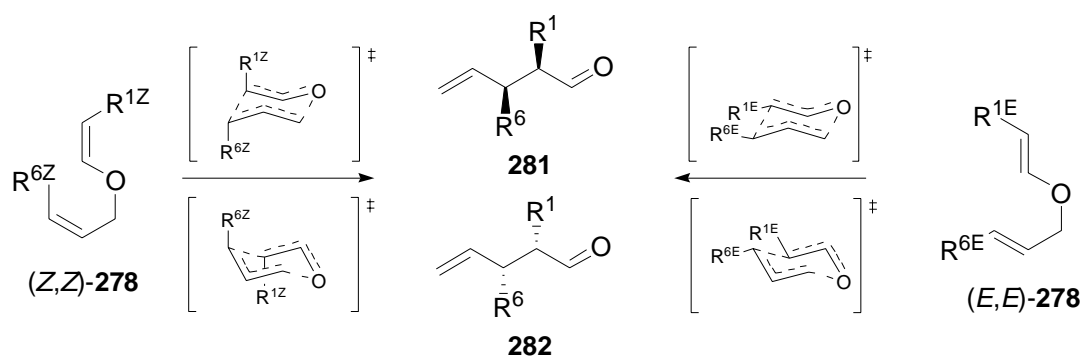
Scheme 72: The allyl fragment can approach either of the two enantiotopic faces of the vinyl ether double bond. Without external asymmetric induction the resulting transition states **272** and **275** are enantiomeric, i.e. they have identical energy values.

According to the concerted nature and the chair-like transition state, the relative configuration of the rearrangement product can be reliably predicted. As a general rule the AVEs (*E,Z*)- and (*Z,E*)-**278** rearrange to *anti*-**279/280** (Scheme 73).



Scheme 73: Rearrangement of (*E,Z*)- and (*Z,E*)-**278** affords *anti*-configured rearrangement products.

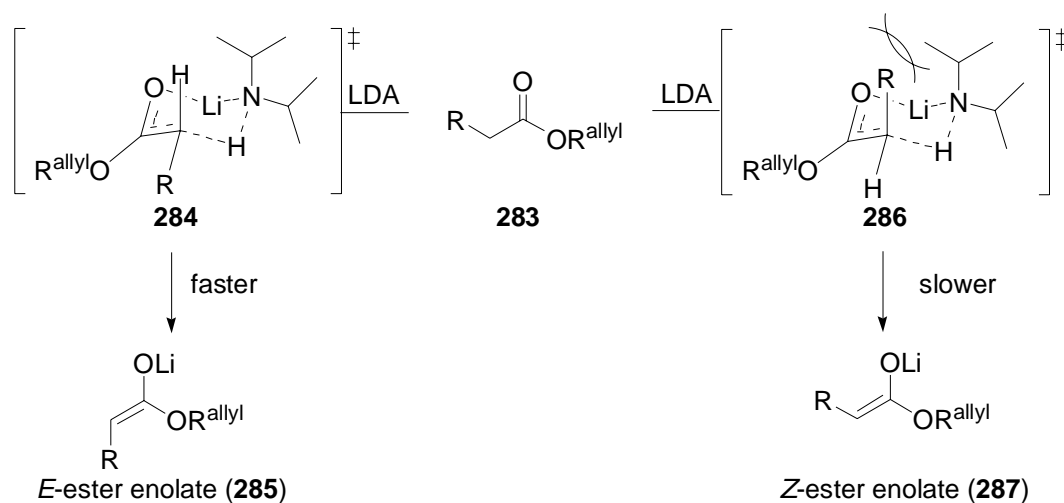
In contrast, the AVEs (*Z,Z*)- and (*E,E*)-**278** afford *syn*-**281/282** (Scheme 74).



Scheme 74: Rearrangement of (Z,Z) - and (E,E) -**278** affords *syn*-configured rearrangement products.

11.2.3 Strategies for the Diastereoselective Formation of the Vinyl Ether Double Bond

In order to achieve the rearrangement products as single diastereomers it is essential to create the starting materials as single double bond isomers - a synthetic hurdle that is often troublesome and there are only few reliable strategies to overcome this problem. The Ireland-Claisen rearrangement offers the most convenient strategy. As mentioned earlier, the choice of the deprotonation conditions may control the vinyl ether double bond configuration. The Ireland-model provides a good rationalization for the preferential formation of an *E*-ester enolate double bond during the deprotonation with LDA.²⁴³ Stronger 1,3-diaxial interactions in transition state **286** were accounted for the preferred formation of *E*-ester enolate **285** (Scheme 75).

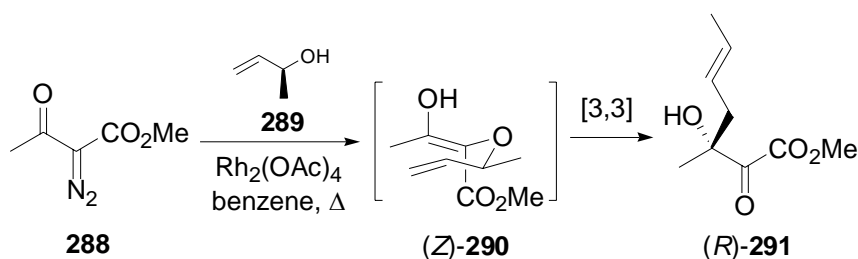


Scheme 75: Less dominant, unfavourable 1,3-diaxial interactions may be accounted to explain the preferred formation of *E*-ester enolates **285** during the deprotonation with LDA. LDA= lithium diisopropylamide.

²⁴³ Ireland, R. E.; Willard, A. K. *Tetrahedron Lett.* **1975**, *16*, 3975-3978.

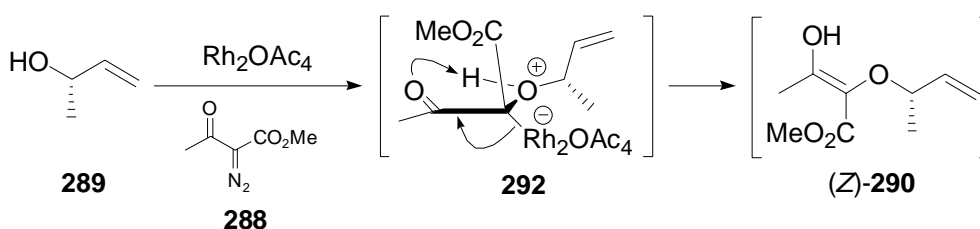
If the formation of a *Z*-ester enolate **287** is required, two of the following options may be employed. Addition of a donor solvent (e.g. HMPA) prevents the formation of the six-membered cyclic transition state. Thus the deprotonation results in the preferred generation of the thermodynamically more stable *Z*-ester enolate **287**. Similarly, utilization of bases other than LDA was found to give *Z*-ester enolate **287** predominantly.

Wood *et al.* reported a rhodium(II)-carbenoid initiated tandem OH-insertion/[3,3]-rearrangement process (Scheme 76).²⁴⁴



Scheme 76: The rhodium(II)-carbenoid initiated Claisen rearrangement proceeds via allyl vinyl ether **290** with *Z*-enol double bond geometry. Ac= acetyl.

The primary addition product of the allylic alcohol with the rhodium(II)-carbenoid is the *Z*-configured enol (*Z*)-**290**. It was speculated,²⁴⁴ that the high preference for the formation of the *Z*-configured enol double bond is a consequence of an intramolecular proton transfer (Scheme 77).

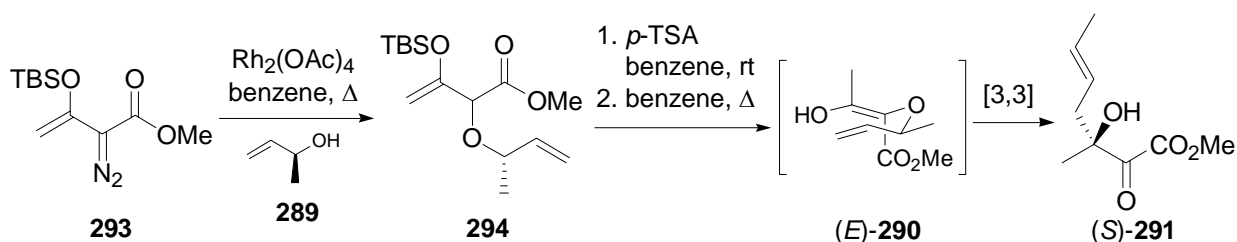


Scheme 77: The highly selective formation of the *Z*-configured enol may be rationalized by an intramolecular proton transfer.

The formation of a silyl enol ether **293** prior to the insertion prevented the intramolecular proton transfer. After the enol ether cleavage the thermodynamically more stable (*E*)-**290** is generated. Consequently, Claisen rearrangement of (*E*)-**290** resulted in the formation of the

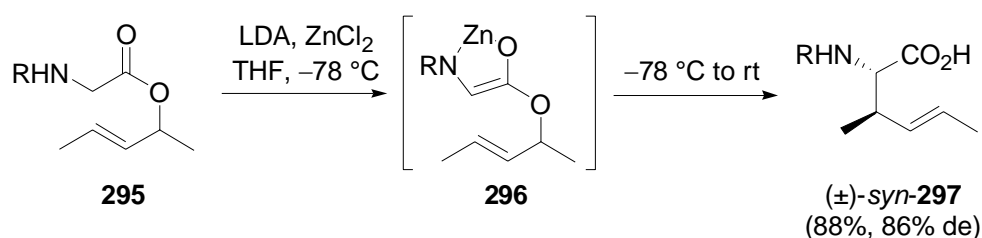
²⁴⁴ Wood, J. L.; Moniz, G. A. *Org. Lett.* **1999**, *1*, 371-374. Even though 1,3-chirality transfer is involved in this example, it is included in this chapter for it represents an interesting variation to allow the diastereoselective formation of the vinyl ether double bond.

enantiomeric rearrangement product (*S*)-**291** (Scheme 78). Employing this strategy allowed an enantioselective access to both of the possible enantiomers of **291**.²⁴⁵



Scheme 78: Enantiomeric rearrangement products (*S*)-**291** are accessible by formation of the silyl enol ether prior to the OH-insertion. Ac= acetyl, TBS= *tert*-butyldimethylsilyl [Si(*t*-Bu)Me₂], TSA= toluene sulfonic acid.

Another interesting alternative is the so-called chelate-enolate-Claisen rearrangement.²⁴⁶ The additional Lewis basic position results in the formation of a chelate complex. Consequently the *E*-enolate is preferentially formed (Scheme 79).



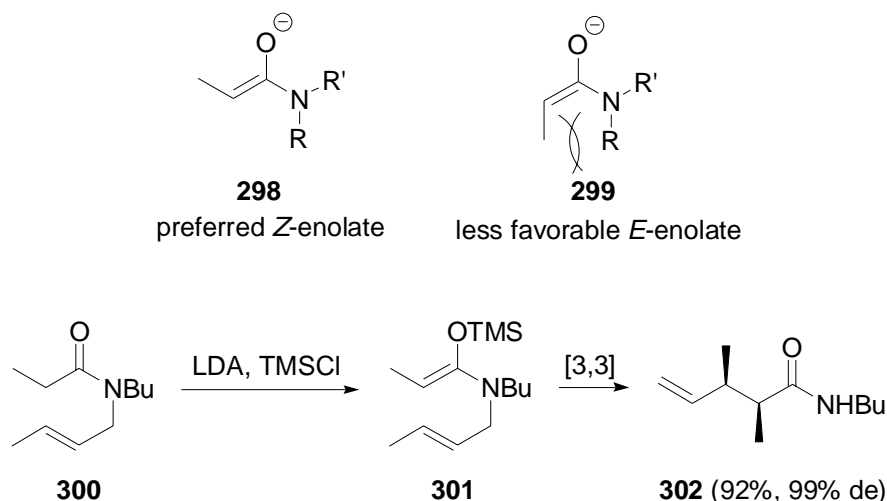
Scheme 79: Chelate formation controls the geometry of the vinyl ether double bond. R= benzyloxycarbonyl, LDA= lithium diisopropylamide.

Aza-Ireland-Claisen rearrangements of (*E*)-**300** afforded *syn*-**302** with excellent diastereoselectivity. It was assumed, that a steric interactions between the methyl group and the substituents on the nitrogen atom led to the preferred formation of the *Z*-enolate **298** and consequently to the generation of the *syn*-configured rearrangement product (Scheme 80).²⁴⁷

²⁴⁵ Wood, J. L.; Monitz, G. A.; Pflum, D. A.; Stoltz, B. M.; Holubec, A. A.; Dietrich, H.-J. *J. Am. Chem. Soc.* **1999**, *121*, 1748-1749.

²⁴⁶ Kazmaier, U. *Angew. Chem.* **1994**, *106*, 1046-1047; *Angew. Chem., Int. Ed. Engl.* **1994**, *33*, 998-999. The chelate formation to control the vinyl ether double bond configuration was as well employed as preliminary step during Ireland-Claisen applications. For instructive examples, see: (a) Mulzer, J.; Mohr, J.-T. *J. Org. Chem.* **1994**, *59*, 1160-1165. (b) Kallmerten, J.; Gould, T. *J. Tetrahedron Lett.* **1983**, *24*, 5177-5180. (c) Burke, S. D.; Fobare, W. F.; Pacofsky, G. J. *J. Org. Chem.* **1983**, *48*, 5221-5228.

²⁴⁷ Tsunoda, T.; Sasaki, O.; Itô, S. *Tetrahedron Lett.* **1990**, *31*, 727-730.



Scheme 80: Preferred formation of *Z*-enolates **298** during aza-Claisen rearrangements. LDA= lithium diisopropylamide, TMS= trimethylsilyl [SiMe₃].

11.3 Induced Diastereo- and Enantioselectivity during Claisen Rearrangements

Beside the simple diastereoselectivity, affords have been made to develop enantioselective and/or diastereoselective variations. There are four different possible strategies for the induction of enantio- or diastereoselectivity:

- substrate induction (11.3.1),
- auxiliary induction (11.3.2),
- reagent induction (11.3.3),
- or catalyst induction (11.3.4).

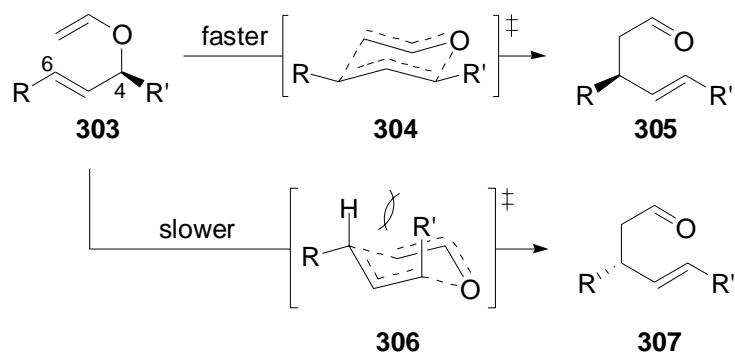
11.3.1 Substrate-Induced Diastereo- and Enantioselectivity: 1,3-Chirality Transfer and Remote Stereocontrol

Numerous applications of substrate-induced diastereo- and enantioselectivity have been successfully employed in total syntheses.²⁴⁸ In those examples, the 1,3-chirality transfer is the most frequently utilized strategy to achieve substrate-induced enantioselectivity.²⁴⁹ The

²⁴⁸ For some instructive examples, see: (a) Mulzer, J.; Mohr, J.-T. *J. Org. Chem.* **1994**, *59*, 1160-1165. (b) Kawasaki, T.; Ogawa, A.; Takashima, Y.; Sakamoto, M. *Tetrahedron Lett.* **2003**, *44*, 1591-1593.

²⁴⁹ We prefer to use a different numbering for the allyl vinyl ether with the vinyl ether double bond located between the carbon atoms C1 and C2 and the allyl ether double bond between carbon atoms C5 and C6. The historical numbering is reflected in the terms '[3,3]-sigmatropic rearrangement' and '1,3-chirality transfer'. In

absolute configuration of the oxygen-substituted carbon atom C4 will merge into the newly formed stereogenic center with complete stereocontrol.²⁵⁰ As depicted in Scheme 81, the presence of the chirality center leads to the availability of two energetically distinct transition states.



Scheme 81: Representative scenario for a 1,3-chirality transfer. The presence of a substituent at C4 results in two diastereomorphous transition states for the Claisen rearrangement.²⁴²

Remote stereocontrol has also been reported. In those examples, the chirality center is attached to carbon atom C1 or C6. A number of instructive examples were reviewed and thoroughly discussed recently by Nubbemeyer.²⁵¹

11.3.2 Auxiliary-Induced Diastereoselectivity

Chiral auxiliaries might be employed for diastereoselective versions of the Claisen rearrangement. The presence of the additional stereogenic center(s) in the auxiliary enables the more easy separation of the resulting diastereomers. Auxiliary-induced diastereoselectivity may be detected by usual NMR-techniques. The major drawback is the requirement of two additional synthetic steps: one for the introduction and the second for the removal of the auxiliary. The principles of the induction are similar to those of the remote stereocontrol. Some applications of this strategy are given below.

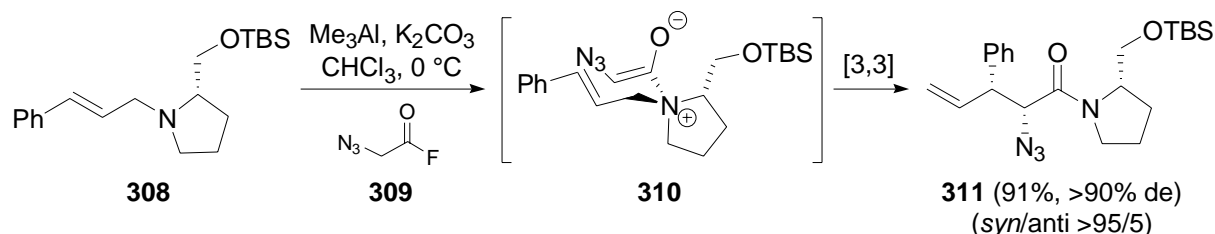
The aza-Claisen rearrangement allows the introduction of a chiral auxiliary bound to the nitrogen. However, high temperatures were required to initiate the aza-Ireland Claisen

this thesis, numbering starts at the potentially broken bond in either direction with 1 and 1' respectively. The new bond will be formed between carbon atoms C3 and C3'.

²⁵⁰ Fujii, K. *Chem. Rev.* **1993**, *93*, 2037-2066.

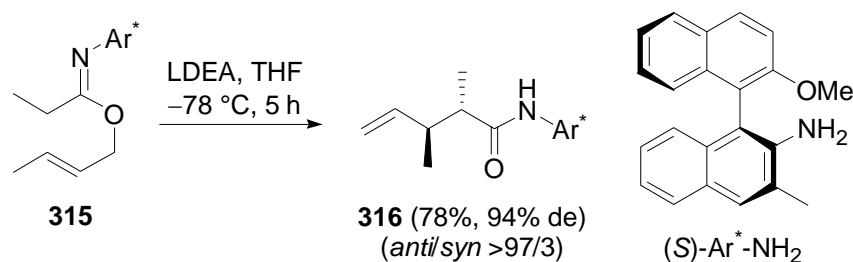
²⁵¹ Nubbemeyer, U. *Synthesis* **2003**, 961-1008.

rearrangement resulting in low diastereoselectivities.²⁵² This problem was solved by the application of a zwitterionic aza-Claisen rearrangement (Scheme 82).²⁵³ The presence of the OTBS-group in the rearrangement product **311** enabled the smooth cleavage of the auxiliary.²⁵⁴



Scheme 82: Zwitterionic aza-Claisen rearrangement according to Nubbemeyer. TBS= *tert*-butyldimethylsilyl [Si(*t*-Bu)Me₂].

During the Eschenmoser-Claisen rearrangements, nitrogen-bound auxiliaries allow the generation of the corresponding γ,δ -unsaturated amides **316** with high auxiliary-induced diastereoselectivity (Scheme 83).²⁵⁵

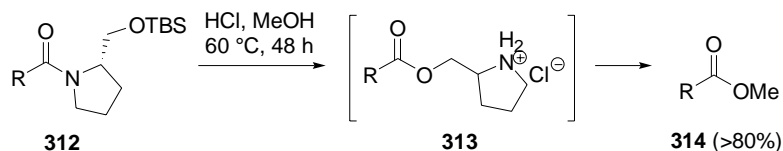


Scheme 83: Auxiliary induced diastereoselectivity in the Eschenmoser-Claisen rearrangement. LDEA= lithium diethylamide.

²⁵² (a) Tsunoda, T.; Ozaki, F.; Shirakata, N.; Tamaoka, Y.; Yamamoto, H.; Itô, S. *Tetrahedron Lett.* **1996**, *37*, 2463-2466. (b) Tsunoda, T.; Nishii, T.; Yoshizuka, M.; Yamasaki, C.; Suzuki, T.; Itô, S. *Tetrahedron Lett.* **2000**, *41*, 7667-7671.

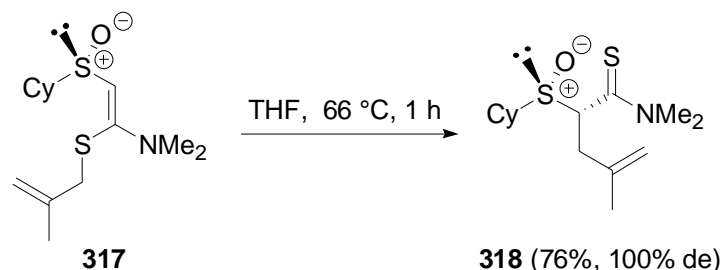
²⁵³ (a) Laabs, S.; Scherrmann, A.; Sudau, A.; Diedrich, M.; Kierig, C.; Nubbemeyer, U. *Synlett* **1999**, 25-28. (b) Laabs, S.; Münch, W.; Bats, J.-W.; Nubbemeyer, U. *Tetrahedron* **2002**, *58*, 1317-1334. (c) Zhang, N.; Nubbemeyer, U. *Synthesis* **2002**, 242-252.

²⁵⁴ Cleavage of the silylether led to the formation of ammonium ester **313** that, upon transesterification, provided ester **314**.

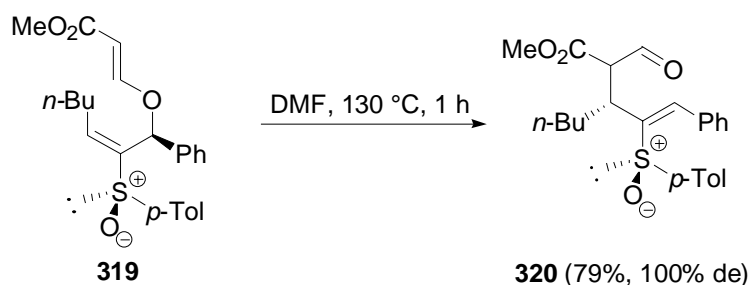


²⁵⁵ (a) Hungerhoff, B.; Metz, P. *Tetrahedron* **1999**, *55*, 14941-14946. (b) Hungerhoff, B.; Metz, P. *J. Org. Chem.* **1997**, *62*, 4442-4448.

Metzner *et al.* successfully employed chiral sulfoxides as highly efficient stereodirecting groups. Representative examples with the sulfoxide bound to C1 or C5 are depicted in Eq. 39²⁵⁶ and Eq. 40²⁵⁷.

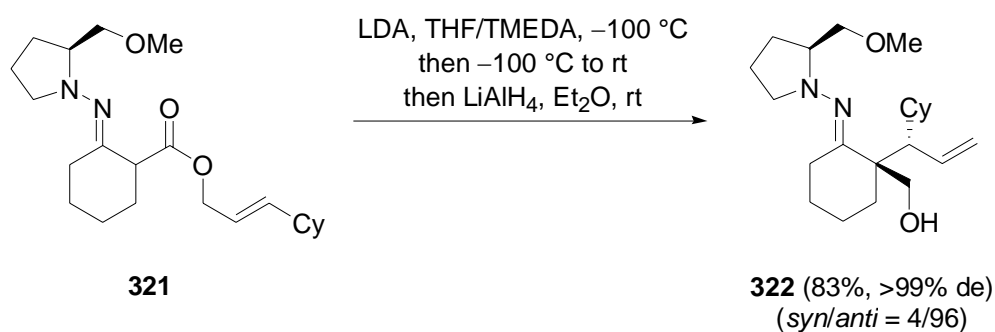


Eq. 39 Cy= cyclohexyl.



Eq. 40 Tol= toluenyl.

The successful utilization of the RAMP/SAMP-methodology for a Carroll-Claisen rearrangement was reported by Enders *et al.*²⁵⁸ The hydrazones **321** rearranged in good yields and usually with high auxiliary induced diastereoselectivity (Scheme 84).



Scheme 84: The chiral SAMP auxiliary efficiently induced diastereoselectivity during the Carroll-Claisen rearrangement LDA= lithium diisopropylamide, TMEDA= *N,N,N',N'*-tetramethylethylenediamine, Cy= cyclohexyl.

²⁵⁶ Nowaczyk, S.; Alayrac, C.; Reboul, V.; Metzner, P.; Averbuch-Pouchot, M.-T. *J. Org. Chem.* **2001**, *66*, 7841-7848.

²⁵⁷ Fernandez de la Pradilla, R.; Montero, C.; Tortosa, M. *Org. Lett.* **2002**, *4*, 2373-2376.

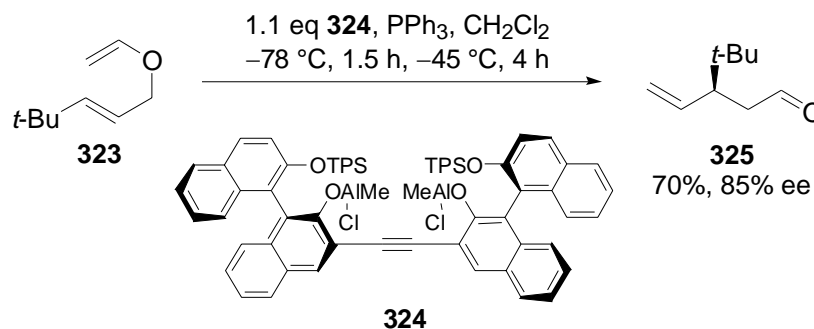
²⁵⁸ (a) Enders, D.; Knopp, M.; Runsink, J.; Raabe, G. *Angew. Chem.* **1995**, *107*, 2442-2445; *Angew. Chem., Int. Ed. Eng.* **1995**, *34*, 2278-2280. (b) Enders, D.; Knopp, M.; Runsink, J.; Raabe, G. *Liebigs Ann.* **1996**, 1095-1116.

11.3.3 Reagent-Induced Enantioselectivity

In recent years, various examples for reagent-induced enantioselectivity have been developed.²⁵⁹ Important examples are highlighted below.

Aluminium(III)

Lewis acids based on aluminium were found to accelerate the Claisen rearrangement.²⁶⁰ Maruoka and Yamamoto developed different chiral Lewis acids based on aluminium. The focus of Maruoka's work is laid upon bidentate Lewis acids.²⁶¹ The efforts culminated in the development of the chiral bidentate organoaluminium Lewis acid **324** that was successfully tested as chiral accelerator of the Claisen rearrangement of **323** (Eq. 41).²⁶²



Eq. 41 TPS= *tert*-butyldiphenylsilyl [$\text{Si}(t\text{-Bu})\text{Ph}_2$].

Yamamoto *et al.* developed the C_3 -symmetric chiral Lewis acids **326** based on aluminium.²⁶³ One example of a successful application is given in Scheme 85.

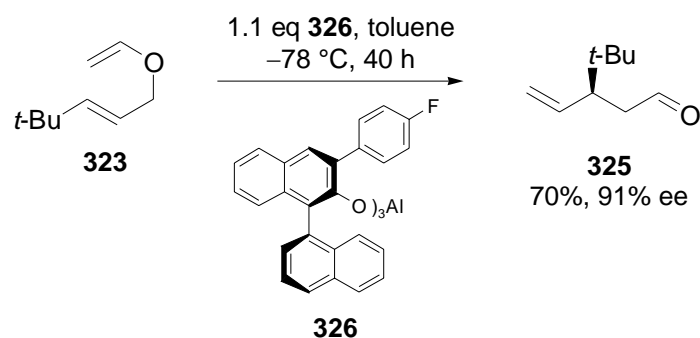
²⁵⁹ For reviews concerning the enantioselective Claisen rearrangement see: (a) Ito, H.; Taguchi, T. *Chem. Soc. Rev.* **1999**, 28, 43-50. (b) Enders, D.; Knopp, M.; Schiffrers, R. *Tetrahedron: Asymmetry* **1996**, 7, 1847-1882.

²⁶⁰ Takai, K.; Mori, I.; Oshima, K.; Nozaki, H. *Tetrahedron Lett.* **1981**, 22, 3985-3988.

²⁶¹ (a) Ooi, T.; Takahashi, M.; Maruoka, K. *J. Am. Chem. Soc.* **1996**, 118, 11307-11308. (b) Ooi, T.; Takahashi, M.; Yamada, M.; Tayama, E.; Omoto, K.; Maruoka, K. *J. Am. Chem. Soc.* **2004**, 126, 1150-1160.

²⁶² Tayama, E.; Saito, A.; Ooi, T.; Maruoka, K. *Tetrahedron* **2002**, 58, 8307-8312.

²⁶³ Maruoka, K.; Saito, S.; Yamamoto, H. *J. Am. Chem. Soc.* **1995**, 117, 1165-1166.

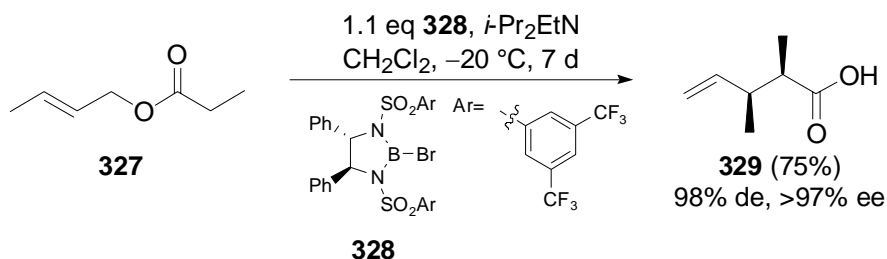


Scheme 85: Enantioselective Claisen rearrangement using the chiral Lewis acid **326** based on aluminium(III).

Unfortunately, the rearrangement products have a stronger affinity to the reagent than the substrate preventing the potential use of Lewis acids based on aluminium(III) as catalysts.²⁶⁴

Boron(III)

Corey and co-workers developed the chiral boron(III) Lewis acid **328** as accelerator of the Ireland Claisen rearrangement.²⁶⁵ The boron(III)-mediated Ireland Claisen rearrangement of **327** afforded **329** with excellent diastereo- and enantioselectivity (Scheme 86).



Scheme 86: Corey's version of a reagent-induced enantioselective Ireland-Claisen rearrangement. Ph= phenyl.

A transannular variation of the reaction was successfully employed in the total synthesis of dolabellatrienone.^{237b} However - as for the aluminium(III)-based accelerators - the reagent had to be added in at least stoichiometric amounts to give good enantioselectivities.

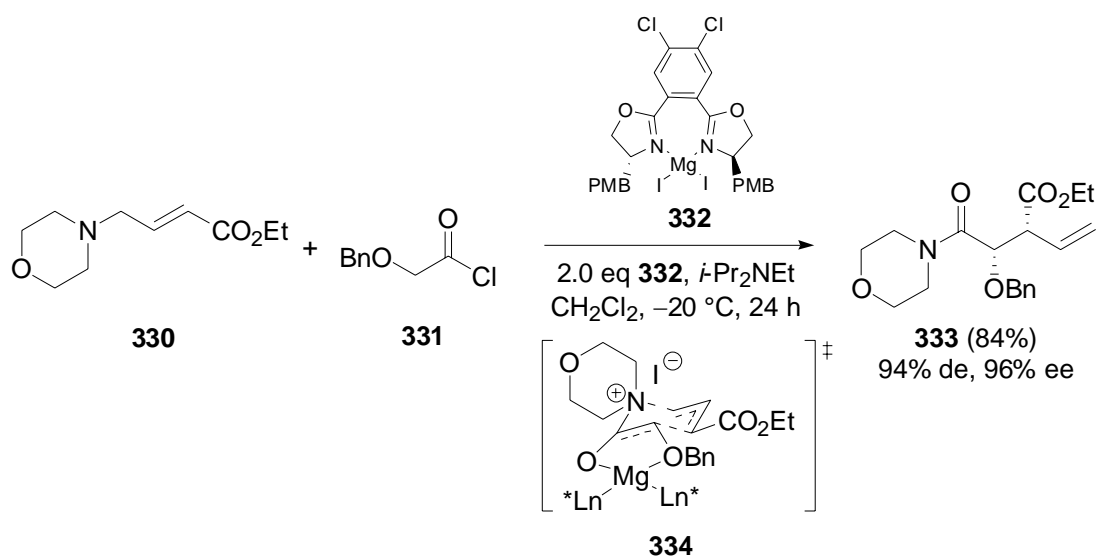
Magnesium(II)

In 2001 MacMillan *et al.* reported a chiral Lewis acid **332** based on magnesium(II) as reagent for the aza-Claisen rearrangement of morpholin derivatives (Scheme 87).²⁶⁶

²⁶⁴ The only catalytic application of an Al^{III}-based Lewis acid was published in 1996: Saito, S.; Shimada, K.; Yamamoto, H. *Chem. Lett.* **1996**, 720-722.

²⁶⁵ Corey, E. J.; Lee, D.-H. *J. Am. Chem. Soc.* **1991**, *113*, 4026-4028.

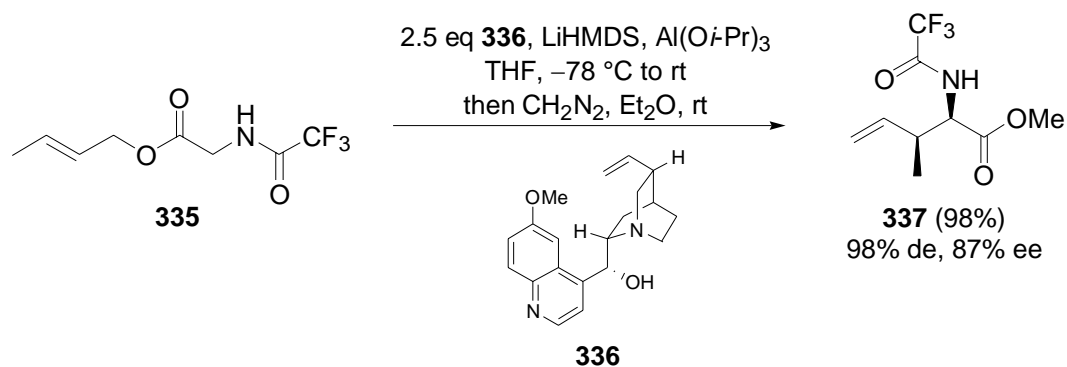
²⁶⁶ Yoon, T. P.; MacMillan, D. W. C. *J. Am. Chem. Soc.* **2001**, *123*, 2911-2912.



Scheme 87: MacMillan's asymmetric aza-Claisen rearrangement was induced by the chiral magnesium(II) complex **332**. PMB= *p*-methoxy benzyl, Bn= benzyl, Ln*= chiral Arbox ligand.

Chelate-Enolate-Claisen

In the research group of Kazmaier *et al.* chiral Lewis acids were employed for enantioselective versions of the chelate-enolate-Claisen rearrangement.²⁶⁷ Best results were achieved using the cinchona alkaloids (e.g. quinine (**336**)), Al(*Oi*-Pr)₃ as chelating metal salt and LiHMDS instead of LDA for the deprotonation. The resulting γ,δ -unsaturated amino acids **337** were formed in excellent yields. Beside high diastereoselectivity, good enantioselectivities up to 87% ee could be achieved (Scheme 88).



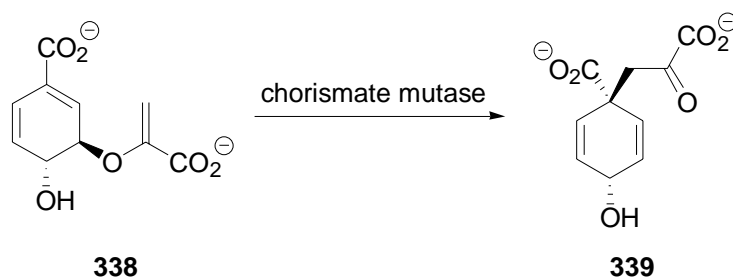
Scheme 88: Cinchona alkaloids **336** gave the best enantioselectivities when employed as chiral ligands for the chelate-enolate-Claisen rearrangement. LiHMDS= Li[N(SiMe₃)₂].

²⁶⁷ Kazmaier, U.; Mues, H.; Krebs, A. *Chem. Eur. J.* **2002**, *8*, 1850-1855.

11.3.4 Catalyst-Induced Enantioselectivity

Catalyzed Claisen Rearrangement in Biological Systems

There is only one known example for the Claisen rearrangement catalyzed by enzymes in biological systems. The Claisen rearrangement of chorismate (**338**) to prephenate (**339**) – a key step in the biosynthesis of shikimic acid which is a precursor for folate, anthranilate and aromatic amino acids²⁶⁸ - is catalyzed by the chorismate mutase (Eq. 42).²⁶⁹ The catalytic activity is believed to be the result of various non-covalent interactions.²⁷⁰



Eq. 42

Attempts, to employ organo catalyst (e.g. Brønstedt acids) for the Claisen rearrangement are limited. Pioneering work was performed by Curran *et al.*²⁷¹ Ureas were used as organo catalysts. They are assumed to cause rate acceleration by forming two hydrogen bonds to the Lewis basic oxygen atom of the substrate.²⁷² However, to induce reasonable reaction rates at 80 °C stoichiometric amounts of the Brønstedt acid were required.

First Attempts: Application of the Late Transition Metal Palladium

With the importance and the high potential of the Claisen rearrangement in mind, it is somewhat surprising that there are only few catalytic versions of the rearrangement. As it was

²⁶⁸ For a concise presentation of biosynthetic pathways involved in the biosynthesis of shikimic acids see: <http://www.chem.qmul.ac.uk/iubmb/enzyme/reaction/misc/shikim.html>

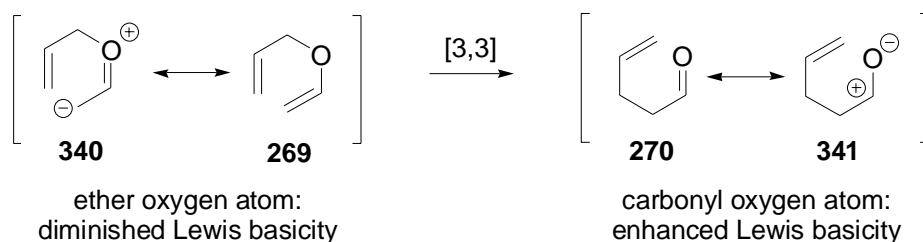
²⁶⁹ Ganem, B. *Tetrahedron* **1978**, *34*, 3353-3383.

²⁷⁰ (a) Repasky, M. P.; Guimaraes, C. R. W.; Chandrasekhar, J.; Tirado-Rives, J.; Jørgensen, W. L. *J. Am. Chem. Soc.* **2003**, *125*, 6663-6672. (b) Wiest, O.; Houk, K. N. *J. Am. Chem. Soc.* **1995**, *117*, 11628-11639. (c) Marti, S.; Andres, J.; Moliner, V.; Silla, E.; Tunon, I.; Bertran, J. *J. Phys. Chem. B* **2000**, *104*, 11308-11315. (d) Wiest, O.; Houk, K. N. *J. Org. Chem.* **1994**, *59*, 7582-7584.

²⁷¹ Curran, D. P.; Kuo, L. H. *Tetrahedron Lett.* **1995**, *36*, 6647-6650.

²⁷² (a) Connon, S. J. *Chem. Eur. J.* **2006**, *12*, 5418-5424. (b) Takemoto, Y. *Org. Biomol. Chem.* **2005**, *3*, 4299-4306.

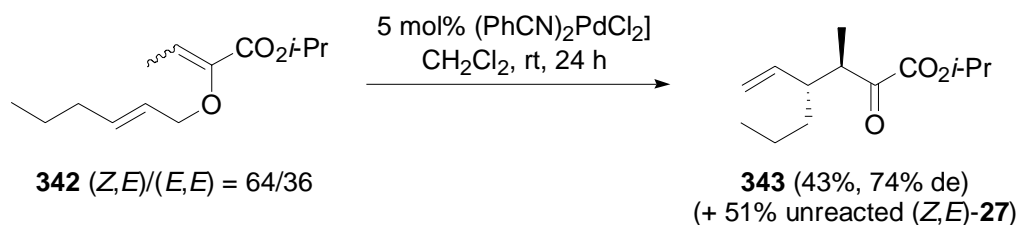
shown in the above examples (see chapter 11.3.3), Lewis acids are capable to accelerate the Claisen rearrangement. However, the major drawback results from the obvious higher Lewis basic characteristics of the rearrangement products compared to the starting materials. The reason can be rationalized by the possible mesomeric structures of starting material **269** and rearrangement product **270** (Scheme 89).



Scheme 89: The product inhibition observed often for Lewis acid accelerated Claisen rearrangements may be the result of different Lewis basic characteristics of the starting material and the rearrangement product.

The first example of a catalyzed aliphatic Claisen rearrangement was reported by van der Baan and Bickelhaupt.²⁷³ They utilized $(\text{CH}_3\text{CN})_2\text{PdCl}_2$ for their studies. Application of this catalyst to various differently substituted allyl vinyl ethers showed that the result of the rearrangement was strongly dependent on the substitution pattern of the AVEs. Only for a limited number of the tested allyl vinyl ethers the reaction afforded the rearrangement product in preparatively useful yields. As a late transition metal, palladium has a stronger affinity toward the ‘softer’ electron rich double bonds than to the ‘harder’ Lewis basic oxygen atoms. Therefore, it was proposed that the coordination to one or both of the double bonds is the reason for the catalytic effect.²⁷⁴

In initial attempts of our research group, the ability of palladium(II)-complexes to catalyze the Claisen rearrangement of 2-alkoxycarbonyl substituted allyl vinyl ethers was investigated. Only the (*E,E*)-configured AVE **342** rearranged under those conditions (Eq. 43).²⁷⁵



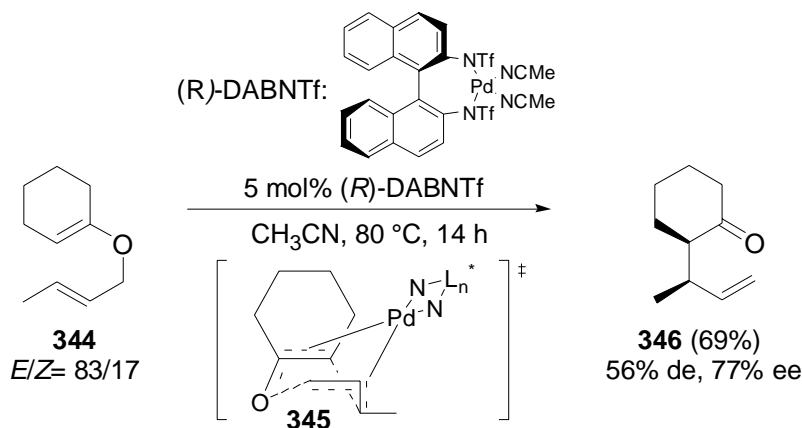
Eq. 43

²⁷³ van der Baan, J. L.; Bickelhaupt, F. *Tetrahedron Lett.* **1986**, 27, 6267-6270.

²⁷⁴ Sugiura, M.; Nakai, T. *Chem. Lett.* **1995**, 697-698.

²⁷⁵ Hiersemann, M. *Synlett* **1999**, 1823-1825.

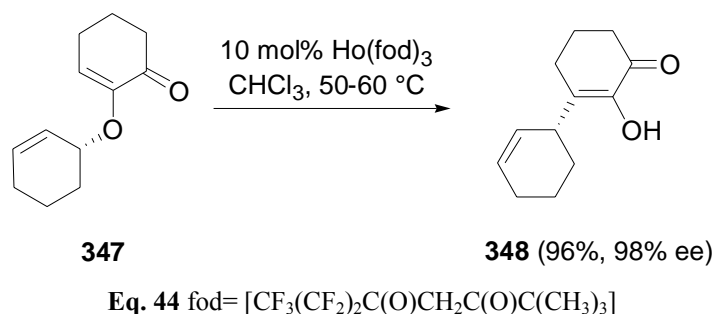
The most recent development in the field of the palladium(II) catalyzed Claisen rearrangement was published in 2004. A catalytic enantioselective Claisen rearrangement using [(*R*)-diamino-binaphthyl trifluoromethane sulfonyl amide]-Pd complex (*R*)-DABNTf was reported by Mikami and co-workers (Scheme 90).²⁷⁶ The author proposed a mechanism similar to that suggested by Nakai *et al.*²⁷⁴ The rearrangement was assumed to proceed via a boat-like transition state **345** with the palladium coordinated to both double bonds.²⁷⁴



Scheme 90: Catalytic asymmetric Claisen rearrangement employing a chiral palladium(II)-complex. Tf= trifluoromethane sulfonyl [CF_3SO_2].

New Catalysts for the Claisen Rearrangement

A milestone observation for the development of the catalytic asymmetric Claisen rearrangement (CAC) was made in 2000 by Trost *et al.* Lanthanide(III) cations were found to catalyse the Claisen rearrangement of aliphatic allyl vinyl ethers **347** (Eq. 44).²⁷⁷

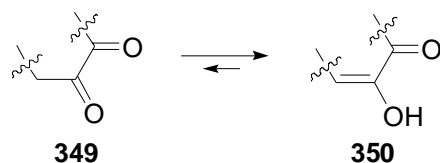


Surprisingly no product inhibition of the catalyst was observed in this case what might be rationalized by the tendency of 1,2-diketones to tautomerize to the corresponding enols

²⁷⁶ Akiyama, K.; Mikami, K. *Tetrahedron Lett.* **2004**, *45*, 7217-7220.

²⁷⁷ Trost, B. M.; Schroeder, G. M. *J. Am. Chem. Soc.* **2000**, *122*, 3785-3786.

(Scheme 91). In contrast to the carbonyl oxygen atom which possesses Lewis basic characteristics, the enol oxygen atom owns a partially positive charge due to resonance stabilization.

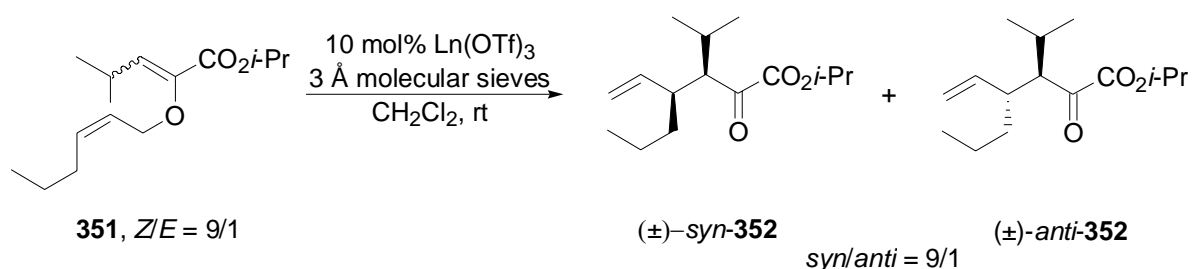


Scheme 91

Therefore, the coordination of the rearrangement product to the Lewis acid might be rendered unfavourable.

In our research group we are interested in the rearrangement of 2-alkoxycarbonyl substituted AVEs. Beside the ether oxygen atom they include a second binding site (the ester oxygen atoms) for a Lewis acidic catalyst at a spatially close position.

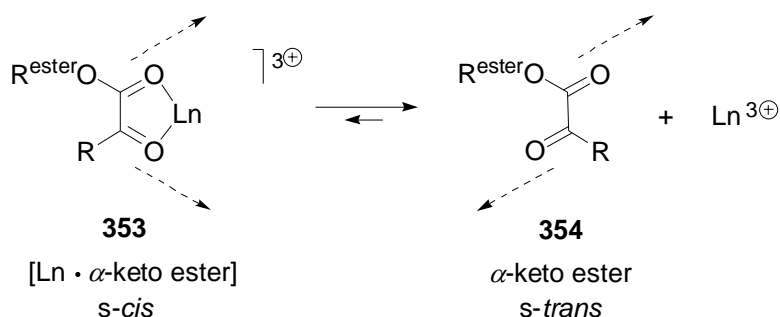
Inspired by Trosts's finding, we employed different lanthanide(III) triflates and $\text{Ce}(\text{OTf})_4$ as catalysts for the Claisen rearrangement of the AVE **351**.^{202b} With 10 mol% of the catalyst ($\text{Ln} = \text{Lu}, \text{Yb}, \text{Tm}, \text{Er}, \text{Ho}$) clean conversion was observed in CH_2Cl_2 within 6-24 h (Table 17).



| Entry | $\text{Ln}(\text{OTf})_3$ | Reaction time [h] | Yield [%] |
|-------|---------------------------|-------------------|-----------|
| 1 | $\text{Lu}(\text{OTf})_3$ | 6 | 98 |
| 2 | $\text{Yb}(\text{OTf})_3$ | 6 | 98 |
| 3 | $\text{Er}(\text{OTf})_3$ | 24 | 100 |
| 4 | $\text{Ho}(\text{OTf})_3$ | 24 | 100 |

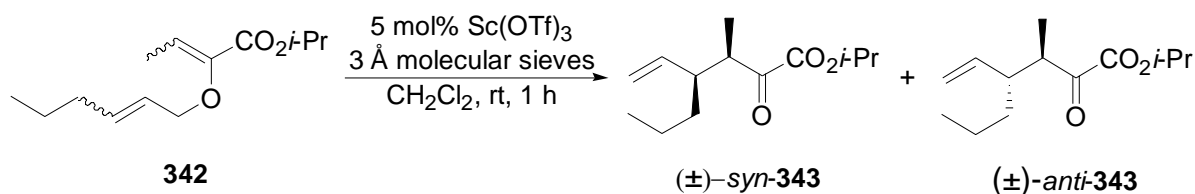
Table 17: Catalytic Claisen rearrangement using lanthanide triflates. Tf= trifluoromethane sulfonyl [CF_3SO_2]

In contrast to other Lewis acid accelerated Claisen rearrangements, no product inhibition was observed. As a reason for this finding, we suggest an unfavourable *s-cis* conformation of the two carbonyl groups present in the catalyst-product-complex (Scheme 92).



Scheme 92: An unfavourable *s-cis* arrangement of the carbonyl groups in the (lanthanide- α -keto ester) complex might enable the release of the catalyst. Ln= lanthanide(III)-cation.

Subsequent reactions were performed with the more reactive $\text{Sc}(\text{OTf})_3$ as catalyst. The isolated yields were quantitative. Interestingly, the diastereoselectivities were found to be dependent on the allyl ether double bond configuration (Table 18).

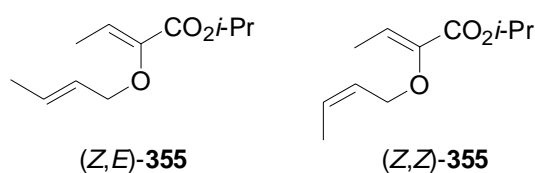


| Entry | Configuration of 342 | Yield [%] | <i>syn/anti</i> |
|-------|-----------------------------|-----------|-----------------|
| 1 | <i>Z,Z</i> | 95 | 96/4 |
| 2 | <i>E,Z</i> | 100 | 4/96 |
| 3 | <i>Z,E</i> | 98 | 44/56 |
| 4 | <i>E,E</i> | 99 | 70/30 |

Table 18: $\text{Sc}(\text{OTf})_3$ -catalysed Claisen rearrangement. Tf= trifluoromethane sulfonyl [CF_3SO_2].

AVEs with *Z*-configured allyl ether double bond rearranged with high diastereoselectivity to the corresponding α -keto esters. As expected (see chapter 11.2), (*E,Z*)-**342** gave (±)-*syn*-**343** (entry 1) while (*Z,Z*)-**342** lead to the formation of (±)-*anti*-**343** (entry 2). In contrast, for the catalyzed rearrangement of the (*Z,E*)-**342** and (*E,E*)-**342** with *E*-configured allyl ether double bond the observed diastereoselectivities are surprisingly low (entry 3 and 4).

This unexpected poor selectivity was verified by calculations performed by Julia Rehbein in our research group.²⁷⁸ It was shown, that the formation of the substrate-catalyst complex results in increased bond lengths of the **355** and therefore a formal ‘destabilization’ of the substrate. On the other hand, the smaller deviation from planarity of the vinyl ether double bond and the ester carbonyl group is enforced by the copper(II)-catalyst. This allows a better conjugation compared to the thermal rearrangement and hence contributes to a better stabilization of the transition state. This transition state stabilization in concert with the formal substrate destabilization results in a smaller activation barrier and can be accounted for the catalytic activity of the transition state metal complexes (Table 19).



| AVE | ΔG^\ddagger [kcal/mol] | |
|-----------|--------------------------------|------------------|
| | (Z,Z)-355 | (Z,E)-355 |
| Thermal | 29.9 | 28.7 |
| Catalytic | 13.0 | 8.5 |

Table 19: Calculated activation barriers for the thermal and the catalytic Claisen rearrangement of *(Z,Z)*-**355** and *(Z,E)*-**355**.

Furthermore, the transition state of the catalyzed Claisen rearrangement is significantly more dissoziative than the transition state of the thermal Claisen rearrangement (Table 20). To achieve high diastereoselectivities, a significant energy gap between boat-like and chair-like transition state is required. The calculations revealed that this energy gap is significantly decreased for the catalyzed process (Table 20).

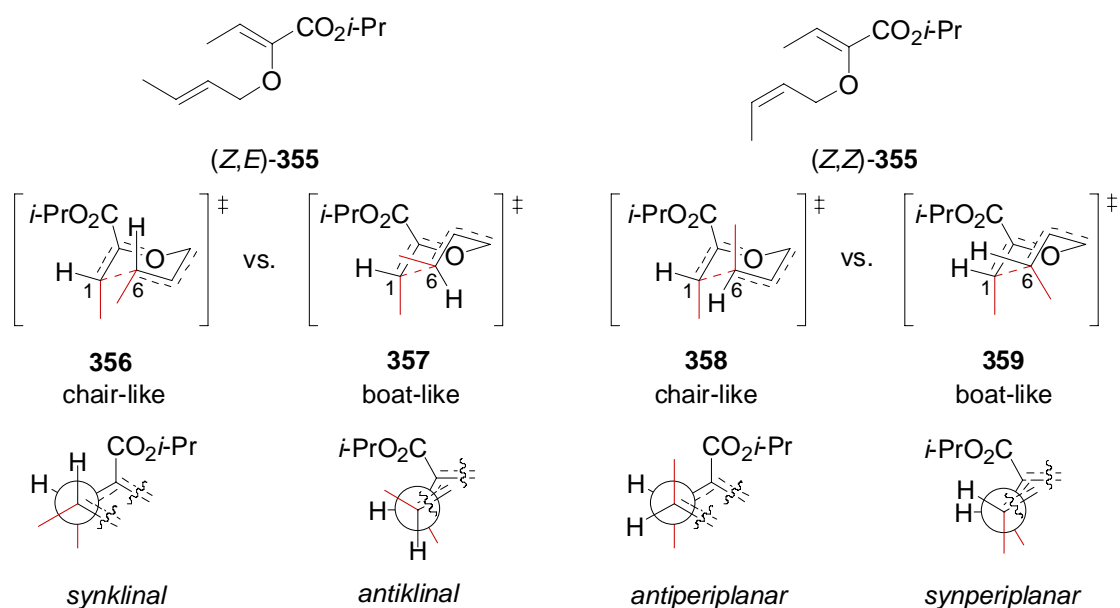
²⁷⁸ Rehbein, J.; Hiersemann, M. *The Catalytic Asymmetric Claisen Rearrangement: How the [Cu^{II}(box)]-Catalyst Achieves Rate Acceleration and Stereodifferentiation – A Computational Study*. Poster for *Synthetic, Mechanistic and Reaction Engineering. Aspects of Metal Containing Catalysts*, **2005**, Berlin, and unpublished results.

| AVE | Critical bond length $r_{(C1-C6)}$ [\AA] ^a | | $\Delta\Delta G^{\ddagger}_{(\text{chair-boat})}$ [kcal/mol] | |
|-----------|--|----------------------------|--|----------------------------|
| | (<i>Z,Z</i>)- 355 | (<i>Z,E</i>)- 355 | (<i>Z,Z</i>)- 355 | (<i>Z,E</i>)- 355 |
| Thermal | 2.375 | 2.370 | -6.2 | -3.9 |
| Catalytic | 2.888 | 2.814 | -1.1 | -0.2 |

Table 20: Critical bond lengths and energy gaps between chair-like transition state and boat-like transition state using (*Z,Z*)-**355** and (*Z,E*)-**355** as representative examples. ^a Values for the chair-like transition state. Similar extensions were calculated for $r_{(O3-C4)}$. Comparable results were obtained for the boat-like transition state.

Additionally, $\Delta\Delta G$ was found to be considerably greater for the rearrangement of the (*Z,Z*)-**355**. The latter finding nicely mirrors the experimentally found better diastereoselectivity observed for the catalytic rearrangement of AVEs with *Z*-configured allyl ether double bond.²⁷⁹ The calculated value of 0.2 kcal/mol should result in a diastereomeric ratio of 58/42 what is in very good agreement with the experimental verified diastereoselectivity of 57/43.²⁸⁰ How can these results be explained? Normally, 1,3-diaxial interactions as well as steric repulsions due to the eclipsed arrangement of the substituent render the boat-like transition state less favourable. These interactions are expected to be less dominant in the more dissoziative transition states of the catalyzed rearrangement. To rationalize the greater gap between the activation energies of the possible transition states found for the catalyzed rearrangement of (*Z,Z*)-**355** compared with (*Z,E*)-**355** may be explained by analyzing the graphical representation of the transition states (Scheme 93).

²⁷⁹ Level of theory: uB3LYP/6-31G*, gas phase, T = 298.15 K. Calculated with Gaussian 98: Gaussian 03, Revision C.02, Frisch, M. J.; Trucks, G. W.; Schlegel, H. B.; Scuseria, G. E.; Robb, M. A.; Cheeseman, J. R.; Montgomery, Jr., J. A.; Vreven, T.; Kudin, K. N.; Burant, J. C.; Millam, J. M.; Iyengar, S. S.; Tomasi, J.; Barone, V.; Mennucci, B.; Cossi, M.; Scalmani, G.; Rega, N.; Petersson, G. A.; Nakatsuji, H.; Hada, M.; Ehara, M.; Toyota, K.; Fukuda, R.; Hasegawa, J.; Ishida, M.; Nakajima, T.; Honda, Y.; Kitao, O.; Nakai, H.; Klene, M.; Li, X.; Knox, J. E.; Hratchian, H. P.; Cross, J. B.; Bakken, V.; Adamo, C.; Jaramillo, J.; Gomperts, R.; Stratmann, R. E.; Yazyev, O.; Austin, A. J.; Cammi, R.; Pomelli, C.; Ochterski, J. W.; Ayala, P. Y.; Morokuma, K.; Voth, G. A.; Salvador, P.; Dannenberg, J. J.; Zakrzewski, V. G.; Dapprich, S.; Daniels, A. D.; Strain, M. C.; Farkas, O.; Malick, D. K.; Rabuck, A. D.; Raghavachari, K.; Foresman, J. B.; Ortiz, J. V.; Cui, Q.; Baboul, A. G.; Clifford, S.; Cioslowski, J.; Stefanov, B. B.; Liu, G.; Liashenko, A.; Piskorz, P.; Komaromi, I.; Martin, R. L.; Fox, D. J.; Keith, T.; Al-Laham, M. A.; Peng, C. Y.; Nanayakkara, A.; Challacombe, M.; Gill, P. M. W.; Johnson, B.; Chen, W.; Wong, M. W.; Gonzalez, C.; and Pople, J. A.; Gaussian, Inc., Wallingford CT, 2004.²⁸⁰ Catalyzed process with Cu(OTf)₂ as catalyst.



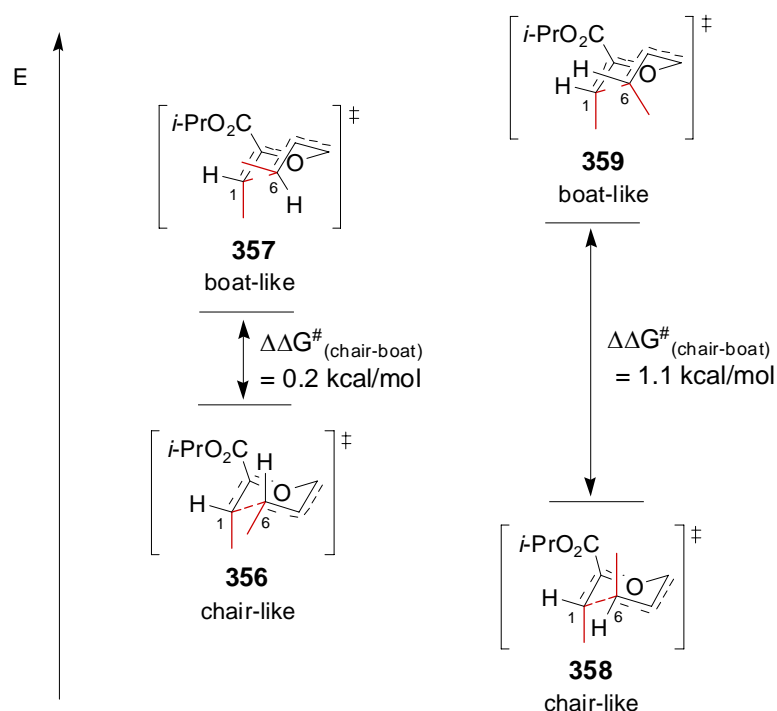
Scheme 93: Chair- and boat-like transition states for (Z,E)- and (Z,Z)-AVE **355**.²⁸¹

The following important characteristics may be emphasized. In all cases the chair-like transition states **356/358** are expected to be more attractive than the corresponding boat-like transition states **357/359**. In the transition states for the rearrangement of the (Z,E)-**355** (**356** and **357**), the spatial relationship of R¹ and R⁶ may be described as *synclinal* (chair-like transition state) versus *anticlinal* (boat-like transition state). In contrast, in the transition states for the rearrangement of (Z,Z)-**355** (**358** and **359**), R¹ and R⁶ are in *antiperiplanar* (chair-like transition state) versus *synperiplanar* (boat-like transition state) relation. Analysis of the spatial 1,6-arrangement gives the following results:

- The chair-like transition state **356** is destabilized by a *gauche* interaction between the two methyl substituents. This interaction is absent in the chair-like transition state **358**. Therefore, **358** is more attractive than **356**.
- In contrast, the boat-like transition state **359** suffers from strong interactions between the methyl groups that are in eclipsed arrangement. This interaction is much less dominant for boat-like transition state **357**, since only a repulsion between a methyl group and a hydrogen atom (instead of another methyl group) has to be considered.

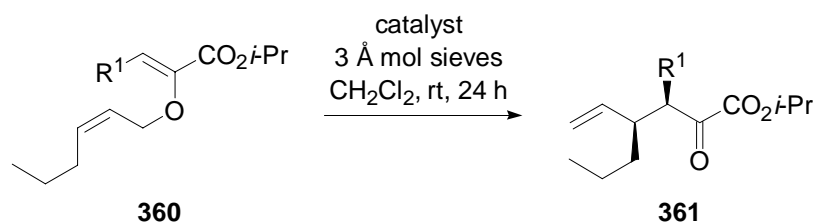
The above analysis may be illustrated by Scheme 94 that once again shows the destabilization of the boat-like transition state **359** compared to **357** and the stabilization of the chair-like transition state **358** in comparison to **356** and consequently results in a smaller energy gap for the rearrangement of (Z,E)-**355**. With this representation the different diastereoselectivities can be easily rationalized

²⁸¹ For descriptors of the steric relationship across single bonds, see: Klyne, W.; Prelog, V. *Experientia* **1960**, *16*, 521-523.



Scheme 94: Illustration of the relative energy values of the different possible transition states for the catalyzed rearrangement of (*Z,E*)-**355** (left) and (*Z,Z*)-AVE **355** (right).

With the successful catalysis of the Claisen rearrangement of 2-alkoxycarbonyl substituted AVEs by lanthanide(III) triflates in hand, we next turned our attention toward $\text{Cu}(\text{OTf})_2$ and $\text{Yb}(\text{OTf})_3$.²⁸² It was found that in the presence of 3 Å molecular sieves both triflates were able to catalyze the transformation. Both, diastereoselectivity and reactivity showed strong dependency on the substrate structure. However, the two catalysts usually gave comparable results (Table 21).



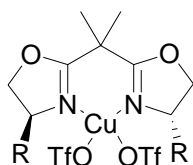
| Entry | R ¹ | Catalyst | Yield [%] | syn/anti |
|-------|----------------|------------------------------------|-----------|----------|
| 1 | Bn | 5 mol% $\text{Cu}(\text{OTf})_2$ | 98 | 93/7 |
| 2 | Bn | 7.5 mol% $\text{Yb}(\text{OTf})_3$ | 99 | 96/4 |
| 3 | <i>i</i> -Pr | 5 mol% $\text{Cu}(\text{OTf})_2$ | 99 | 93/7 |
| 4 | <i>i</i> -Pr | 7.5 mol% $\text{Yb}(\text{OTf})_3$ | 99 | 91/9 |

Table 21: $\text{Cu}(\text{OTf})_2$ and $\text{Yb}(\text{OTf})_3$ catalyzed Claisen rearrangement. Tf= trifluoromethane sulfonyl [CF_3SO_2].

²⁸² Hiersemann, M.; Abraham, L. *Org. Lett.* **2001**, *3*, 49-52.

Catalytic Asymmetric Claisen Rearrangement

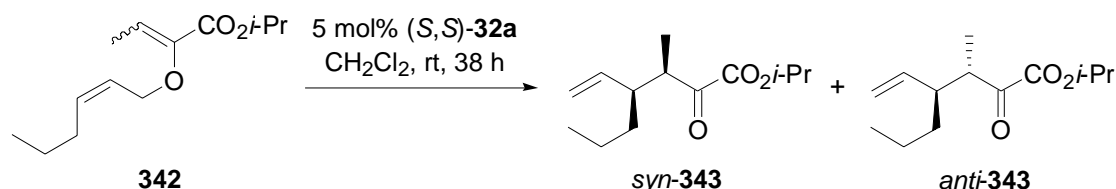
These promising results guided us to the development of an enantioselective variation of the Claisen rearrangement. To induce enantioselectivity, a chiral ligand is required to provide the chiral environment that is essential to discriminate between the two possible enantiomeric transition states. In our first attempts we employed the well known copper(II) bis(oxazolines) (*S,S*)-**362** (Figure 16).²⁰⁶



R= *t*-Bu (*S,S*)-**362a**
R= Ph (*S,S*)-**362b**

Figure 16: Copper(II)-bis(oxazoline)-complex. Tf= trifluoromethane sulfonyl [CF_3SO_2].

We concentrated on AVEs with *Z*-configured allyl ether double bond or lacking a stereogenic allyl ether double bond.²⁸³ Generally, isolated yields were very good. When applied to different test substrates, copper(II) bis(oxazoline) complex (*S,S*)-**362b** afforded the corresponding rearrangement products with high diastereoselectivities and enantioselectivities up to 88% ee (Table 22).^{202b}

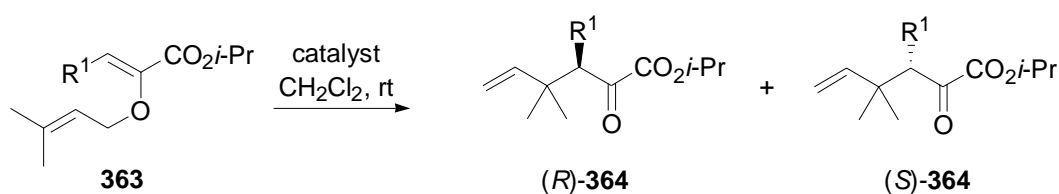


| Entry | Configuration | Yield [%] | <i>syn/anti</i> | ee [%] |
|-------|---------------|-----------|-----------------|--------|
| 1 | <i>E</i> | 99 | 3/97 | 88 |
| 2 | <i>Z</i> | 98 | 99/1 | 84 |

Table 22: Application of $[\text{Cu}\{(S,S)\text{-Ph-box}\}](\text{OTf})_2$ [(*S,S*)-**362b**] for the catalytic asymmetric Claisen rearrangement (CAC). Tf= trifluoromethane sulfonyl [CF_3SO_2].

Comparison of the copper(II)-bis(oxazoline) catalysts (*S,S*)-**362a** and (*S,S*)-**362b** as catalysts for the Claisen rearrangement was performed next (Table 23).^{202b}

²⁸³ AVEs with *E*-configured allyl ether double bond rearrange with decreased diastereoselectivities. See preceding paragraph.



| Entry | R ¹ | Z/E | Catalyst | Reaction time [h] | Yield [%] | (R)/(S) |
|-------|----------------|------|-------------------------------------|-------------------|-----------|---------|
| 1 | Me | 96/4 | 5 mol% (<i>S,S</i>)- 362b | 1 | 100 | 91/9 |
| 2 | Me | 96/4 | 10 mol% (<i>S,S</i>)- 362a | 24 | 99 | 6/94 |
| 3 | Bn | 97/3 | 5 mol% (<i>S,S</i>)- 362b | 1 | 99 | 88/12 |
| 4 | Bn | 97/3 | 10 mol% (<i>S,S</i>)- 362a | 72 | 94 | 8/92 |

Table 23: Comparison of [Cu{(S,S)-Ph-box}](OTf)₂ [(S,S)-**362b**] and [Cu{(S,S)-*t*-Bu-box}](OTf)₂ [(S,S)-**362a**] as catalysts for the catalytic asymmetric Claisen rearrangement (CAC). Tf= trifluoromethane sulfonyl [CF₃SO₂], Bn= benzyl.

We found that the copper(II)-*t*-Bu-box catalyst (*S,S*)-**362a** is less reactive than the copper(II)-Ph-box catalyst (*S,S*)-**362b** (Table 23, entry 2 and 4). Often, the addition of molecular sieves was required to enhance the reaction rate if (*S,S*)-**362a** was used as catalyst. However, the observed enantioselectivities were found to be slightly higher (Table 23, entry 2 and 4). Another interesting result is the reversed absolute configuration of the product **364** that was observed for the rearrangement with (*S,S*)-**362a** compared to (*S,S*)-**362b** (Table 23, entry 1 and 3).

The enhanced enantioselectivity and the reversal of the absolute configuration may be a result of the geometry of the complexes (*S,S*)-**362a** and (*S,S*)-**362b**. In an effort to explain the finding, a set of quantum chemical calculations was performed by Julia Rehbein in our research group.²⁸⁴ For [Cu{(S,S)-*t*-Bu-box}](H₂O)₂(SbF₆)₂ [(S,S)-**234a**] a distorted square-planar coordination geometry around the copper(II) central atom was determined (Figure 17, right) that is even more pronounced for [Cu{(S,S)-Ph-box}](H₂O)₂(SbF₆)₂ [(S,S)-**234b**] (Figure 17, left).

²⁸⁴ Rehbein, J.; unpublished results.

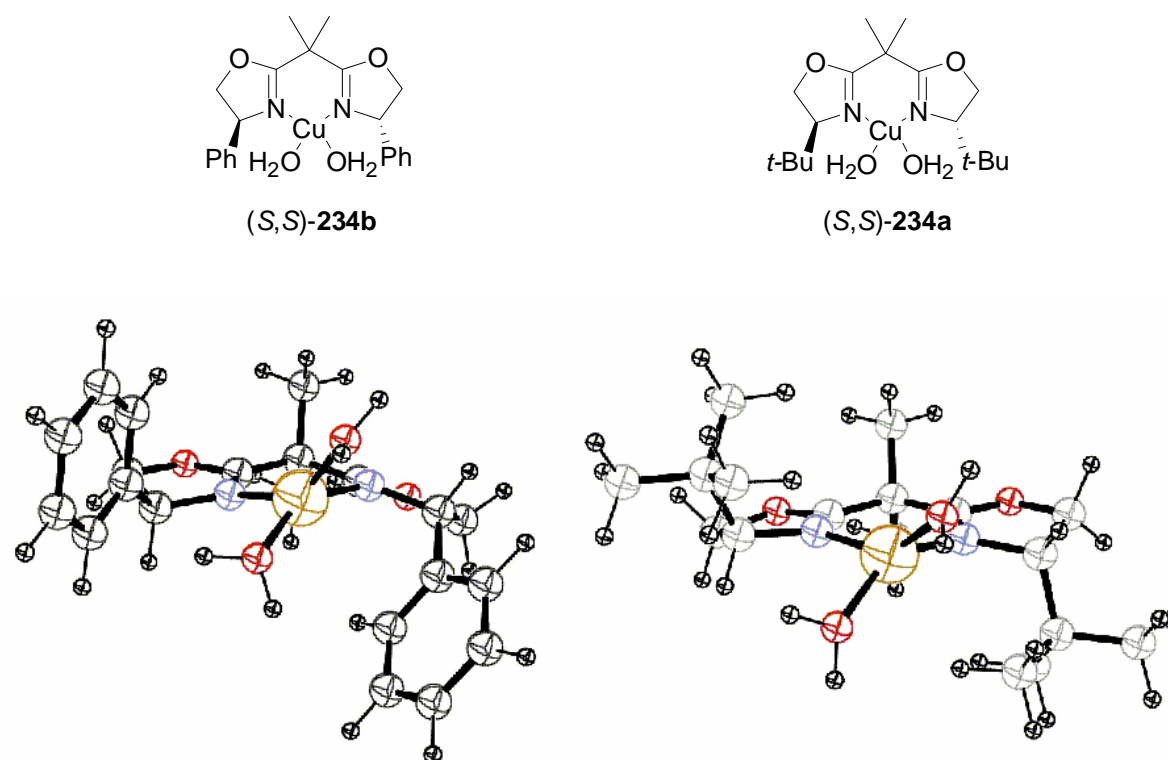
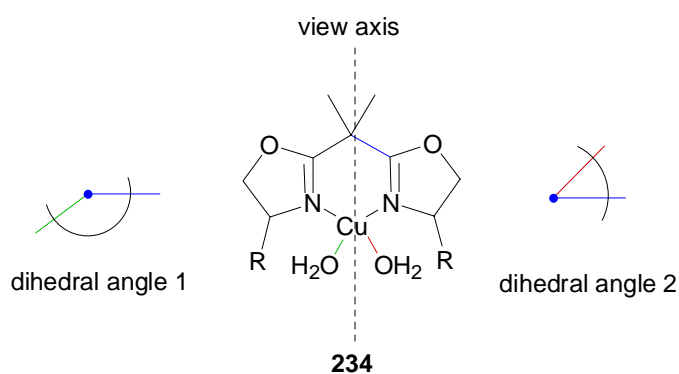


Figure 17: Calculated distorted square-planar coordination of (S,S)-234a and (S,S)-234b.^{279,285}

The degree of distortion may be expressed by the dihedral angle. With an assumed plane spread out between the copper central atom and the two nitrogen atoms coordinatively bound to it, the dihedral angles may be defined as deviation of the water ligands from this plane assuming an almost planar arrangement of the oxazoline rings in this plane and a view axis along the copper atom and the C₁-linker connecting the two oxazolines rings (Scheme 95).



Scheme 95: Visualization of the position of the dihedral angles.²⁸⁵

²⁸⁵ Charges and counter ions are not depicted for concise reasons.

Calculated values are represented in Table 24.

| | (<i>S,S</i>)- 234a | (<i>S,S</i>)- 234b |
|------------------|-----------------------------|-----------------------------|
| Dihedral angle 1 | 136.1 | 125.1 |
| Dihedral angle 2 | -53.0 | -72.6 |

Table 24: Dihedral angles for (*S,S*)-**234a** and (*S,S*)-**234b**.^{279,284}

As a consequence of this distortion, the attack of the allyl fragment from the opposite enantiotopic face of the vinyl ether double bond appears possible.²⁸⁶

Since the [Cu{(S,S)-*t*-Bu-box}](OTf)₂ [(S,S)-**362a**] - that gave the better enantioselectivities - showed only limited reactivity, we sought for a related catalyst with increased Lewis acidity that at the same time maintains the capability to differentiate between the two enantiotopic faces of the vinyl ether double bond. Exchange of the triflate counter ion with the less coordinating hexafluoro antimonate resulted in the “cationic” complex [Cu{(S,S)-*t*-Bu-box}](H₂O)₂(SbF₆)₂ [(S,S)-**234a**] which was originally described by Evans and co-workers (Figure 18).²⁸⁷

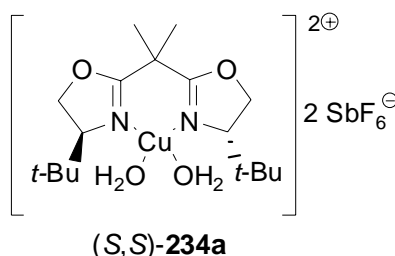


Figure 18: Cationic copper(II)-bis(oxazoline)-complex (*S,S*)-**234a**.

Replacing (*S,S*)-**362a** by the “cationic” copper(II)-bis(oxazoline) complex (*S,S*)-**234a** enhanced both reaction rates and enantioselectivities.^{202d} Different AVEs were successfully rearranged under those conditions (Table 25). The presence of protected alcohol functionalities allows further manipulation of the rearrangement products and therefore renders them versatile intermediates for target oriented synthesis.

²⁸⁶ For a more detailed discussion, see chapter 11.3.4 – Proposed Mechanism.

²⁸⁷ (a) Evans, D. A.; Murry, J. A.; von Matt, P.; Norcross, R. D.; Miller, S. J. *Angew. Chem., Int. Ed. Engl.* **1995**, *34*, 798-800; *Angew. Chem.* **1995**, *107*, 864-867. (b) Evans, D. A.; Miller, S. J.; Lectka, T.; Matt, v. P. *J. Am. Chem. Soc.* **1999**, *121*, 7559-7573.

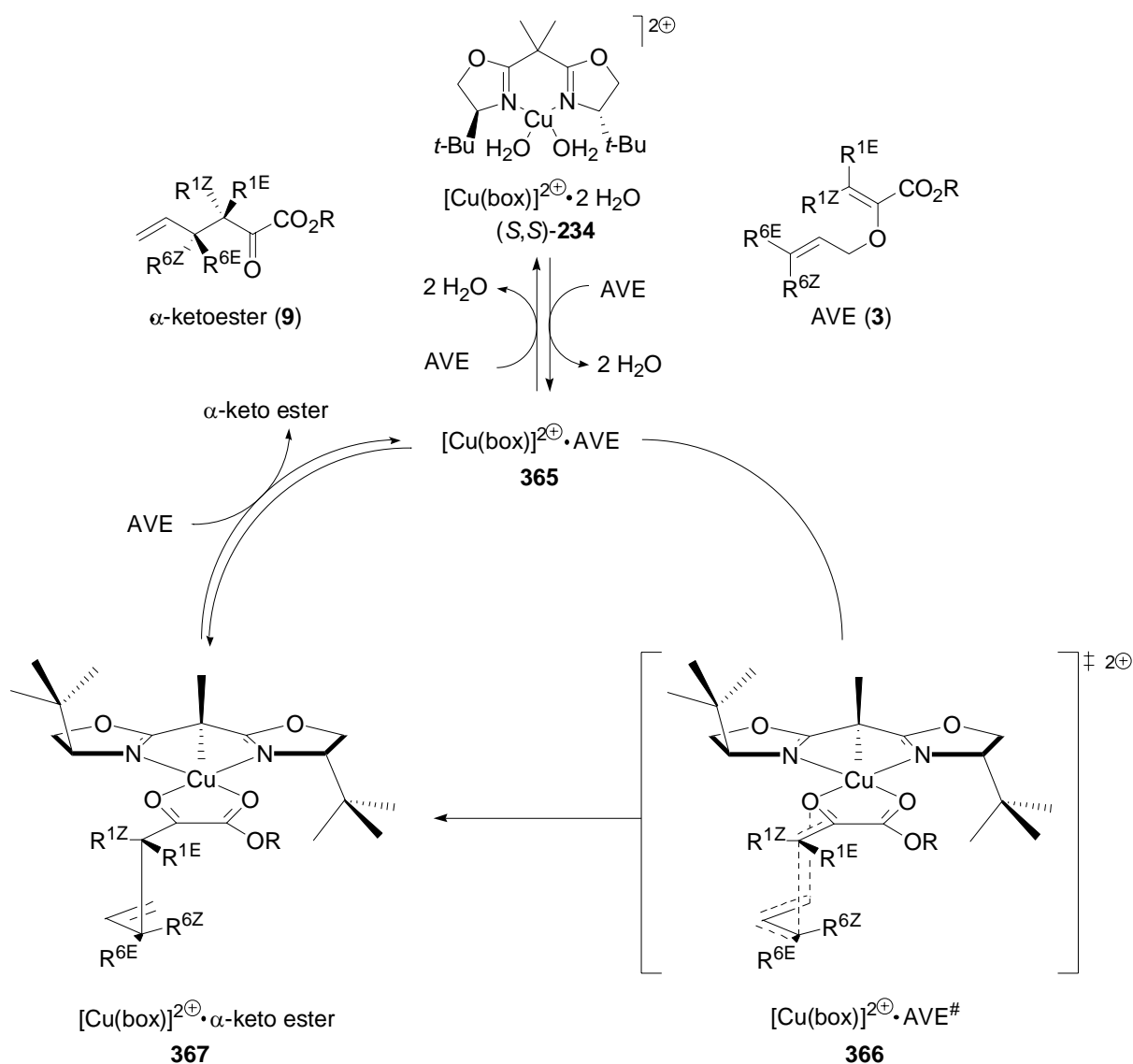
| Entry | Allyl vinyl ether | Rearrangement product | Catalyst loading [mol%] | Reaction time [h] | Yield [%] | de [%] | ee [%] |
|-------|-------------------|-----------------------|-------------------------|-------------------|-----------|--------|--------|
| 1 | | | 10 | 3 | 99 | 98 | 99 |
| 2 | | | 2.5 | 1.5 | 99 | 98 | 99 |
| 3 | | | 2.5 | 1.5 | 99 | 98 | 99 |
| 4 | | | 10 | 1.5 | 98 | - | 99 |
| 5 | | | 10 | 48 | 98 | 98 | 99 |

Table 25: Different allyl vinyl ethers that have been successfully applied to the CAC using $[\text{Cu}\{(S,S)\text{-}t\text{-Bu-box}\}(\text{SbF}_6)_2(\text{H}_2\text{O})_2]$ (*S,S*)-**234a** as catalyst.

Proposed catalytic cycle

As a result of our studies we propose the following catalytic cycle. We assume that the rate determining step of the catalytic asymmetric Claisen rearrangement is the formation of the catalyst-substrate complex **365** rather than the rearrangement itself. Thus according to the Izumi-Tai classification,²⁸⁸ the CAC with $[\text{Cu}\{(S,S)\text{-}t\text{-Bu-box}\}(\text{H}_2\text{O})_2(\text{SbF}_6)_2]$ [(*S,S*)-**234a**] has to be classified as enantiotopos and not as enantioface differentiating reaction. Once the complex **365** is formed, the reorganisation is fast leading to the product-catalyst complex **367**. In a final step the α -keto ester **9** has to be replaced by another molecule **3** to regenerate the substrate-catalyst complex **365** (Scheme 96).

²⁸⁸ Izumi, Y.; Tai, A. *Stereodifferentiating Reactions* Academic Press New York, 1977.



Scheme 96: Proposed catalytic cycle for the Claisen rearrangement of 2-alkoxycarbonyl substituted allyl vinyl ethers catalyzed by $[Cu\{(S,S)\text{-}t\text{-Bu}\text{-box}\}(\text{SbF}_6)_2(\text{H}_2\text{O})_2][(S,S)\text{-}234\text{a}]$.

Transition state and enantioselectivity

Steric repulsions direct the coordination of the catalyst with one of the two enantiotopic lone pairs of the ether oxygen atom of O3. As illustrated in Scheme 96 a conformation is adopted that allows a maximal spatial distance between the allyl moiety and the *tert*-butyl substituent of the ligand. Figure 19 shows the calculated transition state for the copper(II)-*t*-Bu-*box*-catalyzed rearrangement.

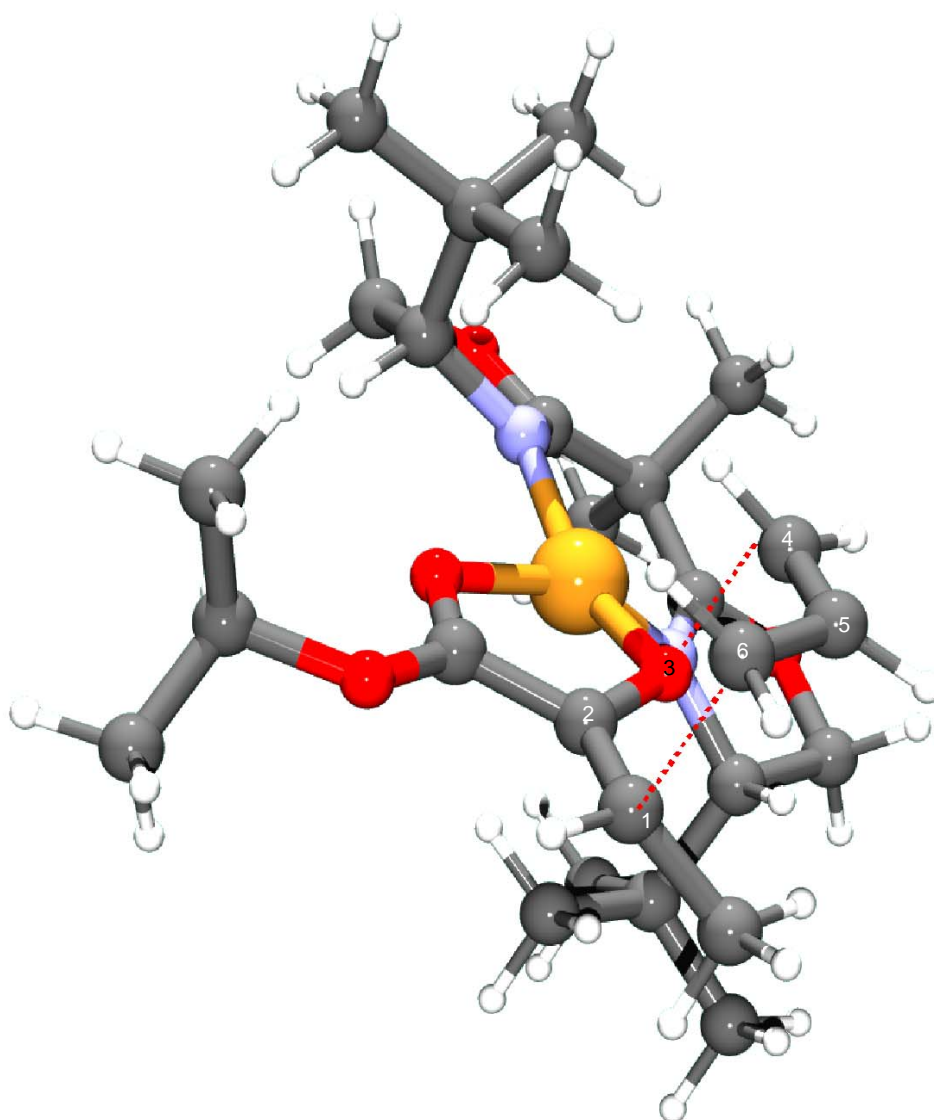
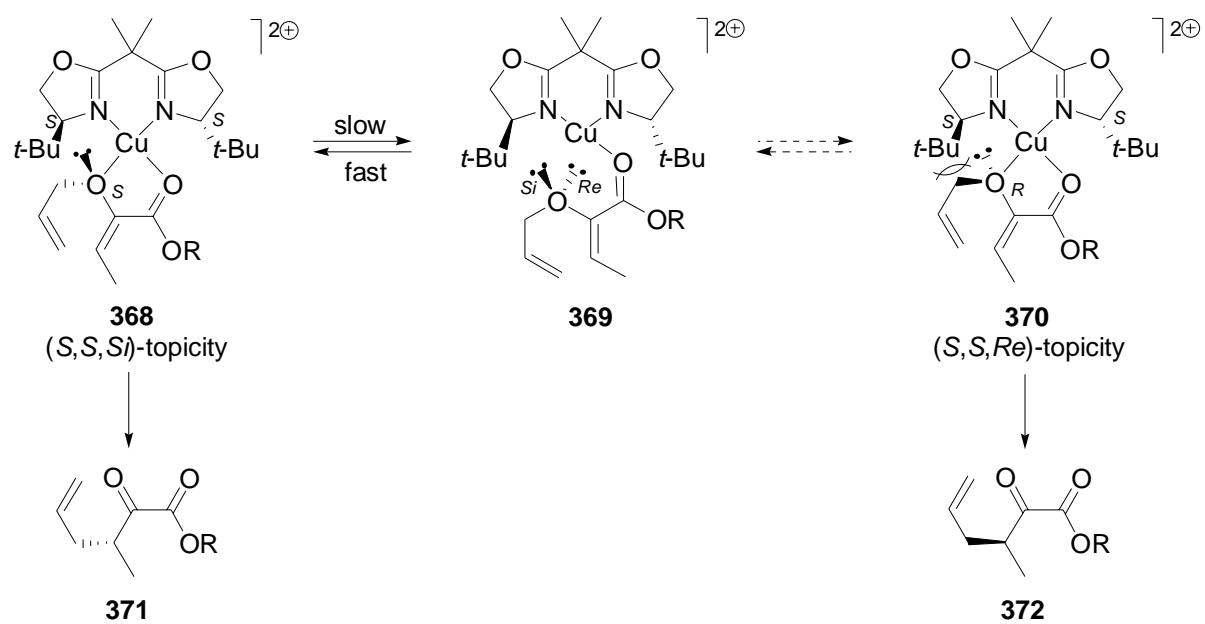


Figure 19: Transition state for the $[\text{Cu}\{(S,S)\text{-}t\text{-Bu-box}\}]$ -catalysed Claisen rearrangement of a 2-alkoxycarbonyl substituted allyl vinyl ether.²⁷⁹

Once coordinated to the catalyst, the approach of the opposite enantiotopic face of the vinyl ether double bond by the allyl moiety would require the energetically unfavourable breaking of the copper oxygen bond (Scheme 97).



Scheme 97: For the formation of the diastereomorph complex **370** the Cu-O(ether)-bond of **368** needs to be ceased - an energetically disfavoured process. The formation of the complex **370** suffers from a disadvantageously steric interaction.

12 Copper(II) Bis(oxazoline) Complexes

Since the copper(II) bis(oxazoline) complexes are of fundamental importance for our synthetic strategy, some important information concerning bis(oxazoline) complexes in general and the copper(II) bis(oxazoline) complexes in particular shall be summarized in the following section.²⁸⁹ The introduction of the “cationic” copper(II) bis(oxazoline) complex (*S,S*)-**234a** for asymmetric synthesis was the result of a long-standing development process toward catalytic enantioselective transformations.^{206b} Chiral bis(oxazoline) ligands have been introduced since 1989.²⁹⁰ A small selection of the various structurally diverse examples that have been developed over the years is depicted in Figure 20. They can be subdivided according to the number of atoms that link the two oxazoline rings of the bis(oxazoline). Depending on the linker different metal chelate ring sizes will be formed: bis(oxazolines) with a C₀ linker (e.g. **373**) will form five-membered rings. The widely used bis(oxazoline) ligands with C₁ linker (e.g. **374-376**) result in six-membered rings. Further increased linker sizes (e.g. **377** and **378**) consequently generate seven- or eight-membered rings. The latter bis(oxazolines) often contain an additional coordination site which renders the ligand tridentate (e.g. **378**).

²⁸⁹ Desimoni, G.; Faita, G.; Jørgensen, K. A. *Chem. Rev.* **2006**, *106*, ASAP, DOI: 101021/cr0505324.

²⁹⁰ (a) Nishiyama, H.; Sakaguchi, H.; Nakamura, T.; Horihata, M.; Kondo, M.; Itoh, K. *Organometallics* **1989**, *8*, 846-848. (b) Balavoine, G.; Clinet, J. C.; Lellouche, I. *Tetrahedron Lett.* **1989**, *30*, 5141-5144.

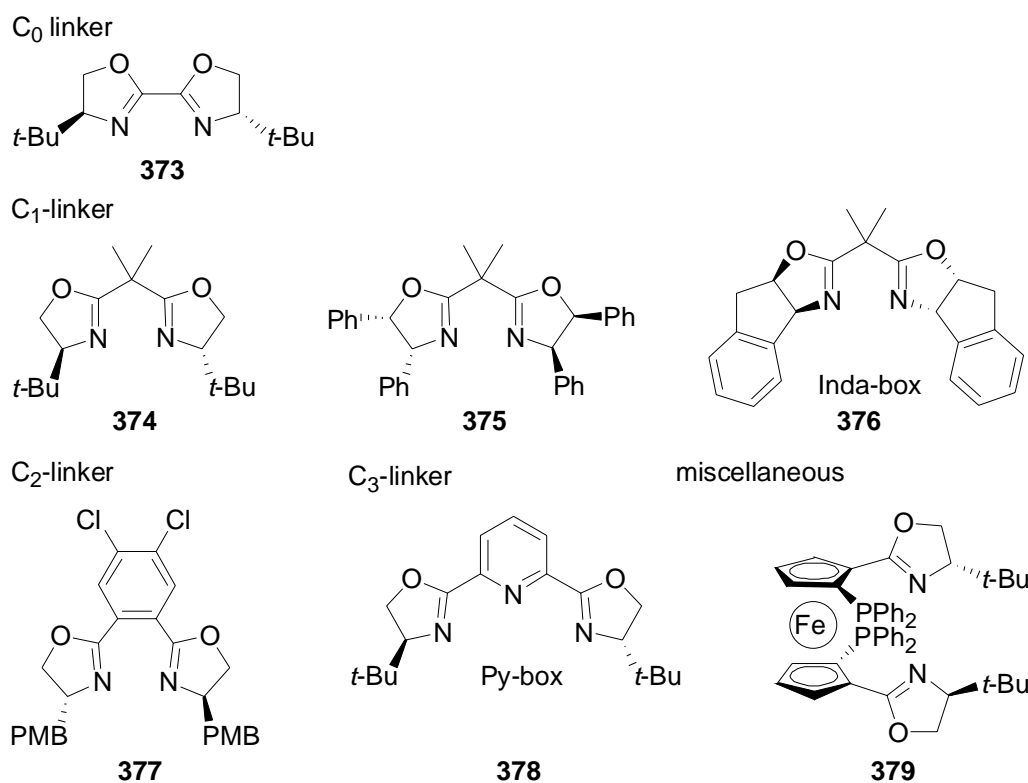


Figure 20: Selected bis(oxazoline) ligands that were successfully employed in catalytic asymmetric transformations.

The ligands are usually bidentate bearing two nitrogen donor sites and form chelate complexes with metal cations. They are derived from a wide variety of readily available optical active amino acids (ex-chiral-pool). This results in a great variability of bis(oxazoline) ligands thus allowing the optimization of the ligand with respect to a specific asymmetric process.^{206d} The synthesis of the bis(oxazolines) is usually straight forward and the generally high stability allows an easy handling. Among the various bis(oxazoline) ligands, those where the two oxazoline rings are connected by a one carbon spacer are most frequently utilized for asymmetric induction during metal catalyzed reactions.

For different applications, specific metal cations had to be employed. With the following examples it is not intended to give a comprehensive overview. Instead, the chosen applications should illustrate the versatility of bis(oxazoline) ligands.

Ruthenium based bis(oxazoline) catalyst for example, have been employed in catalytic enantioselective cyclopropanation reactions.²⁹¹ The same research group employed nickel

²⁹¹ (a) Nishiyama, H.; Aoki, K.; Itoh, H.; Iwamura, T.; Sakata, N.; Kurihara, O.; Motoyama, Y. *Chem. Lett.* **1996**, 1071-1072. (b) Park, S.-B.; Sakata, N.; Nishiyama, H. *Chem. Eur. J.* **1996**, 2, 303-306. (c) Park, S.-B.; Murata, K.; Matsumoto, H.; Nishiyama, H. *Tetrahedron: Asymmetry* **1995**, 6, 2487-2494. (d) Nishiyama, H.; Itoh, Y.; Matsumoto, H.; Aoki, Y.; Itoh, K. *Bull. Chem. Soc. Jpn.* **1995**, 68, 1247-1262. (e) Nishiyama, H.; Itoh,

bis(oxazolines) complexes for asymmetric 1,3-dipolar cycloadditions.²⁹² Another application of ruthenium in concert with bis(oxazoline) ligands was found in the asymmetric epoxidation of alkenes.²⁹³ Pfaltz *et al.* developed an asymmetric allylic substitution based on palladium and molybdenum bis(oxazoline) complexes.²⁹⁴ Iron²⁹⁵ and magnesium²⁹⁶ bis(oxazoline) complexes were utilized for catalytic asymmetric Diels-Alder and hetero Diels-Alder reactions. Rhodium bis(oxazoline) complexes have proved to be useful catalysts for asymmetric hydrosilylations^{296b,297} and asymmetric conjugate reductions of α,β -unsaturated ketones and esters.²⁹⁸ As well they were employed for the enantioselective allylation of aldehydes.²⁹⁹

However, far the greatest impact was achieved by copper(II) bis(oxazoline) complexes with its most dominant representative (*S,S*)-**234a** (Scheme 98, Table 26,).²⁰⁶ Soon after its development, [Cu{(S,S)-*t*-Bu-box}](H₂O)₂(SbF₆)₂ [(S,S)-**234a**] proved its potential for the asymmetric induction. Results of these efforts have been reviewed earlier.²⁰⁶ (*S,S*)-**234a** was employed for various pericyclic reactions, e.g. Diels-Alder²⁰⁶ and Hetero-Diels-Alder²⁰⁶ or carbonyl ene reactions,²⁰⁶ as well as for carbonyl reactions e.g. Michael additions²⁰⁶ and Mukaiyama-Aldol reactions.²⁰⁶ It could be applied to cycloadditions e.g. [2+2]-cycloadditions of silyl ketenes³⁰⁰ and for the asymmetric carbene or nitrene transfer to olefins.³⁰¹ When

Y.; Matsumoto, H.; Park, S.-B.; Itoh, K. *J. Am. Chem. Soc.* **1994**, *116*, 2223-2224. (f) Iwasa, S.; Tsushima, S.; Nishiyama, K.; Tsuchiya, Y.; Takezawa, F.; Nishiyama, H. *Tetrahedron: Asymmetry* **2003**, *14*, 855-865.

²⁹² Iwasa, S.; Maeda, H.; Nishiyama, K.; Tsushima, S.; Tsukamoto, Y.; Nishiyama, H. *Tetrahedron* **2002**, *58*, 8281-8287.

²⁹³ Tse, M. K.; Bhor, S.; Klawonn, M.; Anilkumar, G.; Jiao, H.; Döbler, C.; Spannenberg, A.; Mägerlein, W.; Hugl, H.; Beller, M. *Chem. Eur. J.* **2006**, *12*, 1855-1874.

²⁹⁴ Palladium: (a) Müller, D.; Umbricht, G.; Weber, B.; Pfaltz, A. *Helv. Chim. Acta* **1991**, *74*, 232-240. (b) von Matt, P.; Lloyds-Jones, G. C.; Minidis, A. B. E.; Pfaltz, A.; Macko, L.; Neuburger, M.; Zehnder, M.; Ruegger, H.; Pregosin, P. S. *Helv. Chim. Acta* **1995**, *78*, 265-284. (c) Mazet, C.; Köhler, V.; Pfaltz, A. *Angew. Chem.* **2005**, *117*, 4966-4969; *Ang. Chem., Int. Ed.* **2005**, *44*, 4888-4891. Molybdenum: Glorius, F.; Pfaltz, A. *Org. Lett.* **1999**, *1*, 141-144. For a review concerning allylic substitution reactions, see: Pfaltz, A.; Lautens, M. *Compr. Asym. Catal.* **1999**, *2*, 813-830.

²⁹⁵ (a) Corey, E. J.; Imai, N.; Zhang, H. *J. Am. Chem. Soc.* **1991**, *113*, 728-729. (b) Takacs, J. M.; Weidner, J. J.; Takacs, B. E. *Tetrahedron Lett.* **1993**, *34*, 6219-6222. (c) Takacs, J. M.; Bioto, S. C. *Tetrahedron Lett.* **1995**, *36*, 2941-2944. (d) Usuda, H.; Kuramochi, A.; Kanai, M.; Shibasaki, M. *Org. Lett.* **2004**, *6*, 4387-4390. (e) Kanemasa, S.; Adachi, K.; Yamamoto, H.; Wada, E. *Bull. Chem. Soc. Jpn.* **2000**, *73*, 681-687.

²⁹⁶ (a) Corey, E. J.; Ishihara, K. *Tetrahedron Lett.* **1992**, *33*, 6807-6810. (b) Desimoni, G.; Faita, G.; Righetti, P. P.; Sardone, N. *Tetrahedron* **1996**, *52*, 12019-12030. (c) Sibi, M. P.; Matsunaga, H. *Tetrahedron Lett.* **2004**, *45*, 5925-5929.

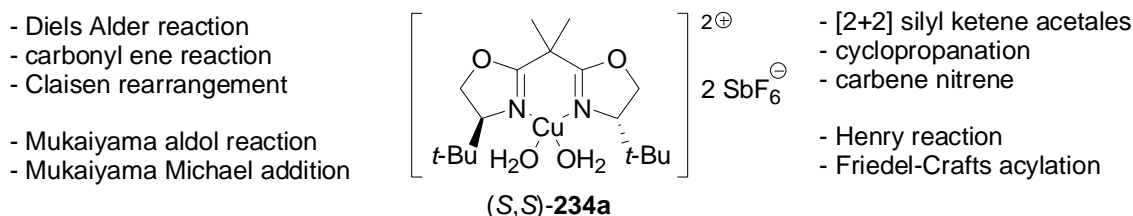
²⁹⁷ (a) Nishiyama, H.; Yamaguchi, S.; Kondo, M.; Itoh, K. *J. Org. Chem.* **1992**, *57*, 4306-4309. (b) Nishiyama, H.; Yamaguchi, S.; Park, S.-B.; Itoh, K. *Tetrahedron: Asymmetry* **1993**, *4*, 143-150. (c) Nishiyama, H.; Park, S.-B.; Itoh, K. *Tetrahedron: Asymmetry* **1992**, *3*, 1029-1034.

²⁹⁸ Kanazawa, Y.; Tsuchiya, Y.; Kobayashi, K.; Shiomi, T.; Itoh, J.-i.; Kikuchi, M.; Yamamoto, Y.; Nishiyama, H. *Chem. Eur. J.* **2006**, *12*, 63-71.

²⁹⁹ (a) Motoyama, Y.; Narusawa, H.; Nishiyama, H. *Chem. Comm.* **1999**, 131-132. (b) Motoyama, Y.; Okano, M.; Narusawa, H.; Makihara, N.; Aoki, K.; Nishiyama, H. *Organometallics* **2001**, *20*, 1580-1589.

³⁰⁰ Evans, D. A.; Janey, J. M. *Org. Lett.* **2001**, *3*, 2125-2128.

employed in the catalysis of the Henry reaction varying enantioselectivities were reported depending on the substrate structure and the reaction conditions.³⁰² More recently it was shown that excellent enantioselectivities could be achieved when (*S,S*)-**234a** was applied to the Claisen rearrangement of 2-alkoxycarbonyl substituted allyl vinyl ethers^{202c,d} and during Friedel-Crafts alkylation of pyrroles and indoles.³⁰³



Scheme 98: A selection of different reactions successfully employed for catalytic asymmetric variations using **16b** as catalyst.

³⁰¹ (a) Evans, D. A.; Faul, M. M.; Bilodeau, M. T.; Anderson, B. A.; Barnes, D. M. *J. Am. Chem. Soc.* **1993**, *115*, 5328-5329. (b) Evans, D. A.; Woerpel, K. A.; Hinman, M. M.; Faul, M. M. *J. Am. Chem. Soc.* **1991**, *113*, 726-728. (c) Evans, D. A.; Woerpel, K. A.; Scott, M. J. *Angew. Chem.* **1992**, *104*, 439-441; *Angew. Chem.; Int. Ed. Engl.* **1992**, *31*, 430-432. (d) A new bis(oxazoline) ligand expanded by secondary binding site was employed recently for the cyclopropanation of furans: Schinnerl, M.; Böhm, C.; Seitz, M.; Reiser, O. *Tetrahedron: Asymmetry* **2003**, *14*, 765-771.

³⁰² Christensen, C.; Juhl, K.; Hazell, R. G.; Jørgensen, K. A. *J. Org. Chem.* **2002**, *67*, 4875-4881.

³⁰³ Palomo, C.; Oiarbide, M.; Kardak, B. G.; García, J. M.; Linden, A. *J. Am. Chem. Soc.* **2005**, *127*, 4154-4155.

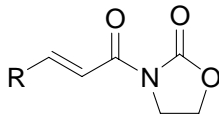
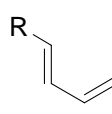
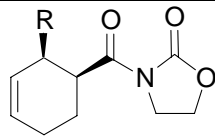
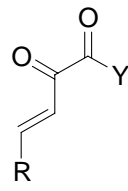
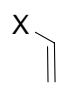
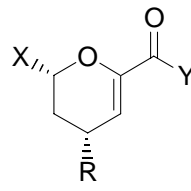
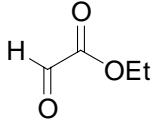
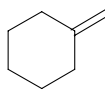
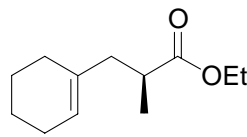
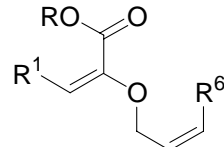
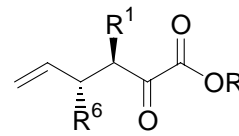
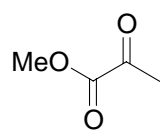
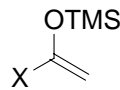
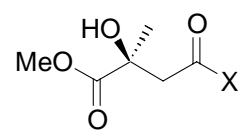
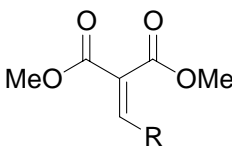
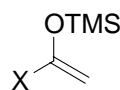
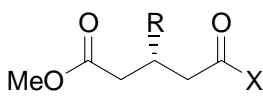
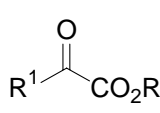
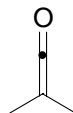
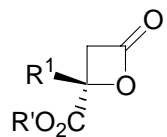
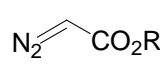
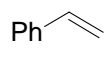
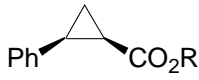
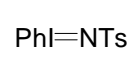
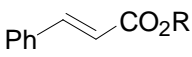
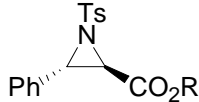
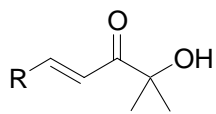
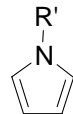
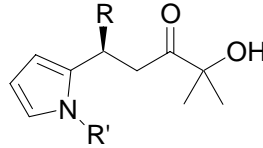
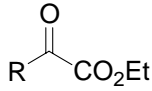

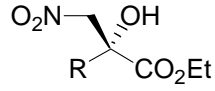
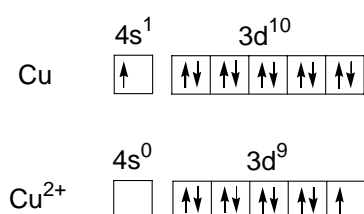
| Entry | Reaction | Substrate | Reaction partner | Product |
|-------|---|---|--|---|
| 1 | Diels-Alder ²⁰⁶ |  |  |  |
| 2 | Hetero-Diels-Alder ²⁰⁶ |  |  |  |
| 3 | Carbonyl ene ²⁰⁶ |  |  |  |
| 4 | Claisen rearrangement ²⁰² |  | - |  |
| 5 | Mukaiyama aldol ²⁰⁶ |  |  |  |
| 6 | Mukaiyama-Michael ²⁰⁶ |  |  |  |
| 7 | [2+2] cycloaddition ³⁰⁰ |  |  |  |
| 8 | Cyclopropanation ³⁰¹ |  |  |  |
| 9 | Carbene-Nitrene addition ³⁰¹ |  |  |  |
| 10 | Friedel-Crafts acylation ³⁰³ |  |  |  |
| 11 | Henry-Reaction ³⁰² |  |  |  |

Table 26: A selection of different reaction employed for catalytic asymmetric variations using (*S,S*)-**234ab** as catalyst. TMS= trimethylsilyl [SiMe₃], Ts= *para*-toluene sulfonyl.

The common feature of all these very different reactions is the ability of the substrates to act as bidentate ligands. According to empirical data, the bidentate coordination is an essential feature to achieve high enantioselectivities.²⁰⁶ The variety of very different transformations that proceed in a catalytic enantioselective way in the presence of [(*S,S*)-**234a**] clearly illustrate the impressive success of this specific catalyst system.

General features of the central cation in bis(oxazoline) complexes

The electron configuration of elemental copper is [Ar]3d¹⁰4s¹. Consequently, for the copper(II) cation the electron configuration would be [Ar]3d⁹4s⁰ (Scheme 99).



Scheme 99: Valenz electron configuration of the copper atom and the copper(II) cation.

Cu^{II} is known to act as a Lewis acid. According to the Irving-Williams order for divalent metal ions in the first transition series, copper(II) cations form the thermodynamically most stable complexes.³⁰⁴ This is an important feature with respect to the desired stereodifferentiation. The dissociation of the chiral ligand from the catalytically active center would cause the rescindment of the chiral environment and therefore, it needs to be prevented to achieve optimal enantioselectivities. Common coordination numbers of copper(II) ions are 4 and 6. Due to the 3d⁹ valenz electron configuration of the copper(II) cation, octahedral complexes show a strong Jahn-Teller distortion with the apical ligands being more weakly bond to the central cation or even completely detached (Figure 21).

³⁰⁴ Irving, H.; Williams, J. P. *J. Chem. Soc.* **1953**, 3192-3210.

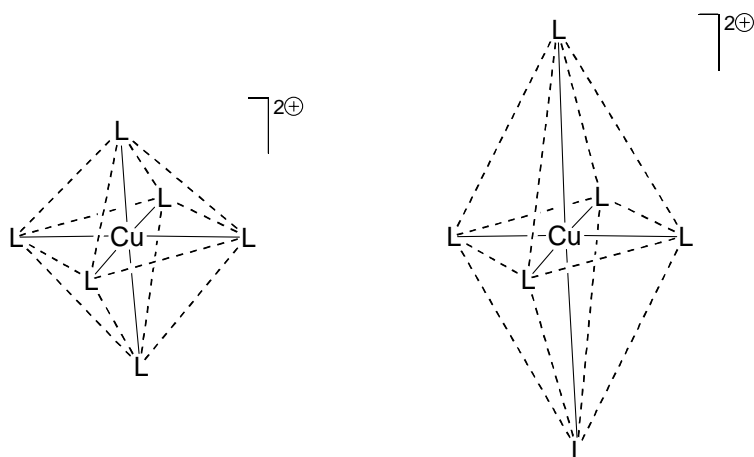


Figure 21: Visualization of the Jahn-Teller distortion. The octahedral structure (symbolized by the dashed lines) appears to be elongated vertically. Due to the increased distance between the central ion and the apical ligands the latter are more weakly bonded.

In 4-coordinated complexes, the square-planar coordination geometry is commonly found.³⁰⁵

Features of the complex

Copper(II) bis(oxazoline)-complexes are usually 4-coordinated and display a propensity to adopt square-planar geometry around the coordination center. The bidentate bis(oxazoline) ligand will occupy two of the four coordination sites (Figure 22).

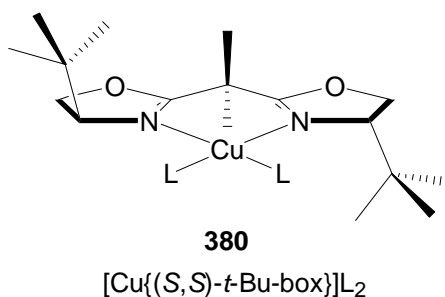


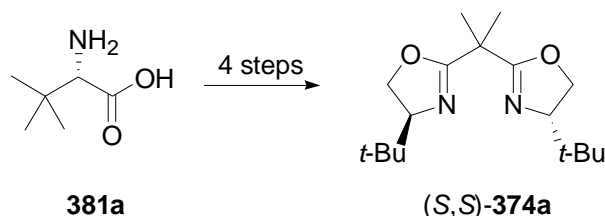
Figure 22: Square planar arrangement around the copper(II) coordination center. Two of the four coordination sites are occupied by the bidentate bis(oxazoline) ligand. (L= monodentate ligand).

Replacement of the other two monodentate ligands by a bidentate substrate is entropically favoured. Complexation of two bidentate ligands results in a highly ordered situation around the complex center. As mentioned earlier, this appears to be a crucial criterion to achieve high enantioselectivities. An important feature of the bis(oxazoline) ligands is that the nitrogen donor sites are located at a spatially close position to the stereodifferentiating chiral carbon atoms. The C₂-symmetry minimizes the number of possible transition states.

³⁰⁵ Greenwood, N. N.; Earnshaw, A. *Chemie der Elemente*; VCH Weinheim, 1990.

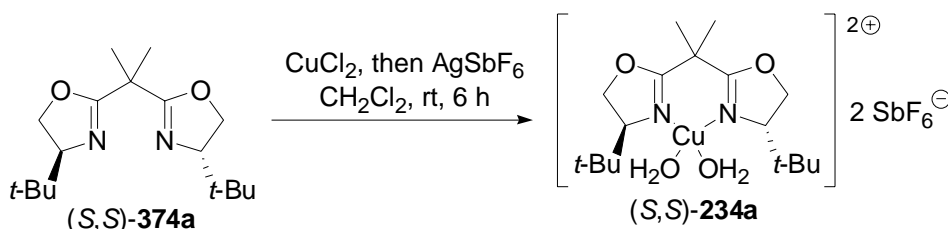
Synthesis of the ligand

The catalyst (*S,S*)-**234a** may be synthesized following a four step procedure starting from amino acid (*S*)-*tert*-leucine **381a** (Scheme 100).³⁰⁶



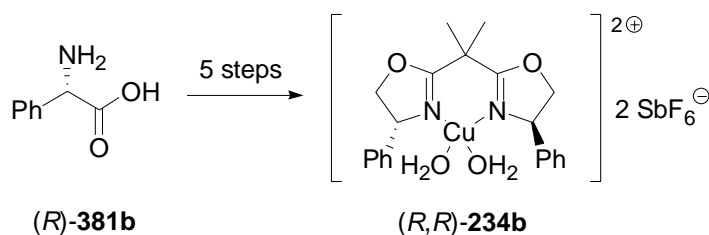
Scheme 100: Synthesis of the ligand (*S,S*)-**374a** can be realized in four steps.

Subsequent reaction with CuCl_2 and AgSbF_6 would provide the catalyst (*S,S*)-**234a** (Scheme 101).



Scheme 101

The corresponding copper(II)-Ph-box catalyst (*R,R*)-**234b** may be synthesized analogue to the above procedure starting from *R*-phenylglycine (**381b**) (Scheme 102).



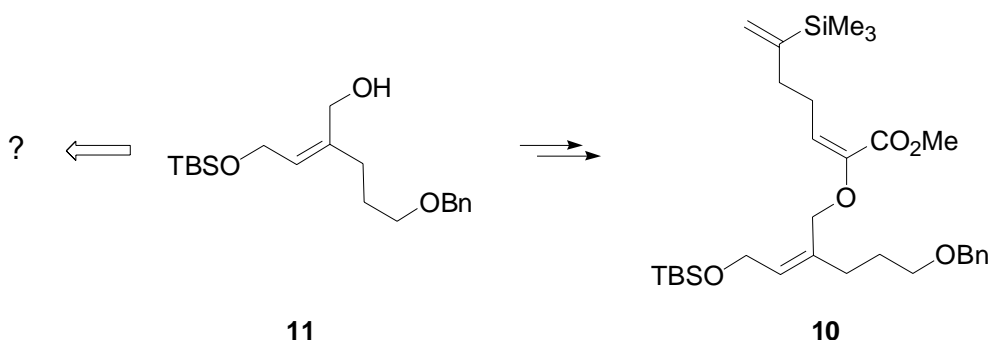
Scheme 102

Having discussed the theoretical background of the thermal and the catalytic asymmetric Claisen rearrangement as well as the involved copper(II)-bis(oxazoline) complex (*S,S*)-**234a**, the following chapter will cover results and perspectives of the synthetic effort toward (-)-xeniolide **F** (**2a**). The underlying synthetic plan was outlined previously and - if required - the interested reader is kindly referred to chapter 10 (page 96) to recapitulate the intended strategy.

³⁰⁶ Evans, D. A.; Peterson, G. S.; Johnson, J. S.; Barnes, D. M.; Capos, K. R.; Woerpel, K. A. *J. Org. Chem.* **1998**, *63*, 4541-4544.

13 Stereoselective Synthesis of the Allylic Alcohol

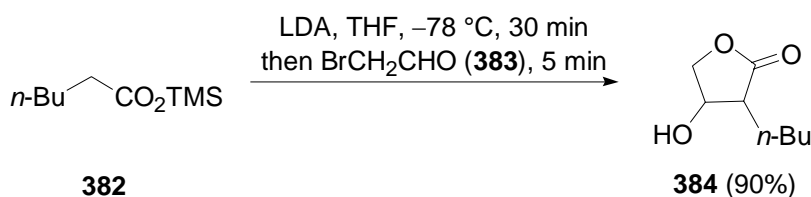
The synthetic plan for the total synthesis of (–)-xeniolide F (**2a**) is founded on the accessibility of the allyl vinyl ether **10**. For the generation of the allyl vinyl ether **10** a reliable and stereoselective synthetic route toward the *Z*-configured allylic alcohol **11** had to be developed (Scheme 103).



Scheme 103: The synthesis of the AVE **10** requires a reliable and stereoselective access toward allylic alcohol **11**. TBS= *tert*-butyldimethylsilyl [Si(*t*-Bu)Me₂], Bn= benzyl.

13.1 Butyrolactone Route

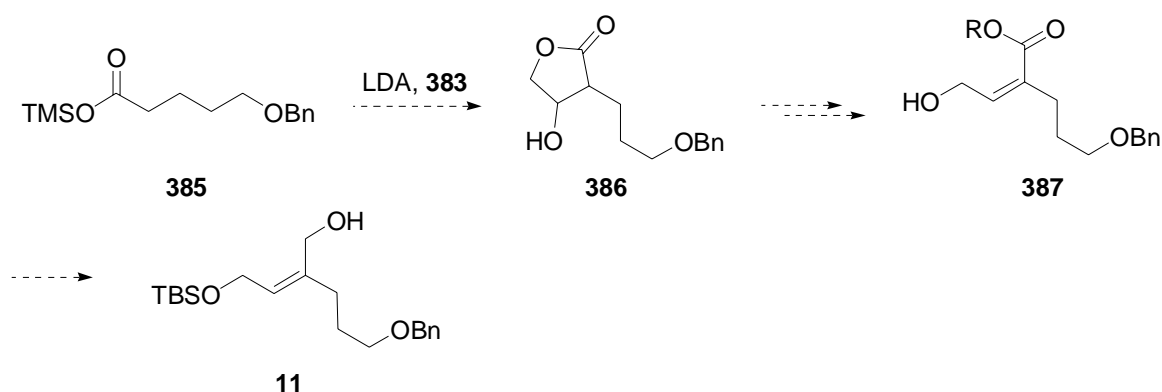
The initial approach was founded on the successful synthesis of β -hydroxybutyrolactones **384** developed by Kraus *et al.*³⁰⁷



Eq. 45 LDA= lithium diisopropylamide, TMS= trimethylsilyl [SiMe₃].

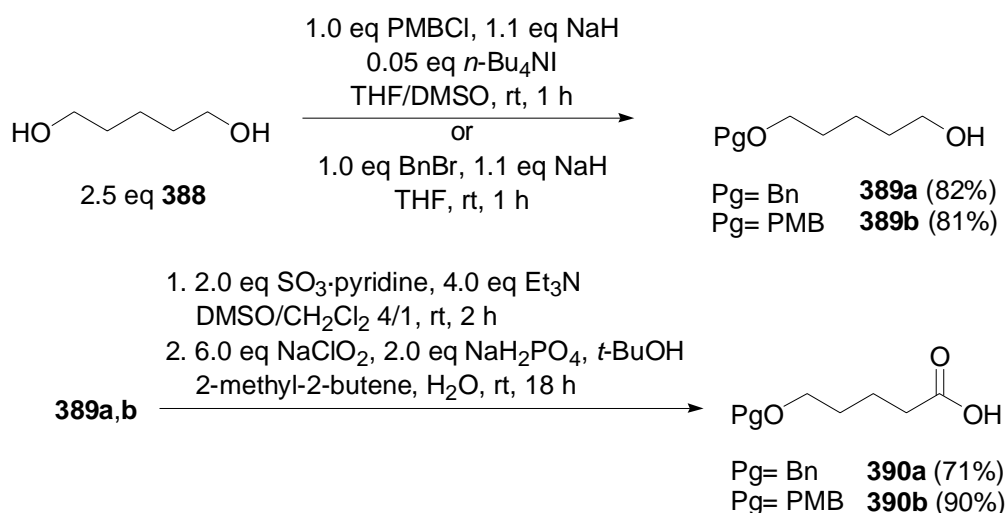
We intended to utilize this strategy to synthesize β -hydroxybutyrolactone **386** with a protected hydroxyl group in the side chain. Mesylation, elimination and lacton cleavage was expected to afford α,β -unsaturated ester **387**. After protection of the hydroxyl group and reduction of the ester functionality, the desired allylic alcohol **11** should be accessible.

³⁰⁷ Kraus, G. A.; Gottschalk, P. *J. Org. Chem.* **1983**, *48*, 5356-5357.



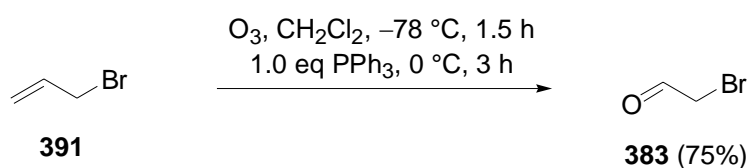
Scheme 104: Envisioned synthesis of the allylic alcohol **11** based on the formation of β -hydroxybutyrolactone **386**. Bn= benzyl, TBS= *tert*-butyldimethylsilyl [Si(*t*-Bu)Me₂], LDA= lithium diisopropylamide, R= alkyl.

Starting material **385** was generated by monoprotection of pentane-1,5-diol (**388**) and subsequent oxidation of the free hydroxyl group using a two step protocol (Scheme 105).³⁰⁸ A one-step variation using TEMPO for the direct transformation of the alcohol into the acid³⁰⁹ furnished the desired acids with unsatisfying yields.



Scheme 105: Synthesis of acids **390a** and **390b**. PMB= *para*-methoxybenzyl, Bn= benzyl.

Aldehyde **383** was synthesized by ozonolysis of allyl bromide (**391**) (Eq. 46). After distillation it was obtained as solution in CH₂Cl₂.³⁰⁷

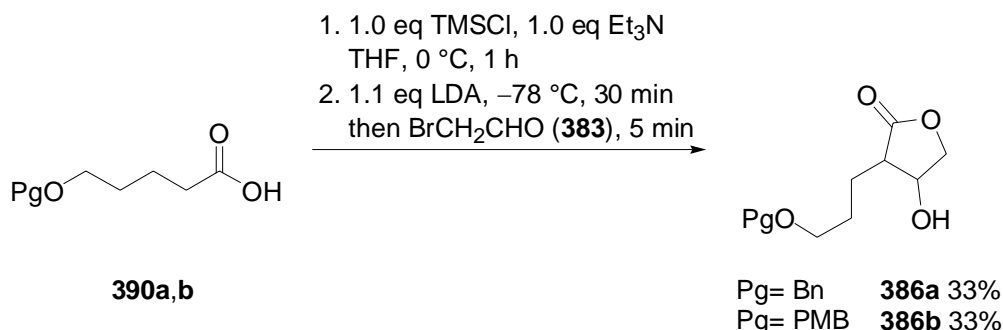


Eq. 46

³⁰⁸ Parikh, J. P.; Doering, W. v. E. *J. Am. Chem. Soc.* **1967**, *89*, 5505-5507.

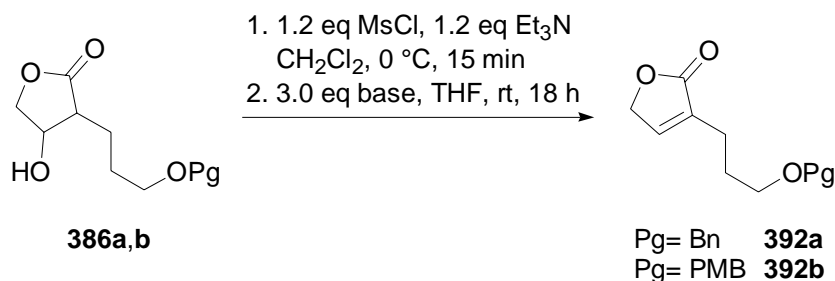
³⁰⁹ De Luca, L.; Giacomelli, G.; Masala, S.; Porcheddu, A. *J. Org. Chem.* **2003**, *68*, 4999-5001.

For the formation of the β -hydroxybutyrolactones **386a,b**, acids **390a,b** were first transformed to the corresponding trimethylsilyl esters **385**. Subsequent deprotonation and reaction with the aldehyde **383** afforded the β -hydroxybutyrolactones **386a,b** in low yield (Scheme 106).



Scheme 106 Formation of the β -hydroxybutyrolactones **386a,b**. TMS= trimethylsilyl [SiMe₃], LDA= lithium diisopropylamide, PMB= *para*-methoxybenzyl, Bn= benzyl.³¹⁰

The β -hydroxybutyrolactones **386a,b** were then mesylated and subjected to basic conditions to induce β -elimination (Table 27). Utilization of tetramethyl guanidine resulted in slightly higher yields compared to DBU. However, the α,β -unsaturated lactones **392a,b** were formed with low yields.



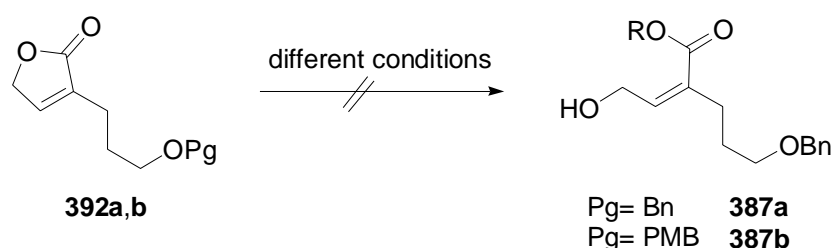
| Entry | Pg | Base | Yield [%] |
|-------|-----|-----------------------|-----------|
| 1 | Bn | DBU | 30 |
| 2 | Bn | tetramethyl guanidine | 34 |
| 3 | PMB | DBU | 31 |
| 4 | PMB | tetramethyl guanidine | 43 |

Table 27: The α,β -unsaturated lactones **391** were formed only with unsatisfying yields. PMB= *para*-methoxybenzyl, Bn= benzyl, DBU=1,8-diazabicyclo[5.4.0]undec-7-ene.

Initial experiments to induce lactone cleavage by treatment of **391a,b** with sodium methanolate only led to the recovery of the starting materials. Attempts to trap a potentially

³¹⁰ Diastereoselectivity was not determined. Yields not optimized.

formed γ -hydroxyl ester **387a,b** that could possibly relactonize under the reaction conditions proved to be unsuccessful (Scheme 107).³¹¹

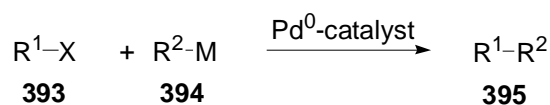


Scheme 107: Initial experiments for the lactone cleavage were unsuccessful. PMB= *para*-methoxybenzyl, Bn= benzyl.

Therefore, and with respect to the low yields obtained for the previous steps, we turned our attention toward an alternative route employing a palladium(0)-catalyzed cross-coupling.

13.2 Cross-Coupling Approach

Palladium(0)-catalyzed cross-coupling reactions have evolved into fundamental synthetic tools for carbon-carbon bond formation. Highly efficient and exceptionally mild methods were introduced that now have a proven track of successful applications in natural product synthesis.³¹² Several variations have been developed with respect of the organometallic coupling partner **394**.



Eq. 47 M= metal (e.g. Sn, Zn, B, Mg), R¹,R²= alkyl, alkenyl, aryl, alkynyl.

Grignard reagents as nucleophiles for the cross-coupling reaction were first reported by Kumada and co-workers in 1972.³¹³ Negishi *et al.* found zinc organyls versatile cross-coupling partners.³¹⁴ Only a short time later, organostannans were introduced as highly useful

³¹¹ Reaction conditions not optimized.

³¹² De Meijere, A.; Diederich, F. (Eds.) *Metal-Catalyzed Cross-Coupling Reactions (2nd Edn.)* **2004**, Wiley-VCH, Weinheim.

³¹³ Nickel-catalyzed: (a) Kumada, M. *J. Am. Chem. Soc.* **1972**, *94*, 4374-4376. Palladium-catalyzed: (b) Hayashi, T.; Konishi, M.; Kumada, M. *Tetrahedron Lett.* **1979**, *20*, 1871-1874.

³¹⁴ Negishi, E.-i.; King, A. O.; Okukada, N. *J. Org. Chem.* **1977**, *42*, 1821-1823. For a review, see: Negishi, E.-i. *Acc. Chem. Res.* **1982**, *15*, 340-348.

cross-coupling partners by Migita and Stille.³¹⁵ A less toxic alternative was found by the application of organo boron compounds.³¹⁶ The reaction requires the presence of a base. Without the addition of the base, the highly covalent characteristic of the boron-carbon bond prevents the transmetallation step.

Palladium(0)-catalyzed cross-couplings, that utilize alkenylcopper(I)-compounds are referred to as Normant-couplings.³¹⁷ The successful application of organosilicon compounds was reported by Hiyama and co-workers.³¹⁸ Another important variation is the so-called Sonogashira-coupling that employs alkynylcopper(I) compounds.³¹⁹

It is generally agreed that cross-couplings proceed via a catalytic cycle that involves the oxidative addition of the palladium(0) species into the carbon-halogen bond (alternatively a carbon-OTf bond), followed by transmetallation - the transfer of the organic group from the organometallic compound to the palladium - and finally the reductive elimination releasing the coupling product and at the same time regenerating the catalyst for another turnover (Scheme 108). Each of the steps involves further complicated processes, e.g. ligand exchanges. However, the presence of the intermediates **396** and **397** was verified by isolation and spectroscopic analysis.^{316a}

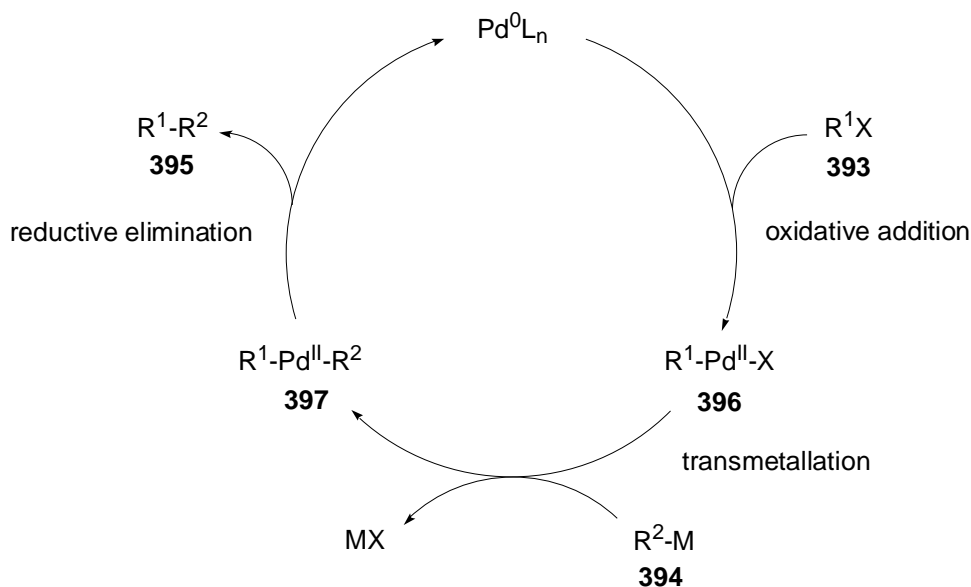
³¹⁵ (a) Kosugi, M.; Sasazawa, K.; Shimizu, Y.; Migita, T. *Chem. Lett.* **1977**, 301-302. (b) Milstein, D.; Stille, J. K. *J. Am. Chem. Soc.* **1978**, *100*, 3636-3638. For reviews see: (c) Farina, V.; Krishnamurthy, V.; Scott, W. *J. Org. React.* **1997**, *50*, 1-652. (d) Fugami, K.; Kosugi, M. *Top. Curr. Chem.* **2002**, *219*, 87-130.

³¹⁶ Miyaura, N.; Yamada, K.; Suzuki, A. *Tetrahedron Lett.* **1979**, *20*, 3437-3440. For reviews see: (a) Miyaura, N.; Suzuki, A. *Chem. Rev.* **1995**, *95*, 2457-2483. (b) Suzuki, A. *J. Organomet. Chem.* **1999**, *576*, 147-168.

³¹⁷ Alexakis, N. J. A.; Normant, J. F. *Tetrahedron Lett.* **1981**, *22*, 959-962.

³¹⁸ Hatanaka, Y.; Hiyama, T. *J. Org. Chem.* **1988**, *53*, 918-920.

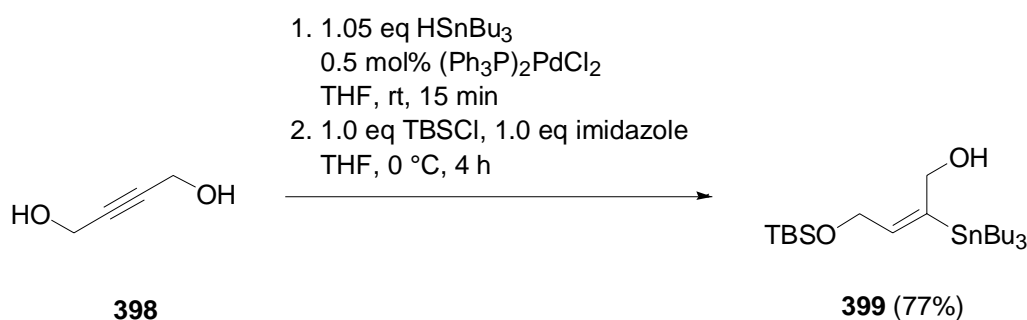
³¹⁹ Sonogashira, K.; Tohda, Y.; Hagihara, N. *Tetrahedron Lett.* **1975**, *16*, 4467-4470.



Scheme 108: Simplified catalytic cycle for palladium(0)-catalyzed cross-couplings. X= halogen or trifluoromethane sulfonyl (OTf), M= metal (e.g. B, Mg, Zn, Sn, Cu, Si), R¹,R²= alkyl, alkenyl, aryl, alkynyl.

13.2.1 Stille Cross-Coupling

In 2001, Parrain *et al.* reported the synthesis of the monoprotected vinyl stannane **399** as intermediate during their efforts toward the synthesis of marine sesquiterpenes.³²⁰ Reproduction of the two step procedure afforded vinylstannane **399** with improved isolated yields (lit. 64%³²⁰) (Eq. 48).

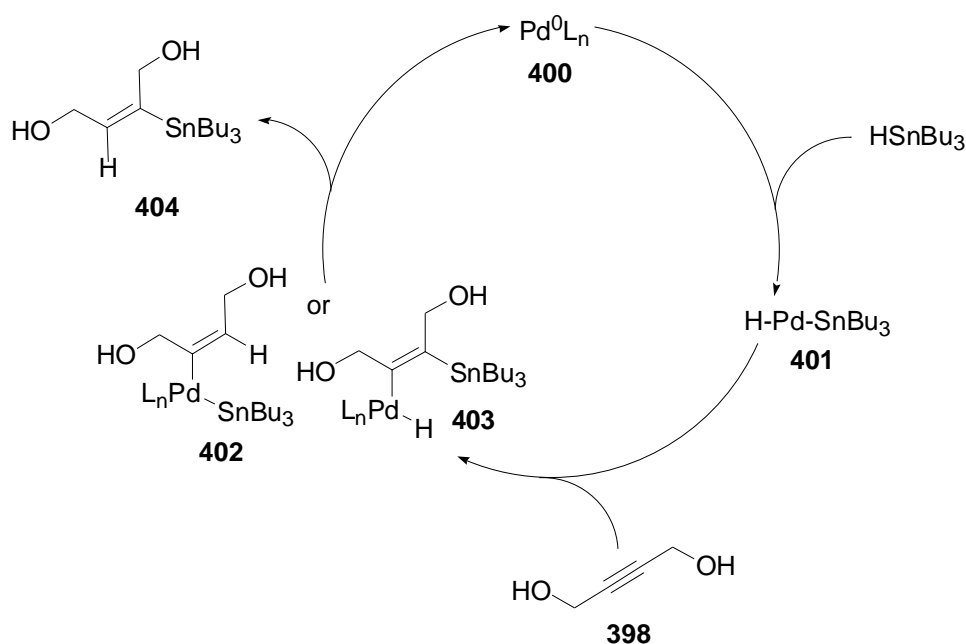


Eq. 48 TBS= *tert*-butyldimethylsilyl [Si(*t*-Bu)Me₂].

The palladium(0)-catalyzed hydropalladation is believed to proceed via the simplified mechanism illustrated in Scheme 109.³²¹

³²⁰ Commeiras, L.; Santelli, M.; Parrain, J.-L. *Org. Lett.* **2001**, *3*, 1713-1715.

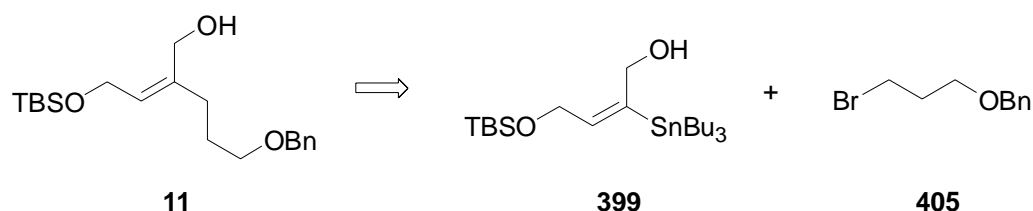
³²¹ (a) Ichinose, Y.; Oda, H.; Oshima, K.; Utimoto, K. *Bull. Chem. Jpn. Soc.* **1987**, *60*, 3468-3470. (b) Kikukawa, K.; Umekawa, H.; Wada, F.; Matsuda, T. *Chem. Lett.* **1988**, 881-884. (c) Zhang, H. X.; Guibé, F.; Balavoine, G. *Tetrahedron Lett.* **1988**, *29*, 619-622. (d) Guibé, F. *Main Group Met. Chem.* **1989**, *12*, 437-446. (e) Zhang, H.



Scheme 109: Model-mechanism for the palladium(0)-catalyzed hydrostannation of alkyne **398**.

Initially, the Pd^{II} hydrido stannyl complex **401** is formed by oxidative addition of the palladium(0) catalyst **400** into the hydrogen-tin-bond of HSnBu₃. *Cis*-addition (either of Pd-H or Pd-Sn of **401**) to the alkyne **398** and subsequent reductive elimination generates the desired (*E*)-vinylstannane **404**. The steric demand of the trialkyl stannyl group in **404** allowed the selective protection of the less hindered hydroxyl group of **404**.³²² Therefore, **399** was formed exclusively.

Structure **399** represents a prospective candidate for the formation of allylic alcohol **11**. It possesses the correct double bond configuration and a stannyl functionality located at the desired position to allow regioselective cross-coupling.

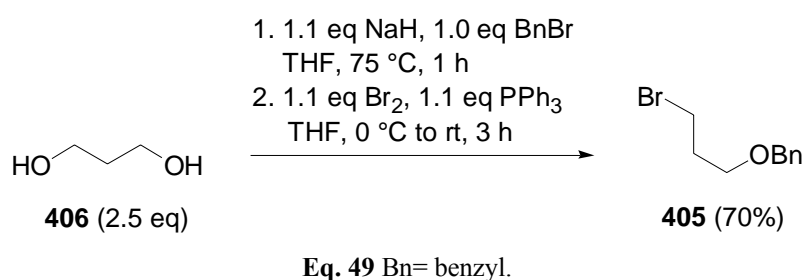


Scheme 110: Retrosynthetic analysis of **11** involving a Stille cross-coupling. TBS= *tert*-butyldimethylsilyl [Si(*t*-Bu)Me₂], Bn= benzyl.

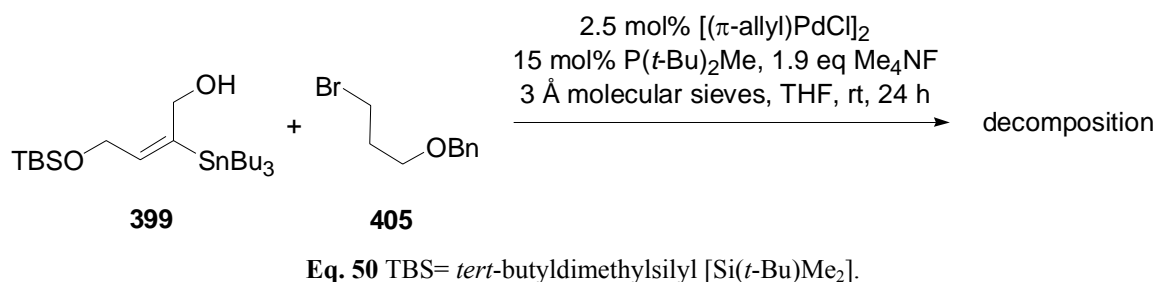
X.; Guibé, F.; Balavoine, G. *J. Org. Chem.* **1990**, *55*, 1857-1867. (f) Miyake, H.; Yamamura, K. *Chem. Lett.* **1989**, 981-984. (g) Cochran, J. C.; Bronk, B. S.; Terrence, K. M.; Phillips, H. K. *Tetrahedron Lett.* **1990**, *31*, 6621-6624. (h) Lautens, M.; Smith, N. D.; Ostrovsky, D. *J. Org. Chem.* **1997**, *62*, 8970-8971.

³²² Barrett, A. G. M.; Barta, T. E.; Flygare, J. A. *J. Org. Chem.* **1989**, *54*, 4246-4249.

However, the trialkylstannyl group is part of a tri-substituted double bond. Stille cross-couplings involving such starting materials are rarely found among the literature.³²³ Moreover, the utilization of alkyl electrophiles is sometimes complicated.³²⁴ In 2003, Fu *et al.* reported reaction conditions, which were successfully utilized for the Stille cross-coupling with various alkyl bromides bearing β -hydrogen atoms.³²⁵ Therefore, encouraged by this report, the cross-coupling between **399** and **405** as possible route to **11** was investigated. Alkyl bromide **405** was synthesized in two steps starting from propane-1,3-diol (**406**) by monoprotection and redox condensation (Eq. 49).⁶³ Using carbon tetrabromide instead of bromine resulted in reduced yields.



Unfortunately, exposure of vinyl stannane **399** to **405** using the conditions described by Fu³²⁵ led to the complete decomposition of the starting materials and the formation of unidentified side products (Eq. 50).



However, none of the isolated products exhibited aromatic signals in the ¹H NMR spectrum a result that could have been accounted as evidence for a successful coupling between stannane **399** and the bromide **405**.

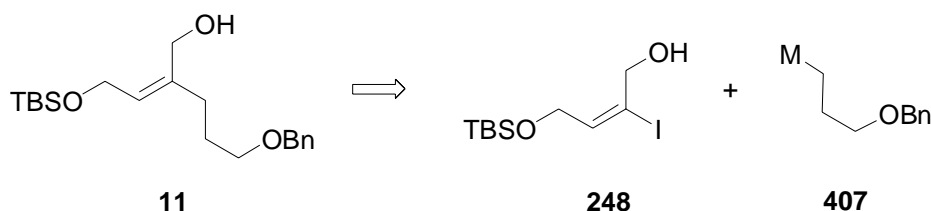
³²³ (a) Bellina, F.; Carpita, A.; De Santis, M.; Rossi, R. *Tetrahedron* **1994**, *50*, 12029-12046. (b) Burke, B.; Overman, L. E. *J. Am. Chem. Soc.* **2004**, *126*, 16829-16833.

³²⁴ For difficulties concerned with the utilization of alkyl electrophiles, see: (a) Cárdenas, D. J. *Angew. Chem., Int. Ed.* **2003**, *42*, 384-387; *Angew. Chem.* **2003**, *115*, 398-401. (b) Cárdenas, D. J. *Angew. Chem., Int. Ed.* **1999**, *38*, 3018-3020; *Angew. Chem.* **1999**, *111*, 3201-3203. (c) Luh, T.-Y.; Leung, M.-k.; Wong, K.-T. *Chem. Rev.* **2000**, *100*, 3187-3204.

³²⁵ Menzel, K.; Fu, G. C. *J. Am. Chem. Soc.* **2003**, *125*, 3718-3719.

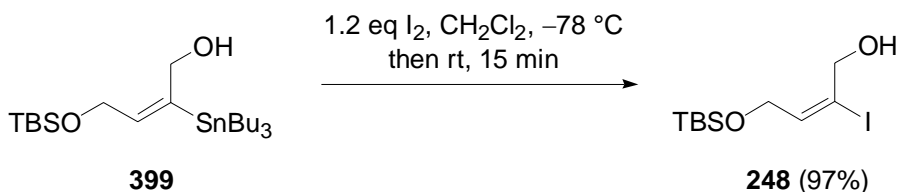
13.2.2 Negishi and Suzuki-Miyaura Cross-Coupling

Since the efforts to generate **11** by Stille cross-coupling have not met the desired success, a different strategy with reversed reactivity of the coupling partners was attempted. As shown in Scheme 111 this strategy involves a C(sp³)-C(sp²) bond formation between the vinyl halogenid **248** and the metallated alkyl compound **407**. Even though this variation is not as highly developed as its C(sp²)-C(sp²) counterparts, reliable procedures emerged over the past twenty years.³²⁶ Therefore, the *B*-alkyl-Suzuki-Miyaura³²⁷ and the Negishi^{314,328} cross-couplings which have been shown to provide a well tried access to such carbon-carbon bond formations were chosen (Scheme 111).



Scheme 111: Retrosynthetic analysis of allylic alcohol **11** based on the *B*-alkyl-Suzuki-Miyaura- (M= B) or Negishi- (M= Zn) cross-coupling. TBS= *tert*-butyldimethylsilyl [Si(*t*-Bu)Me₂], Bn= benzyl.

Subjecting vinylstannane **399** to iodine resulted in a clean and almost quantitative conversion to the vinyl iodide **248** by iododestannylation (Eq. 51).³²⁹



Eq. 51 TBS= *tert*-butyldimethylsilyl [Si(*t*-Bu)Me₂].

The vinyl iodide **248** appears to be light sensitive and degenerates upon storing for prolonged times.³³⁰

³²⁶ Tamao, K. *Coupling Reactions Between sp³ and sp² Carbon Centers*, in *Comprehensive Organic Synthesis*, Vol. 3, Trost, B. M.; Fleming, I. (Eds.) **1991**, Pergamon Press, Oxford.

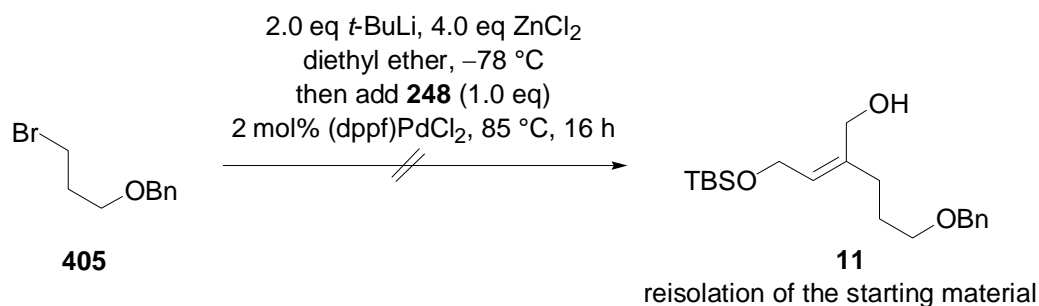
³²⁷ (a) See reference 222. For a review see: (b) Chemler, S. R.; Trauner, D.; Danishefsky, S. J. *Angew. Chem.* **2001**, *113*, 4676-4701; *Angew. Chem., Int. Ed.* **2001**, *40*, 4544-4568.

³²⁸ (a) Kobayashi, M.; Negishi, E.-i. *J. Org. Chem.* **1980**, *45*, 5223-5225. (b) Negishi, E.-i.; Owczarczyk, Z. *Tetrahedron Lett.* **1991**, *32*, 6683-6686. (c) Williams, D. R.; Kissel, W. S. *J. Am. Chem. Soc.* **1998**, *120*, 11198-11199. (d) Ohgiya, T.; Nishiyama, S. *Tetrahedron Lett.* **2004**, *45*, 8273-8275.

³²⁹ Aoyagi, S.; Wang, T. C.; Kibayashi, C. *J. Am. Chem. Soc.* **1993**, *115*, 11393-11409.

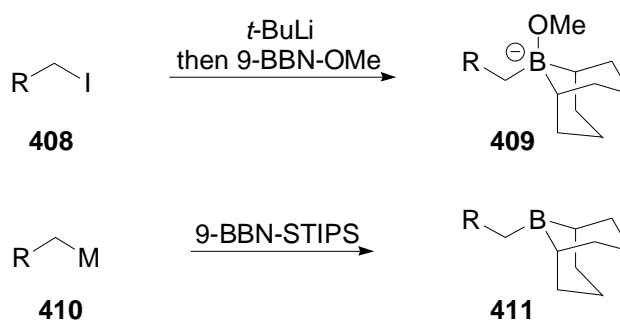
³³⁰ We found **248** being sufficiently stable for storing for about two weeks at 4 °C.

Motivated by the work of Nishiyama,^{328d} we attempted a Negishi coupling of vinyl iodide **248** with the corresponding zinc organyl derived from alkyl bromide **405**. Halogen lithium exchange and addition of zinc chloride was expected to produce the zinc organyl ready for palladium(0)-catalyzed cross-coupling. Neither in diethyl ether nor in THF the reaction produced any cross coupling product **11** (Eq. 52).



Eq. 52 TBS= *tert*-butyldimethylsilyl [Si(*t*-Bu)Me₂], Bn= benzyl.

Therefore, the *B*-alkyl-Suzuki-Miyaura cross-coupling was addressed next.³²⁷ In this version of the Suzuki-Miyaura coupling,³¹⁶ the originally employed aryl and alkenyl boron compounds were replaced by alkyl boron compounds.³²⁷ Trialkylboranes may be generated by transmetallation of alkyl lithium or Grignard compounds **408/410** (Scheme 112).³³¹



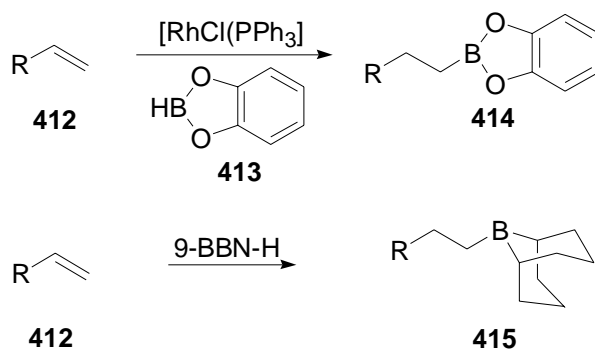
Scheme 112: Formation of trialkylboranes by transmetallation. BBN= borabicyclo[3.3.1]nonane, TIPS= triisopropylsilyl [Si(*i*-Pr)₃], M= MgBr or Li.

However, most often the facile transformation of alkene double bonds into alkyl boranes using hydroboration³³² with catechol borane **413** (Scheme 113, top) or 9-borabicyclo[3.3.1]nonane 9-BBN-H (Scheme 113, bottom) is employed for the generation of the starting material. The less reactive alkyl boronic acids derivatives **414** obtained by

³³¹ (a) Marshall, J. A.; Johns, B. A. *J. Org. Chem.* **1998**, *63*, 7885-7892. (b) Kalesse, M. *ChemBioChem* **2000**, *1*, 171-175. (c) Soderquist, J. A.; Justo de Pomar, J. C. *Tetrahedron Lett.* **2000**, *41*, 3537-3539. (d) Matteson, D. S. *Tetrahedron* **1989**, *45*, 1859-1885.

³³² Miyaura, N.; Ishiyama, T.; Sasaki, H.; Ishikawa, M.; Satoh, M.; Suzuki, A. *J. Am. Chem. Soc.* **1989**, *111*, 314-321.

hydroboration with catechol borane **413** usually required special conditions for the cross coupling. It was shown, that thallium salts (e.g. TlOH or Tl₂CO₃) are efficient bases to enable the transformation.³³³ However, their major drawback is the high toxicity. Therefore, 9-BBN-H is the most commonly hydroboration agent for the generation of the starting materials **415** of the *B*-alkyl-Suzuki-Miyaura cross-coupling.

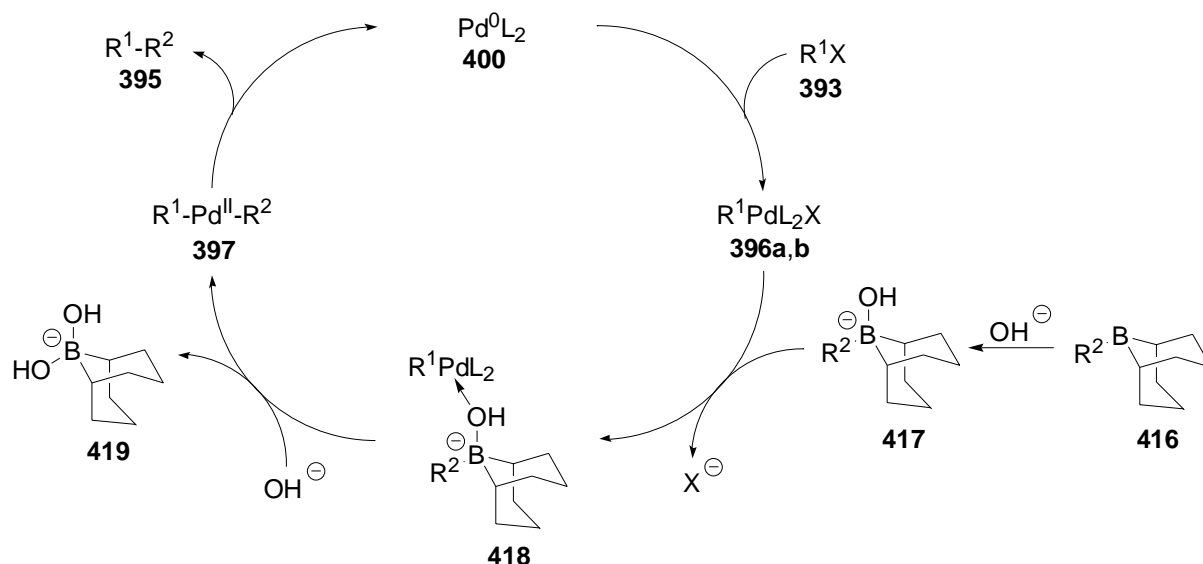


Scheme 113: Formation of trialkylboranes **414/415** by hydroboration.

The hydroboration step proceeds with high *anti*-Markovnikov selectivity. It is best suited for electron rich double bonds. Advantageously for the *B*-alkyl-Suzuki-Miyaura cross-coupling reactions are the different transfer tendencies of primary and secondary alkyl groups bound at the boron atom. Since primary alkyl groups are transferred preferentially, this prevents transmission of the secondary alkyl groups of 9-BBN. As priorly mentioned, the addition of a base is required. During their studies, Soderquist and Matos ascertained that the base is involved in various steps of the catalytic cycle (Scheme 114).³³⁴ The hydroxy group will bind to the Lewis acidic boron atom of the trialkylborane **416** affording a negatively charged boronate **417** which is believed to be the reactive species for the transformation. The oxygen atom of the hydroxy group of **417** enables coordination to the Lewis acidic palladium(II) intermediate **396** to form the π -complex **418**. The base will as well facilitate the transmetallation step leading to the formation of **397** by replacing the alkyl moiety of **418** that is transferred to palladium. Finally, it was shown that addition of the base causes the hydrolysis of the primary formed product **396a** (X= Hal/OTf) of the oxidative addition to the more reactive complex **396b** (X= OH).

³³³ Sato, M.; Miyaura, N.; Suzuki, A. *Chem. Lett.* **1999**, 1405-1408.

³³⁴ Matos, K.; Soderquist, J. A. *J. Org. Chem.* **1998**, *63*, 461-470.



Scheme 114: Mechanism of the *B*-alkyl-Suzuki-Miyaura cross-coupling. X= Hal/OTf or OH.

The choice of the catalyst applied for the reaction is an important parameter to influence the cross-coupling. Although various catalysts have been successfully employed for the transformation (e.g. $\text{Pd}(\text{PPh}_3)_4$ and Pd_2dba_3), the most successful and frequently used palladium complex is the ferrocenyl complex $(\text{dppf})\text{PdCl}_2$.³³⁵ The success of this specific catalyst may be accounted to the following reasons:

- As shown in Figure 23 the structure of the ligand enforces a *cis*-arrangement of R^1 and R^2 which facilitates the reductive elimination. This is essential to avoid β -hydride elimination that has always been taken into consideration when substrates bearing β -hydrogen atoms are employed.
- The voluminous iron atom causes a small bite angle resulting in a closer position of the residues that will be coupled what may as well facilitate the reductive elimination step of the coupling.

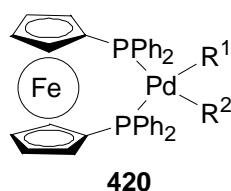
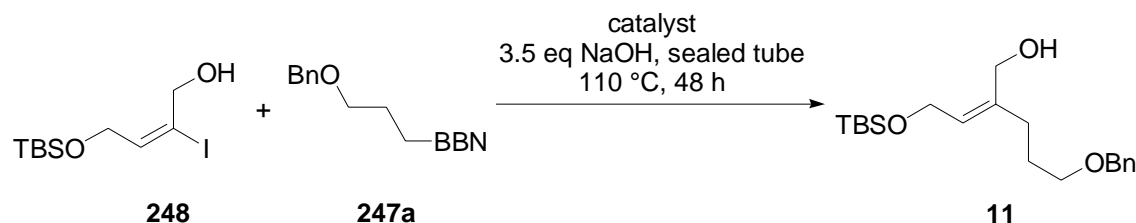


Figure 23: Representation of the palladium complex **420** prior to the reductive elimination step.

Since the reaction takes place in an aquatic environment, it was expected that the unprotected hydroxyl group of vinyl iodide **248** would be tolerated by the reaction conditions. Initial

³³⁵ Hayashi, T.; Konishi, M.; Kobori, Y.; Kumada, M.; Higuchi, T.; Hirotsu, K. *J. Am. Chem. Soc.* **1984**, *106*, 158-163.

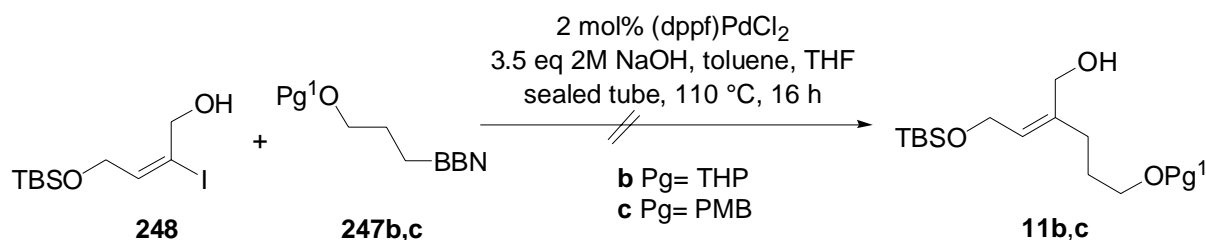
attempts with Pd(PPh₃)₄ (Table 28, entry 1) and Pd₂dba₃ (Table 28, entry 2) according to the procedures published by Kwochka³³⁶ and Shibasaki³³⁷ respectively have been unsuccessful. We next tested the palladium(II) ferrocenyl complex (dppf)PdCl₂. With an aqueous solution of NaOH as base and THF or a mixture of THF and toluene (1/1) as solvent **11** was formed as minor product (Table 28, entry 3 and 4).³³⁸



| Entry | Catalyst | Solvent | Yield[%] |
|-------|--|-------------|----------|
| 1 | 20 mol% Pd(PPh ₃) ₄ | THF | 0 |
| 2 | 20 mol% Pd ₂ dba ₃ | THF | 0 |
| 3 | 5 mol% (dppf)PdCl ₂ | THF | 7 |
| 4 | 5 mol% (dppf)PdCl ₂ | toluene/THF | 3 |

Table 28 TBS= *tert*-butyldimethylsilyl [Si(*t*-Bu)Me₂], Bn= benzyl.

We tested different protection groups of the allylic alcohol employed in the hydroboration step. Neither introduction of the THP-protecting group³³⁹ nor utilization of PMB-protected allylic alcohol³⁴⁰ resulted in the isolation of the desired coupling product.



Scheme 115: TBS= *tert*-butyldimethylsilyl [Si(*t*-Bu)Me₂], PMB= *para*-methoxybenzyl, THP= tetrahydropyranyl.

³³⁶ Smith, B. B.; Kwochka, W. R.; Damrauer, R.; Swope, R. J.; Smyth, J. R. *J. Org. Chem.* **1997**, *62*, 8589-8590.

³³⁷ Cho, S. Y.; Shibasaki, M. *Tetrahedron: Asymmetry* **1998**, *9*, 3751-3754.

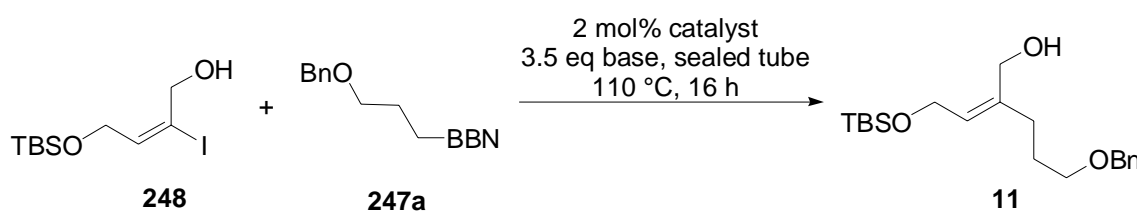
³³⁸ Kamatani, A.; Overman, L. E. *J. Org. Chem.* **1999**, *64*, 8743-8744.

³³⁹ For a successful hydroboration of a THP-protected allylic alcohol, see: Mori, K.; Puapoomchareon, P. *Liebigs Ann. Chem.* **1990**, 159-162.

³⁴⁰ For the hydroboration of alkenes containing PMB-ethers, see: Meng, D.; Danishefsky, S. J. *Angew. Chem.* **1999**, *111*, 1582-1585; *Angew. Chem., Int. Ed.* **1999**, *38*, 1485-1478.

TLC-control indicated that in the case of THP-protected allylic alcohol **247b** already the hydroboration was problematic. Using PMB as protecting group resulted in the consumption of the starting material during the hydroboration step (followed by TLC). Nevertheless, the following cross-coupling reaction of **247c** has not been successful.

With the strong dependency of the *B*-alkyl-Suzuki-Miyaura cross-coupling from the base and the solvent in mind, we performed the reaction at several other reaction conditions which were successfully employed for other systems (Table 29).



| Entry | Catalyst | Solvent | Base | Yield [%] |
|-------|------------------------------------|---------|--------------------------------|----------------|
| 1 | Pd(PPh ₃) ₄ | dioxane | K ₃ PO ₄ | 0 ^a |
| 2 | Pd ₂ dba ₃ | dioxane | K ₃ PO ₄ | 0 ^a |
| 3 | (dppf)PdCl ₂ | dioxane | K ₃ PO ₄ | 21 |
| 4 | (dppf)PdCl ₂ | DMF | K ₃ PO ₄ | 14 |
| 5 | (dppf)PdCl ₂ | DMF | CsCO ₃ ^b | 20 |

Table 29: ^a catalyst loading 20 mol% ^b 2 mol% AsPh₃ were added in this attempt. TBS= *tert*-butyldimethylsilyl [Si(*t*-Bu)Me₂], Bn= benzyl.

K₃PO₄ in dioxane in combination with Pd(PPh₃)₄³⁴¹ (Table 29, entry 1) or Pd₂dba₃³³⁷ (Table 29, entry 2) did not furnish the desired coupling product. However, combination of K₃PO₄ with the ferrocenyl complex (dppf)PdCl₂ performed in dioxane³⁴² (Table 29, entry 3) provided an improved access to the allylic alcohol **11**. Performed in DMF (Table 29, entry 4) as reported by Mori *et al.*³³⁹ the reaction afforded **11** with lower yields while application of CsCO₃ in combination with triphenylarsine³⁴³ (Table 29, entry 5) gave comparable results. However, the isolated yields remain unsatisfactory.

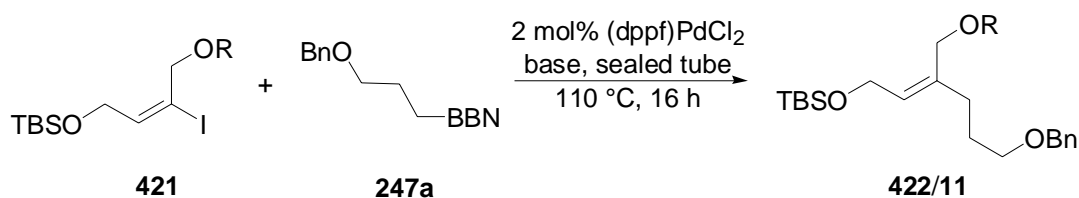
In a next step, we protected the free hydroxyl group prior to the coupling (Table 30). While the PMB-protected vinyl iodide did not react (Table 30, entry 1), application of TES

³⁴¹ Ishiyama, T.; Miyaura, N.; Suzuki, A. *Bull. Chem. Soc. Jpn.* **1991**, *64*, 1999-2001.

³⁴² Oh-e, T.; Miyaura, N.; Suzuki, A. *J. Org. Chem.* **1993**, *58*, 2201-2208.

³⁴³ Johnson, C. R.; Miller, M. W.; Golebiowski, A.; Sundram, H.; Ksebati, M. B. *Tetrahedron Lett.* **1994**, *35*, 8991-8994.

protection group resulted in an inseparable product mixture (Table 30, entry 2). Using thallium salts for the desired reaction did not result in the formation of the coupling product (Table 30, entry 3 and 4). Employment of the trimethylsilyl protected vinyl iodide **421** afforded fully protected allylic alcohol **422** (Table 30, entry 5) which was easily deprotected by treatment with K_2CO_3 in methanol. It should be emphasized at this point that the reaction of unprotected vinyl iodide **248** afforded **11** under comparable conditions only in trace amounts (Table 28, entry 4). With this pleasing result, we tested the reaction conditions that previously gave the best yields (Table 29, entry 3). Unluckily, for TMS-protected vinyl iodide **421** unsatisfactory 11% of the mono deprotected allylic alcohol **11** were isolated after treatment of the raw product with K_2CO_3 (Table 30, entry 6).

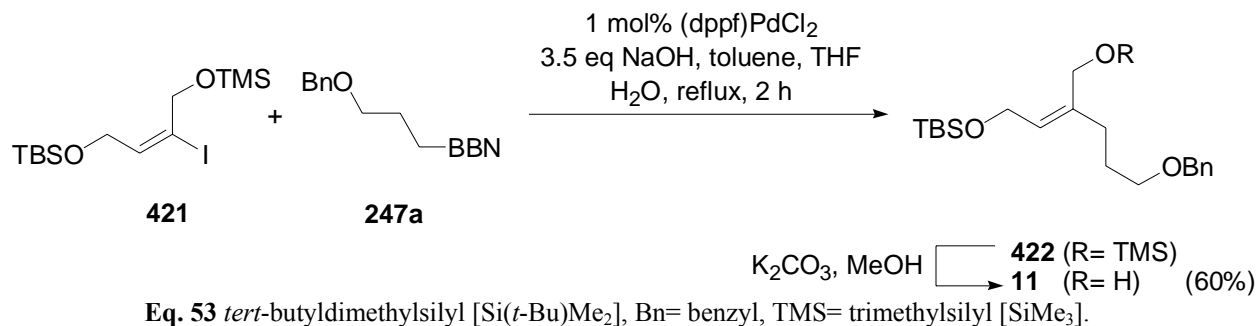


| Entry | R | Solvent | Base | Yield of 422 (R= TMS) | Yield of 11 after deprotection (R= H) ^a |
|-------|-----|-------------|-------------------------------------|---------------------------------|--|
| 1 | PMP | THF/toluene | 3.5 eq NaOH | Reisolated starting material | - |
| 2 | TES | THF/toluene | 3.5 eq NaOH | Inseparable product mixture | - ^b |
| 3 | TMS | THF/toluene | 1.5 eq $TiClO_3$ | 0 | - |
| 4 | TMS | THF/toluene | 3.0 eq $TiOEt_3$ 2 mol% $AsPh_3$ | 0 | - |
| 5 | TMS | toluene/THF | 3.5 eq NaOH | 66 ^c | 25 |
| 6 | TMS | dioxane | 3.5 eq K_3PO_4 | 43 ^c | 11 |

Table 30 ^a After treatment with K_2CO_3 in MeOH for 30 minutes at room temperature. ^b The raw product was subjected to acetic acid in CH_2Cl_2 at 0 °C which immediately resulted in the cleavage of both silyl ethers. ^c Contaminated by a not identified unpolar by-product. PMB= *para*-methoxybenzyl, TMS= trimethylsilyl [$SiMe_3$], Bn= benzyl, TBS= TBS= *tert*-butyldimethylsilyl [$Si(t-Bu)Me_2$].

In contrast to the reaction of vinyl iodide **248**, TMS protected **421** afforded a new, with TLC clearly detectable product which appeared to have a higher R_f value than the other various by-products of this rather grubby reaction. Cleavage of the TMS-ether was realized by the treatment with K_2CO_3 in methanol. Depending on the reaction conditions (bath temperature,

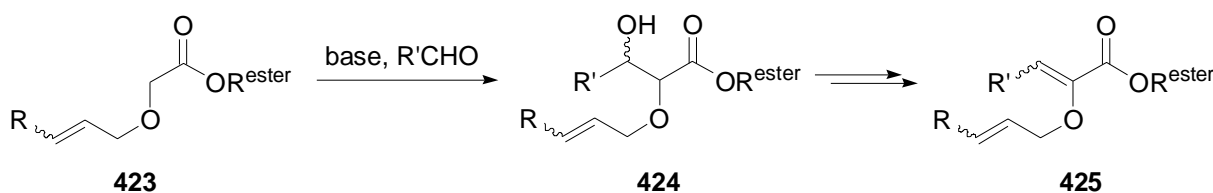
reaction time) we noticed that together with the fully protected allylic alcohol **422** varying amounts of monodeprotected allylic alcohol **11** were formed. Careful optimization of the reaction conditions guided us to the reaction conditions given below - the best result so far.



In summary, allylic alcohol **11** can be synthesized in a four-step sequence with moderate yield as single double bond isomer. Routinely, about 8 g (~30 mmol) of **248** were used for the transformation to afford about 5 g (~20 mmol) of the allylic alcohol **11**.

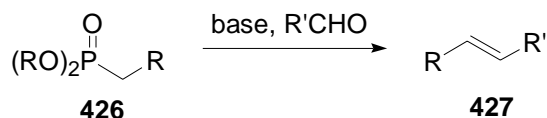
14 Stereoselective Synthesis of Allyl Vinyl Ethers via Horner-Wadsworth-Emmons Olefination

Since the discovery of the Claisen rearrangement the convenient synthesis of the allyl vinyl ether substrates has been a major concern. In our research group we have developed a strategy based on aldol condensation of an α -allyloxy substituted acetic acid ester **423** providing 2-alkoxycarbonyl substituted allyl vinyl ethers **425** (Scheme 116).⁶⁴



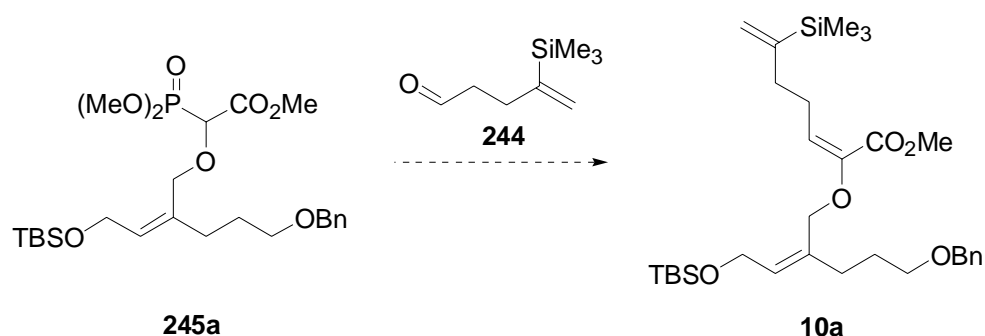
Scheme 116: Synthesis of AVEs **425** based on the aldol condensation strategy.

The aldol condensation provided mixtures of vinyl double bond isomers. The allyl vinyl ethers (*E*)- and (*Z*)-**425** were easily separable by preparative HPLC in multigram scale. They were usually produced with low selectivity or slightly preferred *Z*-selectivity. However, our synthetic plan for (–)-xeniolide **F** (**2a**) requires a selective access to AVE **10** with an *E*-configured vinyl ether double bond. Therefore, efforts were aimed at a new, selective access of such AVEs. We identified the inherently *E*-selective HWE reaction²¹⁶ as potential solution to overcome this hurdle (Eq. 54).



Eq. 54

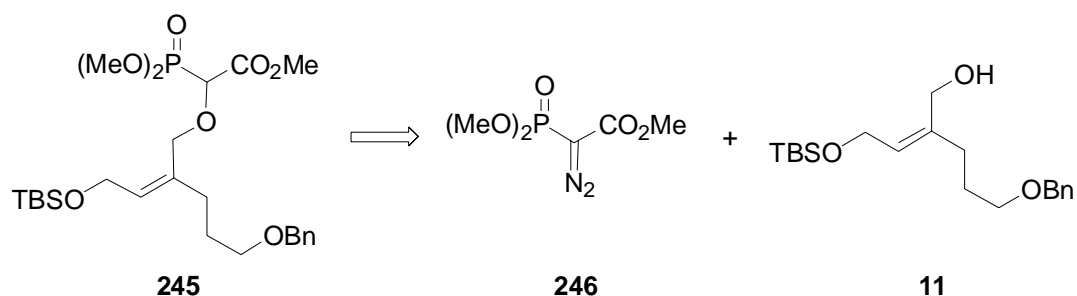
Starting from an appropriately substituted phosphonate **245a** deprotonation and subsequent reaction with aldehyde **244** should provide the AVE **10a** with *E*-configured vinyl ether double bond.



Scheme 117: Allyl vinyl ether **10a** may be synthesized by a HWE olefination of phosphonate **245a** with aldehyde **244**. TBS= *tert*-butyldimethylsilyl [$\text{Si}(t\text{-Bu})\text{Me}_2$], Bn= benzyl.

14.1 Rhodium-Catalyzed OH-Insertion

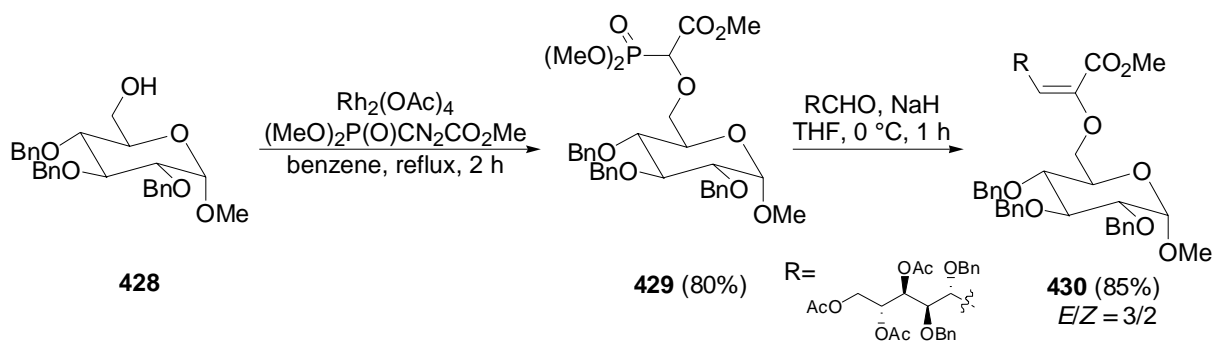
Required for the successful implementation of the HWE is a reliable access to the phosphonate **245a**. In our case, Rhodium catalysed OH-insertion²¹⁷ should enable the formation of the phosphonate **245a** starting from allylic alcohol **11** (Scheme 118).



Scheme 118: Access of the phosphonate **245** may be realized by rhodium catalyzed OH-insertion. TBS= *tert*-butyldimethylsilyl [$\text{Si}(t\text{-Bu})\text{Me}_2$], Bn= benzyl.

The rhodium(II)-catalyzed OH-insertion as preliminary step for the Horner-Wadsworth-Emmons olefination was first published by Sinaÿ and co-workers.³⁴⁴

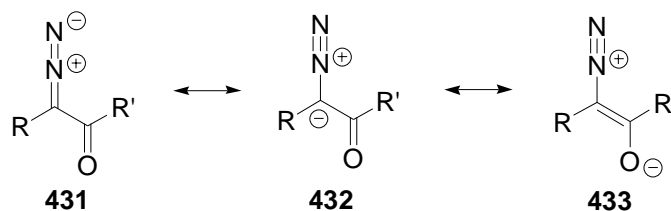
³⁴⁴ See reference 218a,b.



Scheme 119: The first example of a sequence of rhodium-catalyzed OH-insertion and HWE-olefination. Bn= benzyl, Ac= acetyl.

Further successful applications of this two step strategy were realised independently by Ganem,²¹⁹ and Berchtold.²²⁰ An intramolecular approach was developed by Moody and co-workers.^{221,345}

The starting diazo carbonyl compounds **431** have been widely applied for various chemical transformations.³⁴⁶ The carbonyl group plays an essential role during the generation of the carbene.³⁴⁷ It was postulated, that the resonance stabilization of diazo carbonyl compounds between keto and enolate form delocalizes the negative charge away from the diazo group (Scheme 120).³⁴⁸ Consequently, this would facilitate the nitrogen extrusion and therefore the formation of the carbene.



Scheme 120: Resonance stabilization of diazo carbonyl compounds.

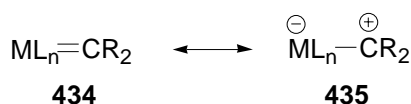
With transition metals diazo carbonyl compounds form electrophilic carbenes. The reactivity of the carbenes may be visualized by its resonance structure **435** (Scheme 121).

³⁴⁵ Davies, M. J.; Moody, C. J. *Tetrahedron Lett.* **1991**, 32, 6947-6948.

³⁴⁶ Ye, T.; McKerver, A. *Chem. Rev.* **1994**, 94, 1091-1160.

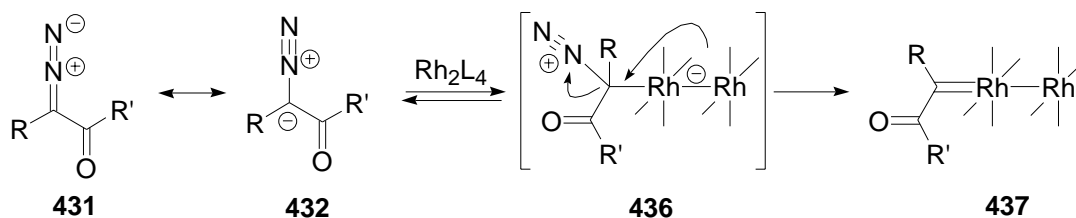
³⁴⁷ Cox, G. G.; Miller, D. J.; Moody, C. J.; Sie, E.-R. H. B. *Tetrahedron* **1994**, 50, 3195-3212.

³⁴⁸ Regitz, M.; Bartz, W. *Chem. Ber.* **1970**, 103, 1477-1485.



Scheme 121 M= metal (e.g. Rh, Cu).

However, there has been considerable controversy concerning the exact nature of the carbene. Studies performed by Wang *et al.* provided some experimental evidence favouring the build-up of a partial positive charge in the Rh^{II}-carbene.³⁴⁹ The results as well support the suggested mechanism of the metal catalysed decomposition of the diazo compounds (Scheme 122).³⁵⁰ After complexation of the negatively polarized carbon atom of the diazo compound to the axial site of the Rh^{II} catalyst subsequent irreversible extrusion of nitrogen results in the formation of the rhodium(II) carbene intermediate **437**.



Scheme 122: Exemplary formation of a carbene **437** with a binuclear rhodium(II)-complex as catalyst. In structures **436** and **437** the ligands are not depicted for concise reason and would be bound at the four remaining single bonds present at each of the rhodium atoms. L= bidentate ligand.

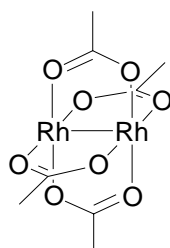
Due to the electrophilic character, the metal carbene **437** reacts preferentially with electron rich substrates. Insertions (α,α -substitutions) into Het-H and Het-Het bonds, cyclopropanations, C-H-insertions, dipolar cycloaddition and sigmatropic rearrangements as result of ylide formations are the predominant examples.²¹⁷ The most important catalyst for such transformations was found to be the binuclear complex Rh₂(OAc)₄ (Figure 24). Teyssié *et al.* was the first to discover the potential of Rh₂(OAc)₄ as catalyst in reactions with diazo compounds.³⁵¹ Variation of the ligands both resulted in the basic understanding of carbenoid transformations and to the evolution of chiral catalysts for enantioselective transformations.³⁵²

³⁴⁹ Qu, Z., Shi, W.; Wang, J. *J. Org. Chem.* **2001**, *66*, 8139-8144.

³⁵⁰ Doyle, M.; P. *Chem. Rev.* **1986**, *86*, 919-939.

³⁵¹ Paulissen, R.; Hubert, A. J.; Teyssié, Ph. *Tetrahedron Lett.* **1972**, *23*, 1465-1466.

³⁵² Doyle, M. P.; Forbes, D. C. *Chem. Rev.* **1998**, *98*, 911-935.



438

Figure 24

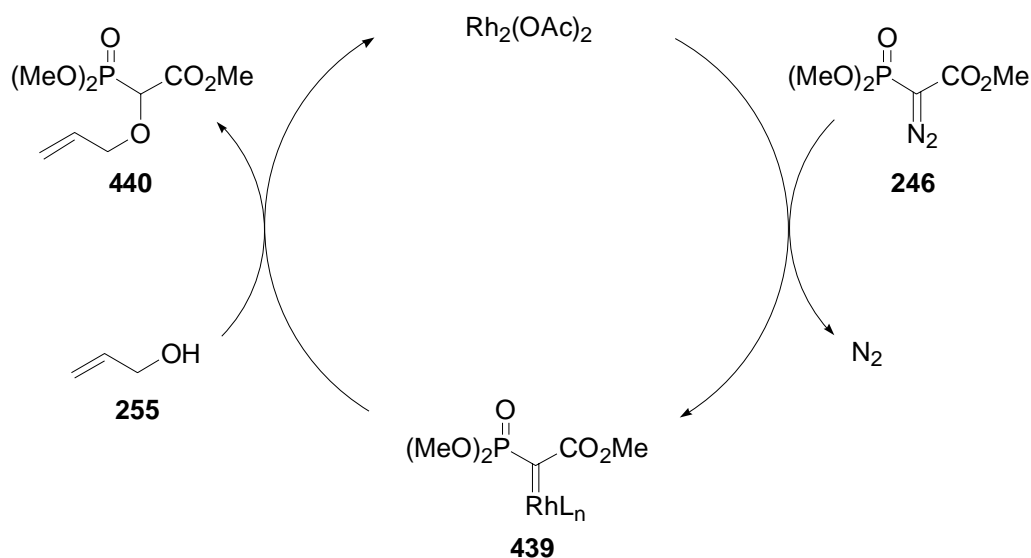
Subjected to substrates possessing OH-groups, the reaction causes a formal insertion of the carbene into the OH-bond.³⁵³ Probably the most common example of the insertion of a carbene (derived from a diazo compound) into an OH-bond is the esterification of carboxylic acids with diazomethane.³⁵⁴ For the formation of ethers, the carbene insertion into the OH-bond of alcohols has to be addressed. Phosphonate **245a** - the starting material for a Horner-Wadsworth-Emmons olefination - may be generated using diazophosphonoacetate **246** as the appropriated substrate. In contrast to diazo carbonyl compounds **431**, diazophosphonoacetate **246** often exhibited reduced reactivities and afford the application of the more reactive rhodium(II) trifluoroacetamide $[\text{Rh}_2(\text{tfacm})_4]$ to induce insertion reactions.³⁵⁵ Competing cyclopropanation reactions have to be considered if unsaturated alcohols are utilized as reaction partners. However, several experiments indicated that allylic alcohols (e.g. **11**) show a high preference for OH-insertion over cyclopropanations.³⁵⁶ The presumed mechanism of the transformation is depicted in Scheme 123.

³⁵³ Paulissen, R.; Reimlinger, H.; Hayez, E.; Hubert, A. J.; Teyssié, Ph. *Tetrahedron Lett.* **1973**, *24*, 2233-2236.

³⁵⁴ For recent examples, see: (a) Hanessian, S.; Gauchet, C.; Charron, G.; Marin, J.; Nakache, P. *J. Org. Chem.* **2006**, *71*, 2760-2778. (b) Kim, S.; Ko, H.; Lee, T.; Kim, D. *J. Org. Chem.* **2005**, *70*, 5756-5759. (c) Sohn, J.-H.; Waizumi, N.; Zhong, H. M.; Rawal, V. H. *J. Am. Chem. Soc.* **2005**, *127*, 7290-7291.

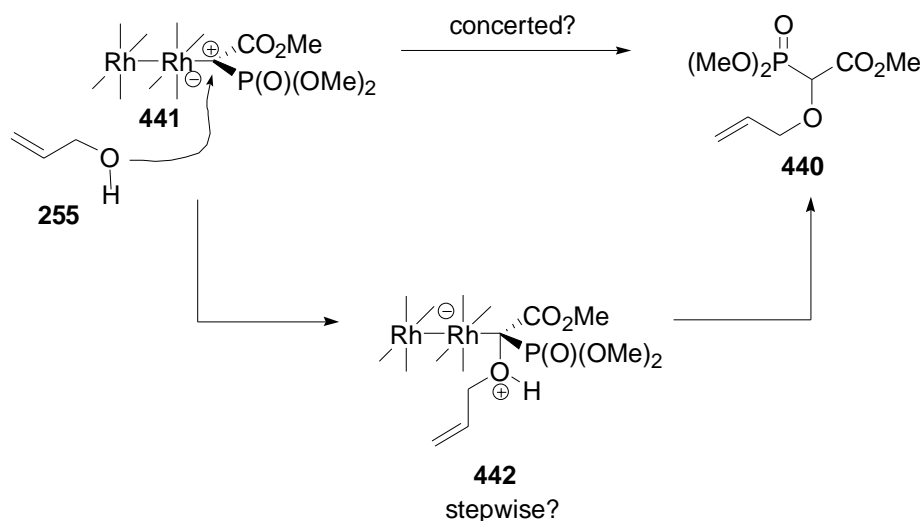
³⁵⁵ Cox, G. G.; Kulagowski, J. J.; Moody, C. J.; Sie, E.-R. H. B. *Synlett* **1992**, 975-976.

³⁵⁶ Petiniot, N.; Anciaux, A. J.; Noels, A. F.; Hubert, A. J.; Teyssié, P. *Tetrahedron Lett.* **1978**, *19*, 1239-1242.



Scheme 123: Mechanism of the rhodium-catalyzed OH-insertion.

The formation of the carbene **439** occurs with nitrogen extrusion. Formal OH-insertion of the carbene **439** into the OH-bond of the allylic alcohol **255** results in the formation of the phosphonate **440**. The insertion may proceed either in a single step or by a stepwise mechanism (Scheme 124).



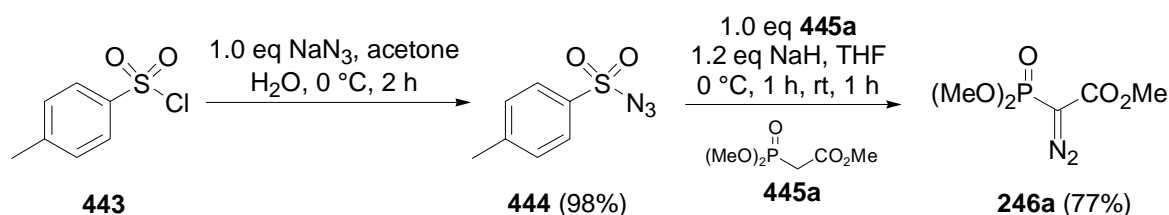
Scheme 124: Possible mechanism for the OH-insertion step.

However, to the best of my knowledge, the mechanism of the OH-insertion process has not been revealed, yet.

14.1.1 Synthesis of the Phosphonates

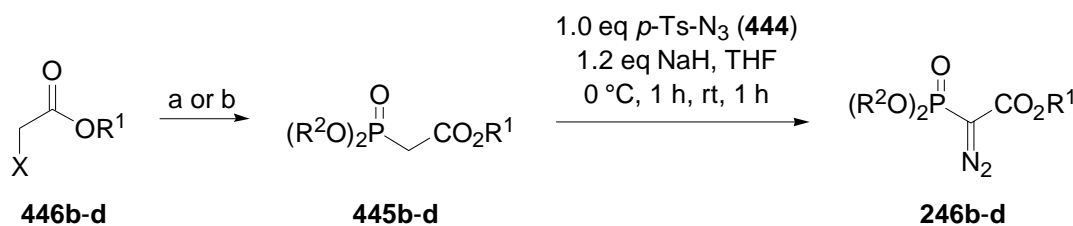
Different possibilities for the formation of diazo compounds are known and have been reviewed earlier.³⁴⁶ We utilized the standard procedure involving the diazo transfer reagent tosyl azide **444** in the presence of a base. This method was developed by Regitz and co-workers.³⁵⁷

Tosyl azide **444** was easily synthesized from *p*-toluene sulfonyl chloride **443** and sodium azide (Scheme 125). Treatment of commercially available trimethylphosphonoacetate **445a**³⁵⁸ with *p*-tosyl azide **444** afforded diazo phosphonate **246a** in 75% yield.



Scheme 125: Formation of the diazophosphonoacetate **246a**.

The related diazophosphonoacetates **246b-d** were generated by a two step procedure involving Arbuzov reaction of halo acetic acids **446b-d** with either trimethylphosphite (Table 31, entry 2 and 3) or triethylphosphite (Table 31, entry 1) to afford the phosphonoacetates **445a-c** followed by the treatment with NaH and *p*-tosyl azide **444** (Table 31).³⁵⁹



| Entry | X | R ¹ | Conditions | R ² | Yield (445) [%] | Yield (246) [%] | Product |
|-------|----|----------------|----------------|----------------|--------------------------|--------------------------|-----------------|
| 1 | Br | Me | a ^a | Et | 94 | 62 | 445/246b |
| 2 | Cl | <i>i</i> -Pr | b ^b | Me | 39 ^{c,d} | 89 | 445/246c |
| 3 | Cl | <i>t</i> -Bu | b ^b | Me | 48 ^{c,d} | 87 | 445/246d |

Table 31 ^a Reaction conditions: P(OEt)₃, reflux with distillation off of the side products. ^b First step: NaI, acetone, rt. Second step: P(OMe)₃, reflux with distillation off of the side products. ^c Contaminated by small amounts of *para*-toluene sulfonyl amine. ^d Yields not optimized

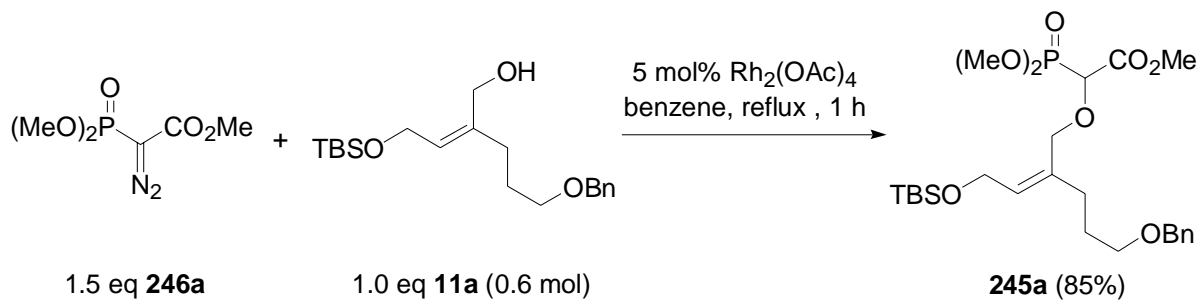
³⁵⁷ Regitz, M.; Anschütz, W.; Liedhengener, A. *Chem. Ber.* **1968**, *101*, 3734-3743.

³⁵⁸ Trimethylphosphonoacetate **445a** may be generated by Arbuzov reaction of chloro acetic acid methyl ester **446a** with trimethylphosphite (analogue to **445c,d** (Table 31)).

³⁵⁹ House, H. O.; Jones, V. K.; Frank, G. A. *J. Org. Chem.* **1964**, *29*, 3327-3333.

14.1.2 Application of the Rhodium-Catalyzed OH-Insertion

Initial experiments concerning the rhodium-catalyzed OH-insertion afforded the desired phosphonate **245a** with good yields (Eq. 55, Table 32, entry 1).



Eq. 55 TBS= *tert*-butyldimethylsilyl [Si(*t*-Bu)Me₂], Bn= benzyl, Ac= acetyl.

However, reproduction of the reaction under comparable conditions afforded **245a-d** with strongly varying yields (Table 32, entry 2). Upscaling of the reaction size resulted in a significant reduction of the isolated yields (Table 32, entry 3). After some experimentation we found 1,2-dichloro ethane the best solution both according to isolated yields and reproducibility (Table 32, entry 4 and 5).

| Entry | Reaction size [mmol] | Solvent ^a | Yield [%] |
|-------|----------------------|----------------------|-----------|
| 1 | 0.6 | benzene | 85 |
| 2 | 0.8 | benzene | 17-67 |
| 3 | 4.7 | benzene | 20 |
| 4 | 0.5 | 1,2-dichloroethane | 60 |
| 5 | 3.5 | 1,2-dichloroethane | 59 |

Table 32: Results of the rhodium(II) catalyzed OH-insertion. ^a Reaction conditions: A solution of 1.5 eq **246a** in 1,2-dichloroethane or benzene was added dropwise within 15 min to a refluxing solution of 1.0 eq **11a** and 5 mol% of Rh₂OAc₄ in 1,2-dichloroethane or benzene. The reaction mixture was stirred at reflux for one hour, cooled to rt and concentrated. TBS= *tert*-butyldimethylsilyl [Si(*t*-Bu)Me₂]

We found that 1.2 g (3.5 mmol) of **11a** was the reaction size of choice affording the product in acceptable and reproducible yields. Upscaling was realized by running the reaction in parallel vessels each equipped with the above amount of the starting materials.³⁶⁰ After the completion of the reaction the raw materials were combined and purified as one single

³⁶⁰ 4.8 g (13.4 mmol) of the allyl alcohol **11** were converted at the same time by application of this procedure.

product. The raw material of the OH-insertion had to be purified immediately after the reaction. Storing of the raw product even at $-32\text{ }^{\circ}\text{C}$ resulted in the degradation of the phosphonate **245a** and reduced isolated yields were observed.

Phosphonates **245b-d** were synthesized in analogy to the above procedure. Results are summarized in Table 33.

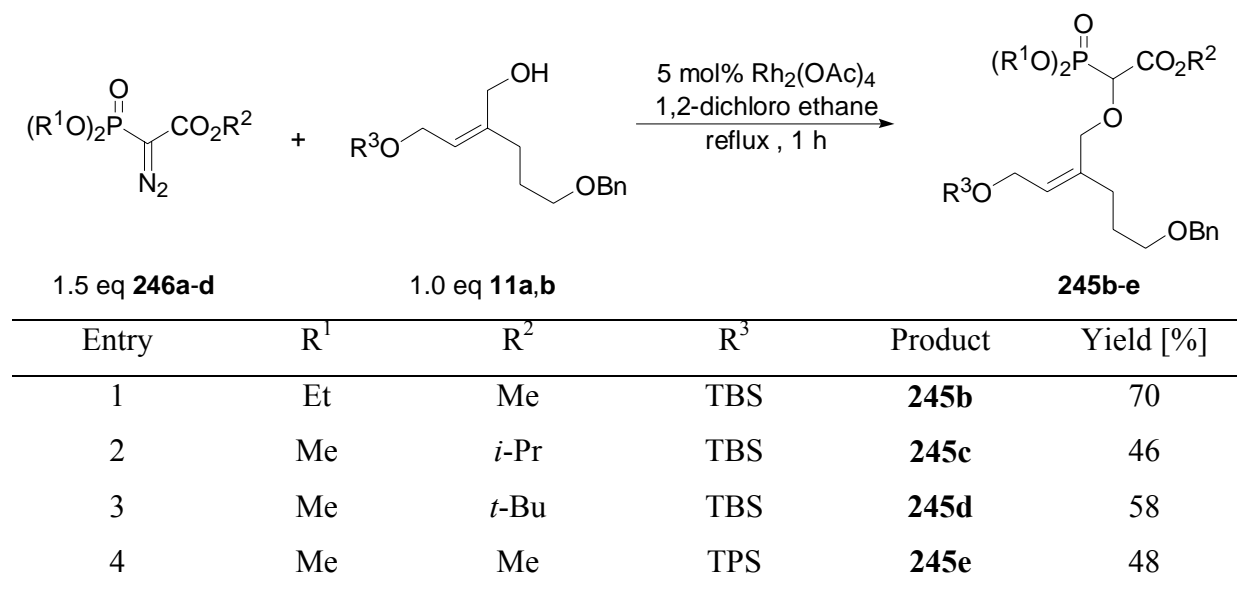


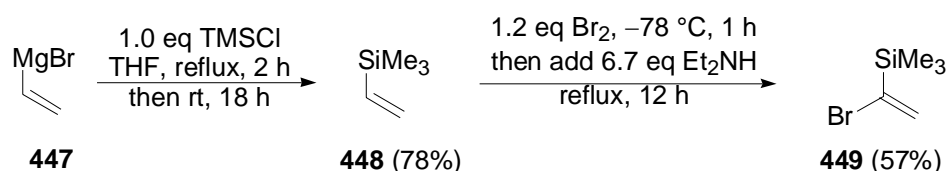
Table 33 Synthesis of the phosphonates **245b-e**. TBS= *tert*-butyldimethylsilyl [$\text{Si}(t\text{-Bu})\text{Me}_2$], TPS= *tert*-butyldiphenylsilyl [$\text{Si}(t\text{-Bu})\text{Ph}_2$], Bn= benzyl, Ac= acetyl.

14.2 Horner-Wadsworth-Emmons Olefination

Aldehyde **244** - required for the generation of AVE **10a** by HWE olefination - was synthesized according to a procedure published by Overman *et al.*³⁶¹ The starting 1-bromo-1-vinyl trimethylsilane **449** is commercially available but for economic reasons it may be synthesized using a two step procedure starting from vinyl magnesium bromide **447** (Scheme 126).³⁶² Attempts to use the less expensive vinyl magnesium chloride instead of vinyl magnesium bromide **447** for the first step did not result in the formation of the desired vinyl trimethylsilane **448**.

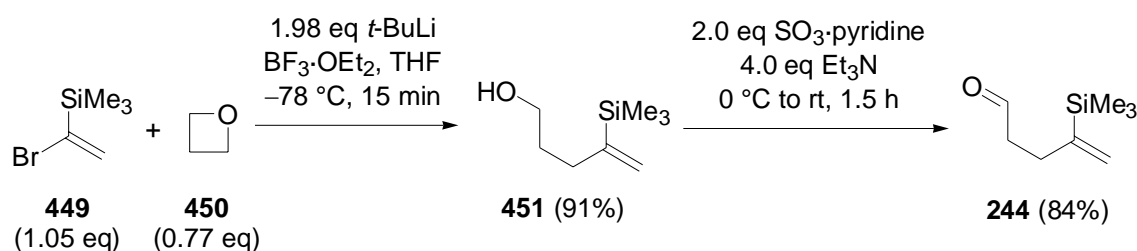
³⁶¹ Overman, L. E.; Thompson, A. S. *J. Am. Chem. Soc.* **1988**, *110*, 2248-2256.

³⁶² Boeckman, R. K., Jr.; Blum, D. M.; Ganem, B.; Halvey, N. *Org. Synth.* **1980**, *58*, 152-157.



Scheme 126: Formation of 1-bromo-1-vinyl trimethylsilane **449**. TMS= trimethylsilyl [SiMe₃].

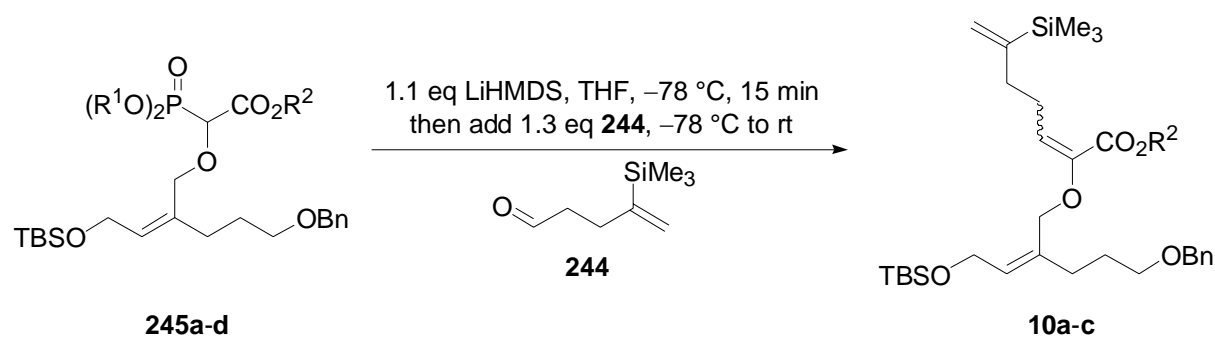
Lithiation of 1-bromo-1-vinyl trimethylsilane **449** using *t*-BuLi and subsequent addition of trimethylene oxide **450** and boron trifluoride etherate afforded alcohol **451** (Scheme 127). After initial good results, the formation of a side product was observed several times during later experiments. This side product was difficult to remove and resulted in various problems during the following steps.³⁶³ However, careful flash chromatography enabled the separation of this side product. Oxidation using Parikh-Doering conditions³⁰⁸ resulted in the formation of aldehyde **244** in good yields (Scheme 127).



Scheme 127: Formation of the aldehyde **244** according to Overman.

The stereochemical result of the HWE is known to be affected by the steric demand of the substituents present at the phosphonate and by the base employed for the generation of the cation. Consequently, phosphonates **245** bearing ester residues with varying steric demands were tested.

³⁶³ For details, see: Experimental Section.

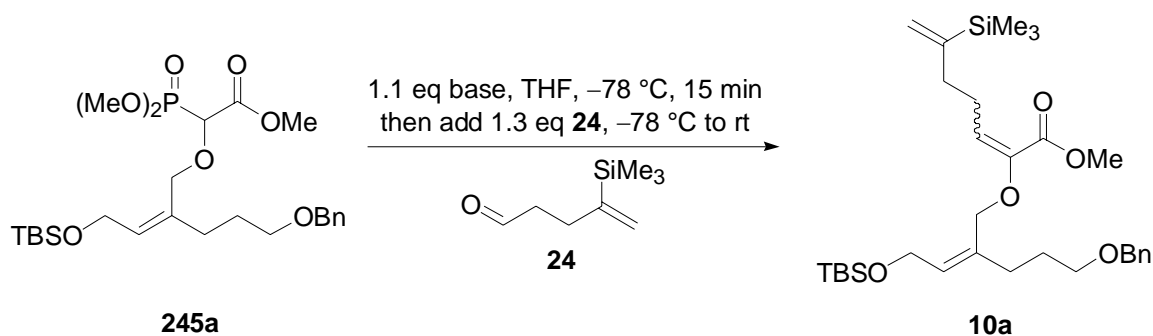


| Entry | R ¹ | R ² | n ₍₂₄₅₎ [mmol] | Product | <i>E/Z</i> | Yield [%] |
|-------|----------------|----------------|---------------------------|------------|------------|-----------|
| 1 | Me | Me | 0.4 | 10a | 12/1 | 82 |
| 2 | Et | Me | 0.05 | 10a | 3/1 | 61 |
| 3 | Me | <i>i</i> -Pr | 0.05 | 10b | 8/1 | 72 |
| 4 | Me | <i>t</i> -Bu | 0.05 | 10c | 7/1 | 50 |

Table 34 Results of the HWE olefination of phosphonates **245a-d** bearing phosphonate and ester residue with different steric demands. TBS= *tert*-butyldimethylsilyl [$Si(t\text{-Bu})Me_2$], Bn= benzyl, LiHMDS= lithium hexamethyl disilazide $\{Li[N(SiMe_3)_2]\}$.

Obviously, substituents at the ester residues had an influence on the selectivity (Table 34, entry 1,3 and 4) but the differences are rather small. In contrast, small variation of the phosphonate residue (methyl replaced by ethyl) significantly decreased the *E*-selectivity (Table 34, entry 2).

We then checked the effect of different bases. Accordingly LDA, LiHMDS, KHMDS, NaHMDS and LiCl/TMG (Masamune Roush)³⁶⁴ were compared.



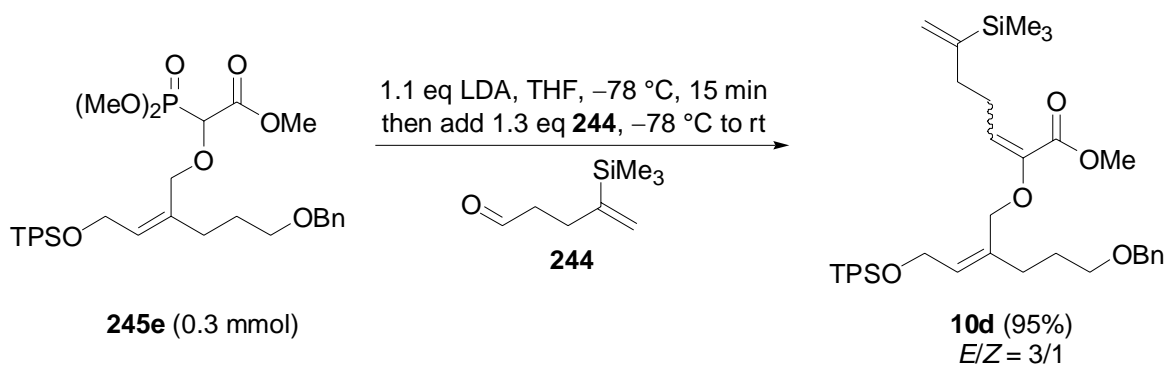
³⁶⁴ Blanchette, M. A.; Choy, W.; Davis, J. T.; Essinfeld, A. P.; Masamune, S. S.; Roush, W. R.; Sakai, T. *Tetrahedron Lett.* **1984**, *25*, 2183-2186.

| Entry | n _(245a) [mmol] | Base | t [h] | E/Z | Yield [%] |
|-------|----------------------------|----------|-------|------|-----------|
| 1 | 0.9 | LDA | 0.5 | 9/1 | 78 |
| 2 | 0.4 | LiHMDS | 0.5 | 12/1 | 82 |
| 3 | 0.5 | KHMDS | 1 | 3/1 | 36 |
| 4 | 0.1 | NaHMDS | 4 | 3/1 | 54 |
| 5 | 0.5 | LiCl/TMG | 0.5 | 4/1 | 29 |

Table 35 Results of the HWE olefination for the reaction of phosphonate **245a** with aldehyde **244**. TBS= *tert*-butyldimethylsilyl [Si(*t*-Bu)Me₂], Bn= benzyl, LDA= lithium diisopropylamide, LiHMDS= lithium hexamethyl disilazide {Li[N(SiMe₃)₂]}, KHMDS= potassium hexamethyl disilazide {K[N(SiMe₃)₂]}, NaHMDS= sodium hexamethyl disilazide {Na[N(SiMe₃)₂]}, TMG= tetramethyl guanidine.

LiHMDS resulted in enhanced diastereoselectivities compared with LDA (Table 35, entry 1 and 2). KHMDS, NaHMDS and Masamune Roush conditions³⁶⁴ exhibited reduced reactivities and significantly decreased *E*-selectivities (Table 35, entry 3, 4 and 5).

Surprisingly, when applied to TPS-protected phosphonate **245e** reduced diastereoselectivities were observed as well (Eq. 56).

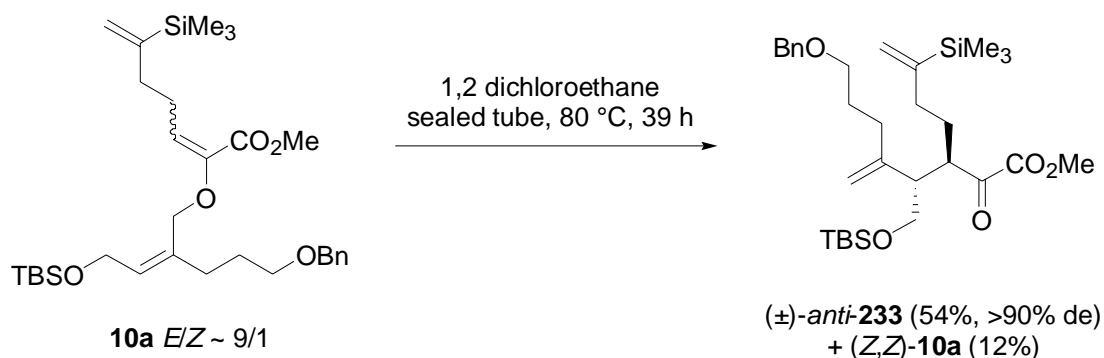


Eq. 56 TPS= *tert*-butyldiphenylsilyl [Si(*t*-Bu)Ph₂], Bn= benzyl, LDA= lithium diisopropylamide.

For economic reasons, I decided to employ LDA as method of choice for the further progress. However, later results (see chapter 15) revealed, that utilization of LiHMDS might be advantageously for the further development of the synthetic route.

15 Catalytic Asymmetric Claisen Rearrangement (CAC)

The initial experiments were performed with the mixtures of double bond isomers of the AVE **10a**. When AVE **10a** was subjected to the conditions of the thermal Claisen rearrangement we noticed incomplete conversion even after prolonged heating. This is in contrast to earlier results that ascertained the complete conversion of double bond mixtures under thermal conditions.²⁰² Separation of the rearrangement products resulted in α -keto ester (\pm)-*anti*-**233** in moderate yields³⁶⁵ and the reisolation of the starting material that almost exclusively consisted of the *Z*-isomer (*Z,Z*)-**10a**. Apparently, the allyl vinyl ether (*Z,Z*)-**10a** did not rearrange under these conditions.



Eq. 57 TBS= *tert*-butyldimethylsilyl [Si(*t*-Bu)Me₂], Bn= benzyl.

Separation of the α -keto ester enantiomers (*2S,10R*)-**233** and (*2R,10S*)-**233** was realized by chiral analytical HPLC (Figure 25).³⁶⁶ Even though the first peak appears to be slightly higher, integral sizes confirm that it is indeed a racemate with both enantiomers being in 1/1 ratio.

³⁶⁵ Yields not optimized.

³⁶⁶ Analytical HPLC: Hewlett-Packard 1090, DAD detection at 210 and 220 nm, column: Chiracel OD 14025 (4.6×255 mm, 10 μ m), solvent: *n*-hexane/*i*-PrOH, 1 mL/min, 35 °C. For details, see: Experimental Section.

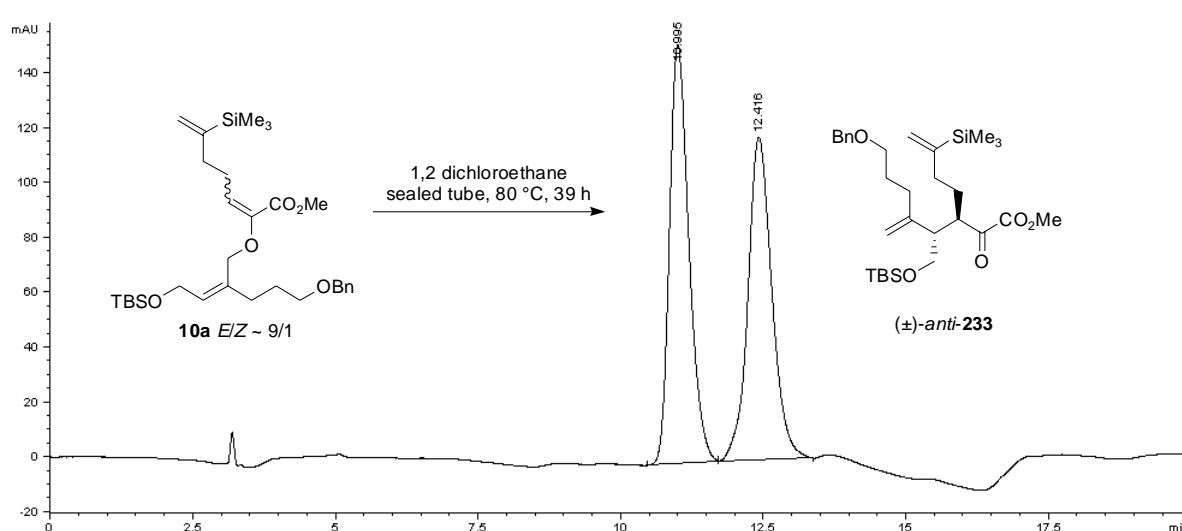


Figure 25: Chromatogram of the racemic product (\pm)-*anti*-**233** of the thermal Claisen rearrangement. TBS= *tert*-butyldimethylsilyl [$\text{Si}(t\text{-Bu})\text{Me}_2$], Bn= benzyl.

We then attempted the catalytic asymmetric Claisen rearrangement. Initial experiments under standard conditions (5 mol% (*S,S*)-**234a**, 4 Å molecular sieves,³⁶⁷ CH_2Cl_2 , rt, 24 h) did not result in the formation of α -keto ester **233** in considerable amounts. We assumed that the higher steric demand of the AVE **10a** featuring a three substituted double bond may interfere with the highly ordered situation at the catalytic center of the *t*-Bu-box-catalyst (*S,S*)-**234a**. Therefore, we performed the same experiments with the less demanding Ph-box catalyst (*R,R*)-**234b**. Similarly, standard conditions did not result in the desired rearrangement. However, treatment of AVE **10a** with equimolar amounts of (*R,R*)-**234b** resulted in the conversion to the α -keto ester **233** within 16 hours.³⁶⁸ However, if the enantiomers were separated by chiral, analytical HPLC the results were not very encouraging (Figure 26). There was almost no asymmetric induction if (*R,R*)-**234b** was used.

³⁶⁷ Unless otherwise state, freshly activated, manually crushed 4 Å molecular sieves were used. For details, see: Experimental Section.

³⁶⁸ Reaction time not optimized.

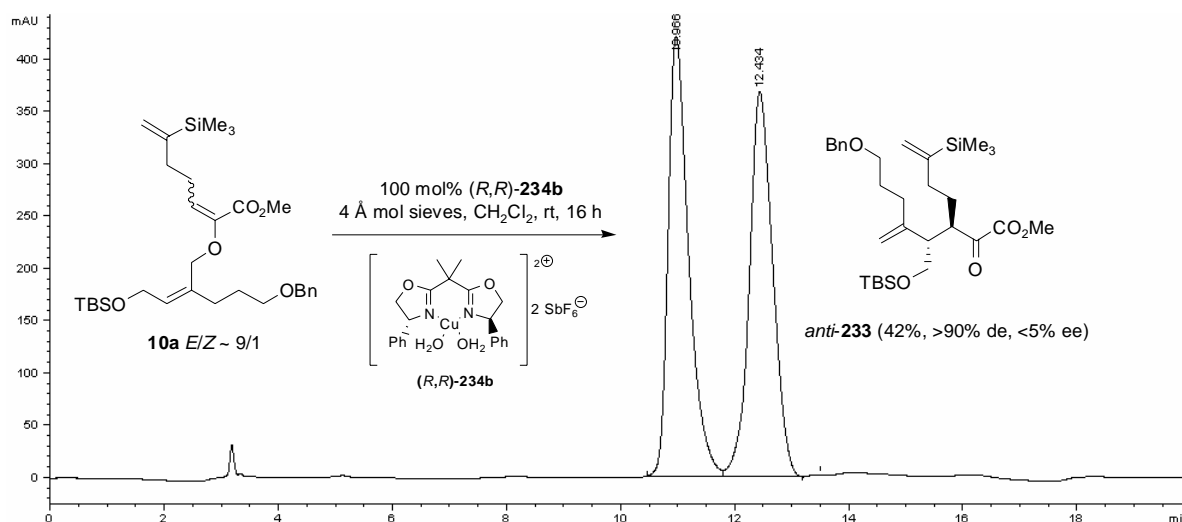


Figure 26: Chromatogram of the product *anti*-**233** of the Claisen rearrangement ‘catalyzed’ by **(*R,R*)-234b**. TBS= *tert*-butyldimethylsilyl [$\text{Si}(t\text{-Bu})\text{Me}_2$], Bn= benzyl.

Consequently, we tested ‘cationic’ copper(II)-complex **(*S,S*)-234a** next. Treatment of the AVE **10a** with equimolar amounts of the **(*S,S*)-234a** afforded the rearrangement product (**2*S*,10*R***)-**233** within less than 2 h. In this case excellent enantioselectivities were observed (Figure 27).³⁶⁹

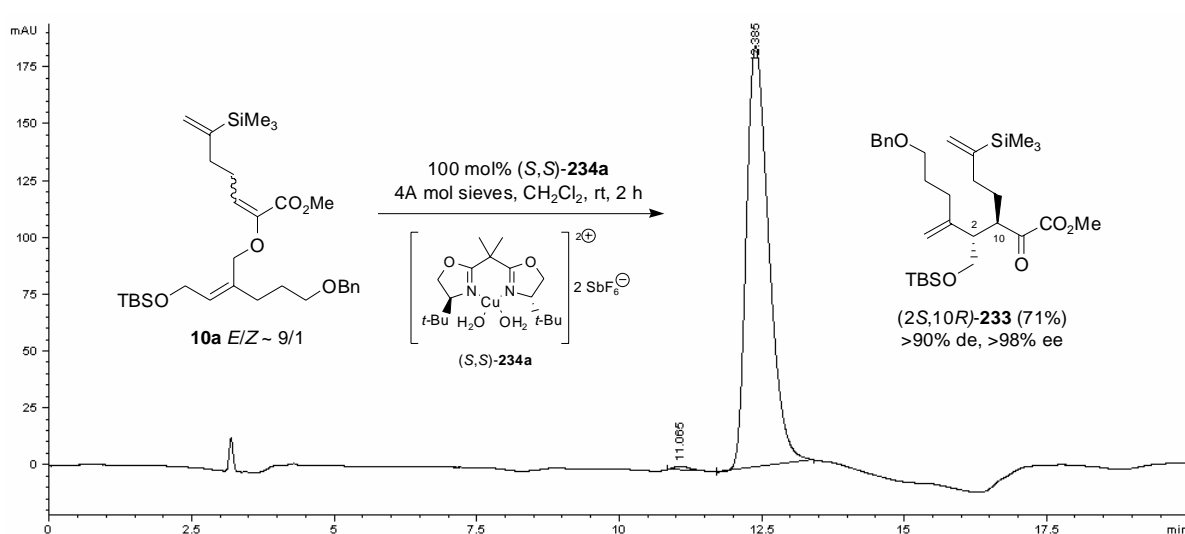


Figure 27: Chromatogram of the α -keto ester product (**2*S*,10*R***)-**233** of the Claisen rearrangement ‘catalyzed’ by **(*S,S*)-234a**. TBS= *tert*-butyldimethylsilyl [$\text{Si}(t\text{-Bu})\text{Me}_2$], Bn= benzyl.³⁷⁰

³⁶⁹ First implementations were analyzed by chiral HPLC (Hewlett-Packard 1090) with DAD detection. In these cases no second enantiomer was detectable. The old machine was later replaced by a modern Agilent 1100 series with DAD detection. During the analysis of the rearrangement product with this newer HPLC the second enantiomer was within the limits of detectability exhibiting 98% ee.

³⁷⁰ Identical chromatograms were obtained for experiments using 25 mol% (or less) of the catalyst **(*S,S*)-234a**.

To control that the minor peak was indeed the second enantiomer an artificial mixture of the product of the CAC and the thermal Claisen rearrangement was produced. Figure 28 represents the resulting chromatogram that clearly shows an increased intensity of the first peak.

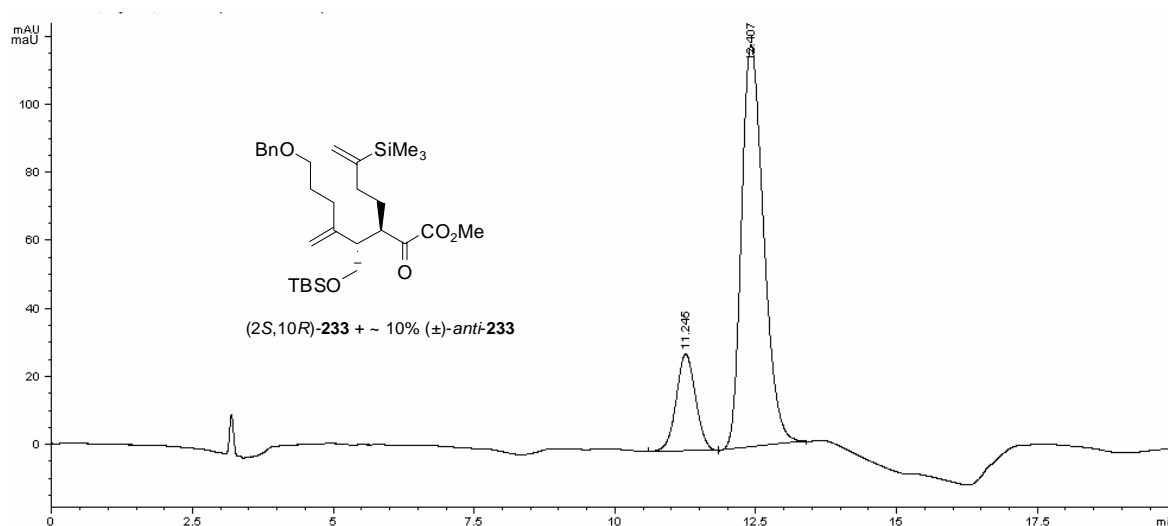
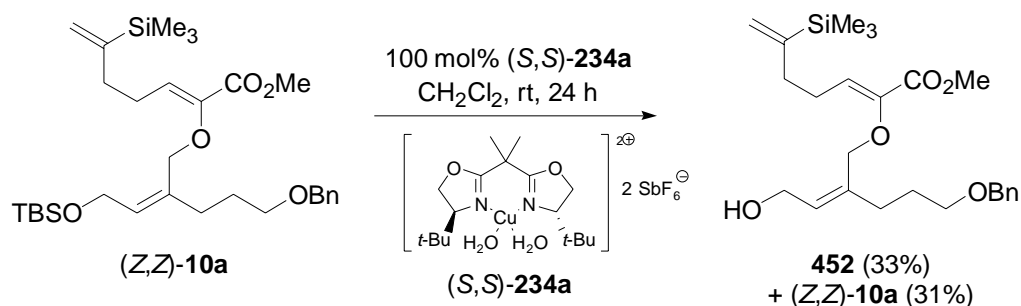


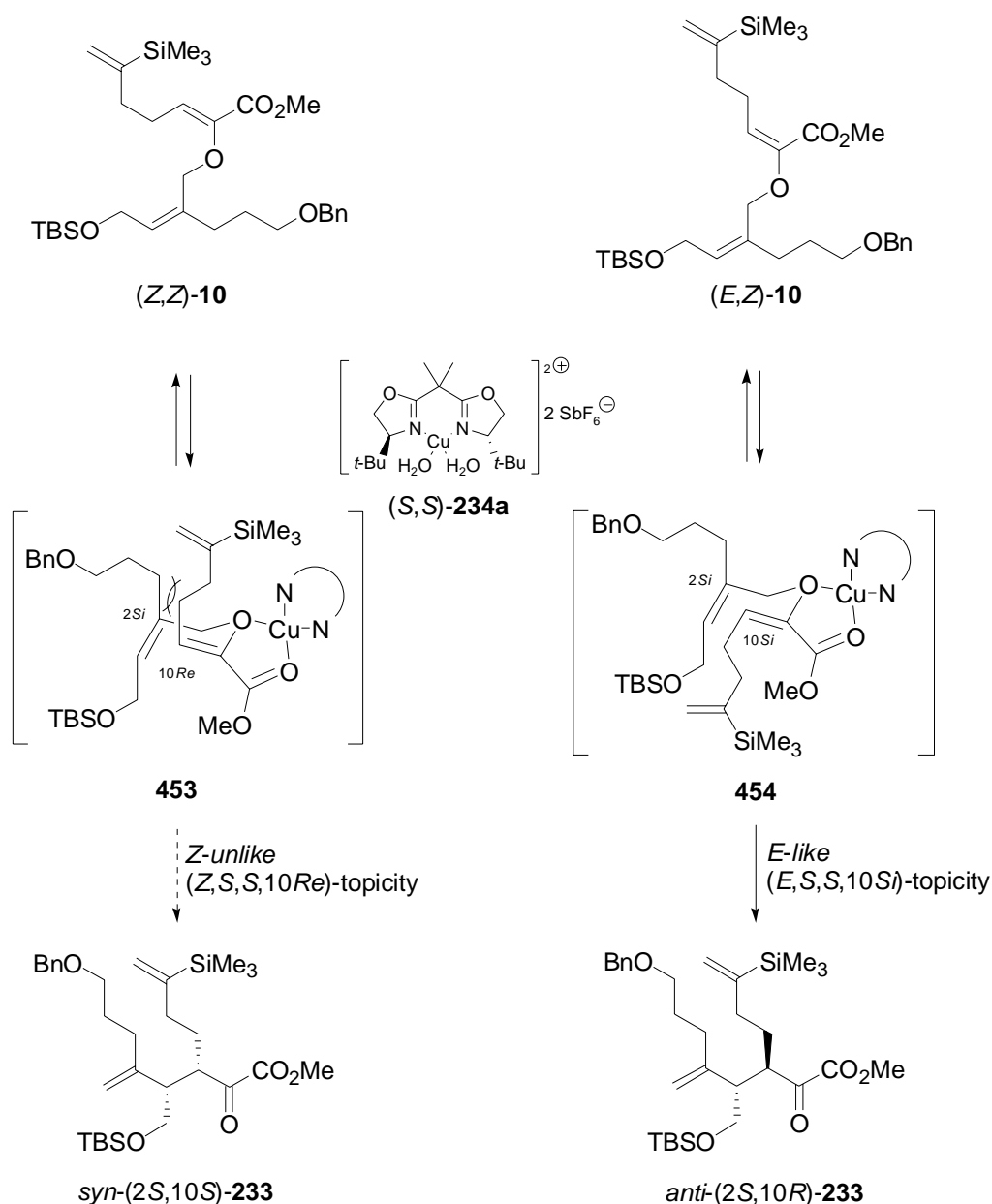
Figure 28: Chromatogram of an artificial mixture of (2*S*,10*R*)-**233** and (±)-*anti*-**233**. TBS= *tert*-butyldimethylsilyl [Si(*t*-Bu)Me₂], Bn= benzyl.

We noticed that even with stoichiometric amounts of the catalyst the reaction did not proceed to completion. Interestingly, as it was observed for the thermal Claisen rearrangement *Z*-configured AVE **10a** did not undergo the catalyzed Claisen rearrangement. If reisolated pure *Z*-AVE (*Z,Z*)-**10a** was subjected to stoichiometric amounts of the catalyst (*S,S*)-**234a** no rearrangement at all occurred. Instead subsequent cleavage of the TBS ether was observed (Eq. 58).



Eq. 58 TBS= *tert*-butyldimethylsilyl [Si(*t*-Bu)Me₂], Bn= benzyl.

A proposal of the stereochemical course of rearrangement may explain the different reactivities of (*E,Z*)-**10a** and (*Z,Z*)-**10a** (Scheme 128).

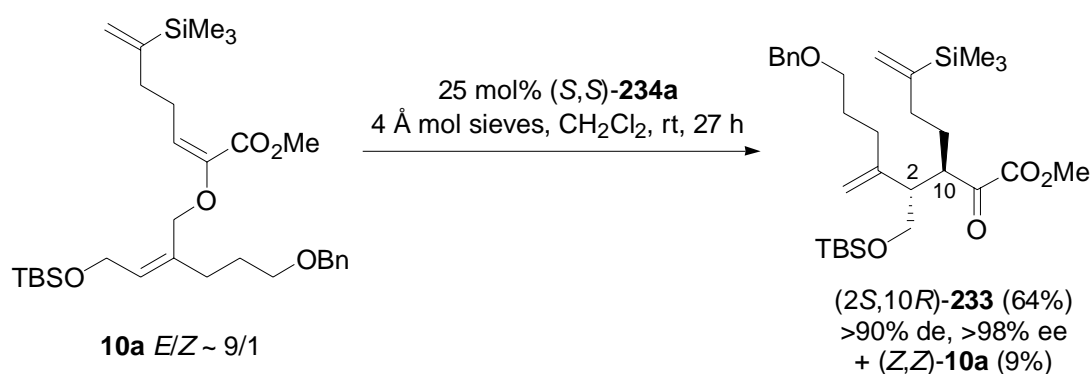


Scheme 128: The different reactivities of (E,Z) -**10a** and (Z,Z) -**10a** may be accounted to steric interactions that should be significantly stronger for intermediate **453** than for intermediate **454**. TBS= *tert*-butyldimethylsilyl [$\text{Si}(t\text{-Bu})\text{Me}_2$], Bn= benzyl.

Steric interactions between the vinylic side chain and the substituent at C2 should be more predominant in the complex **453**. Consequently, (Z,Z) -**10a** is expected to be less prone to form this complex and/or adopt the reactive conformation that would lead to a *Z-unlike* transition state and consequently to the *syn*-diastereomer of **233** (Scheme 128, left). On the other hand, this pseudo-1,3-diaxial repulsion is expected to be significantly smaller if (E,Z) -**10a** (vinyl- $\text{R}^E = \text{H}$) is employed. Therefore, the activation barrier for the catalyzed (and for the thermal) Claisen rearrangement of (E,Z) -**10a** should be lower than for (Z,Z) -**10a**.

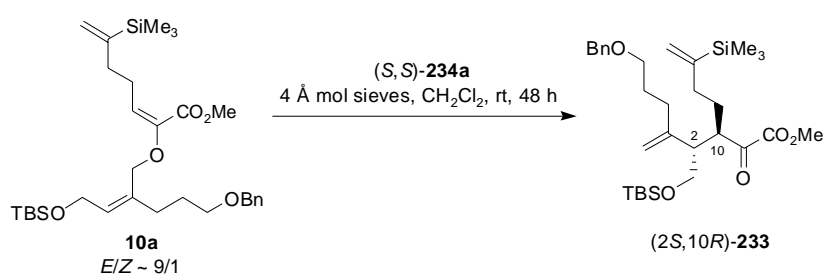
The presence of unreacted (*Z,Z*)-**10a** perturbed the reaction control via TLC since the complete conversion of (*E,Z*)-**10a** can not easily be detected. However, the different reactivities of the double bond isomers are not without advantage. No separation of the double bond isomers is required. Thus, the α -keto ester **233** will be formed as single diastereomer. The rearrangement product **233** is easily separable from unreacted starting material (*Z,Z*)-**10a** by flash chromatography.

Subsequent optimization resulted in the reaction conditions given below. 25 mol% of (*S,S*)-**234a** were found to be the minimum amount of catalyst to initiate the rearrangement of **10a** if used as mixture of double bond isomers (Eq. 59).



Eq. 59 TBS= *tert*-butyldimethylsilyl [Si(*t*-Bu)Me₂], Bn= benzyl

Further reduction of the catalyst loading resulted in unacceptable long reaction times. After 48 hours incomplete conversion of the starting material **10a** was observed (Table 36).³⁷¹

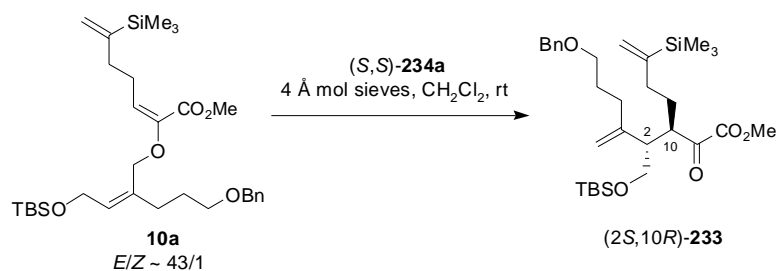


| Entry | Catalyst loading ^a [mol%] | Conversion ^b [%] |
|-------|--------------------------------------|-----------------------------|
| 1 | 20 | 81 |
| 2 | 15 | 63 |
| 3 | 10 | ~10 |

Table 36 ^a Reaction size: 25 mg (0.045mmol) **10a**, 4 ml CH₂Cl₂. ^b Deduced from ¹H NMR. TBS= *tert*-butyldimethylsilyl [Si(*t*-Bu)Me₂], Bn= benzyl

³⁷¹ The term ‘incomplete conversion’ does not take into consideration that (*Z,Z*)-**10a** does not rearrange. It is used to express, that incomplete conversions was observed for the reactive AVE (*E,Z*)-**10a**.

The required substoichiometric amount of the catalyst (turnover rate: 4) and the back isolation of (*Z,Z*)-**10a** guided us to the question whether or not the pure *E*-AVE (*E,Z*)-**10a** would rearrange with lower catalyst loading. Attempts to separate the double bond isomers by preparative HPLC have been successfully challenged.³⁷² However, long retention times and lacking base line separation make the separation of the double bond isomers (*Z,E*)-**10a** and (*Z,Z*)-**10a** prior to the rearrangement an unreasonable option. However, results that were made with almost pure *E*-AVE **10a** (*E/Z* = 43/1) were very promising (Table 37). Complete consumption of the starting material was detected within a few minutes if 25 mol% of (*S,S*)-**234a** were employed. Furthermore, increased isolated yields of satisfying 80% were observed. Consequently, the reaction was performed with lower catalyst loading. We found that the minimum catalyst loading was 10 mol% what now fits in the description of the transformation as *catalytic* asymmetric Claisen rearrangement. The reaction was complete within 3.5 hours. 5 mol% (*S,S*)-**234a** exhibited no significant acceleration of the Claisen rearrangement of **10a**.



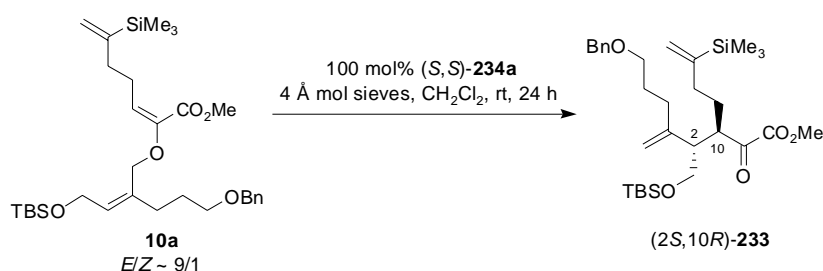
| Entry | Catalyst loading ^a [mol%] | Reaction time | Conversion ^b [%] | Isolated yield ^c [%] |
|-------|--------------------------------------|---------------|-----------------------------|---------------------------------|
| 1 | 25 | 10 min | 100 | 80 (100) |
| 2 | 10 | 3.5 h | 100 | 70 (100) |
| 3 | 5 | 9 d | ~5 | - (100) |

Table 37 ^a Reaction size: 25 mg (0.045mmol) **10a**, 4 ml CH₂Cl₂. ^b Deduced from ¹H NMR. ^c After purification by column chromatography. Yields in parentheses are obtained after filtration of the reaction mixture through a plug of silica gel (0.5×2 cm). TBS= *tert*-butyldimethylsilyl [Si(*t*-Bu)Me₂], Bn= benzyl.

The exact role of the molecular sieves remains still speculative. We assume that it is involved in the rate determining formation of the catalyst substrate complex by absorbing the water that is displaced by the substrate. This might however not be the only role. With this uncertainty in mind we performed a set of reactions with varying molecular sieve amounts. Without molecular sieves the reaction rate significantly decreases and various side products were

³⁷² For details, see: Experimental Section.

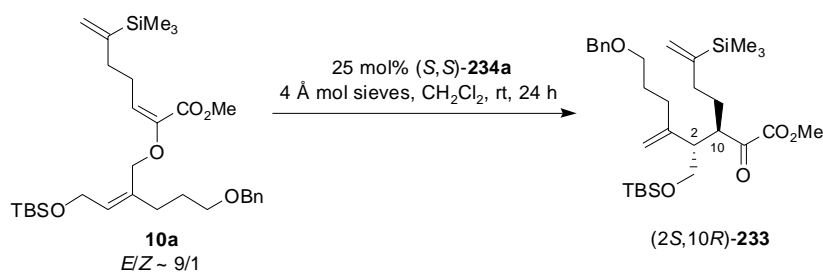
detected by TLC. Subsequent enhancement of the molecular sieves loading increased the reaction rate. At the same time, reduced side product formation was detected (Table 38).



| Entry | 4 Å mol sieves ^a [mg/mmol 10a] | Conversion ^b [%] | Side product formation ^c |
|-------|---|-----------------------------|-------------------------------------|
| 1 | - | 50 | Strong |
| 2 | 9 | 66 | Significant |
| 3 | 18 | >95 | Little |
| 4 | 36 | >95 | Hardly detectable |

Table 38 ^a Reaction size: 25 mg (0.045mmol) **10a**, 4 ml CH_2Cl_2 . ^b Deduced from ^1H NMR. ^c Detected by TLC control. TBS= *tert*-butyldimethylsilyl [$\text{Si}(t\text{-Bu})\text{Me}_2$], Bn= benzyl.

Since the reaction proceeded significantly faster with higher amounts of molecular sieves, the following reactions were performed with 25 mol% catalyst loading (Table 39). In all cases only small side product formation was observed.

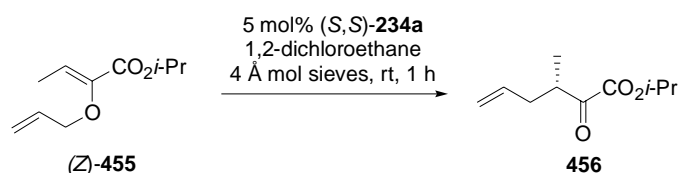


| Entry | 4 Å molecular sieves ^a [mg/mmol 10a] | Conversion ^b [%] |
|-------|---|-----------------------------|
| 1 | 50 | 70 |
| 2 | 82 | 37 |
| 3 | 164 | 18 |

Table 39 ^a Reaction size: 25 mg (0.045mmol) **10a**, 4 ml CH_2Cl_2 . ^b Deduced from ^1H NMR. TBS= *tert*-butyldimethylsilyl [$\text{Si}(t\text{-Bu})\text{Me}_2$], Bn= benzyl.

Apparently, there is an optimum amount of molecular sieves loading.

Routinely, we used freshly activated 4 Å molecular sieves that were manually pulverized.³⁷³ Other commercially available molecular sieves (e.g. 4 Å molecular sieves beads or powder) may be used as well. Earlier observations in our research group revealed a correlation between particle size and conversion rate.³⁷⁴ Lowest conversion rates were found for molecular sieves powder (Table 40).



| Entry | Molecular sieves | Conversion [%] |
|-------|------------------|----------------|
| 1 | beads | 95 |
| 2 | manually crushed | 50 |
| 3 | powder | 3 |
| 4 | - | 20 |

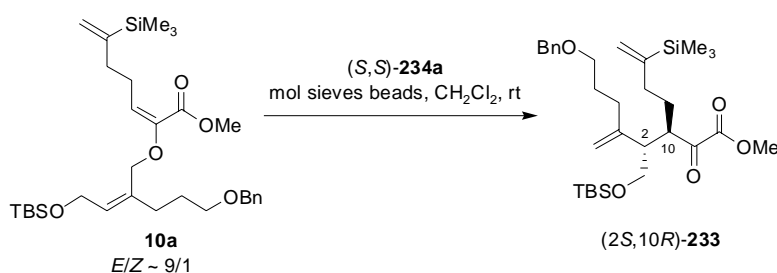
Table 40: Different molecular sieves types have a strong influence on the conversion rate.

For the rearrangement of **10a** the following molecular sieves types were tested: Baker 3 Å molecular sieves beads (corn diameter 2.5-5 mm), Baker 4 Å molecular sieves beads (corn diameter 1.7-2.4 mm), ACROS 4 Å molecular sieves powder (particle size <5 μm).³⁷⁵ Similar to Julia's results, increased reaction rates were observed if 4 Å molecular sieves beads were used (Table 41, entry 2 and 4). However, utilization of the 3 Å molecular sieves beads with further increased particle size resulted in lower reaction rates (Table 41, entry 3). For all cases a significantly higher side product formation was detected by TLC (Figure 29). Interestingly, lower catalyst loading was required (5 mol% (S,S)-**234a**). Complete conversion was observed within 48 hours (Table 41, entry 4).

³⁷³ For details, see: Experimental Section.

³⁷⁴ Rehbein, J., unpublished results.

³⁷⁵ All molecular sieves were freshly activated before use. For details, see: Experimental Section.



| Entry | Catalyst loading ^a [mol%] | Molecular sieves beads [Å] | Reaction time [h] | Yield [%] ^b | Yield of 233 [%] |
|-------|---|-------------------------------|----------------------|------------------------|----------------------------|
| 1 | 10 | 3 | 24 | 90 | 50 |
| 2 | 10 | 4 | 24 | 100 | 55 |
| 3 | 5 | 3 | 48 | 92 ^c | 28 |
| 4 | 5 | 4 | 48 | 80 | 48 |

Table 41 ^a Reaction size: 25 mg (0.045mmol) **10a**, 4 ml CH₂Cl₂. ^b Obtained after filtration of the reaction mixture through a plug of silica gel (0.5×2 cm), unless otherwise stated conversion of (*E,Z*)-**10a** = 100%. ^c Conversion ~75%. TBS= *tert*-butyldimethylsilyl [Si(*t*-Bu)Me₂], Bn= benzyl.

The other commercially available molecular sieves type (powder, particle size <5 μm) was tested next. Surprisingly and in contrast to earlier observations (Table 40) AVE **10a** reacted with enhanced reaction rates if molecular sieves powder was used (Table 42, entry 1). In contrast to the uncrushed molecular sieves almost no side product formation was detected (Figure 29).

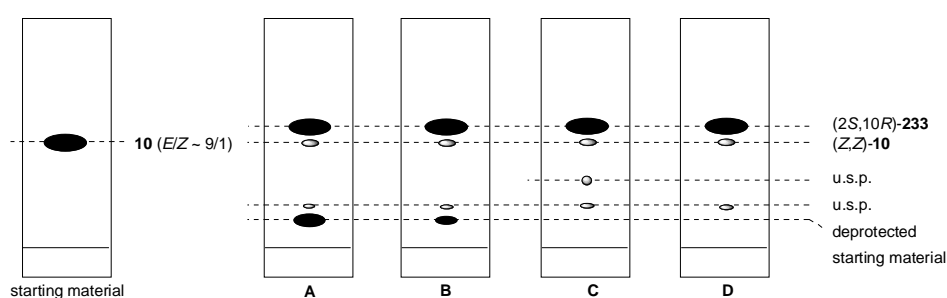
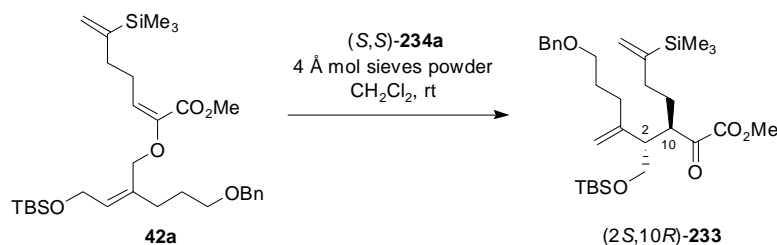


Figure 29: TLC-control of the CAC using 3 Å molecular sieves beads of ~4 mm diameter (**A**), 4 Å molecular sieves beads of ~2 mm diameter (**B**), manually crushed molecular sieves (**C**) and molecular sieves powder (**D**). u.s.p.= unspecified side product.

Catalyst loading was decreased next. Unexpectedly, there was hardly any reaction if only the catalyst loading was reduced leaving all other reaction conditions constant (Table 42, entry 2 and 3). Reduction of both the catalyst loading and the amount of 4 Å molecular sieves powder in the same relation afforded the rearrangement product as expected (Table 42, entry 4 and 5). Using 10 mol% of the catalyst (*S,S*)-**234a** resulted in complete conversion of the starting material within 45 hours (Table 42, entry 4), the corresponding reaction with 5 mol% of (*S,S*)-

234a resulted in about 90% conversion (Table 42, entry 5). If these reaction conditions were applied to the *E*-**10** enriched fraction of the HPLC purification, the reaction was significantly faster (Table 42, entry 6 and 7). However, if 2.5 mol% (*S,S*)-**234a** were used, only 40% conversion could be detected even after 7 days (Table 42, entry 8).



| Entry | <i>E/Z</i> | Catalyst | Molecular | Reaction | Conversion ^b [%] | Yield ^c [%] |
|-------|------------|--------------------------------|-----------------------------|-------------|--------------------------------|---------------------------|
| | | loading ^a [mol%] | sieves/catalyst [g/mmol] | time [h] | | |
| 1 | 15/1 | 18 | 4.2 | 0.5 | 100 | 82 |
| 2 | 9/1 | 10 | 10.2 | 95 | ~5 | n.i. |
| 3 | 9/1 | 5 | 20.2 | 95 | ~5 | n.i. |
| 4 | 9/1 | 10 | 4.1 | 45 | 100 | 60 |
| 5 | 9/1 | 5 | 4.1 | 45 | 90 | n.i. |
| 6 | 43/1 | 10 | 4.1 | 1.25 | 98 | 80 |
| 7 | 43/1 | 5 | 4.1 | 3 | 95 | 85 |
| 8 | 43/1 | 2.5 | 4.1 | 168 | 40 | - |

Table 42 ^a Reaction size: 25 mg (0.045mmol) **10a**, 4 ml CH₂Cl₂. ^b Deduced from ¹H NMR. ^c After purification by column chromatography. All reaction proceeded with 100% yield after filtration through a silica gel plug (0.5×2 cm). n.i.: not isolated. TBS= *tert*-butyldimethylsilyl [Si(*t*-Bu)Me₂], Bn= benzyl.

In summary, two results may be emphasized:

- Using molecular sieves powder, lower catalyst loadings could be realized.
- At least for this type of molecular sieves the relation between catalyst and molecular sieves amount has to be considered.

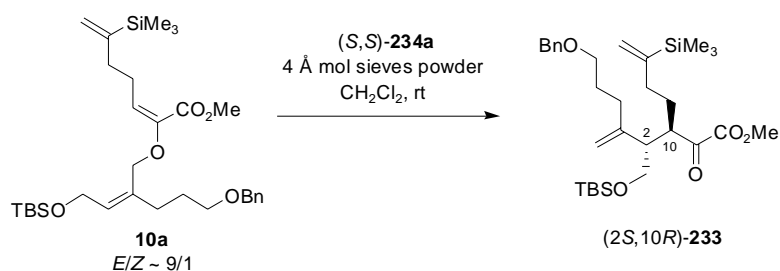
However, if this finding was projected to the CAC using manually crushed molecular sieves, no significant reaction rates were observed if 5 mol% of the catalyst were utilized in concert with a reduced amount of molecular sieves (Table 43).



| Entry | Catalyst loading | Molecular sieves/catalyst | Reaction time | Conversion |
|-------|------------------|---------------------------|---------------|------------|
| | [mol%] | [g/mmol] | [h] | [%] |
| 1 | 25 | 4.1 | 48 | 100 |
| 2 | 5 | 4.1 | 93 | ~5 |

Table 43 ^a Reaction size: 25 mg (0.045mmol) **10a**, 4 ml CH₂Cl₂. ^b Deduced from ¹H NMR. TBS= *tert*-butyldimethylsilyl [Si(*t*-Bu)Me₂], Bn= benzyl.

Upscaling experiments were performed based on the promising results illustrated in Table 42. At first we performed the reaction with 0.5 g **10a** using a 0.1 mol/l concentration (Table 44, entry 1 and 2). Disappointingly, again an increased side product formation was observed. Even though the conversion was found to be 100% both for 5 and 10 mol% catalyst within 48 hours only 41 and 48% yield of the rearrangement product **233** could be isolated respectively. Reproduction of the reaction with 10-fold dilution resulted in a faster transformation that at the same time produced less side products. The α -keto ester **233** was isolated with 63 and 66% yield respectively. However, 100 ml solvent/mmol substrate appears to be a rather inappropriate dilution for routine synthesis.



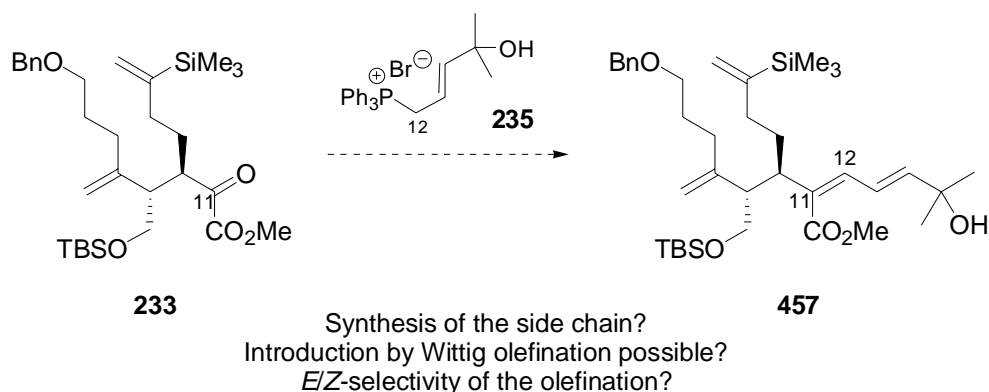
| Entry | Catalyst loading ^a | Concentration | Reaction time | Yield ^b |
|-------|-------------------------------|---------------|---------------|--------------------|
| | [mol%] | [mol/l] | [h] | [%] |
| 1 | 5 | 0.1 | 48 | 41 (82) |
| 2 | 10 | 0.1 | 14 | 49 (94) |
| 3 | 5 | 0.01 | 24 | 63 (99) |
| 4 | 10 | 0.01 | 14 | 66 (100) |

Table 44 ^a Reaction size: 0.5 g (0.89 mmol) **10a**. ^b After purification by column chromatography. Yields in parentheses: after filtration through a silica gel plug (1.5×3 cm). TBS= *tert*-butyldimethylsilyl [Si(*t*-Bu)Me₂], Bn= benzyl.

In summary, even though lower catalyst loading could be realized by changing the molecular sieves type, the originally employed crushed molecular sieves still appears to give the best results. While the application of molecular sieves beads with increased diameter resulted in increased side product formation, application of molecular sieves powder required high dilutions to give optimal chemical yields. The reasons for this dependency remain still unclear. It is somehow a drawback that various parameters have to be optimized for each individual starting material of the catalytic asymmetric Claisen rearrangement without an appropriate rationalization of the different behaviour at hand. Nevertheless, it could be shown that the high potential of the CAC may be successfully applied for the generation of highly functionalized α -keto esters.

16 Side Chain Synthesis and Introduction

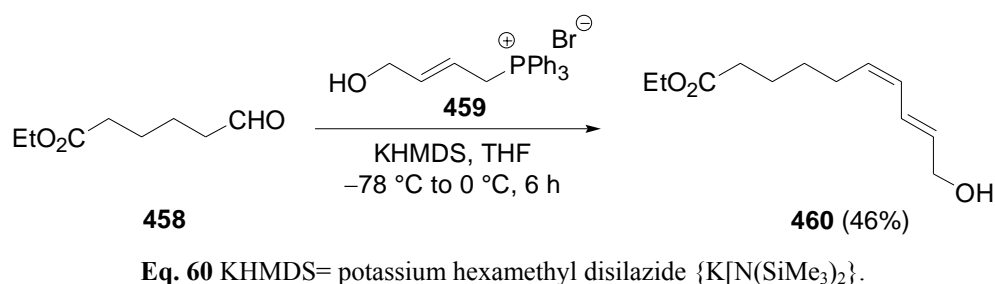
Our synthetic plan involves a Wittig olefination for the introduction of the side chain at C11 (Scheme 129).



Scheme 129: Envisioned introduction of the side chain by Wittig olefination between α -keto ester **233** and Wittig salt **235**.

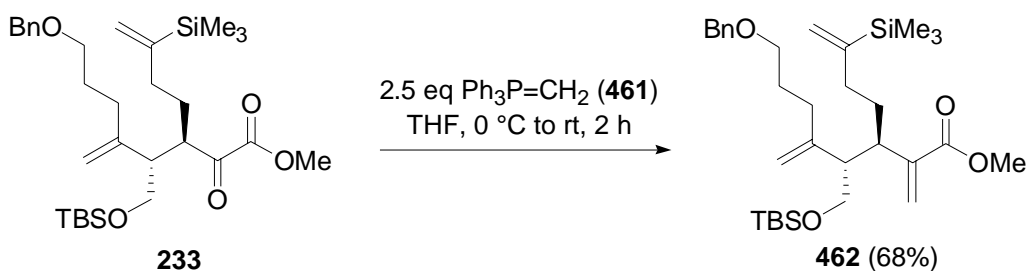
Although not very frequently used, examples for Wittig olefinations employing Wittig salts with free hydroxyl groups have been reported and successfully applied for natural product syntheses.²⁰⁹

A recent application of a Wittig salt very similar to **235** is depicted in Eq. 60.



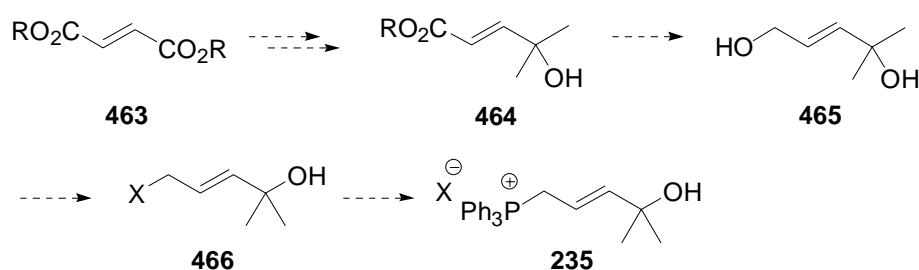
The Wittig reaction of α -keto esters (e.g. **233**) is yet not developed as synthetic tool. An initial test reaction was performed with the simplest Wittig ylene Ph₃P=CH₂ (**461**).³⁷⁶ After some optimizations **462** was synthesized with promising 68% (Eq. 61).

³⁷⁶ Formed *in situ* by treatment of methyl triphenyl phosphonium bromide with an appropriated base. For details, see: Experimental Section.



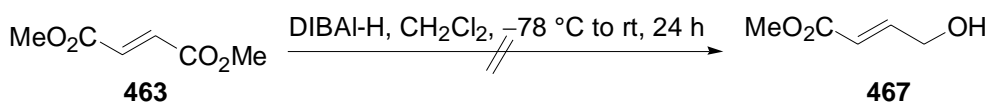
Eq. 61 TBS= *tert*-butyldimethylsilyl [$\text{Si}(t\text{-Bu})\text{Me}_2$], Bn= benzyl.

Consequently, the synthesis of the side chain **235** was explored. The original plan was to take advantage of the preformed *E*-configured double bond present in fumaric acid esters **463**. Reduction to the corresponding allylic alcohol, and a sequence of oxidation to an aldehyde, alkylation of this aldehyde, oxidation of the resulting secondary alcohol to the corresponding ketone and another alkylation might provide alcohol **464**. Subsequent reduction of the other ester functionality of **464** might afford the alcohol **465** ready for functional group transformation (replacement of OH by a halogen) by Mitsunobu redox condensation. **Fehler! Textmarke nicht definiert.** Halogenide **466** might then be transformed to the Wittig salt **235**.



Scheme 130: Envisioned access of **235** starting from fumaric acid esters **463**. R= alkyl, X= halogen.

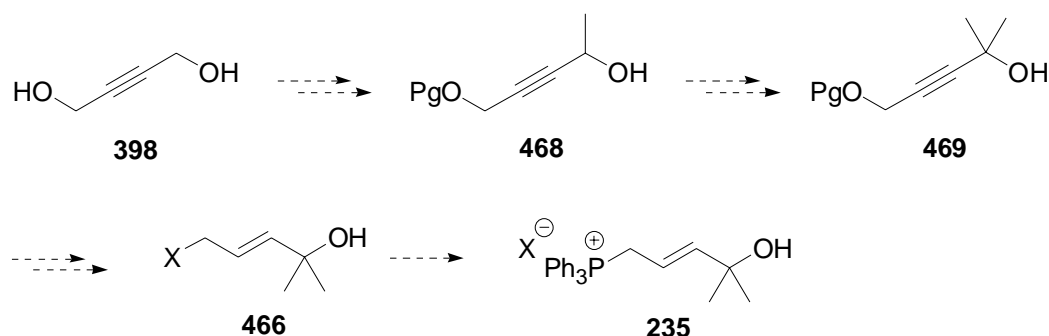
Unfortunately, the initial reduction step failed to give the desired allylic alcohol **467** (Eq. 62). At low temperatures incomplete conversion was observed. Increasing of the reaction temperature led to complex product mixtures.



Eq. 62

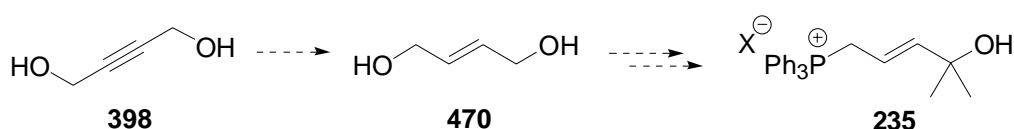
Therefore, a strategy starting from 2-butyn-1,4-diol **398** was utilized. The diol **398** might be monoprotected, oxidized to the corresponding aldehyde and alkylated to afford alcohol **468**. After oxidation to the corresponding ketone and another methylation protected alcohol **469**

might be reduced to the corresponding alkene by *E*-selective reduction using LiAlH_4 or Red-Al .³⁷⁷ Deprotection and functional group transformation as described above should afford halogenide **466** ready for the formation of the Wittig salt **235** (Scheme 131).



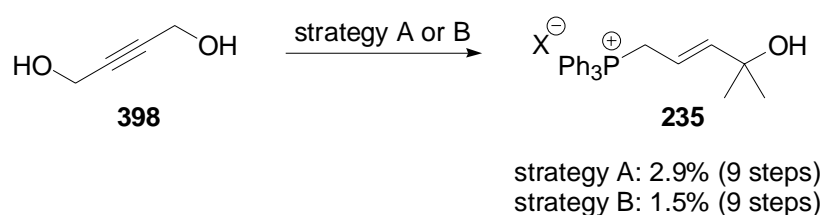
Scheme 131: Alternative route for the synthesis of the Wittig salt **235** involving *E*-selective reduction of the propargylic alcohol **469** (strategy A). *Pg*= protecting group, *X*= halogen.

Instead, *E*-configured alkene **470** might be formed starting from **398** prior to the oxidation alkylation sequence (Scheme 132).



Scheme 132 Reversed order of *E*-selective reduction and the oxidation-/alkylation-sequence may as well lead to the desired Wittig salt **235** (strategy B). *X*= halogen.

Both reaction paths were found to be feasible. However, the obtained yields are rather low and the procedure rather steppy.³⁷⁸

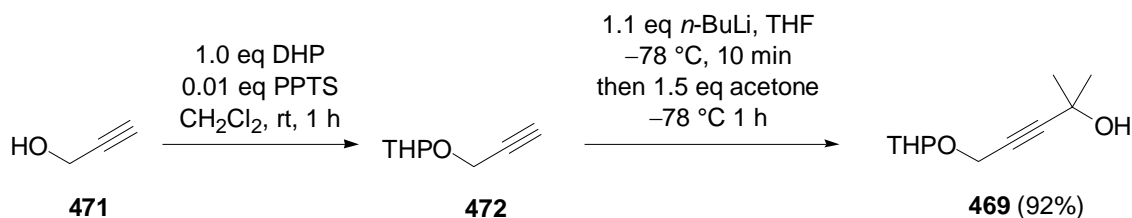


Scheme 133: Summarized results for the synthesis of **235** following strategy A or B.

³⁷⁷ For mechanistic considerations, see: (a) Blunt, J. W.; Hartshorn, M. P.; Munro, M. H. G.; Soong, L. T.; Thompson, R. S.; Vaughan, J. J. *Chem. Soc., Chem. Comm.* **1980**, 820-821. (b) Baldwin, J. E.; Black, K. A. *J. Org. Chem.* **1983**, *48*, 2778-2779. (c) Corey, E. J.; Katzenellenbogen, J. A.; Posner, G. H. *J. Am. Chem. Soc.* **1967**, *89*, 4245-4247. For recent examples, see: (d) Bode, J. W.; Carreira, E. M. *J. Org. Chem.* **2001**, *66*, 6410-6424. (e) Ahmed, A.; Hoegenauer, E. K.; Enev, V. S.; Hanbauer, M.; Kaehlig, H.; Ohler, E.; Mulzer, J. *J. Org. Chem.* **2003**, *68*, 3026-3042. (f) Trost, B. M.; Gunzner, J. L. *J. Am. Chem. Soc.* **2001**, *123*, 9449-9450.

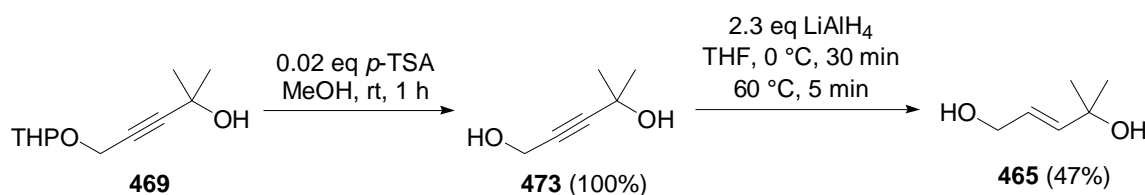
³⁷⁸ For details, see: Experimental section.

Consequently, a shorter sequence had to be revealed. A more efficient approach was stimulated by the work of Díez Martín *et al.*³⁷⁹ In this attempt propargylic alcohol **471** was conveniently protected as THP ether **472**. Subsequent lithiation of the terminal alkyne carbon atom and addition of the alkynyl lithium compound to acetone afforded alcohol **496** (Scheme 134).



Scheme 134: Synthesis of the protected propargyl alcohol **469** according to Díez Martín. DHP= dihydropyrane, PPTS= pyridinium *para*-toluenyl sulfonate, THP= tetrahydropyranyl.

Attempts to reduce the alkyne **469** prior to the deprotection had only limited success. Therefore, **469** was deprotected to provide diol **473** which in turn was subjected to the *E*-selective reduction to afford the desired allylic alcohol **465** (Scheme 135).³⁷⁷

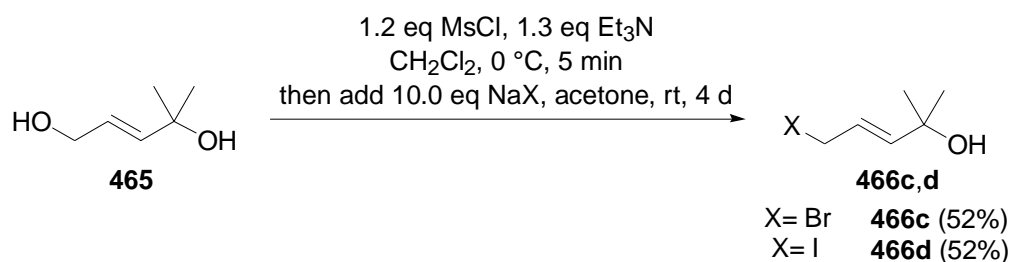


Scheme 135: Synthesis of allylic alcohol **465** was realized in two steps starting from **469**. *p*-TSA= *para*-toluene sulfonic acid, THP= tetrahydropyranyl.

With the alcohol **465** in hand, the functional group transformation was investigated. Mitsunobu redox condensation⁶³ using CBr₄ or bromine did not furnish the desired halogenide **466**. Therefore, a two-step protocol was utilized. Alcohol **465** was first subjected to methane sulfonyl chloride and triethylamine. To the reaction mixture acetone and excess of sodium halogenide was added. Short reaction times and low temperatures (0 °C) resulted in the predominant formation of the chloride. However, prolonged reaction times at room temperature afforded the desired halogenides **466c,d** in moderate not optimized yields (Scheme 136). Allyl iodide **466d** was found to be highly instable and degenerates within a

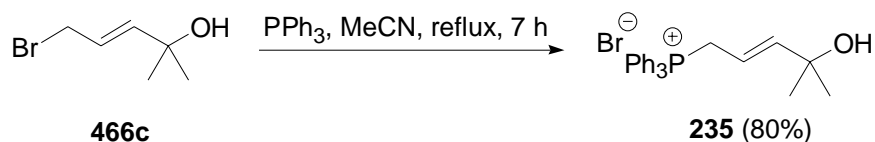
³⁷⁹ Díez Martín, D.; Marcos, I. S.; Basabe, P.; Romero, R. E.; Moro, R. F.; Lumeras, W.; Rodríguez, L.; Urones, J. G. *Synthesis* **2001**, 1013-1022.

short period of time. Furthermore, the reaction generates undesired mixtures of double bond isomers. Consequently, the efforts were concentrated on bromide **466c**.



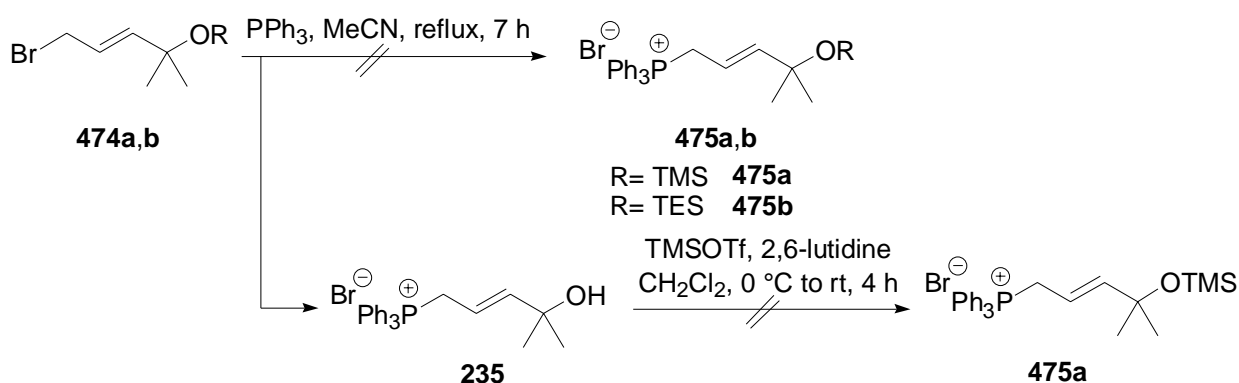
Scheme 136: Formation of halogenides **466** was realized by a one-pot, two step procedure.

The Wittig salt **235** was synthesized by treatment of **466c** with triphenylphosphine in refluxing acetonitrile (Eq. 63).



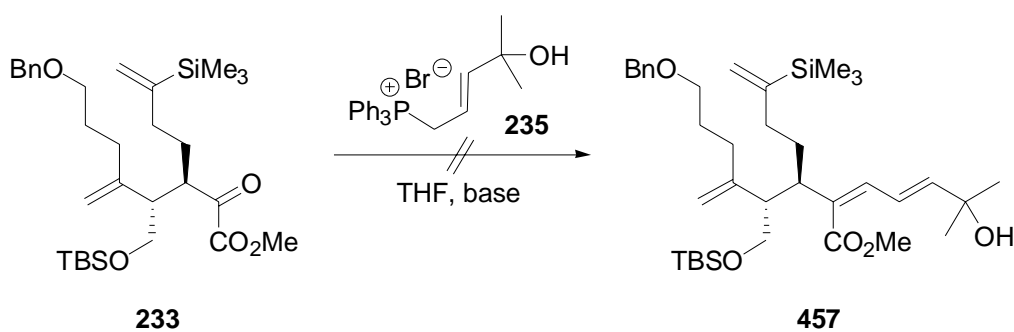
Eq. 63

Attempts, to synthesize the protected Wittig salts **475a,b** were unsuccessful. Utilization of protected halogenides **474a,b** as starting materials resulted in the cleavage of the protection groups. Further trials to introduce the protection group after the formation of the Wittig salt **235** have been unsuccessful too (Scheme 137).



Scheme 137: Unsuccessful trials to generate the protected Wittig salts **475a,b**. TMS= trimethylsilyl [SiMe₃], TES= triethylsilyl [SiEt₃], Tf= trifluoromethyl sulfonyl [CF₃SO₂].

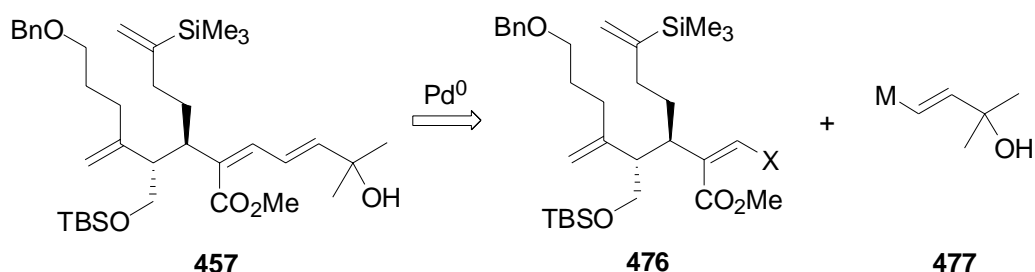
A number of conditions were tested for the Wittig olefination between **233** and **235** (Table 45). None of them furnished the desired coupling product.



| Entry | base | Reaction conditions | Equivalents of the ylene |
|-------|-----------------|---|--------------------------|
| 1 | NaH/DMSO | DMSO, rt, overnight | 1.7 |
| 2 | NaH/DMSO | DMSO, $-78\text{ }^{\circ}\text{C}$ to rt, 48 h | 5.0 |
| 3 | NaH/DMSO | THF, $-78\text{ }^{\circ}\text{C}$ to rt, 48 h | 5.0 |
| 4 | NaH | THF, $-78\text{ }^{\circ}\text{C}$ to rt, 48 h | 5.0 |
| 5 | <i>n</i> -BuLi | THF, $-78\text{ }^{\circ}\text{C}$ to rt, 48 h | 5.0 |
| 6 | LDA | THF, $-78\text{ }^{\circ}\text{C}$ to rt, 48 h | 5.0 |
| 7 | KHMDS | THF, $-78\text{ }^{\circ}\text{C}$ to rt, 48 h | 5.0 |
| 8 | LiHMDS | THF, $-78\text{ }^{\circ}\text{C}$ to rt, 48 h | 5.0 |
| 9 | K <i>Ot</i> -Bu | THF, $-78\text{ }^{\circ}\text{C}$ to rt, 48 h | 5.0 |

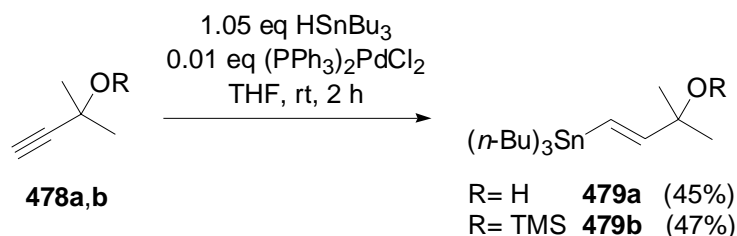
Table 45: Tested reaction conditions for the Wittig olefination of **233** with **235**. DMSO= dimethylsulfoxide, LDA= lithium diisopropylamide, KHMDS= potassium hexamethyldisilazide $\{\text{K}[\text{N}(\text{SiMe}_3)_2]\}$, LiHMDS= lithium hexamethyldisilazide $\{\text{Li}[\text{N}(\text{SiMe}_3)_2]\}$.

Therefore, a stepwise introduction of the side chain was considered. The presence of a halomethylen group should enable palladium catalyzed cross coupling (Scheme 138).



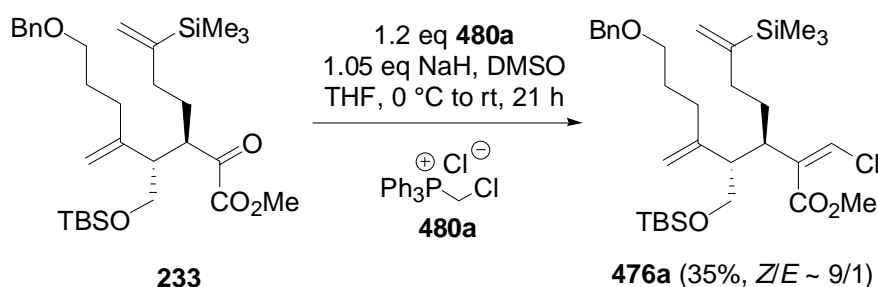
Scheme 138: Alternative route toward **457** by palladium-catalyzed cross-coupling. TBS= *tert*-butyldimethylsilyl $[\text{Si}(t\text{-Bu})\text{Me}_2]$, Bn= benzyl, X= halogen, M= metal.

The coupling partner **477** may be synthesized by hydrostannation of commercially available **478a** or **478b**. *Cis*-selectivity hydrostannation (see chapter 13.2) is expected to provide **479a,b** as *trans*-olefins.



Scheme 139: Formation of the vinyl stannanes **479a,b** by hydrostannation.³⁸⁰

Preliminary experiments for the synthesis of **476** have been performed with the commercially available Wittig salt **480a**.³⁸¹ The reaction of **233** with **480a** furnished the desired olefination product **476a** with 35% not optimized yield (Eq. 64).



Eq. 64 TBS= *tert*-butyldimethylsilyl [$\text{Si}(t\text{-Bu})\text{Me}_2$], Bn= benzyl, DMSO= dimethylsulfoxide.

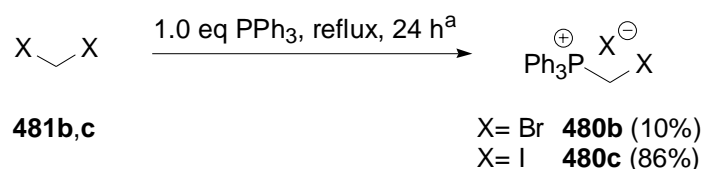
One of the two possible double bond isomers was preferentially formed. NOE experiments conducted for **476a** revealed that indeed the required *Z*-isomer is the major product.³⁸² The double bond isomers were found to be separable by careful flash chromatography.

For the generation of the corresponding vinyl bromides and iodides **476b,c** the bromine and iodine containing Wittig salts **480b,c** were required. **480b,c** may be prepared by the reaction of dihalomethanes **481a,b** with PPh_3 (Scheme 140).

³⁸⁰ Yields not optimized.

³⁸¹ Frye, L. L.; Robinson, C. H. *J. Org. Chem.* **1990**, *55*, 1579-1584.

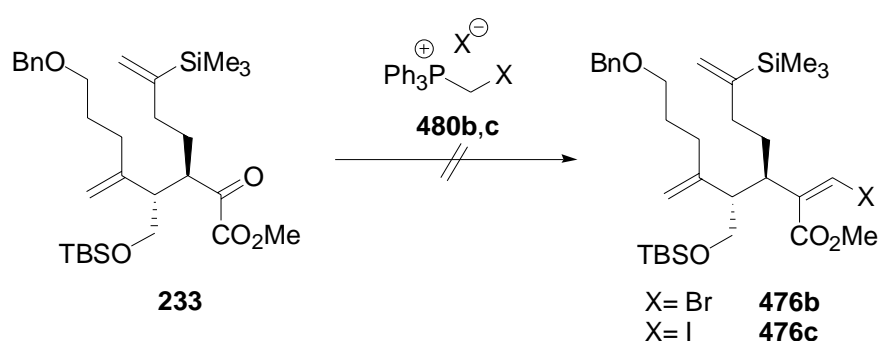
³⁸² For a more detailed analysis, see chapter 19.



^a **481b** in toluene, **481c** in MeCN

Scheme 140: Formation of the Wittig salts **480b**³⁸³ and **480c**.

Various conditions were tested for the reaction of α -keto ester **233** with either of the Wittig salts **480b,c** (Table 46). However, none of the tested procedures delivered the olefination product **476b,c**.

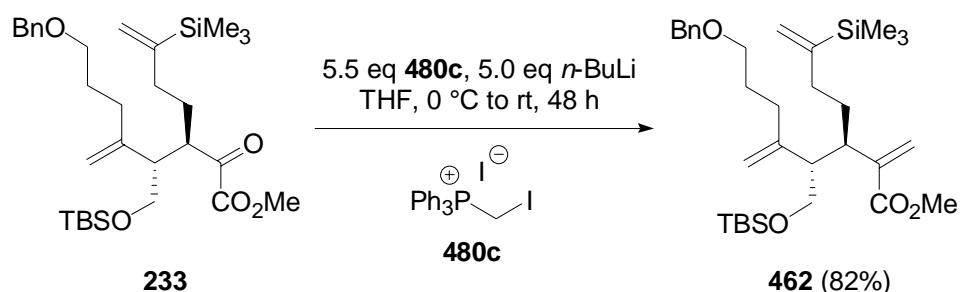


| Entry | Base | Reaction conditions | Equivalents of the ylene |
|-------|-----------------------------|-----------------------|--------------------------|
| 1 | NaH ^a | DMSO, rt, overnight | 1.1 |
| 2 | NaH ^b | DMSO, rt, overnight | 5.0 |
| 3 | NaH ^b | DMSO, 80 °C, 12 h | 5.0 |
| 4 | <i>n</i> -BuLi | THF, 0 °C to rt, 48 h | 1.1 |
| 5 | <i>n</i> -BuLi ^b | THF, 0 °C to rt, 48 h | 5.0 |
| 6 | NaHMDS ^a | THF, 0 °C to rt, 48 h | 1.1 |
| 7 | NaHMDS ^b | THF, 0 °C to rt, 12 h | 5.0 |
| 8 | KOt-Bu | THF, 0 °C to rt, 48 h | 1.1 |
| 9 | KOt-Bu ^b | THF, 0 °C to rt, 48 h | 5.0 |

Table 46 Reaction conditions for the Wittig olefination of **233** with **480b,c**. ^a Only applied to **480b**. ^b Only applied to **480c**. TBS= *tert*-butyldimethylsilyl [Si(*t*-Bu)Me₂], Bn= benzyl, DMSO= dimethylsulfoxide, NaHMDS= sodium hexamethyldisilazide {Na[N(SiMe₃)₂]}.

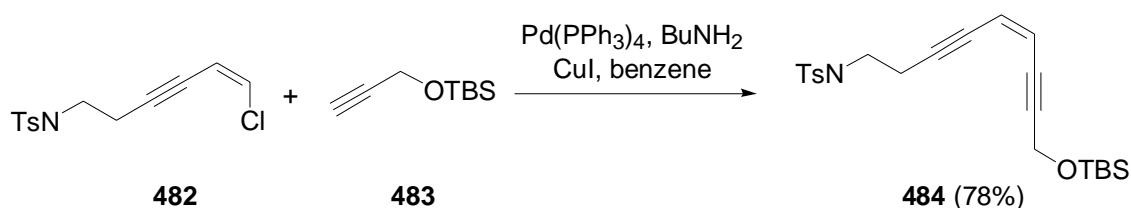
³⁸³ Following the procedure published earlier: Rodríguez, J. G.; Martín-Villamil, R.; Lafuente, A. *Tetrahedron* **2003**, *59*, 1021-1032. Yields not optimized.

Starting material **233** was reisolated in all cases except for the utilization of *n*-BuLi for the Wittig reaction with **480c** (Table 46, entry 5). Under those conditions the reaction delivered dehalogenated Wittig olefination product **462** with 82% isolated yield (Eq. 65).

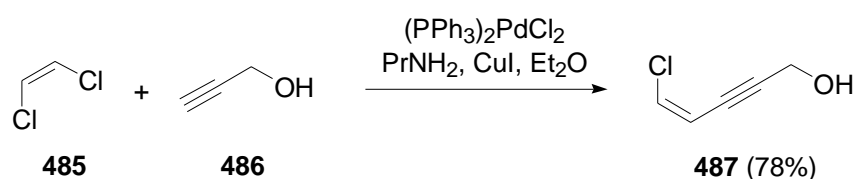


Eq. 65 Bn= benzyl.

Since the efforts to generate **476b,c** have not been successful and consequently, common palladium-catalyzed cross-coupling could not be challenged, a different approach that involves the vinyl chloride **476a** was envisioned. Castro-Stephens coupling might offer such an alternative.³⁸⁴ Two successful examples are depicted in Eq. 66^{384a} and Eq. 67.^{384b}



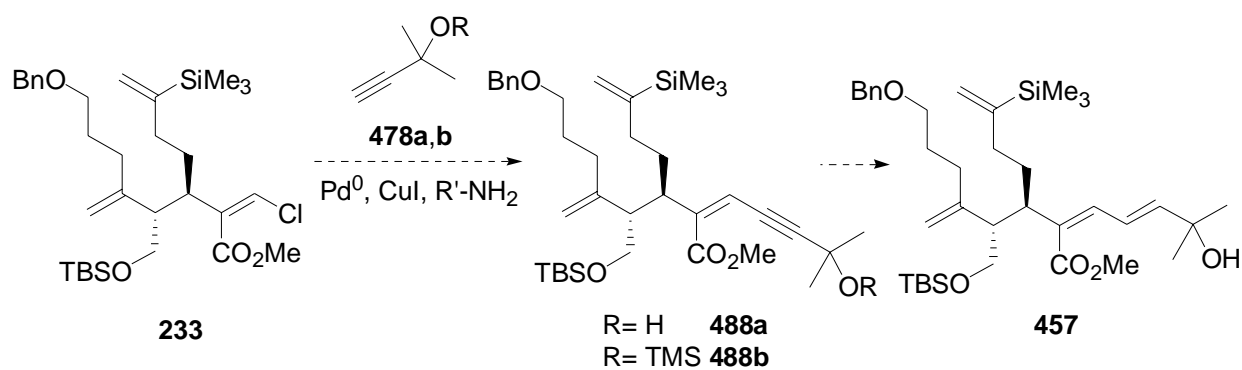
Eq. 66 Ts= *para*-toluene sulfonyl, TBS= *tert*-butyldimethylsilyl [Si(*t*-Bu)Me₂].



Eq. 67

Accordingly, **476a** may be subjected to **478a,b** in the presence of copper(I)-iodide, (PPh₃)₂PdCl₂ and a primary amine (Scheme 141). The desired coupling product **488** may be reduced to the conjugated diene **457** by the above mentioned *E*-selective reduction of propargylic alcohols (see Scheme 135).

³⁸⁴ Stephens, R. D.; Castro, C. E. *J. Org. Chem.* **1963**, *24*, 3313-3315. For recent examples involving vinyl chlorides instead of phenyl chlorides, see: (a) Basak, A.; Shain, J. C.; Khamrai, U. K.; Rudra, K. R.; Basak, A. *J. Chem. Soc., Perkin Trans. 1* **2000**, 1955-1964. (b) Myers, A. G.; Dragovich, P. S.; Kuo, E. Y. *J. Am. Chem. Soc.* **1992**, *114*, 9369-9386.

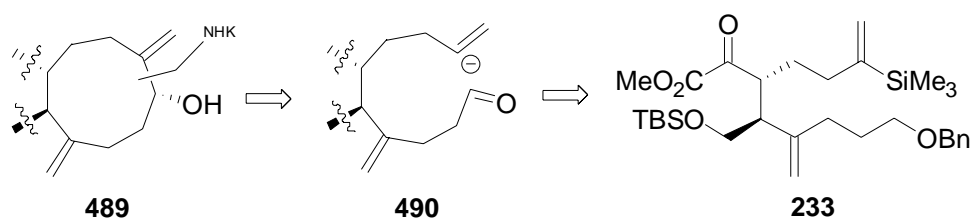


Scheme 141: Alternative introduction of the side chain by Castro-Stephens cross-coupling. TBS= *tert*-butyldimethylsilyl [$\text{Si}(t\text{-Bu})\text{Me}_2$], Bn= benzyl, TMS= trimethylsilyl [SiMe_3], R'= alkyl.

Even though a preliminary experiment for the coupling of **233** with **478a** has not been successful this reaction offers further potential for optimization.

17 Preliminary Experiments for the Envisaged Nozaki-Hiyama-Kishi Reaction

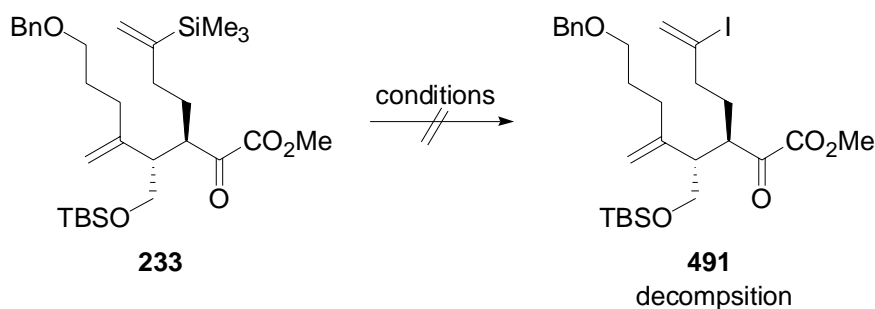
The formation of the nine-membered ring of xeniolide F (represented by the fragment **489**) by Nozaki-Hiyama-Kishi reaction requires a vinyl iodide fragment as precursor of the vinyl anion and an aldehyde functionality as present in **490**. The aldehyde might be generated from the benzyl protected hydroxyl group present in the Claisen rearrangement product **233** (Scheme 142). As ‘masked’ vinyl iodide utilization of a vinyl trimethylsilane moiety was envisioned.



Scheme 142: The vinyl anion and the aldehyde functionality of **490** required for a NHK coupling might be generated by iododesilylation and a deprotection-oxidation sequence.

Iododesilylation has been reported frequently to provide a reasonable strategy to form vinyl iodides. Depending on the structure of the substrate, a variety of conditions for this transformation are known.³⁸⁵ Several iododesilylation conditions were screened (Table 47). Disappointingly, none of them afforded the desired vinyl iodide **491**.

³⁸⁵ (a) NIS in EtCN: Morit, R.; Shirakawa, E.; Tsuchimoto, K. *Org. Biomol. Chem.* **2005**, *3*, 1263-1268. (b) NIS in concert with ClCH₂CN in MeCN: Stamos, D. P.; Taylor, A. G.; Kishi, Y. *Tetrahedron Lett.* **1996**, *37*, 8647-8650. (c) NIS in MeCN: Durham, T. B.; Blanchard, N.; Savall, B. M.; Powell, N. A.; Roush, W. R. *J. Am. Chem. Soc.* **2004**, *126*, 9307-9317. (d) I₂ in CH₂Cl₂: Chan, T.; Fleming, I. *Synthesis* **1979**, 761-786. (e) ICl in DMSO: Chan, T. H.; Koumaglo, K. *J. Organomet. Chem.* **1985**, *285*, 109-119. (f) Py₂IBF₄ in CH₂Cl₂: Barluenga, J.; Alvarez-García, L. J.; González, J. M. *Tetrahedron Lett.* **1995**, *36*, 2153-2156.

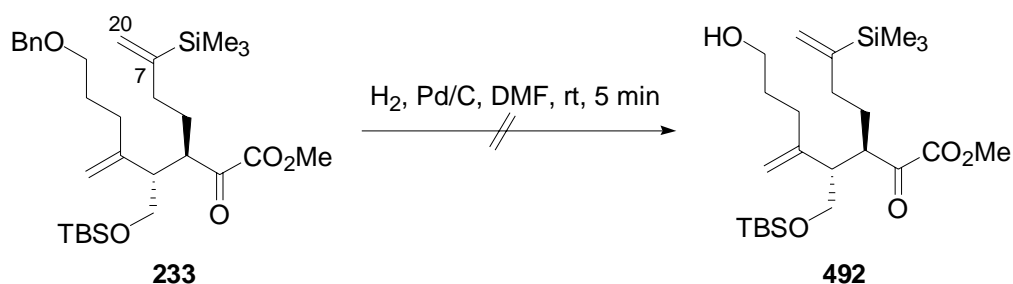


| Entry | Iodonium ion source | Solvent |
|-------|---------------------|---------------------------------|
| 1 | NIS | MeCN |
| 2 | NIS | ClCH ₂ CN:MeCN (1/4) |
| 3 | NIS | EtCN |
| 4 | I ₂ | CH ₂ Cl ₂ |

Table 47: Screening of frequently used iododesilylation conditions. NIS= *N*-iodo succinimide. TBS= *tert*-butyldimethylsilyl [Si(*t*-Bu)Me₂], Bn= benzyl.

All reaction conditions resulted in the decomposition of the starting material **233** into various unidentified side-products. In contrast, subjection of allyl vinyl ether **10a** to *N*-iodo succinimide in acetonitrile gave reisolated starting material. Therefore, it might be concluded that the reactivity of the α -keto ester **233** interferes with iododesilylation conditions and the transformation has to be performed at a later stage of the total synthesis.

Another preliminary experiment was performed for the debenylation. In analogy to earlier results,^{65j,k} hydrolytic cleavage of the benzyl ether was investigated. The reaction was carefully monitored using TLC and stopped as soon as TLC indicated the complete consumption of the starting material (~5 min). Disappointingly, the C7-C20 double bond was affected as well under those conditions.



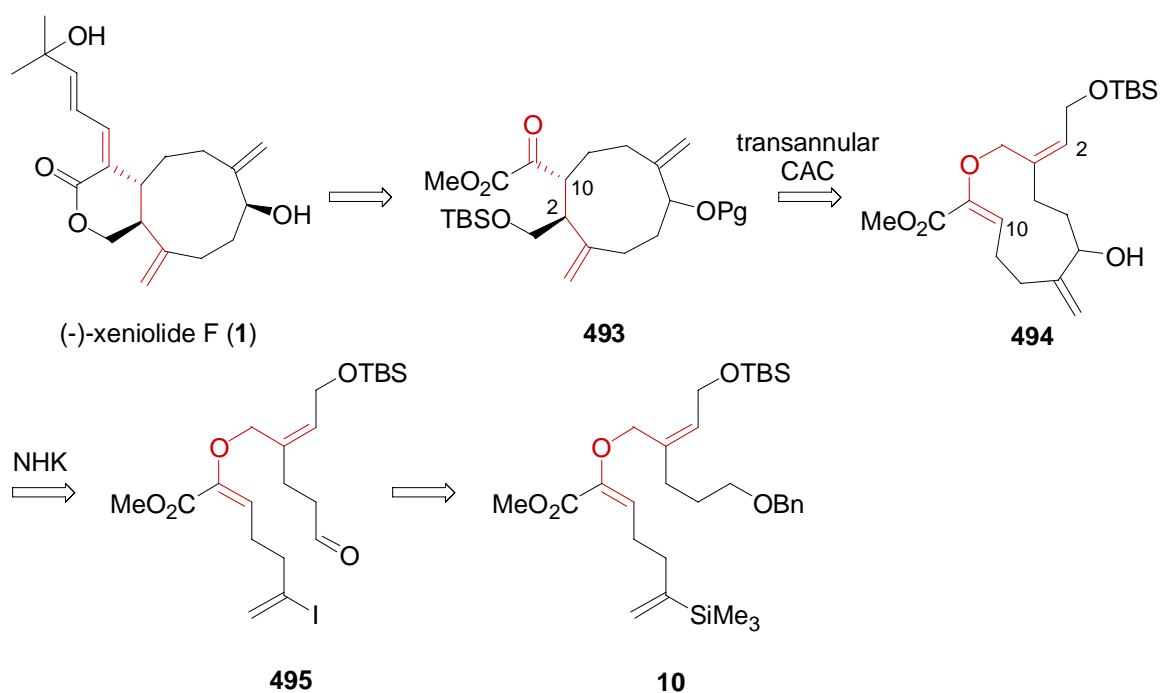
Eq. 68 TBS= *tert*-butyldimethylsilyl [Si(*t*-Bu)Me₂], Bn= benzyl.

18 Summary and Future Prospects

In summary, a reliable strategy was developed for the generation of α -keto ester **233**. Preliminary experiments were performed that showed that vinyl chloride **476a** is in principle accessible by Wittig olefination. Expansion of this strategy to bromo- or iodo-analogues thereof has yet not met the desired success. If reaction conditions can be found to generate the required vinyl iodide or vinyl bromide **476b,c**, palladium-catalyzed cross-coupling might provide a strategy to introduce the side chain. In case that only the vinyl chloride is accessible at this way, Castro-Stephens cross-coupling might be employed for the completion of the side chain. Even though the preliminary experiment for this route has been unsuccessful, variations are possible both concerning the reaction conditions and the protection groups of the reaction partners.

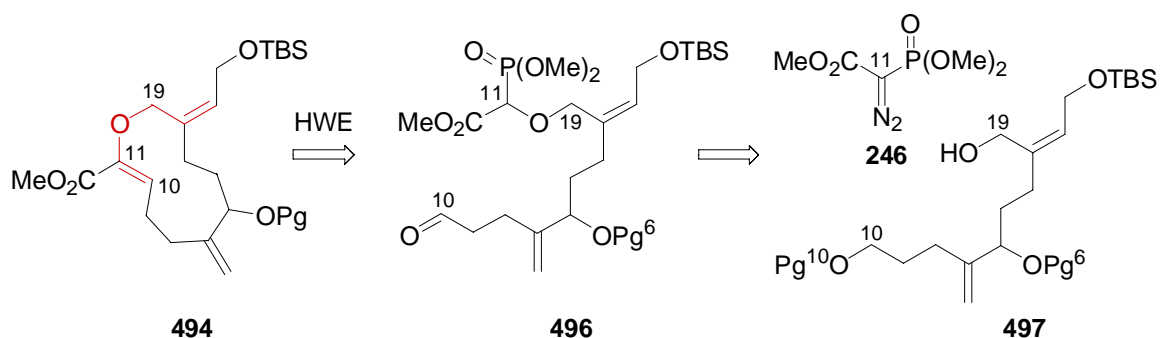
As mentioned earlier, the iododesilylation might prove successful at a later stage of the synthesis. Alternatively, the vinyl iodide moiety could be formed at an earlier stage of the synthesis presupposed that it express reasonable stability. Utilization of a vinyl stannane instead of the vinyl silane is an additional option.

As pointed out earlier, a possible intramolecular Michael-addition of the vinyl anion that would be formed intermediary during the Nozaki-Hiyama-Kishi coupling could prevent this strategy for the formation of the nine-membered ring. An alternative route that bypasses that difficulty is depicted in Scheme 143. This strategy involves a transannular Claisen rearrangement of the allyl vinyl ether **494**. The Claisen rearrangement causes ring contraction to form the nine-membered carbocycle of **493**. For the synthesis of **494** a NHK coupling of **495** is envisioned.



Scheme 143: Alternative strategy for the synthesis of (-)-xeniolide F involving a transannular catalytic asymmetric Claisen rearrangement CAC. TBS= *tert*-butyldimethylsilyl [$\text{Si}(t\text{-Bu})\text{Me}_2$], Bn= benzyl, NHK= Nozaki-Hiyama-Kishi coupling.

If the NHK-coupling fails to generate **494** an alternative route could be applied. Thus, analogue to the formation of phosphonate **245** (chapter 14.1.2) the rhodium(II)-catalyzed OH-insertion employing the allylic alcohol **497** would provide **496** after deprotection and oxidation. Intramolecular HWE olefination might afford the desired allyl vinyl ether **494** (Scheme 144).



Scheme 144: Alternative strategy for the generation of **494** involving an intramolecular Horner-Wadsworth-Emmons olefination HWE. TBS= *tert*-butyldimethylsilyl [$\text{Si}(t\text{-Bu})\text{Me}_2$], Pg= unspecified protecting groups.

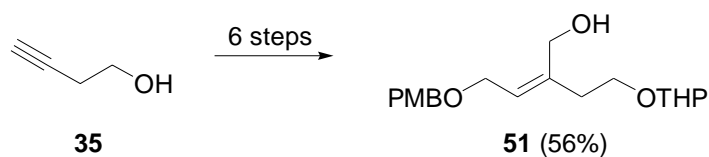
An improvement of the synthesis might be achieved by using a different strategy for the synthesis of the allylic alcohol **11**. The realized synthetic route is summarized in Scheme 145.³⁸⁶

³⁸⁶ For details, see chapter 13.2.2.



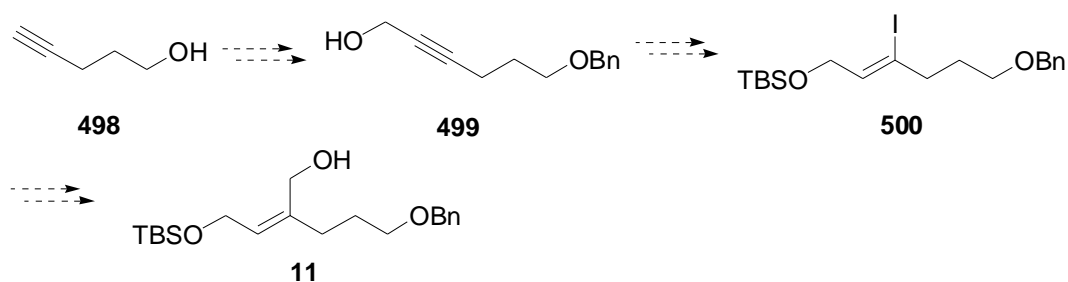
Scheme 145: Realized synthesis of allylic alcohol **11**. TBS= *tert*-butyldimethylsilyl [$\text{Si}(t\text{-Bu})\text{Me}_2$], Bn= benzyl.

The total synthesis of viridiofungin A (**1a**) involved the allylic alcohol **51** generated by a six-step procedure in 56% yield (Scheme 146).³⁸⁷



Scheme 146: Synthetic route toward allylic alcohol **11**. PMB= *para*-methoxybenzyl, THP= tetrahydropyranyl.

Even though six steps are required instead of five steps in the present synthetic route, due to the higher yields this strategy appears to be an attractive alternative. Starting from 5-pentyn-1-ol (**498**) an analogue route should provide allylic alcohol **11**.



Scheme 147: Application of the alternative strategy for the generation of allylic alcohol **11**. TBS= *tert*-butyldimethylsilyl [$\text{Si}(t\text{-Bu})\text{Me}_2$], Bn= benzyl.

³⁸⁷ See chapter 2.3.4.

19 Verification of the Proposed Structure

The most advanced compound during the attempted synthesis of (–)-xeniolide F (**2a**) that was realized during the thesis work is vinyl chloride **476a**.

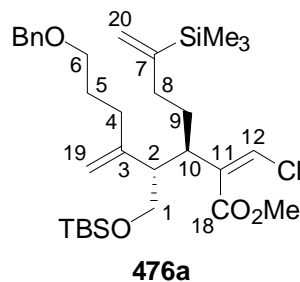


Figure 30 TBS= *tert*-butyldimethylsilyl [$\text{Si}(t\text{-Bu})\text{Me}_2$], Bn= benzyl.

IR-analysis of **476a** revealed signals between 3120 and 3050 cm^{-1} as well as between 2955 and 2855 cm^{-1} indicating the presence of CH-vibrations of aromatic and aliphatic CH-groups. A strong signal at 1730 cm^{-1} shows the presence of at least one carbonyl group.

Analysis of the ^{13}C NMR spectrum of **476a** shows signals of five non-hydrogen substituted carbon atoms at 166.6, 151.9, 148.4, 138.6 and 137.3 ppm. The signal at 166.6 ppm indicates the presence of an ester carbonyl group. HMBC experiments allowed the correlation of the four following signals to 7-C=, 3-C=, C-Ar, and 11-C=. The three signals of the five aromatic CH-groups are located at 128.3, 127.6 and 127.5 ppm. While the two signals of vinylic CH_2 -groups at 124.2 and 111.1 ppm belong to 20- $\text{CH}_2=$ and 19- $\text{CH}_2=$ respectively, the signal at 121.2 ppm can be attributed to 12- $\text{CH}=$. The downfield shift of the three CH_2 -signals at 72.9, 70.2 and 64.0 ppm indicates the presence of an adjacent oxygen atom. COSY cross peaks allowed the assignment that the three signals belong to OCH_2Ph , 6- CH_2 and 1- CH_2 (starting from higher ppm value). The following three signals which indicate the presence of CH- or CH_3 -groups were assigned to OCH_3 (51.8 ppm) and the two stereogenic centers 2-CH (50.4 ppm) and 10-CH (45.0 ppm). The four remaining CH_2 -group signals at 34.1, 32.4, 30.6 and 27.7 ppm are attributed to 8- CH_2 , 4- CH_2 , 9- CH_2 and 5- CH_2 . A CH_3 -signal with high intensity located at 25.9 ppm in concert with the signal of a non-hydrogen substituted carbon atom at 18.2 is characteristic for the *tert*-butyl group of the TBS-protecting group. The upfield shift of the following three CH_3 -group signals (-1.5 , -5.5 and -5.6 ppm) is in agreement with a silicon atom directly attached to them.

In addition to the aromatic signals between 7.35 and 7.25 ppm, five prominent singlets were detected between 6.20 and 4.83 ppm in the ^1H NMR spectrum of **476a**. Each of those signals was found to have an integral height of one proton. The chlorine atom bond to 12-CH= provoked the significant downfield shift (6.20 ppm) of the corresponding signal. The association of the following singlets (5.48 and 5.27 ppm) with 20-CH₂= as well as the singlets at 4.88 and 4.83 ppm with 19-CH₂= was achieved by the interpretation of the HMBC and HSQC data of **476a**. The singlets at 4.48 and 3.79 ppm as well as the signals at 3.63, 3.55 and 3.48 ppm show typical chemical shifts that indicate the presence of an adjacent oxygen atom. The exceeding down field shift of the first of these signals can be attributed to a neighbouring aryl group. Therefore, it was identified as the OCH₂Ph signal – an assignment that is supported by the integral height indicating two protons. Consequently, the other singlet with an integral height of three protons belongs to the OCH₃-group. Analysis of the HSQC- and the COSY spectrum of **476a** allowed to correlation of the signals at 3.63 and 3.55 ppm to 1-CH₂ that exhibited an AB-system splitting. Consequently, the signal at 3.48 ppm originates from the 6-CH₂-group. The following signal was assigned as 10-CH by its multiplicity (ddd). Between 2.20 and 1.24 ppm several multiplets can be identified. HSQC analysis allowed the correlation of the multiplets with 2-CH, 8-CH₂, 4-CH₂, 5-CH₂ and 9-CH₂. The signals of 8-CH₂ and 9-CH₂ are both split into two multiplets of one proton (integral size). The singlets of the silyl groups are located at 0.85 ppm (OSi(CCH₃)), 0.03 ppm (Si(CH₃)₃) and -0.03 ppm (OSi(CH₃)₂).

The constitution of **476a** was verified by the analysis of the COSY-spectrum. It could be approved that 4-CH₂ is connected with a non-hydrogen substituted carbon atom and with 5-CH₂ which is connected with 6-CH₂. Furthermore, it could be confirmed that there is a linear connection of 1-CH₂, 2-CH, 10-CH, 9-CH₂ and 8-CH₂.

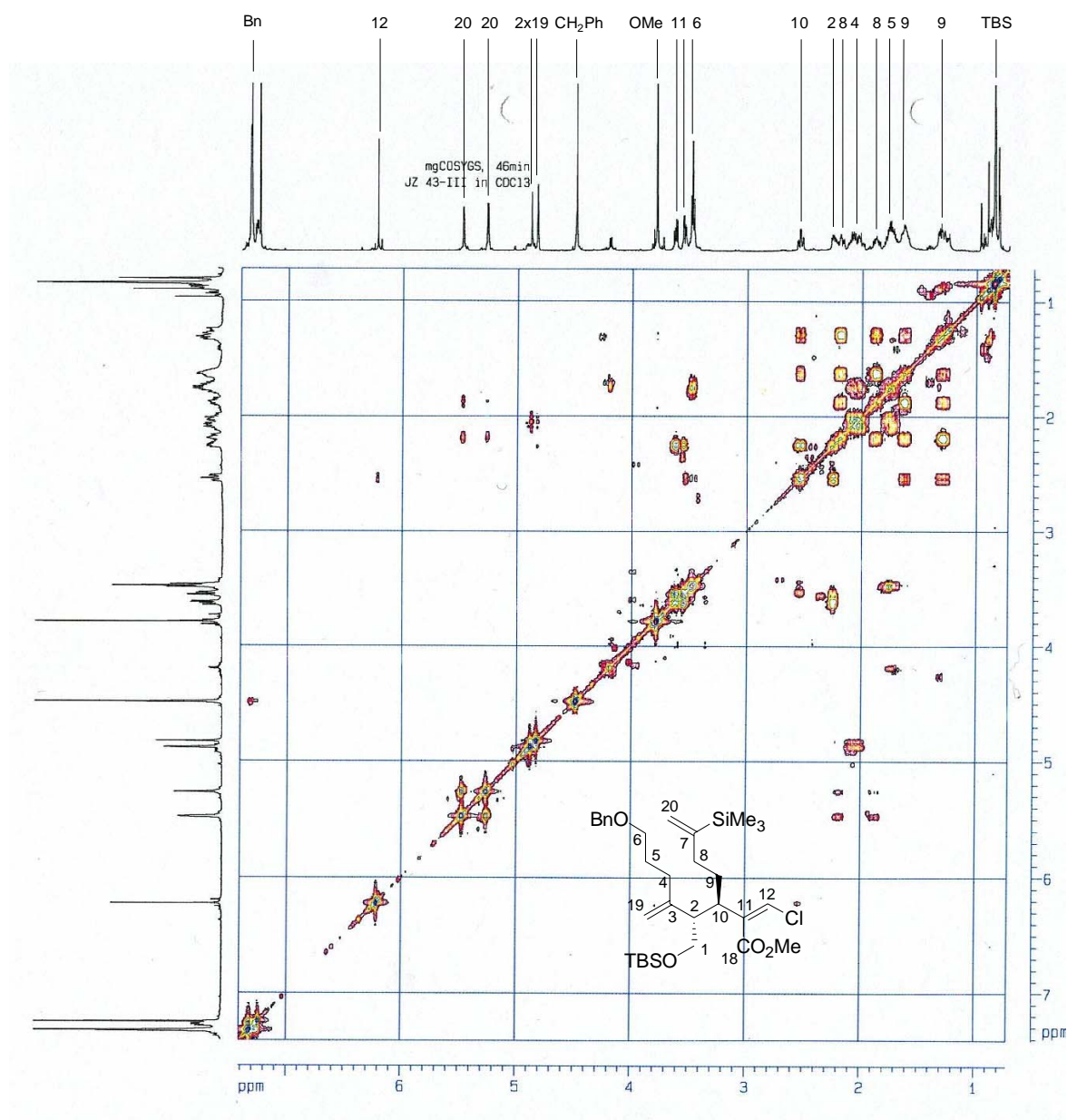
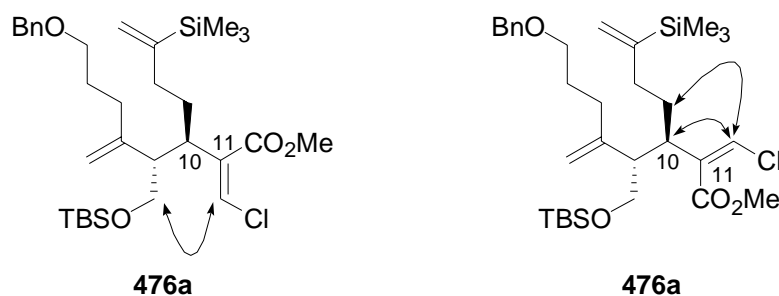


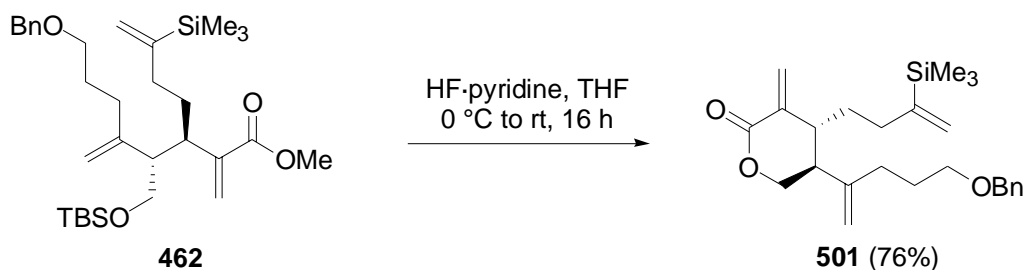
Figure 31: COSY spectrum of **476a**: signals from left to right: Ph-H, 12-CH=, 20-CH₂ (two singlets), 19-CH₂ (two singlets), OCH₂Ph, OCH₃, 1-CH₂ (two separate dd), 6-CH₂, 10-CH, 2-CH, 8-CH₂ (one of two protons), 4-CH₂, 8-CH₂ (one of two protons), 5-CH₂, 9-CH₂ (two multiplets), SiC(CH₃)₃, two further singlets of SiMe₃ and Si(CH₃)₂ appear at upfield shift and are not included in the COSY. TBS= *tert*-butyldimethylsilyl [Si(*t*-Bu)Me₂], Bn= benzyl.

The presumption of a *Z*-configured C11-C12 double bond was supported by NOESY-spectroscopy. It was found that 12-CH= exhibits NOE-cross peaks with 1-CH₂, 10-CH and 9-CH₂. No cross peaks was found between 12-H and the ester residue.



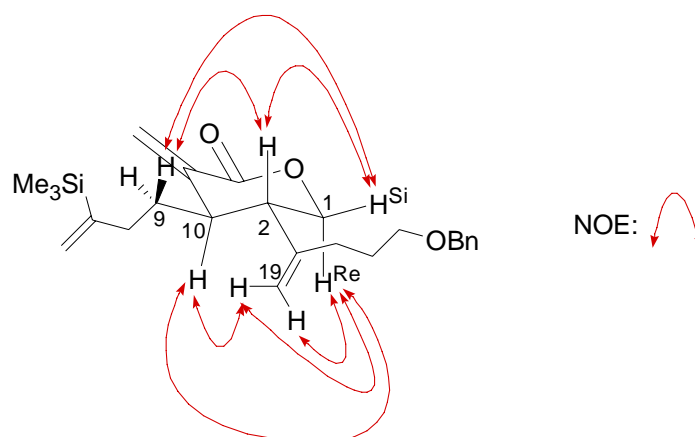
Scheme 148: Selected NOEs of **476a**. The two structures represent different conformations that result from the rotation around the C-10-C11 bond. TBS= *tert*-butyldimethylsilyl [Si(*t*-Bu)Me₂], Bn= benzyl.

To confirm the relative configuration of *anti*-(2*S*,10*R*)-**233** lactone **501** was generated. Cleavage of the silyl ether protecting group of **462** caused in situ lactonization affording δ -lactone **501**.



Eq. 69 TBS= *tert*-butyldimethylsilyl [Si(*t*-Bu)Me₂], Bn= benzyl.

Analysis of NOE data supports the assigned *anti*-configuration of the rearrangement product with respect to substituents at C-2 and C-10 (Scheme 149).



Scheme 149: Selected NOEs for **501**. Bn= benzyl.

Due to the 1,2-relation between 10-H and 2-H, NOE correlations with 1-H have to be considered. The two diastereotopic protons at C-1 exhibit clearly separated signals. Analysis

of the NOE data allowed the assignment of the diastereotopic protons. The signal at 3.63 ppm has a prominent cross peak with 10-H but no cross peak with 9-H and it is therefore assigned as 1-H^{Re}. Consequently, the 1-H signal at 3.55 ppm that does not exhibit a cross peak with 10-H is assigned as 1-H^{Si}. NOE cross peaks were identified between 1-H^{Si} and 9-H as well as between 1-H^{Si} and 2-H. Even though the latter cross peak is a result of a 1,2-relation it should be mentioned because it exhibits a significantly higher intensity than the corresponding 1-H^{Re}/2-H cross peak. As well, a strong NOE cross peak was detected between the protons 9-H and 2-H. In contrast, no cross peak was visible for 1-H^{Re}/9-H. The latter results support the assumption of a spatial relation between 9-H, 2-H and 1-H^{Si}.

Neither 9-H/19-H nor 1-H^{Si}/19H exhibited cross coupling peaks. In contrast, NOE cross peaks were prominent between 19-H and 10-H as well as between 19-H and 1-H^{Re}.

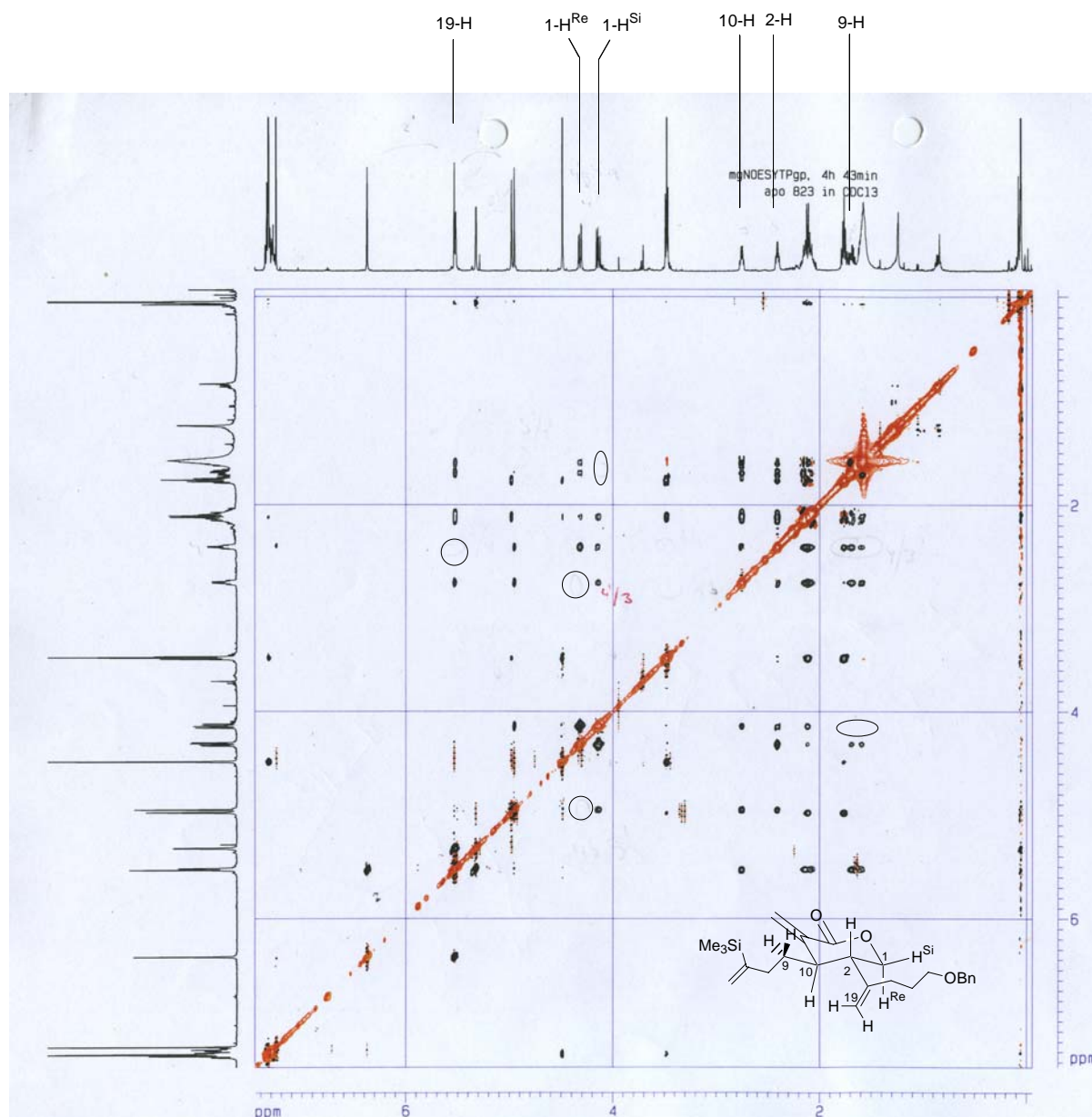


Figure 32: NOESY spectrum of **501**. Encircled are lacking NOE-cross peaks that further support the stereochemical assignment.

In summary, good arguments can be found that strongly support the assumed *anti*-configuration. However, the unambiguous verification of the relative configuration could not be assured.

Part 3: Experimental Section

20 Experimental Section³⁸⁸

20.1 General Experimental Methods

Nomenclature

The nomenclature of the compounds is based on the characteristic, structural elements present in a specific molecule. For the atom numbering we followed the common numbering of the natural products as it was suggested in the literature. If 2D-NMR experiments allowed the unambiguous correlation between NMR-signals and the associated carbon or hydrogen atoms this numbering will be used to specify the signals in the reported data.

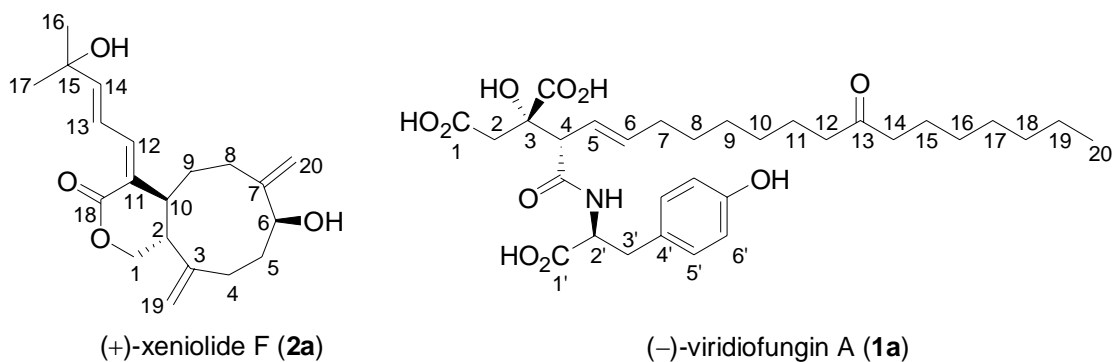


Figure 33

Flash Chromatography

Silica gel 60 (0.040-0.063, MERCK[®]) was used as stationary phase for flash chromatography and filtration. Depending on the amount of crude product, columns with diameters of 10-100 mm were applied. Employed eluents are specified for each individual compound. The starting solvent should cause a R_f value of <0.5 . Usually a gradient was utilized starting with a less polar mixture which composition was gradually changed toward the more polar solvent. If necessary, a manual air compressor was utilized to enable a reasonable flow rate. During my thesis work in our research group the heptane as solvent for flash chromatography was replaced by hexanes.

Thin Layer Chromatography

³⁸⁸ The total synthesis of viridifungin triesters and preliminary results for the total synthesis of (-)-xeniolide F has been published previously (reference 65k and 202e respectively). Parts of the Supporting Informations of these papers have been taken over with minor changes for the present Experimental Section.

Analytical thin layer chromatography (TLC) was performed using pre-coated silica gel foils 60 F₂₅₄ (layer thickness: 0.2 mm, MERCK[®]). Routine reaction control was accomplished using plates 4 cm in length (maximum front length: 3.4 cm). Visualization was achieved by UV-light irradiation ($\lambda = 254$ nm) or by heating of the plates after immersion into an anisaldehyde based staining reagent (2.53 vol% of anisaldehyde, 0.096 vol% of acetic acid, 93.06 vol% of ethanol, 0.034 vol% of conc. H₂SO₄).

High Pressure Liquid Chromatography

A) Normal phase HPLC

- Preparative HPLC: WATERS System 3000; RI-Detection (KNAUER K2400); Column: Nucleosil 50-5 (32 × 250 mm, 5 μ m); Eluent: *n*-heptane/ethyl acetate; Flow: 30 mL/min; Temperature: ambient temperature. Probe preparation: All substances were filtered through a plug of silica gel (20 mm, heptane/ethyl acetate) immediately before the separation and it was ensured that the substance was free of baseline pollutions ($R_f = 0$). The solvents were evaporated at reduced pressure and a solution (heptane/ethyl acetate) of the substance was prepared. In case of unsolved particles, the solution had to be filtered *before* the analysis is performed! Depending on the compound, mass concentrations between 0.2 and 0.5 g/mL could be employed.

- Analytical HPLC: either Hewlett-Packard 1090; DAD-Detection at 210 and 220 nm; Column: Chiracel OD 14025 (4.6 × 255 mm, 10 μ m); Eluent: *n*-hexane/*i*-PrOH, 1 mL/min; Temperature: 35 °C, or Agilent 1100 Series; DAD-Detection at 210 and 220 nm; Column: Chiracel OD 14025 (4.6 × 255 mm, 10 μ m); Eluent: *n*-hexane/*i*-PrOH, 1 mL/min; Temperature: 35 °C. Probe preparation: all substances were filtered through a plug of silica gel (20 × 5 mm, hexanes/ethyl acetate) and it was ensured that the substance was free of baseline pollutions ($R_f = 0$). The solvents were evaporated at reduced pressure and a solution of the substance in *n*-hexane was prepared (1-10 mg/mL) and filled into a HPLC-probe vessel that was sealed with an aluminum foil cap. In case of unsolved particles, the solution had to be filtered *before* the analysis is performed!

B) Reversed phase HPLC

- Preparative HPLC: VARIAN Pro Star; ELDS detection (PL-ELS 1000, POLYMER LABORATORIES); Column: VYDAC 208TP1030 – C8 (30 × 250 mm, 10 μ m); Eluent: isocratic A/B (solvent A: H₂O + 5 % CH₃CN + 5 % CH₃OH + 0.1 % TFA, solvent B: CH₃CN + 0.1 % TFA); Flow: 40 mL/min; Temperature: ambient temperature. Probe preparation: All

substances were filtered through a plug of silica gel (20 mm, ethyl acetate) immediately before the separation and it was ensured that the substance was free of baseline pollutions ($R_f = 0$). The solvents were evaporated at reduced pressure and a solution (MeCN) of the substance was prepared. The solution was drawn up into a syringe and pressed through a 5 μm PTFE filter into the probe vessel. Depending on the compound, mass concentrations between 0.05 and 0.1 g/mL could be employed.

- Analytical HPLC: AGILENT 1100 Series; DAD-Detection at 215, 260 and 280 nm; Column: ECLIPSE XDB-C8 (4.6 \times 150 mm, 5 μm); Eluent: isocratic A/B (solvent A: H₂O + 0.1 % TFA, solvent B: CH₃CN + 0.1 % TFA); Flow: 1 mL/min; Temperature: 35 °C. Probe preparation: All substances were filtered through a plug of silica gel (20 mm, ethyl acetate) immediately before the separation and it was ensured that the substance was free of baseline pollutions ($R_f = 0$). The solvents were evaporated at reduced pressure and a solution (MeCN) of the substance was prepared. The solution was drawn up into a syringe and pressed through a 2 μm PTFE filter into the HPLC-probe vessel that was sealed with an aluminum foil cap.

NMR-Spectroscopy

¹H NMR spectra were recorded either on an ASP-300 (BRUKER) at 300.13 MHz or on a DRX-500 (BRUKER) at 500.13 MHz and the data are listed as follows: chemical shift δ in ppm using tetramethylsilane as internal standard (δ 0 ppm), multiplicity (s = singlet, d = doublet, t = triplet, q = quartet, br = broad, quint = quintet, m = multiplet or overlap of non equivalent resonances), coupling constant (H-H or P-H) in Hz,³⁸⁹ integration. ¹³C NMR spectra were recorded either on an ASP-300 (BRUKER) at 75.48 MHz or on a DRX-500 (BRUKER) at 125.77 MHz and the data are listed as follows: chemical shift δ in ppm using CDCl₃ as internal standard (δ 72.2 ppm), coupling constant (only for P-C) in Hz, multiplicity with respect to proton (deduced from DEPT³⁹⁰ experiments). The assignments of atom connectivity and spatial relationships are exclusively based on 2D NMR correlation (NOESY³⁹¹, ¹H/¹H-COSY³⁹², ¹H/¹³C-HMBC³⁹³ and ¹H/¹³C-HSQC³⁹⁴).

³⁸⁹ Deduced from the spectra using Win-NMR 1D (version 6.0). All unspecified coupling constants are H-H couplings, P-H couplings are specified.

³⁹⁰ DEPT = Distortionless Enhancement by Polarization Transfer

³⁹¹ NOESY = Nuclear Overhauser Spectroscopy

³⁹² COSY = Correlated Spectroscopy

³⁹³ HMBC = Heteronuclear Multiple Bond Coherence

³⁹⁴ HSQC = Heteronuclear Single Quantum Coherence

FT-IR-Spectroscopy

FT-IR-spectra were recorded on Nicolet 205 FT-IR spectrometer (NICKOLET[®]) as ATR (Attenuated Total Reflectance). Probe preparation was carried out on a KBr-disc. The utilization of a thin substance film between two KBr-discs for the measurement is reflected in the term ‘in substance’.

Elemental Analysis

Molecular formula assignment was confirmed by combustion elemental analysis using an Elemental Analyzer EA 1108 (CARLO ERBA INSTRUMENTS[®]) or Euro EA 3000 (HEKATECH[®]).

Optical Rotation Values

Optical rotation values were recorded on polarimeter 341 LC (PERKIN ELMER[®]) with the solvent specified for the respective compound. In all cases a wave length of $\lambda = 589$ nm was applied. The actual temperature during the measurement will be reported as well. For the calculation of the specific optical rotation the following formula was employed.

$$[\alpha]_d^T = \frac{\alpha \cdot 100}{l \cdot c}$$

α = measured optical rotation angle [°]
 l = layer thickness [dm]
 c = concentration [g/100 ml solvent].

Specification of Percentage Values

Percentage values are used to describe the mass portion of a specific compound with respect to the total mass of the mixture. The ratios given for solvent mixtures refer to volume units.

Amounts of Starting Materials and Reaction Products

Mass, volume and mol amount values are rounded as following: >100 mmol: full numbers; 0.1-99.9 mmol: one decimal place, <0.1 mmol: two decimal places; >0.5 g: one decimal place, <0.5 g: two decimal palces, <0.1g: amount given in mg; >20 mL: full numbers, 0.5-19.9 mL: one decimal place, 0.10-0.49 mL: two decimal places, <0.1 mL: volume given in μ L.

All moisture-sensitive **reactions** were performed in flame-dried septum-sealed glassware under an atmosphere of argon. The argon stream was supplied to the flask by piercing a

needle connected with an argon source through the septum. Addition of solids was realized in a continuing argon stream. Liquids were added by cannula equipped syringes. Sealed tubes were obtained from SIGMA-ALDRICH[®] (Ace pressure tube, 35 ml, PTFE bushing, FETFE O-ring, type A). Polyethylene vials were not pre-heated but only filled with argon before use.

Chemicals and Solvents

Chemicals were obtained from ALDRICH, ACROS, MERCK, ABCR, FLUKA, FISCHER CHEMICALS, ROTH and J.T. BAKER. Unless otherwise noted, commercially available chemicals were used as received without further purification. Before use, solvents were refluxed over the appropriated drying agent and distilled under nitrogen: tetrahydrofuran from potassium, dichloromethane, 1,2-dichloroethane and triethylamine from CaH₂; methanol from magnesium. DIBAL and *n*-BuLi was obtained in 1 L bottles. 100 mL portions were transferred into flame dried, argon filled and septum sealed vessels. The concentration of *n*-BuLi and *t*-BuLi was determined employing 4-biphenylmethanol as indicator.³⁹⁵

Molecular Sieves

Molecular sieves were obtained from Baker (4 Å, Ø 1.7-2.4 mm and 3 Å, Ø 2.5-5.2 mm) and from Aldrich (4 Å, particle size <5 µm). For the making of 'manually crushed' molecular sieves, 4 Å mol sieves beads were pulverized in a ceramic mortar and the finely grinded material was stored under argon at 80 °C. Before use, all molecular sieves were freshly activated by heating them at high vacuum (0.05 mbar, 200 °C, 2 h), cooling at 0.05 mbar and venting of the storing flask with argon.

Standard Workup Procedure

Unless otherwise stated, the following workup procedure was employed. To quench a reaction approximately the same amount of an aqueous solution (specified in the procedures in the following section) is added at the appropriated temperature. The magnetic stir bar was removed and the reaction mixture was diluted with CH₂Cl₂ and transferred to a separation funnel. The phases were separated and the aqueous layer was extracted with CH₂Cl₂. The combined organic layers were dried over MgSO₄. The solid was removed by filtration through a borsilicate stem frit (Por.4) at reduced pressure. The solvents were removed using a Rotavapor[®] evaporator (40 °C). After purification the product was filtered through a small

³⁹⁵ Juaristi, E.; Martinez-Richa, A.; Garcia-Rivera, A.; Cruz-Sanchez, J. S. *J. Org. Chem.* **1983**, *48*, 2603-2606.

pipette stuffed with a small cotton pad using CH_2Cl_2 as solvent. The solvent was removed at reduced pressure and then non-volatile products were exposed to high vacuum.

Ozonolysis

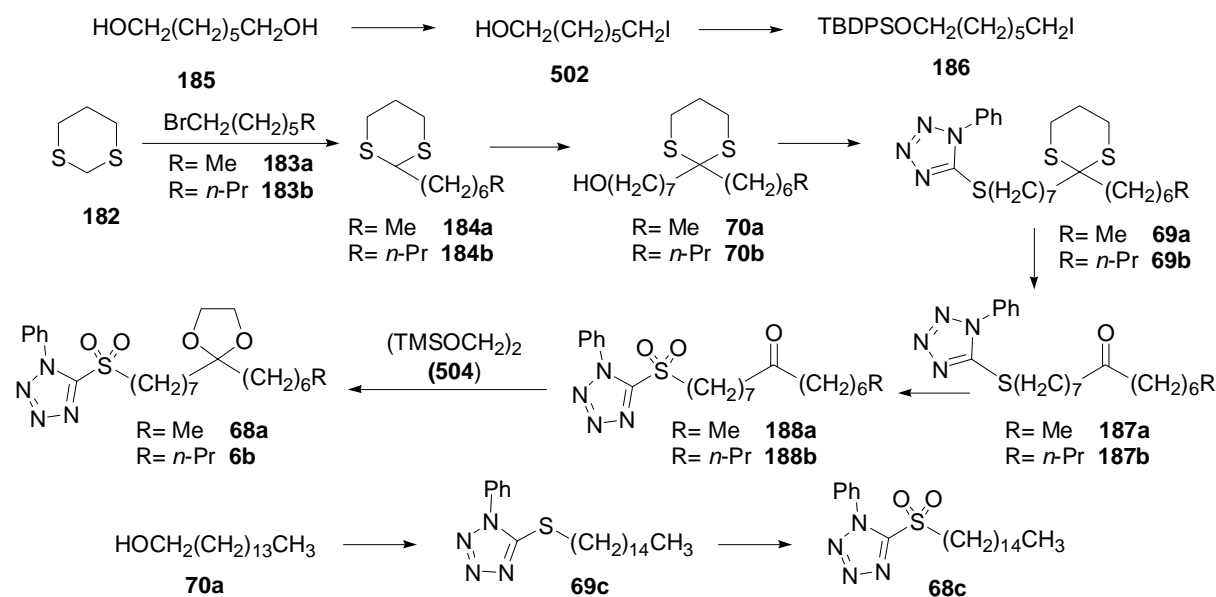
For the production of ozone a Labor Ozonisorator (SANDERS[®]) was used.

Technical Gas

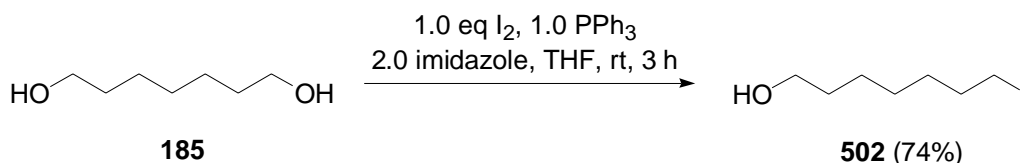
Prefilled pressure bottles (MESSER-GRIESHEIM[®]) of argon (quality: 4.8) were utilized as argon supply. The argon was additionally predried by leading it through a U-tube filled with, P_2O_5 , kieselgur[™] and CaCl_2 .

20.2 Viridifungins

20.2.1 Synthesis of the Eastern Half



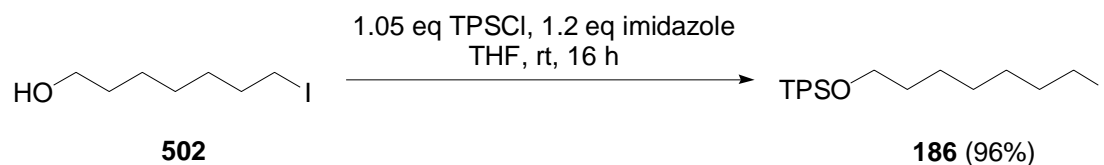
Scheme 150: Synthesis of the eastern half (68a-c).



7-Iodo-1-heptanol (502).³⁸⁸ To an ice cooled solution of 1,7-heptanediol (185) (6.0 g, 45.5 mmol, 2.5 eq), imidazole (2.5 g, 36.3 mmol, 2.0 eq) and triphenylphosphine (4.8 g, 18.2

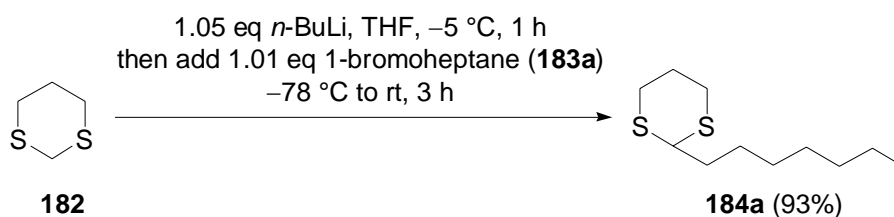
mmol, 1.0 eq) in THF (250 mL, 5 mL/mmol **185**) was added a solution of iodine (4.6 g, 18.2 mmol, 1.0 eq) in THF (45 mL, 1 mL/mmol **185**) over a period of 1 h. After additional 3 h at rt, the mixture was quenched with saturated aq Na₂S₂O₃. The aqueous layer was extracted with CH₂Cl₂ (3 × 50 mL). The combined organic phases were dried over MgSO₄ and concentrated. Flash chromatography (heptane/ethyl acetate 2/1) afforded **502** (3.3 g, 13.4 mmol, 74%) as pale yellow oil (*R_f* 0.24 heptane/ethyl acetate 1/1).

¹H NMR (300 MHz, CDCl₃) δ 3.58 (t, *J* = 6.7 Hz, 2H), 3.12 (t, *J* = 7.0 Hz, 2H), 1.76 (dt, *J* = 14.3, 7.1 Hz, 2H), 1.51 (dt, *J* = 13.6, 6.7 Hz, 2H), 1.40-1.25 (m, 6H) no OH-resonance observed; ¹³C NMR (CDCl₃, 75 MHz) δ 62.9 (CH₂), 33.4 (CH₂), 32.6 (CH₂), 30.4 (CH₂), 28.3 (CH₂), 25.5 (CH₂), 7.2 (CH₂). Anal. Calcd for C₇H₁₅IO: C, 34.73; H, 6.25; I, 52.42.



Iodide 186.³⁸⁸ To a solution of 7-iodo-1-heptanol (**502**) (3.2 g, 13.2 mmol, 1.0 eq) in THF (1.5 mL/mmol **502**) was added imidazole (1.1 g, 15.9 mmol, 1.2 eq) and *tert*-butyldiphenylchlorosilane TPSCl (3.8 g, 13.9 mmol, 1.05 eq) and stirred over night. The reaction mixture was quenched by the addition of saturated aq NaHCO₃ and the aqueous layer was extracted with CH₂Cl₂ (3 × 50 mL). The combined organic phases were dried over MgSO₄ and concentrated. Flash chromatography (heptane/ethyl acetate 20/1) afforded iodide **186** (6.0 g, 12.5 mmol, 96%) as colorless oil (*R_f* 0.41 heptane/ethyl acetate 20/1).

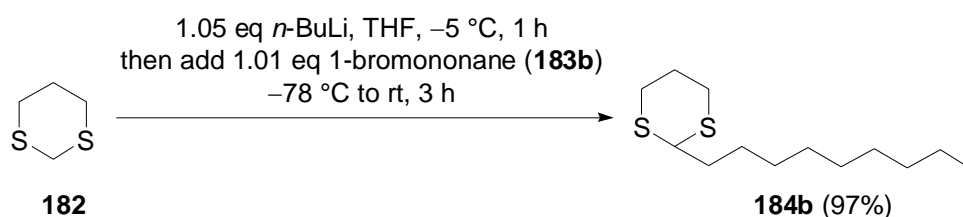
¹H NMR (300 MHz, CDCl₃) δ 7.69-7.64 (m, 4H), 7.47-7.33 (m, 6H), 3.65 (t, *J* = 6.3 Hz, 2H), 3.17 (t, *J* = 7.0 Hz, 2H), 1.82 (dt, *J* = 14.3, 7.3 Hz, 2H), 1.62-1.50 (m, 2H), 1.43-1.22 (m, 6H), 1.05 (s, 9H); ¹³C NMR (75 MHz, CDCl₃) δ 135.6 (4 × CH), 134.1 (2 × C), 129.5 (2 × CH), 127.6 (4 × CH), 63.8 (CH₂), 33.5 (CH₂), 32.4 (CH₂), 30.5 (CH₂), 28.2 (CH₂), 26.9 (3 × CH₃), 25.5 (CH₂), 19.2 (CH₂), 7.2 (CH₂); IR (in substance) ν 3070-3050, 2930-2855 cm⁻¹. Anal. Calcd for C₂₃H₃₃IOSi: C, 57.49; H, 6.92. Found: C, 57.65; H, 7.11.



Dithiane 184a.³⁸⁸ To a stirred solution of 1,3-dithiane (**182**) (0.8 g, 6.3 mmol, 1.0 eq) in THF (13 mL, 2 mL/mmol **182**) was added *n*-BuLi (2.45 M in hexanes, 2.7 mL, 6.6 mmol,

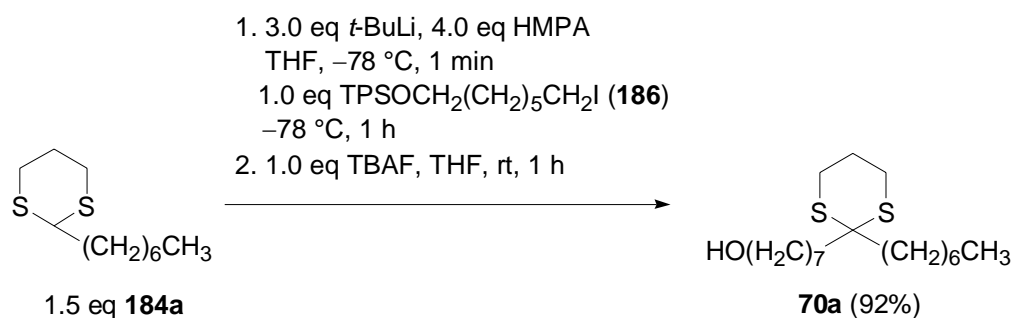
1.05 eq) at $-78\text{ }^{\circ}\text{C}$ and stirred for 1 h at $-5\text{ }^{\circ}\text{C}$. 1-Bromoheptane (**183a**) (1.0 ml, 6.4 mmol, 1.01 eq) was added at $-78\text{ }^{\circ}\text{C}$ and the reaction mixture was allowed to warm to ambient temperature over 3 h. The reaction was quenched with water (5 mL) and extracted with CH_2Cl_2 ($3 \times 25\text{ mL}$). The combined organic phases were dried over MgSO_4 and concentrated. Flash chromatography (heptane) afforded dithiane **184a** (1.3 g, 5.8 mmol, 93%) as a pale yellow oil (R_f 0.47 heptane/ethyl acetate 20/1).

^1H NMR (300 MHz, CDCl_3) δ 4.03 (t, $J = 7.0\text{ Hz}$, 1H), 2.94-2.76 (m, 4H), 2.16-1.95 (m, 1H), 1.87-1.63 (series of m, 3H), 1.53-1.42 (m, 2H), 1.32-1.20 (m, 8H), 0.87 (t, $J = 6.7\text{ Hz}$, 3H); ^{13}C NMR (75 MHz, CDCl_3) δ 47.7 (CH), 35.5 (CH_2), 31.7 (CH_2), 30.5 ($2 \times \text{CH}_2$), 29.2 (CH_2), 29.0 (CH_2), 26.6 (CH_2), 26.1 (CH_2), 22.6 (CH_2), 14.1 (CH_3); IR (in substance) ν 2925-2855 cm^{-1} . Anal. Calcd for $\text{C}_{11}\text{H}_{22}\text{S}_2$: C, 60.49; H, 10.15; S, 29.36. Found: C, 60.26; H, 10.17; S, 29.26.



Dithiane 184b.³⁸⁸ As described in the preceding paragraph, consecutive treatment of 1,3-dithiane (**182**) (3.0 g, 25.0 mmol) with $n\text{-BuLi}$ (2.36 M in hexane, 11.1 ml, 26.2 mmol) and 1-bromononane **183b** (5.3 g, 25.5 mmol) afforded the monoalkylated dithiane **184b** (6.0 g, 24.2 mmol, 97%) as a pale yellow oil (R_f 0.36 heptane/ethyl acetate 20/1).

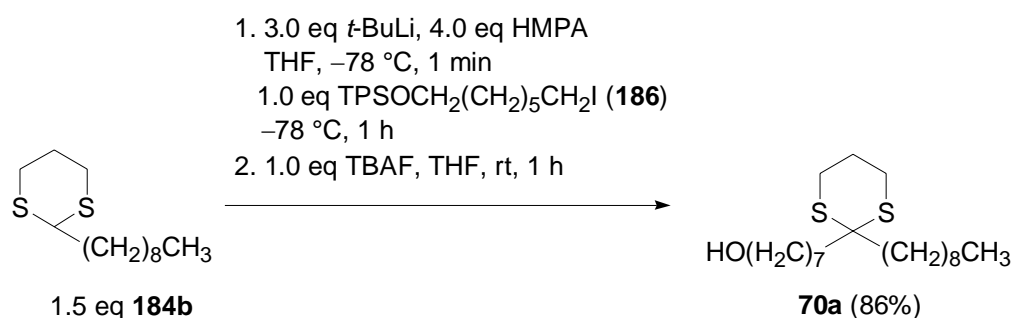
^1H NMR (300 MHz, CDCl_3) δ 4.03 (t, $J = 6.8\text{ Hz}$, 1H), 2.93-2.75 (m, 4H), 2.17-2.05 (m, 1H), 1.93-1.66 (series of m, 3H), 1.57-1.41 (m, 2H), 1.35-1.17 (m, 12H), 0.87 (t, $J = 7.0\text{ Hz}$, 3H); ^{13}C NMR (75 MHz, CDCl_3) δ 47.7 (CH), 35.5 (CH_2), 31.9 (CH_2), 30.5 ($2 \times \text{CH}_2$), 29.5 (CH_2), 29.4 (CH_2), 29.2 (CH_2), 29.2 (CH_2), 26.6 (CH_2), 26.1 (CH_2), 22.6 (CH_2), 14.1 (CH_3); IR (in substance) ν 2920-2850 cm^{-1} . Anal. Calcd for $\text{C}_{13}\text{H}_{26}\text{S}_2$: C, 63.35; H, 10.63; S, 26.02. Found: C, 63.5; H, 11.03; S, 25.97.



C₁₅-Alcohol 70a.³⁸⁸ To a stirred solution of the monoalkylated dithiane **184a** (1.3 g, 6.0 mmol, 1.5 eq) in HMPA (2.9 mL, 16 mmol, 4.0 eq) and THF (22 mL, 7.5 mL/mmol **186**) was added *t*-BuLi (1.5 M in pentane, 8.0 mL, 12.0 mmol, 3.0 eq) at -78 °C. Within 1 minute, a cooled solution (-78 °C) of iodide **186** (1.9 g, 4.0 mmol, 1.0 eq) in THF (5 mL) was added via cannula. The reaction mixture was stirred for 1 h at -78 °C and then quenched with saturated aq NH₄Cl and extracted with CH₂Cl₂ (3 × 75 mL). The combined organic phases were dried over MgSO₄ and concentrated.

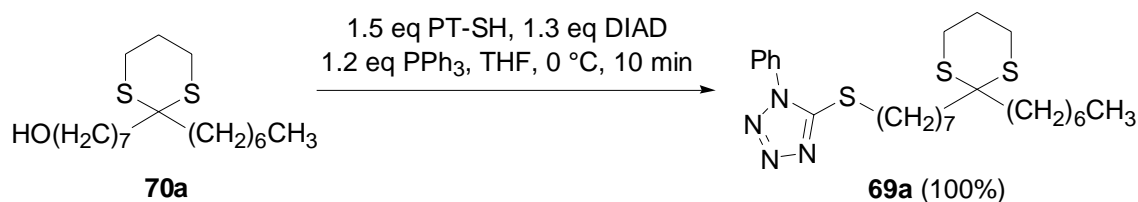
The resulting crude product was diluted with THF (15 mL, 5 mL/mmol **186**) and solid tetrabutyl ammonium fluoride TBAF (1.3 g, 4.0 mmol, 1.0 eq) was added. After stirring for 1 h at rt, the reaction was quenched with saturated aq NaHCO₃ and extracted with CH₂Cl₂ (3 × 75 mL). The combined organic phases were dried over MgSO₄ and concentrated. Flash chromatography (heptane/ethyl acetate 10/1 to 5/1) afforded alcohol **70a** (1.2 g, 3.7 mmol, 92%) as a colorless oil (*R_f* 0.52 heptane/ethyl acetate 1/1).

¹H NMR (300 MHz, CDCl₃) δ 3.63 (t, *J* = 6.5 Hz, 2H), 2.84-2.73 (m, 4H), 1.99-1.89 (m, 2H), 1.89-1.79 (m, 4H), 1.63-1.20 (series of m, 20H), 0.87 (t, *J* = 6.7 Hz, 3H) no OH-resonance observed; ¹³C NMR (75 MHz, CDCl₃) δ 63.0 (CH₂), 53.4 (C), 38.2 (2 × CH₂), 32.8 (CH₂), 31.8 (CH₂), 29.8 (2 × CH₂), 29.3 (CH₂), 29.2 (CH₂), 26.0 (2 × CH₂), 25.7 (CH₂), 25.6 (CH₂), 24.1 (CH₂), 24.0 (CH₂), 22.6 (CH₂), 14.1 (CH₃); IR (in substance) ν 3345, 2925-2855 cm⁻¹. Anal Calcd for C₁₈H₃₆OS₂: C, 65.00; H, 10.91; S, 19.28. Found: C, 65.28; H, 11.15; S, 18.95.



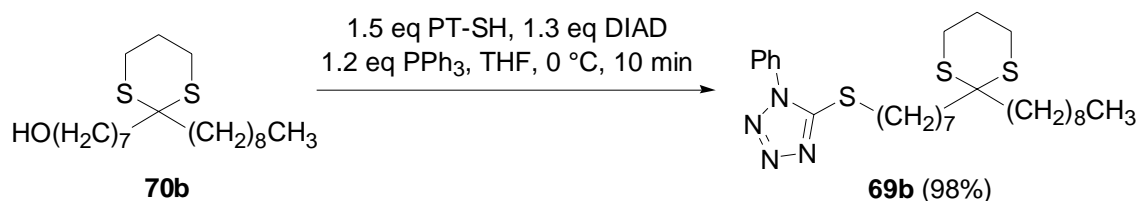
C₁₇-Alcohol 70b.³⁸⁸ As described for C₁₅-alcohol **70a**, the monoalkylated dithiane **184b** (1.1 g, 4.6 mmol) in HMPA (2.2 ml, 12.1 mmol) and THF was treated with *t*-BuLi (1.5 M in pentane, 6.0 ml, 9.0 mmol) and iodide **186** (1.46 g, 3.0 mmol). The crude product was subjected to tetrabutyl ammonium fluoride TBAF (1.0 g, 3.0 mmol). Flash chromatography (heptane/ethyl acetate 10/1 to 5/1) provided alcohol **70b** (0.9 g, 2.6 mmol, 86%) as a colorless oil (*R_f* 0.49 heptane/ethyl acetate 1/1).

^1H NMR (300 MHz, CDCl_3) δ 3.56 (dt, $J = 5.7, 5.7$ Hz, 2H), 2.74-2.66 (m, 4H), 1.90-1.80 (m, 2H), 1.79-1.70 (m, 4H), 1.53-1.09 (series of m, 24H), 0.79 (t, $J = 6.7$ Hz, 3H) no HO-resonance observed; ^{13}C NMR (75 MHz, CDCl_3) δ 63.0 (CH_2), 53.4 (C), 38.2 (CH_2), 32.8 (CH_2), 31.9 (CH_2), 29.81 (CH_2), 29.78 (CH_2), 29.54 (CH_2), 29.47 (CH_2), 29.3 (CH_2), 26.0 (CH_2), 25.7 (CH_2), 25.6 (CH_2), 24.1 (CH_2), 24.0 (CH_2), 22.6 (CH_2), 14.1 (CH_3) (several overlapping signals between 38.2 and 22.7, total number (CH_2): 18); IR (in substance) ν 3345, 2925-2850 cm^{-1} . Anal Calcd for $\text{C}_{20}\text{H}_{40}\text{OS}_2$: C, 66.60; H, 11.18; S, 17.78. Found: C, 66.26; H, 11.38; S, 17.58.



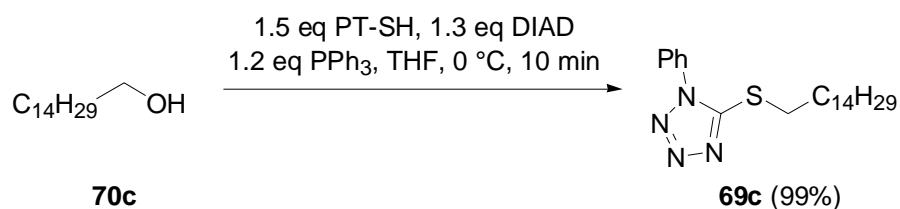
Phenyl-1H-Tetrazole 69a.³⁸⁸ To an ice-cooled solution of the alcohol **70a** (1.4 g, 4.3 mmol, 1.0 eq) in THF (4 mL, 1 mL/mmol **70a**) was added PPh_3 (1.4 g, 5.2 mmol, 1.2 equiv), 1-phenyl-1H-tetrazole-5-thiol PT-SH (1.3 g, 6.5 mmol, 1.5 eq) and diisopropyl azodicarboxylate DIAD (1.1 g, 5.6 mmol, 1.3 eq). After stirring for 10 min, saturated aq NaHCO_3 (5 mL) was added and the aqueous layer was extracted with CH_2Cl_2 (3×20 mL). The combined organic phases were dried over MgSO_4 and concentrated. Flash chromatography (heptane/ethyl acetate 10/1) afforded tetrazole **69a** (2.1 g, 4.3 mmol, 100%) as a yellow oil (R_f 0.33 heptane/ethyl acetate 1/1).

^1H NMR (300 MHz, CDCl_3) δ 7.63-7.50 (m, 5H), 3.39 (t, $J = 7.5$ Hz, 2H), 2.88-2.75 (m, 4H), 1.99-1.89 (m, 2H), 1.88-1.78 (m, 6H), 1.67-1.17 (series of m, 18H), 0.87 (t, $J = 7.0$ Hz, 3H); ^{13}C NMR (75 MHz, CDCl_3) δ 154.5 (C), 133.8 (C), 130.1 (CH), 129.8 ($2 \times \text{CH}$), 123.9 ($2 \times \text{CH}$), 53.3 (C), 38.2 (CH_2), 38.1 (CH_2), 33.3 (CH_2), 31.8 (CH_2), 29.8 (CH_2), 29.6 (CH_2), 29.2 (CH_2), 29.1 (CH_2), 29.0 (CH_2), 28.9 (CH_2), 28.6 (CH_2), 26.0 (CH_2), 25.6 (CH_2), 24.1 (CH_2), 24.0 (CH_2), 22.6 (CH_2), 14.1 (CH_3); IR (in substance) ν 3055, 2925-2855 cm^{-1} . Anal. Calcd for $\text{C}_{25}\text{H}_{40}\text{N}_4\text{S}_3$: C, 60.93; H, 8.18; N, 11.37; S, 19.52. Found: C, 61.15; H, 8.40; N, 11.63; S, 19.67.



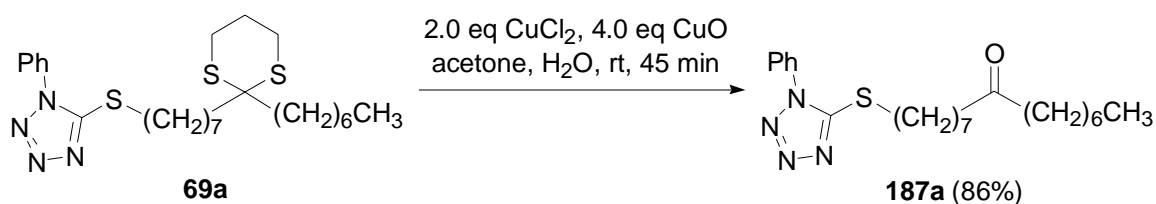
Phenyl-1*H*-Tetrazole 69b.³⁸⁸ As described for tetrazole **69a**, alcohol **70b** (0.9 g, 2.5 mmol) was treated with PPh₃ (0.8 g, 3.0 mmol), 1-phenyl-1*H*-tetrazole-5-thiol PT-SH (0.7 g, 3.8 mmol) and diisopropylazodicarboxylate DIAD (0.7 g, 3.3 mmol). Flash chromatography (heptane/ethyl acetate 5/1) provided the tetrazole **69b** (1.3 g, 2.5 mmol, 98%) as a yellow oil (*R_f* 0.53 heptane/ethyl acetate 1/1).

¹H NMR (300 MHz, CDCl₃) δ 7.60-7.50 (m, 5H), 3.38 (t, *J* = 7.3 Hz, 2H), 2.83-2.73 (m, 4H), 1.98-1.88 (m, 2H), 1.87-1.76 (m, 6H), 1.52-1.18 (series of m, 22H), 0.87 (t, *J* = 6.7 Hz, 3H); ¹³C NMR (CDCl₃, 75 MHz) δ 154.4 (C), 142.6 (C), 130.0 (CH), 129.7 (2 × CH), 123.9 (2 × CH), 53.4 (C), 38.3 (CH₂), 38.2 (CH₂), 33.3 (CH₂), 31.9 (CH₂), 29.8 (CH₂), 29.6 (CH₂), 29.53 (CH₂), 29.47 (CH₂), 29.3 (CH₂), 29.1 (CH₂), 28.9 (CH₂), 28.6 (CH₂), 26.0 (2 × CH₂), 25.6 (CH₂), 24.1 (CH₂), 24.0 (CH₂), 22.6 (CH₂), 14.1 (CH₃); IR (in substance) ν 2925-2850 cm⁻¹. Anal. Calcd for C₂₇H₄₄N₄S₃: C, 62.26; H, 8.51; N, 10.76; S, 18.47. Found: C, 62.32; H, 8.59; N, 10.96; S, 18.45.



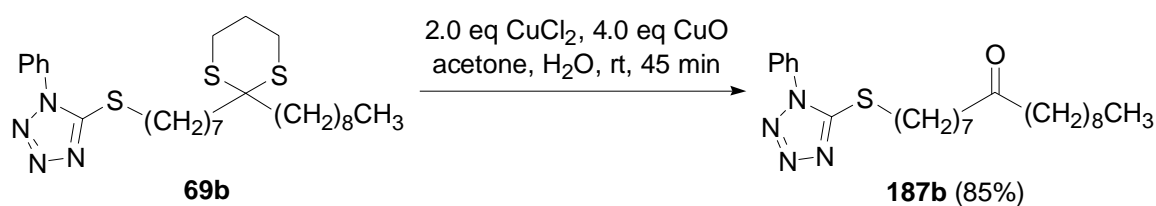
Phenyl-1*H*-Tetrazole 69c.³⁸⁸ As described for tetrazole **69a**, pentadecanol **70c** (0.9 g, 4.0 mmol) was treated with PPh₃ (1.3 g, 4.8 mmol), 1-phenyl-1*H*-tetrazole-5-thiol PT-SH (1.1 g, 6.0 mmol) and diisopropyl azodicarboxylate DIAD (1.1 g, 5.2 mmol, 1.3 eq). Flash chromatography (heptane/ethyl acetate 5/1) afforded the corresponding phenyl-1*H*-tetrazole **69c** (1.6 g, 4.0 mmol, 99%) as a white solid (*R_f* 0.70 heptane/ethyl acetate 1/1).

¹H NMR (300 MHz, CDCl₃) δ 7.61-7.51 (m, 5H), 3.38 (t, *J* = 7.3 Hz, 2H), 1.83 (td, *J* = 15.2, 7.6 Hz, 2H), 1.48 – 1.37 (m, 2H), 1.36-1.19 (m, 22H), 0.87 (t, *J* = 7.0 Hz, 3H); ¹³C NMR (75 MHz, CDCl₃) δ 154.5 (C), 133.9 (C), 130.0 (CH), 129.7 (2 × CH), 123.9 (2 × CH), 33.4 (CH₂), 31.9 (CH₂), 29.59 (CH₂), 29.56 (CH₂), 29.5 (CH₂), 29.4 (CH₂), 29.3 (CH₂), 29.1 (CH₂), 29.0 (CH₂), 28.6 (CH₂), 22.6 (CH₂) (several overlapping signals between 33.5 and 22.6, total number (CH₂): 14), 14.0 (CH₃); IR (in substance) ν 2970-2850 cm⁻¹. Anal. Calcd for C₂₂H₃₆N₄S: C, 67.69; H, 9.34; N, 14.48; S, 8.39. Found: C, 67.85; H, 9.26; N, 14.47; S, 8.54.



Ketone 187a.³⁸⁸ To a solution of 1,3-dithiane **69a** (1.0 g, 2.0 mmol, 1.0 eq) in acetone/water (99/1, 8 mL/mmol **69a**) was added CuCl₂ (0.5 g, 4.1 mmol, 2.0 eq) and CuO (0.6 g, 8.1 mmol, 4.0 eq). The mixture was stirred at rt for 45 min and filtered through a Celite pad. The pad was washed with Et₂O and the combined organic phases were concentrated under reduced pressure. The residue was dissolved in CH₂Cl₂ (75 mL) and extracted with saturated aq NaHCO₃ (10 mL). The aqueous layer was extracted with CH₂Cl₂ (3 × 15 mL) and the combined organic phases were dried over MgSO₄ and concentrated. Flash chromatography (heptane/ethyl acetate 10/1) afforded the corresponding ketone **187a** (0.7 g, 1.7 mmol, 86%) as pale yellow oil (*R_f* 0.44 heptane/ethyl acetate 1/1).

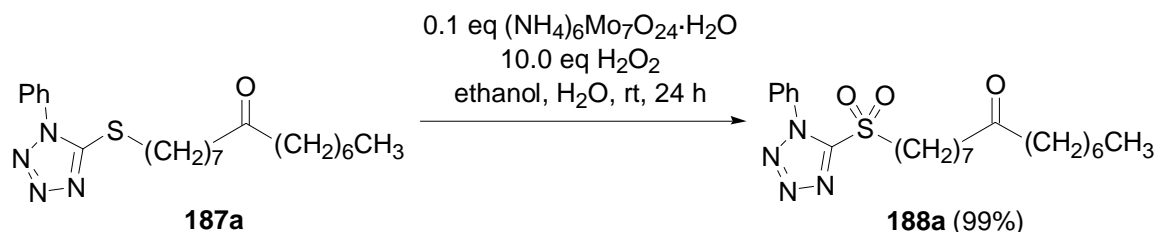
¹H NMR (300 MHz, CDCl₃) δ 7.62-7.48 (m, 5H), 3.38 (t, *J* = 7.3 Hz, 2H), 2.37 (t, *J* = 7.4 Hz, 2H), 2.36 (t, *J* = 7.4 Hz, 2H), 1.83 (td, *J* = 14.8, 7.4 Hz, 2H), 1.64-1.18 (series of m, 18H), 0.86 (t, *J* = 6.8 Hz, 3H); ¹³C NMR (75 MHz, CDCl₃) δ 211.5 (C), 154.5 (C), 133.8 (C), 130.1 (CH), 129.8 (2 × CH), 123.9 (2 × CH), 42.9 (CH₂), 42.6 (CH₂), 33.3 (CH₂), 31.7 (CH₂), 29.2 (CH₂), 29.1 (2 × CH₂), 29.0 (CH₂), 28.8 (CH₂), 28.4 (CH₂), 23.9 (CH₂), 23.6 (CH₂), 22.6 (CH₂), 14.0 (CH₃); IR (in substance) ν 2930-2855, 1710 cm⁻¹. Anal. Calcd for C₂₂H₃₄N₄OS: C, 65.63; H, 8.51; N, 13.92; S, 7.96. Found: C, 65.60; H, 8.40; N, 13.44; S, 8.16.



Ketone 187b.³⁸⁸ As described for the synthesis of ketone **187a** in the preceding paragraph, 1,3-dithiane **69b** (1.2 g, 2.4 mmol) was treated with CuCl₂ (0.6 g, 4.8 mmol) and CuO (0.8 g, 9.2 mmol). Flash chromatography (heptane/ethyl acetate 10/1) provided the ketone **187b** (0.9 g, 2.0 mmol, 85%) as pale yellow oil (*R_f* 0.36 heptane/ethyl acetate 1/1).

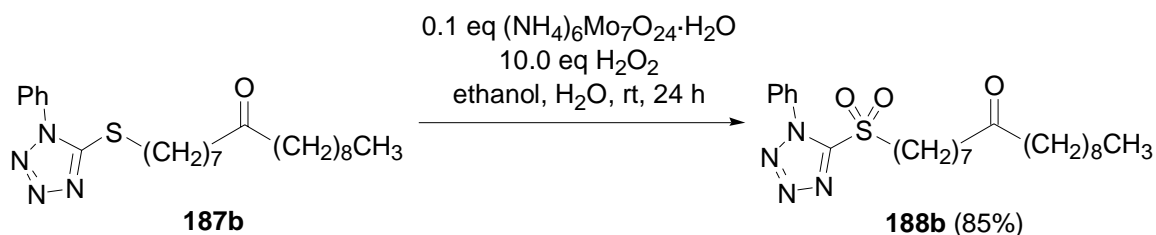
¹H NMR (300 MHz, CDCl₃) δ 7.60-7.50 (m, 5H), 3.37 (t, *J* = 7.3 Hz, 2H), 2.37 (t, *J* = 7.3 Hz, 2H), 2.36 (t, *J* = 7.4 Hz, 2H), 1.83 (td, *J* = 15.0, 7.6 Hz, 2H), 1.60-1.19 (series of m, 22H), 0.86 (t, *J* = 6.7 Hz, 3H); ¹³C NMR (75 MHz, CDCl₃) δ 211.5 (C), 154.5 (C), 133.8 (C), 130.1 (CH), 129.8 (2 × CH), 123.9 (2 × CH), 42.6 (CH₂), 42.7 (CH₂), 33.3 (CH₂), 31.7 (CH₂), 29.2 (2 × CH₂), 29.1 (2 × CH₂), 29.0 (2 × CH₂), 28.8 (CH₂), 28.4 (CH₂), 23.9 (CH₂), 23.6 (CH₂),

22.6 (CH₂), 14.0 (CH₃); IR (in substance) ν 2915-2850, 1700 cm⁻¹. Anal. Calcd for C₂₄H₃₈N₄OS: C, 66.94; H, 8.89; N, 13.01; S, 7.45. Found: C, 66.99; H, 8.82; N, 13.06; S, 7.25.



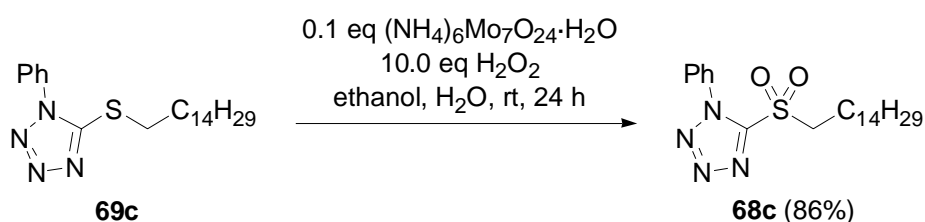
Sulfone 188a.³⁸⁸ To an ice-cooled solution of the ketone **187a** (1.6 g, 4.1 mmol, 1.0 eq) in ethanol (40 mL, 10 mL/mmol **187a**) a solution of (NH₄)₆Mo₇O₂₄·H₂O (0.5 g, 0.4 mmol, 0.1 eq) in hydrogen peroxide (30% in H₂O, 4.5 mL, 41 mmol, 10.0 eq) was added. The reaction mixture was stirred at ambient temperature for 24 h, then added to brine (30 mL) and extracted with CH₂Cl₂ (3 × 30 mL). The combined organic phases were dried over MgSO₄ and concentrated. Flash chromatography (heptane/ethyl acetate 3/1) afforded the sulfone **188a** (1.7 g, 4.1 mmol, 99%) as pale yellow oil (*R_f* 0.29 heptane/ethyl acetate 1/1).

¹H NMR (300 MHz, CDCl₃) δ 7.72-7.54 (m, 5H), 3.76-3.66 (m, 2H), 2.35 (t, *J* = 7.4 Hz, 2H), 2.33 (t, *J* = 7.4 Hz, 2H), 2.00-1.88 (m, 2H), 1.61-1.20 (series of m, 18H), 0.87 (t, *J* = 6.7 Hz, 3H); ¹³C NMR (75 MHz, CDCl₃) δ 211.3 (C), 153.5 (C), 133.0 (C), 131.5 (CH), 129.7 (2 × CH), 125.1 (2 × CH), 56.0 (CH₂), 42.9 (CH₂), 42.5 (CH₂), 31.7 (CH₂), 29.2 (CH₂), 29.1 (CH₂), 28.8 (CH₂), 28.7 (CH₂), 27.9 (CH₂), 23.9 (CH₂), 23.5 (CH₂), 22.6 (CH₂), 21.9 (CH₂), 14.0 (CH₃); IR (in substance) ν 2925-2855, 1710 cm⁻¹. Anal. Calcd for C₂₂H₃₄N₄O₃S: C, 60.80; H, 7.89; N, 12.89; S, 7.38. Found: C, 60.92; H, 7.91; N, 12.91; S, 7.10.



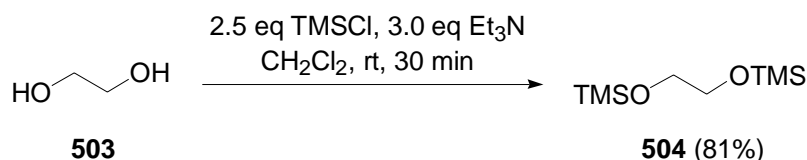
Sulfone 188b.³⁸⁸ According to the procedure for the preparation of sulfone **188a**, the ketone **187b** (0.8 g, 1.9 mmol) was treated with (NH₄)₆Mo₇O₂₄·H₂O (0.25 g, 0.2 mmol) in hydrogen peroxide (30% in H₂O, 2.30 mL, 20.3 mmol). Flash chromatography (heptane/ethyl acetate 5/1) afforded the corresponding sulfone **188b** (0.8 g, 1.7 mmol, 85%) as pale yellow oil (*R_f* 0.56 heptane/ethyl acetate 1/1).

^1H NMR (300 MHz, CDCl_3) δ 7.71-7.55 (m, 5H), 3.75-3.67 (m, 2H), 2.38 (t, $J = 7.3$ Hz, 2H), 2.37 (t, $J = 7.5$ Hz, 2H), 2.00-1.88 (m, 2H), 1.61-1.19 (series of m, 22H), 0.86 (t, $J = 6.8$ Hz, 3H); ^{13}C NMR (75 MHz, CDCl_3) δ 211.2 (C), 153.5 (C), 133.1 (C), 131.4 (CH), 129.7 (2 \times CH), 125.1 (2 \times CH), 56.0 (CH_2), 42.9 (CH_2), 42.5 (CH_2), 31.8 (CH_2), 29.4 (2 \times CH_2), 29.2 (2 \times CH_2), 28.8 (CH_2), 28.7 (CH_2), 27.9 (CH_2), 23.9 (CH_2), 23.5 (CH_2), 22.6 (CH_2), 21.9 (CH_2), 14.0 (CH_3); IR (in substance) ν 2920-2850, 1700 cm^{-1} . Anal. Calcd for $\text{C}_{24}\text{H}_{38}\text{N}_4\text{O}_3\text{S}$: C, 62.31; H, 8.28; N, 12.11; S, 6.93. Found: C, 62.46; H, 8.32; N, 12.06; S, 7.11.



Sulfone 68c.³⁸⁸ As described for the synthesis of sulfone **188a**, tetrazole **69c** (1.6 g, 4.0 mmol) was treated with $(\text{NH}_4)_6\text{Mo}_7\text{O}_{24}\cdot\text{H}_2\text{O}$ (0.49 g, 0.4 mmol) and 30 % aq hydrogen peroxide (4.4 mL, 40.0 mmol) to provide sulfone **68c** (1.4 g, 3.4 mmol, 86%) as a white solid (R_f 0.68 heptane/ethyl acetate 1/1).

^1H NMR (300 MHz, CDCl_3) δ 7.71-7.57 (m, 5H), 3.76-3.69 (m, 2H), 2.00-1.88 (m, 2H), 1.54-1.43 (m, 2H), 1.39-1.20 (m, 22H), 0.87 (t, $J = 6.7$ Hz, 3H); ^{13}C NMR (75 MHz, CDCl_3) δ 153.6 (C), 133.1 (C), 131.4 (CH), 129.7 (2 \times CH), 125.1 (2 \times CH), 56.0 (CH_2), 31.9 (CH_2), 29.7 (CH_2), 29.62 (CH_2), 29.59 (CH_2), 29.5 (CH_2), 29.4 (CH_2), 29.3 (CH_2), 29.2 (CH_2), 28.9 (CH_2), 28.1 (CH_2), 22.6 (CH_2), 21.9 (CH_2), 14.1 (CH_3) (several overlapping signals between 31.9 and 22.0, total number (CH_2): 14); IR (in substance) ν 2920-2850 cm^{-1} . Anal. Calcd for $\text{C}_{22}\text{H}_{36}\text{N}_4\text{O}_2\text{S}$: C, 62.82; H, 8.63; N, 13.32; S, 7.62. Found: C, 63.12; H, 8.71; N, 13.43; S, 7.61.

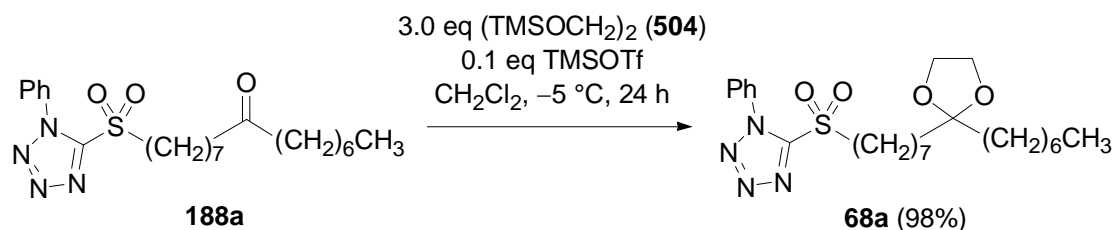


Protected Diol 504.³⁹⁶ To a solution of 1,2-ethanediol (**503**) (1.8 g, 1.7 mL, 30.0 mmol, 1.0 eq) in CH_2Cl_2 (5 mL/mmol **502**) was added triethylamine (9.1 g, 8.9 mL, 90.0 mmol, 3.0 eq) and trimethylchlorosilane TMSCl (8.2 g, 9.5 mL, 75.0 mmol, 2.5 eq). The reaction mixture was stirred for 30 min at rt. The precipitate was then removed by filtration and

³⁹⁶ Compound **504** is commercially available from Aldrich. For an analogue synthesis, see: Mash, E. A.; Hemperly, S. B. *J. Org. Chem.* **1990**, *55*, 2055-2060.

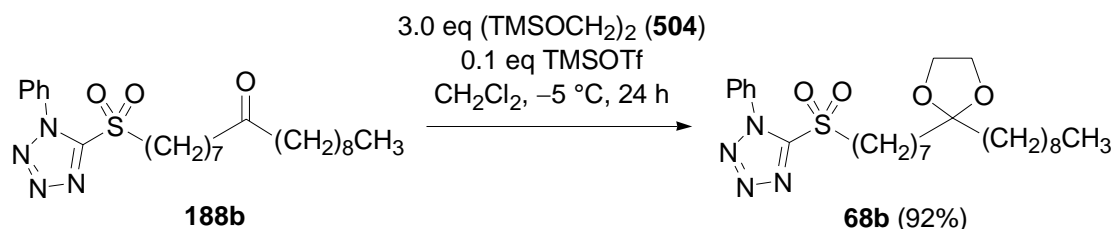
washed with diethylether. The solvents were removed under reduced pressure to afford the protected diol **502** (5.01 g, 24.3 mmol, 81%) which was used without further purification.

^1H NMR (300 MHz, CDCl_3) δ 3.52 (s, 4H), 0.01 (s, 18H). Anal. Calcd for $\text{C}_8\text{H}_{22}\text{O}_2\text{Si}_2$: C, 46.55; H, 10.74.



Ketale 68a.³⁸⁸ A solution of the sulfone **188a** (1.7 g, 4.0 mmol, 1.0 eq) and 1,2-bis-trimethylsilyloxyethane (**504**) (2.5 g, 12.0 mmol, 3.0 eq) in CH_2Cl_2 (8 mL, 2 mL/mmol **188a**) was cooled to $-5 \text{ }^\circ\text{C}$ and treated with TMSOTf (88 mg, 0.4 mmol, 0.1 eq). The mixture was stirred for 24 h at $-5 \text{ }^\circ\text{C}$. The reaction was then quenched by the addition of pyridine (4 mL, 1 mL/mmol **188a**) and added to saturated aq NaHCO_3 . The aqueous layer was extracted with CH_2Cl_2 ($3 \times 25 \text{ mL}$). The combined organic phases were dried over MgSO_4 and concentrated. Flash chromatography (heptane/ethyl acetate 5/1) provided ketale **68a** (1.9 g, 4.0 mmol, 98%) as a pale yellow oil (R_f 0.29 heptane/ethyl acetate 1/1).³⁹⁷

^1H NMR (300 MHz, CDCl_3) δ 7.72-7.58 (m, 5H), 3.91 (s, 4H), 3.76-3.67 (m, 2H), 2.00-1.88 (m, 2H), 1.62-1.20 (series of m, 22H), 0.88 (brt, $J = 6.8 \text{ Hz}$, 3H); ^{13}C NMR (75 MHz, CDCl_3) δ 153.5 (C), 133.0 (C), 131.4 (CH), 129.7 ($2 \times \text{CH}$), 125.0 ($2 \times \text{CH}$), 111.7 (C), 64.9 ($2 \times \text{CH}_2$), 56.0 (CH_2), 37.2 (CH_2), 37.0 (CH_2), 31.8 (CH_2), 29.9 (CH_2), 29.4 (CH_2), 29.3 (CH_2), 28.9 (CH_2), 28.0 (CH_2), 23.9 (CH_2), 23.6 (CH_2), 22.6 (CH_2), 21.9 (CH_2), 14.1 (CH_3); IR (in substance) ν 2925-2855 cm^{-1} . Anal. Calcd for $\text{C}_{24}\text{H}_{38}\text{N}_4\text{O}_4\text{S}$: C, 60.22; H, 8.00; N, 11.71; S, 6.70. Found: C, 60.27; H, 8.13; N, 11.83; S, 6.38.



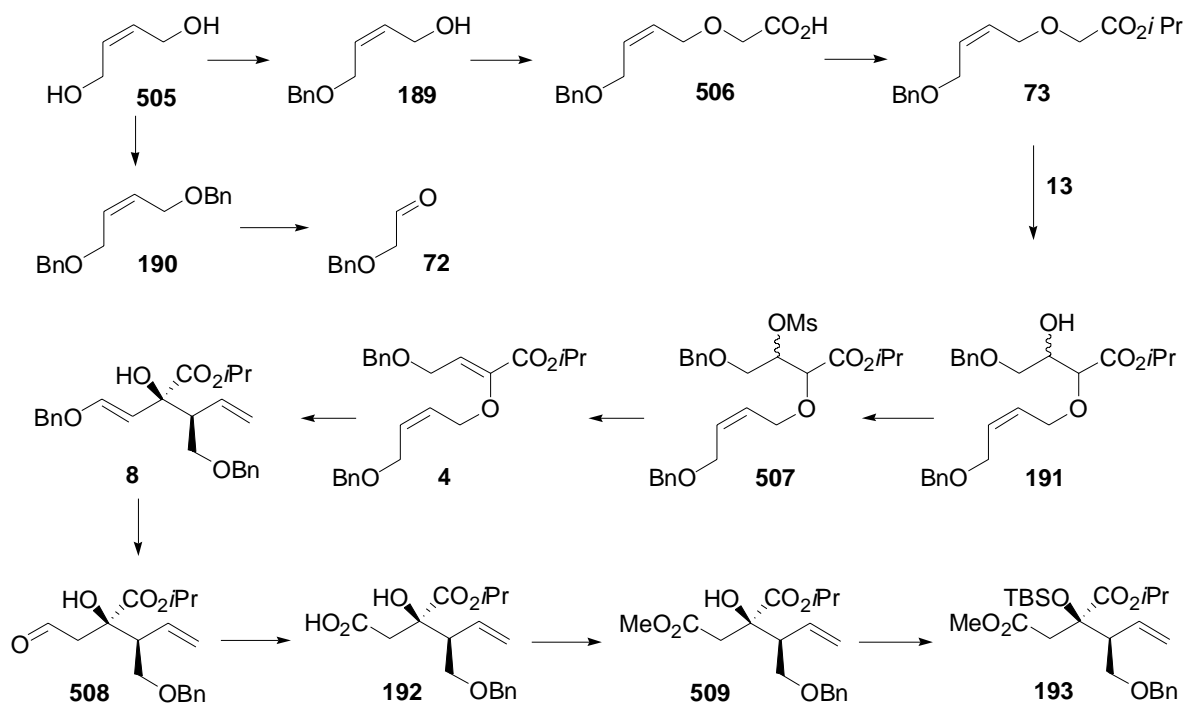
Ketale 68b.³⁸⁸ As described in the preceding paragraph, sulfone **188b** (0.7 g, 1.4 mmol) was treated with 1,2-bis-trimethylsilyloxy-ethane (**504**) (0.9 g, 4.3 mmol) and TMSOTf (32

³⁹⁷ CDCl_3 used for NMR probe preparation should be filtered through a plug of basic Alox to prevent cleavage of the ketal protecting group.

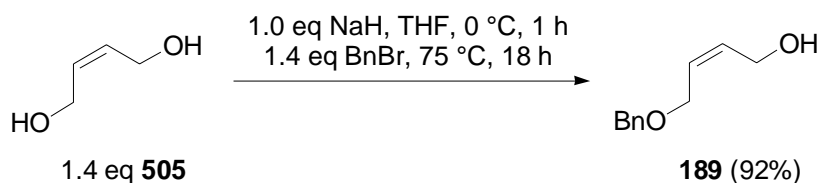
mg, 0.14 mmol). Flash chromatography (heptane/ethyl acetate 5/1) afforded ketale **68b** (0.7 g, 1.3 mmol, 92%) as pale yellow oil (R_f 0.61 heptane/ethyl acetate 1/1).³⁹⁷

^1H NMR (300 MHz, CDCl_3) δ 7.69-7.57 (m, 5H), 3.91 (s, 4H), 3.73-3.70 (m, 2H), 1.97-1.91 (m, 2H), 1.59-1.22 (series of m, 26H), 0.86 (br t, $J = 6.9$ Hz, 3H); ^{13}C NMR (75 MHz, CDCl_3) δ 153.5 (C), 133.1 (C), 131.4 (CH), 129.7 (2 \times CH), 125.1 (2 \times CH), 111.8 (C), 64.9 (2 \times CH_2), 56.0 (CH_2), 37.2 (CH_2), 37.0 (CH_2), 31.9 (CH_2), 29.9 (CH_2), 29.6 (CH_2), 29.5 (CH_2), 29.4 (CH_2), 29.3 (CH_2), 28.8 (CH_2), 28.0 (CH_2), 23.9 (CH_2), 23.6 (CH_2), 22.6 (CH_2), 21.9 (CH_2), 14.1 (CH_3); IR (in substance) ν 2925-2855, 1710 cm^{-1} . Anal. Calcd for $\text{C}_{26}\text{H}_{42}\text{N}_4\text{O}_4\text{S}$: C, 61.63; H, 8.35; N, 11.06; S, 6.33. Found: C, 61.85; H, 8.15; N, 11.27; S, 6.39.

20.2.2 Synthesis of the Western Half

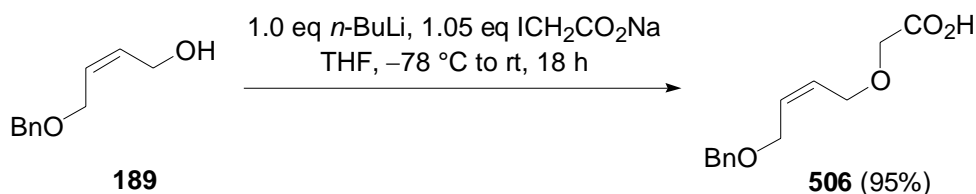


Scheme 151: Synthesis of **193** – the immediate precursor of the western half **67**.



Benzyl Ether 189.³⁹⁸ To a stirred solution of *cis*-butene-1,4-diole (**505**) (19.8 g, 225 mmol, 1.4 eq) in THF (45 mL, 0.2 mL/mmol of the diol) was carefully added sodium hydride (5.8 g, 146 mmol, 1.0 eq) at 0 °C. After stirring for 1 h at rt benzyl bromide (25.1 mL, 209 mmol, 1.4 eq) was added and the resulting mixture was stirred over night at 75 °C. The reaction was quenched at ambient temperature with saturated aq NH₄Cl and extracted with CH₂Cl₂ (3 × 50 mL). The combined organic phases were dried over MgSO₄ and concentrated. Flash chromatography (heptane/ethyl acetate 10/1 to 5/1 to 1/1) afforded the protected diol **189** (12.3 g, 69.2 mmol, 92%) as colorless oil (*R_f* 0.21 heptane/ethyl acetate 1/1). Small amounts of dibenzyl ether **190** (*R_f* 0.85 heptane/ethyl acetate 1/1) that are formed as side product of the monoprotection may be isolated as well.

¹H NMR (300 MHz, CDCl₃) δ 7.36-7.27 (m, 5H), 5.87-5.67 (m, 2H), 4.53 (s, 2H), 4.18 (d, *J* = 5.88 Hz, 2H), 4.09 (d, *J* = 5.63 Hz, 2H); ¹³C NMR (75 MHz, CDCl₃) δ 137.9 (C), 132.3 (CH), 128.5 (2 × CH), 128.4 (CH), 127.84 (2 × CH), 127.80 (CH), 72.5 (CH₂), 65.7 (CH₂), 58.8 (CH₂). Anal. Calcd for C₁₁H₁₄O₂: C, 74.13; H, 7.92.

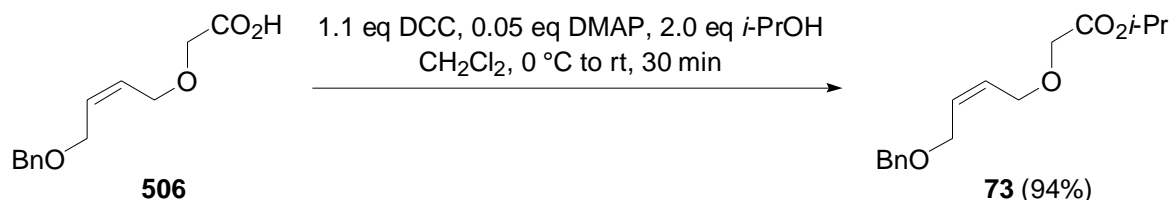


Acid 506.³⁸⁸ To a stirred solution of (*Z*)-4-benzyloxybut-2-en-1-ol **189** (11.1 g, 62.2 mmol, 1.0 eq) in THF (62 mL, 1 mL/mmol) was added *n*-BuLi (2.4 M in hexane, 25.9 mL, 62.2 mmol, 1.0 eq) at -78 °C followed by the addition of solid iodoacetic acid sodium salt (13.6 g, 65.3 mmol, 1.05 equiv). The cooling bath was removed and the suspension was stirred over night. The reaction was then quenched by the addition of aq 1 N KOH (90 mL). The phases were separated and the organic phase was extracted twice with aq 1 N KOH (30 mL). The aqueous phase was acidified by the addition of concd HCl (pH < 4) and extracted with CH₂Cl₂ (3 × 100 mL). The combined organic phases were dried over MgSO₄ and the solvent was removed under reduced pressure. Purification by kugelrohr distillation (150 °C, 0.1 mbar) afforded (*Z*)-(4-benzyloxybut-2-enyloxy)acetic acid **506** (14.0 g, 59.3 mmol, 95%) as brown oil.

¹H NMR (300 MHz, CDCl₃) δ 8.95 (br s, 1H), 7.39-7.28 (m, 5H), 5.91-5.80 (m, 1H), 5.80-5.70 (m, 1 H), 4.52 (s, 2H), 4.17 (d, *J* = 5.8 Hz, 2H), 4.09 (d, *J* = 4.9 Hz, 2H), 4.09 (s, 2H);

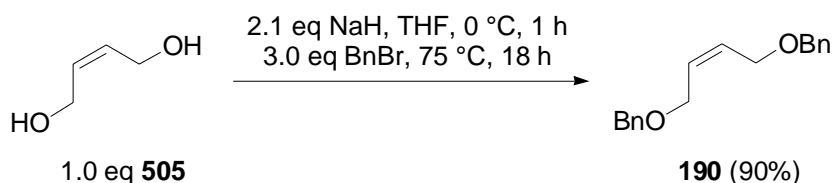
³⁹⁸ Compound **189** is commercially available from Aldrich. For an analogue synthesis, see: Schmidt, B.; Pohler, M.; Costisella, B. *Tetrahedron* **2002**, *58*, 7951-7958.

^{13}C NMR (75 MHz, CDCl_3) δ 173.9 (C), 137.9 (C), 130.7 (CH), 128.4 ($2 \times \text{CH}$), 127.1 (CH), 127.81 ($2 \times \text{CH}$), 127.76 (CH), 72.4 (CH_2), 67.1 (CH_2), 66.8 (CH_2), 65.5 (CH_2); IR (in substance) ν 3250-3030, 2860, 1685 cm^{-1} . Anal. Calcd for $\text{C}_{13}\text{H}_{16}\text{O}_4$: C, 66.09; H, 6.83. Found: C, 66.27, H, 6.95.



Ester 73.^{399,388} To an ice cooled solution of the acid (7.1 g, 30.1 mmol, 1.0 equiv) in CH_2Cl_2 (2 ml/mmol of the acid) at 0 $^\circ\text{C}$ was added DMAP (0.18 g, 1.5 mmol, 0.05 equiv), DCC (6.8 g, 33.1 mmol, 1.1 equiv) and the *iso*-propanol (4.6 ml, 60.2 mmol, 2.0 equiv). The resulting suspension was stirred for 30 min at ambient temperature. The precipitate was then removed by filtration, washed with CH_2Cl_2 and the solvent was evaporated under reduced pressure. Flash chromatography (heptane/ethyl acetate 5/1) afforded the ester **73** (7.9 g, 28.4 mmol, 94%) as yellow oil (R_f 0.65 heptane/ethyl acetate 1/1).

^1H NMR (300 MHz, CDCl_3) δ 7.36-7.23 (m, 5H), 5.88-5.70 (m, 2H), 5.10 (sept, $J = 6.3$ Hz, 1H), 4.50 (s, 2H), 4.15 (d, $J = 5.7$ Hz, 2H), 4.09 (d, $J = 5.6$ Hz, 2H), 4.01 (s, 2H), 1.25 (d, $J = 6.2$ Hz, 6H); ^{13}C NMR (75 MHz, CDCl_3) δ 169.8 (C), 138.1 (C), 130.3 (CH), 128.6 (CH), 128.4 ($2 \times \text{CH}$), 127.8 ($2 \times \text{CH}$), 127.7 (CH), 72.3 (CH_2), 68.5 (CH_2), 67.5 (CH_2), 66.9 (CH), 65.7 (CH_2), 21.8 ($2 \times \text{CH}_3$); IR (in substance) ν 2980-2860, 1750 cm^{-1} . Anal. Calcd for $\text{C}_{16}\text{H}_{22}\text{O}_4$: C, 69.04; H, 7.97. Found: C, 69.06; H, 8.19.



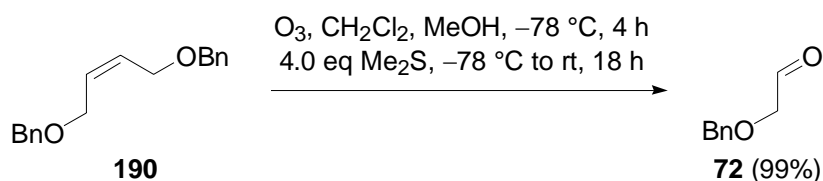
Dibenzyl Ether 190.⁴⁰⁰ According to the procedure for the preparation of **189**, *Z*-butene-1,4-diol **505** (6.13 g, 69.6 mmol, 1.0 eq) was treated with sodium hydride (5.84 g, 146.1 mmol, 2.1 eq) and benzyl bromide (25.1 ml, 208.7 mmol, 3.0 eq). Flash chromatography (heptane/ethyl acetate 20/1 to 5/1) afforded the dibenzyl ether **190** (16.81 g, 62.6 mmol, 90%) as a colorless oil (R_f 0.85 heptane/ethyl acetate 1/1). Small amounts of benzyl ether **189** (R_f

³⁹⁹ Prepared analogue to: Hiersemann, M. *Synthesis* **2000**, 1279-1290.

⁴⁰⁰ Compound **190** is commercially available, e.g. from Aldrich. For an analogue synthesis, see reference 398.

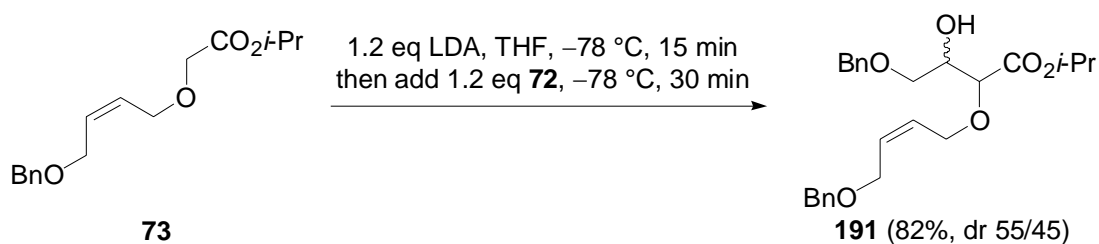
0.21 heptane/ethyl acetate 1/1) that are formed as side product of the dibenylation may be isolated as well.

^1H NMR (300 MHz, CDCl_3) δ 7.36-7.27 (m, 10H), 5.81-5.75 (m, 2H), 4.49 (s, 4H), 4.06 (d, $J = 4.7$ Hz, 4H); ^{13}C NMR (75 MHz, CDCl_3) δ 138.2 ($2 \times \text{C}$), 129.5 ($2 \times \text{CH}$), 128.4 ($4 \times \text{CH}$), 127.8 ($4 \times \text{CH}$), 127.6 ($2 \times \text{CH}$), 72.3 ($2 \times \text{CH}_2$), 65.8 ($2 \times \text{CH}_2$). Anal. Calcd for $\text{C}_{18}\text{H}_{20}\text{O}_2$: C, 80.56; H, 7.51.



Aldehyde 72.⁴⁰¹ Through a solution of **190** (8.9 g, 33.1 mmol, 1.0 eq) in $\text{CH}_2\text{Cl}_2/\text{MeOH}$ (3/1, 80 mL, 2.5 mL/mmol of **190**) at -78 $^\circ\text{C}$ was bubbled a stream of ozone until the color turned blue (~ 4 h). The excess ozone was removed by a nitrogen stream (disappearance of the blue color) and then dimethylsulfide (9.8 mL, 132.2 mmol, 4.0 eq) was added at -78 $^\circ\text{C}$. The reaction mixture was warmed to ambient temperature and stirred over night. The solvents were removed under reduced pressure. Flash chromatography (heptane/ethyl acetate 1/1) afforded the aldehyde **72** (9.9 g, 65.6 mmol, 99%) as a colorless oil (R_f 0.52 heptane/ethyl acetate 1/1) that was immediately used after purification.

^1H NMR (300 MHz, CDCl_3) δ 9.72 (s, 1H), 7.48-7.31 (m, 5H), 4.62 (s, 2H), 4.09 (s, 2H). Anal. Calcd for $\text{C}_9\text{H}_{10}\text{O}_2$: C, 71.98; H, 6.71.

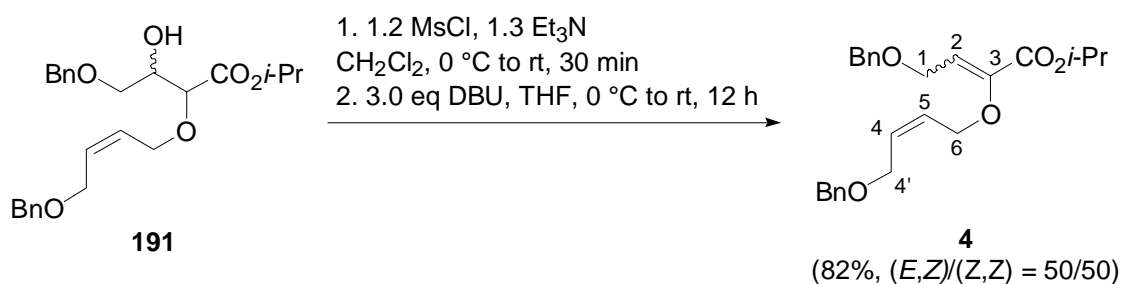


β -Hydroxy Ester 191.^{399,388} To a stirred solution of LDA [prepared in situ from diisopropylamine (7.8 mL, 55.4 mmol, 1.3 eq) and *n*-BuLi (2.31 M in hexanes, 22.2 mL, 51.2 mmol, 1.2 equiv)] in THF (43 mL, 1 mL/mmol **73**) was added a cooled solution (-78 $^\circ\text{C}$) of the ester **73** (11.9 g, 42.6 mmol, 1.0 eq) in THF (43 mL, 1 mL/mmol **73**) at -78 $^\circ\text{C}$. The solution was stirred for 15 min, and the freshly prepared aldehyde **72** (8.3 g, 55.4 mmol, 1.2 equiv) was added as cooled solution (-78 $^\circ\text{C}$) in THF (21 mL, 0.5 mL/mmol **73**). The mixture

⁴⁰¹ Compound **72** is commercially available, e.g. from Aldrich. For an analogue synthesis, see: Daub, G. W.; Edwards, J. P.; Okada, C. R.; Allen, J. W.; Maxey, C. T.; Wells, M. S.; Goldstein, A. S.; Dibley, M. J.; Wang, C. J.; Ostercamp, D. P.; Chung, S.; Cunningham, P. S.; Berliner, M. A. *J. Org. Chem.* **1997**, *62*, 1976-1985.

was stirred 30 min at $-78\text{ }^{\circ}\text{C}$ and then quenched by the addition of saturated aq NH_4Cl at $-78\text{ }^{\circ}\text{C}$. After dilution with H_2O and CH_2Cl_2 , the layers were separated and the aqueous phase was extracted with CH_2Cl_2 ($3 \times 100\text{ ml}$). The combined organic phases were dried over MgSO_4 and concentrated. Flash chromatography (heptane/ethyl acetate 3/1 to 1/1) afforded the β -hydroxy ester **191** [15.0 g, 34.9 mmol, 82%, mixture of diastereomers (dr 55/45)] as pale yellow oil (R_f 0.35 heptane/ethyl acetate 1/1).

^1H NMR (500 MHz, CDCl_3), mixture of diastereomers δ 7.38-7.27 (m, 10H), 5.84-5.75 (m, 1H), 5.73-5.67 (m, 1H), 5.08 (br sept, $J = 6.3\text{ Hz}$, 1H), 4.52 (dd, $J = 8.2, 4.4\text{ Hz}$, 2H), 4.48 (d, $J = 1.6\text{ Hz}$, 2H), 4.28 (dd, $J = 12.5, 5.8\text{ Hz}$, 1 H^{minor}), 4.21 (dd, $J = 12.1, 6.2\text{ Hz}$, 1 H^{major}), 4.11-3.93 (m, 4H), 4.00 (d, $J = 3.6\text{ Hz}$, 1 H^{minor}), 3.96 (d, $J = 5.8\text{ Hz}$, 1 H^{major}), 3.64-3.53 (m, 2H), 2.58 (d, $J = 6.5\text{ Hz}$, 1 H^{major}), 2.46 (d, $J = 7.5\text{ Hz}$, 1 H^{minor}), 1.28-1.16 (m, 6H); ^{13}C NMR (75 MHz, CDCl_3), mixture of diastereomers δ 170.3 (C-minor), 170.2 (C-major), 138.0 (C), 137.8 (C), 130.33 (CH-major), 130.28 (CH-minor), 128.5 ($2 \times \text{CH}$), 128.4 ($4 \times \text{CH}$), 127.80 ($2 \times \text{CH}$), 127.76 ($2 \times \text{CH}$), 127.7 (CH), 78.9 (CH-major), 77.8 (CH-minor), 73.45 (CH_2 -major), 73.42 (CH_2 -minor), 72.4 (CH_2), 71.2 (CH), 70.1 (CH_2 -minor), 70.0 (CH_2 -major), 68.92 (CH-minor), 68.88 (CH-major), 66.43 (CH_2 -minor), 66.40 (CH_2 -major), 65.7 (CH_2), 21.8 (CH_3), 21.7 (CH_3); IR (in substance) ν 3550-3420, 2980-2875, 1730 cm^{-1} . Anal. Calcd for $\text{C}_{25}\text{H}_{32}\text{O}_6$: C, 70.07; H, 7.53. Found: C, 70.26, H, 7.83.

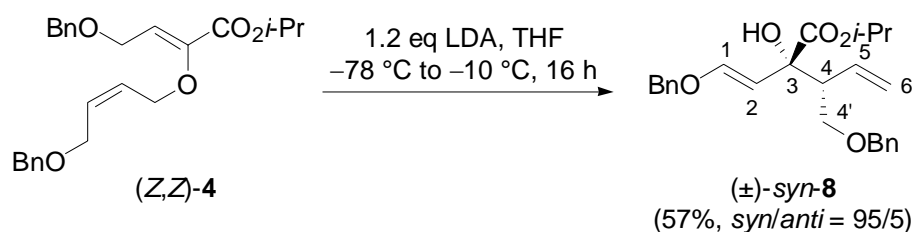


Allyl Vinyl Ether 4.^{399,388} To a solution of the diastereomeric β -hydroxy ester **191** (15.0 g, 35.1 mmol, 1.0 eq) in CH_2Cl_2 (105 mL, 3 mL/mmol **191**) at $0\text{ }^{\circ}\text{C}$ was added triethylamine (6.3 mL, 45.6 mmol, 1.3 eq) and methane sulfonyl chloride MsCl (3.3 mL, 42.1 mmol, 1.2 eq). The reaction mixture was stirred for 30 min at ambient temperature, quenched with saturated aq NaHCO_3 and extracted with CH_2Cl_2 ($2 \times 50\text{ mL}$). The combined organic phases were dried over MgSO_4 and concentrated under reduced pressure to afford the crude mesylate **507** which was dissolved in THF (70 mL, 2 mL/mmol **191**) and cooled to $0\text{ }^{\circ}\text{C}$. DBU (16.0 mL, 105 mmol, 3.0 equiv) was added at $0\text{ }^{\circ}\text{C}$. The reaction mixture was stirred at ambient temperature until TLC indicated complete consumption of the starting material (about 12 h). The reaction was then quenched with H_2O (70 mL) and extracted with CH_2Cl_2 ($2 \times 50\text{ mL}$).

The combined organic phases were dried over MgSO_4 and concentrated. Flash chromatography (heptane/ethyl acetate 10/1) afforded the allyl vinyl ether **4** (11.8 g, 28.8 mmol, 82%) as mixture of double bond isomers [(*E,Z*)/(*Z,Z*) = 50/50] as pale yellow oil (R_f 0.59 heptane/ethyl acetate 1/1). The double bond isomers were separated by preparative HPLC, column: 32×250 mm, Nucleosil 50-5, $5 \mu\text{m}$, solvent: (heptane/ethyl acetate 4/1, flow: 30 mL/min, r_t (*Z,Z*-**4**) \sim 16 min, r_t (*E,Z*-**4**) \sim 19 min, performance: \sim 1 g/h).

(*E,Z*)-**4**. ^1H NMR (500 MHz, CDCl_3) δ 7.34-7.26 (m, 10H, CH-Ar), 5.81-5.79 (m, 2H, 4- and 5- CH=), 5.29 (t, $J = 5.8$ Hz, 1H, 2- CH=), 5.10 (sept, $J = 6.3$ Hz, 1H, -*Oi*-Pr CH), 4.53 (s, 2H, 1- CH_2Ph), 4.51 (s, 2H, 4'- CH_2Ph), 4.48 (d, $J = 5.8$ Hz, 2H, 1- CH_2OBn), 4.34 (brd, $J = 3.7$ Hz, 2H, 6- CH_2), 4.10 (brd, $J = 4.3$ Hz, 2H, 4'- CH_2OBn), 1.26 (d, $J = 6.3$ Hz, 6H, -*Oi*-Pr CH_3); ^{13}C NMR (126 MHz, CDCl_3) δ 162.7 (3'- C), 145.4 (3- C=), 138.1 (C-Ar), 137.9 (C-Ar), 129.8 (4- CH=), 128.41 ($2 \times \text{CH-Ar}$), 128.39 ($2 \times \text{CH-Ar}$), 127.83 ($2 \times \text{CH-Ar}$), 127.77 ($2 \times \text{CH-Ar}$), 127.70 (CH-Ar), 127.67 (CH-Ar), 127.4 (5- CH=), 112.1 (2- CH=), 72.5 (1- CH_2Ph), 72.4 (4'- CH_2Ph), 69.1 (-*Oi*-Pr CH), 66.6 (1- CH_2), 65.9 (4'- CH_2), 64.7 (6- CH_2), 21.7 ($2 \times$ -*Oi*-Pr CH_3); IR (in substance) ν 3090-3030, 2980-2860, 1720 cm^{-1} . Anal. Calcd for $\text{C}_{25}\text{H}_{30}\text{O}_5$: C, 73.15; H, 7.37. Found: C 73.31; H 7.64.

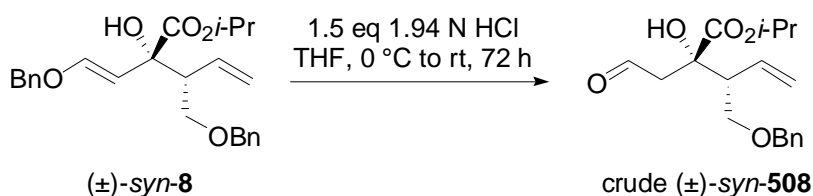
(*Z,Z*)-**4**. ^1H NMR (500 MHz, CDCl_3) δ 7.34-7.28 (m, 10H, CH-Ar), 6.35 (t, $J = 6.3$ Hz, 1H, 2- CH=), 5.80-5.73 (m, 2H, 4- and 5- CH=), 5.07 (sept, $J = 6.3$ Hz, 1H, -*Oi*-Pr CH), 4.50 (s, 2H, 1- CH_2Ph), 4.47 (s, 2H, 4'- CH_2Ph), 4.44 (d, $J = 6.2$ Hz, 2H, 6- CH_2), 4.24 (d, $J = 6.3$ Hz, 2H, 1- CH_2), 4.06 (d, $J = 6.4$ Hz, 2H, 4'- CH_2), 1.27 (d, $J = 6.3$ Hz, 6H, -*Oi*-Pr CH_3); ^{13}C NMR (126 MHz, CDCl_3) δ 162.6 (3'- C), 145.7 (3- C=), 138.0 (C-Ar), 137.9 (C-Ar), 130.6 (4- CH=), 128.43 ($2 \times \text{CH-Ar}$), 128.41 ($2 \times \text{CH-Ar}$), 127.9 (CH-Ar), 127.83 ($2 \times \text{CH-Ar}$), 127.78 (CH-Ar), 127.76 ($2 \times \text{CH-Ar}$), 127.7 (5- CH=), 124.3 (2- CH=), 72.8 (1- CH_2Ph), 72.4 (4'- CH_2Ph), 68.9 (-*Oi*-Pr CH), 67.5 (6- CH_2), 65.6 (4'- CH_2), 64.5 (1- CH_2), 21.8 ($2 \times$ -*Oi*-Pr CH_3); IR (in substance) ν 3090-3030, 2980-2860, 1720 cm^{-1} . Anal. Calcd for $\text{C}_{25}\text{H}_{30}\text{O}_5$: C, 73.15; H, 7.37. Found: C, 73.03; H, 7.58.



α -Hydroxyester (\pm)-*syn*-**8**.³⁸⁸ To a stirred solution of LDA [prepared in situ from diisopropylamine (1.7 mL, 12.0 mmol, 1.2 eq) and *n*-BuLi (2.3 M in hexanes, 4.6 mL, 10.5 mmol, 1.05 eq)] in THF (40 mL, 4 mL/mmol **4**) was added a cooled solution ($-78 \text{ }^\circ\text{C}$) of the

allyl vinyl ether (*Z,Z*)-**4** (4.1 g, 10.0 mmol, 1.0 eq) in THF (20 mL, 2 mL/mmol **4**) at -78 °C. The solution was allowed to warm to -10 °C over night, quenched with saturated aq NH_4Cl and extracted with CH_2Cl_2 (3×30 mL). The combined organic phases were dried over MgSO_4 and concentrated. Flash chromatography (heptane/ethyl acetate 20/1 to 10/1) afforded of the rearrangement product **8** (2.4 g, 5.7 mmol, 57%, *syn/anti* = 95/5) as pale yellow oil (R_f 0.59 heptane/ethyl acetate 1/1).

^1H NMR (500 MHz, CDCl_3) δ 7.37-7.24 (m, 10H), 6.71 (d, $J = 12.7$ Hz, 1H, 1- $\text{CH}=\text{C}$), 5.84 (ddd, $J = 16.8, 10.5, 9.4$ Hz, 1H, 5- $\text{CH}=\text{C}$), 5.18 (d, $J = 1.3$ Hz, 1H, 4- $\text{CH}_2=\text{C}$), 5.15 (dd, $J = 9.7, 1.9$ Hz, 1H, 4- $\text{CH}_2=\text{C}$), 4.99 (d, $J = 12.5$ Hz, 1H, 2- $\text{CH}=\text{C}$), 4.99 (sept, $J = 6.3$ Hz, 1H, -*Oi-PrCH*), 4.74 (d^{AB} , $J = 11.9$ Hz, 1H, 1- CH_2Ph), 4.70 (d^{AB} , $J = 12.0$ Hz, 1H, 1- CH_2Ph), 4.48 (d^{AB} , $J = 11.9$ Hz, 1H, 4'- CH_2Ph), 4.42 (d^{AB} , $J = 11.7$ Hz, 1H, 4'- CH_2Ph), 3.71 (dd^{AB} , $J = 9.6, 4.1$ Hz, 1H, 4'- CH_2OBn), 3.65 (s, 1H, OH), 3.57 (dd^{AB} , $J = 9.4, 7.5$ Hz, 1H, 4'- CH_2OBn), 2.75-2.65 (m, 1H, 4- CH), 1.23 (d, $J = 6.2$ Hz, 3H, -*Oi-Pr-CH}_3*), 1.17 (d, $J = 6.2$ Hz, 3H, *Oi-PrCH}_3*); ^{13}C NMR (126 MHz, CDCl_3) δ 174.0 (3'- C), 148.4 (1- $\text{CH}=\text{C}$), 138.2 (C-Ar), 136.7 (C-Ar), 135.2 (5- $\text{CH}=\text{C}$), 128.5 ($2 \times \text{CH-Ar}$), 128.3 ($2 \times \text{CH-Ar}$), 127.9 (CH-Ar), 127.6 ($2 \times \text{CH-Ar}$), 127.5 (CH-Ar), 127.4 ($2 \times \text{CH-Ar}$), 118.9 (4- $\text{CH}_2=\text{C}$), 105.3 (2- $\text{CH}=\text{C}$), 77.1 (3- C), 73.2 (1- CH_2Ph), 71.6 (4'- CH_2Ph), 70.0 (-*Oi-PrCH*), 69.8 (4'- CH_2OBn), 51.6 (4- CH), 21.6 ($2 \times \text{-Oi-PrCH}_3$); IR (in substance) ν 3500, 3070-3030, 2980-2870, 1720 cm^{-1} . Anal. Calcd for $\text{C}_{25}\text{H}_{30}\text{O}_5$: C, 73.15; H, 7.37. Found: C, 73.09; H, 7.80.

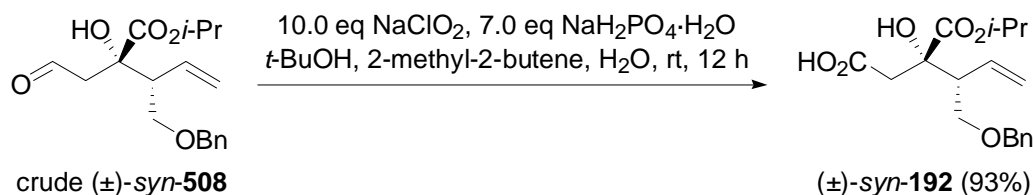


Aldehyde (\pm)-(*syn*)-**508**.^{402,388} To an ice-cooled solution of the benzyl enol ether **8** (2.4 g, 5.8 mmol, 1.0 eq) in THF (3 mL, 0.5 mL/mmol **8**) was added aq HCl (1.94 M, 4.3 mL, 8.4 mmol, 1.5 eq) and stirred for 72 h at ambient temperature. The reaction mixture was then quenched with saturated aq NaHCO_3 and extracted with CH_2Cl_2 (3×30 mL). The combined organic phases were dried over MgSO_4 and concentrated under reduced pressure to afford the crude aldehyde (R_f 0.44 heptane/ethyl acetate 1/1) that was used without further purification. (analyzed as a mixture of crude (\pm)-*syn*-**508** and benzyl alcohol).

^1H NMR (300 MHz, CDCl_3) δ 9.53 (t, $J = 1.6$ Hz, 1H), 7.23-7.11 (m, 5H), 5.66 (ddd, $J = 16.9, 10.2$ Hz, 1H), 5.04-4.95 (m, 2H), 4.88 (sept, $J = 6.3$ Hz, 1H), 4.38 (d^{AB} , $J = 12.0$ Hz,

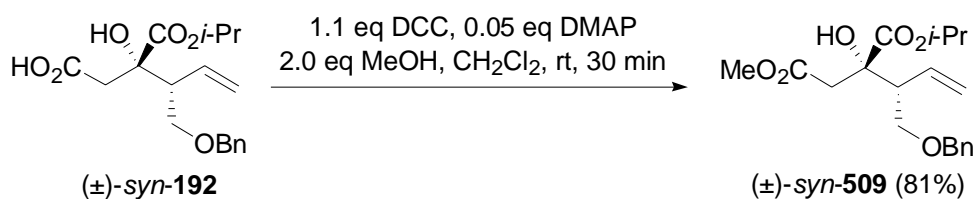
⁴⁰² Fully characterized after esterification.

1H), 4.32 (d^{AB}, $J = 12.0$ Hz, 1H), 3.60 (dd^{AB}, $J = 9.7, 7.1$ Hz, 1H), 3.42 (dd^{AB}, $J = 9.7, 5.2$ Hz, 1H), 2.85 (dd^{AB}, $J = 17.4, 1.8$ Hz, 1H), 2.72 (dd^{AB}, $J = 17.2, 1.3$ Hz, 1H), 2.57 (ddd, $J = 9.7, 7.2, 5.1$ Hz, 1H), 1.06 (d, $J = 6.3$ Hz, 6H) no OH-resonance observed; ¹³C NMR (75 MHz, CDCl₃) δ 199.9 (CH), 140.9 (C), 137.7 (C), 134.1 (CH), 128.6 (CH), 128.4 (CH), 127.8 (CH), 127.7 (CH), 127.0 (CH), 119.3 (CH₂), 75.7 (C), 73.4 (CH₂), 70.2 (CH), 70.1 (CH₂), 65.4 (CH₂), 52.2 (CH), 50.8 (CH₂), 21.8 (2 \times CH₃). Anal. Calcd for C₁₈H₂₄O₅: C, 67.48; H, 7.55.



Acid (±)-*syn*-192.^{402,388} To a solution of the crude aldehyde **508** (5.8 mmol, 1.0 eq) in *t*-BuOH (58 mL, 10 mL/mmol **508**) and 2-methyl-2-butene (58 mL, 10 mL/mmol **508**) was added a solution of NaClO₂ (5.2 g, 57.5 mmol, 10.0 eq) and NaH₂PO₄·H₂O (5.6 g, 40.2 mmol, 7.0 eq) in water (120 mL, 20 mL/mmol **508**). The reaction mixture was stirred at ambient temperature for 12 hours, diluted with water and extracted with CH₂Cl₂ (3 \times 50 mL). The combined organic phases were dried over MgSO₄ and concentrated. Purification by flash chromatography (heptane/ethyl acetate 10/1 to 1/2) provided the acid (±)-*syn*-**192** (1.8 g, 5.3 mmol, 93%) as pale yellow oil (R_f 0.09 heptane/ethyl acetate 1/1).⁴⁰³

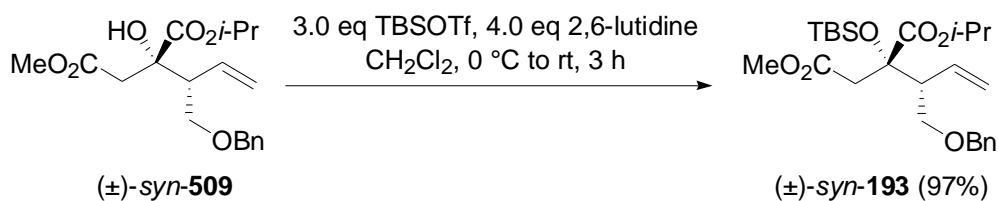
¹H NMR (300 MHz, CDCl₃) δ 7.40-7.22 (m, 5H), 5.81 (ddd, $J = 16.3, 11.0, 9.7$ Hz, 1H), 5.18 (s, 1H), 5.15 (dd, $J = 7.5, 1.6$ Hz, 1H), 5.03 (sept, $J = 6.3$ Hz, 1H), 4.53 (d^{AB}, $J = 11.7$ Hz, 1H), 4.46 (d^{AB}, $J = 11.7$ Hz, 1H), 3.72 (dd^{AB}, $J = 9.7, 7.1$ Hz, 1H), 3.56 (dd^{AB}, $J = 9.6, 5.0$ Hz, 1H), 3.00 (d^{AB}, $J = 16.3$ Hz, 1H), 2.90 (d^{AB}, $J = 16.5$ Hz, 1H), 2.71 (ddd, $J = 9.7, 7.0, 5.0$ Hz, 1H), 1.23 (d, $J = 6.2$ Hz, 3H), 1.21 (d, $J = 6.2$ Hz, 3H); ¹³C NMR (75 MHz, CDCl₃) δ 174.3 (C), 173.0 (C), 137.8 (C), 134.2 (CH), 128.4 (2 \times CH), 127.8 (2 \times CH), 127.0 (CH), 119.2 (CH₂), 76.5 (C), 73.5 (CH₂), 70.1 (CH₂), 70.1 (CH), 52.2 (CH), 42.1 (CH₂), 21.7 (CH₃), 21.6 (CH₃). Anal. Calcd for C₁₈H₂₄O₆: C, 64.27; H, 7.19.



⁴⁰³ The benzyl alcohol (R_f 0.47 heptane/ethyl acetate 1/1, clearly detectable by UV irradiation), cleaved in the previous step, had to be carefully removed from the acid to avoid undesired side reactions during the following esterification

Ester (\pm)-*syn*-509.³⁸⁸ To an ice cooled solution of the acid **192** (1.8 g, 5.3 mmol, 1.0 eq) in CH₂Cl₂ (21 mL, 4 mL/mmol **192**) was added DMAP (32 mg, 0.3 mmol, 0.05 eq), DCC (1.21 g, 5.9 mmol, 1.1 eq) and MeOH (1 mL, 15.9 mmol, 2.0 eq). The resulting suspension was stirred for 30 min at ambient temperature. The precipitate was then removed by filtration, washed with CH₂Cl₂ and the solvent was evaporated under reduced pressure. Flash chromatography (heptane/ethyl acetate 10/1 to 5/1) afforded of the ester (\pm)-*syn*-**509** (1.5 g, 4.3 mmol, 81%) as pale yellow oil (*R*_f 0.32 heptane/ethyl acetate 1/1).

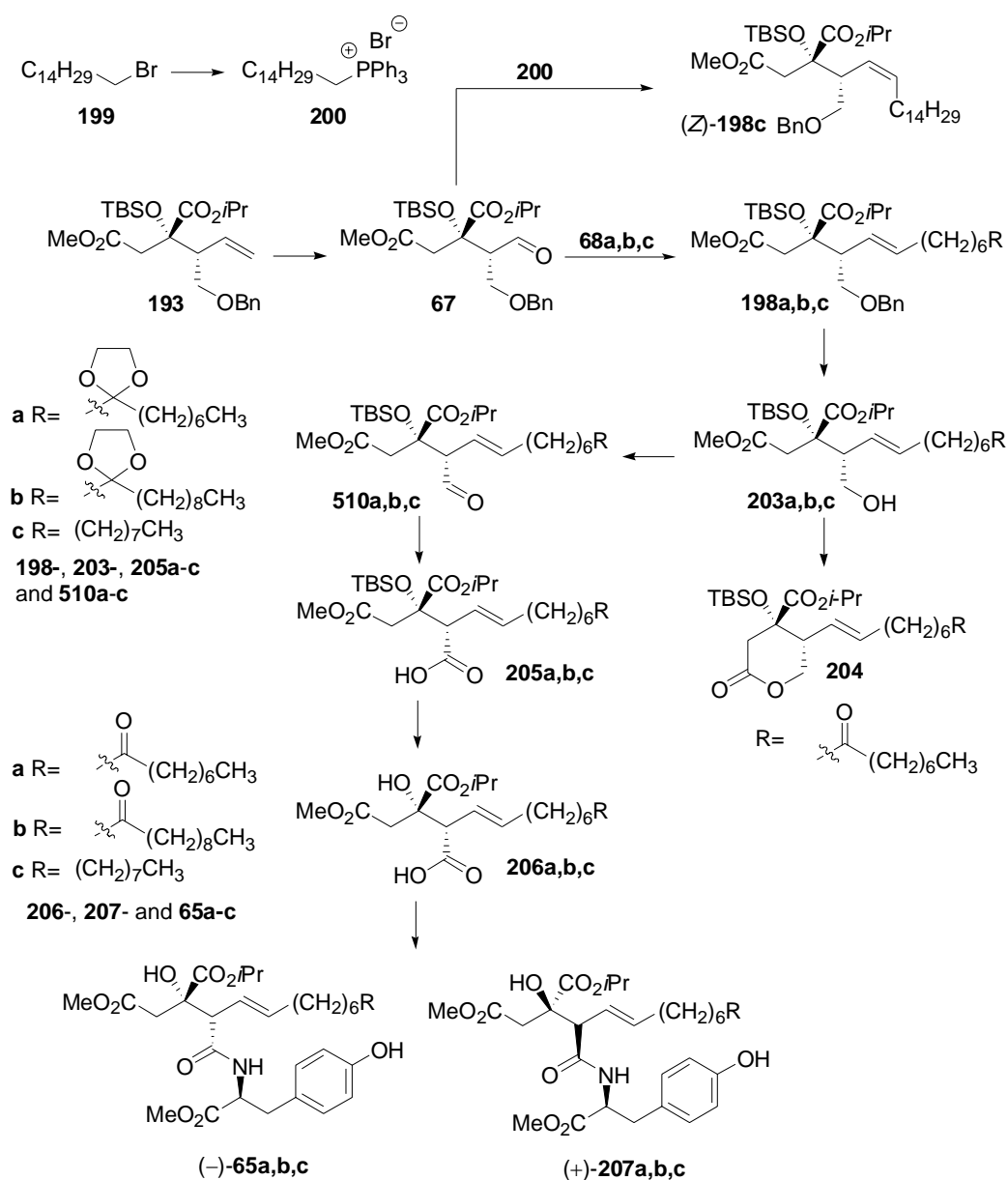
¹H NMR (500 MHz, CDCl₃) δ 7.34-7.24 (m, 5H), 5.77 (ddd, *J* = 16.8, 10.3, 10.3 Hz, 1H), 5.15 (s, 1H), 5.13 (dd, *J* = 8.7, 1.6 Hz, 1H), 5.04 (sept, *J* = 6.3 Hz, 1H), 4.50 (d^{AB}, *J* = 12.0 Hz, 1H), 4.45 (d^{AB}, *J* = 11.7 Hz, 1H), 4.00 (s, 1H), 3.70 (dd^{AB}, *J* = 9.6, 6.5 Hz, 1H), 3.64 (s, 3H), 3.52 (dd^{AB}, *J* = 9.8, 5.4 Hz, 1H), 2.94 (d^{AB}, *J* = 16.8 Hz, 1H), 2.86 (d^{AB}, *J* = 16.1 Hz, 1H), 2.67-2.61 (m, 1H), 1.29 (d, *J* = 6.0 Hz, 3H), 1.21 (d, *J* = 6.0 Hz, 3H); ¹³C NMR (126 MHz, CDCl₃) δ 173.4 (C), 171.1 (C), 137.9 (C), 134.5 (CH), 128.3 (2 \times CH), 127.7 (2 \times CH), 127.6 (CH), 119.0 (CH₂), 76.1 (C), 73.3 (CH₂), 69.9 (CH₂), 52.4 (CH or CH₃), 51.7 (CH or CH₃), 42.4 (CH₂), 21.7 (CH₃), 21.6 (CH₃); IR (in substance) ν 3480-2980, 2920-2835, 1740 cm⁻¹. Anal. Calcd for C₁₉H₂₆O₆: C, 65.13; H, 7.48. Found: C, 65.17; H, 7.65.



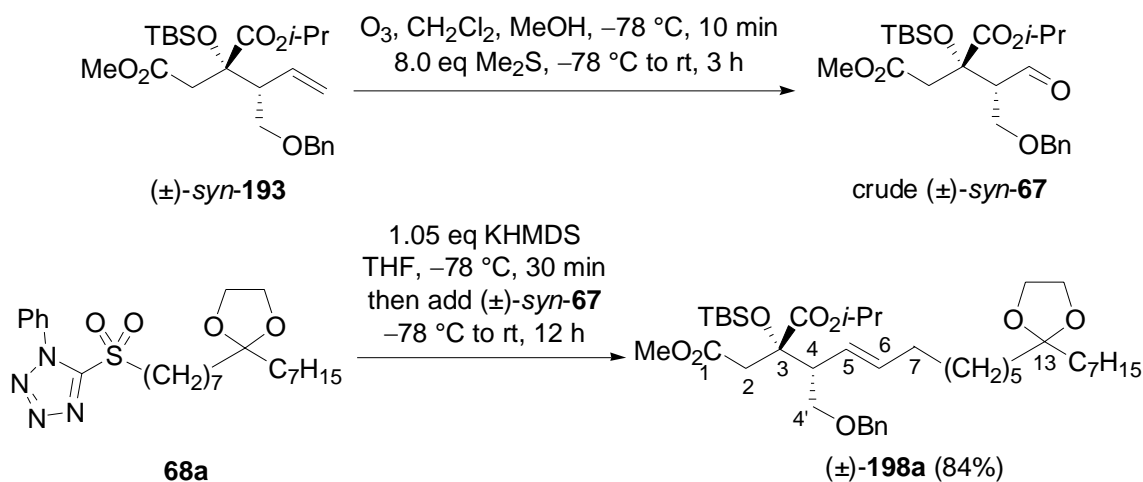
Silyl Ether (\pm)-*syn*-193.³⁸⁸ To an ice cooled solution of the ester **509** (1.1 g, 3.1 mmol, 1.0 eq) in CH₂Cl₂ (15 mL, 5 mL/mmol **509**) was added 2,6-lutidine (1.4 mL, 12.4 mmol, 4.0 eq) and TBSOTf (2.5 g, 9.3 mmol, 3.0 eq). The resulting mixture was stirred at ambient temperature until TLC indicated complete consumption of the starting material (~3 h). The reaction was quenched with saturated aq NaHCO₃ and extracted with CH₂Cl₂ (3 \times 10 mL). The combined organic layers were dried over MgSO₄ and concentrated. Flash chromatography (heptane/ethyl acetate 20/1 to 10/1) afforded silyl ether (\pm)-*syn*-**193** (1.4 g, 3.0 mmol, 97%) as pale yellow oil (*R*_f 0.79 heptane/ethyl acetate 1/1).

¹H NMR (300 MHz, CDCl₃) δ 7.21-7.04 (m, 5H), 5.61 (ddd, *J* = 16.9, 10.2, 10.2 Hz, 1H), 4.97 (d, *J* = 1.9 Hz, 1H), 4.94 (dd, *J* = 10.2, 1.8 Hz, 1H), 4.80 (sept, *J* = 6.3 Hz, 1H), 4.30 (s, 2H), 3.63 (dd^{AB}, *J* = 5.4, 9.6 Hz, 1H), 3.44 (s, 3H), 3.28 (dd^{AB}, *J* = 6.5, 9.7 Hz, 1H), 2.81 (d^{AB}, *J* = 15.3 Hz, 1H), 2.68 (d^{AB}, *J* = 15.3 Hz, 1H), 2.61-2.51 (m, 1H), 1.06 (d, *J* = 6.5 Hz, 3H), 1.02 (d, *J* = 6.5 Hz, 3H), 0.64 (s, 9H), 0.00 (s, 3H), -0.12 (s, 3H); ¹³C NMR (75 MHz,

CDCl_3) δ 171.9 (C), 170.4 (C), 138.1 (C), 135.7 (CH), 128.3 (2 \times CH), 127.7 (2 \times CH), 127.6 (CH), 118.5 (CH₂), 79.8 (C), 73.1 (CH₂), 69.5 (CH₂), 69.1 (CH), 53.5 (CH or CH₃), 51.5 (CH or CH₃), 43.9 (CH₂), 26.0 (3 \times CH₃), 21.8 (CH₃), 21.7 (CH₃), 18.9 (C), -2.5 (CH₃), -2.9 (CH₃); IR (in substance) ν 2975-2855, 1745 cm^{-1} . Anal. Calcd for C₂₅H₄₀O₆Si: C, 64.62; H, 8.68. Found: C, 64.68; H, 8.85.

20.2.3 Synthesis of the Viridiofungin A, A₄, A₂ Triesters

Scheme 152: Completion of the viridiofungin triester synthesis.

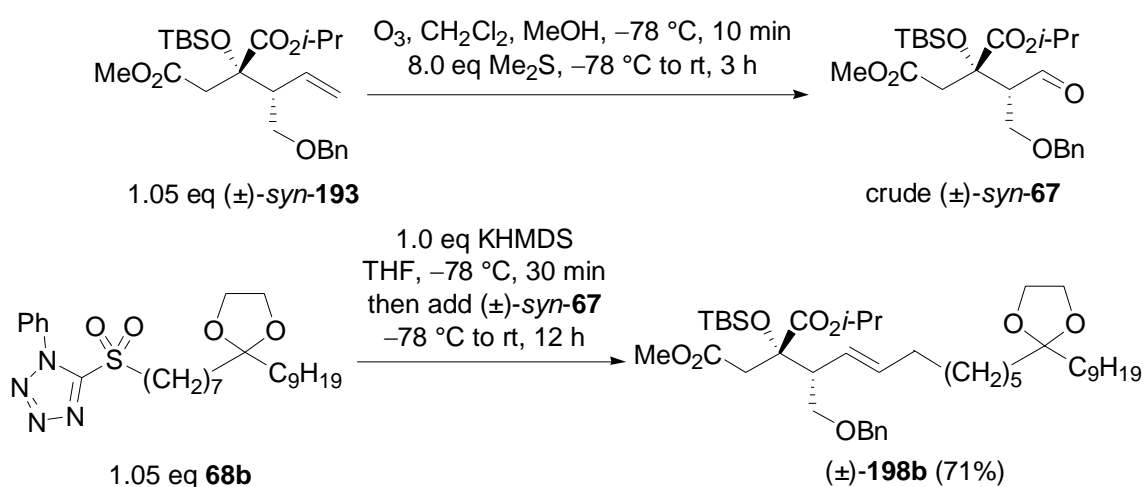


Olefin (\pm)-198a**.**³⁸⁸ Through a solution of the terminal olefin (\pm)-**syn-193** (0.23 g, 0.5 mmol, 1.0 eq) in CH_2Cl_2 and MeOH (4/1, 10 mL, 20 mL/mmol **193**) at $-78\text{ }^\circ\text{C}$ was bubbled a stream of ozone until the color of the reaction mixture turned blue (~ 10 min). The excess ozone was removed by a nitrogen stream (disappearance of the blue color) and then Me_2S (0.3 mL, 4.0 mmol, 8.0 eq) was added at $-78\text{ }^\circ\text{C}$. The reaction mixture was allowed to warm to ambient temperature and stirred at this temperature until TLC indicated complete consumption of the ozonide (~ 3 h). The reaction mixture was then concentrated at reduced pressure to provide the crude aldehyde (\pm)-**syn-67** (R_f 0.23 heptane/ethyl acetate 5/1) which was used without further purification.

To a solution of the sulfone **68a** (0.23 g, 0.5 mmol, 1.0 equiv) in THF (5 mL, 10 mL/mmol **68a**) at $-78\text{ }^\circ\text{C}$ was added KHMDS (0.5 M solution in THF , 0.9 mL, 0.5 mmol, 1.05 eq) and the resulting mixture was stirred for 30 min. A pre-cooled ($-78\text{ }^\circ\text{C}$) solution of the aldehyde (\pm)-**syn-67** (0.5 mmol, 1.0 eq) in THF (2.5 mL, 5 mL/mmol **67**) was then added and the mixture was warmed to ambient temperature over night. The resulting slurry was diluted with water, the phases were separated and the organic layer was washed with brine (2 x 10 mL), dried over MgSO_4 and then concentrated. Flash chromatography (heptane/ethyl acetate 20/1) afforded the olefin (\pm)-**198a** (0.29 g, 0.4 mmol, 84%) as a colorless oil (R_f 0.38 heptane/ethyl acetate 5/1).³⁹⁷

$^1\text{H NMR}$ (500 MHz, CDCl_3) δ 7.31-7.18 (m, 5H, CH-Ar), 5.44 (ddd, $J = 15.0, 6.5, 6.5$ Hz, 1H, 6- CH=), 5.24 (ddd, $J = 15.2, 9.6$ Hz, 1H, 5- CH=), 4.91 (sept, $J = 6.3$ Hz, 1H, - $\text{O}i\text{-PrCH}$), 4.41 (s, 2H, 4''- CH_2Ph), 3.87 (s, 4H, 13'- CH_2), 3.73 (dd^{AB} , $J = 9.6, 5.4$ Hz, 1H, 4'- CH_2), 3.56 (s, 3H, CO_2CH_3), 3.32 (dd^{AB} , $J = 9.6, 6.3$ Hz, 1H, 4'- CH_2), 2.89 (d^{AB} , $J = 15.3$ Hz, 1H, 2- CH_2), 2.80 (d^{AB} , $J = 15.3$ Hz, 1H, 2- CH_2), 2.68-2.57 (m, 1H, 4- CH), 1.98-1.86 (m, 2H, 7- CH_2), 1.58-1.46 (m, 4H, 12- and 14- CH_2), 1.36-1.24 (m, 18H, 8-, 9-, 10-, 11- and 15-, 16-, 17-, 18-, 19- CH_2), 1.22 (d, $J = 6.3$ Hz, 3H, - $\text{O}i\text{-PrCH}_3$), 1.20 (d, $J = 6.3$ Hz, 3H, - $\text{O}i\text{-PrCH}_3$),

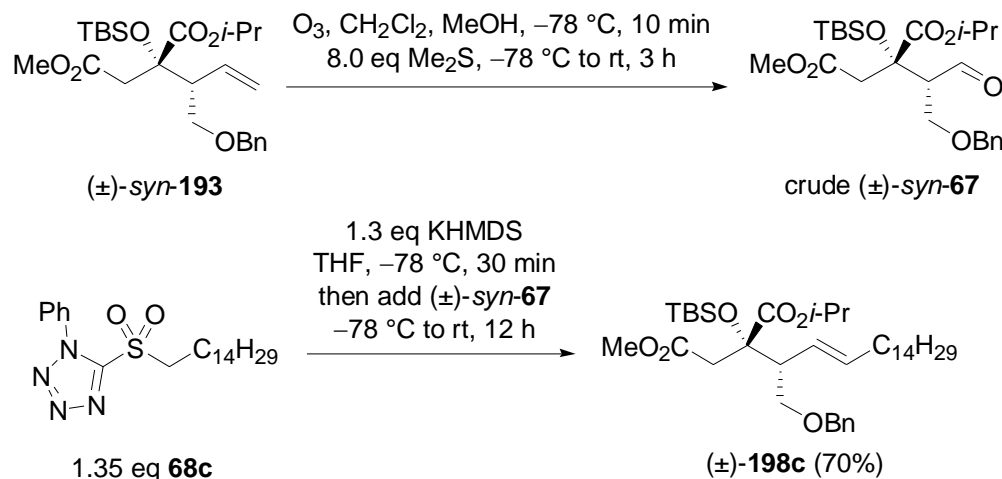
0.87 (t, $J = 6.9$ Hz, 3H, 20-CH₃), 0.81 (s, 9H, SiC(CH₃)₃), 0.13 (s, 3H, SiCH₃), 0.00 (s, 3H, SiCH₃); ¹³C NMR (126 MHz, CDCl₃) δ 172.0 (CO₂*i*-Pr), 170.6 (CO₂Me), 138.3 (C-Ar), 134.4 (6-CH=), 128.3 (2 × CH-Ar), 127.7 (2 × CH-Ar), 127.5 (CH-Ar), 127.0 (5-CH=), 111.9 (13-C), 80.3 (3-C), 73.0 (4''-CH₂), 70.0 (4'-CH₂), 68.9 (-*Oi*-PrCH), 64.9 (2 × 13'-CH₂), 52.2 (4-CH), 51.4 (-OCH₃), 44.0 (2-CH₂), 37.1 (12- and 14-CH₂), 32.6 (7-CH₂), 31.8 (18-CH₂), 29.9 (CH₂), 29.8 (CH₂), 29.3 (CH₂), 29.23 (CH₂), 29.16 (CH₂), 26.0 (3 × SiC(CH₃)₃), 23.84 (11- or 15-CH₂), 23.82 (11- or 15-CH₂), 22.6 (CH₂), 21.9 (-*Oi*-PrCH₃), 21.7 (-*Oi*-PrCH₃), 19.0 (SiC(CH₃)₃), 14.1 (20-CH₃), -2.4 (SiCH₃), -2.9 (SiCH₃); IR (in substance) ν 2930-2850, 1745 cm⁻¹. Anal. Calcd for C₄₁H₇₀O₈Si: C, 68.48; H, 9.81. Found: C 68.63; H 9.98.



Olefin (±)-198b.³⁸⁸ As outlined for the preparation of olefin (±)-**198a**, sulfone **68b** (0.18 g, 0.36 mmol, 1.05 equiv) was treated with KHMDS (0.5 M solution in THF, 0.7 ml, 0.34 mmol, 1.0 equiv) and the aldehyde (±)-*syn*-**67** (0.36 mmol, 1.05 equiv). Flash chromatography afforded olefin (±)-**198b** (0.19 g, 0.3 mmol, 71%) as a colorless oil (R_f 0.35 heptane/ethyl acetate 3/1).³⁹⁷

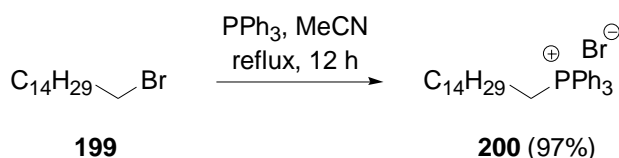
¹H NMR (300 MHz, CDCl₃) δ 7.33-7.29 (m, 5H), 5.47 (ddd, $J = 14.9, 6.6, 6.6$ Hz, 1H), 5.29 (dd, $J = 15.4, 9.6$ Hz, 1H), 4.96 (sept, $J = 6.2$ Hz, 1H), 4.47 (s, 2H), 3.92 (s, 4H), 3.78 (dd^{AB}, $J = 9.6, 5.7$ Hz, 1H), 3.62 (s, 3H), 3.38 (dd^{AB}, $J = 9.6, 6.2$ Hz, 1H), 2.95 (d^{AB}, $J = 15.2$ Hz, 1H), 2.86 (d^{AB}, $J = 15.2$ Hz, 1H), 2.72-2.64 (m, 1H), 1.97 (ddd, $J = 6.6, 6.5, 6.5$ Hz, 2H), 1.61-1.55 (m, 4H), 1.38-1.13 (m, 22H), 1.23 (d, $J = 6.1$ Hz, 3H), 1.21 (d, $J = 6.1$ Hz, 3H), 0.82 (s, 9H), 0.88 (t, $J = 6.7$ Hz, 3H), 0.18 (s, 3H), 0.05 (s, 3H); ¹³C NMR (75 MHz, CDCl₃) δ 172.0 (C), 170.6 (C), 138.3 (C), 134.4 (CH), 128.3 (2 × CH), 127.7 (2 × CH), 127.5 (CH), 127.0 (CH), 111.9 (C), 80.3 (C), 73.0 (CH₂), 70.1 (CH₂), 68.9 (CH), 64.9 (2 × CH₂), 52.3 (CH or CH₃), 51.3 (CH or CH₃), 44.0 (CH₂), 37.2 (2 × CH₂), 34.1 (CH₂), 32.6 (CH₂), 31.9 (CH₂), 30.0 (CH₂), 29.8 (CH₂), 29.61 (CH₂), 29.55 (CH₂), 29.3 (CH₂), 29.23 (CH₂), 29.16 (CH₂),

26.1 (3 × CH₃), 23.8 (CH₂), 22.7 (CH₂), 21.8 (CH₃), 21.7 (CH₃), 19.0 (C), 14.1 (CH₃), -2.4 (CH₃), -2.9 (CH₃); IR (in substance) ν 2955-2855, 1745 cm⁻¹. Anal. Calcd for C₄₃H₇₄O₈Si: C, 69.13; H, 9.98. Found: C, 69.37; H, 10.03.



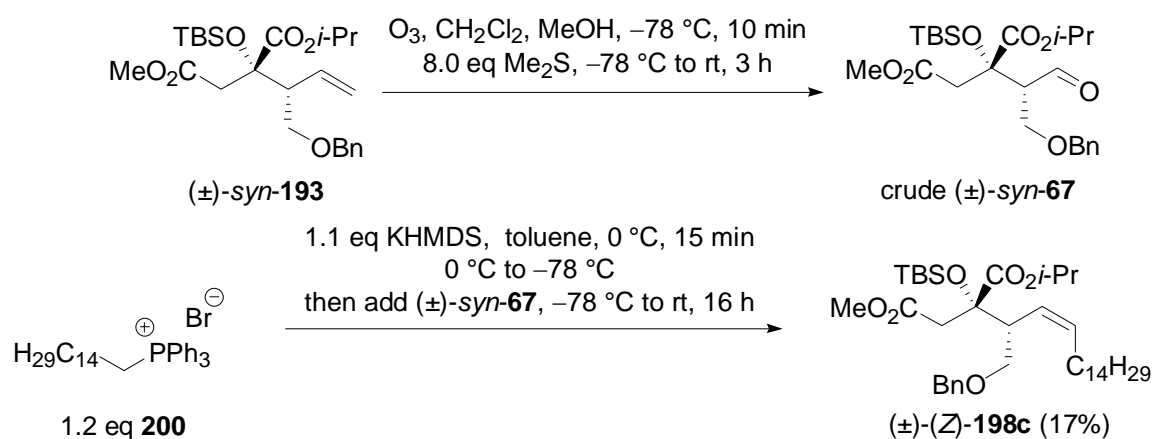
Olefin (±)-(*E*)-198c.³⁸⁸ Analogous to the procedure for the preparation of olefin (±)-198a, sulfon **68c** (0.28 g, 0.7 mmol, 1.35 eq) was treated with KHMDS (0.5 M solution in THF, 1.3 ml, 0.7 mmol, 1.3 eq) and the aldehyde (±)-*syn*-67 (0.5 mmol, 1.0 eq). Flash chromatography afforded olefin (±)-(*E*)-198c (0.23 g, 0.35 mmol, 70%) as a colorless oil (*R_f* 0.56 heptane/ethyl acetate 5/1).

¹H NMR (500 MHz, CDCl₃) δ 7.34-7.23 (m, 5H), 5.50 (dt, *J* = 15.1, 6.2 Hz, 1H), 5.31 (dd, *J* = 15.3, 9.6 Hz, 1H), 4.95 (sept, *J* = 6.2 Hz, 1H), 4.46 (s, 2H), 3.79 (dd^{AB}, *J* = 9.6, 5.8 Hz, 1H), 3.61 (s, 3H), 3.39 (dd^{AB}, *J* = 9.5, 6.3 Hz, 1H), 2.95 (d^{AB}, *J* = 15.1 Hz, 1H), 2.86 (d^{AB}, *J* = 15.1 Hz, 1H), 2.69 (ddd, *J* = 9.7, 5.9 Hz, 1H), 1.97 (dt, *J* = 6.8, 6.8 Hz, 2H), 1.40-1.16 (m, 30H), 0.88 (t, *J* = 6.9 Hz, 3H), 0.81 (s, 9H), 0.17 (s, 3H), 0.04 (s, 3H); ¹³C NMR (75 MHz, CDCl₃) δ 171.9 (C), 170.5 (C), 138.4 (C), 134.4 (CH), 128.2 (2 × CH), 127.7 (2 × CH), 127.4 (CH), 127.0 (CH), 80.3 (C), 73.0 (CH₂), 70.2 (CH₂), 68.9 (CH), 52.3 (CH or CH₃), 51.2 (CH or CH₃), 43.9 (CH₂), 32.6 (CH₂), 31.9 (CH₂), 29.63 (CH₂), 29.60 (CH₂), 29.58 (CH₂), 29.5 (CH₂), 29.3 (CH₂), 29.2 (CH₂), 26.1 (3 × CH₃), 22.6 (CH₂) (several overlapping signals between 44.0 and 22.7, total number (CH₂): 16), 21.8 (CH₃), 21.6 (CH₃), 18.9 (C), 14.0 (CH₃), -2.5 (CH₃), -2.9 (CH₃); IR (in substance) ν 2925-2855, 1745 cm⁻¹. Anal. Calcd for C₃₉H₆₈O₆Si: C, 70.86; H, 10.37. Found: C, 70.63; H, 10.62.



Wittig Salt 200.⁴⁰⁴ To a solution of bromopentadecane (**199**) (0.6 mL, 2.0 mmol, 1.0 eq) in acetonitrile (20 mL, 10 mL/mmol) was added PPh₃ (0.5 g, 2.1 mmol, 1.03 eq). The reaction mixture was refluxed for 12 h, cooled to rt and concentrated to yield about 2 mL of a solution of the crude product. To that solution diethyl ether was added dropwise until a little turbidity appeared in the solution. When considerable crystallization became apparent further diethyl ether (10 mL) were slowly added and the reaction flask was stored at 4 °C overnight. The precipitate was obtained by filtration and thoroughly washed with 10 mL diethyl ether. The mother liquor was concentrated to yield about 1 mL solution. Again, diethyl ether (3 mL) was slowly added and the precipitate was obtained as described above. The combined solids were dried at high vacuum to yield **200** (1.0 g, 1.9 mmol, 97%) as white solid (*R_f* 0.00 ethyl acetate).

¹H NMR (300 MHz, CDCl₃) δ 8.32-7.45 (m, 15H), 3.91-3.79 (m, 2H), 1.70-1.16 (series of m, 26H), 0.88 (t, *J* = 6.9 Hz, 3H). Anal. Calcd for C₃₃H₄₆BrP: C, 71.60; H, 8.38; Br, 14.43.



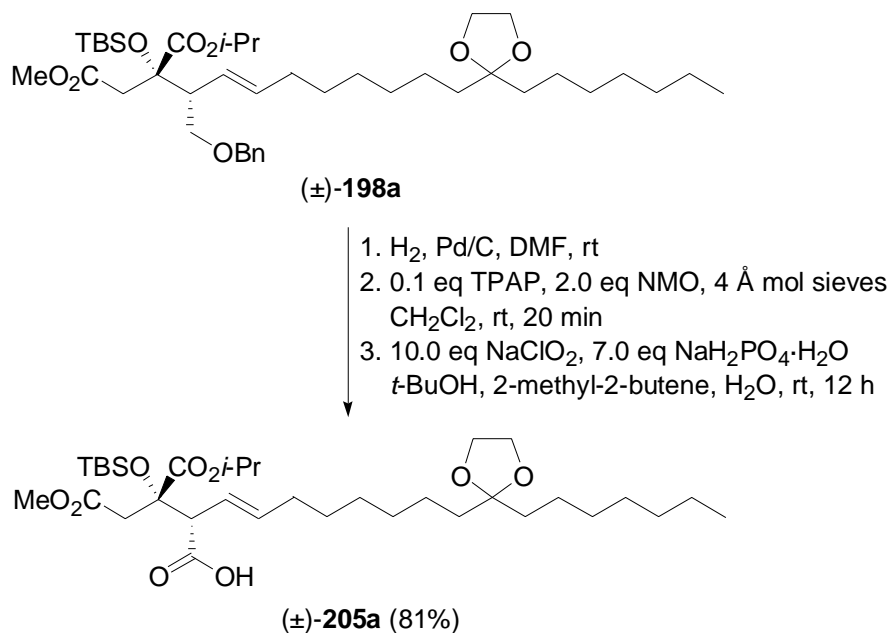
Olefin (±)-(Z)-198c. Through a solution of the terminal olefin $(\pm)\text{-syn-193}$ (20 mg, 0.05 mmol, 1.0 eq) in CH₂Cl₂ and MeOH (4/1, 5 mL) at -78 °C was bubbled a stream of ozone until the color of the reaction mixture turned blue (~2 min). The excess ozone was removed by a nitrogen stream (disappearance of the blue color) and then Me₂S (0.26 μL, 0.4 mmol, 8.0 eq) was added at -78 °C. The reaction mixture was allowed to warm to ambient temperature and stirred at this temperature until TLC indicated complete consumption of the ozonide (~3 h). The reaction mixture was then concentrated at reduced pressure to provide the crude aldehyde $(\pm)\text{-syn-67}$ (*R_f* 0.24 heptane/ethyl acetate 5/1) which was used without further purification.

To a solution of the Wittig salt **200** (30 mg, 0.05 mmol, 1.2 equiv) in toluene (2 mL) was added KHMDS (0.5 M solution in THF, 0.1 mL, 0.05 mmol, 1.1 eq) at 0 °C and the resulting

⁴⁰⁴ Kumar, V.; Dev, S. *Tetrahedron* **1987**, *43*, 5933-5948.

suspension was stirred for 15 min at 0 °C. The solution was cooled to -78 °C and a pre-cooled (-78 °C) solution of the aldehyde (\pm)-*syn*-**67** (0.05 mmol, 1.0 eq) in toluene (2 mL) was added. The reaction mixture was warmed to ambient temperature, stirred over night, quenched by the addition of saturated aq NH₄Cl and extracted (3 × 3 mL). The combined organic layers were dried over MgSO₄ and concentrated. Flash chromatography (heptane/ethyl acetate 20/1) afforded the olefin (\pm)-(*Z*)-**198a** (5.1 mg, 0.01 mmol, 17%) as a pale yellow oil (*R_f* 0.5 heptane/ethyl acetate 5/1).

¹H NMR (300 MHz, CDCl₃) δ 7.28-7.22 (m, 5H), 7.45 (ddd, *J* = 11.3, 7.2, 7.2 Hz, 1H), 5.27 (dd, *J* = 10.7, 10.7 Hz, 1H), 4.90 (sept, *J* = 6.2 Hz, 1H), 4.41 (s, 2H), 3.73 (dd, *J* = 9.5, 6.1 Hz, 1H), 3.56 (s, 3H), 3.24 (dd, *J* = 9.6, 5.8 Hz, 1H), 3.05-2.97 (m, 1H), 2.97 (d^{AB}, *J* = 15.3 Hz, 1H), 2.84 (d^{AB}, *J* = 15.3 Hz, 1H), 2.11-1.84 (m, 2H), 1.27-1.18 (m, 24H), 1.17 (d, *J* = 6.6 Hz, 3H), 1.14 (d, *J* = 6.3 Hz, 3H), 0.82 (t, *J* = 7.1 Hz, 3H), 0.78 (s, 9H), 0.13 (s, 3H), 0.00 (s, 3H); ¹³C NMR (147 MHz, CDCl₃) δ 172.1 (C), 170.6 (C), 138.3 (C), 133.3 (CH), 128.3 (2 × CH), 127.6 (2 × CH), 127.5 (CH), 79.8 (C), 73.1 (CH₂), 70.4 (CH₂), 69.0 (CH), 51.4 (CH₃), 46.8 (CH), 44.0 (CH₂), 31.9 (CH₂), 29.7 (CH₂), 29.63 (CH₂), 29.57 (CH₂), 29.5 (CH₂), 29.4 (CH₂), 27.9 (CH₂), 26.0 (3 × CH₃), 22.7 (CH₂), 21.72 (CH₃), 21.67 (CH₃), 19.0 (C), 14.1 (CH₃), -2.5 (CH₃), -2.8 (CH₃); IR (in substance) ν 2925-2855, 1750 cm⁻¹. Anal. Calcd for C₃₉H₆₈O₆Si: C, 70.86; H, 10.37. Found: C, 70.93; H, 10.22.



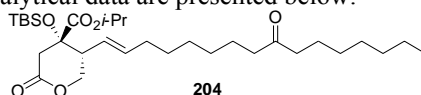
Acid (\pm)-205a.³⁸⁸ To a solution of the olefin (\pm)-**198a** (0.19 g, 0.26 mmol, 1.0 eq) in DMF (5 mL, 20 mL/mmol **198a**) was added palladium on activated carbon (Pd/C) (110 mg, 50 mg/0.1 mmol). The flask was then equipped with a three way faucet connected to a hydrogen

balloon. The suspension was carefully degassed, recharged with hydrogen and vigorously stirred until TLC indicated complete consumption of the starting material (R_f 0.56 heptane/ethyl acetate 1/1). The Pd/C-catalyst was removed by filtration and the solvents were evaporated under *high vacuum at ambient temperature* in order to avoid lactonization. The crude alcohol (\pm)-**203a** (R_f 0.38 heptane/ethyl acetate 1/1) was immediately used for the next reaction due to its susceptibility to lactonization.⁴⁰⁵

To a solution of the crude alcohol (\pm)-**203a** in CH_2Cl_2 (5 mL, 20 mL/mmol **203a**) was added freshly activated 4 Å molecular sieves (200 mg), *N*-methylmorpholine-*N*-oxide (NMO) (61 mg, 0.51 mmol, 2.0 eq) and tetrapropylammoniumperuthenate (TPAP) (12.7 mg, 0.03 mmol, 0.1 equiv). The resulting black suspension was stirred for 20 min at rt and then filtrated through a plug of silica gel (washing with heptane/ethylacetate 20/1). The solvents were then evaporated under reduced pressure and the crude aldehyde (\pm)-**510a** (R_f 0.59 heptane/ethyl acetate 1/1) was dissolved in *t*-BuOH (5 mL, 20 mL/mmol **203a**) and 2-methyl-2-butene (1 mL, 4 mL/mmol **203a**) to which a solution of NaClO_2 (0.24 g, 2.6 mmol, 10.0 eq) and $\text{NaH}_2\text{PO}_4 \cdot \text{H}_2\text{O}$ (0.25 mg, 1.8 mmol, 7.0 eq) in water (1 mL, 4 mL/mmol **203a**) was added. The reaction mixture was vigorously stirred at ambient temperature for 12 h, diluted with water and extracted with CH_2Cl_2 (3 × 20 mL). The combined extracts were dried over MgSO_4 and concentrated. Flash chromatography (heptane/ethylacetate 10/1 to 5/1 to 1/1) afforded the acid (\pm)-**205a** (0.13 g, 0.21 mmol, 81%) as pale yellow oil (R_f 0.29 heptane/ethyl acetate 1/1).

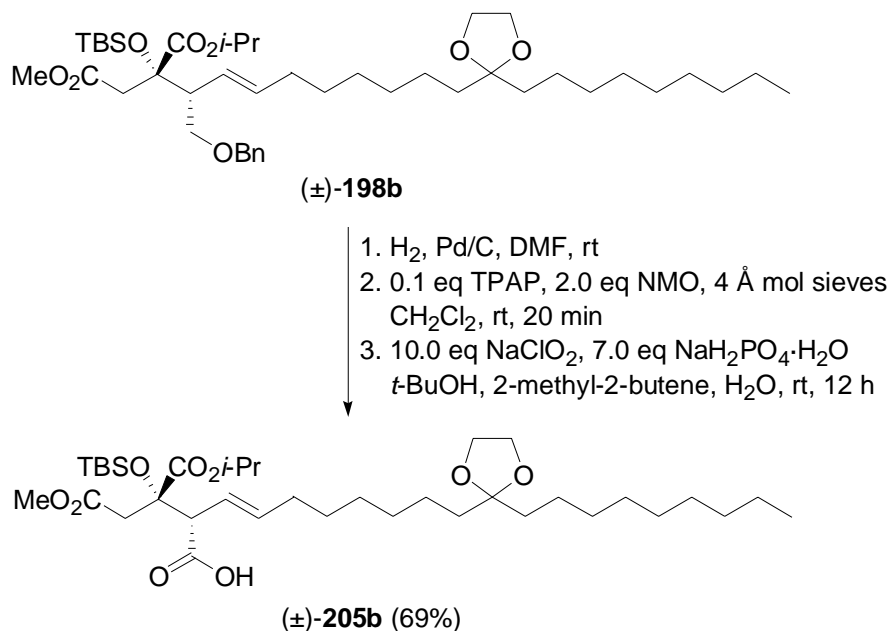
^1H NMR (500 MHz, CDCl_3) δ 5.50-5.42 (m, 2H), 4.94 (sept, $J = 6.2$ Hz, 1H), 3.82 (s, 4H), 3.55 (s, 3H), 3.36 (d, $J = 8.3$ Hz, 1H), 2.95 (d^{AB}, $J = 15.2$ Hz, 1H), 2.72 (d^{AB}, $J = 15.2$ Hz, 1H), 1.91 (ddd, $J = 7.0, 6.7, 6.7$ Hz, 2H), 1.51-1.49 (m, 4H), 1.27-1.14 (m, 24H), 0.91 (t, $J = 6.6$ Hz, 3H), 0.75 (s, 9H), 0.11 (s, 3H), 0.00 (s, 3H) no CO_2H -resonance observed; ^{13}C NMR (126 MHz, CDCl_3) δ 175.0 (C), 170.7 (C), 170.1 (C), 137.1 (C), 122.7 (CH), 111.9 (C), 79.7 (C), 69.7 (CH), 64.9 (2 × CH_2), 58.3 (CH or CH_3), 51.7 (CH or CH_3), 43.4 (CH_2), 37.14 (CH_2), 37.08 (CH_2), 32.5 (CH_2), 31.8 (CH_2), 29.9 (CH_2), 29.7 (CH_2), 29.3 (CH_2), 29.1 (CH_2),

⁴⁰⁵ For one representative lactone analytical data are presented below:



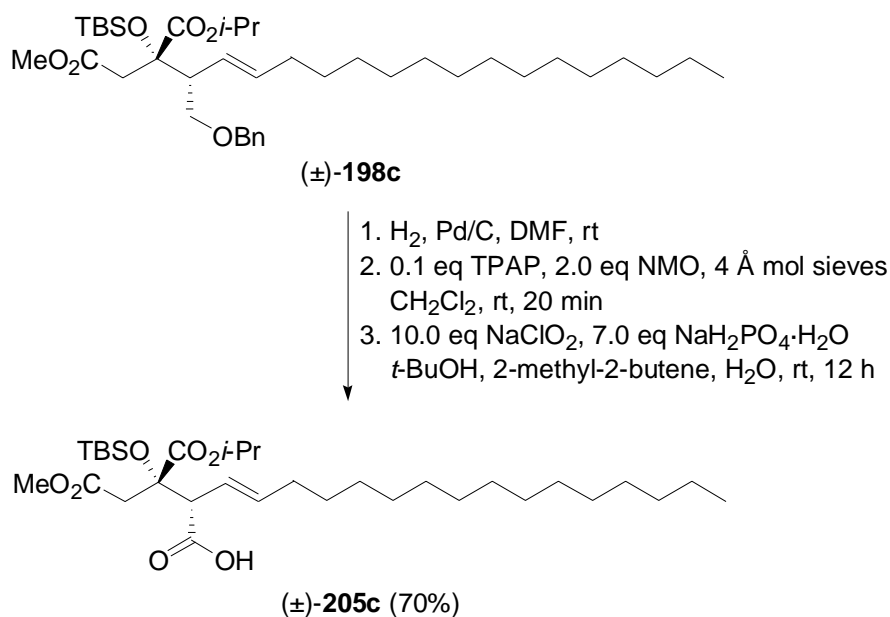
Lactone 204. ^1H NMR (300 MHz, CDCl_3) δ 5.62 (ddd, $J = 15.3, 6.9, 6.9$ Hz, 1H), 5.17 (dd, $J = 15.3, 8.8$ Hz, 1H), 5.01 (sept, $J = 6.3$ Hz, 1H), 4.38 (dd, $J = 11.4, 11.4$ Hz, 1H), 4.16 (dd, $J = 11.0, 5.5$ Hz, 1H), 3.06 (d, $J = 17.9$ Hz, 1H), 2.89 (ddd, $J = 11.7, 8.6, 5.5$ Hz, 1H), 2.70 (d, $J = 18.2$ Hz, 1H), 2.37 (dd, $J = 7.5, 7.5$ Hz, 4H), 1.96 (ddd, $J = 6.5, 6.5, 6.5$ Hz, 2H), 1.60-1.47 (m, 2H), 1.33-1.20 (m, 20H), 0.89 (s, 9H), 0.87 (t, $J = 7.3$ Hz, 3H), 0.20 (s, 3H), 0.10 (s, 3H); ^{13}C NMR (75 MHz, CDCl_3) δ 211.6 (C), 171.1 (C), 168.3 (C), 137.2 (CH), 121.9 (CH), 76.8 (C), 69.8 (CH), 69.2 (CH_2), 45.6 (CH), 42.8 (CH_2), 42.7 (CH_2), 41.1 (CH_2), 32.6 (CH_2), 31.7 (CH_2), 29.7 (CH_2), 29.2 (CH_2), 29.1 (CH_2), 28.9 (CH_2), 28.8 (CH_2), 25.9 (3 × CH_3), 23.9 (CH_2), 23.7 (CH_2), 22.6 (CH_2), 21.9 (CH_3), 21.8 (CH_3), 18.7 (C), 14.1 (CH_3), -3.0 (CH_3), -3.1 (CH_3); IR (in substance) ν 2925-2855, 1745, 1715 cm^{-1} . Anal. Calcd for $\text{C}_{31}\text{H}_{56}\text{O}_6\text{Si}$: C, 66.87; H, 10.10.

28.8 (CH₂), 25.9 (3 × CH₃), 23.84 (CH₂), 23.76 (CH₂), 22.6 (CH₂), 21.8 (CH₃), 21.6 (CH₃), 18.8 (C), 14.1 (CH₃), -2.7 (CH₃), -2.9 (CH₃); IR (in substance) ν 2930-2855, 1750, 1715 cm⁻¹. Anal. Calcd for C₃₄H₆₂O₉Si: C, 63.52; H, 9.72. Found: C, 63.45; H, 9.41.



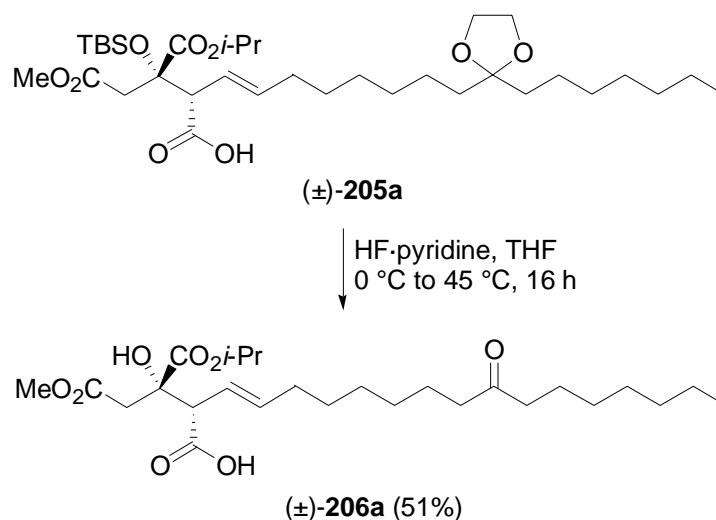
Acid (±)-205b.³⁸⁸ As described for the preparation of the acid (±)-**205a**, olefin (±)-**198b** (79 mg, 0.11 mmol, *R_f* 0.67 heptane/ethyl acetate 1/1) was debenzylated to afford the corresponding alcohol (±)-**203b** (*R_f* 0.50 heptane/ethyl acetate 1/1). (±)-**203b** was then treated with NMO (25 mg, 0.21 mmol) and TPAP (4 mg, 0.01 mmol). The resulting crude aldehyde (±)-**510b** (*R_f* 0.62 heptane/ethyl acetate 1/1) was oxidized with NaClO₂ (96 mg, 1.1 mmol) and NaH₂PO₄·H₂O (101 mg, 0.7 mmol). Flash chromatography (heptane/ethylacetate 10/1 to 1/1) afforded the acid (±)-**205b** (49 mg, 0.07 mmol, 69%) as pale yellow oil (*R_f* 0.38 heptane/ethyl acetate 1/1).

¹H NMR (300 MHz, CDCl₃) δ 5.58-5.54 (m, 2H), 5.02 (sept, *J* = 6.3 Hz, 1H), 3.90 (s, 4H), 3.62 (s, 3H), 3.40 (d, *J* = 8.9 Hz, 1H), 3.04 (d, *J* = 15.2 Hz, 1H), 2.80 (d, *J* = 15.3 Hz, 1H), 2.01-1.97 (m, 2H), 1.58-1.53 (m, 4H), 1.35-1.22 (m, 28H), 0.82 (s, 9H), 0.86 (t, *J* = 6.9 Hz, 3H), 0.18 (s, 3H), 0.07 (s, 3H), no CO₂H-resonance observed; ¹³C NMR (75 MHz, CDCl₃) δ 175.2 (C), 170.7 (C), 170.1 (C), 137.1 (CH), 122.7 (CH), 111.9 (C), 79.7 (C), 69.7 (CH), 64.9 (2 × CH₂), 58.4 (CH or CH₃), 51.6 (CH or CH₃), 43.4 (CH₂), 37.2 (CH₂), 37.1 (CH₂), 32.5 (CH₂), 31.9 (CH₂), 30.0 (CH₂), 29.7 (CH₂), 29.5 (CH₂), 29.4 (CH₂), 29.3 (CH₂), 29.1 (CH₂), 28.8 (CH₂), 25.9 (3 × CH₃), 23.8 (CH₂), 23.7 (CH₂), 22.7 (CH₂), 21.8 (CH₃), 21.6 (CH₃), 18.8 (C), 14.1 (CH₃), -2.7 (CH₃), -2.9 (CH₃); IR (in substance) ν 2925-2855, 1745, 1710 cm⁻¹. Anal. Calcd for C₃₆H₆₆O₉Si: C, 64.49; H, 9.92. Found: C, 64.18; H, 9.92.



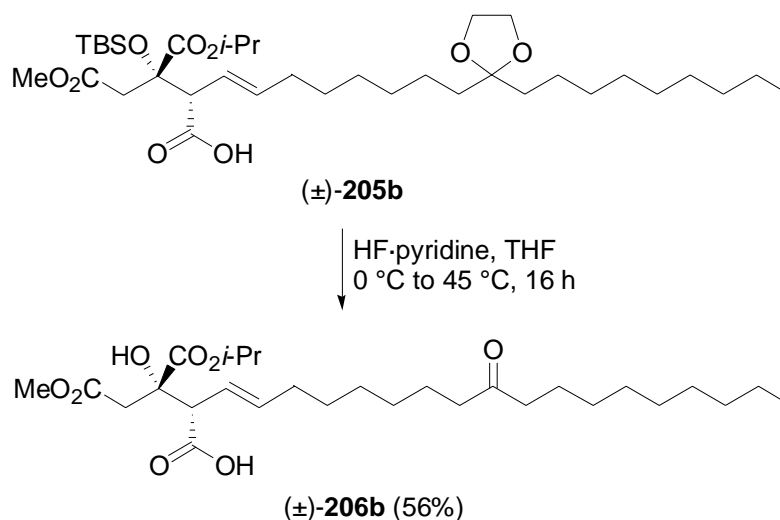
Acid (±)-205c.³⁸⁸ As described for the preparation of the acid (±)-**205a**, olefin (±)-*syn*-**198c** (0.35 g, 0.53 mmol) (R_f 0.71 heptane/ethyl acetate 1/1) was debenzylated to provide the corresponding alcohol (±)-**203** (R_f 0.50 heptane/ethyl acetate 1/1) that was treated with NMO (0.13 g, 1.1 mmol) and TPAP (26 mg, 0.05 mmol). The resulting crude aldehyde (±)-**510c** (R_f 0.59 heptane/ethyl acetate 1/1) was subjected to NaClO₂ (0.16 g, 5.3 mmol) and NaH₂PO₄·H₂O (0.13 g, 3.7 mmol). Flash chromatography (heptane/ethyl acetate 10/1 to 1/1) afforded the acid **205c** (0.22 g, 0.37 mmol, 70%) as a pale yellow oil (R_f 0.35 heptane/ethyl acetate 1/1).

¹H NMR (300 MHz, CDCl₃) δ 5.70 (dt, J = 15.3, 6.8 Hz, 1H), 5.51 (dd, J = 15.3, 9.7 Hz, 1H), 5.01 (sept, J = 6.2 Hz, 1H), 4.37 (br s, 1H), 3.67 (s, 3H), 3.34 (d, J = 9.8 Hz, 1H), 3.02 (d^{AB}, J = 16.1 Hz, 1H), 2.83 (d^{AB}, J = 15.3 Hz, 1H), 2.02 (td, J = 6.6, 6.6 Hz, 2H), 1.29-1.21 (m, 30H), 0.88 (t, J = 7.1 Hz, 3H), 0.84 (s, 9H), 0.20 (s, 3H), 0.09 (s, 3H), no CO₂H-resonance observed; ¹³C NMR (75 MHz, CDCl₃) δ 174.1 (C), 170.6 (C), 170.0 (C), 137.3 (CH), 122.6 (CH), 79.7 (C), 69.7 (CH), 58.2 (CH or CH₃), 51.5 (CH or CH₃), 43.4 (CH₂), 32.5 (CH₂), 31.9 (CH₂), 29.6 (CH₂), 29.5 (CH₂), 29.4 (CH₂), 29.3 (CH₂), 29.2 (CH₂), 28.8 (CH₂), 25.9 (3 × CH₃), 22.6 (CH₂), (several overlapping signals between 43.4 and 22.6, total number of (CH₂): 14) 21.7 (CH₃), 21.6 (CH₃), 18.8 (C), 14.0 (CH₃), -2.7 (CH₃), -2.9 (CH₃); IR (in substance) ν 2980-2855, 1748, 1710 cm⁻¹. Anal. Calcd for C₃₂H₆₀O₇Si: C, 65.71; H, 10.34. Found: C, 65.98; H, 10.53.



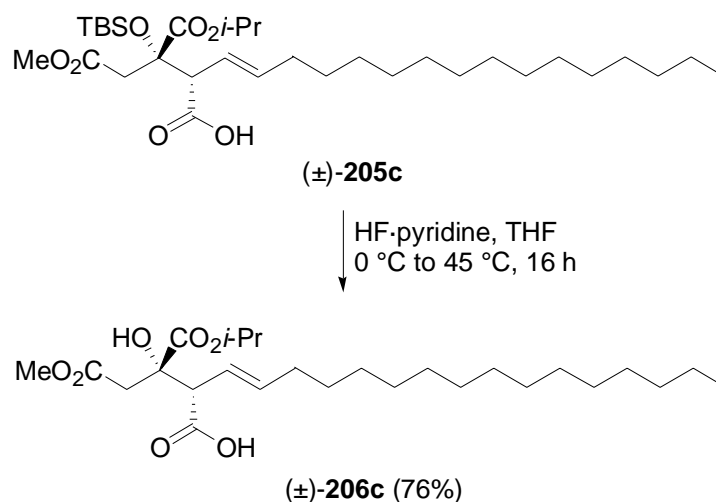
β -Hydroxy Acid (±)-206a.³⁸⁸ To a solution of the acid (±)-**205a** (60 mg, 0.09 mmol, 1.0 eq) in THF (4 mL, 4 mL/0.1 mmol **205a**) was added HF·pyridine (0.15 mL, 0.15 mL/0.1 mmol **205a**) at 0 °C. The reaction mixture was stirred over night at 45 °C. If TLC indicates incomplete consumption of the starting material, additional HF·pyridine (0.15 mL, 0.15 mL/0.1 mmol **205a**) is added and stirring is continued for another 3 h at 45 °C. The reactions was quenched by the careful addition of saturated aq NaHCO₃ and extracted with CH₂Cl₂ (3 x 5 mL). The combined organic layers were dried over MgSO₄ and concentrated. Flash chromatography (heptane/ethyl acetate 1/1 to ethyl acetate) afforded the β -hydroxy acid (±)-**206a** (22 mg, 0.045 mmol, 51%) as colorless oil (*R_f* 0.21 ethyl acetate).

¹H NMR (300 MHz, CDCl₃) δ 5.65 (ddd, *J* = 15.1, 6.6, 6.6 Hz, 1H), 5.52 (dd, *J* = 15.3, 9.6 Hz, 1H), 5.08 (sept, *J* = 6.3 Hz, 1H), 4.25 (s, 1H), 3.66 (s, 3H), 3.32 (d, *J* = 9.6 Hz, 1H), 3.00 (d^{AB}, *J* = 16.3 Hz, 1H), 2.83 (d^{AB}, *J* = 16.3 Hz, 1H), 2.37 (t, *J* = 7.5 Hz, 4H), 2.00 (ddd, *J* = 6.9, 6.8, 6.8 Hz, 2H), 1.57-1.50 (m, 4H), 1.35-1.23 (m, 20H), 0.86 (t, *J* = 6.9 Hz, 3H), no CO₂H-resonance observed; ¹³C NMR (75 MHz, CDCl₃) δ 211.8 (C), 173.8 (C), 171.7 (C), 170.3 (C), 138.1 (CH), 121.2 (CH), 75.7 (C), 70.8 (CH), 56.9 (CH or CH₃), 51.9 (CH or CH₃), 42.8 (CH₂), 42.7 (CH₂), 41.6 (CH₂), 32.4 (CH₂), 31.7 (CH₂), 29.2 (CH₂), 29.1 (CH₂), 29.0 (CH₂), 28.9 (CH₂), 28.6 (CH₂), 23.9 (CH₂), 23.7 (CH₂), 22.6 (CH₂), 21.7 (CH₃), 21.5 (CH₃), 14.1 (CH₃); IR (in substance) ν 3495, 2930-2855, 1740, 1715 cm⁻¹. Anal. Calcd for C₂₆H₄₄O₈: C, 64.44; H, 9.15. Found: C, 64.50; H, 9.18.



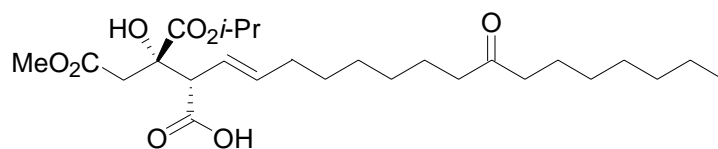
β -Hydroxyacid (±)-206b.³⁸⁸ As described for the β -hydroxy acid (±)-**206a**, the acid (±)-**205b** (55 mg, 0.08 mmol) was treated with HF·pyridine (0.12 ml). Flash chromatography (heptane/ethyl acetate 1/1 to ethyl acetate) afforded the β -hydroxy acid (±)-**206b** (23 mg, 0.45 mmol, 56%) as a colorless oil (R_f 0.26 ethyl acetate).

¹H NMR (300 MHz, CDCl₃) δ 5.70-5.51 (m, 2H), 5.10 (sept, $J = 6.2$ Hz, 1H), 4.23 (br s, 1H (OH)), 3.67 (s, 3H), 3.33 (d, $J = 9.0$ Hz, 1H), 3.02 (d^{AB}, $J = 16.2$ Hz, 1H), 2.85 (d^{AB}, $J = 16.2$ Hz, 1H), 2.38 (t, $J = 7.4$ Hz, 4H), 2.02 (ddd, $J = 6.6, 6.4, 6.4$ Hz, 2H), 1.61-1.50 (m, 4H), 1.31-1.24 (m, 24H), 0.88 (t, $J = 6.6$ Hz, 3H), no CO₂H resonance observed; ¹³C NMR (75 MHz, CDCl₃) δ 211.7 (C), 174.5 (C), 171.8 (C), 170.4 (C), 137.9 (CH), 121.5 (CH), 75.8 (C), 70.7 (CH), 57.0 (CH or CH₃), 51.9 (CH or CH₃), 42.8 (CH₂), 42.7 (CH₂), 41.6 (CH₂), 32.4 (CH₂), 31.8 (CH₂), 31.6 (CH₂), 29.4 (CH₂), 29.2 (CH₂), 29.04 (CH₂), 28.99 (CH₂), 28.8 (CH₂), 28.6 (CH₂), 23.9 (CH₂), 23.7 (CH₂), 22.6 (CH₂), 21.7 (CH₃), 21.5 (CH₃), 14.0 (CH₃); IR (in substance) ν 3480, 2925-2855, 1735, 1710 cm⁻¹. Anal. Calcd for C₂₈H₄₈O₈: C, 65.60; H, 9.44. Found: C, 65.70; H, 9.57.



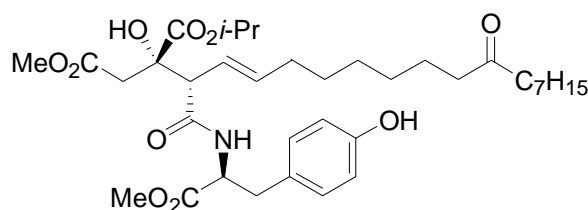
β -Hydroxy Acid (\pm)-206c.³⁸⁸ According to the procedure for the preparation of β -hydroxy acid (\pm)-206a, acid (\pm)-205c (50 mg, 0.09 mmol) was treated with HF·pyridine (0.13 ml). Flash chromatography (heptane/ethyl acetate 1/1 to ethyl acetate) afforded β -hydroxy acid (\pm)-206c (31 mg, 0.07 mmol, 76%) as colorless oil (R_f 0.23 ethyl acetate).

¹H NMR (300 MHz, CDCl₃) δ 5.70 (ddd, J = 15.3, 6.8, 6.8 Hz, 1H), 5.51 (dd, J = 15.3, 9.7 Hz, 1H), 5.01 (sept, J = 6.2 Hz, 1H), 4.37 (br s, 1H), 3.67 (s, 3H), 3.34 (d, J = 9.8 Hz, 1H), 3.02 (d^{AB}, J = 16.1 Hz, 1H), 2.83 (d^{AB}, J = 16.1 Hz, 1H), 2.01 (td, J = 7.2, 7.2 Hz, 2H), 1.36-1.17 (m, 30 H), 0.86 (t, J = 7.1 Hz, 3H) no CO₂H-resonance observed; ¹³C NMR (75 MHz, CDCl₃) δ 171.8 (C), 171.5 (C), 170.2 (C), 138.6 (CH), 120.6 (CH), 75.7 (C), 71.0 (CH), 56.7 (CH or CH₃), 52.0 (CH or CH₃), 41.5 (CH₂), 32.5 (CH₂), 31.9 (CH₂), 29.68 (CH₂), 29.65 (CH₂), 29.6 (CH₂), 29.43 (CH₂), 29.36 (CH₂), 29.1 (CH₂), 28.8 (CH₂), 22.7 (CH₂), (several overlapping signals between 41.5 and 22.7, total number of (CH₂): 14) 21.7 (CH₃), 21.5 (CH₃), 14.1 (CH₃); IR (in substance) ν 2980-2855, 1745 cm⁻¹. Anal. Calcd for C₂₆H₄₆O₇: C, 66.35; H, 9.85. Found: C, 66.43; H, 9.69.

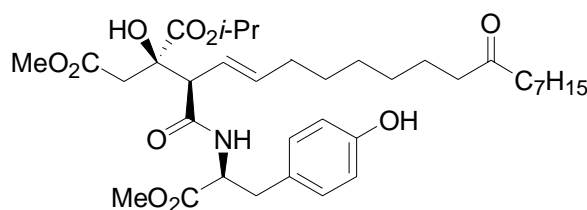


(\pm)-206a

1. 1.5 eq PyBOP, 4.4 eq NMM
1.5 eq (*S*)-TyrMe, CH₂Cl₂, rt, 18 h (71%)
2. separation of diastereomers by
reversed phase HPLC



(-)-65a



(+)-207a

Viridifungin A Ester (-)-65a and (+)-207a.³⁸⁸ To a solution of the β -hydroxy acid (\pm)-206a (27 mg, 0.06 mmol, 1.0 eq) in CH₂Cl₂ (1 mL, 20 mL/mmol 206a) was added benzotriazol-1-yloxytripyrrolidino-phosphonium-hexafluorophosphate (PyBOP) (44 mg, 0.08 mmol, 1.5 eq), *N*-methylmorpholine (NMM) (27 μ l, 0.24 mmol, 4.4 eq) and (*S*)-tyrosine methyl ester (16 mg, 0.08 mmol, 1.5 eq) at ambient temperature. The resulting mixture was stirred over night and then added to saturated aq NaHCO₃. The aqueous layer was extracted

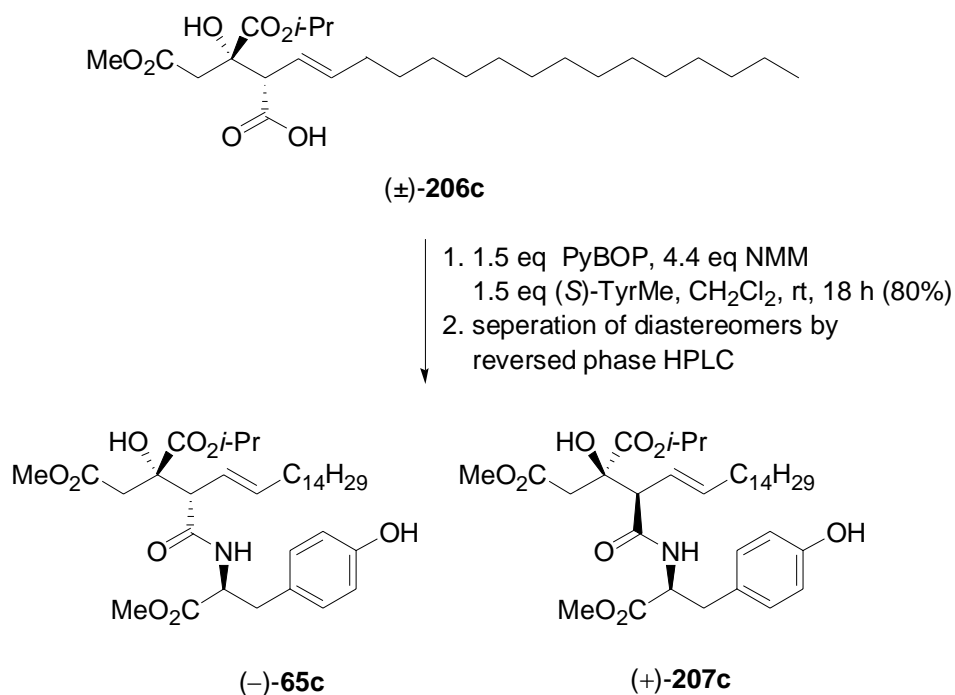
with CH_2Cl_2 (3 x 5 mL). The combined organic phases were dried over MgSO_4 and concentrated. Flash chromatography (heptane/ethyl acetate 1/1 to ethyl acetate) afforded (-)-**65a** and (+)-**207a** as a 1/1 mixture (26 mg, 0.04 mmol, 71%) as pale yellow oil (R_f 0.53 ethyl acetate). The diastereomers were separated by reversed-phase HPLC: Column: VYDAC 208TP1030 – C8, 30 x 250 mm, 10 μm ; Eluent: isocratic A/B (solvent A: H_2O + 5 % CH_3CN + 5 % CH_3OH + 0.1 % TFA, solvent B: CH_3CN + 0.1 % TFA, 40 ml/min). (-)-**65a** /(+)-**207a**: A/B 57/43 R_t (-)-**65a**: 58 min, R_t (+)-**207a**: 63 min.

(-)-**65a**: ^1H NMR (500 MHz, CDCl_3) δ 6.95 (d, J = 8.4 Hz, 2H, 5'-CH-Ar), 6.76 (d, J = 8.5 Hz, 2H, 6'-CH-Ar), 6.67 (d, J = 7.9 Hz, 1H, NH), 6.34 (s, 1H, Ph-OH), 5.63 (ddd, J = 15.2, 6.6, 6.6 Hz, H, 6-CH=), 5.49 (dd, J = 15.3, 9.6 Hz, 1H, 5-CH=), 5.05 (sept, J = 6.3 Hz, 1H, $\text{CO}_2i\text{-Pr-CH}$), 4.74 (ddd, J = 7.1, 7.0, 5.1 Hz, 1H, 2'-CH), 4.49 (s, 1H, 3-OH), 3.72 (s, 3H, 1'- CO_2CH_3), 3.65 (s, 3H, 1- CO_2CH_3), 3.16 (d, J = 9.5 Hz, 1H, 4-CH), 3.09 (dd^{AB}, J = 14.1, 4.9 Hz, 1H, 3'- CH_2), 3.00 (dd^{AB}, J = 14.1, 6.8 Hz, 1H, 3'- CH_2), 2.85 (d^{AB}, J = 16.0 Hz, 1H, 2- CH_2), 2.68 (d^{AB}, J = 16.0 Hz, 1H, 2- CH_2), 2.42 (t, J = 7.2 Hz, 2H, 12- or 14- CH_2), 2.41 (t, J = 7.4 Hz, 2H, 12- or 14- CH_2), 2.01-1.92 (m, 2H, 7- CH_2), 1.59-1.48 (m, 4H, 11- and 15- CH_2), 1.34-1.18 (m, 20 H, $Oi\text{-Pr-CH}_3$, 8-, 9-, 10- CH_2 and 16-, 17-, 18-, 19- CH_2), 0.86 (t, J = 6.9 Hz, 3H, 20- CH_3); ^{13}C NMR (CDCl_3 , 126 MHz) δ 213.4 (13-C=O), 172.2 ($\text{CO}_2i\text{-Pr}$), 171.6 (1'- CO_2CH_3), 170.6 (CONH), 170.5 (1- CO_2CH_3), 155.4 (7'-COH-Ar), 137.8 (6-CH=), 130.4 (2 x 5'-CH-Ar), 127.3 (4'-C-Ar), 122.4 (5-CH=), 115.5 (2 x 6'-CH-Ar), 76.1 (3-C), 70.2 (- $Oi\text{-Pr-CH}$), 57.6 (4-CH), 53.3 (2'-CH), 52.3 (CO_2CH_3), 51.8 (CO_2CH_3), 43.0 (12- or 14- CH_2), 42.7 (12- or 14- CH_2), 41.6 (2- CH_2), 36.6 (3'- CH_2), 32.5 (7- CH_2), 31.7 (18- CH_2), 29.7 (CH_2), 29.2 (CH_2), 29.0 (CH_2), 28.9 (CH_2), 28.5 (CH_2), 23.9 (11- or 15- CH_2), 23.5 (11- or 15- CH_2), 22.6 (19- CH_2), 21.7 (- $Oi\text{-Pr-CH}_3$), 21.6 (- $Oi\text{-Pr-CH}_3$), 14.1 (20- CH_3); IR (in substance) ν 3334, 2926, 2464, 1743 cm^{-1} . Anal. Calcd. for $\text{C}_{36}\text{H}_{55}\text{NO}_{10}$: C, 65.33; H, 8.38. Found: C, 65.47; H, 8.48. $[\alpha]_{\text{D}}^{25}$ -6.6 (c 0.15, CHCl_3), literature for trimethylester: $[\alpha]_{\text{D}}^{25}$ -23.0 (c 0.47, MeOH).

(+)-**207a**: ^1H NMR (500 MHz, CDCl_3) δ 7.05 (d, J = 7.7 Hz, 1H, NH), 7.01 (br s, 1H, Ph-OH), 6.94 (d, J = 8.5 Hz, 2H, 5'-CH-Ar), 6.77 (d, J = 8.5 Hz, 2H, 6'-CH-Ar), 5.55 (ddd, J = 15.2, 6.4, 6.4 Hz, 1H, 6-CH=), 5.23 (dd, J = 15.3, 9.6 Hz, 1H, 5-CH=), 5.03 (sept, J = 6.2 Hz, 1H, - $Oi\text{-Pr-CH}$), 4.73 (ddd, J = 7.9, 7.9, 4.7 Hz, 1H, 2'-CH), 4.23 (s, 1H, 3-OH), 3.75 (s, 3H, 1'- CO_2CH_3), 3.64 (s, 3H, 1- CO_2CH_3), 3.15-3.08 (m, 1H, 3'- CH_2), 3.13 (d, J = 9.5 Hz, 1H, 4-CH), 3.05 (d, J = 16.3 Hz, 1H, 2- CH_2), 2.89 (d, J = 16.1 Hz, 1H, 2- CH_2), 2.91-2.86 (m, 1H, 3'- CH_2), 2.45 (t, J = 7.0 Hz, 2H, 12- or 14- CH_2), 2.43 (t, J = 7.5 Hz, 2H, 12- or 14- CH_2), 1.92-1.83 (m, 2H, 7- CH_2), 1.62-1.48 (m, 4H, 11- and 15- CH_2), 1.30-1.15 (m, 20H, - $Oi\text{-Pr-CH}_3$, 8-, 9-, 10- CH_2 and 16-, 17-, 18-, 19- CH_2), 0.86 (t, J = 6.9 Hz, 3H, 20- CH_3); ^{13}C NMR (CDCl_3 ,

(ddd, $J = 7.5, 7.4, 5.0$ Hz, 1H, 2'-CH), 4.47 (s, 1H, 3-OH), 3.72 (s, 3 H, 1'-CO₂CH₃), 3.65 (s, 3H, 1-CO₂CH₃), 3.15 (d, $J = 9.5$ Hz, 1H, 4-H), 3.09 (dd^{AB}, $J = 14.2, 4.9$ Hz, 1H, 3'-CH₂), 2.98 (dd^{AB}, $J = 14.1, 6.8$ Hz, 1H, 3'-CH₂), 2.83 (d^{AB}, $J = 16.0$ Hz, 1H, 2-CH₂), 2.62 (d^{AB}, $J = 16.0$ Hz, 1H, 2-CH₂), 2.45 (t, $J = 7.2$ Hz, 2H, 12- or 14-CH₂), 2.43 (t, $J = 7.5$ Hz, 2H, 12- or 14-CH₂), 1.98-1.92 (m, 2H, 7-CH₂), 1.58-1.50 (m, 4H, 11- and 15-CH₂), 1.29-1.20 (m, 24H, *Oi*-Pr-CH₃, 8-,9-,10-CH₂ and 16-,17-,18-,19-,20-,21-CH₂), 0.86 (t, $J = 6.9$ Hz, 3H, 22-CH₃) no signal detected for 7'-OH; ¹³C NMR (CDCl₃, 126 MHz) δ 213.3 (13-C=O), 172.1 (C=O*Pr*), 171.6 (1'-CO₂CH₃), 170.7 (CONH), 170.5 (1-CO₂CH₃), 155.5 (7'-COH-Ar), 137.8 (6-CH=), 130.4 (2 × 5'-CH-Ar), 127.1 (4'-C-Ar), 122.3 (5-CH=), 115.5 (2 × 6'-CH-Ar), 76.1 (3-C), 70.2 (*Oi*-Pr-CH), 57.6 (4-CH), 53.3 (2'-CH), 52.3 (CO₂CH₃), 51.8 (CO₂CH₃), 43.0 (12- or 14-CH₂), 42.7 (12- or 14-CH₂), 41.5 (2-CH₂), 36.7 (3'-CH₂), 32.4 (7-CH₂), 31.8 (20-CH₂), 29.40 (CH₂), 29.36 (CH₂), 29.24 (CH₂), 29.20 (CH₂), 28.9 (2 × CH₂), 28.6 (CH₂), 23.9 (11- or 15-CH₂), 23.5 (11- or 15-CH₂), 22.6 (21-CH₂), 21.7 (*Oi*-Pr-CH₃), 21.5 (*Oi*-Pr-CH₃), 14.1 (22-CH₃); IR (in substance) ν 3346, 2926, 2854, 1741 cm⁻¹. Anal. Calcd for C₃₈H₅₉NO₁₀: C, 66.16; H, 8.62; N, 2.03. Found: C, 66.50; H, 8.78; N, 2.09. $[\alpha]_D^{25} -5.1$ (*c* 1.4, CHCl₃).

(+)-**207b**: ¹H NMR (500 MHz, CDCl₃) δ 7.06 (d, $J = 7.7$ Hz, 1H, NH), 6.93 (d, $J = 8.4$ Hz, 2H, 5'-CH-Ar), 6.77 (d, $J = 8.4$ Hz, 2H, 6'-CH-Ar), 5.54 (ddd, $J = 15.2, 6.4, 6.4$ Hz, 1H, 6-CH=), 5.23 (dd, $J = 15.3, 9.6$ Hz, 1H, 5-CH=), 5.03 (sept, $J = 6.3$ Hz, 1H, *Oi*-Pr-CH), 4.73 (ddd, $J = 7.8, 7.8, 4.7$ Hz, 1H, 2'-H), 4.23 (s, 1H, 3-OH), 3.75 (s, 3H, 1'-CO₂CH₃), 3.64 (s, 3H, 1-CO₂CH₃), 3.16 (dd^{AB}, $J = 14.3, 4.7$ Hz, 1H, 3'-CH₂), 3.13 (d, $J = 9.6$ Hz, 1H, 4-H), 3.05 (d^{AB}, $J = 16.4$ Hz, 1H, 2-CH₂), 2.89 (d^{AB}, $J = 16.4$ Hz, 1 H, 2-CH₂), 2.88 (dd^{AB}, $J = 14.4, 8.0$ Hz, 1H, 3'-CH₂) 2.45 (t, $J = 7.0$ Hz, 2H, 12- or 14-CH₂), 2.42 (t, $J = 7.6$ Hz, 2H, 12- or 14-CH₂), 1.91-1.86 (m, 2H, 7-CH₂), 1.59-1.52 (m, 4H, 11- and 15-CH₂), 1.29-1.20 (m, 24H, *Oi*-Pr-CH₃, 8-,9-,10-CH₂ and 16-,17-,18-,19-,20-,21-CH₂), 0.86 (t, $J = 7.0$ Hz, 3H, 22-CH₃), no signal detected for 7'-OH; ¹³C NMR (CDCl₃, 126 MHz) δ 214.2 (13-C=O), 172.3 (C=O*Pr*), 171.9 (1'-CO₂CH₃), 170.6 (1-CO₂CH₃), 170.4 (CONH), 155.6 (7'-COH), 137.1 (6-CH), 130.2 (2 × 5'-CH), 127.1 (4'-C), 121.6 (5-CH), 115.4 (2 × 6'-CH), 75.8 (3-C), 70.5 (*Oi*-Pr-CH), 58.0 (4-CH), 53.2 (2'-CH), 52.4 (CO₂CH₃), 51.8 (CO₂CH₃), 43.0 (12- or 14-CH₂), 42.7 (12- or 14-CH₂), 41.0 (2-CH₂), 36.5 (3'-CH₂), 32.3 (7-CH₂), 31.8 (20-CH₂), 29.4 (CH₂), 29.3 (CH₂), 29.24 (CH₂), 29.20 (CH₂), 28.8 (CH₂), 28.7 (CH₂), 28.0 (CH₂), 23.9 (11- or 15-CH₂), 23.4 (11- or 15-CH₂), 22.6 (21-CH₂), 21.7 (*Oi*-Pr-CH₃), 21.5 (*Oi*-Pr-CH₃), 14.1 (22-CH₃); IR (in substance) ν 3354, 2926, 2490, 2854, 1741 cm⁻¹. Anal. Calcd for C₃₈H₅₉NO₁₀: C, 66.16; H, 8.62; N, 2.03. Found: C, 66.55; H, 8.62; N, 2.01. $[\alpha]_D^{25} +22.9$ (*c* 1.0, CHCl₃).



Viridiofungin A₂ Ester (-)-65c and (+)-207c.³⁸⁸ As described for the preparation of (-)-**65a** and (+)-**207a**, β -hydroxy acid (±)-**206c** (30 mg, 0.06 mmol) was treated with PyBOP (50 mg, 0.10 mmol), NMM (31 μ l, 0.28 mmol) and (*S*)-tyrosine methyl ester (19 mg, 0.10 mmol). Flash chromatography (heptane/ethyl acetate 1/1 to ethyl acetate) afforded (-)-**65c** and (+)-**207c** as a 1/1 mixture (33 mg, 0.05 mmol, 80%) as pale yellow oil (R_f 0.38 ethyl acetate). The diastereomers were separated by reversed-phase HPLC: Column: VYDAC 208TP1030 – C8, 30 \times 250 mm, 10 μ m; Eluent: isocratic A/B (solvent A: H₂O + 5 % CH₃CN + 5 % CH₃OH + 0.1 % TFA, solvent B: CH₃CN + 0.1 % TFA, 40 ml/min). (-)-**65c**/(+)-**207c**: A/B40/60 R_t (-)-**65c**: 33 min, R_t (+)-**207c**: 35 min.

(-)-**65c**: ¹H NMR (500 MHz, CDCl₃) δ 7.01 (d, J = 8.4 Hz, 2H, 5'-CH-Ar), 6.90 (d, J = 8.1 Hz, 1H, NH), 6.71 (d, J = 8.5 Hz, 2H, 6'-CH-Ar), 5.63 (ddd, J = 15.3, 6.6, 6.6 Hz, 1H, 6-CH=), 5.45 (dd, J = 15.1, 9.7 Hz, 1H, 5-CH=), 5.03 (sept, J = 6.5 Hz, 1H, CO₂*i*-Pr-CH), 5.01 (br s, 1H, 7'-OH), 4.80 (ddd, J = 7.8, 7.8, 5.3 Hz, 1H, 2'-CH), 4.29 (s, 1H, 3-OH), 3.71 (s, 3H, 1'-CO₂CH₃), 3.66 (s, 3H, 1-CO₂CH₃), 3.13 (d, J = 9.4 Hz, 1H, 4-H), 3.11 (dd^{AB}, J = 13.9, 5.7 Hz, 1H, 3'-CH₂), 2.96 (dd^{AB}, J = 14.1, 7.5 Hz, 1H, 3'-CH₂), 2.81 (d^{AB}, J = 16.1 Hz, 1H, 2-CH₂), 2.52 (d^{AB}, J = 16.3 Hz, 1H, 2-CH₂), 2.01-1.94 (m, 2H, 7-CH₂), 1.27-1.21 (m, 30H, -*Oi*-Pr-CH₃, 8-,9-,10-,11-,12-,13-,14-,15-,16-,17-,18-,19-CH₂), 0.87 (t, J = 6.9 Hz, 3H, 20-CH₃); ¹³C NMR (CDCl₃, 126 MHz) δ 172.2 (CO₂*i*-Pr), 171.8 (1'-CO₂CH₃), 170.5 (CONH or 1-CO₂CH₃), 170.4 (1-CO₂CH₃ or CONH), 154.8 (7'-COH-Ar), 137.8 (6-CH=), 130.5 (2 \times 5'-CH-Ar), 127.9 (4'-C-Ar), 122.0 (5-CH=), 115.5 (2 \times 6'-CH-Ar), 75.9 (3-C), 70.4 (-*Oi*-Pr-CH), 57.9 (4-CH), 53.3 (2'-CH), 52.3 (CO₂CH₃), 51.8 (CO₂CH₃), 41.3 (2-CH₂), 37.0 (3'-CH₂), 32.6 (7-CH₂), 31.9 (18-CH₂), 29.69 (CH₂), 29.65 (CH₂), 29.6 (CH₂), 29.5 (CH₂), 29.4

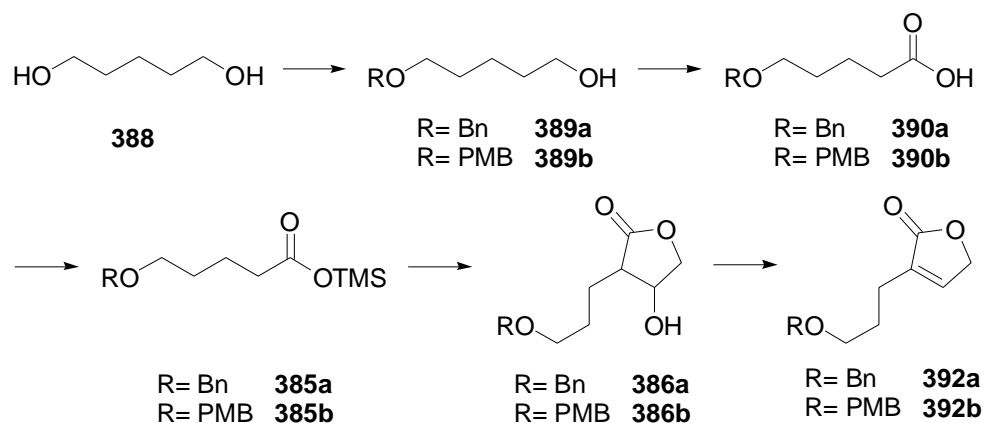
(CH₂), 29.2 (CH₂), 29.0 (CH₂) (several overlapping signals between 29.7 and 29.0, total number of (CH₂): 15), 22.7 (19-CH₂), 21.7 (-*Oi*-Pr-CH₃), 21.5 (-*Oi*-Pr-CH₃), 14.1 (20-CH₃); IR (in substance) ν 3343, 2924, 2854, 1743 cm⁻¹. Anal. Calcd for C₃₆H₅₇NO₉: C, 66.74; H, 8.87. Found: C, 65.47; H, 8.48. $[\alpha]_D^{25}$ -3.9 (*c* 0.19, CHCl₃).

(+)-**207c**: ¹H NMR (500 MHz, CDCl₃) δ 7.06 (d, *J* = 7.9 Hz, 1H, NH), 6.96 (d, *J* = 8.5 Hz, 2H, 5'-CH-Ar), 6.71 (d, *J* = 8.5 Hz, 2H, 6'-CH-Ar), 5.56 (ddd, *J* = 14.8, 6.6, 6.6 Hz, 1H, 6-CH=), 5.31 (dd, *J* = 15.2, 9.6 Hz, 1H, 5-CH=), 5.04 (sept, *J* = 6.2 Hz, 1H, *Oi*-Pr-CH), 5.02 (br s, 1H, 7'-OH), 4.77 (ddd, *J* = 7.1, 7.1, 5.6 Hz, 1H, 2'-H), 4.24 (s, 1H, 3-OH), 3.73 (s, 3H, 1'-CO₂CH₃), 3.63 (s, 3H, 1-CO₂CH₃), 3.14 (d, *J* = 9.6 Hz, 1H, 4-H), 3.08 (dd^{AB}, *J* = 14.1, 5.4 Hz, 1H, 3'-CH₂), 2.98 (d^{AB}, *J* = 16.3 Hz, 1H, 2-CH₂), 2.97 (dd^{AB}, *J* = 14.0, 7.0 Hz, 1H, 3'-CH₂), 2.87 (d^{AB}, *J* = 16.3 Hz, 1H, 2-CH₂), 1.96-1.91 (m, 2H, 7-CH₂), 1.27-1.21 (m, 30H, *Oi*-Pr-CH₃, 8-, 9-, 10-, 11-, 12-, 13-, 14-, 15-, 16-, 17-, 18-, 19-, 20-, 21-CH₂), 0.87 (t, *J* = 6.9 Hz, 3H, 20-CH₃); ¹³C NMR (CDCl₃, 126 MHz) δ 172.3 (CO₂*i*-Pr), 171.9 (1'-CO₂CH₃), 170.6 (CONH or 1-CO₂CH₃), 170.5 (1-CO₂CH₃ or CONH), 154.8 (7'-COH), 137.5 (6-CH), 130.4 (2 × 5'-CH), 127.8 (4'-C), 121.9 (5-CH), 115.4 (2 × 6'-CH), 75.9 (3-C), 70.5 (-*Oi*-Pr-CH), 58.1 (4-CH), 53.1 (2'-CH), 52.3 (CO₂CH₃), 51.8 (CO₂CH₃), 41.1 (2-CH₂), 36.7 (3'-CH₂), 32.6 (7-CH₂), 31.9 (18-CH₂), 29.69 (CH₂), 29.65 (CH₂), 29.6 (CH₂), 29.5 (CH₂), 29.4 (CH₂), 29.2 (CH₂), 29.0 (CH₂) (several overlapping signals between 29.7 and 29.0, total number of (CH₂): 15), 22.7 (19-CH₂), 21.8 (-*Oi*-Pr-CH₃), 21.5 (-*Oi*-Pr-CH₃), 14.1 (20-CH₃); IR (in substance) ν 3343, 2925, 2853, 1743 cm⁻¹. Anal. Calcd for C₃₆H₅₇NO₉: C, 66.74; H, 8.87. Found: C, 66.35; H, 8.87. $[\alpha]_D^{25}$ +20.7 (*c* 0.14, CHCl₃).

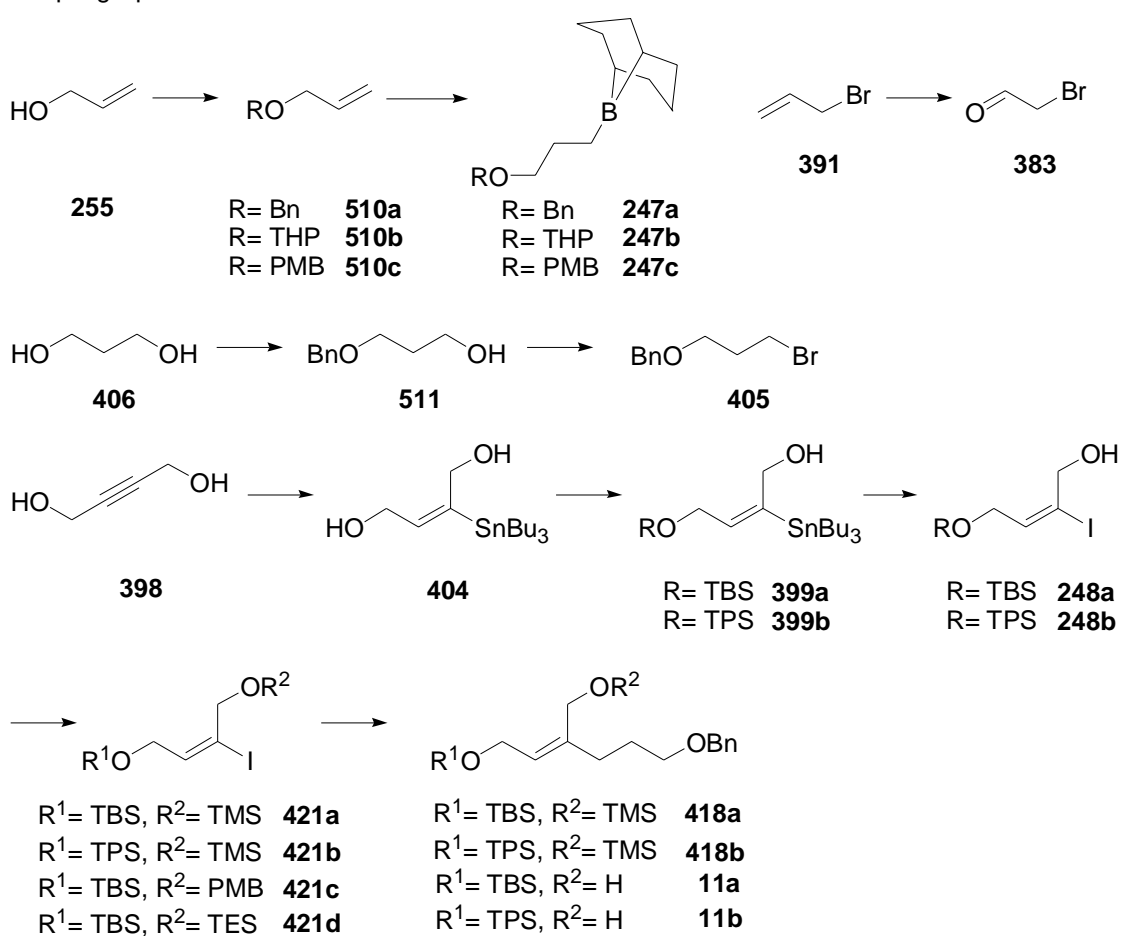
20.3 (-)-Xeniolide F

20.3.1 Stereoselective Synthesis of the Allylic Alcohol

Butyrolactone Route

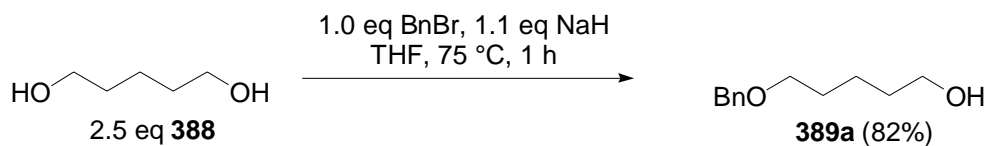


Cross-Coupling Approach



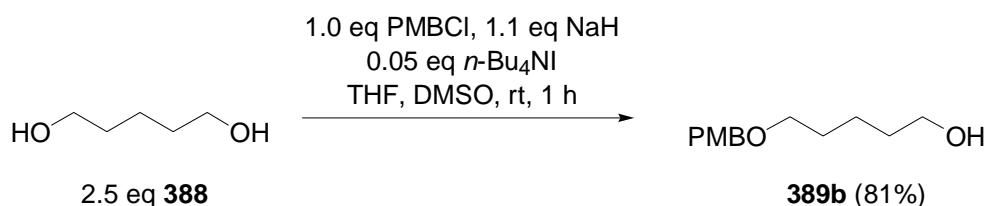
Scheme 153: Synthesis of the allylic alcohol 11.

Butyrolactone Route



Protected Diol 389a.⁴⁰⁶ To an ice-cooled solution of pentane-1,5-diol (**388**) (10.4 g, 100.0 mmol, 2.5 eq) in THF (50 ml, 0.5 mL/mmol) was carefully added sodium hydride (60% suspension in mineral oil, 1.8 g, 44.0 mmol, 1.1 eq). After stirring for 1 h at rt benzyl bromide (4.8 ml, 40.0 mmol, 1.0 eq) was added and the resulting mixture was stirred for 1 h at 75 °C. The reaction was quenched at ambient temperature with saturated aq NH_4Cl and extracted with CH_2Cl_2 (3 × 20 ml). The combined organic phases were dried over MgSO_4 and concentrated. Flash chromatography (heptane/ethyl acetate 1/1) afforded the protected diol **389a** (6.3 g, 32.8 mmol, 82%) as colorless oil. (R_f 0.24 heptane/ethyl acetate 1/2).

^1H NMR (300 MHz, CDCl_3) δ 7.36-7.26 (m, 5H), 4.50 (s, 2H), 3.62 (t, $J = 6.5$ Hz, 2H), 3.48 (t, $J = 6.3$ Hz, 2H), 1.68-1.38 (series of m, 6H), no OH-resonance observed. Anal. Calcd for $\text{C}_{12}\text{H}_{18}\text{O}_2$: C, 74.19; H 9.34.



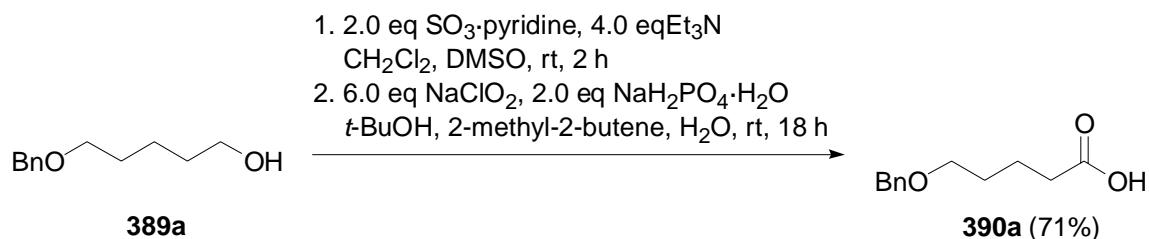
Protected Diol 389b.⁴⁰⁷ To an ice-cooled solution of pentane-1,5-diol (**388**) (10.4 g, 100.0 mmol, 2.5 eq) in THF/DMSO (3/1, 100 mL, 1 mL/mmol) was carefully added sodium hydride (60 % suspension in mineral oil, 1.8 g, 44.0 mmol, 1.1 eq). After stirring for 30 min at rt *para*-methoxybenzyl chloride (5.5 mL, 40.0 mmol, 1.0 eq) was added. The resulting mixture was stirred for 1 h at ambient temperature, quenched with saturated aq NH_4Cl and extracted with CH_2Cl_2 (3 × 40 ml). The combined organic phases were dried over MgSO_4 and concentrated. Flash chromatography (heptane/ethyl acetate 5/1 to 1/1) afforded the protected diol **389b** (7.2 g, 32.4 mmol, 81%) as colorless oil. (R_f 0.15 heptane/ethyl acetate 1/2).

^1H NMR (300 MHz, CDCl_3) δ 7.26 (d, $J = 8.8$ Hz, 2H), 6.88 (d, $J = 8.4$ Hz, 2H), 4.42 (s, 2H), 3.80 (s, 3H), 3.63 (t, $J = 3.6$ Hz, 2H), 3.44 (t, $J = 6.3$ Hz, 2H), 1.70-1.37 (series of m, 6H); ^{13}C NMR (75 MHz, CDCl_3) δ 159.1 (C), 130.6 (C), 129.2 (2 × CH), 113.7 (2 × CH),

⁴⁰⁶ Compound **49a** is commercially available (e.g. from Aldrich). For an analogue synthesis, see: Boerjesson, L.; Csoeregh, I.; Welch, C. J. *J. Org. Chem.* **1995**, *60*, 2989-2999.

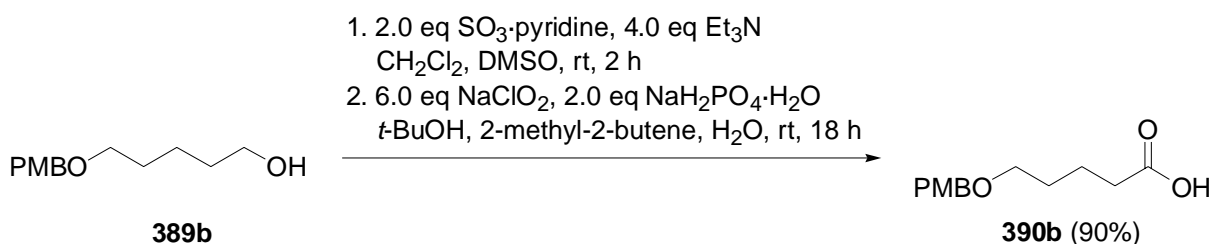
⁴⁰⁷ For an analogue synthesis, see: Zheng, T.; Narayan, R.; Schomaker, J. M.; Borhan, B. *J. Am. Chem. Soc.* **2005**, *127*, 6946-6947.

72.6 (CH₂), 70.0 (CH₂), 62.8 (CH₂), 55.2 (CH₃), 32.5 (CH₂), 29.4 (CH₂), 22.4 (CH₂); IR (in substance) ν 3360, 3020, 2935-2860 cm⁻¹. Anal. Calcd for C₁₃H₂₀O₃: C, 69.61; H 8.99. Found: C, 69.22; H, 8.96.



Acid 390a.⁴⁰⁸ To a solution of protected diol **389a** (6.1 g, 31.5 mmol, 1.0 eq) in CH₂Cl₂/DMSO (4/1, 300 mL, 10 mL/mmol) was added triethylamine (17.7 mL, 126.0 mmol, 4.0 eq) and sulfur trioxide·pyridine complex (10.0 g, 63.0 mmol, 2.0 eq) at ambient temperature. The reaction mixture was stirred for 2 h at rt, quenched by the addition of water and extracted with CH₂Cl₂ (3 × 20 mL). The combined organic layers were dried over MgSO₄ and concentrated and the resulting crude aldehyde (*R_f* 0.68 heptane/ethyl acetate 1/2) was dissolved in *t*-BuOH (125 mL, 4 mL/mmol **389a**) and 2-methyl-2-butene (63 mL, 2 mL/mmol **389a**) to which a solution of NaClO₂ (17.1 g, 189 mmol, 6.0 eq) and NaH₂PO₄·H₂O (8.6 g, 63.0 mmol, 2.0 eq) in water (63 mL, 2 mL/mmol **389a**) was added. The mixture was vigorously stirred at ambient temperature until TLC indicated the complete consumption of the starting material (~18 h), diluted with water (50 mL), and extracted with CH₂Cl₂ (3 × 20 mL). The combined extracts were dried over MgSO₄ and concentrated. Flash chromatography (heptane/ethyl acetate 5/1 to 1/1) afforded the acid **390a** (4.7 g, 22.4 mmol, 71%) as pale yellow oil (*R_f* 0.38 heptane/ethyl acetate 1/2).

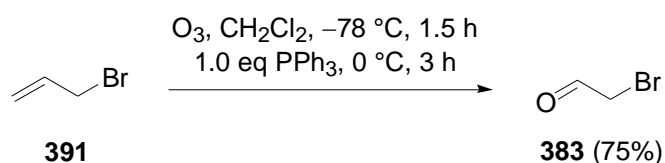
¹H NMR (300 MHz, CDCl₃) δ 7.36-7.26 (m, 5H), 4.50 (s, 2H), 3.49 (t, *J* = 6.0 Hz, 2H), 2.38 (t, *J* = 7.1 Hz, 2H), 1.80-1.61 (m, 4H), no CO₂H-resonance observed; ¹³C NMR (75 MHz, CDCl₃) δ 179.3 (C), 138.4 (C), 128.4 (2 × CH), 127.6 (2 × CH), 127.5 (CH), 72.9 (CH₂), 69.7 (CH₂), 33.7 (CH₂), 29.0 (CH₂), 21.5 (CH₂); IR (in substance) ν 3090-3030, 2940-2860, 1705 cm⁻¹. Anal. Calcd for C₁₂H₁₆O₃: C, 69.21; H 7.74. Found: C, 69.01; H, 7.63.



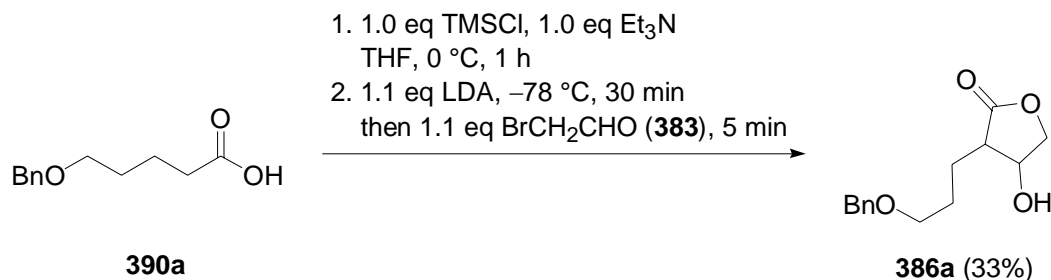
⁴⁰⁸ For reference data, see: Jacobi, P. A.; Li, Y. *Org. Lett.* **2003**, *5*, 701-704.

Acid 390b.⁴⁰⁸ As described for the preparation of the acid **390a**, protected diol **389b** (5.8 g, 26.0 mmol) was oxidized with sulfur trioxide-pyridine complex (8.3 g, 52.0 mmol). The resulting crude aldehyde (R_f 0.41 heptane/ethyl acetate 1/2) was treated with NaClO_2 (14.1 g, 156 mmol) and $\text{NaH}_2\text{PO}_4 \cdot \text{H}_2\text{O}$ (7.1 g, 52.0 mmol). Flash chromatography (heptane/ethyl acetate 1/2) afforded the acid **390b** (5.6 g, 23.4 mmol, 90%) as white solid (R_f 0.08 heptane/ethyl acetate 1/2).

^1H NMR (300 MHz, CDCl_3) δ 7.25 (d, $J = 8.8$ Hz, 2H), 6.87 (d, $J = 8.8$ Hz, 2H), 4.42 (s, 2H), 3.80 (s, 3H), 3.46 (t, $J = 6.0$ Hz, 2H), 2.37 (t, $J = 7.6$ Hz, 2H), 1.79-1.60 (m, 4H), no CO_2H -resonance observed; ^{13}C NMR (75 MHz, CDCl_3) δ 178.8 (C), 159.2 (C), 130.5 (C), 129.2 (2 \times CH), 113.8 (2 \times CH), 72.6 (CH_2), 69.4 (CH_2), 55.3 (CH_3), 33.6 (CH_2), 29.0 (CH_2), 21.6 (CH_2); IR (in substance) ν 3100-3030, 2940-2860, 1710 cm^{-1} . Anal. Calcd for $\text{C}_{13}\text{H}_{18}\text{O}_4$: C, 65.53; H 7.61. Found: C, 65.27; H, 7.56.



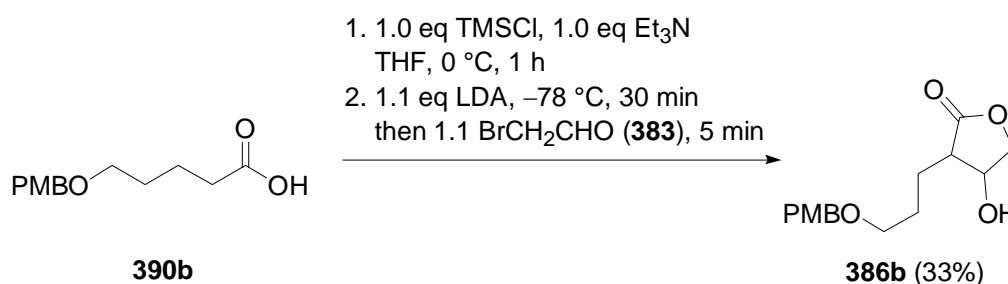
Aldehyde 383.⁴⁰⁹ Through a solution of allyl bromide (**391**) (3.5 mL, 40.0 mmol, 1.0 eq) in CH_2Cl_2 (60 mL, 1.5 mL/mmol) at -78°C was bubbled a stream of ozone until the color turned blue (~ 1.5 h). The excess ozone was removed by a nitrogen stream (disappearance of the blue color) and then triphenylphosphine (10.5 g, 40.0 mmol, 1.0 eq) was added at -78°C . The reaction mixture was warmed to 0°C and stirred for 3 h. Dichloromethane was removed by distillation (120 mbar, 0°C). The residue was then distilled into a receiving flask at -78°C (1.3 mbar, 0 - 50°C) and afforded the aldehyde **383** (3.7 g, 30.1 mmol, 75%) as solution in CH_2Cl_2 (**383**/ CH_2Cl_2 1/1.5).⁴¹⁰ ^1H NMR (300 MHz, CDCl_3) δ 9.53 (t, $J = 2.6$ Hz, 1H), 3.84 (d, $J = 2.6$ Hz, 2H). Anal. Calcd for $\text{C}_2\text{H}_3\text{BrO}$: C, 19.54; H, 2.46; Br, 64.99.



⁴⁰⁹ Prepared analogue to: Jachak, M.; Mittelbach, M.; Junek, H. *Org. Prep.* **1993**, *25*, 469-473. For reference data, see: Kraus, G. A.; Gottschalk, P. *J. Org. Chem.* **1983**, *48*, 2111-2112.

⁴¹⁰ Deduced from ^1H NMR spectrum of the mixture.

Hydroxybutyrolactone 386a.⁴¹¹ To an ice-cooled solution of the acid **390a** (0.8 g, 4.0 mmol, 1.0 eq) in THF (8 mL, 2 mL/mmol) was subsequently added trimethylamine (0.6 mL, 4.0 mmol, 1.0 eq) and trimethylchlorosilane (0.5 mL, 4.0 mmol, 1.0 eq). After stirring for 1 h at 0 °C, the precipitate was removed by filtration and washed with diethylether. The solution was concentrated and afforded protected acid **385a** which was used without further purification. To a solution of LDA [prepared in situ from diisopropyl amine (0.6 mL, 4.4 mmol, 1.1 eq) and *n*-BuLi (2.1 M in hexanes, 2.1 mL, 4.4 mmol, 1.1 eq)] in THF (12 mL, 3.0 mL/mmol) at -78 °C was added **385a** (4.0 mmol, 1.0 eq). After 30 min the aldehyde **383** (7.6% in CH₂Cl₂, 0.5 g, 4.4 mmol, 1.1 eq) was added and the reaction mixture was stirred until TLC indicated the complete consumption of the starting material (~10 min). The reaction was quenched by the addition of acetic acid (0.5 mL, 8.8 mmol, 2.2 eq) and saturated aq NaHCO₃ at 0 °C, extracted with CH₂Cl₂ (3 x 10 mL) and concentrated. The crude product was dissolved in CH₂Cl₂ (4 mL, 1 mL/mmol) and treated with TBAF (1.0 M in THF, 0.5 mL, mmol, eq). The reaction was quenched by the addition of saturated aq NH₄Cl, extracted with CH₂Cl₂ (3 x 5 mL) and concentrate. The crude product was purified by flash chromatography (heptane/ ethyl acetate 1/1) to afford the hydroxybutyrolactone **386a** (0.33 g, 1.3 mmol, 33%) as pale yellow oil (*R_f* 0.06 heptane/ethyl acetate 1/1). ¹H NMR δ 7.37-7.31 (m, 5H), 4.51 (s, 2H), 4.40 (dd, *J* = 9.0, 6.5 Hz, 1H), 4.33 (dd, *J* = 12.0, 6.0 Hz, 1H), 3.97 (dd, *J* = 9.0, 5.4 Hz, 1H), 3.60-3.56 (m, 2H), 2.59-2.53 (m, 1H), 2.04-1.60 (series of m, 4H); ¹³C NMR (75 MHz, CDCl₃) δ 177.3 (C), 137.6 (C), 128.5 (2 × CH), 128.0 (2 × CH), 127.8 (CH), 73.3 (CH₂), 72.33 (CH), 72.27 (CH₂), 70.3 (CH₂), 47.8 (CH), 26.8 (CH₂), 26.3 (CH₂); IR (in substance) ν 3435, 3030, 2925-2860 cm⁻¹. Anal. Calcd for C₁₄H₁₈O₄: C, 67.18; H, 7.25.

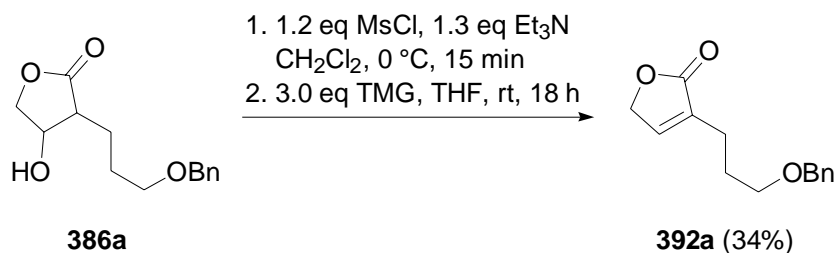


Hydroxybutyrolactone 386b.⁴¹¹ As described in the preceding paragraph, acid **390b** (4.3 g, 18.0 mmol) was treated with triethylamine (2.5 mL, 18.0 mmol) and trimethylchlorosilane (2.3 mL, 18.0 mmol). The crude acid **385** was deprotonated and aldehyde **383** (19% in CH₂Cl₂, 12.8 g, 19.8 mmol) was added. After treatment with TBAF (1.0 M in THF, 9.0 mL,

⁴¹¹ Not fully characterized. **386a/386b** are part of a dead-end synthetic route. For that reason, the complete set of analytical data was not acquired. Yields not optimized.

4.5 mmol), flash chromatography (heptane/ethyl acetate 1/1) afforded hydroxybutyrolactone **386b** (1.8 g, 6.5 mmol, 33%) as pale yellow oil (R_f 0.47 ethyl acetate).

$^1\text{H NMR}$ δ 7.25 (d, $J = 9.4$ Hz, 2H), 6.87 (dd, $J = 8.9, 2.3$ Hz, 2H), 4.45-4.41 (m, 2H), 4.37 (dd, $J = 9.1, 6.5$ Hz, 1H), 4.26-4.22 (m, 1H), 3.95 (dd, $J = 9.1, 5.5$ Hz, 1H), 3.79 (s, 3H), 3.58-3.50 (m, 2H), 2.57-2.41 (m, 1H), 2.06-1.75 (series of m, 4H). Anal. Calcd for $\text{C}_{15}\text{H}_{20}\text{O}_5$: C, 64.27; H, 7.19.

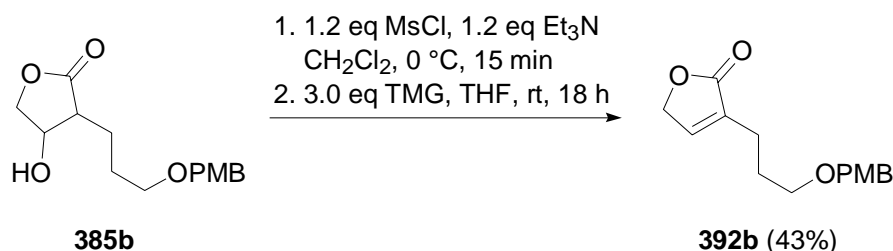


Lactone 392a.⁴¹² To an ice-cooled solution of hydroxybutyrolactone **386a** (1.8 g, 6.5 mmol, 1.0 eq) in CH_2Cl_2 (20 mL, 3 mL/mmol) at 0 °C was subsequently added triethylamine (1.2 mL, 8.5 mmol, 1.3 eq) and methane sulfonyl chloride MsCl (0.6 mL, 7.8 mmol, 1.2 eq). The reaction mixture was stirred for 15 min at 0 °C, quenched by the addition of saturated aq. NaHCO_3 and extracted with CH_2Cl_2 (3 x 5 mL). The combined organic layers were dried over MgSO_4 and concentrated. The crude product (3.3 mmol)⁴¹³ was dissolved in THF (6.5 mL, 2 mL/mmol **386a**) and treated with tetramethylguanidine TMG (1.2 mL, 9.8 mmol, 3.0 eq) at 0 °C. After stirring for 18 h at rt the reaction was quenched by the addition of water (7 mL, 2 mL/mmol) and extracted with CH_2Cl_2 (3 x 5 mL). The combined extracts were dried over MgSO_4 and concentrated. Flash chromatography (heptane/ethyl acetate 1/1) afforded the lactone **392a** (0.29 g, 1.1 mmol, 34%) as pale yellow oil (R_f 0.41 ethyl acetate).

$^1\text{H NMR}$ (300 MHz, CDCl_3) δ 7.36-7.26 (m, 5H), 7.06 (t, $J = 1.6$ Hz, 1H), 4.73 (ddd, $J = 2.0, 2.0, 2.0$ Hz, 2H), 4.49 (s, 2H), 3.50 (t, $J = 6.2$ Hz, 2H), 2.41 (td, $J = 7.7, 1.7$ Hz, 2H), 1.94-1.83 (m, 2H); $^{13}\text{C NMR}$ (75 MHz, CDCl_3) δ 174.3 (C), 144.5 (CH), 138.3 (C), 133.9 (C), 128.4 (2 x CH), 127.7 (2 x CH), 127.6 (CH), 73.0 (CH_2), 70.1 (CH_2), 69.2 (CH_2), 27.5 (CH_2), 22.3 (CH_2); IR (in substance) ν 3080-3030, 2930-2860, 1745 cm^{-1} . Anal. Calcd for $\text{C}_{14}\text{H}_{16}\text{O}_3$: C, 72.39; H 6.94.

⁴¹² Not fully characterized. Compounds **392a,b** are part of a dead-end synthetic route. For that reason, the complete set of analytical data was not acquired. Yields not optimized.

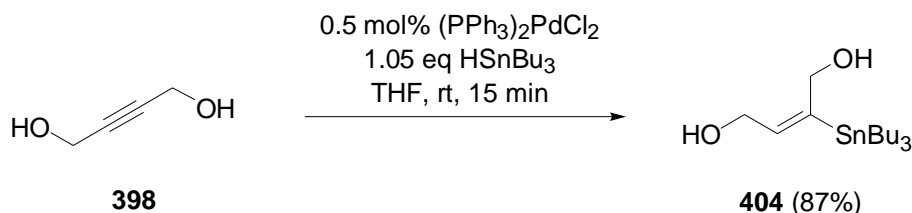
⁴¹³ The crude product was divided into two parts with equal amount of the mesylate. Only one half was used for the conditions described above. The other half was treated with DBU and afforded lower yields. Yields not optimized.



Lactone 392b.⁴¹² As described for lactone **392a**, hydroxybutyrolactone **385b** (1.1 g, 4.5 mmol, 1.0 eq) was treated with triethylamine (0.8 mL, 5.8 mmol) and methane sulfonyl chloride MsCl (0.41 mL, 5.4 mmol). Tetramethylguanidine (0.8 mL, 6.8 mmol) was then added to the resulting crude mesylate (2.3 mmol). Flash chromatography (heptane/ethyl acetate 1/1) afforded the lactone **392b** (0.22 g, 1.0 mmol, 43%) as pale yellow oil (R_f 0.43 ethyl acetate).

$^1\text{H NMR}$ (300 MHz, CDCl_3) δ 7.25 (d, $J = 8.4$ Hz, 2H), 7.06 (t, $J = 1.5$ Hz, 1H), 6.87 (d, $J = 8.8$ Hz, 2H), 4.73 (ddd, $J = 1.9, 1.9, 1.9$ Hz, 2H), 4.42 (s, 2H), 3.80 (s, 3H), 3.47 (t, $J = 6.2$ Hz, 2H), 2.39 (td, $J = 7.6, 1.6$ Hz, 2H), 1.91-1.81 (m, 2H); $^{13}\text{C NMR}$ (75 MHz, CDCl_3) δ 174.3 (C), 159.2 (C), 144.5 (CH), 133.9 (C), 130.4 (C), 129.3 (2 \times CH), 113.8 (2 \times CH), 72.6 (CH_2), 70.1 (CH_2), 68.9 (CH_2), 55.3 (CH_3), 27.5 (CH_2), 22.3 (CH_2); IR (in substance) ν 3000-2860, 1745 cm^{-1} . Anal. Calcd for $\text{C}_{15}\text{H}_{18}\text{O}_4$: C, 68.68; H 6.92. Found: C, 68.73; H, 6.99.

Cross-Coupling Approach

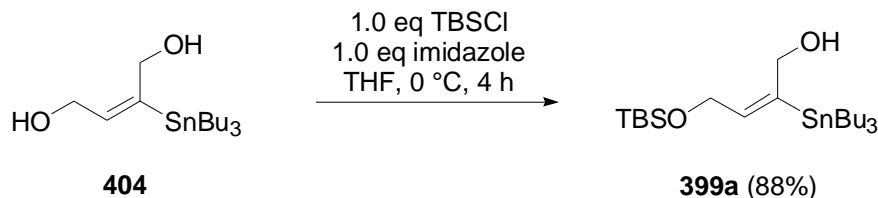


Vinyl Stannane 404.^{414,388} To a solution of 2-butyne-1,4-diol (**398**) (3.4 g, 40.0 mmol, 1.0 eq) and $(\text{PPh}_3)_2\text{PdCl}_2$ (0.14 g, 0.2 mmol, 0.5 mol%) in THF (20 mL, 0.5 mL/mmol) at rt was slowly added a solution of tri-*n*-butyltin hydride HSnBu_3 (11.3 mL, 42.0 mmol, 1.05 eq) in THF (30 mL, 0.7 mL/mmol). The color of the solution turned from light yellow to orange-brown during the addition. The reaction mixture was stirred for 15 min at ambient temperature, concentrated and purified by column chromatography (hexanes/ethyl acetate 10/1 to 2/1) to afford the vinyl stannane **404** (13.1 g, 35.3 mmol, 87%) as a yellow oil (R_f 0.47 hexanes/ethyl acetate 3/1).

$^1\text{H NMR}$ (300 MHz, CDCl_3) δ 5.78 (tt, $J = 5.9, 2.0$ Hz, 1H), 4.39 (bd, $J = 1.9$ Hz, 2H), 4.19 (bt, $J = 4.8$ Hz, 2H), 1.81 (bs, 1H), 1.65-1.57 (m, 1H), 1.54-1.43 (m, 6H), 1.36-1.24 (m, 6H),

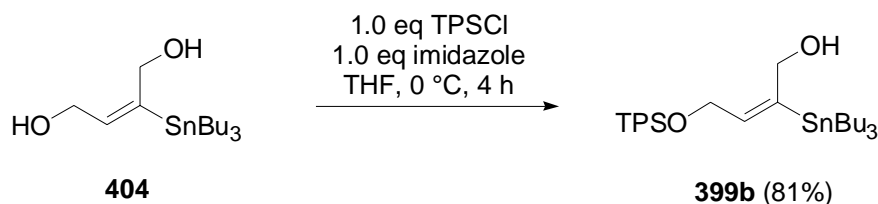
⁴¹⁴ (a) Commeiras, L.; Valls, R.; Santelli, M.; Parrain, J.-L. *Synlett* **2003**, 1719-1721. (b) Commeiras, L.; Santelli, M.; Parrain, J.-L. *Org. Lett.* **2001**, *3*, 1713-1715.

1.02-0.80 (m, 6H), 0.88 (t, $J = 7.2$ Hz, 9H); ^{13}C NMR (75 MHz, CDCl_3) δ 149.3 (C), 138.1 (CH), 63.6 (CH_2), 59.8 (CH_2), 29.1 ($3 \times \text{CH}_2$), 27.4 ($3 \times \text{CH}_2$), 13.7 ($3 \times \text{CH}_3$), 10.0 ($3 \times \text{CH}_2$); IR (in substance) ν 3305, 2955-2855 cm^{-1} . Anal. Calcd for $\text{C}_{16}\text{H}_{34}\text{O}_2\text{Sn}$: C, 50.95; H 9.09. Found: C, 50.95; H, 9.11.



TBS-Protected Vinyl Stannane 399a.^{414,388} To an ice-cooled solution of the vinyl stannane **404** (13.1 g, 35.3 mmol, 1.0 eq) in THF (35 mL, 1 mL/mmol) was added imidazole (2.4 g, 35.3 mmol, 1.0 eq) and *t*-butyldimethylchlorosilane TBSCl (5.3 g, 35.3 mmol, 1.0 eq). After 4 h at 0 °C, the reaction was quenched by the addition of saturated aq NH_4Cl and extracted with CH_2Cl_2 (3×30 mL). The combined organic layers were dried and concentrated. The crude product was purified by column chromatography (hexanes/ethyl acetate 100/1 to 10/1) to afford the protected vinyl stannane **399a** (15.2 g, 30.9 mmol, 88%) as a pale yellow oil (R_f 0.26 hexanes/ethyl acetate 100/1).

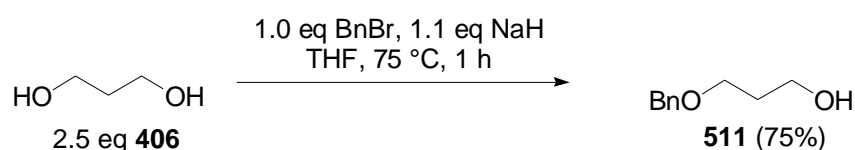
^1H NMR (300 MHz, CDCl_3) δ 5.63 (tt, $J = 5.4, 2.0$ Hz, 1H), 4.34 (d, $J = 5.5$ Hz, 2H), 4.22 (d, $J = 5.4$ Hz, 2H), 1.82 (brt, $J = 5.5$ Hz, 1H), 1.57-1.38 (m, 6H), 1.30-1.26 (m, 6H), 0.91 (s, 9H), 0.94-0.86 (m, 15H), 0.08 (s, 6H); ^{13}C NMR (75 MHz, CDCl_3) δ 147.2 (C), 138.9 (CH), 63.8 (CH_2), 60.7 (CH_2), 29.2 ($3 \times \text{CH}_2$), 27.4 ($3 \times \text{CH}_2$), 25.9 ($3 \times \text{CH}_3$), 18.3 (C), 13.7 ($3 \times \text{CH}_3$), 10.1 ($3 \times \text{CH}_2$), -5.1 ($2 \times \text{CH}_3$); IR (in substance) ν 3435, 2950-2855 cm^{-1} . Anal. Calcd for $\text{C}_{22}\text{H}_{48}\text{O}_2\text{SiSn}$: C, 53.77; H, 9.85. Found: C, 53.80; H, 9.92.



TPS-Protected Vinyl Stannane 399b.⁴¹⁵ As described in the preceding paragraph, consecutive treatment of vinyl stannane **9** (2.3 g, 6.1 mmol, 1.0 eq) in THF (6 mL, 1 mL/mmol) with imidazole (0.42 g, 6.1 mmol, 1.0 eq) and *t*-butyldiphenylchlorosilane (1.7 g, 1.6 mL, 6.1 mmol, 1.0 eq) afforded the protected vinyl stannane **404b** (3.0 g, 4.9 mmol, 81%) as a pale yellow oil (R_f 0.50 hexanes/ethyl acetate 20/1).

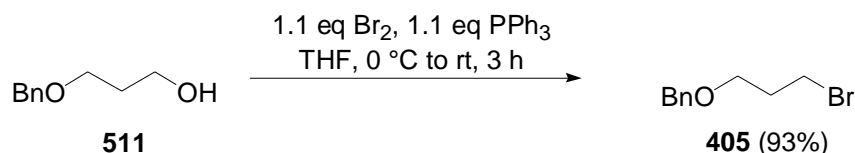
⁴¹⁵ Prepared analogue to reference 414.

^1H NMR (300 MHz, CDCl_3) δ 7.69-7.66 (m, 4H), 7.43-7.34 (m, 6H), 5.74 (tt, $J = 5.5, 2.1$ Hz, 1H), 4.23 (d, $J = 5.6$ Hz, 2H), 4.09 (brd, $J = 3.8$ Hz, 2H), 1.53-1.39 (m, 6H), 1.37-1.25 (m, 6H), 1.03 (s, 9H), 0.87 (t, $J = 7.2$ Hz, 9H), 0.99-0.77 (m, 6H) no OH-resonance observed; ^{13}C NMR (126 MHz, CDCl_3) δ 147.3 (C), 138.2 (CH), 135.6 ($4 \times \text{CH}$), 133.7 ($2 \times \text{C}$), 129.6 ($2 \times \text{CH}$), 127.6 ($4 \times \text{CH}$), 63.5 (CH_2), 61.3 (CH_2), 29.2 ($3 \times \text{CH}_2$), 27.4 ($3 \times \text{CH}_2$), 26.8 ($3 \times \text{CH}_3$), 19.1 (C), 13.7 ($3 \times \text{CH}_3$), 10.0 ($3 \times \text{CH}_2$); IR (in substance) ν 3475, 3070-3055, 2955-2855 cm^{-1} . Anal. Calcd for $\text{C}_{32}\text{H}_{52}\text{O}_2\text{SiSn}$: C, 62.44; H, 8.51. Found: C, 52.56; H, 8.65.



Protected Diol 511.⁴¹⁶ To an ice-cooled solution of propane-1,3-diol (**406**) (2.8 mL, 50.0 mmol, 2.5 eq) in THF (25 mL, 0.5 mL/mmol) was carefully added sodium hydride (60% suspension in mineral oil, 0.9 g, 22.0 mmol, 1.1 eq). After stirring for 1 h at rt benzyl bromide (2.4 mL, 20.0 mmol, 1.0 eq) was added and the resulting mixture was stirred for 1 h at 75 °C. The reaction was quenched at ambient temperature with saturated aq NH_4Cl and extracted with CH_2Cl_2 (3×30 mL). The combined organic phases were dried over MgSO_4 and concentrated. Flash chromatography (heptane/ethyl acetate 1/1) afforded the protected diol **511** (2.5 g, 15.0 mmol, 75%) as colorless liquid (R_f 0.35 heptane/ethyl acetate 1/1).

^1H NMR (300 MHz, CDCl_3) δ 7.38-7.29 (m, 5H), 4.53 (s, 2H), 3.79 (brt, $J = 5.4$ Hz, 2H), 3.67 (t, $J = 5.8$ Hz, 2H), 2.26 (brs, 1H), 1.87 (quint, $J = 5.7$ Hz, 2H); ^{13}C NMR (126 MHz, CDCl_3) δ 138.1 (C), 128.4 ($2 \times \text{CH}$), 127.7 ($2 \times \text{CH}$), 127.6 (CH), 73.3 (CH_2), 69.4 (CH_2), 61.9 (CH_2), 32.1 (CH_2); IR (in substance) ν 3370, 3090-3030, 2940-2865 cm^{-1} . Anal. Calcd for $\text{C}_{10}\text{H}_{14}\text{O}_2$: C, 72.26; H, 8.49.



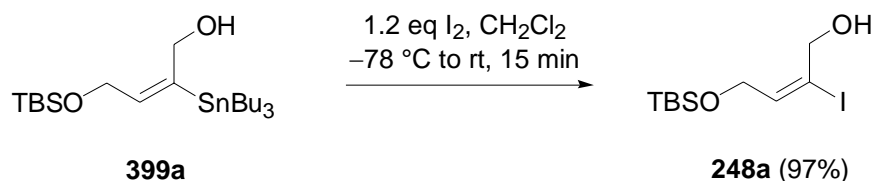
Bromide 405.⁴¹⁷ To an ice-cooled solution of the protected diol **511** (2.4 g, 14.4 mmol, 1.0 eq) in THF (43 mL, 3 mL/mmol) was added triphenylphosphine (4.1 g, 15.8 mmol, 1.1 eq) and bromine (0.8 mL, 15.8 mmol, 1.1 eq). The reaction mixture was warmed to rt and stirred for 3 h at rt. The reaction was quenched by the addition of saturated aq NaS_2O_3 and extracted

⁴¹⁶ Compound **511** is commercially available (e.g. from ALDRICH). For an analogue synthesis, see: Schomaker, J. M.; Pulgam, V. R.; Borhan, B. *J. Am. Chem. Soc.* **2004**, *126*, 13600-13601.

⁴¹⁷ Compound **405** is commercially available (e.g. from ALDRICH). For reference data, see: Ziegler, F. E.; Klein, S. I.; Pati, U. K.; Wang, T. F. *J. Am. Chem. Soc.* **1985**, *107*, 2730-2737.

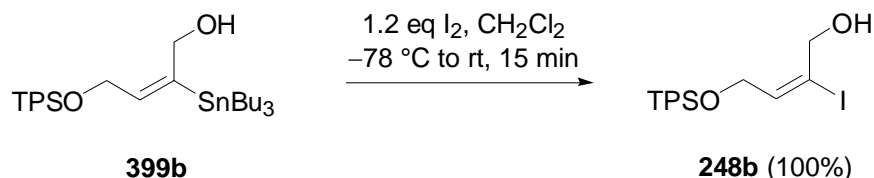
with CH₂Cl₂ (3 × 30 mL). The combined organic layers were dried and concentrated. Flash chromatography (heptane/ethyl acetate 10/1) afforded the bromide **405** (3.1 g, 13.5 mmol, 93%) as colorless liquid (*R*_f 0.61 heptane/ethyl acetate 1/1).

¹H NMR (300 MHz, CDCl₃) δ 7.36-7.31 (m, 5H), 4.52 (s, 2H), 3.61 (t, *J* = 5.4 Hz, 2H), 3.54 (t, *J* = 6.6 Hz, 2H), 2.14 (quint, *J* = 6.4 Hz, 2H); ¹³C NMR (75 MHz, CDCl₃) δ 138.2 (C), 128.4 (2 × CH), 127.6 (3 × CH), 73.2 (CH₂), 67.7 (CH₂), 32.9 (CH₂), 30.6 (CH₂); IR (in substance) ν 3065-3030, 2940-2860 cm⁻¹. Anal. Calcd for C₁₀H₁₃BrO: C, 52.42; H, 5.71. Found: C, 52.48; H, 5.49.



Vinyl Iodide 248a.^{418,388} To a solution of the protected vinyl stannane **399a** (12.9 g, 26.2 mmol, 1.0 eq) in CH₂Cl₂ (100 mL, 4 mL/mmol) was added iodine (8.0 g, 31.4 mmol, 1.2 eq) at -78 °C. The reaction mixture was warmed to rt, quenched by the addition of saturated aq Na₂S₂O₃ and extracted with CH₂Cl₂ (3 × 70 mL). The combined organic layers were dried and concentrated. The crude product was purified by column chromatography (hexanes/ethyl acetate 10/1 to 3/1) to afford the light sensitive vinyl iodide **248a** (8.3 g, 25.3 mmol, 97%) as a pale yellow oil (*R*_f 0.32 hexanes/ethyl acetate 20/1).⁴¹⁹

¹H NMR (300 MHz, CDCl₃) δ 6.44 (bt, *J* = 6.2 Hz, 1H), 4.27 (d, *J* = 6.4 Hz, 2H), 4.21 (d, *J* = 6.2 Hz, 2H), 2.51 (t, *J* = 6.7 Hz, 1H), 0.90 (s, 9H), 0.08 (s, 6H); ¹³C NMR (75 MHz, CDCl₃) δ 141.6 (CH), 104.7 (C), 66.7 (CH₂), 61.2 (CH₂), 25.8 (3 × CH₃), 18.2 (C), -5.3 (2 × CH₃); IR (in substance) ν 3355, 2955-2855 cm⁻¹. Anal. Calcd for C₁₀H₂₁IO₂Si: C, 36.59; H, 6.45. Found: C, 36.76; H, 6.97.



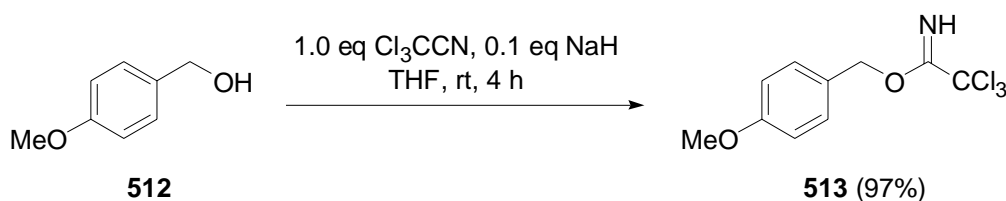
Vinyl Iodide 248b.⁴¹⁸ As described for the preparation of vinyl iodide **248a**, TPS-protected vinyl stannane **399b** (3.0 g, 4.9 mmol, 1.0 eq) was treated with iodine (1.48 g, 5.8 mmol, 1.2

⁴¹⁸ Prepared analogue to: Aoyagi, S.; Wang, T. C.; Kibayashi, C. *J. Am. Chem. Soc.* **1993**, *115*, 11393-11409.

⁴¹⁹ We found **248a** stable for storing for about two weeks at 4 °C protected from light.

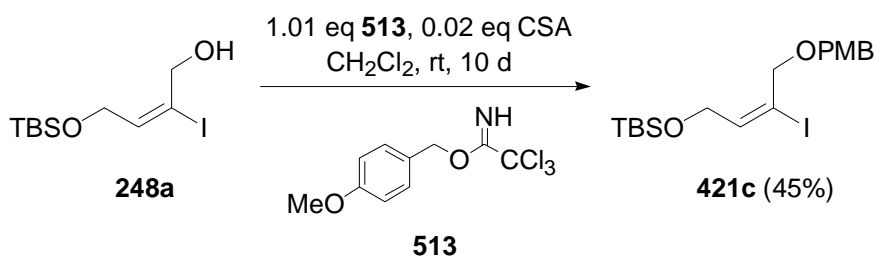
eq) to afford the light sensitive vinyl iodide **248b** (2.2 g, 4.9 mmol, 100%) as a pale yellow oil (R_f 0.26 hexanes/ethyl acetate 10/1).

^1H NMR (300 MHz, CDCl_3) δ 7.68-7.65 (m, 4H), 7.48-7.37 (m, 6H), 6.46 (t, $J = 6.4$ Hz, 1H), 4.20 (d, $J = 6.4$ Hz, 2H), 4.03 (d, $J = 6.2$ Hz, 2H), 1.97 (t, $J = 6.6$ Hz, 1H), 1.05 (s, 9H); ^{13}C NMR (75 MHz, CDCl_3) δ 141.4 (CH), 135.6 (4 \times CH), 132.9 (2 \times C), 129.9 (2 \times CH), 127.8 (4 \times CH), 105.1 (C), 65.9 (CH_2), 61.7 (CH_2), 26.7 (3 \times CH_3), 19.1 (C); IR (in substance) ν 3375, 3070-3060, 2935-2855 cm^{-1} . Anal. Calcd for $\text{C}_{20}\text{H}_{25}\text{IO}_2\text{Si}$: C, 53.10; H, 5.57. Found: C, 53.14; H, 5.63.



Bundle's Reagent (513).⁴²⁰ To a solution of sodium hydride (60% suspension in mineral oil, 0.24 g, 6.0 mmol, 0.1 eq) in THF (18 mL, 0.3 mL/mmol **512**) was carefully added a solution of *para*-methoxy benzyl alcohol (**513**) (7.5 mL, 60.0 mmol, 1.0 eq) in THF (12 mL, 0.2 mL/mmol) at ambient temperature. After stirring for 30 min the reaction mixture was cooled to 0 °C and trichloroacetonitrile (6.0 mL, 60.0 mmol, 1.0 eq) was slowly added whereupon the solution turned yellow. The reaction mixture was warmed to rt and stirred for 4 h. During that time the color darkend and eventually became red. The reaction was diluted with pentane (18 mL, 0.3 mL/mmol) and methanol (0.24 mL, 4 μL /mmol) was added. The mixture was filtered through a plug of Celite and concentrated to afford Bundle's reagent (**513**) (16.4 g, 58.0 mmol, 97%) as deep orange oil (R_f 0.74 heptanes/ethyl acetate 1/1).

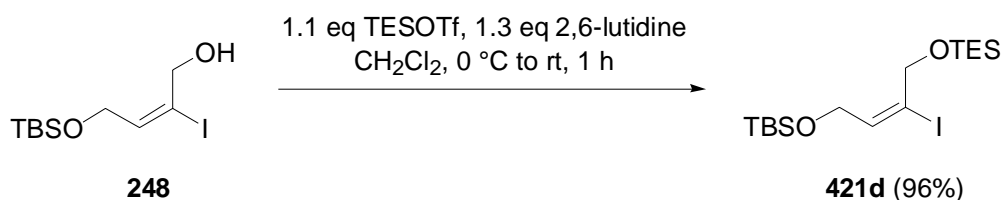
^1H NMR (300 MHz, CDCl_3) δ 8.35 (brs, 1H), 7.36 (d, $J = 8.8$ Hz, 2H), 6.90 (d, $J = 8.4$ Hz, 2H), 5.26 (s, 2H), 3.81 (s, 3H). Anal. Calcd for $\text{C}_{10}\text{H}_{10}\text{Cl}_3\text{NO}_2$: C 42.51; H 3.57; Cl, 37.64, N, 4.96.



⁴²⁰ (a) Paquette, L. A.; Guevel, R.; Sakamoto, K.; In, H.; Crawford, J. *J. Org. Chem.* **2003**, *68*, 6069-6107. (b) Iversen, T.; Bundle, D. R. *J. Chem. Soc., Chem. Comm.* **1981**, 1240-1241.

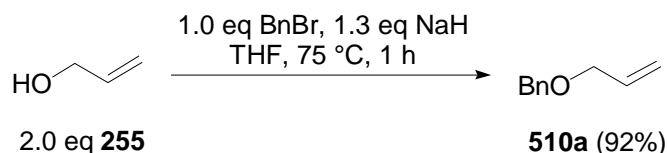
Fully Protected Vinyl Iodide 421c.⁴²¹ To a solution of vinyl iodide **248a** (0.16 g, 0.5 mmol, 1.0 eq) in CH₂Cl₂ (2 mL, 4 mL/mmol) was added Bundle's reagent (**513**) (0.14 g, 0.6 mmol, 1.1 eq) and campher sulfonic acid CSA (2.3 mg, 0.01 mmol, 0.02 eq) at ambient temperature. The reaction was stirred in the dark for 10 d, quenched by the addition of saturated aq NaHCO₃ and extracted with CH₂Cl₂ (3 × 3 mL). The combined organic phases were dried and concentrated. Flash chromatography (hexanes/ethyl acetate 20/1) afforded the vinyl iodide **421c** (0.10 g, 0.23 mmol, 45%) as light sensitive, pale yellow oil (*R_f* 0.59 hexanes/ethyl acetate 3/1).

¹H NMR (300 MHz, CDCl₃) δ 7.26 (d, *J* = 8.4 Hz, 2H), 6.84 (d, *J* = 8.8 Hz, 2H), 6.50 (t, *J* = 6.2 Hz, 1H), 4.39 (s, 2H), 4.13-4.06 (m, 4H), 3.76 (s, 3H), 0.84 (s, 9H), 0.00 (s, 6H). Anal. Calcd for C₁₈H₂₉IO₃Si: C, 48.21; H 6.52; I, 28.30.



Fully Protected Vinyl Iodide 421d.⁴²¹ To an ice-cooled solution of vinyl iodide **248a** (0.7 g, 2.0 mmol, 1.0 eq) in CH₂Cl₂ (2 mL, 2 mL/mmol) was added 2,6-lutidine (0.3 mL, 2.6 mmol, 1.3 eq) and triethylsilyl trifluoromethylsulfonate TESOTf (0.5 mL, 2.2 mmol, 1.1 eq). The reaction was warmed to rt, stirred at ambient temperature for 1 h in the dark, quenched by the addition of saturated aq NaHCO₃ and extracted with CH₂Cl₂ (3 × 3 mL). The combined organic phases were dried and concentrated. Flash chromatography (hexanes/ethyl acetate 20/1 to 3/1) afforded the vinyl iodide **421d** (0.9 g, 1.9 mmol, 96%) as light sensitive, pale yellow oil (*R_f* 0.62 hexanes/ethyl acetate 3/1).

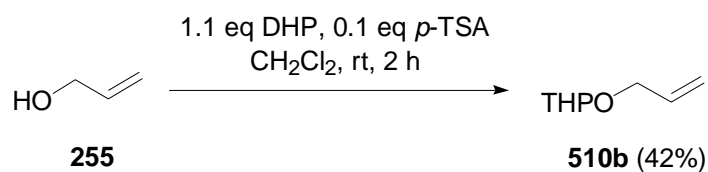
¹H NMR (300 MHz, CDCl₃) δ 6.32 (t, *J* = 6.2 Hz, 1H), 4.23-4.17 (m, 4H), 0.92 (t, *J* = 8.0 Hz, 9H), 0.83 (s, 9H), 0.58 (quart, *J* = 7.9 Hz, 6H), 0.00 (s, 6H). Anal. Calcd for C₁₆H₃₅IO₂Si₂: C, 43.43; H 7.97; I, 28.68.



⁴²¹ Test substrate for the *B*-alkyl-Suzuki-Miyaura cross-coupling. Not fully characterised. Yields not optimized.

Allyl Benzyl Ether (510a).^{422,388} To an ice-cooled solution of the allylic alcohol **255** (5.5 mL, 80.0 mmol, 2.0 eq) in THF (20 mL, 0.5 mL/mmol) was added sodium hydride (2.1 g, 52.0 mmol, 1.3 eq). After 1 h at 0 °C, benzyl bromide (4.8 mL, 40.0 mmol 1.0 eq) was added and the reaction mixture was warmed to 75 °C for 1 h. The reaction was then quenched by the addition of saturated aq NH₄Cl at rt and extracted with CH₂Cl₂ (3 × 30 mL). The combined organic layers were dried and concentrated. The crude product was purified by column chromatography (hexanes/ethyl acetate 20/1) to afford the ether **510a** (5.4 g, 36.5 mmol, 92%) as a colorless oil (*R_f* 0.73 hexanes/ethyl acetate 10/1).

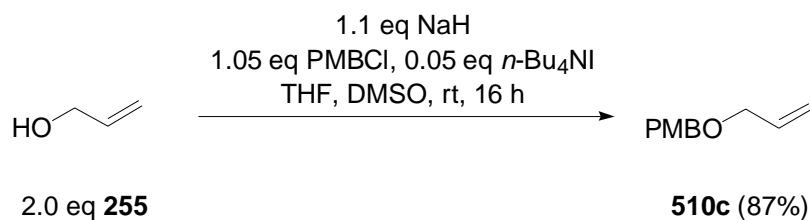
¹H NMR (300 MHz, CDCl₃) δ 7.36-7.28 (m, 5H), 5.96 (tdd, *J* = 17.2, 10.4, 5.6 Hz, 1H), 5.31 (ddd, *J* = 17.2, 3.3, 1.6 Hz, 1H), 5.21 (ddd, *J* = 10.4, 2.9, 1.3 Hz, 1H), 4.53 (s, 2H), 4.03 (td, *J* = 5.6, 1.4 Hz, 2H); ¹³C NMR (75 MHz, CDCl₃) δ 138.3 (C), 134.8 (CH), 128.4 (2 × CH), 127.7 (2 × CH), 127.6 (CH), 117.0 (CH₂), 72.1 (CH₂), 71.1 (CH₂); IR (in substance) ν 3375, 2955-2855 cm⁻¹. Anal. Calcd for C₁₀H₁₂O: C 81.04; H 8.16. Found: C 80.87; H 8.07.



Allyl Tetrahydropyranyl Ether (510b).⁴²¹ To a solution of the allylic alcohol **255** (0.7 mL, 10.0 mmol, 1.0 eq) in CH₂Cl₂ (5 mL, 0.5 mL/mmol) was added 3,4-dihydro-2*H*-pyrane DHP (1.0 g, 11.0 mmol, 1.1 eq) and *p*-TSA (0.18 g, 1.0 mmol, 0.1 eq). The reaction was stirred until TLC indicated complete consumption of the starting material (~2 h), quenched by the addition of saturated aq NaHCO₃ and extracted with CH₂Cl₂ (3 × 10 mL). The combined organic layers were dried and concentrated. The crude product was purified by column chromatography (hexanes/ethyl acetate 20/1) to afford the ether **510b** (0.6 g, 4.2 mmol, 42%) as a colorless liquid (*R_f* 0.63 hexanes/ethyl acetate 1/1).

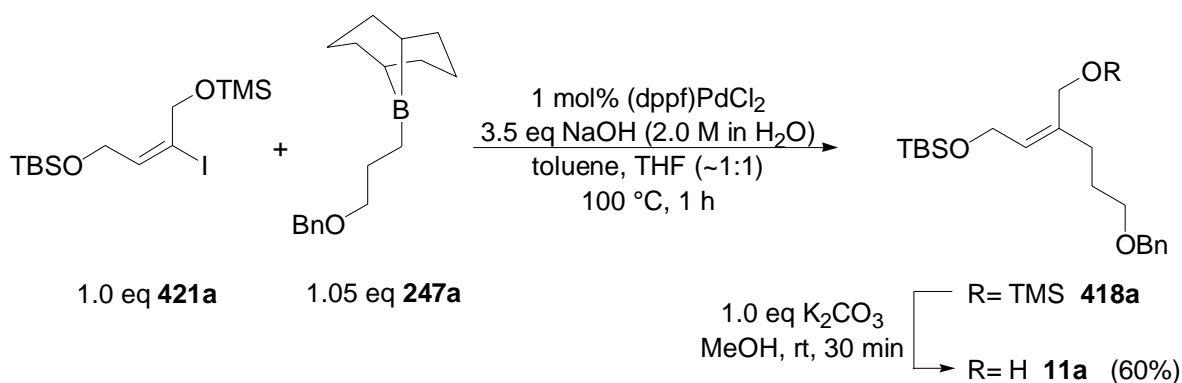
¹H NMR (300 MHz, CDCl₃) δ 6.01-5.87 (m, 1H), 5.30 (dddd, *J* = 17.2, 1.7, 1.7, 1.7 Hz, 1H), 5.17 (dd, *J* = 10.2, 1.8 Hz, 1H), 4.64 (t, *J* = 3.4 Hz, 2H), 4.25 (ddt^{AB}, *J* = 13.0, 5.2, 1.5 Hz, 1H), 3.98 (dd^{AB}, *J* = 13.0, 6.2 Hz, 1H), 3.91-3.83 (m, 1H), 3.55-3.46 (m, 1H), 1.90-1.47 (series of m, 6H). Anal. Calcd for C₈H₁₄O₂: C, 67.57; H, 9.92.

⁴²² (a) Braun, J. V. *Chem. Ber.* **1910**, *43*, 1350-1352. (b) Beinhoff, M.; Karakaya, A.; Schlüter, A. D. *Synthesis* **2003**, 79-90. (c) Bo, Z.; Schlüter, A. D. *J. Org. Chem.* **2002**, *67*, 5327-5332.



Allyl *p*-Methoxybenzyl Ether (510c).⁴²¹ To an ice-cooled solution of the allylic alcohol **255** (0.7 mL, 10.0 mmol, 1.0 eq) and *para*-methoxybenzyl chloride PMBCl (1.4 mL, 10.5 mmol, 1.05 eq) in THF/DMSO (2/1, 40 mL, 4 mL/mmol) was added sodium hydride (0.44 g, 11.0 mmol, 1.1 eq) and *n*-Bu₄NI (0.18 g, 0.5 mmol, 0.05 eq). The reaction mixture was warmed to ambient temperature and stirred overnight. The reaction was then quenched by the addition of saturated aq NH₄Cl and extracted with CH₂Cl₂ (3 × 30 mL). The combined organic layers were dried and concentrated. The crude product was purified by flash chromatography (hexanes/ethyl acetate 20/1) to afford the ether **510c** (1.5 g, 8.7 mmol, 87%) as a colorless liquid (*R*_f 0.51 hexanes/ethyl acetate 1/1).

¹H NMR (300 MHz, CDCl₃) δ 7.21 (d, *J* = 9.1 Hz, 2H), 6.87 (d, *J* = 8.8 Hz, 2H) 5.94 (ddt, *J* = 17.1, 10.6, 5.7 Hz, 1H), 5.29 (dddd, *J* = 17.2, 1.8, 1.8, 1.8 Hz, 1H), 5.19 (dddd, *J* = 10.4, 1.5, 1.5, 1.5 Hz, 1H), 4.45 (s, 2H), 4.01 (dt, *J* = 5.6, 1.3 Hz, 2H), 3.80 (s, 3H). Anal. Calcd for C₁₁H₁₄O₂: C, 74.13; H, 7.92.



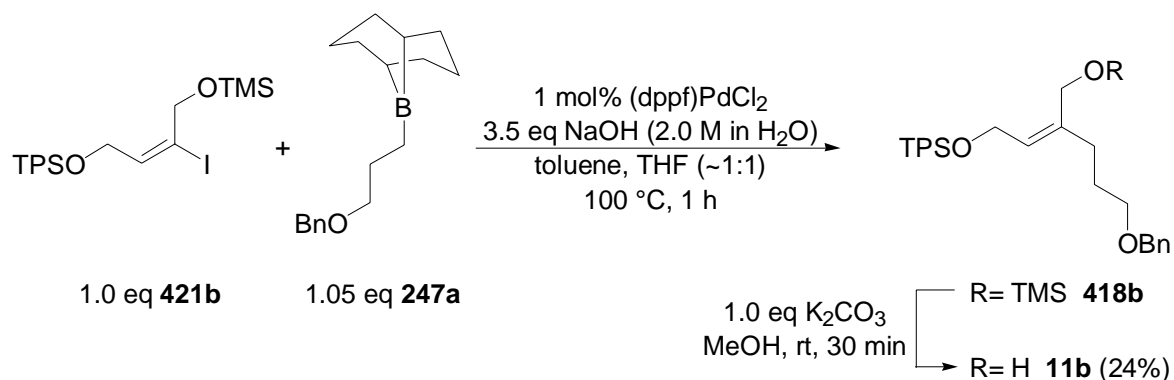
Allylic Alcohol 11a.³⁸⁸ To a solution of allylic benzyl ether (**510a**) (2.1 g, 14.0 mmol, 1.0 eq) in THF (28 mL, 2 mL/mmol) was added a solution of 9-BBN in THF (0.5 M, 29.3 mL, 1.05 eq) at rt. The reaction mixture was stirred at ambient temperature until TLC control indicated complete consumption of the starting material (~48 h). The solution of the borane **247a**^{422b,c} was used without further purification.

To an ice-cooled solution of the vinyl iodide **248a** (4.4 g, 13.3 mmol, 1.0 eq) in CH₂Cl₂ (40 mL, 3 mL/mmol) was added triethylamine (1.9 mL, 13.3 mmol, 1.0 eq) and trimethylchlorosilane (1.7 mL, 13.3 mmol, 1.0 eq). The reaction mixture was stirred in the dark for 30 min at 0 °C and then warmed to rt. The solvents were evaporated and the white

precipitate was removed by filtration and washed with diethyl ether. The ether was then evaporated and the fully protected vinyl iodide **421a** (R_f 0.69 hexanes/ethyl acetate 20/1) was used without further purification.

To the solution of the borane **247a** in THF (0.47 M, 59.3 mL, 1.05 eq) was added the protected vinyl iodide **421a** (13.3 mmol, 1.0 eq) in toluene (52 mL, 4 mL/mmol) and aq NaOH (2.0 M, 23.3 mL, 3.5 eq). The reaction mixture was carefully degassed under reduced pressure, recharged with argon and then (dppf)PdCl₂ (0.11 g, 0.1 mmol, 1 mol%) was added. The orange solution was refluxed for 1 h at 100 °C and turned dark brown. The reaction mixture was then cooled to rt, washed with saturated aq NH₄Cl (100 mL), water (100 mL) and brine (100 mL), and was then dried and concentrated. The crude product was purified by column chromatography (hexanes/ethyl acetate 20/1 to 3/1) to give a mixture of the fully protected diol **418a** (R_f 0.65 hexanes/ethyl acetate 10/1) and a small amount of the monoprotected diol **11a** (R_f 0.38 hexanes/ethyl acetate 10/1). The mixture was dissolved in MeOH (26.0 mL, 2.0 mL/mmol) and K₂CO₃ (1.8 g, 13.3 mmol, 1.0 eq) was added at rt. After 30 min, the salts were removed by filtration and washed with CH₂Cl₂. The organic solvents were then evaporated and the crude product was purified by column chromatography (hexanes/ethyl acetate 10/1) to afford the allylic alcohol **11a** (2.8 g, 8.0 mmol, 60%) as a brown oil (R_f 0.38 hexanes/ethyl acetate 10/1).

¹H NMR (300 MHz, CDCl₃) δ 7.29-7.19 (m, 5H), 5.44 (t, J = 6.3 Hz, 1H), 4.41 (s, 2H), 4.15 (d, J = 6.3 Hz, 2H), 4.02 (s, 2H), 3.42 (t, J = 6.3 Hz, 2H), 2.14 (t, J = 7.5 Hz, 2H), 1.75-1.66 (m, 2H), 0.82 (s, 9H), 0.00 (s, 6H), no OH resonance observed; ¹³C NMR (75 MHz, CDCl₃) δ 142.0 (C), 138.4 (C), 128.4 (2 \times CH), 127.7 (2 \times CH), 127.6 (CH), 127.1 (CH), 72.9 (CH₂), 69.9 (CH₂), 61.0 (CH₂), 59.5 (CH₂), 32.6 (CH₂), 28.1 (CH₂), 25.9 (3 \times CH₃), 18.3 (C), -5.2 (2 \times CH₃); IR (in substance) ν 3395, 3030, 2955-2855 cm⁻¹. Anal. Calcd for C₂₀H₃₄O₃Si: C, 68.52; H, 9.78. Found: C, 68.72; H, 9.90.



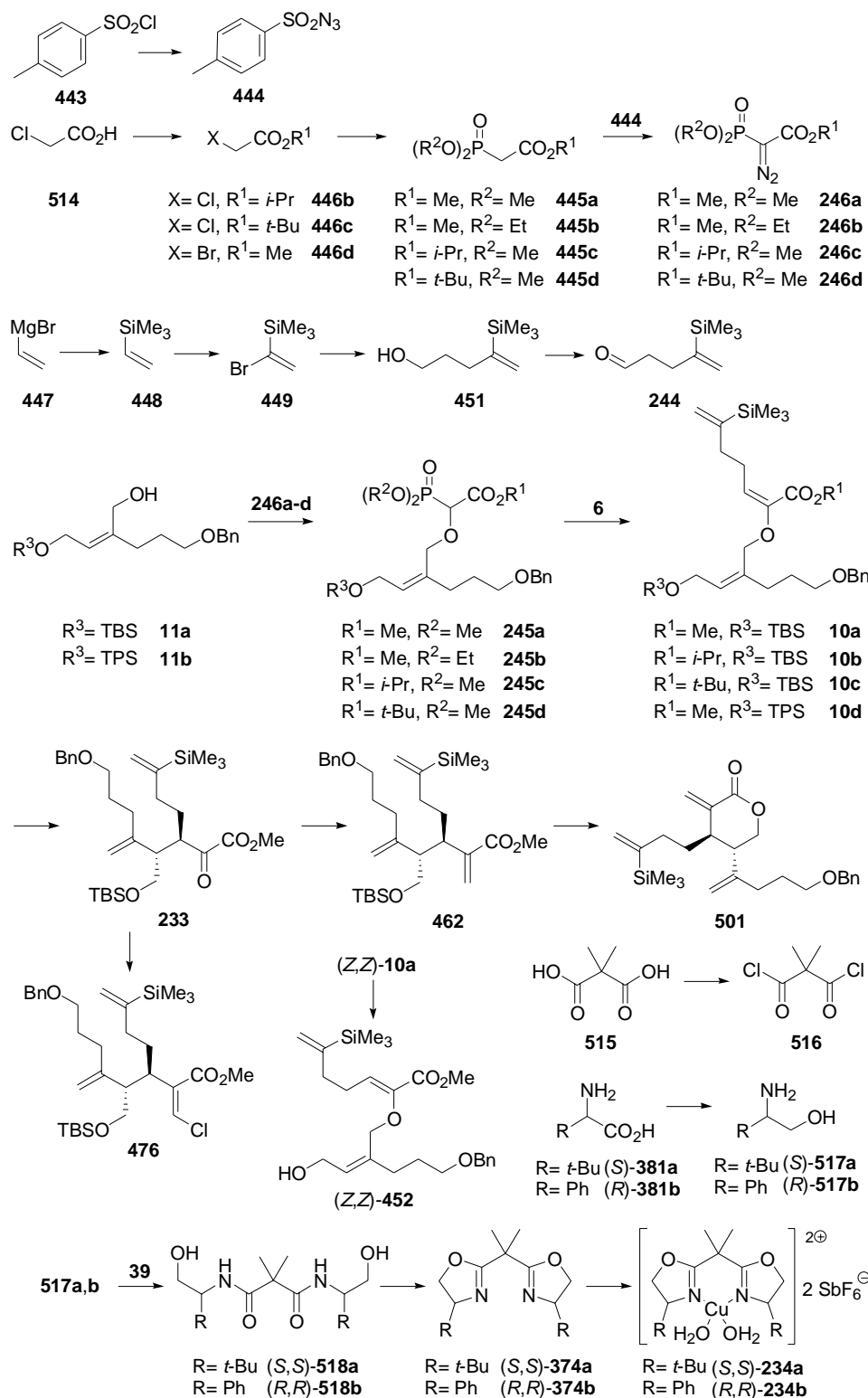
Allylic Alcohol 11b.⁴²³ As described in the preceding paragraph, allyl benzyl ether (**510a**) (0.9 g, 6.0 mmol) was treated with 9-BBN (12.6 mL, 6.3 mmol). The vinyl iodide **248a** (2.2 g, 4.9 mmol) was treated with triethylamine (0.7 mL, 4.9 mmol) and trimethylchlorosilane (0.6 mL, 4.9 mmol).

To the solution of the borane **247a** (6.0 mmol) was added the fully protected vinyl iodide **421b** (17.0 mmol, 1.0 eq) (R_f 0.79 hexanes/ethyl acetate 10/1) aq NaOH (2.0 M, 8.5 mL, 21.0 mmol) and (dppf)PdCl₂ (79 mg, 0.1 mmol). The crude mixture of fully protected diol **418b** (R_f 0.58 hexanes/ethyl acetate 10/1) and a small amount of the monoprotected diol **11b** (R_f 0.10 hexanes/ethyl acetate 10/1) was treated with (0.7 g, 4.9 mmol). Flash chromatography (hexanes/ethyl acetate 10/1) afford the allylic alcohol **11b** (0.5 g, 1.2 mmol, 24%) as a brown oil (R_f 0.12 hexanes/ethyl acetate 5/1).

¹H NMR (300 MHz, CDCl₃) δ 7.70-7.66 (m, 4H), 7.45-7.26 (m, 6H), 5.53 (t, J = 6.4 Hz, 1H), 4.48 (s, 2H), 4.25 (d, J = 6.5 Hz, 2H), 3.95 (s, 2H), 3.48 (t, J = 6.3 Hz, 2H), 2.19 (t, J = 7.5 Hz, 2H), 1.80-1.71 (m, 2H), 1.04 (s, 9H); ¹³C NMR (75 MHz, CDCl₃) δ 141.5 (C), 138.4 (C), 135.6 (4 \times CH), 133.6 (2 \times C), 129.7 (2 \times CH), 128.4 (2 \times CH), 127.7 (6 \times C), 127.6 (CH), 126.9 (CH), 73.0 (CH₂), 69.9 (CH₂), 60.8 (CH₂), 60.3 (CH₂), 32.1 (CH₂), 28.1 (CH₂), 26.8 (3 \times CH₃), 19.1 (C); IR (in substance) ν 3390, 3075-3070, 2930-2855 cm⁻¹. Anal. Calcd for C₃₀H₃₈O₃Si: C, 75.90; H, 8.07. Found: C, 75.84; H, 8.15.

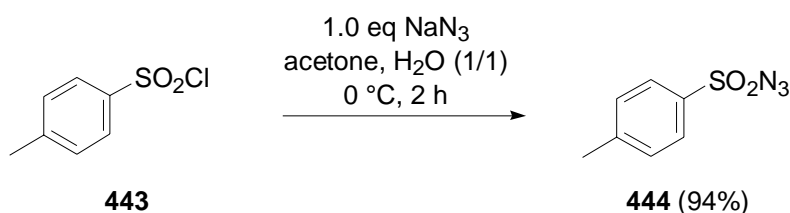
⁴²³ Yields not optimized.

20.3.2 Synthesis of the Allyl Vinyl Ether, Synthesis of the Catalyst, Claisen Rearrangement and Further Steps toward (-)-Xeniolide F



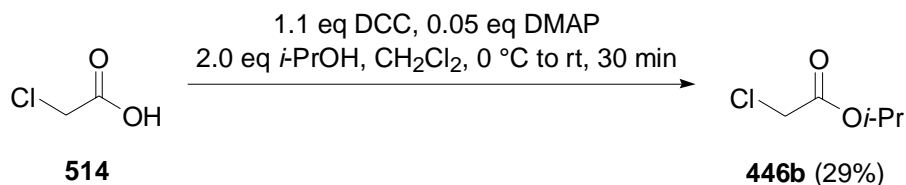
Scheme 154: Synthesis of the AVE, Claisen rearrangement, Wittig olefination, lactonization and synthesis of the catalyst.

Synthesis of the Allyl Vinyl Ether



Sulfonyl Azide 444.^{424,388} To an ice-cooled solution of *p*-toluolsulfonyl chloride (**443**) (8.0 g, 42.0 mmol, 1.0 eq) in acetone/water (1/1, 240 mL, 6 mL/mmol) was added sodium azide (2.7 g, 42.0 mmol, 1.0 eq). The reaction mixture was stirred for 2 h at 0 °C and the acetone was then evaporated (30 °C, 150 mbar). The phases were separated and the aqueous layer was extracted with diethyl ether. The combined organic phases were dried and concentrated to afford *p*-toluolsulfonyl azide (**444**) (7.8 g, 39.4 mmol, 94%) as a pale yellow oil (R_f 0.76 hexanes/ethyl acetate 1/1) which was stored at -32 °C.

¹H NMR (300 MHz, CDCl₃) δ 7.84 (d, J = 8.4 Hz, 2H), 7.40 (d, J = 8.4 Hz, 2H), 2.74 (s, 3H); ¹³C NMR (75 MHz, CDCl₃) δ 146.2 (C), 135.6 (C), 130.3 (2 \times CH), 127.5 (2 \times CH), 21.7 (CH₃). Anal. Calcd for C₇H₇N₃O₂S: C, 42.63; H, 3.58; N, 21.31; S, 16.26.



α -Chloroester 446b.^{425,426} To an ice-cooled solution of α -chloro acetic acid (**514**) (0.19 g, 2.0 mmol, 1.0 eq) in CH₂Cl₂ was subsequently added dicyclohexyl carbodiimide DCC (0.45 g, 2.2 mmol, 1.1 eq), 4-(*N,N*-dimethylamino)-pyridine DMAP (12.0 mg, 0.1 mmol, 0.05 eq) and 2-propanol (0.3 mL, 4.0 mmol, 2.0 eq). After stirring at rt for 30 min the white precipitate was removed by filtration and washed with ethyl acetate. Distillation (1 atm, 149 °C) afforded the α -chloroester **446b** (80 mg, 0.6 mmol, 29%).⁴²⁷

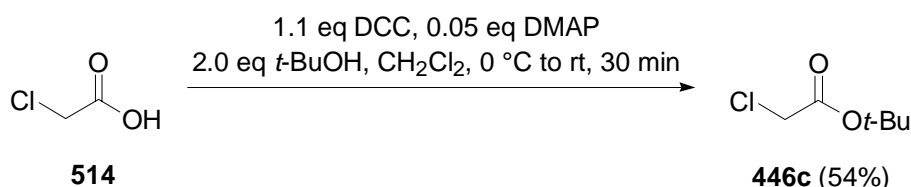
¹H NMR (300 MHz, CDCl₃) δ 5.09 (sept, J = 6.3 Hz, 1H), 4.02 (s, 2H), 1.29 (d, J = 6.2 Hz, 6H). Anal. Calcd for C₅H₉ClO₂: C, 43.97; H, 6.64; Cl, 25.96.

⁴²⁴ McElwee-White, L.; Dougherty, D. A. *J. Am. Chem. Soc.* **1984**, *106*, 3466-3474.

⁴²⁵ Compounds **446a-d** are commercially available (e.g. from ACROS). Synthesis of **446b,c** was performed analogue to the previously described procedure. See reference 64. Yields not optimized.

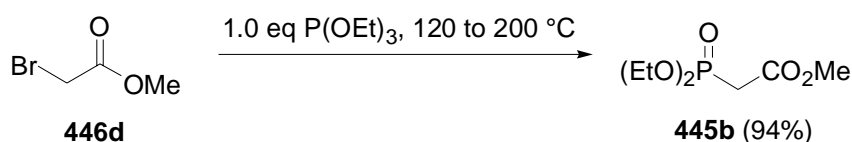
⁴²⁶ Li, Y.-Q. *Synth. Comm.* **1999**, *29*, 3901-3903.

⁴²⁷ According to the ¹H NMR spectrum of the reaction product, **446b** was obtained as 2:1 mixture with ethyl acetate.



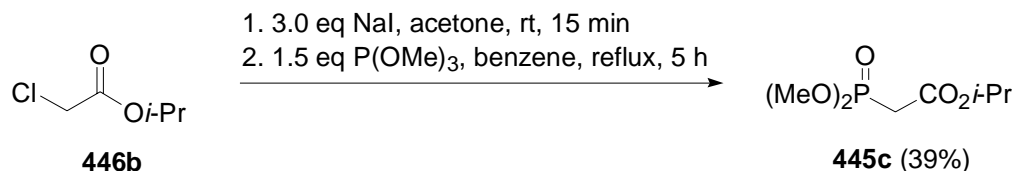
α -Chloroester 446c.^{425,428} As described in the preceding paragraph α -chloro acetic acid (**514**) (0.19 g, 2.0 mmol, 1.0 eq) was treated with DCC (0.45 g, 2.2 mmol, 1.1 eq), 4-(*N,N*-dimethylamino)-pyridine DMAP (12.0 mg, 0.1 mmol, 0.05 eq) and *tert*-butanol (0.4 mL, 4.0 mmol, 2.0 eq) to afford α -chloroester **446c** (0.16 g, 1.1 mmol, 54%) after distillation (1 atm, 157 °C).⁴²⁹

¹H NMR (300 MHz, CDCl₃) δ 3.96 (s, 2H), 1.49 (s, 9H). Anal. Calcd for C₆H₁₁ClO₂: C, 47.85; H, 7.36; Cl, 23.54.



Phosphonoacetate 445b.⁴³⁰ A mixture of bromo acetic acid **446d** (25.0 mL, 263 mmol, 1.0 eq) and triethyl phosphite (45.8 mL, 263 mmol, 1.0 eq) was slowly heated from 130 to 200 °C whereupon volatile by-products were distilled off. The resulting mixture was allowed to cool to 150 °C. The crude product was purified by distillation (0.25 mbar, 150 °C) to afford phosphonoacetate **445b** (46.8 g, 245 mmol, 94%) as colorless oil.⁴³¹

¹H NMR (300 MHz, CDCl₃) δ 4.20-4.10 (m, 4H), 3.73 (s, 3H), 2.96 (d, *J*(P-H) = 21.6 Hz, 2H), 1.33 (t, *J* = 7.0 Hz, 6H); ¹³C NMR (126 MHz, CDCl₃) δ 166.2 (C), 62.74 (CH₂), 62.66 (CH₂), 52.5 (CH₃), 34.1 (d, *J*(P-C) = 134.8 Hz, CH₂), 16.3 (CH₃), 16.2 (CH₃). Anal. Calcd for C₇H₁₅O₅P: C, 40.00; H, 7.19; P, 14.74.



Phosphonoacetate 445c.⁴³² To a solution of α -chloroester **446b** (76% in ethyl acetate, 53 mg, 0.29 mmol, 1.0 eq) in acetone (3 mL, 1 mL/0.1 mmol) was added sodium iodide (0.13 g,

⁴²⁸ Wiener, H.; Gilon, C. *J. Mol. Catal.* **1986**, *37*, 45-52.

⁴²⁹ According to the ¹H NMR spectrum of the reaction product **446c** was obtained as 3:1 mixture with ethyl acetate.

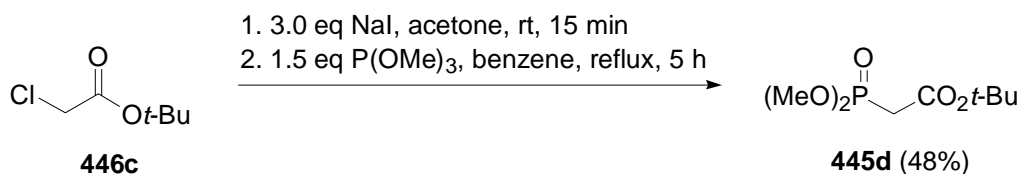
⁴³⁰ Commercially available from Aldrich. Prepared analogue to: House, H.; Jones, V. K.; Frank, G. A. *J. Org. Chem.* **1964**, *29*, 3327-3333.

⁴³¹ No *R_f* value determined.

⁴³² Reetz, M.; von Itzstein, M. *J. Organomet. Chem.* **1987**, *334*, 85-90.

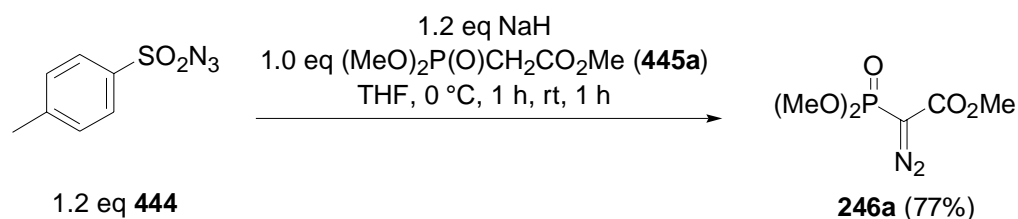
0.9 mmol, 3.0 eq) at rt. After stirring for 15 min in the dark, the resulting mixture was partitioned between ether (10 mL) and water (2 mL). The organic layer was washed with 2-mL portions of saturated aq Na₂S₂O₃, water and brine, dried and concentrated in the dark. The crude product was immediately dissolved in benzene and freshly distilled trimethylphosphite (51 μ L, 0.4 mmol, 1.5 eq) was added. The reaction mixture was heated for 5 h at reflux whereupon volatile by-products were distilled off, cooled to rt and concentrated. Removal of excess of trimethyl phosphite at high vacuum afforded phosphonoacetate **445c** (22 mg, 0.1 mmol, 39%) as colorless oil (R_f 0.26 ethyl acetate).

¹H NMR (300 MHz, CDCl₃) δ 5.05 (sept, J = 6.3 Hz, 1H), 3.82 (s, 3H), 3.79 (s, 3H), 2.94 (d, J (P-H) = 21.7 Hz, 2H), 1.26 (d, J = 6.3 Hz, 6H). Anal. Calcd for C₇H₁₅O₅P: C, 40.00; H, 7.19; P, 14.74.



Phosphonacetate 445d.⁴³³ As outlined for the preparation of phosphonoacetate **445c** α -chloroester **446c** (88% in ethyl acetate, 0.18 g, 1.1 mmol) was treated with sodium iodide (0.48 g, 3.3 mmol). Reaction of the crude product with trimethylphosphite (0.19 mL, 1.6 mmol) afforded phosphonoacetate **445d** (117 mg, 0.5 mmol, 48%) as colorless oil (R_f 0.29 ethyl acetate).

¹H NMR (300 MHz, CDCl₃) δ 3.82 (s, 3H), 3.78 (s, 3H), 2.89 (d, J (P-H) = 21.3 Hz, 2H), 1.47 (s, 9H). Anal. Calcd for C₈H₁₇O₅P: C, 42.86; H, 7.64; P, 13.82.



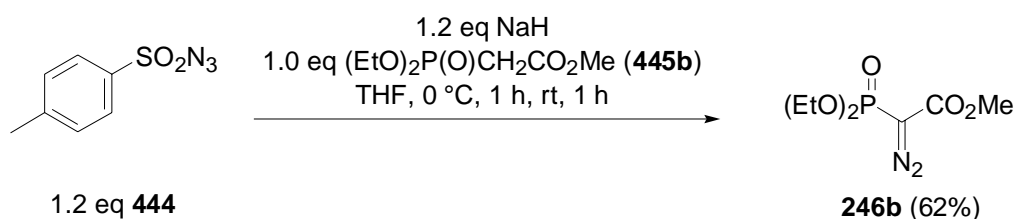
Diazaphosphonoacetate 246a.^{434,388} To a solution of sulfonyl azide **444** (7.8 g, 39.4 mmol, 1.2 eq) in THF (200 mL, 5 mL/mmol) at 0 °C was added sodium hydride (1.6 g, 39.4 mmol, 1.2 eq) and then a solution of trimethylphosphonoacetate (**445a**) (5.3 mL, 33.0 mmol, 1.0 eq) in THF (40 mL, 1 mL/mmol). The reaction mixture was stirred for 1 h at 0 °C, 1 h at rt and then quenched by the addition of water (5 mL/mmol). The phases were separated and the

⁴³³ Commercially available from Fluka. Prepared analogue to **445c**.

⁴³⁴ (a) Regitz, M.; Martin, R. *Tetrahedron* **1985**, *41*, 819-824. Prepared according to (b) Gois, P. M. P.; Afonso, C. A. M. *Eur. J. Org. Chem.* **2003**, 3798-3810.

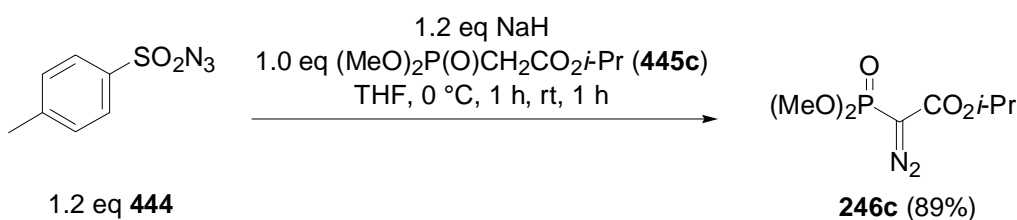
aqueous layer was extracted with diethyl ether. The combined organic phases were dried and concentrated. The crude product was purified by flash chromatography (hexanes/ethyl acetate 1/1) to afford the diazophosphonoacetate **246a** (5.3 g, 25.3 mmol, 77%) as a pale yellow oil (R_f 0.35 ethyl acetate).

^1H NMR (300 MHz, CDCl_3) δ 3.77 (s, 3H), 3.73 (s, 3H), 3.72 (s, 3H); ^{13}C NMR (75 MHz, CDCl_3) δ 163.6 (C), 163.4 (C), 53.83 (CH_3), 53.75 (CH_3), 52.5 (CH_3); IR (in substance) ν 3015-2855, 2125, 1705 cm^{-1} . Anal. Calcd for $\text{C}_5\text{H}_9\text{N}_2\text{O}_5\text{P}$: C, 28.86; H, 4.36; N, 13.46. Found: C, 28.93; H, 4.32; N, 13.27.



Diazophosphonoacetate 246b.⁴³⁵ As described in the preceding paragraph, reaction of *p*-toluenesulfonyl azide (**444**) (4.7 g, 24.0 mmol) with sodium hydride (1.0 g, 24.0 mmol) and phosphonoacetate **445b** (3.8 g, 20.0 mmol) afforded diazophosphonoacetate **246b** (2.9 g, 12.3 mmol, 62%) as pale yellow oil (R_f 0.32 ethyl acetate).

^1H NMR (300 MHz, CDCl_3) δ 4.28-4.10 (m, 4H), 3.79 (s, 3H), 1.35 (t, $J = 7.1$ Hz, 6H). Anal. Calcd for $\text{C}_7\text{H}_{13}\text{N}_2\text{O}_5\text{P}$: C, 35.60; H, 5.55; N, 11.86; P, 13.12.

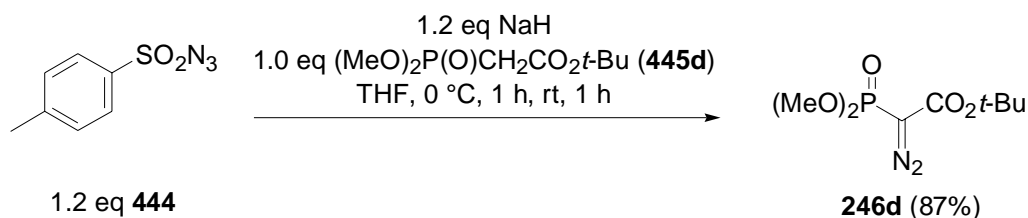


Diazophosphonoacetate 246c.⁴³⁶ As outlined for the preparation of diazophosphonoacetate **246a**, sulfonyl azide **444** (0.7 g, 3.8 mmol) was treated with sodium hydride (0.15 g, 3.8 mmol) and phosphonoacetate **445c** (0.7 g, 3.2 mmol). Flash chromatography (hexanes/ethyl acetate 1/1) afforded diazophosphonoacetate **246c** (0.7 g, 2.8 mmol, 89%) as pale yellow oil (R_f 0.36 ethyl acetate).

^1H NMR (300 MHz, CDCl_3) δ 5.11 (sept, $J = 6.3$ Hz, 1H), 3.85 (s, 3H), 3.81 (s, 3H), 1.28 (d, $J = 6.3$ Hz, 6H). Anal. Calcd for $\text{C}_7\text{H}_{13}\text{N}_2\text{O}_5\text{P}$: C, 35.60; H, 5.55; N, 11.86; P, 13.12.

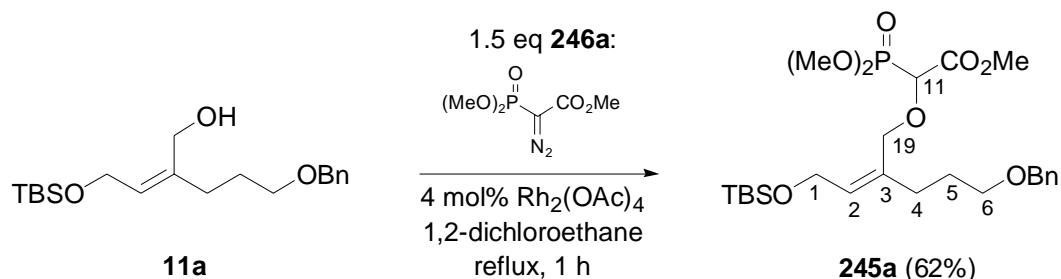
⁴³⁵ Khokhlov, P. S.; Kashemirov, B. A.; Mikityuk, A. D.; Strepikheev, Y. A.; Chimishkyan, A. L. *Z. Obs. Khim.* **1984**, *54*, 2785-2787.

⁴³⁶ Prepared analogue to **246a**. See reference 434.



Diazophosphonoacetate 246d.⁴³⁷ Analogous to the procedure for the preparation of diazophosphonoacetate **246a**, sulfonamide **444** (0.6 g, 2.6 mmol) was treated with sodium hydride (0.12 g, 3.1 mmol) and phosphonoacetate **445d** (0.6 g, 2.6 mmol). Flash chromatography (hexanes/ethyl acetate 1/1) afforded diazophosphonoacetate **246d** (0.6 g, 2.3 mmol, 87%) as pale yellow oil (R_f 0.44 ethyl acetate).

¹H NMR (300 MHz, CDCl₃) δ 3.84 (s, 3H), 3.81 (s, 3H), 1.50 (s, 9H). Anal. Calcd for C₈H₁₁N₂O₅P: C, 38.41; H, 6.04; N, 11.20; P, 12.38.



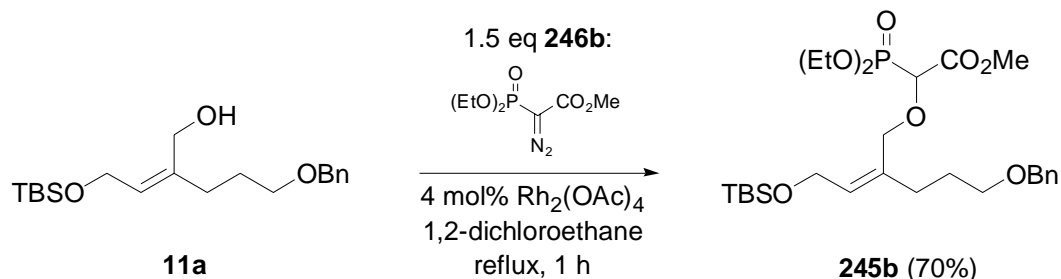
Phosphonate 245a.³⁸⁸ A solution of the allylic alcohol **11a** (1.0 g, 2.8 mmol, 1.0 eq) in 1,2-dichloroethane (21 mL, 7.5 mL/mmol) and Rh₂(OAc)₄ (49 mg, 0.1 mmol, 0.04 eq) was heated to reflux and the diazophosphonate **246a** (0.9 g, 4.2 mmol, 1.5 eq) in 1,2-dichloroethane (21 mL, 7.5 mL/mmol) was added dropwise. The reaction mixture was refluxed for 1 h, cooled to rt and then concentrated. The crude product was immediately purified by column chromatography⁴³⁸ (hexanes/ethyl acetate 1/1) to afford the phosphonate **245a** (0.9 g, 1.7 mmol, 62%) as a colorless oil (R_f 0.53 hexanes/ethyl acetate).

¹H NMR (500 MHz, CDCl₃) δ 7.31-7.26 (m, 5H, Ar-CH), 5.59 (t, J = 6.2 Hz, 1H, 2-CH=), 4.47 (s, 2H, -OCH₂Ph), 4.34 (d, ² J (P-H) = 19.1 Hz, 1H, 11-CH), 4.21-4.18 (m, 3H, 1-CH₂ and 19-CH₂), 4.07 (d^{AB}, J = 11.4 Hz, 1H, 19-CH₂), 3.811 (s, 3H, -OCH₃), 3.806 (s, 3H, -OCH₃), 3.79 (s, 3H, -OCH₃), 3.46 (t, J = 6.5 Hz, 2H, 6-CH₂), 2.20-2.06 (m, 2H, 4-CH₂), 1.78-1.74 (m, 2H, 5-CH₂), 0.88 (s, 9H, SiC(CH₃)₃), 0.04 (s, 6H, Si(CH₃)₂); ¹³C NMR (126 MHz, CDCl₃) δ 167.7 (C=O), 138.5 (C-Ar), 135.0 (3-C), 131.3 (2-CH=), 128.3 (2 × CH-Ar), 127.6 (2 × CH-Ar), 127.5 (CH-Ar), 74.6 (¹ J (P-C) = 158.7 Hz, 11-CH), 72.9 (-OCH₂Ph), 69.8 (6-CH₂), 69.1 (³ J (P-C) = 12.6 Hz, 19-CH₂), 59.3 (1-CH₂), 54.2 (² J (P-C) = 6.3 Hz, P-OCH₃),

⁴³⁷ Moore, J. D.; Sprott, K. T.; Hanson, P. R. *J. Org. Chem.* **2002**, *67*, 8123-8129.

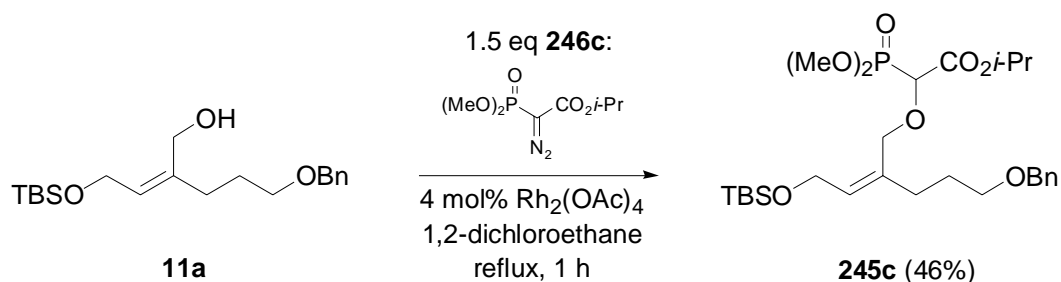
⁴³⁸ Storing of the crude product or the solution of the crude product even at -32 °C led to significant reduction of the isolated yields.

54.1 (2J (P-C) = 7.3 Hz, P-OCH₃), 52.8 (-OCH₃), 31.3 (4-CH₂), 27.8 (5-CH₂), 25.9 (3 × SiC(CH₃)₃), 18.3 (SiC(CH₃)₃), -5.2 (2 × Si(CH₃)₂); IR (in substance) ν 3330, 2980-2855, 1750 cm⁻¹. Anal. Calcd for C₂₅H₄₃O₈PSi: C 56.58; H 8.17. Found: C 56.51; H 8.04.



Phosphonate 245b.⁴³⁹ As described for the preparation of phosphonate **245a**, allylic alcohol **11a** (0.18 g, 0.5 mmol) was treated with $\text{Rh}_2(\text{OAc})_4$ (11 mg, 0.03 mmol) and diazophosphonoacetate **246b** (0.18 g, 0.8 mmol). Flash chromatography (hexanes/ethyl acetate 3/1 to 1/1) afforded the phosphonate **245b** (0.20 g, 0.4 mmol, 70%) as pale yellow oil (R_f 0.56 hexanes/ethyl acetate 2/1).

¹H NMR (300 MHz, CDCl_3) δ 7.34-7.22 (m, 5H), 5.54 (t, J = 6.1 Hz, 1H), 4.43 (s, 2H), 4.26 (d, J (P-H) = 19.1 Hz, 1H), 4.19-3.99 (m, 8H), 3.75 (s, 3H), 3.41 (t, J = 6.4 Hz, 2H), 2.20-2.11 (m, 2H), 1.78-1.66 (m, 2H), 1.26 (t, J = 7.2 Hz, 6H), 0.83 (s, 9H), 0.00 (s, 6H); IR (in substance) ν 3350, 2930-2855, 1750 cm⁻¹. Anal. Calcd for C₂₇H₄₇O₈PSi: C, 58.04; H, 8.48; P, 5.54.

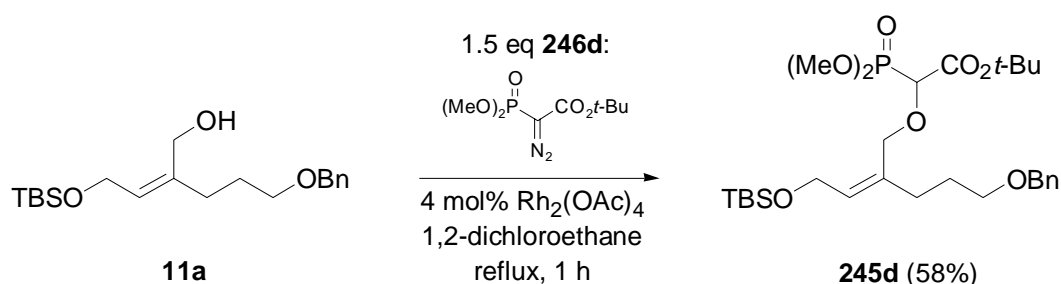


Phosphonate 245c.⁴³⁹ Analogous to the synthesis of phosphonate **245a**, allylic alcohol **11a** (0.15 g, 0.4 mmol) was treated with $\text{Rh}_2(\text{OAc})_4$ (8 mg, 0.02 mmol) and diazophosphonate **246c** (0.15 g, 0.6 mmol). Flash chromatography (hexanes/ethyl acetate 3/1 to 1/1) afforded the phosphonate **245c** (0.11 g, 0.2 mmol, 46%) as pale yellow oil (R_f 0.58 hexanes/ethyl acetate 1/1).

¹H NMR (300 MHz, CDCl_3) δ 7.30-7.22 (m, 5H), 5.54 (t, J = 6.3 Hz, 1H), 5.10 (sept, J = 6.3 Hz, 1H), 4.43 (s, 2H), 4.23 (d, 2J (P-H) = 18.8 Hz, 1H), 4.19-4.12 (m, 3H), 4.02 (d^{AB}, J =

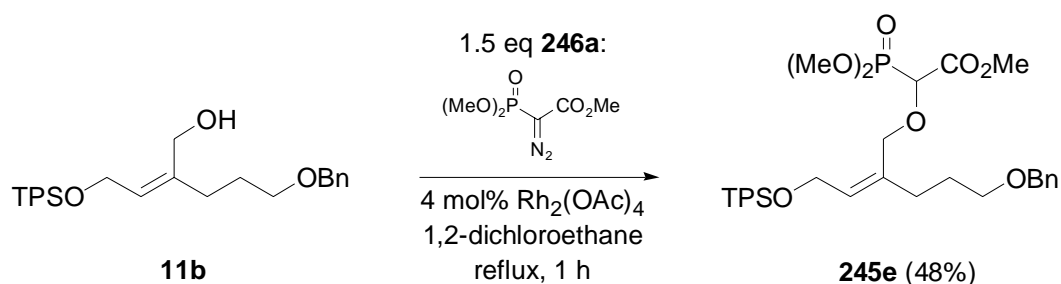
⁴³⁹ Test substrate for the HWE olefination. Not fully characterized.

11.4 Hz, 1H), 3.77 (s, 3H), 3.74 (s, 3H), 3.42 (t, $J = 6.4$ Hz, 2H), 2.16 (brt, $J = 7.5$ Hz, 2H), 1.79-1.66 (m, 2H), 1.25 (d, $J = 6.3$ Hz, 3H), 1.24 (d, $J = 6.3$ Hz, 3H), 0.83 (s, 9H), 0.00 (s, 6H); ^{13}C NMR (75 MHz, CDCl_3) δ 166.6 (C), 138.5 (C), 135.1 (C), 131.2 (CH), 128.3 (2 \times CH), 127.6 (2 \times CH), 127.5 (CH), 75.1 (J (P-C) = 158.2 Hz, CH), 72.9 (CH_2), 69.9 (CH_2), 69.8 (CH), 69.0 (J (P-C) = 12.4 Hz, CH_2), 59.4 (CH_2), 54.0 (J (P-C) = 6.8 Hz, 2 \times CH_3), 31.3 (CH_2), 27.8 (CH_2), 25.9 (3 \times CH_3), 21.7 (CH_3), 21.5 (CH_3), 18.3 (C), -5.1 (2 \times CH_3); IR (in substance) ν 3410, 2960-2850, 1730 cm^{-1} . Anal. Calcd for $\text{C}_{27}\text{H}_{47}\text{O}_8\text{PSi}$: C, 58.04; H, 8.48; P, 5.54.



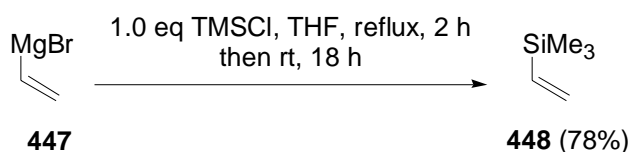
Phosphonate 245d.⁴³⁹ As described for phosphonate **245a**, allylic alcohol **11a** (0.14 g, 0.4 mmol) was treated with $\text{Rh}_2(\text{OAc})_4$ (7 mg, 0.02 mmol) and diazophosphonate **246d** (0.15 g, 0.6 mmol). Flash chromatography (hexanes/ethyl acetate 3/1 to 1/1) afforded phosphonate **245d** (0.13 g, 0.2 mmol, 58%) as pale yellow oil (R_f 0.50 hexanes/ethyl acetate 2/1).

^1H NMR (300 MHz, CDCl_3) δ 7.33-7.21 (m, 5H), 5.70 (t, $J = 7.2$ Hz, 1H^{minor}), 5.54 (t, $J = 6.4$ Hz, 1H^{major}), 4.43 (s, 2H), 4.27-3.99 (m, 5H), 3.77 (s, 3H), 3.73 (s, 3H), 3.42 (brt, $J = 6.43$, 2H), 2.15 (brt, $J = 7.2$ Hz, 2H), 1.78-1.64 (m, 2H), 1.45 (s, 9H), 0.85 (s, 9H^{minor}), 0.83 (s, 9H^{major}), 0.04 (s, 6H^{minor}), 0.00 (s, 6 H^{major}); ^{13}C NMR (126 MHz, CDCl_3) δ 166.1 (C), 138.5 (C), 135.1 (C), 131.1 (CH), 128.3 (2 \times CH), 127.6 (2 \times CH), 127.4 (CH), 83.0 (C), 75.2 (J (P-C) = 157.4 Hz, CH), 72.8 (CH_2), 69.8 (CH_2), 68.9 (J (P-C) = 13.3 Hz, CH_2), 59.4 (CH_2), 53.8 (J (P-C) = 6.1 Hz, CH_2), 31.3 (CH_2), 27.9 (3 \times CH_3), 27.8 (CH_2), 25.9 (3 \times CH_3), 18.3 (C), -3.6 (2 \times CH_3), -5.2 (3 \times CH_3); IR (in substance) ν 3345, 2955-2855, 1740 cm^{-1} . Anal. Calcd for $\text{C}_{28}\text{H}_{49}\text{O}_8\text{PSi}$: C, 58.72; H, 8.62; P, 5.41.



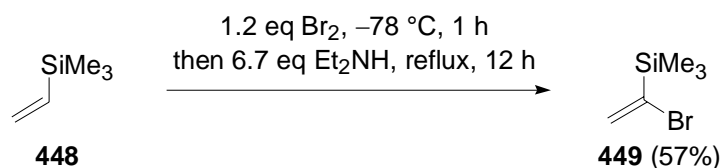
Phosphonate 245e.⁴³⁹ As outlined for the preparation of **245a**, allylic alcohol **11b** (75 mg, 0.2 mmol) was treated with $\text{Rh}_2(\text{OAc})_4$ (3 mg, 0.01 mmol) and diazophosphonate **246a** (52 mg, 0.3 mmol). Flash chromatography (hexanes/ethyl acetate 2/1 to ethyl acetate) afforded phosphonated **245e** (52 mg, 0.1 mmol, 48%) as bluegreen oil (R_f 0.67 ethyl acetate).

^1H NMR (500 MHz, CDCl_3) δ 7.66-7.64 (m, 4H), 7.43-7.34 (m, 6H), 7.33-7.32 (m, 5H), 5.66 (t, $J = 6.3$ Hz, 1H), 4.48 (s, 2H), 4.24-4.19 (m, 3H), 3.99 (d^{AB}, $J = 11.5$ Hz, 1H), 3.86 (d^{AB}, $J = 11.5$ Hz, 1H), 3.74 (d, $J(\text{P-H}) = 5.9$ Hz, 3H), 3.72 (d, $J(\text{P-H}) = 5.9$ Hz, 3H), 3.67 (s, 3H), 3.46 (t, $J = 6.4$ Hz, 2H), 2.18 (dd, $J = 13.8, 6.2$ Hz, 2H), 1.78-1.69 (m, 2H), 1.02 (s, 9H); ^{13}C NMR (126 MHz, CDCl_3) δ 167.6 ($J(\text{P-C}) = 2.4$ Hz, C), 138.5 (C), 135.5 ($4 \times \text{CH}$), 135.2 (C), 133.6 ($2 \times \text{C}$), 130.7 (CH), 129.7 ($2 \times \text{CH}$), 128.3 ($2 \times \text{CH}$), 127.7 ($4 \times \text{CH}$), 127.6 ($2 \times \text{CH}$), 127.5 (CH), 74.6 ($J(\text{P-C}) = 158.6$ Hz, CH), 72.9 (CH_2), 69.8 (CH_2), 69.0 ($J(\text{P-C}) = 13.3$ Hz, CH_2), 60.1 (CH_2), 54.1 ($J(\text{P-C}) = 7.3$ Hz, CH_3), 54.0 ($J(\text{P-C}) = 6.1$ Hz, CH_3), 52.6 (CH_3), 31.2 (CH_2), 27.7 (CH_2), 26.7 ($3 \times \text{CH}_3$), 19.1 (C); IR (in substance) ν 3375, 3070-3000, 2955-2855, 1745 cm^{-1} . Anal. Calcd for $\text{C}_{35}\text{H}_{47}\text{O}_8\text{PSi}$: C, 64.20; H, 7.23; P, 4.73.



Vinyl Silane 448.^{362,388} A solution of vinylmagnesium bromide (**447**) in THF (1.0 M, 100.0 mL, 100.0 mmol, 1.0 eq) was heated to reflux and trimethylchlorosilane (12.6 mL, 100 mmol, 1.0 eq) in THF (10 mL, 0.1 mL/mmol) was added dropwise over 30 min. After heating to reflux for 2 h, the reaction mixture was cooled to rt and stirred for 18 h. The product was distilled from the reaction mixture (bp 60-66 °C, bath temperature 100-180 °C) and then washed with small amounts of water (20×5 mL) to remove the THF. The isolated vinyl silane **448** (7.8 g, 78.2 mmol, 78%) contained small amounts (<5%) of THF.⁴⁴⁰

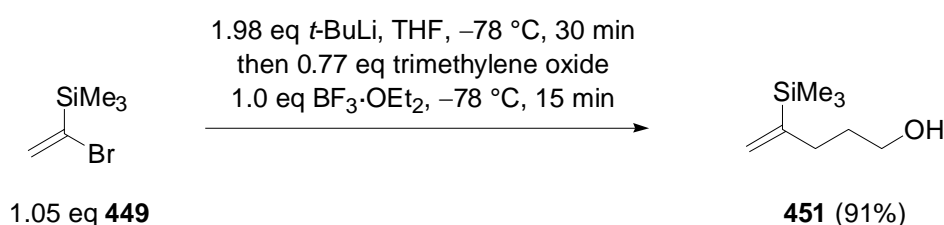
^1H NMR (300 MHz, CDCl_3) δ 6.09 (dd, $J = 20.1, 14.6$ Hz, 1H), 5.85 (dd, $J = 16.7, 4.0$ Hz, 1H), 5.59 (dd, $J = 20.2, 4.0$ Hz, 1H), 0.00 (s, 9H); ^{13}C NMR (75 MHz, CDCl_3) δ 140.3 (CH), 130.8 (CH_2), -1.7 ($3 \times \text{CH}_3$). Anal. Calcd for $\text{C}_5\text{H}_{12}\text{Si}$: C, 59.91; H, 12.07.



⁴⁴⁰ Determined from the 300 MHz ^1H NMR spectrum of **448**.

Vinyl Bromide 449.^{362,388} To the vinyl silane **448** (3.1 g, 31.0 mmol, 1.0 eq) at $-78\text{ }^{\circ}\text{C}$ was added bromine (1.9 mL, 5.8 mmol, 1.2 eq) over 1 h. The reaction mixture was warmed to rt and re-cooled to $0\text{ }^{\circ}\text{C}$. Diethylamine (21.6 mL, 21.0 mmol, 6.7 eq) was added carefully and the reaction mixture was heated to reflux for 12 h. The white precipitate was removed by filtration and washed with diethyl ether. The combined organic phases were washed carefully with 2 N HCl until the pH value of the aqueous layer was <2 . The organic phase was then washed with water (150 mL) and brine (150 mL), dried, concentrated and distilled to afford vinyl bromide **449** (4.3 g, 74% in Et_2O ,⁴⁴¹ 17.9 mmol, 57%) as a colorless liquid (bp.: $125\text{ }^{\circ}\text{C}$, 1 atm).

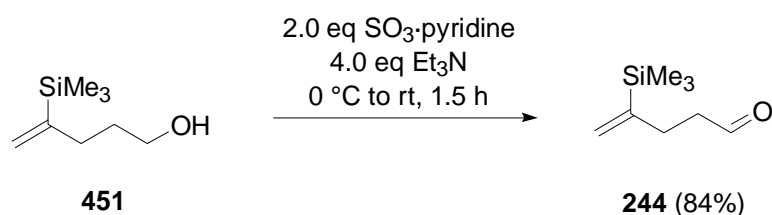
^1H NMR (300 MHz, CDCl_3) δ 6.27 (d, $J = 1.6$ Hz, 1H), 6.18 (d, $J = 1.7$ Hz, 1H), 0.19 (s, 9H); ^{13}C NMR (75 MHz, CDCl_3) δ 138.9 (C), 129.3 (CH_2), -2.2 ($3 \times \text{CH}_3$). Anal. Calcd for $\text{C}_5\text{H}_{11}\text{BrSi}$: C, 33.53; H, 6.19.



Alcohol 451.^{361,388} To a solution of the vinyl bromide **449** (86% in Et_2O , 3.1 g, 15 mmol, 1.05 eq) in THF (45 mL, 3 mL/mmol) was added $t\text{-BuLi}$ (1.5 M, 18.9 mL, 28.3 mmol, 1.98 eq) at $-78\text{ }^{\circ}\text{C}$ and stirred for 30 min. Trimethylene oxide (0.7 mL, 11.0 mmol, 0.77 eq) and $\text{BF}_3\cdot\text{OEt}_2$ (1.7 mL, 14.3 mmol, 1.0 eq) was added and the reaction mixture was stirred for 15 min. The reaction was quenched by the addition of saturated aq NH_4Cl and extracted with CH_2Cl_2 (3×30 mL). The combined organic layers were dried and concentrated. The crude product was purified by column chromatography (pentane/diethyl ether 10/1 to 1/1) to afford the alcohol **451** (1.6 g, 10.0 mmol, 91%) as a colorless liquid (R_f 0.35 hexanes/ethyl acetate 3/1). The unspecified side product that was observed several times is detectable by TLC if longer heating times of the TLC plate (treated with the staining reagent) are employed. R_f (side product) 0.41 hexanes/ethyl acetate 3/1). The spot of the side product has a more bluish appearance than the spot of **451**.

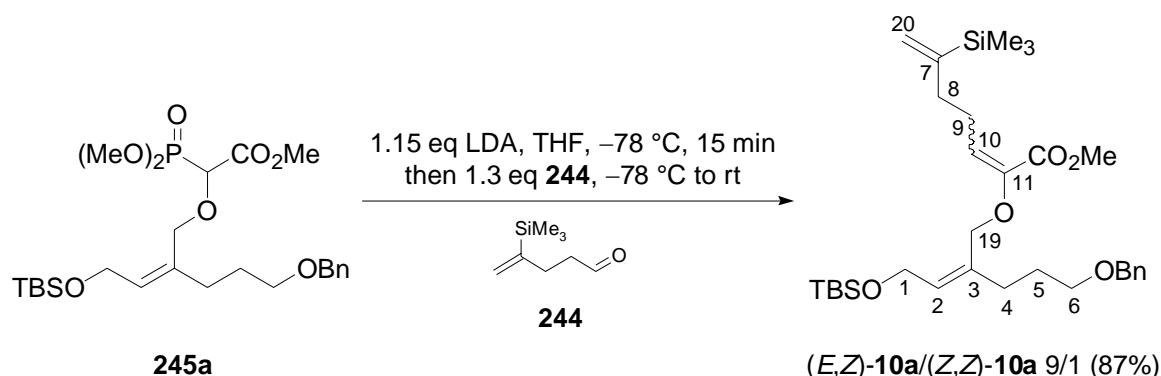
^1H NMR (300 MHz, CDCl_3) δ 5.49 (dt, $J = 2.9, 1.5$ Hz, 1H), 5.25 (bd, 2.9 Hz, 1H), 3.57 (t, $J = 6.5$ Hz, 2H), 2.12 (t, $J = 7.7$ Hz, 2H), 1.66-1.60 (m, 2H), 0.00 (s, 9H); ^{13}C NMR (75 MHz, CDCl_3) δ 151.8 (C), 124.1 (CH_2), 62.8 (CH_2), 32.1 (CH_2), 31.9 (CH_2), -1.5 ($3 \times \text{CH}_3$). Anal. Calcd for $\text{C}_8\text{H}_{18}\text{OSi}$: C, 60.69; H, 11.46.

⁴⁴¹ Determined from the 300 MHz ^1H NMR spectrum of **449**.



Aldehyde 244.^{361,388} To a solution of the alcohol **451** (0.4 g, 2.7 mmol, 1.0 eq) in CH₂Cl₂/DMSO (4/1, 20 mL, 8 mL/mmol) at 0 °C was added triethylamine (1.5 mL, 10.6 mmol, 4.0 eq) and sulfur trioxide-pyridine complex (0.8 g, 5.3 mmol, 2.0 eq). The reaction mixture was stirred for 1.5 h at rt, quenched by the addition of water and extracted with CH₂Cl₂ (3 × 20 mL). The combined organic layers were dried and concentrated. The crude product was purified by column chromatography (pentane) to afford the aldehyde **244** (0.35 g, 2.2 mmol, 84%) as a colorless liquid (*R_f* 0.32 hexanes/ethyl acetate 20/1).

¹H NMR (300 MHz, CDCl₃) δ 9.68 (s, 1H), 5.45-5.42 (m, 1H), 5.28-5.26 (m, 1H), 2.51-2.44 (m, 2H), 2.39-2.32 (m, 2H), 0.00 (s, 9H); ¹³C NMR (75 MHz, CDCl₃) δ 202.2 (C), 150.2 (C), 124.2 (CH₂), 42.6 (CH₂), 27.5 (CH₂), -1.7 (3 × CH₃). Anal. Calcd for C₈H₁₆OSi: C, 61.48; H, 10.32.



Allyl Vinyl Ether 10a.³⁸⁸ To a solution of the phosphonate **245a** (1.1 g, 2.1 mmol, 1.0 eq) in THF (14 mL, 7 mL/mmol) was added a LDA solution [prepared from diisopropylamine (0.4 mL, 2.7 mmol, 1.3 eq) and *n*-BuLi (2.2 M in *n*-hexanes, 1.1 mL, 1.15 eq)] in THF (8 mL, 4 mL/mmol of **245a**) at -78 °C. After 15 min, a cooled (-78 °C) solution of the aldehyde **244** (0.43 g, 2.7 mmol, 1.3 eq) in THF (8 mL, 4 mL/mmol of **245a**) was added at -78 °C. The reaction mixture was stirred for 30 min at -78 °C, warmed to rt, quenched by the addition of saturated aq NH₄Cl and extracted with CH₂Cl₂ (3 × 20 mL). The combined organic layers were dried and concentrated. The crude product was purified by column chromatography (hexanes/ethyl acetate 20/1) to afford the allyl vinyl ether **10a** (1.0 g, 1.8 mmol, 87%) as mixture of double bond isomers (*E,Z*)-**10a**/*Z,Z*-**10a** 9/1 (*R_f* 0.24 hexanes/ethyl acetate 10/1). Allyl vinyl ether **10a** was generally used as mixture of double bond isomers. However, the

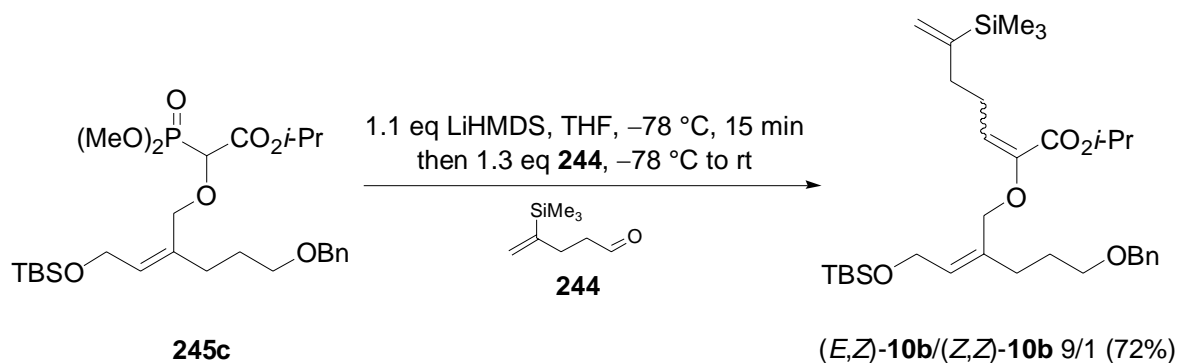
double bond isomers may be separated by preparative HPLC: *n*-heptane/ethyl acetate 30/1, r_t (*Z,Z*-**10a**) ~ 19 min, r_t (*E,Z*-**10a**) ~ 20 min, no baseline separation under these conditions.

(*E,Z*-**10a**/*Z,Z*-**10a** 9/1: ^1H NMR (500 MHz, CDCl_3) δ 7.26-7.17 (m, 5H, CH-Ar), 6.17 (t, $J = 7.3$ Hz, 1H^{minor} , 10-CH=), 5.58-5.57 (m, 1H, 20-CH₂=), 5.54 (t, $J = 5.9$ Hz, 1H, 2-CH=), 5.35 (d, $J = 1.8$ Hz, 1H, 20-CH₂=), 5.28 (t, $J = 7.5$ Hz, 1H^{major} , 10-CH=), 4.48 (s, 2H, OCH₂Ph), 4.28-4.24 (m, 4H^{minor} , 19-CH₂ and 1-CH₂), 4.23-4.22 (m, 4H^{major} , 19-CH₂ and 1-CH₂), 3.75 (s, 3H, -OCH₃), 3.48 (t, $J = 6.5$ Hz, 2H, 6-CH₂), 2.56 (dt, $J = 15.3, 7.6$ Hz, 2H^{major} , 9-CH₂), 2.36-2.32 (m, 2H^{minor} , 9-CH₂), 2.28 (t, $J = 7.0$ Hz, 2H^{minor} , 4-CH₂), 2.27-2.20 (m, 2H^{major} , 4-CH₂ and 2H, 8-CH₂), 1.80-1.75 (m, 2H, 5-CH₂), 0.89 (s, 9H, SiC(CH₃)₃), 0.08 (s, 9H, Si(CH₃)₃), 0.05 (s, 6H, Si(CH₃)₂); ^{13}C NMR (126 MHz, CDCl_3) δ 164.3 ($\text{CO}_2\text{Me}^{\text{minor}}$), 164.0 ($\text{CO}_2\text{Me}^{\text{major}}$), 151.3 (7-C=^{major}), 150.9 (7-C=^{minor}), 144.6 (11-C=^{minor}), 144.5 (11-C=^{major}), 138.6 (C-Ar), 135.8 (3-C=^{minor}), 135.5 (3-C=^{major}), 130.3 (2-CH=^{minor}), 129.5 (2-CH=^{major}), 129.2 (10-CH=^{minor}), 128.3 (2 × CH-Ar), 127.6 (2 × CH-Ar), 127.5 (CH-Ar), 124.4 (20-CH₂^{major}), 124.2 (20-CH₂^{minor}), 117.7 (10-CH=^{major}), 72.9 (-OCH₂Ph), 69.9 (6-CH₂), 69.3 (19-CH₂^{minor}), 66.9 (19-CH₂^{major}), 59.6 (1-CH₂), 51.8 (-OCH₃^{minor}), 51.7 (-OCH₃^{major}), 36.1 (8-CH₂^{major}), 34.3 (8-CH₂^{minor}), 31.7 (4-CH₂^{minor}), 31.5 (4-CH₂^{major}), 27.9 (5-CH₂), 26.1 (9-CH₂^{major}), 25.9 (3 × SiC(CH₃)₃), 24.9 (9-CH₂^{minor}), 18.3 (SiC(CH₃)₃), -1.5 (3 × Si(CH₃)₃), -5.1 (2 × SiCH₃); IR (in substance) ν 2955-2855, 1725 cm^{-1} . Anal. Calcd for C₃₁H₅₂O₅Si₂: C, 66.38; H, 9.34. Found: C, 66.07; H, 9.45.

(*E,Z*-**10a**: ^1H NMR (300 MHz, CDCl_3) δ 7.34-7.26 (m, 5H), 5.58-5.57 (m, 1H), 5.54 (t, $J = 5.9$ Hz, 1H), 5.35 (d, $J = 1.8$ Hz, 1H), 5.28 (t, $J = 7.5$ Hz 1H), 4.49 (s, 2H), 4.24-4.21 (m, 4H), 3.75 (s, 3H), 3.48 (t, $J = 6.5$ Hz, 2H), 2.57 (dt, $J = 15.3, 7.6$ Hz, 2H), 2.24-2.19 (m, 4H), 1.81-1.74 (m, 2H), 0.89 (s, 9H), 0.08 (s, 9H), 0.05 (s, 6H); ^{13}C NMR (75 MHz, CDCl_3) δ 164.1 (C), 151.3 (C), 144.6 (C), 138.6 (C), 135.5 (C), 129.5 (CH), 128.3 (2 × CH), 127.6 (2 × CH), 127.5 (CH), 124.5 (CH₂), 117.8 (CH), 72.9 (CH₂), 69.9 (CH₂), 70.0 (CH₂), 59.6 (CH₂), 51.7 (CH₃), 36.1 (CH₂), 31.6 (CH₂), 28.0 (CH₂), 26.1 (CH₂), 25.9 (3 × CH₃), 18.3 (C), -1.5 (3 × CH₃), -5.1 (2 × CH₃).

(*Z,Z*-**10a**: ^1H NMR (500 MHz, CDCl_3) δ 7.33-7.26 (m, 5H, CH-Ar), 6.25 (t, $J = 7.3$ Hz, 1H, 10-CH=), 5.59-5.45 (m, 2H, 20-CH₂= and 2-CH=), 5.35-5.33 (m, 1H, 20-CH₂=), 4.49 (s, 2H, -OCH₂Ph), 4.28-4.25 (m, 4H, 19-CH₂ and 1-CH₂), 3.75 (s, 3H, -OCH₃), 3.48 (t, $J = 6.5$ Hz, 2H, 6-CH₂), 2.37-2.31 (m, 2H, 9-CH₂), 2.28 (t, $J = 7.0$ Hz, 2H, 4-CH₂), 2.24-2.16 (m, 2H, 8-CH₂), 1.84-1.76 (m, 2H, 5-CH₂), 0.88 (s, 9H, SiC(CH₃)₃), 0.07 (s, 9H, Si(CH₃)₃), 0.05 (s, 6H, Si(CH₃)₂); ^{13}C NMR (126 MHz, CDCl_3) δ 164.3 (CO_2Me), 150.9 (7-C=), 144.7 (11-C=), 138.6 (C-Ar), 135.8 (3-C=), 130.3 (2-CH=), 129.2 (10-CH=) 128.3 (2 × CH-Ar), 127.6 (2 ×

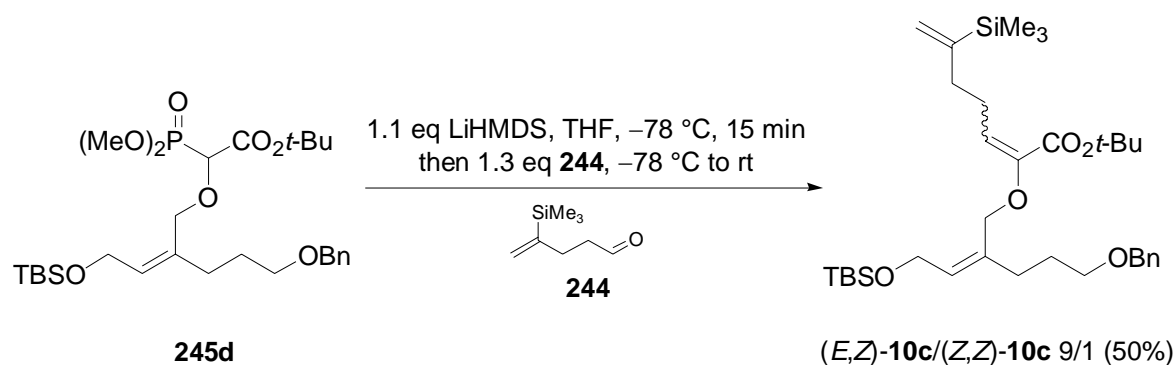
CH-Ar), 127.5 (CH-Ar), 124.2 (20-CH₂), 72.9 (-OCH₂Ph), 69.9 (6-CH₂), 69.3 (19-CH₂), 59.6 (1-CH₂), 51.8 (-OCH₃), 34.3 (8-CH₂), 31.7 (4-CH₂), 27.9 (5-CH₂), 25.9 (3 × SiC(CH₃)₃), 24.9 (9-CH₂), 18.3 (SiC(CH₃)₃), -1.6 (3 × Si(CH₃)₃), -5.1 (2 × SiCH₃).



Allyl Vinyl Ether 10b.⁴⁴² To a solution of the phosphonate **245c** (28 mg, 0.05 mmol, 1.1 eq) in THF (2 mL, 4 mL/0.1 mmol **245c**) was added a LiHMDS solution (1.0 M in hexanes, 55 μ L, 0.06 mmol, 1.1 eq) at -78°C . After stirring for 30 min a pre-cooled (-78°C) solution of the aldehyde **87** (10 mg, 0.07 mmol, 1.3 eq) in THF (2 mL, 4 mL/0.1 mmol **245c**) was added. The reaction mixture was warmed to rt, quenched by the addition of saturated aq NH₄Cl and extracted with CH₂Cl₂ (3 × 4 mL). The combined organic layers were dried and concentrated. Flash chromatography (hexanes/ethyl acetate 20/1) afforded allyl vinyl ether **10b** (21 mg, 0.04 mmol, 72%) as mixture of double bond isomers (*E,Z*-**10b**/*Z,Z*-**10b** 9/1 as colorless oil (*R_f* 0.45 hexanes/ethyl acetate 10/1)

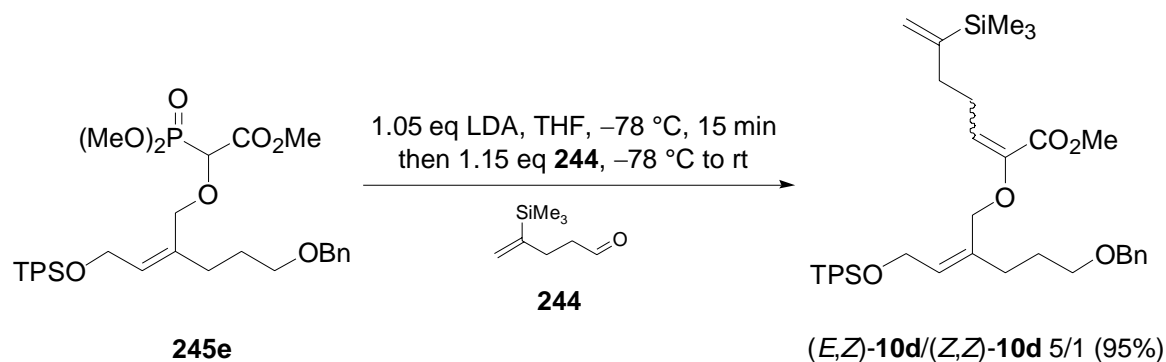
¹H NMR (300 MHz, CDCl₃) δ 7.27-7.13 (m, 5H), 6.15 (t, *J* = 7.5 Hz, 1H^{minor}), 5.52-5.47 (m, 1H), 5.45 (t, *J* = 6.1 Hz, 1H), 5.29-5.24 (m, 1H), 5.17 (t, *J* = 7.4 Hz, 1H^{major}), 5.01 (sept, *J* = 6.3 Hz, 1H), 4.40 (s, 2H), 4.21-4.17 (m, 4H^{minor}), 4.17-4.10 (m, 4H^{major}), 3.40 (t, *J* = 6.4 Hz, 2H), 2.52-2.40 (m, 2H), 2.14 (t, *J* = 7.5 Hz, 2H), 1.77-1.65 (m, 2H), 1.19 (d, *J* = 6.3 Hz, 6H), 0.82-0.78 (m, 9H), 0.02-(-0.01) (m, 9H), -0.01-(-0.04) (m, 6H); ¹³C NMR (75 MHz, CDCl₃) δ 163.2 (C), 151.4 (C), 145.2 (C), 138.6 (C), 135.7 (C), 129.3 (CH), 128.3 (2 × CH), 127.6 (2 × CH), 127.5 (CH), 124.2 (CH₂), 117.3 (CH), 72.9 (CH₂), 70.0 (CH₂), 68.3 (CH), 67.0 (CH₂), 59.6 (CH₂), 36.0 (CH₂), 31.7 (CH₂), 28.0 (CH₂), 27.9 (CH₂), 25.9 (3 × CH₃), 21.8 (2 × CH₃), 18.3 (C), -1.5 (CH₃), -1.6 (CH₃), -5.1 (3 × CH₃); IR (in substance) ν 2955-280, 1720 cm⁻¹. Anal. Calcd for C₃₃H₅₆O₅Si₂: C, 67.30; H, 9.58. Found: C, 67.40; H, 9.44.

⁴⁴² Compounds **10b-d** were not used for the further synthesis of xeniolide F. Therefore, the complete set of analytical data was not acquired.



Allyl Vinyl Ether 10c.⁴⁴² To a solution of the phosphonate **245c** (28 mg, 0.05 mmol, 1.1 eq) in THF (2 mL, 4 mL/0.1 mmol **245c**) was added a LiHMDS solution (1.0 M in hexanes, 55 μL , 0.06 mmol, 1.1 eq) at -78°C . After stirring for 30 min a pre-cooled (-78°C) solution of the aldehyde **244** (10 mg, 0.07 mmol, 1.3 eq) in THF (2 mL, 4 mL/0.1 mmol **245c**) was added. The reaction mixture was warmed to rt, quenched by the addition of saturated aq NH_4Cl and extracted with CH_2Cl_2 (3×4 mL). The combined organic layers were dried and concentrated. Flash chromatography (hexanes/ethyl acetate 20/1) afforded allyl vinyl ether **10b** (21 mg, 0.04 mmol, 50%) as mixture of double bond isomers (*E,Z*)-**10c**/*Z,Z*)-**10c** 9/1 as colorless oil (R_f 0.45 hexanes/ethyl acetate 10/1)

^1H NMR (300 MHz, CDCl_3) δ 7.27-7.19 (m, 5H), 6.07 (t, $J = 7.4$ Hz, 1H^{minor}), 5.48 (brs, 1H), 5.44 (t, $J = 6.1$ Hz, 1H), 5.26 (d, $J = 2.6$ Hz, 1H), 5.10 (t, $J = 7.4$ Hz, 1H^{major}), 4.41 (s, 2H), 4.21-4.09 (m, 4H), 3.40 (t, $J = 6.4$ Hz, 2H), 2.48-2.38 (m, 2H), 2.27-2.08 (m, 2H), 2.14 (t, $J = 6.4$ Hz, 2H), 1.77-1.65 (m, 2H), 1.41 (s, 9H), 0.80 (s, 9H), 0.00 (s, 9H), -0.03 (s, 6H); ^{13}C NMR (75 MHz, CDCl_3) δ 162.9 (C), 151.4 (C), 146.0 (C), 138.6 (C), 135.7 (C), 129.2 (CH), 128.3 ($2 \times \text{CH}$), 127.6 ($3 \times \text{CH}$), 127.5 (CH), 124.0 (CH_2), 115.9 (CH), 72.9 (CH_2), 70.0 (CH_2), 66.9 (CH_2), 59.7 (CH_2), 36.0 (CH_2), 31.6 (CH_2), 28.2 ($3 \times \text{CH}_2$), 28.0 (CH_3), 25.9 ($3 \times \text{CH}_3$ and $1 \times \text{CH}_2$), 18.3 (C), -1.5 ($2 \times \text{CH}_3$), -5.1 ($3 \times \text{CH}_3$); IR (in substance) ν 2935-2855, 1715 cm^{-1} . Anal. Calcd for $\text{C}_{34}\text{H}_{58}\text{O}_5\text{Si}_2$: C, 67.72; H, 9.70.

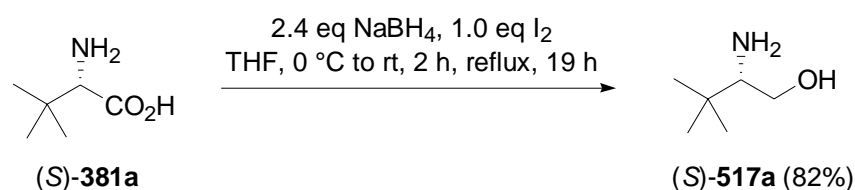


Allyl Vinyl Ether 10d.⁴⁴² As described for the synthesis of **10a**, phosphonate **245e** (0.25 g, 0.3 mmol, 1.0 eq) was treated with LDA [prepared from diisopropylamine (62 μL , 0.4 mmol,

1.15 eq) and *n*-BuLi (0.16 mL, 0.4 mmol, 1.05 eq)] and aldehyde **244** (62 mg, 0.4 mmol, 1.15 eq). Flash chromatography (hexanes/ethyl acetate 20/1) afforded the allyl vinyl ether **10d** (0.22 g, 0.3 mmol, 95%) as mixture of double bond isomers (*E,Z*)-**10d**/*Z,Z*-**10d** 5/1 as pale yellow oil (R_f 0.27 hexanes/ethyl acetate 10/1).

^1H NMR (500 MHz, CDCl_3) δ 7.68-7.64 (m, 4H), 7.41-7.35 (m, 6H), 7.34-7.33 (m, 5H), 6.18 (t, $J = 7.4$ Hz, 1H^{minor}), 5.16 (t, $J = 6.2$ Hz, 1H), 5.55-5.53 (m, 1H^{major}), 5.50-5.48 (m, 1H^{minor}), 5.33-5.31 (m, 1H^{major}), 5.30-5.29 (m, 1H^{minor}), 5.11 (t, $J = 7.6$ Hz, 1H^{major}), 4.49 (s, 2H), 4.25 (d, $J = 6.3$ Hz, 2H^{minor}), 4.24 (d, $J = 6.3$ Hz, 2H^{major}), 4.07 (s, 2H^{minor}), 3.99 (s, 2H^{major}), 3.66 (s, 3H^{major}), 3.60 (s, 3H^{minor}), 3.47 (t, $J = 6.5$ Hz, 2H), 2.51 (dt, $J = 7.8, 7.5$ Hz, 2H^{major}), 2.28-2.22 (m, 2H^{minor}), 2.21-2.10 (m, 4H), 1.78-1.71 (m, 2H), 1.03 (s, 9H), 0.07 (s, 9H^{major}), 0.05 (s, 9H^{minor}); ^{13}C NMR (126 MHz, CDCl_3) δ 164.3 (C^{minor}), 164.0 (C^{major}), 151.3 (C^{major}), 150.8 (C^{minor}), 144.5 (C^{minor}), 144.4 (C^{major}), 138.6 (C), 136.0 (C^{minor}), 135.7 (C^{major}), 135.6 ($4 \times \text{CH}$), 133.72 ($2 \times \text{C}^{\text{minor}}$), 133.68 ($2 \times \text{C}^{\text{major}}$), 129.7 (CH^{minor}), 129.62 ($2 \times \text{CH}$), 129.59 (CH), 129.1 (CH^{minor}), 128.9 ($2 \times \text{CH}^{\text{minor}}$), 128.3 ($2 \times \text{CH}^{\text{major}}$), 127.7 ($4 \times \text{CH}$), 127.6 ($2 \times \text{CH}$), 127.5 (CH^{major}), 124.4 ($\text{CH}_2^{\text{major}}$), 124.2 ($\text{CH}_2^{\text{minor}}$), 117.4 (CH^{major}), 72.9 (CH_2), 69.9 ($\text{CH}_2^{\text{major}}$), 69.1 ($\text{CH}_2^{\text{minor}}$), 66.6 (CH_2), 60.4 (CH_2), 51.7 ($\text{CH}_3^{\text{minor}}$), 51.6 ($\text{CH}_3^{\text{major}}$), 36.0 ($\text{CH}_2^{\text{major}}$), 34.2 ($\text{CH}_2^{\text{minor}}$), 31.6 ($\text{CH}_2^{\text{minor}}$), 31.4 ($\text{CH}_2^{\text{major}}$), 27.89 ($\text{CH}_2^{\text{major}}$), 27.86 ($\text{CH}_2^{\text{minor}}$), 26.8 ($3 \times \text{CH}_3$), 26.1 ($\text{CH}_2^{\text{major}}$), 24.8 ($\text{CH}_2^{\text{minor}}$), 19.1 (C), -1.5 ($3 \times \text{CH}_3^{\text{major}}$), -1.6 ($3 \times \text{CH}_3^{\text{minor}}$); IR (in substance) ν 3070-3020, 2955-2860, 1745 cm^{-1} . Anal. Calcd for $\text{C}_{41}\text{H}_{56}\text{O}_5\text{Si}_2$: C, 71.88; H, 8.24.

Catalyst

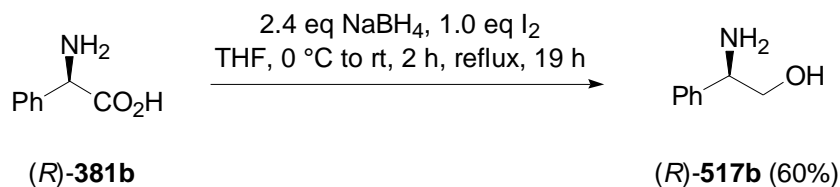


Amino Alcohol (S)-517a.⁴⁴³ To an ice-cooled solution of (*S*)-*tert*-leucine ((*S*)-**381a**) (65.6 g, 500 mmol, 1.0 eq) and sodium borohydride (45.4 g, 1200 mmol, 2.4 eq) in THF (500 mL, 1 mL/mmol **381**) was added a solution of iodine (126.9 g, 500 mmol, 1.0 eq) in THF (250 mL, 0.5 mL/mmol **381**) over 1.5 h. The reaction mixture was warmed to rt and stirred until the brown color had disappeared. Then, the reaction was brought to reflux for 19 h, cooled to 0 °C and carefully treated with MeOH (150 mL, 0.3 mL/mmol **381**). The solvents were

⁴⁴³ Meyers, A. I.; McKennon, M. J. *J. Org. Chem.* **1993**, *58*, 3568-3571.

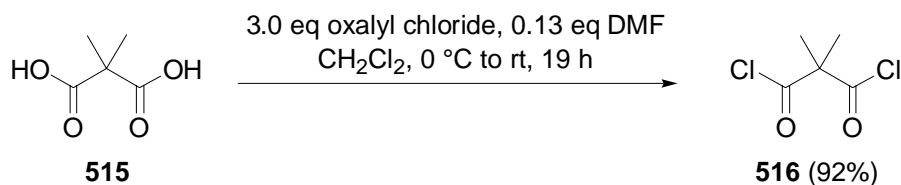
removed at reduced pressure and the crude product was dissolved in 20% aq. KOH (1 L, 2 mL/mmol **381**). After stirring for 6 h at ambient temperature, the reaction mixture was extracted with CH₂Cl₂ (3 × 800 mL). The combined organic extracts were dried and concentrated. Kugelrohr distillation (80 °C, 2.0 mbar) afforded (*S*)-*tert*-leucinol ((*S*)-**517a**) (47.9 g, 409 mmol, 82%) as colorless oil that solidified upon cooling to rt.

¹H NMR (300 MHz, CDCl₃) δ 3.73 (dd, *J* = 10.3, 3.8 Hz, 1H), 3.21 (dd, *J* = 10.3, 10.3 Hz, 1H), 2.51 (dd, *J* = 10.3, 3.8 Hz, 1H), 1.87 (brs, 3H), 0.94 (s, 9H); ¹³C NMR (75.5 MHz, CDCl₃) δ 62.3 (CH₂), 61.8 (CH), 33.2 (C), 26.3 (3 × CH₃). Anal. Calcd for C₆H₁₅NO: C, 61.49; H, 12.90; N, 11.95. [α]_D²⁸ +39.6° (*c* 0.75, CHCl₃) (lit. *tert*-leucinol [α]_D²⁵ +36.5° (*c* 1.22, EtOH).



Amino Alcohol (R)-517b.⁴⁴³ As described for the synthesis of amino alcohol (*S*)-**517a**, (*R*)-phenyl glycine ((*R*)-**381b**) (14.0 g, 92.6 mmol) was treated with sodium borohydride (8.4 g, 223 mmol) and iodine (23.5 g, 92.6 mmol). Distillation (140 °C, 0.1 mbar) yielded the amino alcohol (*R*)-**517b** (7.4 g, 55.7 mmol, 60%) as pale yellow oil that solidified upon standing at rt.

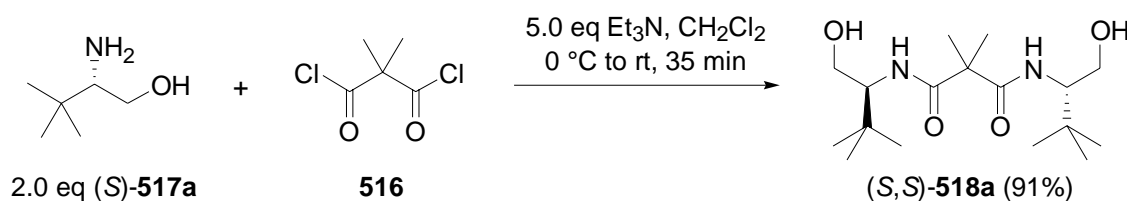
¹H NMR (300 MHz, CDCl₃) δ 7.39-7.20 (m, 5H), 3.99 (dd, *J* = 8.1, 4.2 Hz, 1H), 3.68 (t, *J* = 11.0, 4.2 Hz, 1H), 3.51 (dd, *J* = 10.9, 8.3 Hz, 1H), 2.78 (brs, 3H). Anal. Calcd for C₈H₁₁NO: C, 70.04; H, 8.08; N, 10.21.



Malonyl Dichloride 516.⁴⁴⁴ To solution of dimethyl malonic acid **515** (6.0 g, 45.4 mmol, 1.0 eq) and DMF (0.5 mL, 5.9 mmol, 0.13 eq) in CH₂Cl₂ (70 mL, 1.5 mL/mmol) was added oxalyl chloride (11.9 mL, 136 mmol, 3.0 eq) over 1 h at 0 °C. The reaction mixture was warmed to rt, stirred for 18 h at ambient temperature and concentrated. The crude product was purified by distillation (165 °C, 1 atm) to afford the malonyl dichloride **516** (7.1 g, 42.1 mmol, 92%) as colorless liquid.

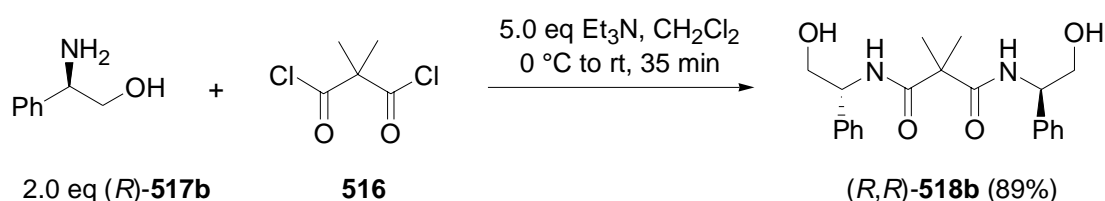
⁴⁴⁴ Prepared according to reference 306.

^1H NMR (300 MHz, CDCl_3) δ 1.67 (s, 6H). Anal. Calcd for $\text{C}_5\text{H}_6\text{Cl}_2\text{O}_2$: C, 35.53; H, 3.58; Cl, 41.95.



Bis(amide) (S,S)-518a.⁴⁴⁴ To an ice-cooled solution of (*S*)-*tert*-leucinol ((*S*)-**517a**) (9.7 g, 82.8 mmol, 2.0 eq) in CH_2Cl_2 (100 mL, 2.5 mL/mmol of **517**) was added triethylamine (28.8 mL, 207 mmol, 5.0 eq) in one portion and a solution of dimethylmalonyl dichloride (7.0 g, 41.4 mmol, 1.0 eq) in CH_2Cl_2 (40 mL, 1 mL/mmol of **517**) over 20 min. The reaction mixture was warmed to rt, stirred for 35 min at ambient temperature and diluted with CH_2Cl_2 (300 mL, 7.5 mL/mmol of **517**). The organic layer was subsequently washed with aq 1N HCl (60 mL), saturated aq NaHCO_3 (60 mL), and brine (60 mL), dried over MgSO_4 and concentrated. Recrystallisation of the crude product from ethyl acetate affords the bis(amide) (*S,S*)-**518a** (12.4 g, 37.5 mmol, 91%) as white solid that is bench stable at rt.

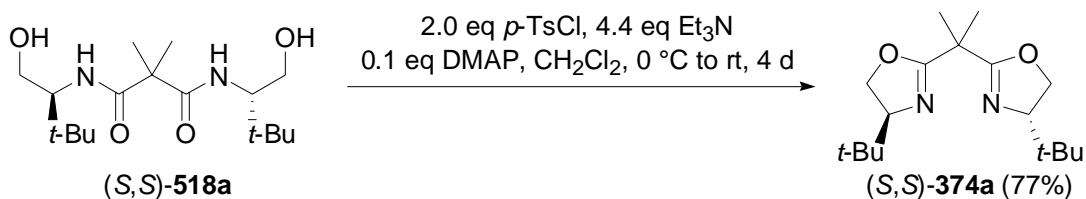
^1H NMR (300 MHz, CDCl_3) δ 6.44 (d, $J = 9.5$ Hz, 2H), 3.90-3.80 (m, 4H), 3.48-3.41 (m, 2H), 1.50 (s, 6H), 0.92 (s, 18H), no OH-resonance observed. Anal. Calcd for $\text{C}_{17}\text{H}_{34}\text{N}_2\text{O}_4$: C, 61.79; H, 10.37; N, 8.48.



Bis(amide) (R,R)-518b.⁴⁴⁵ As outlined in the preceding paragraph, amino alcohol (*R*)-**517b** (2.7 g, 20.7 mmol) was treated with triethylamine (6.5 mL, 46.6 mmol) and dimethylmalonyl dichloride (**516**) (1.8 g, 10.4 mmol). Recrystallation from ethyl acetate afforded bis(amide) (*R,R*)-**518b** (3.4 g, 9.3 mmol, 89%) as pale white-brown solid.

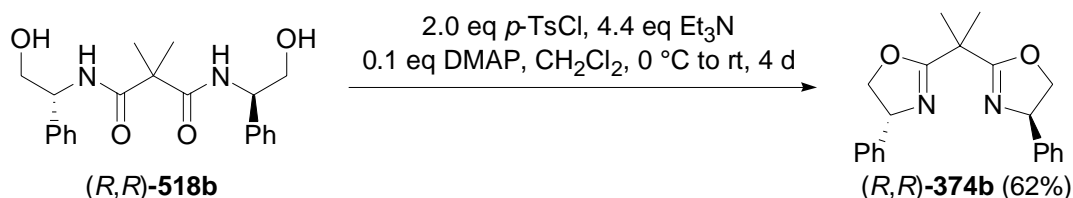
^1H NMR (300 MHz, CDCl_3) δ 7.37-7.12 (m, 10H), 5.12 (ddd, $J = 7.6, 7.6, 3.9$ Hz, 2H), 3.88 (dd, $J = 11.7, 3.9$ Hz, 2H), 3.73 (dd, $J = 11.5, 7.6$ Hz, 2H), 3.31 (brs, 2H), 1.48 (s, 6H), no OH-resonance observed. Anal. Calcd for $\text{C}_{21}\text{H}_{26}\text{N}_2\text{O}_4$: C, 68.09; H, 7.07; N, 7.56.

⁴⁴⁵ Evans, D. A.; Miller, S. J.; Lectka, T.; Matt, P. v. *J. Am. Chem. Soc.* **1999**, *121*, 7559-7573.



Bis(oxazoline) (S,S)-374a.⁴⁴⁴ To a solution of the bis(amide) (S,S)-**518a** (2.0 g, 6.1 mmol, 1.0 eq) and 4-(*N,N*-dimethylamino)-pyridine DMAP (74 mg, 0.6 mmol, 0.1 eq) in CH₂Cl₂ (25 mL, 4 mL/mmol of **518**) was added triethylamine (3.7 mL, 26.4 mmol, 4.4 eq) in one portion and a solution of *para*-toluene sulfonyl chloride (2.3 g, 12.1 mmol, 2.0 eq) in CH₂Cl₂ (12 mL, 2 mL/mmol of **518**) using water bath cooling to maintain the temperature during the addition. The reaction mixture was stirred for 4 d at ambient temperature, quenched with saturated aq. NH₄Cl and extracted with CH₂Cl₂ (3 × 40 mL). The combined organic layers were dried and concentrated. Flash chromatography (heptane/ethyl acetate 10/1 to 1/1) yielded the bis(oxazoline) (S,S)-**374** (1.4 g, 4.8 mmol, 77%) as white solid (*R_f* 0.15 hexanes/ethyl acetate 1/1) which was immediately used for the synthesis of the catalyst (S,S)-**234a**.

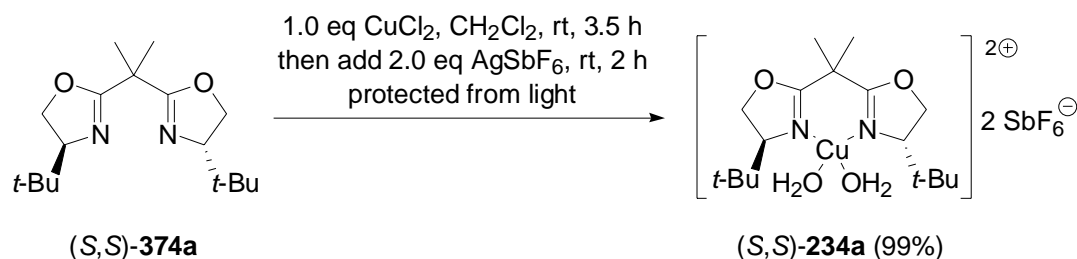
¹H NMR (300 MHz, CDCl₃) δ 4.12 (dd, *J* = 10.0, 8.7 Hz, 2H), 4.07 (dd, *J* = 8.6, 6.9 Hz, 2H), 3.83 (dd, *J* = 10.0, 6.9 Hz, 2H), 1.50 (s, 6H), 0.86 (s, 18H). Anal. Calcd for C₁₇H₃₀N₂O₂: C, 69.35; H, 10.27; N, 9.51. [α]_D²⁸ +93.6° (*c* 1.75, CHCl₃) (lit. **374a** [α]_D²⁵ +113.2° (*c* 1.22, CH₂Cl₂)).



Bis(oxazoline) (R,R)-374b.⁴⁴⁵ To an ice-cooled solution of the bis(amide) (R,R)-**518b** (1.5 g, 4.0 mmol, 1.0 eq) in CH₂Cl₂ (16 mL, 4 mL/mmol) were subsequently added triethylamine (1.9 mL, 13.3 mmol, 3.3 eq) and methane sulfonyl chloride MsCl (0.8 mL, 10.1 mmol, 2.5 eq). The reaction mixture was stirred for 20 min at 0 °C, quenched with saturated aq. NaHCO₃ and extracted with CH₂Cl₂ (3 × 10 mL). The combined organic layers were dried and concentrated. A sealed tube was charged with the crude product dissolved in 1,2-dichloroethane (16 mL, 4 mL/mmol) and triethylamine (1.7 mL, 12.2 mmol, 3.0 eq). The tube was placed into an oil bath and heated for 3 d (bath temperature 90 °C). The reaction mixture was then cooled to rt, quenched with saturated aq. NH₄Cl and extracted with CH₂Cl₂ (3 × 40 mL). The combined organic layers were dried and concentrated. Flash chromatography (ethyl acetate CH₂Cl₂ 4/1) yielded the bis(oxazoline) (R,R)-**374b** (0.9 g, 2.5 mmol, 62%) as white

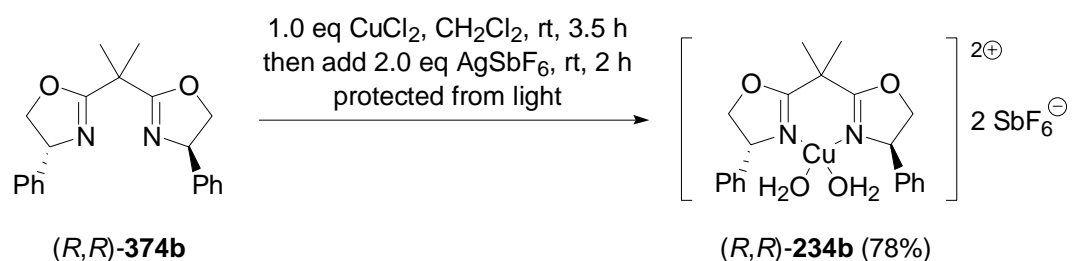
solid (R_f 0.12 ethyl acetate) which was immediately used for the synthesis of the catalyst (*R,R*)-**234b**.

^1H NMR (300 MHz, CDCl_3) δ 7.37-7.22 (m, 10H), 5.23 (dd, $J = 10.1, 7.5$ Hz, 2H), 4.67 (dd, $J = 10.1, 8.4$ Hz, 2H), 4.16 (dd, $J = 8.0, 8.0$ Hz, 2H), 1.68 (s, 6H). Anal. Calcd for $\text{C}_{17}\text{H}_{30}\text{N}_2\text{O}_2$: C, 69.35; H, 10.27; N, 9.51.



Catalyst (*S,S*)-234a. To a solution of bis(oxazoline) (*S,S*)-**374a** (1.2 g, 4.0 mmol, 1.0 eq) in CH_2Cl_2 (10 mL, 2.5 mL/mmol) was added CuCl_2 ⁴⁴⁶ (0.5 g, 4.0 mmol, 1.0 eq) at ambient temperature. The clear green solution was stirred for 3.5 h protected from light at rt. The solution was filtered through a cotton pad and diluted with CH_2Cl_2 (10 mL, 2.5 mL/mmol). To that solution AgSbF_6 ⁴⁴⁷ (2.7 g, 8.0 mmol, 2.0 eq) was added and the resulting blue suspension was stirred at ambient temperature for 2 h protected from light. The reaction mixture was filtered through a plug of Celite and concentrated. The residue was dissolved in CH_2Cl_2 (5 mL) and filtered through a 2 μm PTFE syringe filter to remove any remaining solid silver chloride. The clear blue green solution was slowly concentrated to afford (*S,S*)-**234a** (3.4 g, 4.0 mmol, 99%) as blue solid.

IR (in substance) ν 3700-3000 (br, w, OH), 2970 (w, CH), 1740 (w), 1650 (w, N=C), 1480 (w), 1370 (w), 1250 (w, C-O), 1140 (m, C-N), 1070 (w), 971 (w), 946 (w), 653 (s), 640 (s).⁴⁴⁸



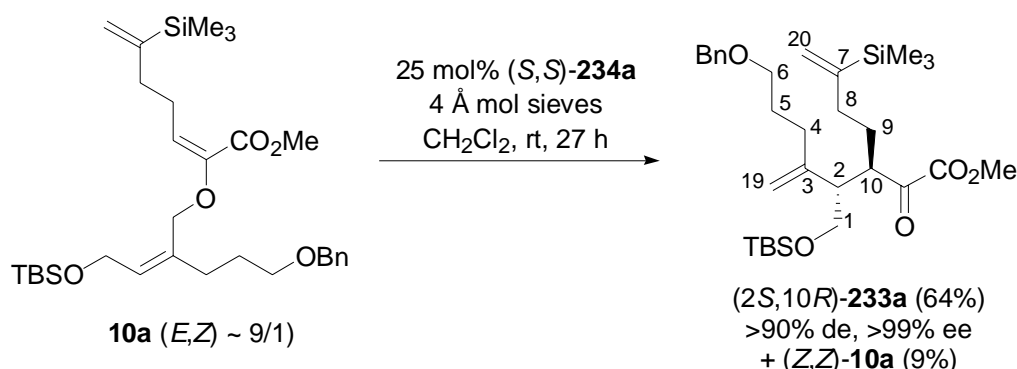
Catalyst (*R,R*)-234b.⁴⁴⁹ As described for the preparation of (*S,S*)-**234a** bis(oxazoline) (*R,R*)-**374b** (0.10 g, 0.3 mmol, 1.0 eq) in CH_2Cl_2 (3 mL, 1 mL/0.1 mmol) was treated with

⁴⁴⁶ $\text{CuCl}_2 \cdot \text{H}_2\text{O}$ (99.999%, obtained from Aldrich), was dried at high vacuum (0.05 mmbar, 50 $^\circ\text{C}$, 1 h).

⁴⁴⁷ AgSbF_6 (98%, obtained from ACROS) was stored protected from light. The substance was quickly weighed out at ambient atmosphere without using a glove box.

⁴⁴⁸ A more detailed analysis of the IR spectrum is given for (*S,S*)-**234a** because we were unable to obtain single crystals of the catalyst for X-ray crystallography. Abbreviations are used as following: s= strong signal, m= signal of medium intensity, w= weak signal, br= broad signal.

CuCl_2 ⁴⁴⁶ (0.39 g, 0.3 mmol) and AgSbF_6 ⁴⁴⁷ (0.21 g, 0.6 mmol) to afford (*R,R*)-**234b** (0.22 g, 0.2 mmol, 78%) as blue solid.

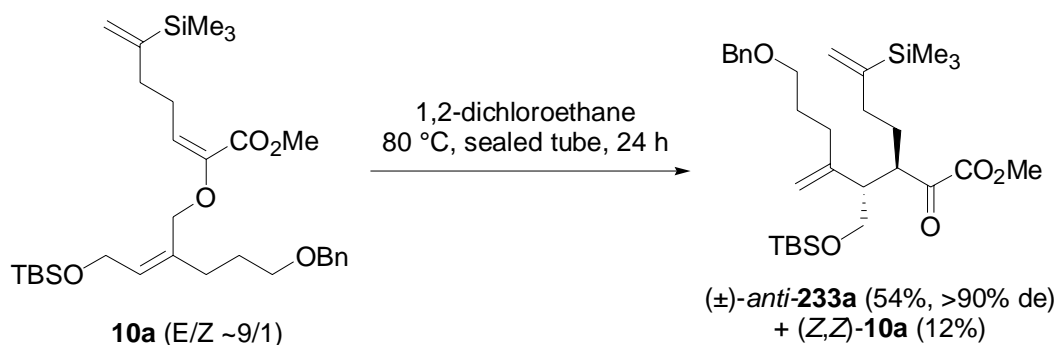


α -Keto Ester (2*S*,10*R*)-233a.³⁸⁸ To a solution of $[\text{Cu}\{(S,S)\text{-tert-Bu-box}\}](\text{SbF}_6)_2(\text{H}_2\text{O})_2$ [(*S,S*)-**234a**] (0.23 g, 0.3 mmol, 0.25 eq) in CH_2Cl_2 (11 mL, 10 mL/mmol of **10a**) was added pulverized and activated 4 Å molecular sieves (1.2 g 110 mg/0.1 mmol of **10a**) at rt. After 5 min, a solution of **10a** (0.6 g, 1.1 mmol, 1.0 eq) in CH_2Cl_2 (11 mL, 10 mL/mmol) was added. The reaction mixture was stirred for 27 h at rt. The mol sieves were removed by filtration and the solution was then concentrated. The crude product was purified by column chromatography (hexanes/ethyl acetate 20/1) to afford the α -keto ester (*2S,10R*)-**233a** (0.38 g, 0.7 mmol, 64%) as a pale yellow oil (R_f 0.35 hexane/ethyl acetate 10/1) and the allyl vinyl ether (*Z,Z*)-**10a** (56 mg, 0.1 mmol, 9%) as a colorless oil (R_f 0.24 hexanes/ethyl acetate 10/1). Only one diastereomer was detectable from the ^1H NMR spectrum of the crude product mixture.

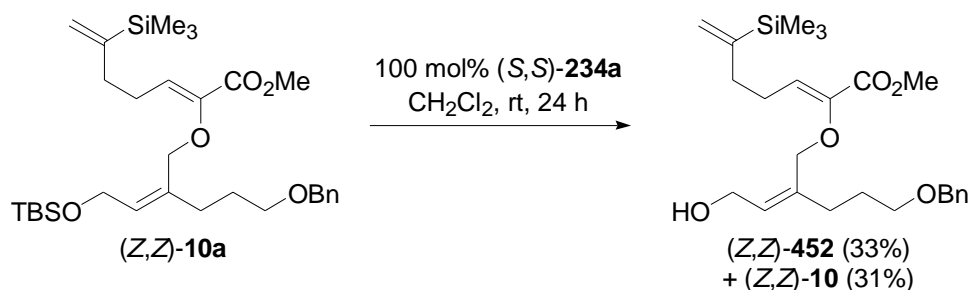
^1H NMR (500 MHz, CDCl_3) δ 7.34-7.27 (m, 5H, CH-Ar), 5.45 (d, $J = 1.8$ Hz, 1H, 20- $\text{CH}_2=$), 5.26 (d, $J = 1.8$ Hz, 1H, 20- $\text{CH}_2=$), 4.93 (s, 1H, 19- $\text{CH}_2=$), 4.87 (s, 1H, 19- $\text{CH}_2=$), 4.50 (s, 2H, $-\text{OCH}_2\text{Ph}$), 3.82 (s, 3H, $-\text{OCH}_3$), 3.54-3.49 (m, 3H, 1- CH_2 and 2-CH), 3.48 (t, $J = 6.3$ Hz, 2H, 6- CH_2), 2.53-2.51 (m, 1H, 10-CH), 2.06 (t, $J = 7.7$ Hz, 2H, 4- CH_2), 1.93 (t, $J = 8.1$ Hz, 2H, 8- CH_2), 1.79-1.75 (m, 2H, 5- CH_2), 1.76-1.52 (m, 2H, 9- CH_2), 0.81 (s, 9H, $\text{Si}(\text{CH}_3)_3$), 0.02 (s, 9H, $\text{Si}(\text{CH}_3)_3$), -0.03 (s, 3H, SiCH_3), 0.04 (s, 3H, SiCH_3); ^{13}C NMR (126 MHz, CDCl_3) δ 195.9 (C=O), 161.3 (CO_2Me), 151.5 (7-C=), 147.1 (3-C=), 138.5 (C-Ar), 128.4 ($2 \times \text{CH-Ar}$), 127.6 ($2 \times \text{CH-Ar}$), 127.5 (CH-Ar), 124.7 (20- $\text{CH}_2=$), 111.7 (19- $\text{CH}_2=$), 72.9 ($-\text{OCH}_2\text{Ph}$), 69.8 (6- CH_2), 66.4 (1- CH_2), 53.4 (2-CH), 52.7 ($-\text{OCH}_3$), 48.6 (10-CH), 33.8 (8- CH_2), 32.5 (4- CH_2), 30.6 (9- CH_2), 27.7 (5- CH_2), 25.8 ($3 \times \text{Si}(\text{CH}_3)_3$), 18.5 ($\text{Si}(\text{CH}_3)_3$), -1.5 ($3 \times \text{Si}(\text{CH}_3)_3$), -5.6 ($\text{Si}(\text{CH}_3)_2$), -5.8 ($\text{Si}(\text{CH}_3)_2$); IR (in substance) ν 2955-2855, 1725

⁴⁴⁹ No analytical data have been obtained for (*R,R*)-**234b**.

cm⁻¹. Anal. Calcd for C₃₄H₅₂O₅Si₂: C, 66.38; H, 9.34. Found: C, 66.46; H, 9.46. [α]_D²⁵ +22.1 (*c* 1.0, CHCl₃).



α -Keto Ester (±)-*anti*-233a.⁴⁵⁰ A solution of the allyl vinyl ether **4a** (50 mg, 0.09 mmol) in 1,2-dichloroethane (4 mL, 4 mL/ 0.1 mmol) was heated in a sealed tube (bath temperature 80 °C). After 24 h, the solvents were evaporated and the crude product was purified by column chromatography (hexanes/ethyl acetate 20/1) to afford the α -keto ester (±)-*anti*-**3a** (27 mg, 0.05 mmol, 54%) as a pale yellow oil (*R_f* 0.35 hexane/ethyl acetate 10/1) and the allyl vinyl ether (Z,Z)-**10a** (6 mg, 0.01 mmol, 12%) as a colorless oil (*R_f* 0.24 hexanes/ethyl acetate 10/1). Only one diastereomer was detectable from the ¹H NMR spectrum of the crude product mixture. Analytical data are identical with (2*S*,10*R*)-**233a**.

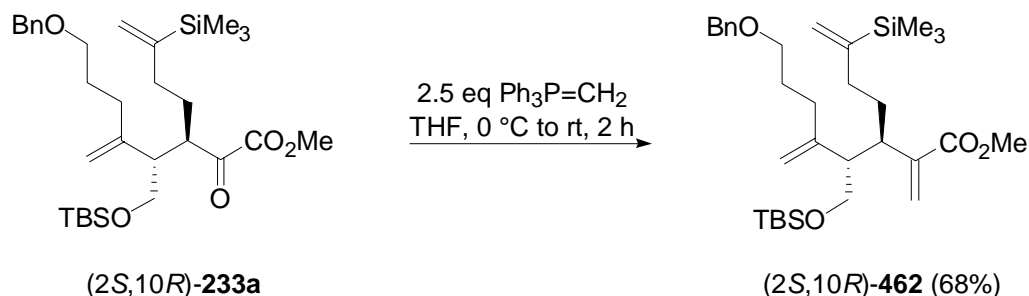


Deprotected Allyl Vinyl Ether (Z,Z)-452. To a solution of (Z,Z)-**10a** (25 mg, 0.05 mmol, 1.0 eq) in CH₂Cl₂ (4 mL) was added (S,S)-**234a** (39 mg, 0.05 mmol, 1.0 eq) at rt. After stirring at ambient temperature for 24 h the reaction mixture was concentrated at reduced pressure. The crude product was purified by flash chromatography (hexanes/ethyl acetate 10/1) and afforded deprotected (Z,Z)-**452** (7 mg, 0.02 mmol, 33%) as pale yellow oil (*R_f* 0.29 hexanes/ethyl acetate 1/1) and unaffected starting material (Z,Z)-**10a** (8 mg, 0.01 mmol, 31%) as pale yellow oil (*R_f* 0.79 hexanes/ethyl acetate 1/1).

¹H NMR (300 MHz, CDCl₃) δ 7.29-7.18 (m, 5H), 6.22 (t, *J* = 7.5 Hz, 1H), 5.64 (t, *J* = 7.4 Hz, 1H), 5.51-5.49 (m, 1H), 5.30-5.28 (m, 1H), 4.43 (s, 2H), 4.25 (s, 2H), 4.11 (d, *J* = 7.4 Hz,

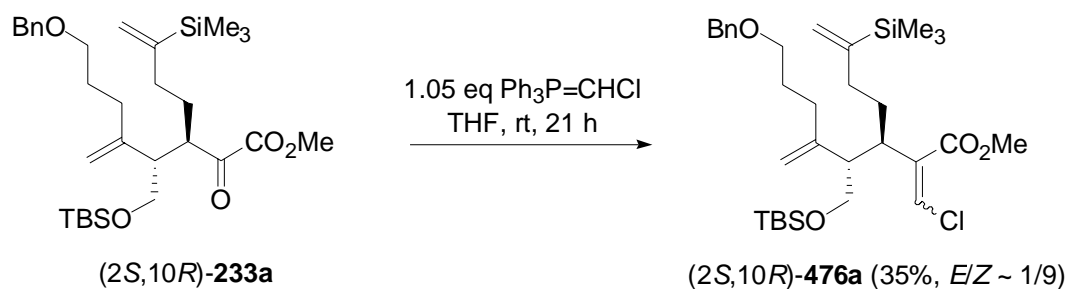
⁴⁵⁰ Yields not optimized.

2H), 3.70 (s, 3H), 2.42 (t, $J = 6.4$ Hz, 2H), 2.34-2.10 (m, 6H), 1.80-1.67 (m, 2H), 0.00 (s, 9H).
 Anal. Calcd for $C_{25}H_{38}O_5Si$: C, 67.23; H, 8.58.



α,β -Unsaturated Ester (2S,10R)-462.³⁸⁸ To a solution of methyl triphenylphosphonium bromide (96 mg, 0.3 mmol, 3.0 eq) in THF (2 mL, 2 mL/0.1 mmol of **3**) at 0 °C was added a LiHMDS solution (1.0 M in THF, 0.23 mL, 0.2 mmol, 2.5 eq). After 1 h at 0 °C, a solution of the α -keto ester (2S,10R)-**233a** (50 mg, 0.09 mmol, 1.0 eq) in THF (2 mL, 2 mL/0.1 mmol) was added and the suspension was warmed to rt. When TLC indicated complete consumption of the starting material (~2 h), the reaction was quenched by the addition of saturated aq NH_4Cl and extracted with CH_2Cl_2 . The combined organic layers were dried and concentrated. The crude product was purified by column chromatography (hexanes/ethyl acetate 20/1) to afford the α,β -unsaturated ester (2S,10R)-**462** (34 mg, 0.06 mmol, 68%) as a pale yellow oil (R_f 0.41 hexanes/ethyl acetate 10/1).

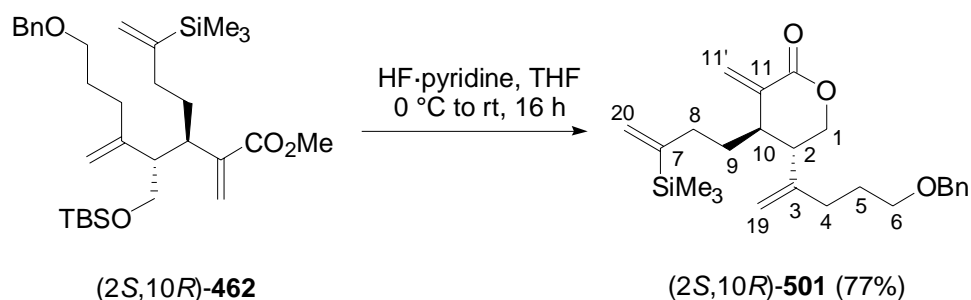
1H NMR (300 MHz, $CDCl_3$) δ 7.34-7.24 (m, 5H), 6.23 (d, $J = 1.0$ Hz, 1H), 5.54 (d, $J = 1.0$ Hz, 1H), 5.46-5.43 (m, 1H), 5.23 (d, $J = 3.0$ Hz, 1H), 4.86 (s, 1H), 4.82 (s, 1H), 4.48 (s, 2H), 3.72 (s, 3H), 3.51-3.44 (m, 4H), 2.63 (td, $J = 10.8, 3.3$ Hz, 1H), 2.38 (dt, $J = 9.6, 5.7$ Hz, 1H), 2.11-1.49 (series of m, 8H), 0.81 (s, 9H), 0.00 (s, 9H), -0.07 (s, 3H), -0.08 (s, 3H); ^{13}C NMR (75 MHz, $CDCl_3$) δ 167.7 (C), 152.3 (C), 149.1 (C), 142.0 (C), 138.6 (C), 128.3 (2 \times CH), 127.6 (2 \times CH), 127.5 (CH), 125.9 (CH₂), 123.9 (CH₂), 110.6 (CH₂), 72.8 (CH₂), 70.3 (CH₂), 64.7 (CH₂), 52.0 (CH), 51.7 (CH₃), 34.0 (CH₂), 32.1 (CH₂), 31.6 (CH₂), 29.7 (CH), 27.6 (CH₂), 25.9 (3 \times CH₃), 18.2 (C), -1.5 (3 \times CH₃), -5.5 (CH₃), -5.6 (CH₃); IR (in substance) ν 2950-2855, 1720 cm^{-1} . Anal. Calcd for $C_{32}H_{54}O_4Si_2$: C, 68.76; H, 9.74. Found: C, 68.88; H, 9.40. $[\alpha]_D^{25} +9.1$ (c 1.0, $CHCl_3$).



Vinyl Chloride (2S,10R)-476a.⁴⁵¹ An ice-cooled suspension of chloromethyl triphenylphosphonium chloride **480a** (74 mg, 0.2 mmol, 1.2 eq) in THF (2 mL, 10 mL/mmol) was treated with *n*-BuLi (2.3 M, 80 μ L, 0.2 mmol, 1.05 eq), warmed to rt and stirred for 2 h. To the yellow suspension was added a solution of the α -ketoester $(2S,10R)$ -**233a** (0.10 g, 0.2 mmol, 1.0 eq) in THF (2 mL, 10 mL/mmol). The reaction mixture was stirred for 21 h at ambient temperature, quenched with saturated aq NH_4Cl and extracted with CH_2Cl_2 (3×5 mL). The combined organic layers were dried and concentrated. Flash chromatography (hexanes/ethyl acetate 50/1) afforded the vinyl chloride $(2S,10R)$ -**476a** (39 mg, 0.06 mmol, 35%) as mixture of double bond isomers ((Z) -**476a**/ (E) -**476a** $\sim 9/1$) as pale yellow oil (R_f 0.56 hexanes/ethyl acetate 5/1). ($R_f(\alpha\text{-keto ester})$ 0.59 hexanes/ethyl acetate 5/1). The double bond isomers may be separated by carefully performed flash chromatography.

1H NMR (500 MHz, $CDCl_3$) δ 7.35-7.25 (m, 5H, CH-Ar), 6.22 (s, $1H^{major}$, 12-CH=), 6.20 (s, $1H^{minor}$, 12-CH=), 5.48 (s, 1H, 20-CH₂), 5.27 (s, 1H, 20-CH₂), 4.88 (s, 1H, 19-CH₂), 4.83 (s, 1H, 19-CH₂), 4.48 (s, 2H, OCH_2Ph), 3.79 (s, 3H, OCH_3), 3.63 (dd^{AB}, $J = 10.1, 5.7$ Hz, 1H, 1-CH₂), 3.55 (dd^{AB}, $J = 9.9, 3.3$ Hz, 1H, 1-CH₂), 3.48 (dd, $J = 6.5, 6.5$ Hz, 2H, 6-CH₂), 2.54 (ddd, $J = 11.2, 11.2, 2.7$ Hz, 1H, 10-CH₂), 2.28-2.21 (m, 1H, 2-CH), 2.20-2.16 (m, 1H, 8-CH₂), 2.13-1.98 (m, 2H, 4-CH₂), 1.92-1.84 (m, 1H, 8-CH₂), 1.79-1.72 (m, 2H, 5-CH₂), 1.67-1.60 (m, 1H, 9-CH₂), 1.34-1.24 (m, 1H, 9-CH₂), 0.85 (s, 9H, $Si(CH_3)_3$), 0.03 (s, 9H, $Si(CH_3)_3$), -0.03 (s, 6H, $Si(CH_3)_2$); ^{13}C NMR (126 MHz, $CDCl_3$) δ 166.6 ($\underline{C}O_2Me$), 151.9 (7-C=), 148.4 (3-C=), 138.6 (C-Ar), 137.3 (11-C=), 128.3 ($2 \times CH\text{-Ar}$), 127.6 ($2 \times CH\text{-Ar}$), 127.5 (CH-Ar), 124.2 (20-CH₂=), 121.2 (12-CH=), 111.1 (19-CH₂=), 72.9 ($-OCH_2Ph$), 70.2 (6-CH₂), 64.0 (1-CH₂), 51.8 ($-OCH_3$), 50.4 (2-CH), 45.0 (10-CH), 34.1 (8-CH₂), 32.4 (4-CH₂), 30.6 (9-CH₂), 27.7 (5-CH₂), 25.9 ($3 \times Si(CH_3)_3$), 18.2 ($Si(CH_3)_3$), -1.5 ($3 \times Si(CH_3)_3$), -5.5 ($Si(CH_3)_2$), -5.6 ($Si(CH_3)_2$); IR (in substance) ν 3080-3045, 2950-2855, 1730 cm^{-1} . Anal. Calcd for $C_{32}H_{53}ClO_4Si_2$: C, 64.77; H, 9.00; Cl, 5.97. Found: C, 64.86; H, 8.92; Cl, 5.74. $[\alpha]_D^{28} -2.3^\circ$ (c 0.48, $CHCl_3$).

⁴⁵¹ Prepared according to: Frye, L. L.; Robinson, C. H. *J. Org. Chem.* **1990**, *55*, 1579-1584.

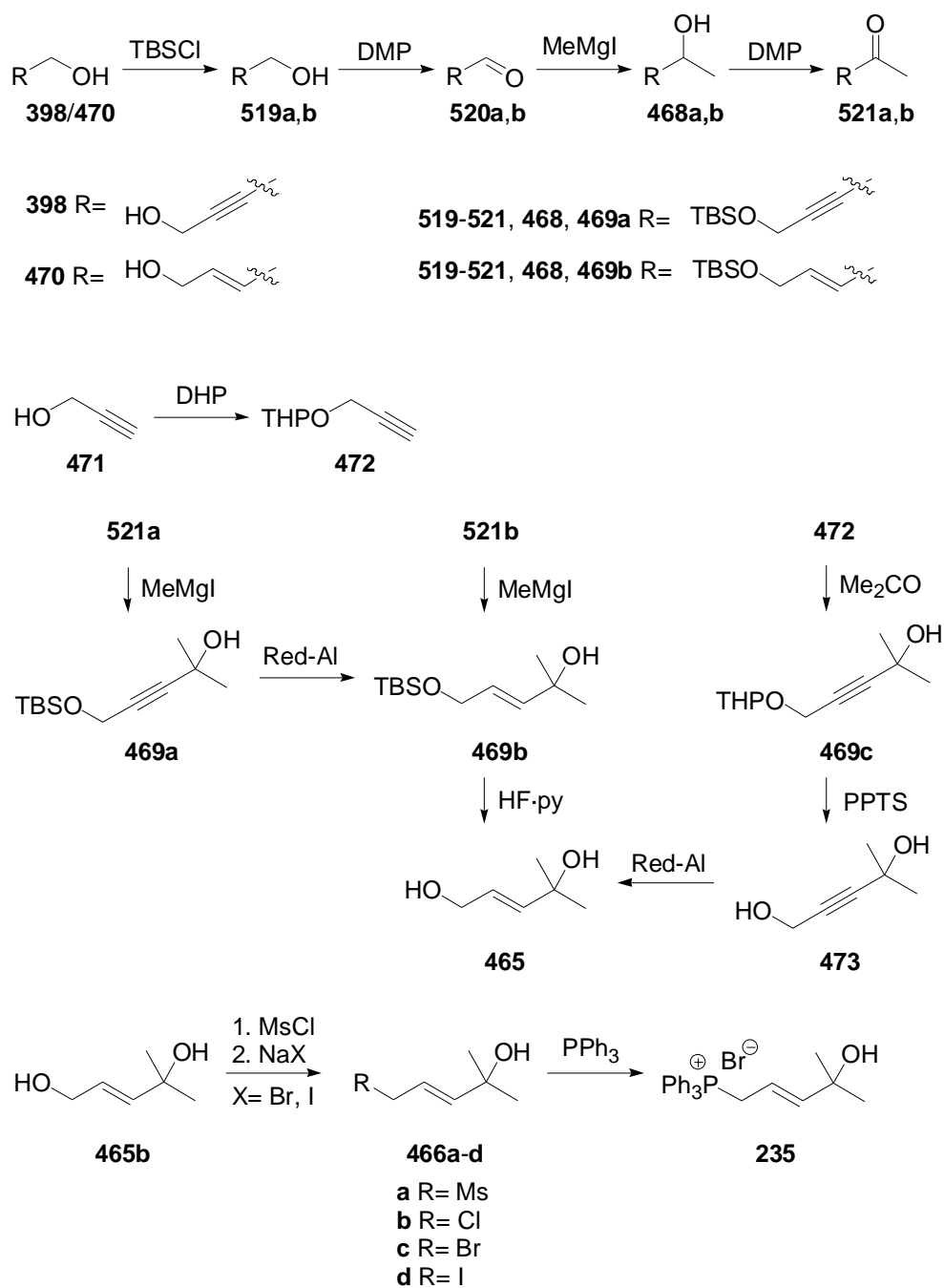


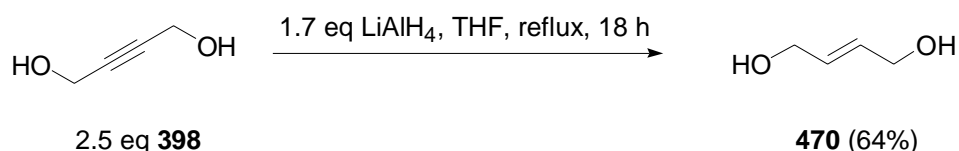
δ -Lacton (2*S*,10*R*)-501.³⁸⁸ To a solution of the α,β -unsaturated ester (2*S*,10*R*)-**462** (11 mg, 0.02 mmol, 1.0 eq) in THF (2 mL) at 0 °C was added HF·pyridine (30 μ L, 0.15 mL/0.1 mmol of **462**).⁴⁵² After 12 h at rt, an additional portion of HF·pyridine (30 μ L, 0.15 mL/0.1 mmol of **462**) was added and the reaction mixture was stirred until TLC indicated complete consumption of the starting material (~4 h). The reaction was then quenched by the careful addition of saturated aq NaHCO₃ and extracted with CH₂Cl₂ (3 \times 5 mL). The combined organic layers were dried and concentrated. The crude product was purified by column chromatography (hexanes/ethyl acetate 10/1) to afford the δ -lacton (2*S*,10*R*)-**501** (6 mg, 0.014 mmol, 77%) as a colorless oil (*R*_f 0.21 hexanes/ethyl acetate 10/1).

¹H NMR (500 MHz, CDCl₃) δ 7.35-7.28 (m, 5H, CH-Ar), 6.37 (s, 1H, 11'-CH₂=), 5.53 (s, 1H, 11'-CH₂=), 5.52 (d, *J* = 2.7 Hz, 1H, 20-CH₂), 5.32 (d, *J* = 2.7 Hz, 1H, 20-CH₂), 4.98 (s, 1H, 19-CH₂=), 4.95 (s, 1H, 19-CH₂=), 4.49 (s, 2H, -OCH₂Ph), 4.32 (dd^{AB}, *J* = 11.4, 4.1 Hz, 1H, 1-CH₂), 4.14 (dd^{AB}, *J* = 11.4, 7.6 Hz, 1H, 1-CH₂), 3.48 (t, *J* = 6.3 Hz, 2H, 6-CH₂), 2.75 (ddd, *J* = 6.2, 6.2, 6.2 Hz, 1H, 10-CH), 2.41 (ddd, *J* = 7.2, 7.2, 4.1 Hz, 1H, 2-CH), 2.16-2.08 (m, 4H, 4-CH₂ and 8-CH₂), 1.76 (quint, *J* = 6.3 Hz, 2H, 5-CH₂), 1.72-1.67 (m, 1H, 9-CH₂), 1.63-1.59 (m, 1H, 9-CH₂), 0.06 (s, 9H, Si(CH₃)₃); ¹³C NMR (126 MHz, CDCl₃) δ 166.7 (C=O), 151.3 (7-C), 146.2 (3-C), 138.3 (C-Ar), 137.9 (11-C), 128.4 (2 \times CH-Ar), 128.1 (11'-CH₂=), 127.6 (3 \times CH-Ar), 124.5 (20-CH₂=), 112.4 (19-CH₂=), 73.0 (-OCH₂Ph), 69.7 (1-CH₂), 69.5 (6-CH₂), 44.3 (2-CH), 41.6 (10-CH), 33.6 (9-CH₂), 32.1 (8-CH₂), 31.4 (4-CH₂), 28.0 (5-CH₂), -1.5 (3 \times SiCH₃); IR (in substance) ν 2925-2850, 1730 cm⁻¹. Anal. Calcd for C₂₅H₃₆O₃Si: C, 72.77; H, 8.79. [α]_D²⁵ -29.7 (*c* 1.0, CHCl₃).

⁴⁵² Performed in a polyethylene vial.

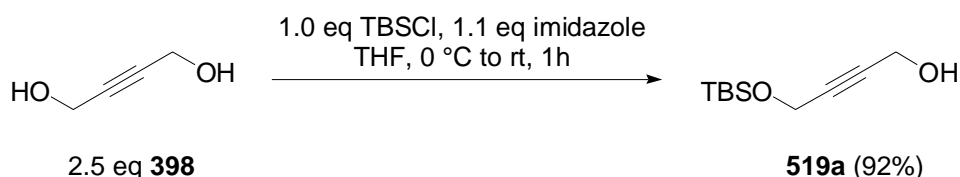
20.3.3 Side Chain Synthesis

Scheme 155: Synthesis of the Wittig salt **235**.



(E)-2-Butene-1,4-diol (470).⁴⁵³ To a suspension of lithium aluminium hydride (9.7 g, 255 mmol, 1.7 eq) in THF (130 mL, 0.5 mL/mmol) was slowly added a solution of 2-butyne-1,4-diol (**398**) (10.0 g, 116 mmol, 1.0 eq) in THF (120 mL, 1 mL/mmol). To enable stirring of the resulting suspension a big magnetic stir barbell should be used. The reaction mixture was refluxed for 18 h, cooled to 0 °C and 2.5 g Celite were added. The reaction was then quenched by the careful addition of saturated aq NH₄Cl (12.5 mL). The precipitates were removed by filtration and washed thoroughly with methanol. The filtrate was concentrated and purified by kugelrohr distillation (3 mbar, 120 °C) to afford (*E*)-butene-1,4-diol **470** (6.5 g, 74.0 mmol, 64%) as colorless oil.

¹H NMR (DMSO-*d*₆, 300 MHz) δ 5.69-5.65 (m, 2H), 4.67-4.61 (m, 2H), 3.92-3.83 (m, 4H).
 Anal. Calcd for C₄H₈O₂: C, 54.53; H, 9.15.

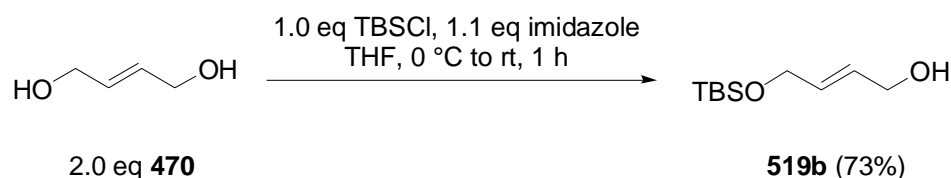


Protected Diol 519a.⁴⁵⁴ To a solution of 2-butyne-1,4-diol **398** (4.3 g, 50.0 mmol, 2.5 eq) and imidazole (3.0 g, 22.0 mmol, 1.1 eq) in THF (40 mL, 0.8 mL/mmol) was added *tert*-butyldimethylchlorosilane TBSCl (3.0 g, 20.0 mmol, 1.0 eq) at 0 °C. The reaction mixture was warmed to rt, stirred for 1 h at ambient temperature, quenched by the addition of saturated aq. NH₄Cl and extracted with CH₂Cl₂ (3 × 20 mL). The combined organic phases were dried with MgSO₄ and concentrated. Flash chromatography (hexanes/ethyl acetates 20/1 to 2/1) afforded protected diol **519a** (3.7 g, 18.5 mmol, 92%) as colorless oil (*R*_f 0.29 hexanes/ethyl acetate 5/1).

¹H NMR (300 MHz, CDCl₃) δ 4.23 (t, *J* = 1.8 Hz, 2H), 4.18 (t, *J* = 1.8 Hz, 2H), 0.79 (s, 9H), 0.00 (s, 6H), no OH-resonance observed; ¹³C NMR (75 MHz, CDCl₃) δ 84.5 (C), 83.0 (C), 51.7 (CH₂), 51.2 (CH₂), 25.8 (3 × CH₃), 18.3 (C), -5.2 (2 × CH₃); IR (in substance) ν 3375, 2955-2855 cm⁻¹. Anal. Calcd for C₁₀H₂₀O₂Si: C, 59.95; H, 10.06.

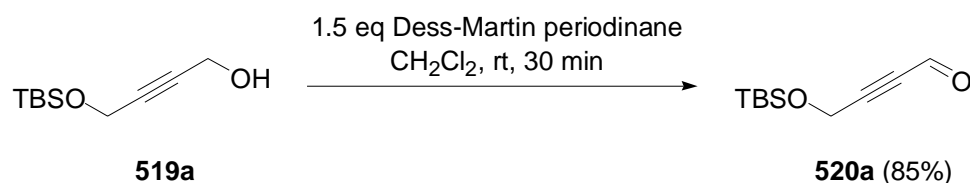
⁴⁵³ Commercially available from Narchem. Synthesized analogue to: Zhao, L.; Lu, X.; Xu, W. *J. Org. Chem.* **2005**, *70*, 4059-4063.

⁴⁵⁴ Padwa, A.; Lipka, H.; Watterson, S. H.; Murphree, S. S. *J. Org. Chem.* **2003**, *68*, 6238-6250.



Protected Diol 519b.⁴⁵⁵ As described in the preceding paragraph, 2-butene-1,4-diol (**470**) (1.8 g, 20.0 mmol) was treated with *tert*-butyldimethylchlorosilane TBSCl (1.5 g, 10.0 mmol) and imidazole (0.7 g, 11.0 mmol). Flash chromatography (hexanes/ethyl acetate 20/1 to 2/1) afforded the protected diol **519b** (1.5 g, 7.3 mmol, 73%) as colorless oil (R_f 0.26 hexanes/ethyl acetate 5/1).

¹H NMR (300 MHz, CDCl₃) δ 5.85-5.68 (m, 2H), 4.13-4.07 (m, 4H), 0.84 (s, 9H), 0.00 (s, 6H), no OH-resonance observed; ¹³C NMR (75 MHz, CDCl₃) δ 131.0 (CH), 128.9 (CH), 63.2 (CH₂), 63.1 (CH₂), 25.9 (3 \times CH₃), 18.4 (C), -5.3 (2 \times CH₃); IR (in substance) ν 3370, 2955-2860 cm⁻¹. Anal. Calcd for C₁₀H₂₂O₂Si: C, 59.35; H, 10.96.



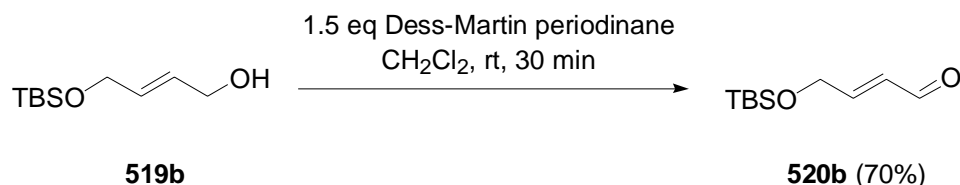
Aldehyde 520a.⁴⁵⁶ To a solution of the protected diol **519a** (50 mg, 0.3 mmol, 1.0 eq) in CH₂Cl₂ (3 mL, 1 mL/0.1 mmol) was added Dess-Martin periodinane⁴⁵⁷ (0.2 mg, 0.4 mmol, 1.5 eq) at ambient temperature. The reaction mixture was stirred for 30 min at rt, diluted with saturated aq. NaHCO₃ and extracted with CH₂Cl₂ (3 \times 3 mL). The combined organic layers were washed with aq Na₂S₂O₅ (1M, 5 mL), dried over MgSO₄, filtered through a plug of Celite and concentrated. Flash chromatography (hexanes/ethyl acetate 50/1 to 20/1) afforded the aldehyde **520a** (43 mg, 0.2 mmol, 85%) as colorless oil (R_f 0.56 hexanes/ethyl acetate 10/1).

¹H NMR (300 MHz, CDCl₃) δ 9.10 (s, 1H), 4.37 (s, 2H), 0.78 (s, 9H), 0.00 (s, 6H); ¹³C NMR (75 MHz, CDCl₃) δ 176.3 (CH), 94.8 (C), 84.2 (C), 51.5 (CH₂), 25.7 (3 \times CH₃), 18.2 (C), -5.3 (2 \times CH₃); IR (in substance) ν 2955-2855, 1675 cm⁻¹. Anal. Calcd for C₁₀H₁₈O₂Si: C, 60.56; H, 9.15.

⁴⁵⁵ Pankett, C. S.; Byrne, P. W.; Teobald, B. J.; Rola, B.; Ozanne, A.; Hitchcock, P. B. *Tetrahedron* **2004**, *60*, 2771-2784.

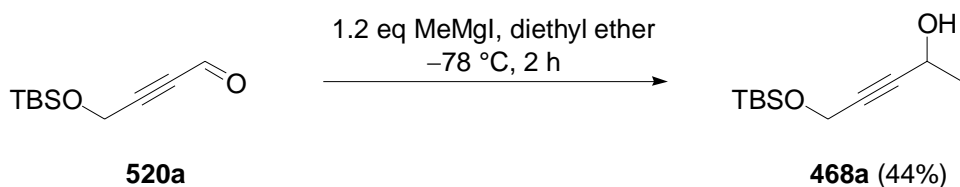
⁴⁵⁶ Morrison, C. F.; Burnell, D. J. *Tetrahedron Lett.* **2001**, *42*, 7367-7369.

⁴⁵⁷ Preparation of Dess-Martin periodinane (**523**) is described below.



Aldehyde 520b.⁴⁵⁸ As described for the synthesis of aldehyde **520a**, protected diol **519b** (50 mg, 0.3 mmol) was treated with Dess-Martin periodinane (0.16 g, 0.4 mmol). Flash chromatography afforded the aldehyde **520b** (35 mg, 0.2 mmol, 70%) as colorless oil (R_f 0.44 hexanes/ethyl acetate 10/1).

¹H NMR (300 MHz, CDCl₃) δ 9.51 (d, $J = 8.1$ Hz, 1H), 6.82 (dt, $J = 15.5, 3.3$ Hz, 1H), 6.31 (ddt, $J = 15.4, 8.1, 2.1$ Hz, 1H), 4.36 (dd, $J = 3.2, 2.2$ Hz, 2H), 0.83 (s, 9H), 0.00 (s, 6H); ¹³C NMR (75.5 MHz, CDCl₃) δ 193.3 (CH), 156.3 (CH), 130.6 (CH), 62.2 (CH₂), 61.7 (CH₂), 25.8 (3 \times CH₃), 18.3 (C), -5.5 (2 \times CH₃); IR (in substance) ν 2955-2855, 1690 cm⁻¹. Anal. Calcd for C₁₀H₂₀O₂Si: C, 59.95; H, 10.06.

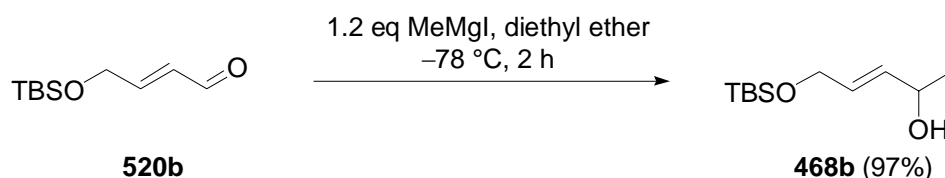


Alcohol 468a.⁴⁵⁹ To a solution of the aldehyde **520a** (2.8 g, 14.3 mmol, 1.0 eq) in diethyl ether (28 mL, 2 mL/mmol) was added a solution of methyl magnesium iodide (2.3 M, 7.5 mL, 17.2 mmol, 1.2 eq) [prepared in situ from magnesium (0.7 g, 30.0 mmol, 1.0 eq) and iodomethane (1.9 mL, 30.0 mmol, 1.0 eq)] at -78 °C. The reaction mixture was stirred for 2 h at -78 °C, quenched by the addition of saturated aq NH₄Cl and extracted with CH₂Cl₂ (3 \times 25 mL). The combined organic phases were dried and concentrated. Flash chromatography (hexanes/ethyl acetate 10/1) afforded alcohol **468a** (1.4 g, 6.3 mmol, 44%) as colorless oil (R_f 0.18 hexanes/ethyl acetate 10/1).

¹H NMR (300 MHz, CDCl₃) δ 4.44 (qt, $J = 6.6, 1.7$ Hz, 1H), 4.22 (d, $J = 1.8$ Hz, 2H), 1.33 (d, $J = 6.6$ Hz, 3H), 0.79 (s, 9H), 0.00 (s, 6H), no OH-resonance observed; ¹³C NMR (75 MHz, CDCl₃) δ 86.6 (C), 82.7 (C), 58.4 (CH), 51.7 (CH₂), 25.8 (3 \times CH₃), 24.2 (CH₃), 18.3 (C), -5.1 (2 \times CH₃); IR (in substance) ν 3400, 2955-2855 cm⁻¹. Anal. Calcd for C₁₁H₂₂O₂Si: C, 61.63; H, 10.34.

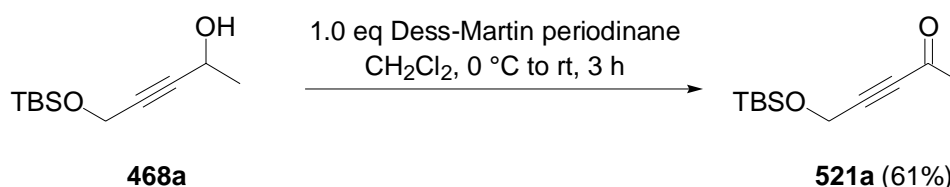
⁴⁵⁸ Crilley, M. M. L.; Golding, B. T.; Pierpoint, C. *J. Chem. Soc., Perkin Trans. 1* **1988**, 2061-2067.

⁴⁵⁹ Wipf, P.; Rahman, L. T.; Rector, S. R. *J. Org. Chem.* **1998**, *63*, 7132-7133.



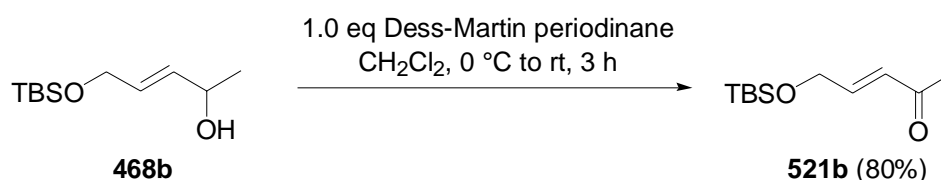
Alcohol 468b.⁴⁶⁰ Analogous to the procedure for the preparation of alcohol **468a**, aldehyde **520b** (1.0 g, 4.9 mmol) was treated with a solution of methyl magnesium iodide (2.3 M, 2.6 mL, 5.9 mmol). Flash chromatography (hexanes/ethyl acetate 10/1) afforded the alcohol **468b** (1.0 g, 4.8 mmol, 97%) as colorless oil (R_f 0.21 hexanes/ethyl acetate 10/1).

¹H NMR (300 MHz, CDCl₃) δ 5.70-5.64 (m, 2H), 4.31-4.21 (m, 1H), 4.10 (d, J = 2.9 Hz, 2H), 1.20 (d, J = 6.6 Hz, 3H), 0.84 (s, 9H), 0.00 (s, 6H), no OH-resonance observed; ¹³C NMR (75 MHz, CDCl₃) δ 134.0 (CH), 129.3 (CH), 68.3 (CH), 63.1 (CH₂), 25.9 (3 \times CH₃), 23.2 (CH₃), 18.4 (C), -5.2 (2 \times CH₃); IR (in substance) ν 3345, 2955-2855 cm⁻¹. Anal. Calcd for C₁₁H₂₄O₂Si: C, 61.05; H, 11.18.



Ketone 521a.⁴⁶¹ To an ice-cooled solution of the alcohol **468a** (1.4 g, 6.3 mmol, 1.0 eq) in CH₂Cl₂ (36 mL, 6 mL/mmol) was added Dess-Martin periodinane⁴⁵⁷ (2.7 g, 6.3 mmol, 1.0 eq). The reaction mixture stirred for 1 h at 0 °C and 2 h at rt, diluted with saturated aq NaHCO₃ and extracted with CH₂Cl₂ (3 \times 3 mL). The combined organic layers were washed with aq Na₂S₂O₅ (1M, 10 mL), dried over MgSO₄, filtered through a plug of Celite and concentrated. Flash chromatography (hexanes/ethyl acetate 20/1) afforded the ketone **521a** (0.8 g, 3.8 mmol, 61%) as colorless oil (R_f 0.47 hexanes/ethyl acetate 10/1).

¹H NMR (300 MHz, CDCl₃) δ 4.33 (s, 2H), 2.21 (s, 3H), 0.78 (s, 9H), 0.00 (s, 6H). Anal. Calcd for C₁₁H₂₀O₂Si: C, 62.21; H, 9.49.



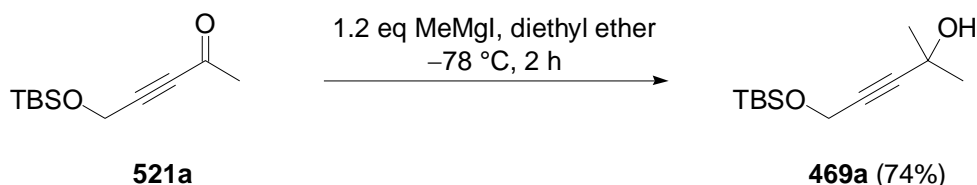
Ketone 521b.⁴⁶¹ As described for the preparation of ketone **521a**, alcohol **468b** (0.13 g, 0.6 mmol) was treated with Dess-Martin periodinane⁴⁵⁷ (0.25 g, 0.6 mmol, 1.0 eq). Flash

⁴⁶⁰ Belelie, J. L.; Chong, J. M. *J. Org. Chem.* **2002**, *67*, 3000-3006.

⁴⁶¹ Piggot, M. J.; Wege, D. *Aust. J. Chem.* **2003**, *56*, 691-702.

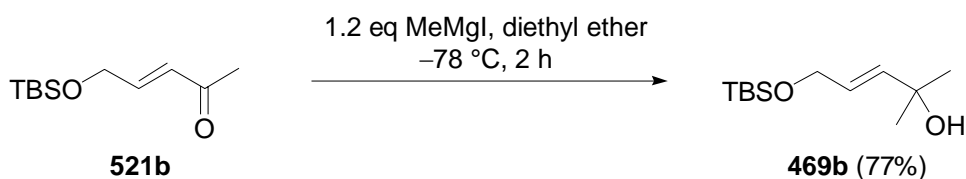
chromatography (hexanes/ethyl acetate 20/1) afforded the ketone **521b** (0.10 g, 0.5 mmol, 80%) as colorless oil (R_f 0.50 hexanes/ethyl acetate 10/1).

^1H NMR (300 MHz, CDCl_3) δ 6.74 (dt, $J = 15.8, 3.5$ Hz, 1H), 6.25 (dt, $J = 15.8, 2.2$ Hz, 1H), 4.28 (dd, $J = 3.3, 2.2$ Hz, 2H), 0.84 (s, 9H), 0.00 (s, 6H); Anal. Calcd for $\text{C}_{11}\text{H}_{22}\text{O}_2\text{Si}$: C, 61.63; H, 10.34.



Alcohol 469a.⁴⁶² To a solution of the ketone **521a** (0.8 g, 3.9 mmol, 1.0 eq) in diethyl ether (8 mL, 2 mL/mmol) was added a solution of methyl magnesium iodide (1.5 M, 3.0 mL, 4.63 mmol, 1.2 eq) [prepared in situ from magnesium (2.9 g, 12.0 mmol, 1.0 eq) and iodomethane (0.8 mL, 12.0 mmol, 1.0 eq)] at -78°C . The reaction mixture was stirred for 1 h at -78°C and 1 h at rt, quenched by the addition of saturated aq NH_4Cl and extracted with CH_2Cl_2 (3×6 mL). The combined organic phases were dried and concentrated. Flash chromatography (hexanes/ethyl acetate 5/1) afforded alcohol **469a** (0.7 g, 2.9 mmol, 74%) as colorless oil (R_f 0.35 hexanes/ethyl acetate 10/1).

^1H NMR (300 MHz, CDCl_3) δ 4.21 (s, 2H), 1.49 (s, 6H), 0.79 (s, 9H), -0.01 (s, 6H), no OH-resonance observed; ^{13}C NMR (75 MHz, CDCl_3) δ 89.4 (C), 80.8 (C), 65.1 (C), 51.7 (CH_2), 31.3 ($2 \times \text{CH}_3$), 25.8 ($3 \times \text{CH}_3$), 18.3 (C), -5.1 ($2 \times \text{CH}_3$). Anal. Calcd for $\text{C}_{12}\text{H}_{24}\text{O}_2\text{Si}$: C, 63.10; H, 10.59.

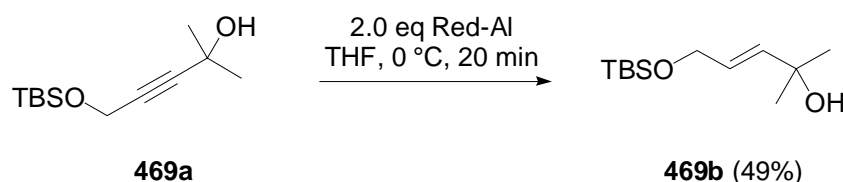


Alcohol 469b.⁴⁶² As outlined in the preceding paragraph, ketone **521b** (0.8 g, 3.5 mmol) was treated with a solution of methyl magnesium iodide (1.5 M, 2.7 mL, 4.3 mmol). Flash chromatography (hexanes/ethyl acetate 5/1) afforded the alcohol **469b** (0.6 g, 2.7 mmol, 77%) as colorless oil (R_f 0.26 hexanes/ethyl acetate 10/1).

^1H NMR (300 MHz, CDCl_3) δ 5.75 (brd, $J = 15.8$ Hz, 1H), 5.67 (dt, $J = 15.6, 4.5$ Hz, 1H), 4.11 (dd, $J = 4.6, 1.3$ Hz, 2H), 1.25 (s, 6H), 0.84 (s, 9H), 0.00 (s, 6H), no OH-resonance observed; ^{13}C NMR (75 MHz, CDCl_3) δ 137.9 (CH), 126.1 (CH), 70.5 (C), 63.4 (CH_2), 29.7

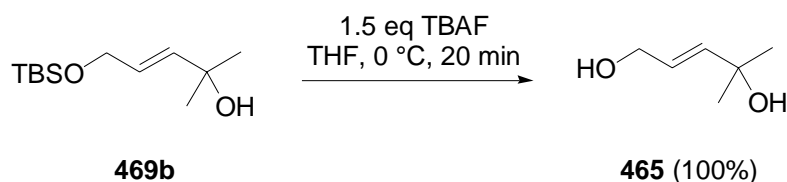
⁴⁶² Trost, B. M.; Corte, J. R.; Gudiksen, M. S. *Angew. Chem., Int. Ed.* **1999**, *38*, 3662-3664.

(2 × CH₃), 25.9 (3 × CH₃), 18.4 (C), -5.2 (2 × CH₃). Anal. Calcd for C₁₂H₂₆O₂Si: C, 62.55; H, 11.37.



Alcohol 469b.⁴⁶² To an ice-cooled solution of alcohol **469a** (40 mg, 0.2 mmol, 1.0 eq) in THF (2 mL, 10 mL/mmol) was added a solution of Red-Al (65% in toluene, 0.1 mL, 0.4 mmol, 2.0 eq). The reaction mixture was stirred for 20 min at 0 °C, carefully quenched with saturated aq NH₄Cl, extracted with CH₂Cl₂ (3 × 3 mL). The combined organic phases were dried and concentrated. Flash chromatography (hexanes/ethyl acetate 5/1) afforded alcohol **469b** (19 mg, 0.08 mmol, 49%) as colorless oil (*R_f* 0.26 hexanes/ethyl acetate 10/1).

¹H NMR (300 MHz, CDCl₃) δ 5.75 (brd, *J* = 15.8 Hz, 1H), 5.67 (dt, *J* = 15.6, 4.5 Hz, 1H), 4.11 (dd, *J* = 4.6, 1.3 Hz, 2H), 1.58, 1.25 (s, 6H), 0.84 (s, 9H), 0.00 (s, 6H), no OH-resonance observed; ¹³C NMR (75.5 MHz, CDCl₃) δ 137.9 (CH), 126.1 (CH), 70.5 (C), 63.4 (CH₂), 29.7 (2 × CH₃), 25.9 (3 × CH₃), 18.4 (C), -5.2 (2 × CH₃). Anal. Calcd for C₁₂H₂₆O₂Si: C, 62.55; H, 11.37.

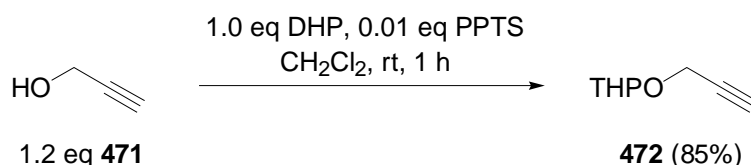


Diol 465.⁴⁶³ To an ice-cooled solution of the alcohol **469b** (0.7 g, 3.2 mmol, 1.0 eq) in THF (10 mL, 3 mL/mmol) was added tetrabutyl ammonium fluoride (1.5 g, 4.8 mmol, 1.5 eq). After stirring for 3 h at 0 °C, solid NaHCO₃ (~0.5 g, 6.2 mmol, 2.0 eq) was added.⁴⁶⁴ The reaction mixture was filtered and concentrated. Flash chromatography (hexanes/ethyl acetate 1/1 to ethyl acetate) afforded the diol **465** (0.36 g, 3.2 mmol, 100%) as colorless oil (*R_f* 0.24 ethyl acetate).

¹H NMR (300 MHz, CDCl₃) δ 5.85-5.75 (m, 2H), 4.14 (d, *J* = 4.0 Hz, 2H), 1.73 (s, 2H), 1.32 (s, 6H); ¹³C NMR (75 MHz, CDCl₃) δ 139.4 (CH), 125.8 (CH), 70.5 (C), 63.0 (CH₂), 29.6 (2 × CH₃). Anal. Calcd for C₆H₁₂O₂: C, 62.04; H, 10.41.

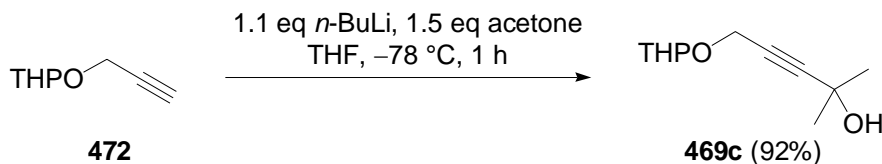
⁴⁶³ Miller, R. B.; Al-Hassan, M. I. *J. Org. Chem.* **1983**, *48*, 4113-4116.

⁴⁶⁴ Aqueous workup of the reaction led to decreased isolated yields due to the high polarity of the diol **465**.



Protected Propargylic Alcohol 472.⁴⁶⁵ To a solution of 2-propyn-1-ol (**471**) (10.0 mL, 171 mmol, 1.2 eq) in CH₂Cl₂ (85 mL, 0.5 mL/mmol) was added 3,4-dihydro-2*H*-pyrane DHP (12.9 mL, 143 mmol, 1.0 eq) and pyridinium-*para*-toluenesulfonate PPTS (0.35 g, 0.01 mmol, 0.01 eq) at ambient temperature. After stirring for 1 h at rt, the reaction was quenched with saturated aq NaHCO₃ and extracted with CH₂Cl₂ (3 × 50 mL). The combined organic phases were dried and concentrated. Flash chromatography (hexanes/ethyl acetate 20/1 to 10/1 to 3/1) afforded the protected alcohol **472** (17.0 g, 121 mmol, 85%) as colorless liquid (*R_f* 0.17 hexanes/ethyl acetate 20/1).

¹H NMR (300 MHz, CDCl₃) δ 4.81 (t, *J* = 3.1 Hz, 1H), 4.29 (dd^{AB}, *J* = 15.6, 2.4 Hz, 1H), 4.22 (dd^{AB}, *J* = 15.8, 2.6 Hz, 1H), 3.88-3.79 (m, 1H), 3.57-3.49 (m, 1H), 3.40 (d, *J* = 2.4 Hz, 1H), 1.89-1.47 (series of m, 6H); ¹³C NMR (126 MHz, CDCl₃) δ 96.8 (CH), 79.7 (C), 74.0 (CH), 62.0 (CH₂), 54.0 (CH₂), 30.2 (CH₂), 25.3 (CH₂), 19.0 (CH₂). Anal. Calcd for C₈H₁₂O₂: C, 68.54, H, 8.63.

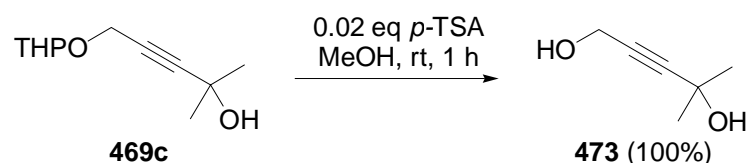


Alcohol 469c.⁴⁶⁵ To a solution of the protected alcohol **472** (0.14 g, 1.0 mmol, 1.0 eq) in THF (2 mL, 2 mL/mmol) was slowly added *n*-BuLi (2.0 M, 0.6 mL, 1.1 mmol, 1.1 eq) at -78 °C. After stirring for 10 min, acetone (0.1 mL, 1.5 mmol, 1.5 eq) was added at -78 °C. The reaction mixture was stirred until TLC indicated the complete consumption of the starting material (*R_f* 0.62 hexanes/ethyl acetate 5/1) (~1 h), quenched with saturated aq. NH₄Cl at -78 °C, diluted with CH₂Cl₂ and water, warmed to rt and extracted with CH₂Cl₂ (3 × 5 mL). The combined organic layers were dried and concentrated. Flash chromatography (hexanes/ethyl acetate 20/1 to 10/1 to 1/1) afforded alcohol **469c** (0.18 g, 0.9 mmol, 92%) as colorless oil (*R_f* 0.32 hexanes/ethyl acetate 5/1).

¹H NMR (500 MHz, CDCl₃) δ 4.79 (t, *J* = 3.3 Hz, 1H), 4.32-4.21 (m, 2H), 3.85-3.79 (m, 1H), 3.55-3.50 (m, 1H), 1.86-1.49 (series of m, 6H), 1.50 (s, 6H), no OH-resonance observed; ¹³C NMR (126 MHz, CDCl₃) δ 96.6 (CH), 90.7 (C), 77.8 (C), 65.0 (C), 61.9 (CH₂), 54.2

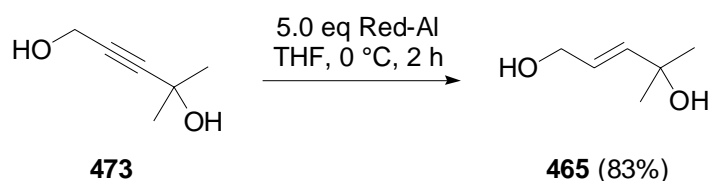
⁴⁶⁵ Díez Martín, D.; Marcos, I. S.; Basabe, P.; Romero, R. E.; Moro, R. F.; Lumeras, W.; Rodríguez, L.; Urones, J. G. *Synthesis* **2001**, 1013-1022.

(CH₂), 31.3 (2 × CH₃), 30.2 (CH₂), 25.3 (CH₂), 18.9 (CH₂). Anal. Calcd for C₁₁H₁₈O₃: C, 66.64; H, 9.15.



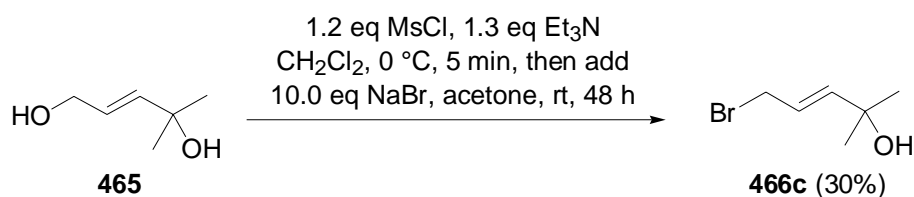
Diol 473.⁴⁶⁶ To a solution of alcohol **469c** (0.18, 0.9 mmol, 1.0 eq) in MeOH (9 mL, 10 mL/mmol) was added *para*-toluene sulfonic acid PTSA (3.5 mg, 0.02 mmol, 0.02 eq) at ambient temperature. After stirring for 1 h at rt solid NaHCO₃ (10 mg, 0.1 mmol, 0.1 eq) was added.⁴⁶⁴ The reaction mixture was stirred for 10 min, filtered and concentrated. Flash chromatography (hexanes/ethyl acetate 10/1 to 1/1) afforded the diol **473** (0.11 g, 0.9 mmol, 100%) as colorless oil (*R_f* 0.26 hexanes/ethyl acetate 1/1).

¹H NMR (300 MHz, CDCl₃) δ 4.27 (s, 2H), 2.79 (brs, 2H), 1.50 (s, 6H); ¹³C NMR (147 MHz, CDCl₃) δ 90.2 (C), 80.2 (C), 65.0 (C), 50.5 (CH₂), 31.1 (2 × CH₃). Anal. Calcd for C₆H₁₀O₂: C, 63.14; H, 8.83.



Diol 465.⁴⁶³ To an ice-cooled solution of the alcohol **473** (52 mg, 0.5 mmol, 1.0 eq) in THF (2 mL, 4 mL/mmol) was added a solution of Red-Al (65% in toluene, 0.7 mL, 4.8 mmol, 1.5 eq). After stirring for 2 h at 0 °C, solid water (54 μL) and MgSO₄ (~100 mg) was added.⁴⁶⁷ The reaction mixture was filtered and concentrated. Flash chromatography (ethyl acetate) afforded the diol **465** (44 mg, 0.4 mmol, 83%) as colorless oil (*R_f* 0.24 ethyl acetate).

¹H NMR (300 MHz, CDCl₃) δ 5.85-5.75 (m, 2H), 4.14 (d, *J* = 4.0 Hz, 2H), 1.73 (s, 2H), 1.32 (s, 6H); ¹³C NMR (75 MHz, CDCl₃) δ 139.4 (CH), 125.8 (CH), 70.5 (C), 63.0 (CH₂), 29.6 (2 × CH₃). Anal. Calcd for C₆H₁₂O₂: C, 62.04; H, 10.41.

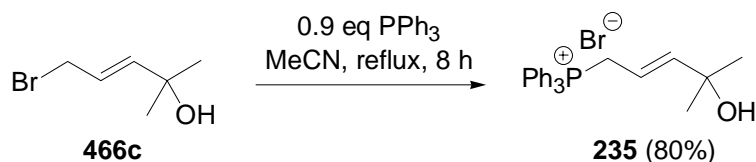


⁴⁶⁶ Commercially available from Scientific Exchange. For reference data, see: reference 465.

⁴⁶⁷ Usual aqueous workup with saturated aq NH₄Cl and extraction with chloroform led to decreased isolated yields due to the high polarity of the diol **465**.

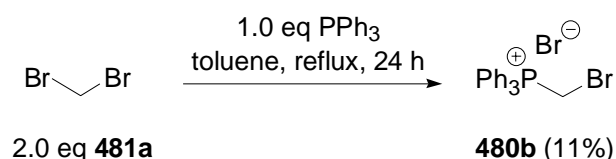
Allylic Bromide 466c.⁴⁶⁸ To a stirred solution of the diol **465** (80 mg, 0.7 mmol, 1.0 eq) in CH_2Cl_2 (1.5 mL, 2 mL/mmol) were added Et_3N (0.1 mL, 0.9 mmol, 1.2 eq) and methane sulfonyl chloride (70 μl , 0.9 mmol, 1.3 eq). After stirring for 5 min NaBr (0.7 g, 7.2 mmol, 10.0 eq) and acetone (3 mL, 4 mL/mmol) were added. The reaction mixture was warmed to rt, stirred in the dark for 48 h at ambient temperature,⁴⁶⁹ filtered and concentrated. Flash chromatography (hexanes/ethyl acetate 10/1) afforded the allylic bromide **466c** (37 mg, 0.2 mmol, 30%) as pale yellow oil (R_f 0.41 hexanes/ethyl acetate 3/1).

^1H NMR (300 MHz, CDCl_3) δ 5.91-5.86 (m, 2H), 3.97-3.93 (m, 2H), 1.59 (brs, 1H), 1.31 (s, 6H); ^{13}C NMR (126 MHz, CDCl_3) δ 142.8 (CH), 123.2 (CH), 70.4 (C), 32.5 (CH_2), 29.5 (2 \times CH_3); IR (in substance) ν 3375, 2975-2865 cm^{-1} . Anal. Calcd for $\text{C}_6\text{H}_{11}\text{BrO}$: C, 40.25; H, 6.19; Cl, 44.63.



Wittig Salt 235. To a solution of the allyl bromide **466c** (0.25 g, 1.4 mmol, 1.0 eq) in acetonitrile (3 mL, 2 mL/mmol) was added triphenylphosphine (0.32 g, 1.2 mmol, 0.9 eq) at ambient temperature. The reaction mixture was refluxed for 8 h, cooled to rt and concentrated. The brown reaction product was suspended in ethyl acetate (70 mL) and heated to reflux for 2 h. The solvent was removed by filtration and the solid was washed thoroughly with ethyl acetate to afford the Wittig salt **235** (0.44 g, 1.0 mmol, 80%) as white solid.

^1H NMR (300 MHz, CDCl_3) δ 7.87-7.60 (m, 15H), 5.93 (dd, J = 15.1, 4.7 Hz, 1H), 5.68-5.59 (m, 1H), 4.58-4.48 (m, 2H), 1.07 (s, 6H); ^{13}C NMR (126 MHz, CDCl_3) δ 150.0 (J (P-C) = 12.1 Hz, CH), 134.9 (J (P-C) = 2.4 Hz, CH), 133.9 (J (P-C) = 9.7 Hz, 2 \times CH), 130.3 (J (P-C) = 13.3 Hz, 2 \times CH), 117.9 (J (P-C) = 86.0 Hz, C), 110.6 (J (P-C) = 9.7 Hz, CH), 70.3 (J (P-C) = 2.4 Hz, C), 29.3 (J (P-C) = 2.4 Hz, 2 \times CH_3), 27.5 (J (P-C) = 49.7 Hz, CH_2); IR (in substance) ν 3290, 3055-2780 cm^{-1} . Anal. Calcd for $\text{C}_{24}\text{H}_{27}\text{BrO}$: C, 40.25; H, 6.19; Cl, 44.63.

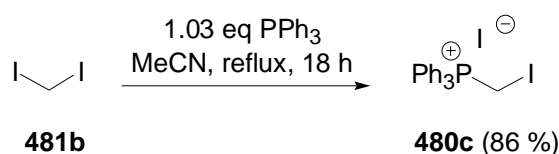


⁴⁶⁸ Kawase, A. *PCT Int. Appl.* **1998**.

⁴⁶⁹ Shorter reaction times afforded mixtures of the bromide **466c** and the corresponding chloride **466b** (^1H NMR (300 MHz, CDCl_3) δ 5.94 (d, J = 15.4 Hz, 1H), 5.81 (dt, J = 5.4, 6.4 Hz, 1H), 4.06 (d, J = 6.3 Hz, 2H), 1.33 (s, 6H); ^{13}C NMR (126 MHz, CDCl_3) δ 142.8 (CH), 123.2 (CH), 70.4 (C), 32.5 (CH_2), 29.5 (2 \times CH_3); IR (in substance) ν 3400, 2975-2865 cm^{-1} . Anal. Calcd for $\text{C}_6\text{H}_{11}\text{ClO}$: C, 53.54; H, 8.24; Cl, 26.34.)

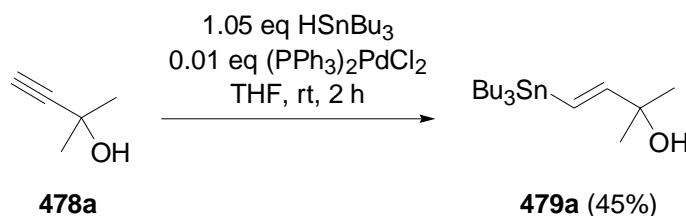
Wittig Salt 480b.⁴⁷⁰ A solution of dibromomethane **481a** (3.5 mL, 50.0 mmol, 2.0 eq) and triphenylphosphine (6.6 g, 25.0 mmol, 1.0 eq) in toluene (50 mL, 1 mL/mmol **481**) was refluxed for 24 h and then cooled to 0 °C whereupon a white precipitate was formed. The solvent was removed by filtration and the solid was washed with toluene (3 × 3 mL) and dried under reduced pressure to afford the Wittig salt **480b** (1.2 g, 2.7 mmol, 11%) as white solid.

¹H NMR (300 MHz, CDCl₃) δ 7.91-7.58 (m, 15H), 5.71 (d, *J* = 5.7 Hz, 2H); ¹³C NMR (126 MHz, CDCl₃) δ 135.4 (*J* (P-C) = 3.4 Hz, 3 × CH), 134.1 (*J* (P-C) = 10.2 Hz, 6 × CH), 130.3 (*J* (P-C) = 13.6 Hz, 6 × CH), 116.6 (*J* (P-C) = 89.3 Hz, 3 × C), 18.3 (*J* (P-C) = 54.3 Hz, CH₂). Anal. Calcd for C₁₉H₁₇Br₂P: C, 52.33; H, 3.83; Br, 36.64.



Wittig Salt 480c.⁴⁷¹ To a solution of diiodomethane **481b** (2.0 mL, 24.8 mmol, 1.0 eq) in acetonitrile (25 mL, 1 mL/mmol) was added triphenylphosphine (6.7 g, 25.5 mmol, 1.03 eq) at rt. The reaction mixture was heated to reflux in the dark for 18 h, cooled to rt and diluted with diethyl ether whereupon a white solid was formed. The solvents were removed by filtration and the reaction product was washed with diethyl ether and dried under reduced pressure to afford the Wittig salt **480c** (11.4 g, 21 mmol, 86%) as light sensitive white solid.⁴⁷²

¹H NMR (300 MHz, CDCl₃) δ 7.95-7.68 (m, 15H), 5.23 (d, *J* = 7.2 Hz, 2H); IR (in substance) ν 3055-2740 cm⁻¹. Anal. Calcd for C₁₉H₁₇I₂P: C, 43.05; H, 3.23. Found: C, 43.06; H, 3.08.



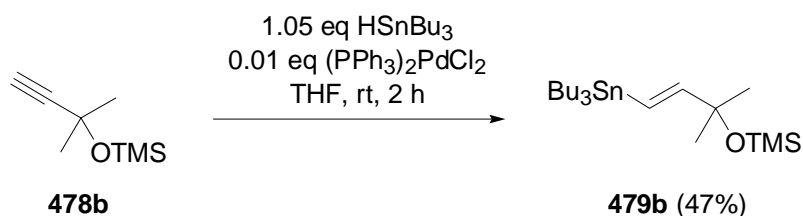
⁴⁷⁰ Commercially available from Aldrich. Lawrence, N. J.; Liddle, J.; Jackson, D. *J. Chem. Soc., Perkin Trans. 1* **2002**, 2260-2267. Prepared analogue to: Rodriguez, J. G.; Martin-Villamil, R.; Lafuente, A. *Tetrahedron* **2003**, *59*, 2021-1032. Yields not optimized.

⁴⁷¹ Commercially available from Aldrich. Vogt, H.; Lauritsen, K.; Riesel, L.; von Loewis, M.; Reck, G. *Z. Nat. B* **1993**, *48*, 1760-1766.

⁴⁷² If stored without light protection, the solid became yellow.

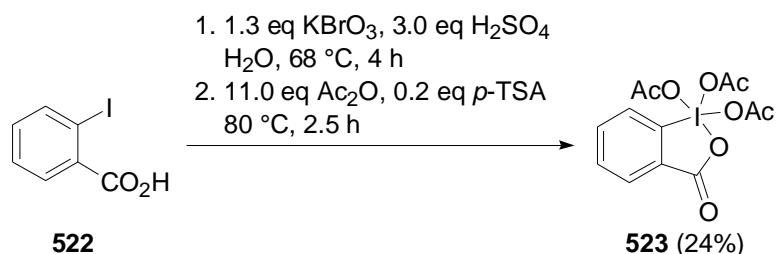
Stannane 479a.⁴⁷³ To a solution of the alkyne **478a** (0.2 mL, 2.0 mmol, 1.0 eq) in THF (2 mL, 1 mL/mmol) were added $(\text{PPh}_3)_2\text{PdCl}_2$ (14 mg, 0.02 mmol, 0.01 eq) and HSnBu_3 (0.6 mL, 2.1 mmol, 1.05 eq) at rt. The yellow solution was stirred for 2 h at ambient temperature and turned dark orange. The solvents were removed and the crude product was purified by flash chromatography to yield stannane **479a** (0.34 g, 0.9 mmol, 45%) as pale yellow oil (R_f 0.62 hexanes/ethyl acetate 5/1).

^1H NMR (300 MHz, CDCl_3) δ 6.22-5.98 (m, 2H), 1.53-1.42 (m, 6H), 1.36-1.22 (m, 6H), 1.29 (s, 6H), 1.00 (m, 6H), 0.88 (t, $J = 7.4$ Hz, 9H), no OH-resonance observed; ^{13}C NMR (126 MHz, CDCl_3) δ 155.2 (CH), 122.4 (CH), 72.4 (C), 29.4 ($2 \times \text{CH}_3$), 29.0 ($3 \times \text{CH}_2$), 27.2 ($3 \times \text{CH}_2$), 13.7 ($3 \times \text{CH}_3$), 9.4 ($3 \times \text{CH}_2$); IR (in substance) ν 3350, 2955-2850 cm^{-1} . Anal. Calcd for $\text{C}_{17}\text{H}_{36}\text{OSn}$: C, 54.42; H, 9.67.



Stannane 479b.⁴⁷⁴ As described for stannane **479a**, alkyne **478b** (0.4 mL, 2.0 mmol, 1.0 eq) was treated with $(\text{PPh}_3)_2\text{PdCl}_2$ (14 mg, 0.02 mmol, 0.01 eq) and HSnBu_3 (0.6 mL, 2.1 mmol, 1.05 eq). Flash chromatography (hexanes/ethyl acetate 100/1) afforded the stannane **479b** (0.42 g, 0.9 mmol, 47%) as pale yellow oil (R_f 0.35 hexanes/ethyl acetate 100/1).

^1H NMR (300 MHz, CDCl_3) δ 6.10-5.97 (m, 2H), 1.55-1.42 (m, 6H), 1.34-1.26 (m, 12H), 0.94-0.84 (m, 15H), 0.10 (s, 9H). ^{13}C NMR (126 MHz, CDCl_3) δ 156.2 (CH), 122.5 (CH), 75.3 (C), 30.1 ($2 \times \text{CH}_3$), 29.1 ($3 \times \text{CH}_2$), 27.3 ($3 \times \text{CH}_2$), 13.7 ($3 \times \text{CH}_3$), 9.4 ($3 \times \text{CH}_2$), 2.6 ($3 \times \text{CH}_3$); IR (in substance) ν 2955-2855 cm^{-1} . Anal. Calcd for $\text{C}_{20}\text{H}_{44}\text{OSiSn}$: C, 53.70; H, 9.91.



⁴⁷³ Gallagher, W. P.; Terstiege, I.; Maleczka, R. E., Jr. *J. Am. Chem. Soc.* **2005**, *123*, 3194-3204. Yields not optimized.

⁴⁷⁴ Lumb, J.-P.; Trauner, D. *J. Am. Chem. Soc.* **2005**, *127*, 2870-2871. Yields not optimized.

Dess-Martin Periodinane 523.⁴⁷⁵ A solution of 2-iodobenzoic acid (**522**) (30.0 g, 121 mmol, 1.0 eq) in aq H₂SO₄ (0.73 M, 0.5 L, 365 mmol, 3.0 eq) was heated to 55 °C and KBrO₃ (26.3 g, 157 mmol, 1.3 eq) was slowly added within 30 min. The reaction mixture was stirred for 4 h at 68 °C whereupon gaseous bromine evolved, cooled to 0 °C and filtered. The solid was washed carefully with water/ethanol (1/1, 500 mL) and then with diethyl ether (200 mL). The white solid was dried at high vacuum (0.05 mmbar) and then dissolved in freshly distilled acetic anhydride (125 mL, 1331 mmol, 11.0 eq). To the reaction mixture *para*-toluene sulfonic acid (4.6 g, 24.2 mmol, 0.2 mmol) was added, the resulting reaction mixture was heated to 80 °C for 2.5 h, cooled to rt and filtered. The resulting white solid was thoroughly washed with diethyl ether (1 L) and dried at reduced pressure to afford Dess-Martin periodinane **523** (12.4 g, 29.3 mmol, 24%) as white solid that was stored at -32 °C protected from light.

¹H NMR (300 MHz, CDCl₃) δ 8.37 (d, *J* = 8.1 Hz, 1H), 8.14-8.06 (m, 2H), 7.98-7.90 (m, 1H), 2.20 (s, 3H), 1.91 (s, 6H).

⁴⁷⁵ Dess, B. D.; Martin, J. C. *J. Am. Chem. Soc.* **1991**, *113*, 7277-7287.

21 Appendix

List of Abbreviations

| | |
|------------|---|
| Å | angstrom, 1/10 of a nanometer |
| abs. | absolute |
| Ac | acetyl |
| α | optical rotation |
| aq | aqueous |
| ATR | attenuate total reflectance |
| AVE | allyl vinyl ether |
| 9-BBN-H | borabicyclo[3.3.1]nonane |
| Bn | benzyl |
| BOC | <i>tert</i> -butyloxycarbonyl |
| Box | bis(oxazoline) |
| Bu | butyl |
| CAC | catalytic asymmetric Claisen rearrangement |
| cal | calory |
| CoA | coenzyme A |
| COSY | correlated spectroscopy |
| conc | concentrated |
| Cp | cyclopentadienyl |
| CSA | camper sulfonic acid |
| Cy | cyclohexyl |
| d | days |
| DBU | 1,8-diazabicyclo[5.4.0]undec-7-ene |
| DCC | <i>N,N</i> -dicyclohexylcarbodiimide |
| DCE | 1,2-dichloroethane |
| DEPT | distortionless enhancement by polarization transfer |
| DDQ | 2,3-dichlor-5,6-dicyano-1,4-benzochinone |
| Δ | heating |
| DAD | diode array detector |
| de | diastereomeric excess |
| ΔG | free enthalpy |
| DIBAL-H | diisobutylaluminiumhydride |

| | |
|------------|---|
| DIAD | diisopropylazodicarboxylate |
| DHP | 1,2-dihydro-2 <i>H</i> -pyrane |
| DMAP | 4-(<i>N,N</i> -dimethylamino)pyridine |
| DMAPP | dimethylallylpyrophosphate |
| DMF | <i>N,N</i> -dimethylformamide |
| DMSO | dimethylsulfoxide |
| dppf | 1,1'-bis(diphenylphosphino)ferrocene |
| dr | diastereomeric ratio |
| E | energy |
| EDCI | <i>N</i> -(3-dimethylaminopropyl)- <i>N'</i> -ethylcarbodiimide-hydrochloride |
| ee | enantiomeric excess |
| e.g. | for example |
| ELSD | Evaporative Light Scattering Detector |
| Eq | equation |
| eq | equivalent |
| Et | ethyl |
| <i>epi</i> | epimeric |
| FPP | farnesylpyrophosphate |
| FT | Fourier transformation |
| g | gram |
| G | carbanion stabilizing group |
| GPP | geranylpyrophosphate |
| GGPP | geranylgeranyldiphosphate |
| h | hours |
| HCV | hepatitis C virus |
| HIV | human immunodeficiency virus |
| Hex | hexyl |
| HMBC | heteronuclear multiple bond coherence |
| HMDS | hexamethyldisilazide |
| HMPA | <i>N,N,N</i> -hexamethylphosphoric acid triamide |
| HPLC | high pressure liquid chromatography |
| HSQC | heteronuclear single quantum coherence |
| HWE | Horner-Wadsworth-Emmons |
| Hz | Hertz |

| | |
|------------------|---|
| <i>i</i> | <i>iso</i> |
| IC ₅₀ | concentration of an inhibitor to induce 50% inhibition of an enzyme |
| i.e. | id est (lat.) = that is |
| IPP | isopentenylpyrophosphate |
| IR | infrared spectroscopy |
| L | ligand |
| lat. | Latin |
| LDA | lithium diisopropylamide |
| LiDBB | lithium di- <i>tert</i> -butylbiphenyl |
| <i>lk</i> | <i>like</i> |
| M | metall |
| MCPBA | <i>meta</i> -chloroperbenzoic acid |
| Me | methyl |
| Mes | mesityl (2,4,6-trimethylphenyl) |
| mL | milliliter |
| mm | millimeter |
| min | minute |
| Ms | methanesulfonyl |
| NADPH | nicotinic amide-adenosine-dinucleotide-phosphate |
| n.i. | not isolated |
| NIS | <i>N</i> -iodosuccinimide |
| NHK | Nozaki-Hiyama-Kishi |
| NMO | <i>N</i> -methyldmorpholine- <i>N</i> -oxide |
| NMM | <i>N</i> -methyldmorpholine |
| NMR | nuclear magnetic resonance spectroscopy |
| NOE | nuclear Overhauser effect |
| Ø | diameter |
| OTf | triflate (trifluoromethanesulfonate) |
| <i>p</i> | <i>para</i> |
| ppm | parts per million |
| Ph | phenyl |
| Pr | propyl |
| Pg | protection group |
| Piv | pivaloyl |

| | |
|----------------|--|
| PMB | <i>para</i> -methoxybenzyl |
| PP | pyrophosphate |
| PPTS | pyridinium- <i>p</i> -toluenesulfonate |
| PT-SH | 1-phenyl-1 <i>H</i> -tetrazole-5-thiole |
| Py | pyridine |
| PyBOP | Benzotriazolylxytris(pyrrolidine)phosphonium hexafluorophosphate |
| quant. | quantitative |
| r | distance between two atoms |
| R | unspecified substituent |
| R_f | ratio of front |
| R_t | retention time |
| rt | room temperature |
| sp. | species |
| SPT | serine palmitoyltransferase |
| TBAF | tetrabutylammoniumfluoride |
| TBS | <i>tert</i> -butyldimethylsilyl |
| TES | triethylsilyl |
| TFA | trifluoroacetic acid |
| THF | tetrahydrofuran |
| THP | tetrahydropyranyl |
| TIPS | triisopropylsilyl |
| TMG | 1,1,3,3-tetramethylguanidin |
| TMS | trimethylsilyl |
| TPAP | tetra- <i>n</i> -propylammoniumperruthenate |
| TPS | <i>tert</i> -butyldiphenylsilyl |
| <i>p</i> -TsOH | <i>para</i> -Toluensulfonic acid |
| Ts | tosyl (<i>p</i> -toluenesulfonyl) |
| Tol | toluene |
| TyrMe | tyrosine methyl ester |
| VF | viridifungin |
| vol | volume |
| vs | versus |
| <i>ul</i> | <i>unlike</i> |

Parts of this thesis work have been covered by recent publications

- Xeniolide F: - Pollex, A.; Hiersemann, M. *Org. Lett.* **2005**, *7*, 5705-5708.
- Virdiofungins: - Pollex, A.; Millet, A.; Müller, J, Hiersemann, M.; Abraham, L. *J. Org. Chem.* **2005**, *70*, 5579-5591.
- Pollex, A.; Abraham, L.; Müller, J.; Hiersemann, M. *Tetrahedron Lett.* **2004**, *45*, 6915-6918.

Acknowledgement

This thesis work is based on results obtained previously in our research group and on contributions of many other committed scientists, past and present. Their work, which is the foundation of this thesis is gratefully acknowledged.

I thank M. Hiersemann for his support and the right balance between demanding work atmosphere and motivation. Great thanks are given to all members of the group: to Lars who was a real friend and who has accompanied me through the whole study time. His contribution to the successful completion of the viridiofungin synthesis is very much appreciated. To Hannes for always being a good example on the ‘cooking job’. And to Julia for always reminding me not to underestimate women’s strength and for accompanying me on an ambitious path. To Marleen, Agnés, Annika and Daniel for keeping the spirits up. And to all undergraduate research participants for a good and productive time.

Many others have contributed to the completion of this work. I thank the members of the Metz group, the Knölker group and the Straßner group for numerous fruitful discussions and memorable spare time activities. Furthermore, this work was supported by very helpful analytic staff. Particularly, I thank Mrs. Böhler, Mrs. Rudolph and Dr. Gruner for numerous quickly elaborated NMR spectra, A. Peritz for the elemental analysis, Mrs. Rößler for recording IR spectra and to Dr. Bauer for performing the mass spectra analysis. G. Schlechtingen supported me during the reversed phase HPLC separation of the viridiofungins. Mrs. Hass’ and Mr. Püschel’s efforts for the prompt supply with all required chemicals and solvents is gratefully appreciated. Last but not least, my thanks are addressed to all other staff of the TU Dresden and the Studentenwerk for contributing to a successful study time.

There are four people to whom I owe more than to any other person. They are my parents, my sister Sylvia and Patrick. They are my greatest confidants and supporters. They shared both the success and the times of uncertainty and I wish to heartily thank them for their love, help and guidance.

Financial support of this thesis work by the Deutsche Forschungsgemeinschaft is gratefully acknowledged.

Versicherung

Hiermit versichere ich, dass ich die vorliegende Arbeit ohne unzulässige Hilfe Dritter und ohne Benutzung anderer als der angegebenen Hilfsmittel angefertigt habe; die aus fremden Quellen direkt oder indirekt übernommenen Gedanken sind als solche kenntlich gemacht. Die Arbeit wurde bisher weder im Inland noch im Ausland in gleicher oder ähnlicher Form einer anderen Prüfungsbehörde vorgelegt.

Die vorliegende Arbeit wurde auf Vorschlag und unter Anleitung von Herrn Prof. M. Hiersemann im Zeitraum von September 2003 bis September 2006 am Institut für Organische Chemie der Technischen Universität Dresden angefertigt.

Es haben bisher keine Promotionsverfahren stattgefunden.

Ich erkenne die Promotionsordnung der Fakultät Mathematik und Naturwissenschaften der Technischen Universität Dresden, vom 16.4.2003 an.

Dresden, den 14.08.2006

Annett Pollex